MARCH 1978

# analytical chemistry

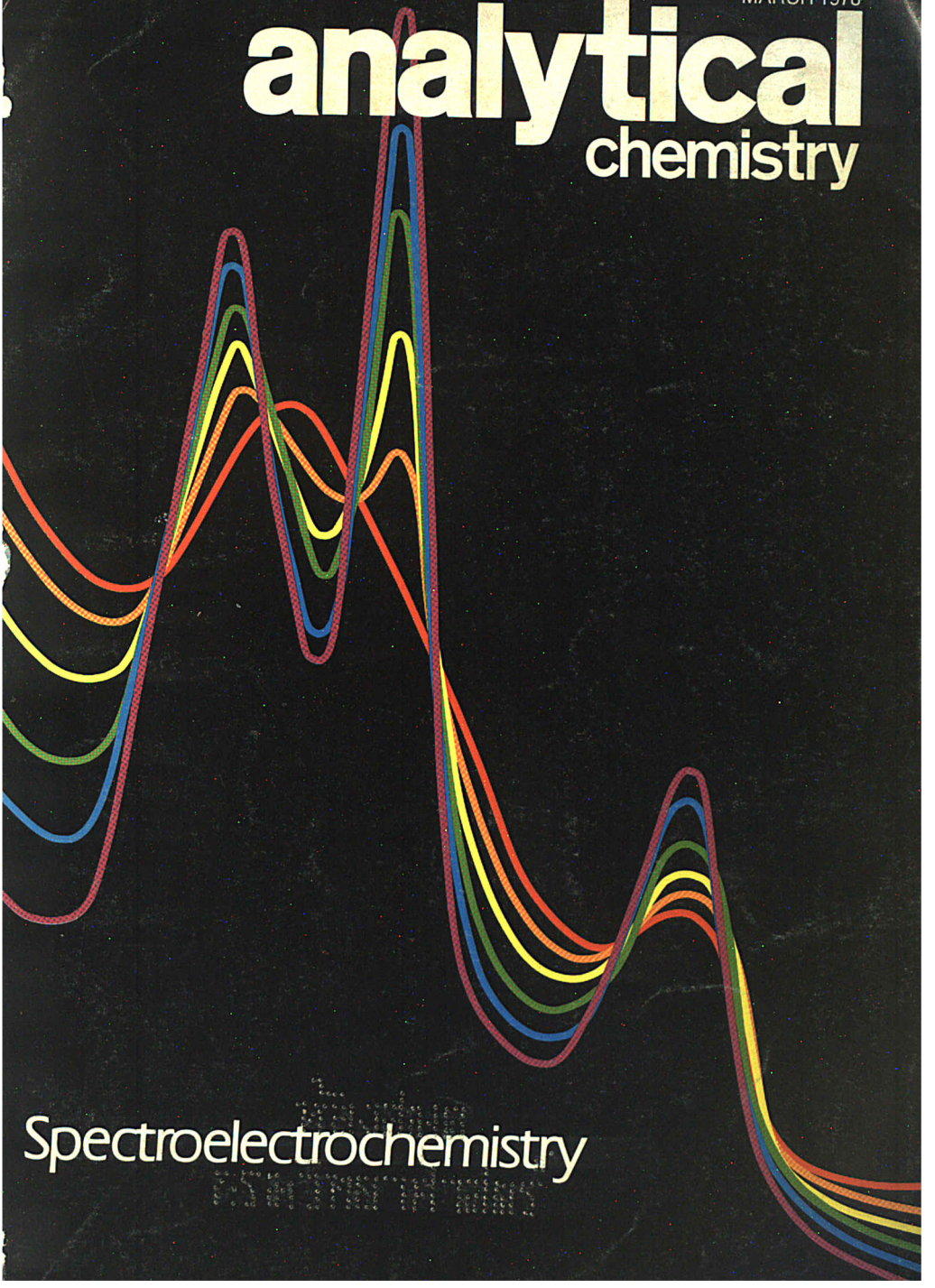

## Spectroelectrochemistry

# NANOpure.

## The New Standard for Reagent Grade Water.

Standard purity meter with dual-range scale provides accurate purity verification at a glance; satisfies quantitative record keeping requirements.

Delivers up to three liters per minute of 10-18 megohm-cm, bacteria-free water at exceptionally low cost.

Optional pump provides pure water instantly; features continuous or 30 second push button rinse-up.

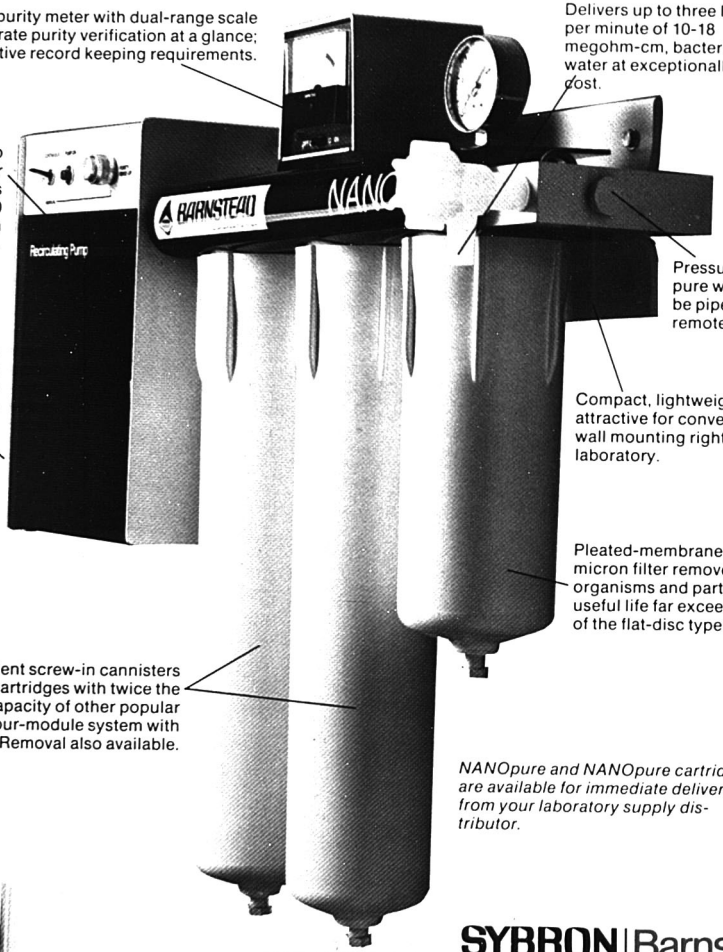


Pressurized pure water can be piped to remote outlets.

Compatible with a range of pretreatment systems including ROpure reverse osmosis.

Compact, lightweight and attractive for convenient wall mounting right in the laboratory.

Pleated-membrane sub-micron filter removes micro-organisms and particulates; useful life far exceeds that of the flat-disc type.

Convenient screw-in cannisters contain cartridges with twice the ion-exchange capacity of other popular systems. Four-module system with Organic Removal also available.

*NANOpure and NANOpure cartridges are available for immediate delivery from your laboratory supply distributor.*

The Barnstead Guide to Reagent Grade Water - everything you need know about reagent grade water. Helps you make an informed decision when evaluating pure water systems. Write for your free copy.

**SYBRON | Barnstead**

Barnstead Company
Division of Sybron Corporation
225 Rivermoor Street
Boston, Massachusetts 02132
(617) 327-1600

CIRCLE 20 ON READER SERVICE CARD

# Announcing the new Ratio II™ Spectrofluorometer

## Your best move in fluorometry

Innovations built into this newest member of the Aminco-Bowman® line of spectrofluorometers provide accurate and reproducible results. Its ease-of-operation makes it useful in a wide variety of applications.

- Increased instrument sensitivity
- Maintains performance stability
- Digital display
- Simplicity of operation
- Selects operating range automatically
- Real-time ratio

Get the most from fluorescence – choose the all-new Ratio II Spectrofluorometer or update your current Aminco-Bowman instrument with a ratio accessory – it's your best move in fluorometry.


AMINCO®

AMERICAN INSTRUMENT COMPANY
DIVISION OF TRAVENOL LABORATORIES, INC.
Silver Spring, Maryland 20910 Phone: 301-589-1727
European Headquarters: Rue Dautzenberg 36-38,
1050 Brussels Belgium, Phone (02) 648-50-02

© 1978, Travenol Laboratories, Inc.

CIRCLE 6 ON READER SERVICE CARD FOR ADVERTISING INFORMATION
CIRCLE 7 ON READER SERVICE CARD TO HAVE A REPRESENTATIVE CALL

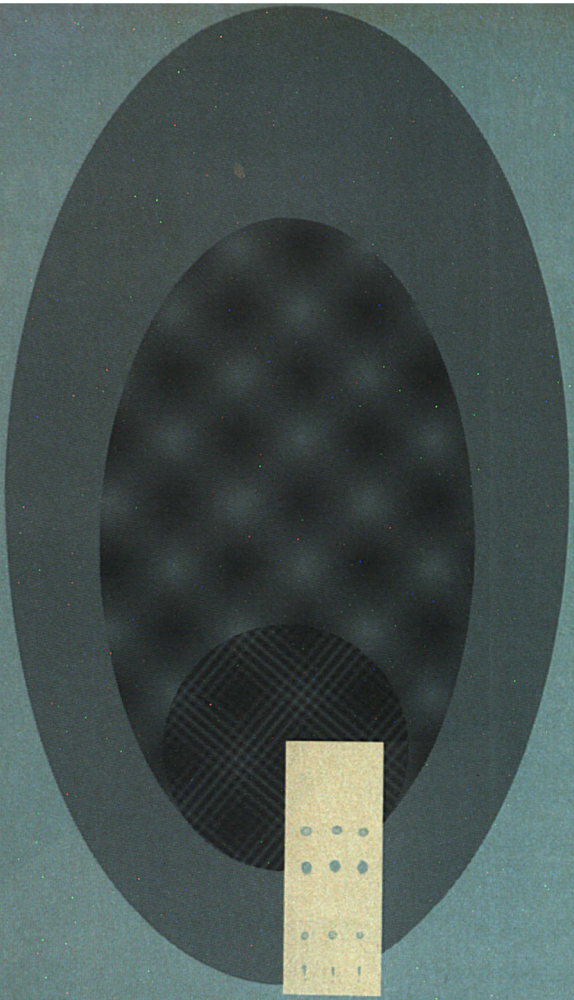

# $KC_{18}$

## *True* $C_{18}$ reversed-phase TLC plates

- Octadecyl groups separate *both* highly polar and highly non-polar compounds.
- $R_f$ Deviation: 0.5%, plate-to-plate.
- Sample Capacity up to 10X that of silica gel plates.
- Correlation with HPLC $C_{18}$ columns.
- High Speed: 2 cm/min, average.

Type $KC_{18}$ plates for reversed-phase TLC. Bonded octadecyl, $C_{18}$, *not* octyl, $C_8$, groups. Use simple solvent systems to separate highly polar and highly non-polar compounds. Typical sample capacity 200 mg per application. Spots 1–10 mm, sharply defined. Highly efficient: HETP approx. 10$\mu$m.

$KC_{18}$ Reversed-Phase TLC Plates. Only from Whatman.

**Whatman Inc.** 9 Bridewell Place,
Clifton, N.J. 07014 • Tel. (201) 777-4825.

Whatman

CIRCLE 234 ON READER SERVICE CARD

Volume 50, No. 3, March 1978
ANCHAM
50(3) 307A–408A/385–544 (1978)
ISSN 0003-2700

© Copyright 1978
by the American Chemical Society

Permission of the American Chemical Society is granted for libraries and other users to make reprographic copies for use beyond that permitted by Sections 107 or 108 of the U.S. Copyright Law, provided that, for all articles bearing an article code, the copying organization pay the stated per-copy fee through the Copyright Clearance Center, Inc. For further information, write to Office of the Director, Books and Journals Division, ACS, 1155 16th St., N.W., Washington, D.C. 20036.

Published monthly with review issue added in April and Laboratory Guide in August by the American Chemical Society, from 20th and Northampton Sts., Easton, Pa. 18042. Executive and Editorial headquarters, American Chemical Society, 1155 16th St. N.W., Washington, D.C. 20036 (202) 872-4600. Second class postage paid at Washington, D.C., and at additional mailing offices.

**1978 Subscription prices—including surface postage**

| | 1 yr | 2 yr | 3 yr |
|---|---|---|---|
| MEMBERS: | | | |
| Domestic | $10.00 | $18.00 | $25.00 |
| Foreign | 19.00 | 36.00 | 52.00 |
| NONMEMBERS—PERSONAL: | | | |
| Domestic | 14.00 | 26.00 | 38.00 |
| Foreign | 23.00 | 44.00 | 65.00 |
| INSTITUTIONAL: | | | |
| Domestic | 14.00 | 26.00 | 38.00 |
| Canada | 23.00 | 44.00 | 65.00 |
| Other foreign | 29.00 | 54.00 | 77.00 |

**Airmail and air freight rates** are available from Membership & Subscription Services, ACS, P.O. 3337, Columbus, Ohio 43210 (614) 421-7230.

**New and renewal subscriptions** should be sent with payment to the Office of the Controller at the ACS Washington address.

**Subscription service inquiries and changes of address** (include both old and new addresses with ZIP code and *recent mailing label*) should be directed to the ACS Columbus address noted above. Please allow six weeks for change of address to become effective.

**Claims for missing numbers** will not be allowed if loss was due to failure of notice of change of address to be received in the time specified; if claim is dated (a) North America: more than 90 days beyond issue date, (b) all other foreign: more than one year beyond issue date; or if the reason given is "missing from files".

**Microfiche subscriptions** are available at the same prices but are mailed first class domestic and airmail foreign. Inquiries and payments to Microform Program, ACS Washington address.

**Single issues,** current year, $3.00 except review issue and Labguide, $4.00; **back issues and volumes; microfilm editions** from volume 1 to present: *write or call* Special Issues Sales, ACS Washington address (202) 872-4365.

**Advertising Management:** Centcom, Ltd., 25 Sylvan Road South, Westport, Conn. 06880 (203) 226-7131

analytical chemistry

## CONTENTS



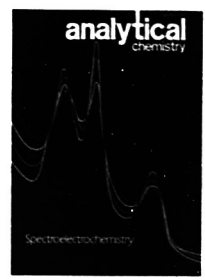


*Our cover illustrates spectroscopy as a probe in monitoring electrochemical processes, the subject of this month's* INSTRUMENTATION

# Briefs

### Wavelength-Modulated Continuum Source Atomic Fluorescence Spectrometer 386

A continuum source atomic fluorescence system with an oscillating interference filter as the wavelength isolation device is constructed and evaluated for Cu and Mg determinations in a flame.

**F. Lipari and F. W. Plankey,*** Department of Chemistry, University of Pittsburg, Pittsburgh, Pa. 15260 *Anal. Chem., 50 (1978)*

### Selective Excitation Fluorometry for the Determination of Chlorophylls and Pheophytins 392

The use of selected monochromatic excitation and emission wavelengths enables each component to be determined with greater selectivity than with previous spectrophotometric or fluorometric methods.

**Kevin G. Boto* and John S. Bunt,** Australian Institute of Marine Science, Cape Ferguson, P.M.B. No. 3, Townsville M.S.O., Q. 4810, Australia *Anal. Chem., 50 (1978)*

### Multicomponent Analysis by Synchronous Luminescence Spectrometry 396

The approach offers several advantages, including narrowing of spectral bands, an enhancement in selectivity by spectral simplification, and a decrease of measurement time in multicomponent analysis.

**Tuan Vo-Dinh,** Health and Safety Research Division, Oak Ridge National Laboratory, Oak Ridge, Tenn. 37830
*Anal. Chem., 50 (1978)*

### Experimental and Theoretical Considerations of Flow Cell Design in Analytical Chemiluminescence 401

A variable geometry, modular flow cell is used to examine the chemiluminescence from two systems, luminol and gallic acid, which have greatly different absorbance characteristics.

**Scott Stieg and Timothy A. Nieman,*** School of Chemical Sciences, University of Illinois, Urbana, Ill. 61801
*Anal. Chem., 50 (1978)*

### Flow Photometric Monitor for Uranium in Carbonate Solutions 404

An unsegmented, continuous flow monitor demonstrates a linear response to uranium in the 0–100 ppm range with good precision. Because of the presence of carbonate, few interferants are observed.

**B. B. Jablonski and D. E. Leyden,*** Department of Chemistry, University of Denver, Denver, Colo. 80208 *Anal. Chem., 50 (1978)*

### Pulsed Radiofrequency-Excited Electrodeless Discharge Lamps for Analytical Atomic Spectrometry 407

The behavior of rf excited electrodeless discharge lamps for Ar, Zn, Cd, and Hg, operated in a pulsed mode, is described.

**John W. Novak, Jr. and Richard F. Browner,*** School of Chemistry, Georgia Institute of Technology, Atlanta, Ga. 30332
*Anal. Chem., 50 (1978)*

* Corresponding author.

### Stationary Cold-Vapor Atomic Absorption Spectrometric Method for Mercury Determination 412

A new stationary cold-vapor method using a 4-cm UV cell is reported with a detection limit of 0.02 ppb Hg(II). Partition constant is also determined by a radiotracer technique.

**Soo-Loong Tong,** Department of Chemistry, University of Malaya, Kuala Lumpur, Malaysia *Anal. Chem., 50 (1978)*

### Discrimination of Monostereoisomers in Asymmetric Solvents by Fourier Transform Infrared Spectrometry 415

The procedure is demonstrated by measurements on all the permutations of both stereoisomers of malic acid dissolved in both stereoisomers of 2-octanol.

**David L. Grieble and Peter R. Griffiths,*** Department of Chemistry, Ohio University, Athens, Ohio 45701, and **Tomas Hirschfeld,** Block Engineering, Inc., 19 Blackstone Street, Cambridge, Mass. 02139 *Anal. Chem., 50 (1978)*

### Dual-Beam Fourier Transform Infrared Spectrometer 418

A dual-beam FT-IR spectrometer is described, which allows intense sources and sensitive detectors to be used for measuring transmittance spectra of weakly absorbing samples without encountering digitization noise.

**Donald Kuehl and Peter R. Griffiths,*** Department of Chemistry, Ohio University, Athens, Ohio 45701 *Anal. Chem., 50 (1978)*

### On-Line Identification of Gas Chromatographic Effluents by Dual-Beam Fourier Transform Infrared Spectrometry 422

A dual-beam FT-IR spectrometer is modified for GC-IR measurements. Detection limits of less than 100 ng are demonstrated for strongly absorbing samples separated on packed GC columns.

**Maria M. Gomez-Taylor and Peter R. Griffiths,*** Department of Chemistry, Ohio University, Athens, Ohio 45701
*Anal. Chem., 50 (1978)*

### Determination of Fluorine in Organic and Inorganic Pharmaceutical Compounds by High Resolution Nuclear Magnetic Resonance Spectrometry Interfaced with a Computer System 426

Organically bonded fluorine is determined by previous combustion or run directly without prior treatment. Inorganic compounds are analyzed directly by dissolving them in appropriate solvents.

**Richard J. Warren,* A. Douglas Bender, David B. Staiger, and John E. Zarembo,** Smith Kline & French Laboratories, 1500 Spring Garden Street, P.O. Box 7929, Philadelphia, Pa. 19101
*Anal. Chem., 50 (1978)*

### Curie-Point Pyrolysis and Field Ionization Mass Spectrometry of Polysaccharides 428

A new method for the controlled thermal degradation of technical and biological macromolecules by Curie-point pyrolysis inside the ion source of a high resolution field ionization mass spectrometer is introduced.

**H.-R. Schulten* and W. Görtz,** Institut für Physikalische Chemie, Universität Bonn, Wegelerstr. 12, 5300 Bonn, West Germany
*Anal. Chem., 50 (1978)*

# ARM your pH meter!

The ARM, a great addition to any pH meter. It holds your electrodes—pH, reference, specific ion, gas sensing—and an automatic temperature compensator, if you use one.

With the ARM you raise and lower your electrodes at a touch. You move your electrodes from beaker to beaker over some 18 square feet of lab bench. The ARM won't rock your meter—it comes with its own heavy swivel base.

You can get an ARM when you buy any of the ORION digital pH and specific ion meters, or you can buy one for your present meter. It's available from most leading lab supply distributors. The ARM, cat. no. 090020.

**ORION RESEARCH**
380 Putnam Avenue, Cambridge, MA 02139
(800) 225-1480

CIRCLE 156 ON READER SERVICE CARD

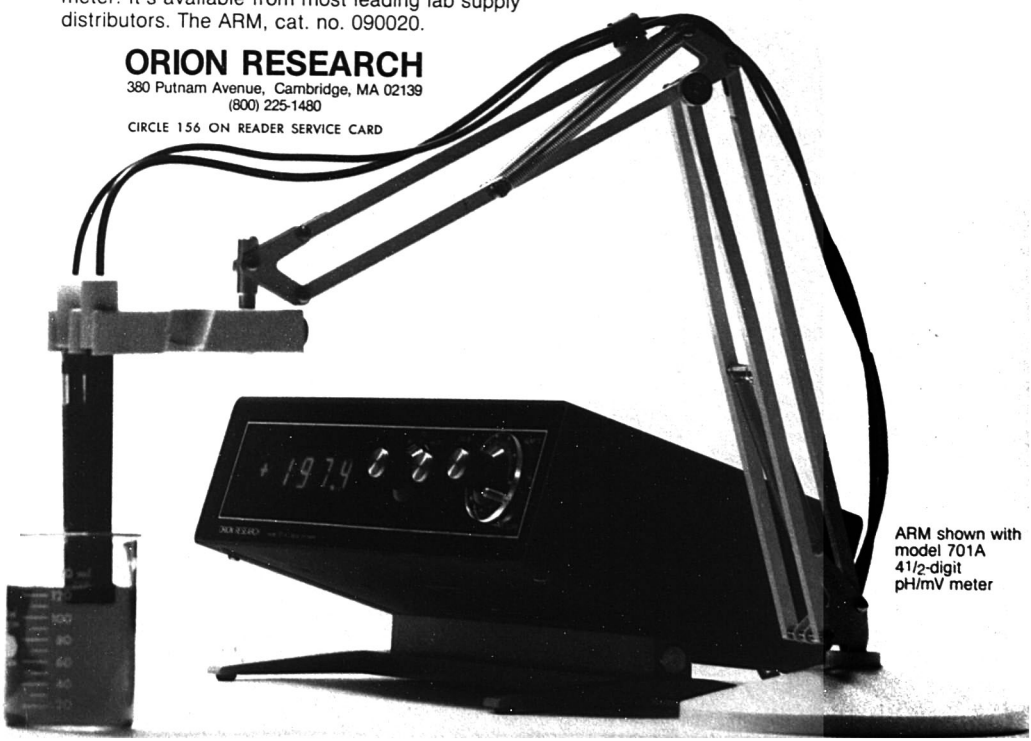

ARM shown with model 701A 4½-digit pH/mV meter

# Briefs

# Really Good Gas Calibration Standards Take 25 Years

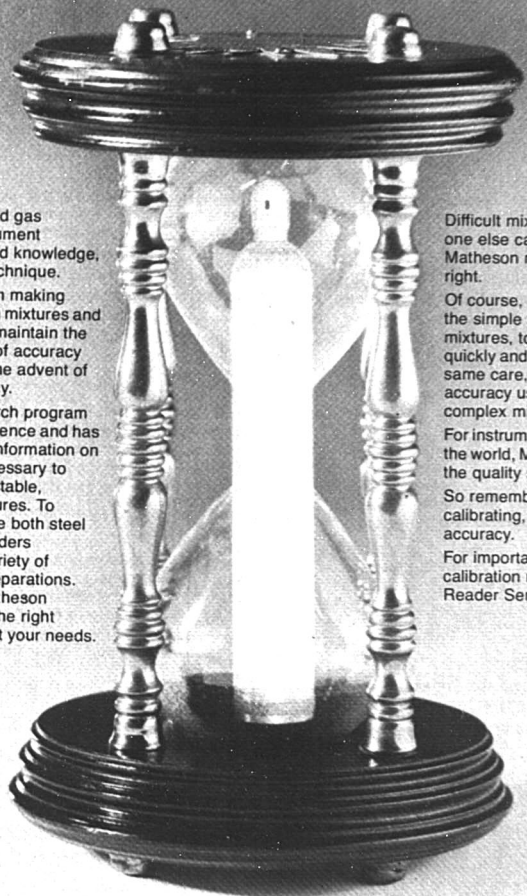

To make really good gas standards for instrument calibration you need knowledge, experience, and technique.

Matheson has been making accurate calibration mixtures and analyzing them to maintain the highest standards of accuracy since long before the advent of gas chromatography.

A continuing research program supports this experience and has provided valuable information on the techniques necessary to prepare accurate, stable, economic gas mixtures. To achieve this, we use both steel and aluminum cylinders combined with a variety of internal cylinder preparations. You can rely on Matheson technology to pick the right combination to meet your needs.

Difficult mixtures...the kind no one else can make...take time. Matheson makes sure they're right.

Of course, Matheson can supply the simple 2- and 3-component mixtures, too. We supply them quickly and economically with the same care, precision, and accuracy used to make the more complex mixtures.

For instrument calibration around the world, Matheson mixtures are the quality standard.

So remember, if it's worth calibrating, it's worth Matheson accuracy.

For important information on calibration mixtures, use the Reader Service No.

**Matheson has what it takes to deliver accurate gas mixtures on time.**

Matheson
Lyndhurst, N.J. 07071

East Rutherford, N.J. 07073/Morrow, Georgia 30260
Gloucester, Massachusetts 01930/Joliet, Illinois 60434
La Porte, Texas 77571/Cucamonga, California 91730
Newark, California 94560/Bridgeport, N.J. 08014
Dorsey, Maryland 21227/Whitby, Ontario, Canada L1N 5R9
Edmonton, Alberta, Canada T5B 4K6/B 2431 Oevel, Belgium
6056 Heusenstamm, West Germany

CIRCLE 140 ON READER SERVICE CARD

# Briefs



## Correspondence

# Gas Chromatography

Nitrogen-Phosphorous

Tracor offers the widest range of superior quality GC detectors—including Flame Photometric, Electron Capture (Ni63), Hall Electrolytic Conductivity, Nitrogen-Phosphorous, Thermal Conductivity, Flame Ionization, Photoionization and Ultrasonic—to compliment a selection of gas chromatographs.

**Reader Service No. 208**

Hall Electrolytic Conductivity

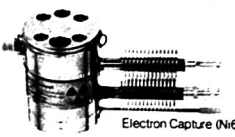

Electron Capture (Ni63)

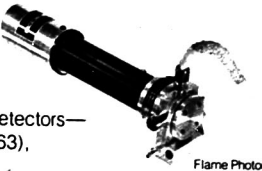

Flame Photometric

# Tracor Chromatography

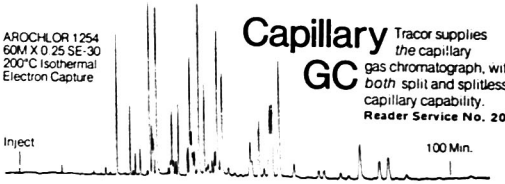


## Capillary GC

Tracor supplies *the* capillary gas chromatograph, with *both* split and splitless capillary capability.

**Reader Service No. 209**

## Water Analysis

Many laboratories are using the Hall Electrolytic Conductivity detector for low concentration detection of halomethanes in drinking water.

1 Methylene Chloride
2 Chloroform
3 1,2 Dichloroethane
4 Trichloroethane
5 Bromodichloromethane
6 Dibromodichloromethane

Tenax Column—
Temp. programmed.

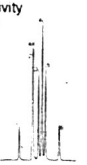

Water Standard
100 ppb each

**Reader Service No. 211**

## Sulfur Analysis

Tracor has supplied many systems for sulfur analysis using the Flame Photometric and Hall Electrolytic conductivity detectors. Applications include natural gas, ambient air, and stack monitoring as well as complete mobile laboratories.

**Reader Service No. 210**

## Data Processing

Tracor's Analytical Processor (TAP) provides the most sophisticated software resulting in highest precision—*and* it's easy to use, too.

**Reader Service No. 212**

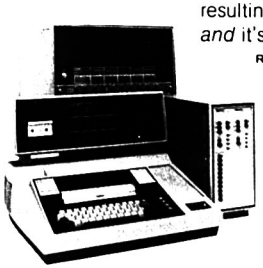

## Liquid Chromatography

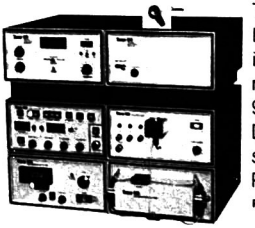

Tracor's line of modular liquid chromatographs includes the highly recommended Model 970A Variable Wavelength Detector and the unique, single pump 980A Solvent Programmer.

**Reader Service No. 213**

## GC/LC News

Send for Tracor's FREE periodical RETENTION TIMES. This will keep you informed of recent developments in both gas and liquid chromatography.

**Reader Service No. 214**

**Tracor Instruments** Tracor, Inc. 6500 Tracor Lane Austin, Texas 78721 Telephone 512:926 2800

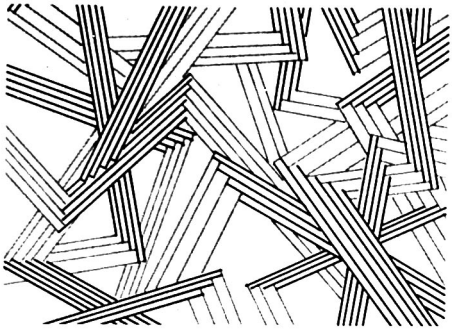

# Copolymers, Polyblends, and Composites

Advances in Chemistry Series No. 142

Norbert A. J. Platzer, *Editor*

***A symposium sponsored by the Division of Industrial and Engineering Chemistry, and co-sponsored by the Division of Polymer Chemistry, the Division of Organic Coatings and Plastics Chemistry, and the Division of Cellulose, Wood, and Fiber Chemistry of the American Chemical Society.***

This timely collection of thirty-eight papers is comprehensive and unique in its coverage of the latest research results on copolymers, polyblends, and composites which are used to toughen brittle polymers with elastomers, to reinforce rubbers with active fillers, and to strengthen or stiffen plastics with fibers or minerals.

Specific topics include:

- determination of MWD in homopolymers; liquid-liquid phase transition phenomena
- grafting kinetics of ABS; rubber-modified polymers; block copolymers; laminating resins; vinylene carbonate
- polymerization and copolymerization behavior; covulcanization of elastomer blends

482 pages (June 1975) $34.50 clothbound (ISBN 0-8412-0214-1).

SIS/American Chemical Society
1155 16th St., N.W./Wash., D.C. 20036

Please send _____ copies of *No. 142 Copolymers, Polyblends, and Composites* at $34.50 per book.

☐ Check enclosed for $_____. ☐ Bill me.
Postpaid in U.S. and Canada, plus 40 cents elsewhere.

Name _____

Address _____

City _____ State _____ Zip _____

# Briefs

## Aids for Analytical Chemists

# With S&S collodion bags you don't lose your concentration.

S&S collodion bags and apparatus are an ideal system for concentrating proteins from cerebral spinal fluid, urine, and other body fluids. In addition, the S&S collodion bag system is used to concentrate strands of RNA or DNA.

Use S&S collodion bags and your fraction collects in the tip of the bag, all together for easy removal without loss. You achieve higher recoveries than with other methods of concentration and dialysis, especially dialysis tubing. S&S bags are ideal for *in vitro* diagnostic use.

You get more of your sample, too. S&S collodion bags are the only practical method on the market that lets you reduce solutions of protein to near-zero volumes. Each bag provides 10cm² of membrane filter surface. The S&S system permits the widest variety of sample volumes, from less than 10ml up to unlimited volumes using the S&S accelerator. Choice of three grades permits a range of MW retentions—10,000, 25,000 and 75,000. And you can withdraw as little as 10μl.

The S&S collodion bag system is faster, lets you dialyze and concentrate simultaneously under a vacuum, and permits you to recover the retentate for further investigation.

S&S collodion bags are inexpensive enough to use once and discard. They're sturdy enough to be cleaned and re-used up to 10 times. The full line of apparatus making up the S&S system is inexpensive glassware. The S&S collodion bag accelerator reduces concentration times up to 43 percent, permits continuous concentration of large volumes, permits easy withdrawal of concentrate during dialysis.

For complete information and specifications send for Instructional Bulletin S-3. Your laboratory supply dealer should have the complete system—collodion bags and apparatus—in stock. You can well afford to be caught holding this bag.

## Schleicher & Schuell

Schleicher & Schuell, Inc.
Keene, New Hampshire 03431

Schleicher & Schüll GmbH, D-3354, Dassel, West Germany
Schleicher & Schüll AG, 8714, Feldbach ZH, Switzerland

CIRCLE 187 ON READER SERVICE CARD

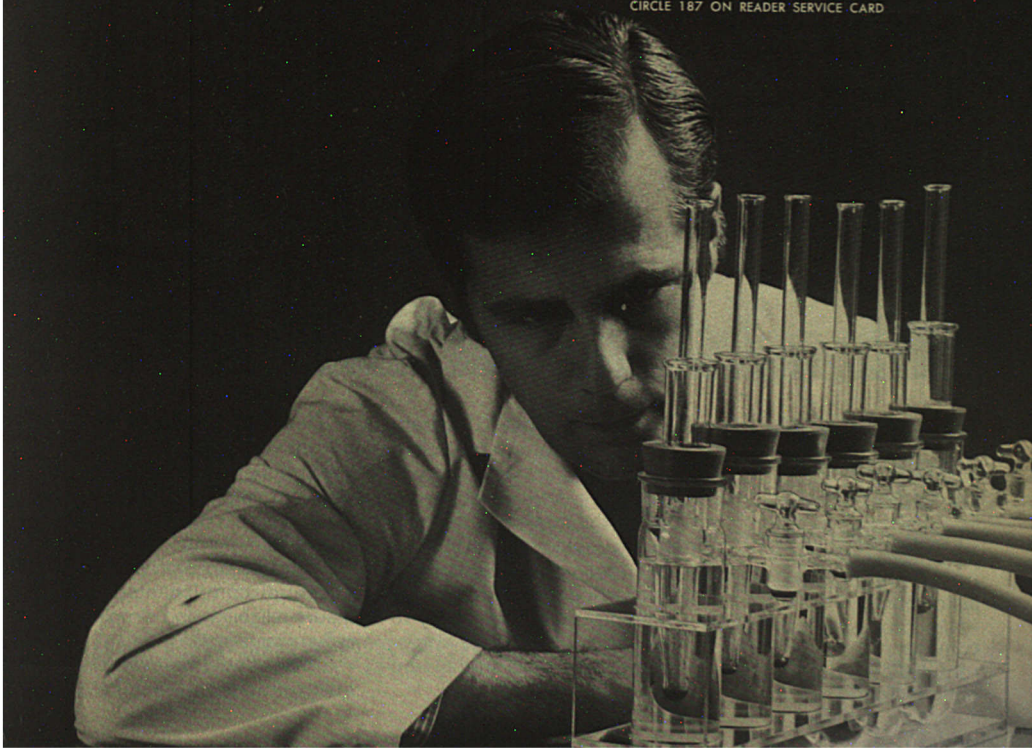

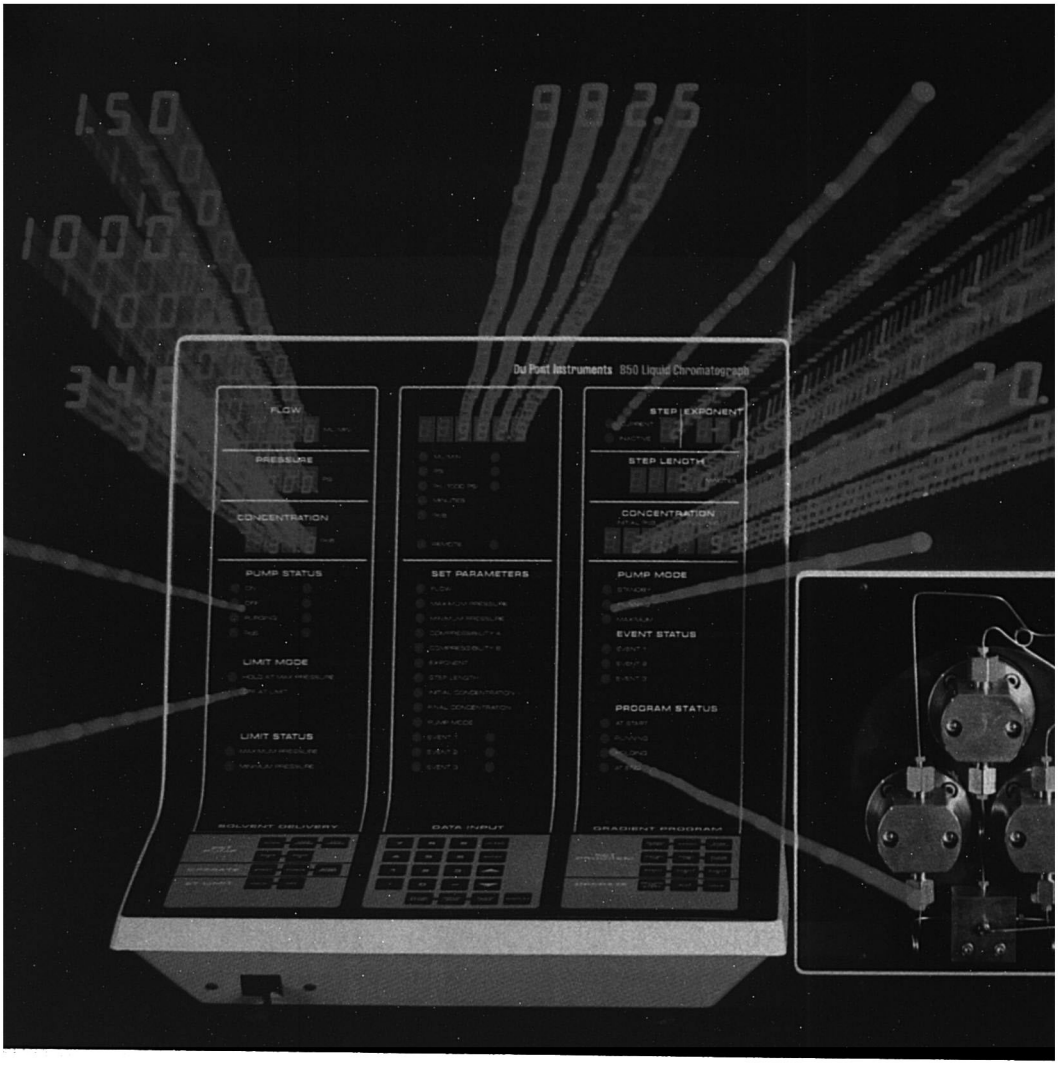


## An outstanding combination of features

- **Visual display of operating parameters**
- **Constant-volume three-piston pump**
- **Microprocessor control of components**
- **Immediate operator access while system is running**

This new DuPont LC system offers the chromatographer more than outstanding reproducibility and reliability. It solves the man-machine interface problem by giving the operator immediate call-out knowledge of all key operating parameters and the ability to effect a change in those parameters while the system is running.

Design features of the innovative system include

- automatic gradient programming
- a precision constant-volume three-piston pump
- a versatile microprocessor to control components, insure reliability and simplify parameter selection
- precise control of thermal environment

# Not just an instrument... a totally new DuPont LC system.

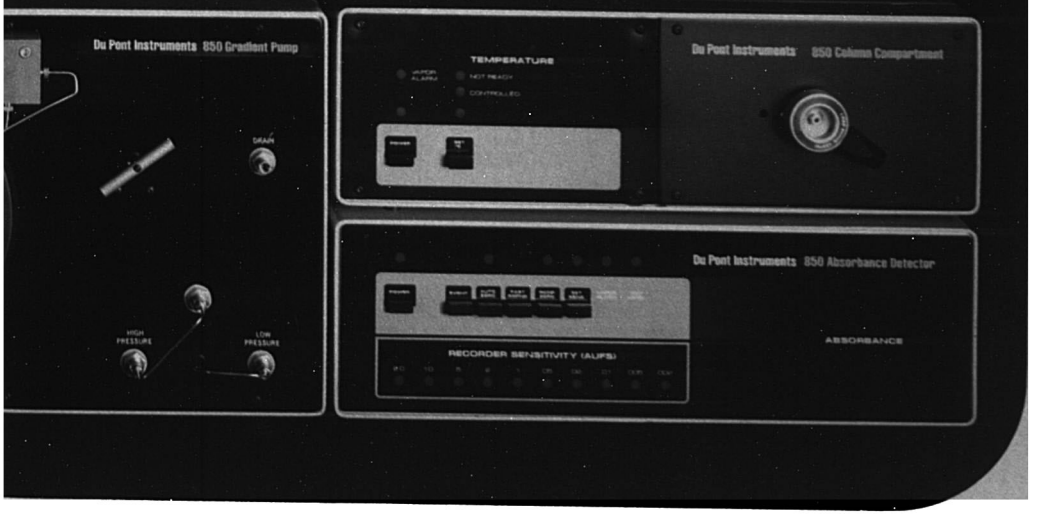


- built-in computerized diagnostics
- universal port for data processing
- guaranteed column performance.

The new system—designated the Model 850—is designed to meet the most demanding requirements of the research scientist as well as the dedicated needs of the quality control analyst. In any situation, the chromatographer is in total charge—with complete authority to change vital parameters without interrupting data reporting.

Get full details by writing DuPont Instruments, Room 36300, Wilmington, DE 19898. Or, if you have immediate need, please telephone 302-772-5139.

## Liquid Chromatographs

Scientific & Process Instruments Division

CIRCLE 51 ON READER SERVICE CARD

DUPONT

# DuPont announces the most

If you want the GC/MS/DS with the best combination of sensitivity, speed, resolution, reproducibility, stability, data handling capability, versatility and ease of operation, you want the new DuPont DP-1 Mass Spectrometer. Here's why:

## Unmatched control and data processing

Fully integrated system controls the GC/MS and acquires data faster than any analytical GC/MS. Dynamic range is unequalled. Special software assures proper abundance and true mass spectra that are comparable with reference data.

Total data display on a single screen with foreground/background processing gives automatic real-time display of routines simultaneously with data acquisition. Selective ion monitoring is standard and quantitative. Routines are written in FORTRAN IV to facilitate user programming. Storage capability is the highest available today—up to 15 megabytes of disc storage, plus provision for archival storage.

## Simple and fast operation

Human engineering for mass spectrometers is at a dramatic new level. Operation and control are greatly simplified, with tuning prompted by the data system. Diagnostic software pinpoints malfunctions and suggests corrective action.

## Instant EI to CI switching

The DP-1 uniquely integrates instant EI to CI switching with

# advanced GC/MS/DS ever built.

data acquisition and programming. Unique ability to program ionization mode and reagent gas during a run helps you use CI to best advantage.

## Automatic source revitalization

Innovative gold sputtering process renews critical ion source surfaces, restores source performance without shutting down, reduces frequency of cleaning.

## Outstanding capillary column interface

Available capillary column inlet provides optimum resolution for high performance GC columns.

To get full details on the DP-1, and explore the potential of mass spectrometry in your work, write to DuPont Instruments, Room 36262, Wilmington, DE 19898. For immediate assistance call our hotline, (302) 772-5429.

See the new DuPont DP-1 GC/MS/DS at the Pittsburgh Conference, Booth 125.

**Mass Spectrometers**

Scientific & Process Instruments Division

DUPONT

CIRCLE 52 ON READER SERVICE CARD

## Computerization of a 4260 Infrared Spectrophotometer.

Several months prior to the 1977 Pittsburgh Conference, Beckman technical staff began private demonstrations of their new Infrared Spectral Information System. Fully integrated were a basic computer, a research grade 4260 instrument, a complete signal interface box, and applications software on floppy disc storage.

Then in Cleveland, workshops and seminars were held to introduce formally IRSIS capabilities to the public. And now, Beckman is ready to put users nationwide on line with a fully tested, turnkey IR system that can digitize and store spectra on floppy disc, process the data fully through 12 operational programs, and output results to a printer or plotter for final answers.

Typical all computer-controlled operations include spectral subtraction, addition, ordinate expansion and averaging, along with a peak pick/search/match routine for compound identification.

Spectra comparison operations have been designed to be completely flexible. For this latter purpose, each user can build a high speed personalized data file to do the exact identification required.

Then, all an operator need do is place the sample in the 4260. Final answers to complex identifications appear in minutes.

So, don't wait a minute longer to get complete information on true IR computer capability. To talk to the experts, contact your local Beckman representative or Scientific Instruments Division, Beckman Instruments, Inc., P.O. Box C-19600, Irvine, CA 92713.

**BECKMAN®**

CIRCLE 26 ON READER SERVICE CARD


# analytical chemistry

## Reader Survey

In 1974 and again in 1976, ANALYTICAL CHEMISTRY sent a survey questionnaire to a randomly selected small group of individual subscribers. Information from surveys of this type helps the publication keep abreast of the interests of our readers and aids us in planning A-page editorial coverage. By extending surveys to the entire readership, we can check on our earlier results, assess trends, and gain additional information.

Please take a few minutes to provide the information requested below. Indicate your answers by circling the appropriate numbers on the Reader Service Card, page 357 A.

Reader survey results will be reported in a future issue of the JOURNAL.

**A. This copy of ANALYTICAL CHEMISTRY is**

301 My own
302 Pass-along copy

**B. Please circle on the Reader Service Card the numbers given below corresponding to the analytical techniques you use:**

303 Affinity chromatography
304 Atomic absorption spectrometry
305 Chemical microscopy
306 Computer techniques, pattern recognition, etc.
307 Electroanalysis and coulometric analysis
308 Electron microscopy
309 Electron spectroscopy: ultraviolet photoexcitation
310 Electron spectroscopy: x-ray and electron excitation
311 Electron spin resonance spectrometry
312 Electrophoresis
313 Emission spectrometry
314 Enzymatic techniques
315 Flame spectrometry
316 Fluorometric analysis
317 Gas chromatography
318 Gas chromatography/mass spectrometry
319 Gel chromatography
320 Infrared spectrometry
321 Ion exchange techniques
322 Ion selective electrodes
323 Kinetic techniques
324 Liquid chromatography
325 Magnetic susceptibility
326 Mass spectrometry
327 Microwave spectrometry
328 Mössbauer spectrometry
329 Nuclear magnetic resonance spectrometry
330 Nucleonics
331 Paper chromatography
332 Potentiometry
333 Raman spectrometry
334 Thermal analysis
335 Thin layer chromatography
336 Ultraviolet/visible spectrometry
337 Voltammetry
338 X-ray spectrometry
339 X-ray diffraction
340 Other, please name

# Simplify your life for only $3,050

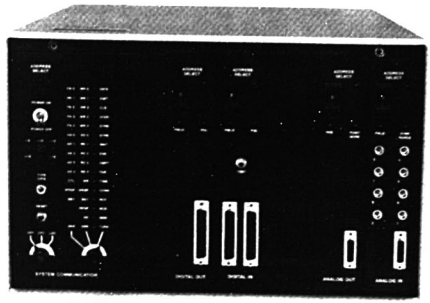

*Actual dimensions: 10-3/4"h x 17-1/8"w x 21-1/2"d*

Here's how three IBM research physicists are getting more experimentation accomplished—with more accurate results than ever before.

Physicist Jim Wynne uses an IBM Device Coupler* to acquire and process data from laser spectroscopy experiments ten times faster than he could before. It's a simple and economical device to facilitate lab experiments by coupling experimental apparatus, analytical instruments and/or test equipment to virtually any computer. It automates data handling and control tasks. It works with most computer languages. It's easy to use and even easier to connect. It's modular, and can be moved quickly from one set-up to another. It helps with the complete job of data acquisition, data analysis, equipment control, reporting of results, and then some.

Jim Wynne, Physicist
*Laser Beam Spectroscopy*

## Laser Beam Spectroscopy

Jim Wynne says: "It simplifies my life. With the Device Coupler, I'm in direct contact with our computer. I don't have to spend time analyzing my data by hand and then manually entering it into the system. We wrote a program that says, 'Find peaks,' and in seconds it finds the locations of 500 new peaks. The computer has located and labeled these 500 peaks in the midst of 10,000 data points. The Device Coupler is a tremendous time and labor saver. It takes one-tenth the time it took in the past to get the same results."

## Surface Spectroscopy

Gary Rubloff says: "In studies of chemical reactions on surfaces, we take many photoemission spectra (sometimes 50 or more) under different surface conditions each day. To analyze these results, we must rescale one spectrum and then subtract it from another. By hand, this procedure takes at least a half hour for each pair of spectra, so we were formerly able to compute and study only a small fraction of the possible 'difference' spectra. Now, using the Device Coupler, the data goes directly into the computer which quickly rescales, subtracts, and plots difference spectra, even between runs of the experiment. Obviously, we can now analyze the results more quickly and thoroughly, and we can better decide during the experiment what to measure next."

Gary Rubloff, Physicist
*Surface Spectroscopy*

## Optical Spectroscopy

"Pep" Perry, says: "The Device Coupler not only controls the running of my experiments, but also handles the vast quantities of data from transmission, absorption, reflectivity and luminescence experiments. With the combination of the Device Coupler and a computer, I can not only convert these data to more useful quantities instantaneously, but I can also perform Kramers-Kronig analyses, line widths and band edge determinations in a matter of seconds—while the experiment is still on line."

"Pep" Perry, Physicist
*Optical Spectroscopy*

We hope the experiences of physicists Wynne, Rubloff and Perry give you some idea of how versatile the Device Coupler can be. Its range of applications is very broad. We'd be delighted to tell you how it can put your data to work for you. Call Dr. Jack Smith collect at (914)696-4575. Or write to IBM Instrument Systems, 1000 Westchester Avenue, White Plains, N.Y. 10604.

The Device Coupler may simplify *your* life, too.

IBM
System Products Division

** The applications described in this advertisement are being implemented with a prototype version of the Device Coupler which is functionally similar to the production IBM 7406.*

CIRCLE 105 ON READER SERVICE CARD

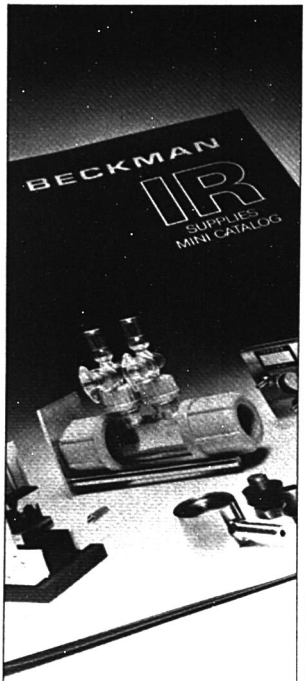


**New IR catalog is free from Beckman.**

Prices, specifications, and full ordering information for your most needed IR supplies and accessories are all included in our new "Mini Catalog."

Get yours free now and solve the supplies search. Just circle the reader service number or contact Scientific Instruments Division, Beckman Instruments, Inc., P.O. Box C-19600, Irvine, CA 92713.

**BECKMAN®**

CIRCLE 27 ON READER SERVICE CARD

# Letters

## New Environmental SRM's

**Sir:** In their comprehensive report, "Metals in Bioenvironmental Systems", which appeared in the December 1977 issue of ANALYTICAL CHEMISTRY, G. B. Morgan and E. W. Brethauer refer to the calibration of analytical instrumentation as a critical problem in analyzing samples at the trace and ultratrace levels. The authors emphasize the importance of having "independent accuracy standards that have certified values of a wide range of trace elements at low concentrations" and refer to the few National Bureau of Standards Standard Reference Materials (SRM's) available for this use. They emphasize the need for additional environmental SRM's.

The readers of ANALYTICAL CHEMISTRY may be interested in other trace element environmental SRM's that have been issued (or planned) by NBS. NBS has recently issued a number of SRM's certified for potentially toxic elements at the trace and ultratrace levels and expects to issue four additional SRM's in the first six months of 1978.

Available now are two water SRM's—SRM 1642a, certified for Hg at the ng/mL level, and SRM 1643, certified for 17 elements at the ng/mL level including Cd, As, and Pb; four botanical SRM's—spinach, orchard leaves, pine needles, and tomato leaves, which provide concentration ranges for a number of elements including Pb from 6.3 to 45 $\mu$g/g and Hg from 0.030 to 0.155 $\mu$g/g; an animal tissue SRM—SRM 1577 Bovine Liver, which has certified concentrations for 13 elements at $\mu$g/g levels. The Certificates of Analysis for the Orchard Leaves and Bovine Liver SRM's that were revised in 1977 contained certified values for six additional elements. In the first six months of 1978, NBS expects to issue new SRM's for the analysis of wheat flour, rice flour, river sediment, and airborne particulates.

**R. Alvarez**
**W. P. Reed**
**G. A. Uriano**
Office of Standard Reference Material
National Bureau of Standards
Washington, D.C. 20234

Contributions from readers are invited for the LETTERS section. Topics should preferably be of broad interest to readers and/or may be comments on material published in the A-pages. See Prof. Laitinen's editorial, page 1281, August 1977.

## Calculations with Words

**Sir:** Your readers may be interested in using their pocket calculators in day-to-day chemical calculations.

Consider the calculation of molecular weight. This turns out to be an addition sum in words. In reply to CH3COOH you expect 60.05 molecular weight.

A way to feed in the atomic symbols is needed, whereupon the calculator can easily recall the atomic weights and add them up. In the case of calculators with labels (user definable keys), this proves to be simple.

Of course, once we can feed in the symbols we can access any stored data whatsoever about the hundred chemical elements, or indeed particular classes of compound. On one HP or TI magnetic card (or solid state memory), one could have properties of the amino-acids, all accessible by name (or formula if desired). One can build up a library, rendering many reference books obsolete!

My associates and I have several years of experience in accessing data by name. It is impossible to say much here because there are applications outside the chemical sphere, and we are actively developing new areas for commercial clients. The purpose of this letter is to make chemists aware of one of the most straightforward and easiest applications.

On calculators with five labels (ABCDE), molecular weights of organic compounds can be calculated by programming the atomic weights of C, H, O, N, Cl at the above label-locations. I have available, free, for HP67/97 users such a program covering C, H, O, N, Cl, Br, F, I, S, P.

**J. Marshall**
850 Bloomfield Ave.
Montclair, N.J. 07042

# HPLC Solvents by J.T. Baker

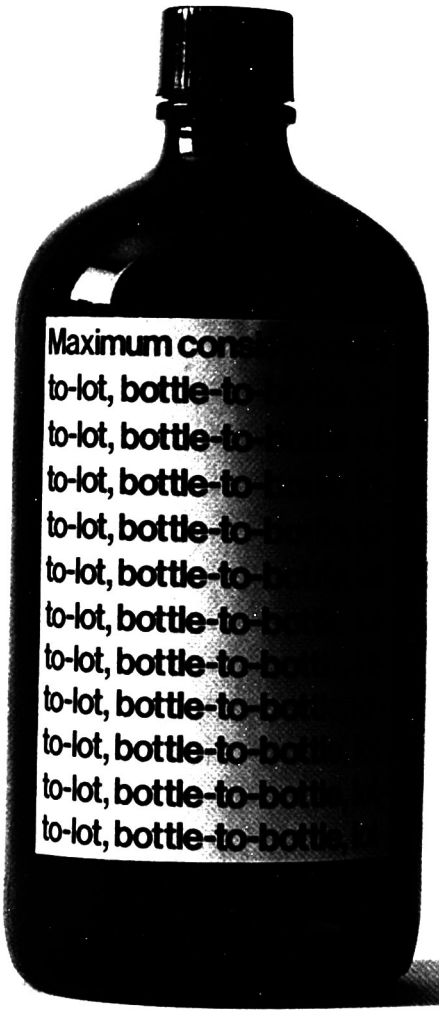


High performance liquid chromatography problems are frequently related to the *variability* of the reagents used. Specifically: spurious UV absorbance, particulate matter, residues, unknown or uncontrolled water, etc. 17 Baker HPLC solvents, however, now provide maximum reproducibility... new predictability... exceptional consistency.

How is such unusual consistency achieved? Extremely tight specifications coupled with superior product definition create consistency.

Examples? HPLC Acetonitrile is controlled for low UV absorbance at 210 nm (0.10 max.), 254 nm (0.05 max.), 280 nm (0.02 max.) and at 350 nm (0.01 max.); water 0.02% max.: residue 0.0005% max. Refractive index: controlled, consistent. Plus physical data. And of course, the actual lot analysis *for the specific lot in question* is always on the 'Baker Analyzed'™ container label. You can always verify our claims for reproducibility beforehand.

Consistency? Here are 10 consecutive lots of Baker HPLC Methanol:

| Lot | 1 | 2 | 3 | 4 | 5 | 6 | 7 | 8 | 9 | 10 |
|---|---|---|---|---|---|---|---|---|---|---|
| Water % | 0.03 | 0.04 | 0.02 | 0.03 | 0.02 | 0.03 | 0.02 | 0.02 | 0.02 | 0.03 |
| Residue % | 0.0003 | 0.0001 | 0.0001 | 0.0001 | 0.0001 | 0.0002 | 0.0002 | 0.00005 | 0.00005 | 0.00005 |
| Abs. at 254 nm | <0.01 | <0.05 | <0.04 | <0.05 | <0.04 | <0.03 | <0.04 | <0.05 | <0.05 | <0.03 |

A tested water content of 0.02-0.04% and a residue after evaporation of 0.00005-0.0003%. Our lot-to-lot product consistency provides you with solvents affording the best reproducibility.

Baker HPLC solvents are stocked where you need them. Contact one of the more than 120 Baker distributor locations in the U.S. and Canada to implement a stocking program to suit your needs.

For emergency shipments on HPLC solvents, your distributor can provide special Baker Super Service by calling a Baker Super Service Center for immediate shipment to you.

For more information, please use the coupon below and send to J.T. Baker Chemical Co., Phillipsburg, N.J. 08865, or call 201/859-5411.

**J. T. Baker**
**"use matched" products and...Super Service**

J.T.Baker®
CHEMICALS

J. T. Baker Chemical Co
Phillipsburg, N.J. 08865

☐ I'm interested in learning more about the Baker HPLC solvents that are consistent bottle-to-bottle, lot-to-lot, bottle-to-bottle, lot-to-lot, bottle-to-bottle, lot-to-lot, bottle-to-bottle, lot-to-lot, bottle-to-bottle,

Name _____
Title _____
Department _____
Organization _____
Address _____
_____ Zip _____

CIRCLE 22 ON READER SERVICE CARD



หอสมุดกลาง กรมวิทยาศาสตร์

# Linear Programmed Thermal

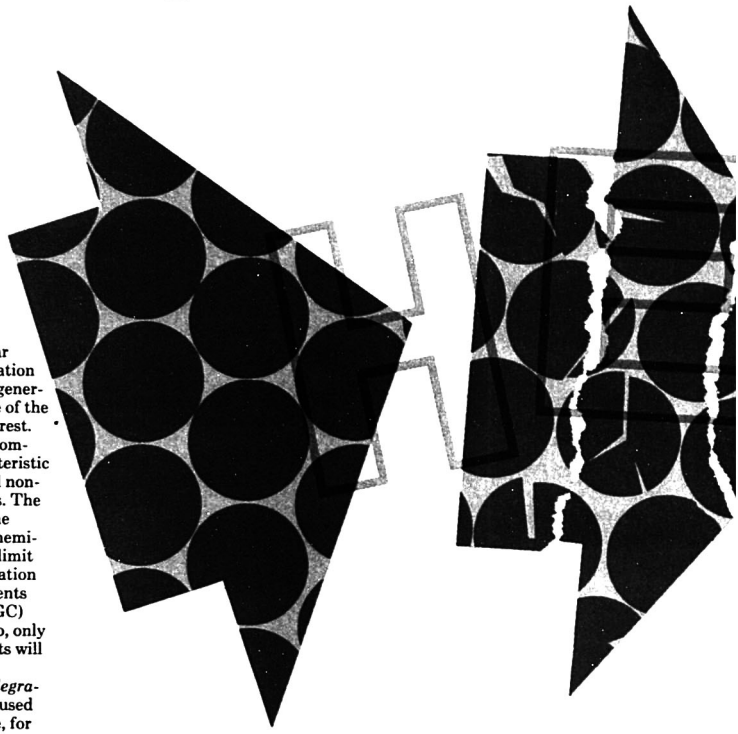

The analysis of high molecular weight substances via fragmentation is limited only by the ability to generate species that still retain some of the character of the material of interest. This limitation is mastered by compromising between large characteristic nonvolatile fragments and small noncharacteristic volatile fragments. The methods for fragmentation of the sample range from thermal to chemical procedures. This report will limit its discussion to thermal degradation and to the analysis of the fragments by either gas chromatography (GC) or mass spectrometry (MS). Also, only the theory, procedure, and results will be discussed here.

Although the terms *thermal degradation* and *pyrolysis* have been used interchangeably in the literature, for the purposes of this discussion we wish to distinguish between them. Thermal degradation is the breakdown of the molecule into smaller molecules by the action of an increase in temperature. Pyrolysis is defined in the same way except that the temperature jump is rapid and may also include subsequent recombination of fragments to form larger species (*1*).

The methodologies for high molecular weight characterizations via thermal degradation can be divided into two areas: isothermal degradation and nonisothermal degradation. Isothermal degradation is a procedure in which the sample is heated as rapidly as possible to a predetermined temperature (pyrolyzed) and then the fragments (pyrolysates) are analyzed. Conversely, with nonisothermal degradation the fragments are analyzed continuously during a slower heating cycle. This latter process is carried out in a flowing gas stream (dynamic system), whereas the former process uses a static system. Direct analysis of the fragments is usually the desirable procedure since the analysis will not be sample-transport limited by contamination or condensation of the fragments. The methodologies that fall into these areas are shown in Figure 1. Although theoretically the same information should be obtained with all these methodologies, the results are different and are often difficult to correlate with each other.

The indirect isothermal degradation methodologies are based on the more traditional pyrolysis methods and can use a range of sample sizes. These procedures have the advantage that the pyrolysis is performed separately from the analytical technique, which means that a number of samples may be pyrolyzed under the same conditions. Also, unlike the other two techniques, the pyrolysis bomb may be manufactured from inert materials that will not affect the degradation processes. However, since the degradation occurs over a period of time, under static conditions, it is probable that side reactions and more complete degradation will occur. This will limit the utility of the methodologies.

Conversely, the direct methodologies attempt to reduce the likelihood of side reactions occurring by degrading the sample as rapidly as possible in a temperature jump device (maximum temperature is reached $\ll 1$ s).

Both these isothermal methodolo-

[1] To whom correspondence should be addressed.
[2] Present address, National Institute of Child Health and Human Development, Bethesda, Md.



0003-2700/78/0350-326A$01.00/0
© 1978 American Chemical Society

Report

# Degradation Mass Spectrometry

**T. H. Risby**[1]
Department of Chemistry
Pennsylvania State University
University Park, Pa. 16802

**A. L. Yergey**[2]
Chemetron Medical Products
Chemetron Corp.
Baltimore, Md. 21207, and
Friends Medical Science Research Center Inc
Catonsville, Md. 21228

gies have used either gas chromatography or mass spectrometry to monitor the fragments. These two techniques are complementary, and the choice is dependent upon the availability and the overall requirements of the analysis. A gas chromatograph is a simple instrument to operate and has minor "down-time" which is exactly the reverse of the operating properties of a mass spectrometer. However, only the fragments that are nonreactive, thermally stable, and volatile can be analyzed by gas chromatography, whereas mass spectrometry has none of these limitations. The fragments eluted from a gas chromatographic column will be separated over a period of time, whereas the mass spectrum will be obtained in a much shorter period of time. Since the mass spectrum will contain ions from all the fragments, as well as fragments produced by ionization, the mass spectrum is collected and analyzed with the aid of a computer. Another problem experienced by gas chromatography is that the column performance is continually degraded by the reactive fragments that modify the column packing material. This will produce irreproducible retention data for the eluting fragments. Characterization based on direct or indirect isothermal degradation methodologies is generally based on empiricism rather than on the identity of specific fragments. The profile of the entire gas chromatogram or mass spectrum is used to characterize the data.

The direct nonisothermal methodologies are similar to the preceding system except that the fragments are analyzed continuously. As a result, only analytical techniques that give rapid selective responses can be used (spectrometric methods of analysis). Mass spectrometry is more suitable than the optical methods since optical methods seldom have sufficient sensitivity and selectivity. The major advantage of these methodologies is that the fragments have temperature or temporal dependence. Also, the fragments are removed continuously, and generally larger characteristic fragments are obtained. The techniques of differential thermal analysis (DTA) (*2*), thermal gravimetric analysis (TGA) (*2*), and evolved gas analysis (EGA) (*2, 3*) are separate from the mass spectrometer and may produce fragment transport problems that will increase with the size of the fragment. However, the methodology linear programmed thermal degradation mass spectrometry (LPTD–MS) (*4, 5*) degrades the sample in a chemical ionization source, which produces a number of advantages over the other nonisothermal methodologies. The first is that since the fragmentation occurs in the mass spectrometer, no transport problems exist, and the possibility of analyzing large characteristic ions is increased. Second, since chemical ionization is used rather than electron impact, less fragmentation due to the ionization process is produced (*6*). Third, since transport time is minimum, it is possible to relate the results of temporal mass spectra to fundamental molecular energetics. Fourth, theoretically it is possible to heat the sample at any rate with any cycle; therefore, greater resolution for the evolution of fragments may be possible, which may be useful for characterization. Finally, once molecular energetics are obtained, it is possible to base characterization on the identity of specific fragments since the thermal degradation process can be well controlled.

Another general advantage of the nonisothermal over the isothermal degradation methodologies is that it is experimentally easier to heat the sample with a constant temperature ramp than it is to heat the sample to an exact temperature, since with the former methodology the final temperature is not critical. However, it is possible that since the equipment for this heating is manufactured from metals, these materials may contribute to the mechanism of fragmentation by acting as a catalyst if the sample is in contact with the metallic surface.

Other procedures are available for the analysis of high molecular weight species. For example, polysaccharides (*7*) and antibiotics and their salts

(*8–9*) have been analyzed by field desorption techniques or by using the $Cf^{252}$ source coupled with a time-of-flight mass spectrometer that has unit mass revolution at 2000 daltons (*10*). Proteins have been sequenced mass spectrometrically (*11–14*) by breaking the molecule into a number of small polypeptide units by various N-terminal degradations and analyzing the polypeptides by GC–MS techniques to deduce the order of amino acids in the original molecule. However, these techniques are not as general as the thermal degradation methodologies.

## Theory

**Nonisothermal Degradation (*15–19*).** Consider the following reaction in which a sample is thermally decomposed into various fragments:

$$(\text{Sample}_j\text{—Fragment}_k)_{\text{solid}} \xrightarrow{\Delta H} (\text{Sample}_j)_{\text{solid}} + (\text{Fragment}_k)_{\text{vapor}} \quad (1)$$

where $(\text{Sample}_j\text{—Fragment}_k)$ represents one of the $j$th variety of ways in which one of the $k$ fragments is present in the sample, and $(\text{Sample}_j)$ represents the pertinent site after the removal of the $k$th fragment.

The general rate expression for this $n$th order reaction is given by

$$\frac{-d[S_j - F_k]}{dt} = \left(\frac{d[F_k]}{dt}\right)_j = K_{kj}[S_j - F_k]^{n_{kj}} \quad (2)$$

in which $[S_j - F_k]$ is the concentration of the $k$th fragment produced by the $j$th process in the sample, $[F_k]$ is the concentration of the $k$th fragment, $n_{kj}$ is the reaction order of the production of the $k$th fragment in the $j$th process, $t$ is the time, and $K_{kj}$ is the specific reaction rate of the $j$th process for the production of the $k$th fragment.

The temperature dependence of the specific reaction rate constant is expressed by the Arrhenius equation:

$$K_{kj} = K_{okj}e^{-E_{kj}/RT} \quad (3)$$

where $K_{okj}$ is the pre-exponential factor, $E_{kj}$ is the activation energy of the production of the $k$th fragment by the $j$th process, $T$ is the temperature, and $R$ is the gas-law constant.

Substituting Equation 3 into 2, the following expression is obtained:

$$\frac{-d[S_j - F_k]}{dt} = K_{okj}e^{-E_{kj}/RT} \times [S_j - F_k]^{n_{kj}} \quad (4)$$

Consider the system where the temperature is not held constant but is varied linearly with a constant temperature ramp $M$, *i.e.*,

$$M = \frac{dT}{dt} \quad (5)$$

If Equation 5 is substituted into 4 and the product is integrated in a similar manner to that reported by Jüntgen and others (*15–19*), the following expression is obtained:

$$\frac{d[F_k]}{dT} = \frac{K_{okj}}{M}e^{-E_{kj}/RT} \times \left[[S_j - F_k]_0^{(1-n_{kj})} + \frac{(n_{kj} - 1)K_{okj}RT^2}{ME_{kj}}\right]^{n_{kj}/1-n_{kj}} \quad (6)$$

which is valid if $n_{kj} \neq 1$ and $E_{kj} \gg RT$ and if the elementary processes establishing thermal equilibrium are rapid as compared with the heating rate.

The initial concentration of the $k$th fragments in the sample is $[S_j - F_k]_0$. The concentration of the $k$th fragment is measured mass spectrometrically as a current of ions $I$, whose magnitude is related to $d[F_k]/dT$ by the following relationship:

$$\frac{d[F_k]}{dT} = \frac{Q}{Mg}\beta_k I_{kj} \quad (7)$$

where $Q$ is the flow rate of the gas passing over the sample, $g$ is the weight of the sample, and $\beta_k$ is a proportionality factor relating a neutral fragment $F_k$ to its mass spectral ion current ($I_{kj}$). There is obviously a different value of $\beta_k$ for each fragment $F_k$.

$$I_{kj} = \frac{g}{Q\beta_k}K_{okj}e^{-E_{kj}/RT} \times \left[[S_j - F_k]_0^{(1-n_{kj})} + \frac{(n_{kj} - 1)K_{ojk}RT^2}{ME_{kj}}\right]^{n_{kj}/1-n_{kj}} \quad (8)$$

If a plot of $I_{kj}$ vs. $T(t)$ were made, it would result in a single peak whose position is dependent upon $K_{ojk}$, $E_{kj}$, $n_{kj}$, and $M$. The expression for the maximum of this peak may be obtained by differentiating Expression 8 and setting this first derivative equal to zero, as follows:

$$\ln\frac{M}{T_{mkj}^2} + \ln\frac{E_{kj}}{RK_{okj}} = -\frac{E_{kj}}{R}\left[\frac{1}{T_{mkj}}\right] \quad (9)$$

$$E_{kj}/2\,RTn_j \gg 1$$

where $T_{mkj}$ is the temperature that corresponds to the maximum evolution of the $k$th fragment by the $j$th process. It should be seen that this expression is independent of the order of the reaction. Therefore, if a series of temperature ramps were used, plots of

Figure 1.
**Thermal characterization methodologies**

| Analysis of Products | Thermal Degradation: isothermal | Thermal Degradation: nonisothermal |
|---|---|---|
| indirect | bomb pyrolysis/GC<br>bomb pyrolysis/GC MS<br>bomb pyrolysis/MS | |
| direct | solids probe pyrolysis/MS<br>Curie point pyrolysis/MS<br>Curie point pyrolysis/GC | DTA/MS<br>TGA/MS<br>EGA/MS<br>LPTD/MS |

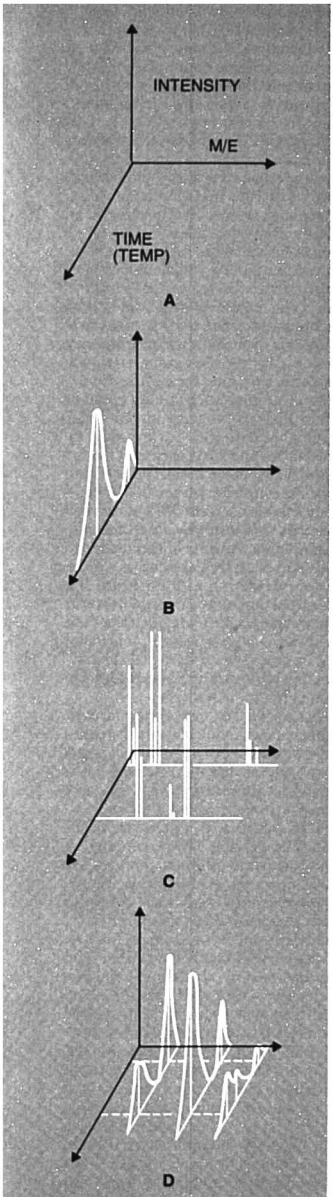


**Figure 2.** Data formats: (A) data axes; (B) total ion plot; (C) sequential mass spectra; (D) specific ion plots (temperature/time profile)

ln $[(M)/(T_{mkj}^2)]$ vs. $1/T_{mkj}$ would provide values for $E_{kj}$ and $K_{okj}$ and hence values for $K_{kj}$.

However, there are $j$ processes which give rise to the production of the $k$th fragment; therefore, the experimental intensity of the $k$th fragment will be the sum of all the individual $j$ processes.

$$I_k = \sum_{m=1}^{j} (I_{kj})_m \qquad (10)$$

Expression 10 will have a series of $j$ maxima, each of which is dependent upon the individual values of $K_o$, $E$, $n$, and $M$.

To this point, the treatment has assumed that the ion intensity at a specific mass is due to a single species. In reality, ions of different chemical composition can contribute to the experimental intensity observed at the $k$th mass. Therefore, if $p$ fragments have the same mass as the $k$th fragment, then Expression 10 must be expanded to include this contribution.

$$I_{k\ \text{total}} = \sum_{y=1}^{p} (I_k)_y = \sum_{y=1}^{p} \left[ \sum_{m=1}^{j} (I_{kj})_m \right]_y \qquad (11)$$

This complicates any attempt to explain the degradation mechanisms. This difficulty may be avoided by the use of high-resolution mass spectrometry.

Consider the complete thermal degradation of the sample in which the $k$ fragments are produced, each by $k_j$ processes.

$$MS = \sum_{z=1}^{k} (I_{k\ \text{total}})_z = \sum_{z=1}^{k} \left\{ \sum_{y=1}^{p} \left[ \sum_{m=1}^{j} (I_{kj})_m \right]_y \right\}_z \qquad (12)$$

The intensities of the $k$ fragments as a function of temperature/time constitute the mass spectral data (MS) that result from the ionization of the fragments.

These fragments will have evolution patterns that consist of a series of maxima and minima. Each maximum will occur at a different temperature and correspond to a particular evolution process. These temperatures are dependent upon the rate of heating of the sample and reflect the activation energies of the fragmentation processes. This assumes that the processes occur in sequence; one reaction is complete before the next begins. In complex materials the evolution processes can be expected to overlap.

Therefore, by consideration of these maxima, it may be possible to describe the molecular structure of the original sample, providing that the origin of the $k$ fragments and the $k_j$ processes that yield these fragments can be deduced. Implicit in this discussion is that the same fragment in different samples with the same molecular environment will have the same maximum evolution temperature, but if the same fragment is present in a different molecular environment, it will evolve at a different temperature. It is this single feature that makes nonisothermal degradation so potentially useful for characterizing samples. A schematic representation of the data is shown in Figure 2. This figure shows how the three variables, temperature, mass/charge ratio, and ion intensity, are related.

The theory of isothermal degradation falls out of the scope of this report since bonds are broken "in concert" rather than successively.

## Methodology

The use of the thermal degradation methodologies for the characterization of high molecular weight materials requires that the physical state of the sample be carefully controlled. Ideally, the sample should be dissolved in a volatile solvent in which the sample's integrity is maintained. However, if the sample cannot be dissolved, it should be ground to a powder. The size and distribution of the particles should be as small as possible, and these parameters should be constant from sample to sample. This size requirement is necessary since the temperature that corresponds to the maximum evolution of the fragment is particle-size dependent. The easiest way that powders can be handled is by a slurry with a volatile solvent. Biological samples such as tissues will require further studies to determine the optimum method of sample preparation without loss of information. If the sample is introduced as a slurry or in solution, then the volume and the concentration of the sample should be maintained constant; otherwise, the coating on the heating element will not be constant. After the sample is added to the reactor, the solvent is evaporated.

## Samples

There are various types of samples that could be analyzed or characterized by these methodologies including biological tissues or cells, polymers,

*The 3700 gets greater all the time.*

# Now there's a nitrogen detector that is selective, sensitive, and stable.

The new Varian Thermionic Specific Detector (TSD) for Model 3700 gas chromatograph is highly selective for nitrogen >5 × $10^4$ with respect to carbon. Minimum nitrogen detectivity is 1 × $10^{-13}$ gN/sec and linearity is $10^5$. It's also excellent for phosphorus detection. selectivity with respect to carbon is >$10^4$

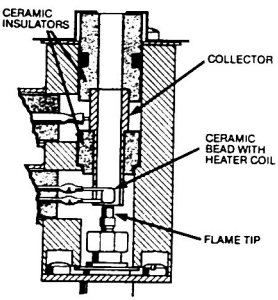


In addition, this detector is stable and easy to operate. The alkali source is a durable ceramic bead with an alkali compound imbedded in the ceramic matrix. The ceramic bead permits operation over a wider temperature range than glass, is more stable and requires less adjustment of bead temperatures. Result: reliable, reproducible operation with long bead lifetime for minimum maintenance and lower cost. It's another reason why the greatest gas chromatograph is getting greater all the time. For details write Varian Instrument Division, 611 Hansen Way, Box D-070, Palo Alto, CA 94303, or circle the Reader Service Number.

varian

CIRCLE 197 ON READER SERVICE CARD

geological specimens, surface coating, and inorganic or organic samples.

**Applications.** *Biological.* The major applications of the thermal degradation methodologies have been and will continue to be the characterization of bacteria and the determination of the chemical structure of biological samples.

Zemany was (*20*) the first person to realize that the pyrolysis of biological samples coupled with mass spectrometry or gas chromatography provides useful chemical information, although Oyama (*21*) first reported its use for characterizing bacteria. These pioneering papers have directed research by other workers in the area of bacterial chemotaxonomy via pyrolysis gas chromatography or mass spectrometry, notably Reiner et al. (PyGC) (*23–29*) and Meuzelaar et al. (PyMS) (*30–36*). These workers and others have had remarkable success even to the extent of showing differences between bacterial strains that may differ only by the absence of the type III polysaccaride antigen in the cell wall (*31*). The obvious advantages of PyMS over PyGC are based on speed of analysis (30–60 times more rapid) and the wealth of useful information obtained by PyMS. In addition, PyMS lends itself to computerization allowing the facile comparison between an unknown spectrum and a library spectrum. In this context an automated PyMS–computer system was recently described for the rapid identification of bacteria (*36*). This system offers to be a very powerful methodology for chemotaxonomy of bacteria.

Other studies have used nonisothermal degradation chemical ionization mass spectrometry to characterize bacteria (*4*). Although preliminary, the results were sufficient to not only differentiate between bacterial species and strains but also to show similarities within a bacterial species. These conclusions were based on the visual examination of data. The uniqueness of the methodology LPTD–MS provides not only the temperature dependence of the degradation processes but also enables larger fragments to be monitored. This latter advantage is a major improvement over other nonisothermal methods in which the degradation occurs apart from the mass spectrometer and therefore monitors small noncharacteristic fragments. Additional studies have used LPTD–MS to examine the chemical differences that account for normal or abnormal white blood cells (*5*). These two studies have shown that the methodologies of the nonisothermal degradation will provide greater information that may be useful for showing minor chemical differences.

The major drawbacks of all these methodologies are that, except in a few instances, the mass spectral or gas chromatographic data were not interpreted and the information was used empirically. While empiricism is sufficient for current applications, it is obvious that if the identities of the characteristic fragments were known, then the biological scientist would be more likely to accept these methodologies. The nonisothermal methodologies are more suitable for identification of fragments since the fragments are resolved temporally which makes the resulting mass spectra easier to interpret. The maximum potential of these techniques has yet to be approached since it is probable that in addition to their use for rapid characterization of bacteria, they may be used for fundamental studies. Such studies could be concerned with why certain bacterial strains are pathogenic or resistant to antibiotics and what occurs in a cell to cause it to mature abnormally. These studies, coupled with the ability to characterize bacteria difficult or impossible to identify by other means, suggest that the area of thermal degradation of biological samples will be a major research area in the future. The identification of mixtures of bacteria will always be difficult since the data are complicated. However, this may not be a problem if bacterial separation is performed by the careful selection of the growth media.

*Polymers.* The use of thermal degradation methodologies for the characterization of polymers was accepted very early; as a result, this area has received the most attention. This acceptance is probably related to the fact that the chemistry of most polymers and their possible thermal degradation fragments (often monomers) are well known. Most of the isothermal pyrolysis studies have been concerned with characterizing and analyzing polymers and copolymers on the basis of the evolved monomers. Other studies that used pyrolysis have been more concerned with the determination of additives such as plasticizers or antioxidants that are volatile or can be thermally degraded. These methodologies are particularly useful when the sample or the condition of the sample is not suitable for infrared analysis. The use of pyrolysis gas chromatography for polymer applications is extensive as shown by a review in 1965 (*44*). Nonisothermal methods will also provide this information; but in addition, they will supply data not available from isothermal pyrolysis. For example, the temperature at which the polymer loses its desired properties may be measured (*47–49*); or more importantly, if oxygen is used the temperature at which the polymer is oxi-

# Get higher resolution and repeatability with new monolayer bonded Zorbax™ columns.

DuPont has developed an innovative new line of monolayer bonded phases for Zorbax™ ODS, Zorbax™ CN and Zorbax™ C-8. This monolayer approach to bonded phases is at the forefront of packing technology utilized by leading researchers in the field.

Zorbax™ monolayer bonded phases (ODS, CN, C-8) are produced from proprietary monofunctional silanes. This technology permits close control of the chemical bonding process. The result is repeatable surface coverage, bringing you columns with the exceptional reproducibility so critical for reliable assays.

## But it all starts with the particle...

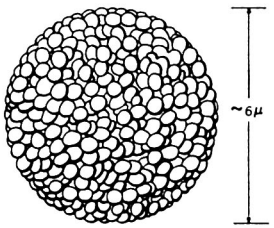


FIGURE 1. ZORBAX™ PARTICLE

Zorbax™ is not a silica gel adapted for HPLC, but a pure siliceous particle designed solely to meet the demanding needs of HPLC (Figure 1). Critical particle parameters that must be controlled for superior performance include:

- Particle size and distribution
- Pore size and distribution
- Surface area

Zorbax™ meets all these criteria through its unique patented structure. Ninety-five percent of all particles are within one micron of the nominal particle diameter (6 μm). This extremely narrow particle size distribution means very high efficiency performance without the high backpressures found with many five to six-micron packings.

The pore structure is also rigidly maintained by the inherent nature of this unique synthetic process. The packing uniformity of Zorbax™ in the column is excellent due to the uniform spherical shape and the narrow particle size distribution.

## ...and ends with performance.

The resolution power of the Zorbax™ ODS column is seen in a separation of polystyrene oligomers (Figure 2). This non-aqueous reversed phase (NARP) separation was achieved with only a fifteen-centimeter column. The fifteen-centimeter Zorbax™ columns provide higher efficiency than many thirty-centimeter columns of 10 μm packings and importantly are less expensive.

FIGURE 2 POLYSTYRENE 800 OLIGOMERS

Column: Zorbax™ ODS, 4.6 mm ID x 15 cm
Mobile Phase:
Primary: MeOH
Secondary: THF
Program: Linear (1.4% min.)
Flow Rate: 1.5 cm³ min.
Detector: UV (254nm)

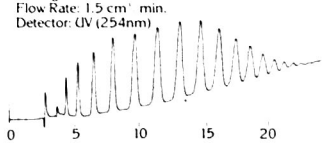


FIGURE 3 SULFA DRUGS

Column: Zorbax™ C-8
4.6 mm ID x 25 cm
Mobile Phase:
40% CH₃CN: 60% NaH PO₄ (.020 M), pH 3.3
Flow Rate: 1 cm³ min.
Detector: UV (254 nm)
PEAK IDENTITY
1 Sodium Sulfathiazole
2 Sulfacetamide
3 Sulfamerazine
4 Sulfisoxazole
5 Sulfabenzamide

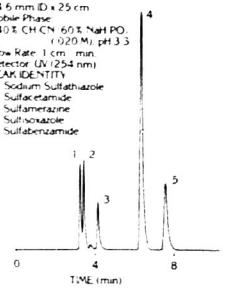


The new member of the DuPont packing team is Zorbax™ C-8. This reversed phase packing shows excellent selectivity for highly polar compounds including water soluble materials. A separation of some common sulfa drugs is readily obtained on Zorbax™ C-8 (Fig. 3).

## Toll-free ordering of columns.

DuPont Instruments is dedicated to giving you the best possible tools for your separation problems. Our toll-free number—800-441-7508 (Delaware 772-5500) is for your convenience in ordering columns.

Make sure you receive DuPont's informative new series of column literature. Send the reader service card, or write to DuPont Instruments, Room 36384, Wilmington, DE 19898.

**Liquid Chromatography Columns**
Scientific & Process Instruments Division
DUPONT
CIRCLE 50 ON READER SERVICE CARD

# Required Reading

**from Waters the Liquid Chromatography People**

**New!**

**Measuring Low-Level Organic Pollutants in WATER**

Easily measure non-volatile hydrocarbons in seawater and pesticide residues in drinking water at ppb levels by LC. This simple technique facilitates high recovery.

CIRCLE 236 ON READER SERVICE CARD

**New!**

**Measuring Low-Level Organic Pollutants from AIR**

Organic particulates from working atmospheres are analyzed with improved sensitivity and reproducibility, turning a problem analysis into a routine measurement.

CIRCLE 237 ON READER SERVICE CARD

**Published Periodically**

**"Environmental Notes"**


This informative bulletin keeps you updated on new applications of LC for environmental analyses. Enter your request now to get issue #1 and those to follow.

CIRCLE 238 ON READER SERVICE CARD

**free from**

**WATERS ASSOCIATES**

137 Maple Street, Milford, MA 01757
Telephone (617) 478-2000


dized may be found (*45, 46*). This information coupled with the products of oxidation is extremely important for those situations where the risk of fire is critical, e.g., materials of construction for aircraft, spacecraft, hospitals, and buildings. Also, nonisothermal methodologies can provide structural information such as the extent and types of cross-linking in polymers and also values for the nonisothermal kinetics of depolymerization. The first report of such studies was by Wilson and Hamaker in 1969 (*50*). These results, in addition to their obvious uses, could be used to study the processes involved in polymer aging or degradation by exposure to the atmosphere. It is apparent from this discussion that these methodologies have already found major applications to polymers and will continue to do so in the future.

*Geological Specimens.* The use of thermal degradation methodologies for the characterization of geological specimens is much less widespread, mainly as a result of the general thermal inertness of the specimens. Two areas have been studied using the nonisothermal methodologies: the hydrodesulfurization of coal (*18*) and the characterization of shale rock (*50–53*). This first study was concerned with characterizing coal via the sulfur content, and it was found that the hydrodesulfurization could be described by five kinetic processes. These processes and their preexponential factors and activation energies were established. This information has been useful for designing processes to remove sulfur from coals for environmental reasons, which is very important due to potential energy shortages. Studies using nonisothermal degradation of shale rock have shown that these methodologies can be used to study the release of organics from these samples. This application will be very important to future attempts to use shale rock as a major source for oil. In related studies, isothermal pyrolysis has been used to examine meteorites (*56*), the soil on the moon (*52, 55, 56*), or Mars for evidence of life. This application is topical, but so far the results have not been definitive.

*Surface Coatings.* For the characterization of surface coatings, isothermal pyrolysis has received little attention until recently (*36*). However, the future of this area looks promising for forensic applications and to study the aging of surface coatings through exposure to the environment. It is probable that in this area the nonisothermal methodologies will have greater application since their information is more detailed.

*Inorganic or Organic Samples.* The application of nonisothermal methodologies to the characterization of inorganic or organic compounds is obvious. Such applications include measurement of activation energies for thermal degradation or dehydration of various samples, for example. So far most reported studies have used thermal methods of analysis without analysis of the evolved products since this information has been sufficient (*2*). However, it is possible that future applications will use the nonisothermal degradation methodologies since the resulting data are more informative.

## Conclusions

The applications of thermal degradation are many and varied, particularly if nonisothermal methodologies are used. Nonisothermal degradations have greater likelihood of characterizing closely related species since the added dimension of temperature provides greater resolution. In addition, nonisothermal methods are free from contamination and can reproduce the temperature ramp more easily than isothermal methods. The most important advantage of nonisothermal methods is that they can be used to measure fundamental molecular energetics and provide molecular structural information.

## References


(1) R. L. Levy, *Chromatogr. Rev.*, **8**, 48 (1966).
(2) W. W. Wendlandt, "Thermal Methods of Analysis", 2nd ed., Wiley-Interscience, New York, N.Y., 1974.
(3) W. Ledding, "Gas Effluent Analysis", Marcel-Dekker, New York, N.Y., 1967.
(4) T. H. Risby and A. L. Yergey, *J. Phys. Chem.*, **80**, 2839 (1976).
(5) A. L. Yergey, T. H. Risby, and H. M. Golomb, *Biomed. Mass Spec.*, **5**, in press (1978).
(6) F. H. Field, *Acc. Chem. Res.*, **1**, 43 (1968).
(7) D. S. Simons, S. N. Colby, and C. A. Evans, Jr., *Int. J. Mass Spectrom. Ion Phys.*, **15**, 291 (1974).
(8) H. D. Beckey, A. Heindricks, and H. V. Winkler, *ibid.*, **3**, 9 (1970).
(9) R. J. Beuhler, E. Flanigan, L. J. Greene, and L. Friedman, *J. Am. Chem. Soc.*, **96**, 3990 (1974).
(10) R. D. MacFarlane and D. F. Torgerson, *Science*, **191**, 920 (1976).
(11) D. F. Torgerson, R. P. Skowronski, and R. D. MacFarlane, *Biochem. Biophys. Res. Commun.*, **60**, 616 (1974).
(12) R. J. Beuhler, E. Flanigan, L. J. Greene, and L. Friedman, *Biochemistry*, **13**, 5060 (1974).
(13) R. Sarges and B. Witkop, *J. Am. Chem. Soc.*, **87**, 2011 (1965).
(14) C. Hignite, "Biochemical Applications of Mass Spectrometry", G. R. Waller, Ed., Wiley-Interscience, New York, N.Y., 1972.
(15) H. Juntgen, *Erdoel Kohle*, **17**, 180 (1964).
(16) H. Juntgen and K. C. Traenckner, *Brennst. Chem.*, **45**, 105 (1964).
(17) H. Juntgen and K. H. Van Heek, *Fuel*, **47**, 103 (1968).
(18) A. L. Yergey, F. W. Lampe, M. L. Vestal, A. G. Day, G. J. Fergusson, W. H. Johnston, J. J. Synderman, R. H. Essen-

*Model 3700, the greatest gas chromatograph, gets greater all the time.*

# Varian announces the first capillary system that is easy to use and the first dual-flame FPD for high selectivity

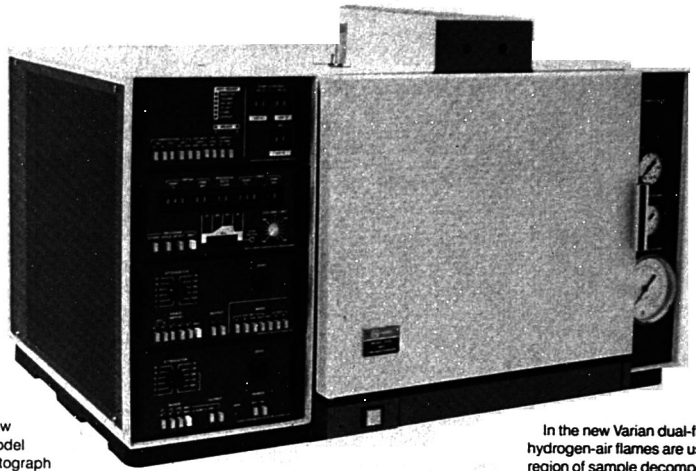

Both advances are now available on Varian Model 3700, the gas chromatograph that brings together all the major chromatographic breakthroughs and offers new applications capabilities in every component.

## NEW CAPILLARY SYSTEM

The entire Model 3700 Chromatograph is optimized for capillary column chromatography: the all-glass injector-splitter; extra large 1350 cubic inch column oven; simple column installation; special thermostatted pneumatics; and full automation capability including the only single channel data system that can handle 0.5 sec peak widths.

**The new all-glass capillary injector-splitter** provides four sample-injection modes. It features a unique positive septum purge to prevent septum bleed problems and a buffer volume for more reproducible splits.

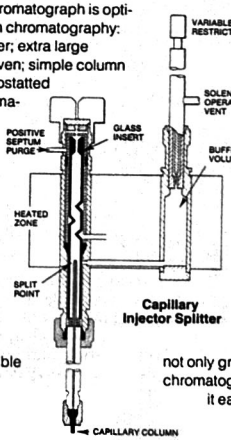


**Capillary Injector Splitter**

**Easy capillary column installation.** In the past, only those with super dexterity and patience could install capillary columns. Now, the 3700 capillary system changes all that. Columns can be installed in a few minutes without straightening the ends and without using a costly cage. Column ends slip directly into the fittings at the glass lined injector and detector inserts. All types of capillary columns can be used: WCOT, SCOT, PLOT, and others. This new column installation design saves at least three hours everytime you install a new column.

**Capillary and packed column chromatography in one instrument.** The 3700's large column oven, and widely separated and independently heated injectors, make it possible to do both capillary and dual packed column chromatography in the same chromatograph. This not only greatly increases the utility of the chromatograph for many labs; it also makes it easier to relate packed column methods to capillary methods.

## NEW DUAL-FLAME FPD

The new flame photometric detector for the 3700 features a proprietary dual-flame design that overcomes many of the limitations of single-flame FPD's such as quenching and compound dependency, and provides high selectivity, linearity and detectivity.

In the new Varian dual-flame design, two hydrogen-air flames are used to separate the region of sample decomposition from the region of emission. Since Flame 1 provides the energy to break down the large molecules in the effluent, Flame 2 can use all of its energy for S and P emission. Consequently, there is no quenching and much less compound dependency. An important benefit of the new design is the greatly improved selectivity of S and P with respect to hydrocarbons and with respect to each other.

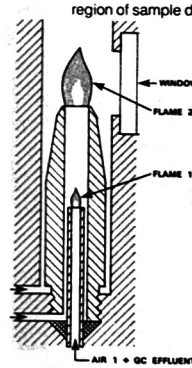


**Dual-Flame FPD**

P/C*>10⁵;
S/C: 10³ to 10⁶
*C in n-hexadecane

**Other major 3700 performance features include:** New ESP* monitor. New non-contaminating FID. New highest sensitivity TCD. New $^{63}$Ni ECD with a *linear* dynamic range > $10^4$ and an MDQ < 0.1 pg of lindane And new carrier gas flow stability because all critical flow control elements are isolated in an independently heated oven.

*Electro Sensor Panel

For full information on the greatest gas chromatograph ever made, circle Reader Service No. 195. To have a Varian representative call, circle Reader Service No. 196.

varian

Varian Instrument Division, 611 Hansen Way, Box D-070, Palo Alto, California 94303

# Sensitive LC Detectors from Varian

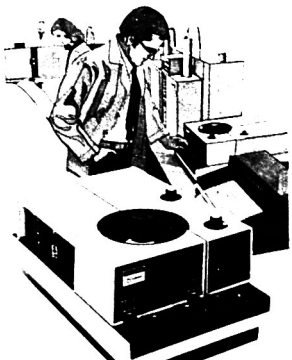

**Varichrom™**

Continuously variable UV-Vis detection from 190 to 700 nm lets you optimize for most organic compounds or for elimination of solvent background. The system's extended wavelength region and low noise permit monitoring many new compound classes such as lipids, mono-olefins and carbohydrates. Dual-beam optics maximize stability and long-term reliability. Unique 8-microliter flow cell with 10 nm path length. Kinematic mount simplifies alignment. Variable spectral bandwidth and time constant. Maximum full scale sensitivity of 0.005 absorbance units.

**Fluorichrom™**

A sensitive, selective filter fluorimeter for ppt trace analysis. For maximum sensitivity in the region where most fluorescent compounds excite, Fluorichrom provides strong continuous excitation from >280 nm through the visible. Dual-filters, at both excitation and emission significantly decrease background noise and increase sensitivity. An optional deuterium source provides low wavelength excitation. A very broad selection of filters is available: bandpass, interference or cut-off, for selectivity or for maximizing cumulative fluorescent emission.

**For Fluorichrom details circle Reader Service No. 223.**

**For Varichrom details circle Reader Service No. 224.**

**To have a representative contact you circle Reader Service No. 225.**

varian



high, and J. E. Hudson, *Ind. Eng. Chem. Process Des. Develop.*, **13**, 233 (1974).
(19) V. M. Gorbachev, *J. Therm. Anal.*, **8**, 349 (1975).
(20) P. D. Zemany, *Anal. Chem.*, **24**, 1709 (1952).
(21) V. I. Oyama, *Nature*, **200**, 1058 (1963).
(22) E. Reiner, *ibid.*, **206**, 1272 (1965).
(23) E. Reiner, *J. Gas Chromatogr.*, **5**, 65 (1967).
(24) E. Reiner and W. H. Ewing, *Nature*, **217**, 191 (1968).
(25) E. Reiner and G. P. Kubica, *Am. Rev. Respir. Dis.*, **99**, 42 (1969).
(26) E. Reiner, R. E. Beam, and G. P. Kubica, *ibid.*, p 750.
(27) E. Reiner, J. J. Hicks, R. E. Beam, and H. L. David, *ibid.*, **104**, 656 (1971).
(28) E. Reiner, J. J. Hicks, M. M. Ball, and W. J. Martin, *Anal. Chem.*, **44**, 1058 (1972).
(29) E. Reiner and J. J. Hicks, *Chromatographia*, **5**, 523 (1972).
(30) H.L.C. Meuzelaar, P. G. Kistemaker, and A. Tom, "New Approaches to the Identification of Microorganisms", Chap. 10, C. G. Heden and T. I. Uleni, Eds., Wiley-Interscience, New York, N.Y., 1975.
(31) P. G. Kistemaker, H.L.C. Meuzelaar, and M. A. Posthumas, *ibid.*, Chap. 11.
(32) H.L.C. Meuzelaar and R. A. in't Veld, *J. Chromatogr. Sci.*, **10**, 213 (1972).
(33) H. R. Schulten, H. D. Beckey, H.L.C. Meuzelaar, and A.J.H. Boerboom, *Anal. Chem.*, **45**, 191 (1973).
(34) H.L.C. Meuzelaar and P. G. Kistemaker, *ibid.*, p 507.
(35) H.L.C. Meuzelaar, P. G. Kistemaker, and M. A. Posthumas, *Biomed. Mass Spec.*, **1**, 312 (1974).
(36) H.L.C. Meuzelaar, P. G. Kistemaker, W.I.M. Eshuis, and M. A. Posthumas, 25th Ann. Meeting of Am. Soc. for Mass Spec., Washington, D.C., May 1977.
(37) V. I. Oyama and G. C. Carle, *J. Gas Chromatogr.*, **5**, 151 (1967).
(38) R. D. Cone and R. V. Lechowich, *Appl. Microbiol.*, **19**, 138 (1970).
(39) P. G. Vincent and M. M. Kulik, *ibid.*, **20**, 957 (1970).
(40) E. E. Medley, P. G. Simmonds, and S. L. Manatt, *Biomed. Mass Spec.*, **2**, 261 (1975).
(41) J. P. Anhalt and C. Fenselau, *Anal. Chem.*, **47**, 219 (1975).
(42) A. S. Sekhow and J. W. Carmichael, *Can. J. Microbiol.*, **18**, 1593 (1972).
(43) P. G. Simmonds, *Appl. Microbiol.*, **20**, 567 (1970).
(44) G. M. Brauer, *J. Polym. Sci.*, **8**, 3 (1965).
(45) G. Dugan, J. D. McCarty, and R. J. Friant, *Anal. Calorimetry Symp. Proc.*, **2**, 417 (1970).
(46) W. K. Rudloff, A. D. O'Donnell, R. G. Scholz, and A. Valaitis, *Therm. Anal.*, **3**, 205 (1971).
(47) I. A. Murdock and L. J. Rigby, "Dynamic Mass Spectrometry", Vol 3, D. Price, Ed., Heydon, London, England, 1972.
(48) A. Zeman, *Therm. Anal.*, **3**, 219 (1971).
(49) I. C. McNeill, *ibid.*, p 229.
(50) D. E. Wilson and F. M. Hamaker, *Int. Conf. Therm. Anal.*, **2**, 517 (1969).
(51) J. W. Smith and D. R. Johnson, *ibid.*, p 1251.
(52) E. K. Gibson, Jr., *Thermochim. Acta*, **5**, 243 (1973).
(53) A. L. Yergey and T. H. Risby, unpublished results, 1977.
(54) E. K. Gibson, Jr., and S. M. Johnson, *Thermochim. Acta*, **4**, 49 (1972).
(55) E. K. Gibson, Jr., and S. M. Johnson, *Proc. Lunar Sci. Conf.*, **2**, 1351 (1971).
(56) E. K. Gibson, Jr., and G. W. Moore, *ibid.*, **3**, 2029 (1972).
(57) H. G. Langer and T. P. Brady, *Int. Conf. Therm. Anal.*, **2**, 295 (1969).
(58) H. G. Langer and T. P. Brady, *Thermochim. Acta*, **5**, 391 (1975).
(59) A. J. Hegedus, *Mikrochim. Acta*, 40 (1971).


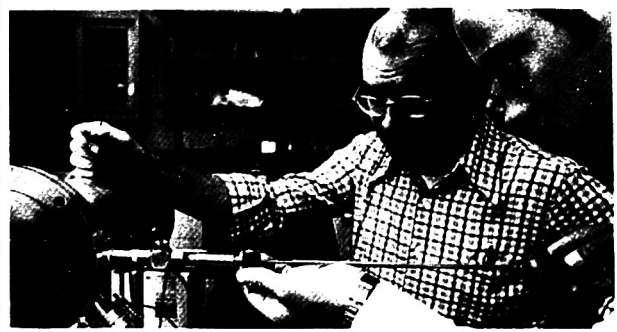

**Terence H. Risby** (right) is an assistant professor of chemistry and a faculty member of the Center for Air Environment Studies at the Pennsylvania State University. His research interests include the significance of metals in biological and environmental systems, electrical discharges, thermodynamics of gas liquid chromatography, trace analysis by chemical ionization mass spectrometry, and the use of linear programmed thermal degradation–mass spectrometry to characterize bacteria.

**Alfred L. Yergey** (left) is a senior scientist at Chemetron Medical Products (formerly Scientific Research Instruments) and at Friends Medical Science Research Center. His research interests include the fundamental design studies of quadrupole mass filters, design of ion optics for quadrupole mass filters, applications of mass spectrometry to clinical and environmental problems, and the application of linear programmed thermal degradation–mass spectrometry to biological systems.

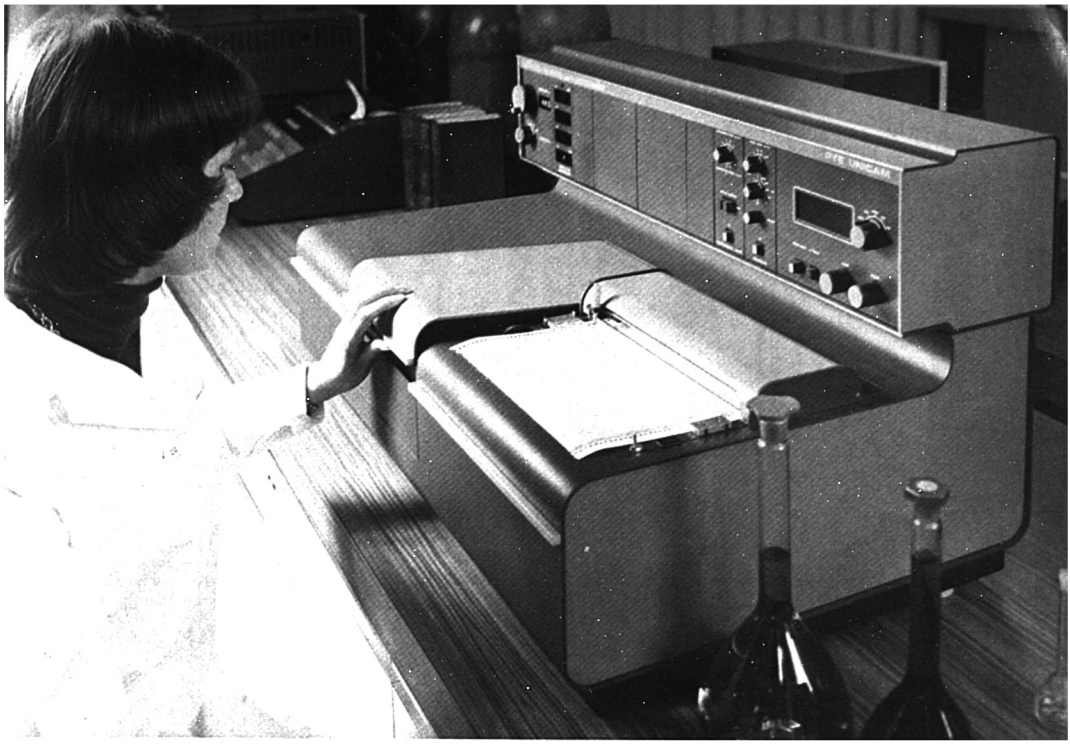

# Get more UV-VIS spectrophotometer than your budget allows!

**Now from Philips, the Pye Unicam SP8-100 high performance spectrophotometer.**

You'll be most pleasantly surprised when you see the features packed into the SP8-100 . . . and learn how affordable it is. Get our brochure and compare this system with any other.

The SP8-100 is built by Pye Unicam, a leader in UV-VIS spectrophotometry, and is backed by Philips, a world leader in high technology systems. Our applications specialists and accessories will help you get the most from your studies, including:

- reaction rate analysis
- color measurements
- fluorescence
- densitometry
- column monitoring
- turbid samples
- automated measurements


Call, write or use the reader reply service for your copy of the SP8-100 brochure.

Stretch your budget . . . and your capabilities . . . with the Pye Unicam SP8-100.

**Philips Electronic Instruments, Inc.**
A North American Philips Company,

85 McKee Drive, Mahwah, N.J. 07430
Telephone (201) 529-3800
International — Contact Pye Unicam Ltd.
York Street, Cambridge, England CB1 2PX
Telephone, Cambridge (0223) 58866
Telex 817331

PHILIPS

**Electronic Instruments**

PHILIPS

CIRCLE 166 ON READER SERVICE CARD

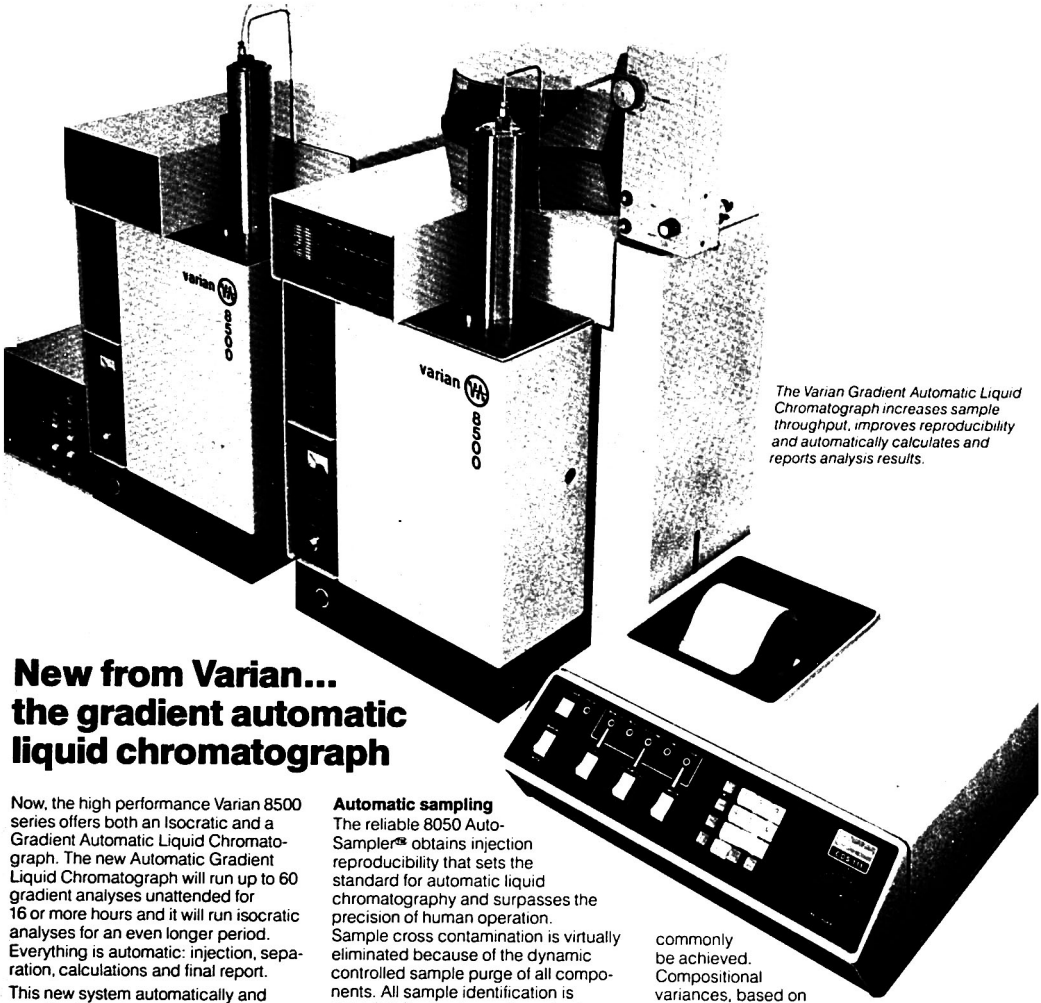


*The Varian Gradient Automatic Liquid Chromatograph increases sample throughput, improves reproducibility and automatically calculates and reports analysis results.*

# New from Varian... the gradient automatic liquid chromatograph

Now, the high performance Varian 8500 series offers both an Isocratic and a Gradient Automatic Liquid Chromatograph. The new Automatic Gradient Liquid Chromatograph will run up to 60 gradient analyses unattended for 16 or more hours and it will run isocratic analyses for an even longer period. Everything is automatic: injection, separation, calculations and final report.

This new system automatically and repetitively performs the most sophisticated gradient analyses. In addition, it has the unique capability to employ different analytical methods, including different gradient profiles for as many as four types of samples in a single unattended period. This is the most versatile and powerful atuomatic liquid chromatograph available today.

**Pulseless flow and versatile gradient generation**

The system's Model 8520 positive displacement pumps provide the pulseless flow required for good accuracy, reproducibility, detectability and high efficiency. The multilinear solvent programmer — the most versatile gradient generation device — controls the dual-pump system to automatically provide gradients of virtually any shape needed to optimize an analysis.

**Automatic sampling**

The reliable 8050 AutoSampler® obtains injection reproducibility that sets the standard for automatic liquid chromatography and surpasses the precision of human operation. Sample cross contamination is virtually eliminated because of the dynamic controlled sample purge of all components. All sample identification is encoded for display on the output report of the CDS-111.

**Automatic data handling**

The third system component, the CDS-111 Chromatography Data System, automatically integrates the chromatogram, calculates the data and reports the results. Area normalization, corrected area normalization, internal standard and external standard calculations can be performed, as well as computation of the appropriate response factors needed in these calculations. Up to eight different analytical method files may be stored in memory. On command from the AutoSampler the CDS-111 will automatically change the analytical method file to handle various sample types with a completely different program. With the Gradient Automatic Liquid Chromatograph, retention time reproducibilities of better than 1% can commonly be achieved. Compositional variances, based on peak area, will be in the range of 1% to 2%.

The components of this system: the 8500, the AutoSampler, and the CDS-111, are also available separately. Together, they form the finest Gradient and Isocratic Automatic Liquid Chromatographs available today.

For details, circle the indicated Reader Service Number:

Automatic Liquid Chromatographs ..... 218
Automatic LC System Components:
- Model 8500 Liquid Chromatographs ... 219
- CDS-111 Chromatography Data System 220
- Model 8050 AutoSampler ..... 221

To have a representative contact you .... 222

varian

# Collaborative Study Procedures of the AOAC

## Association of Official Analytical Chemists

The Association of Official Analytical Chemists (AOAC) is a unique, nonprofit scientific organization whose primary purpose is to serve the needs of government regulatory and research agencies for analytical methods. The goal of the Association is to provide methods which will perform with the necessary accuracy and precision under usual laboratory conditions (*1*). Since its formation in 1884 the AOAC has provided a mechanism to select methods of analysis from published literature or develop new methods, collaboratively test them through interlaboratory studies, approve them, and publish the approved methods for a wide variety of materials relating to foods, drugs, cosmetics, agriculture, forensic science, and products affecting the public health and welfare. Its membership is composed of scientists from Federal, State, Provincial, and other regulatory bodies who work within the AOAC's established procedures as researchers, methods collaborators, and committee members. Although most of the members are from North America, many nations throughout the world are represented.

The AOAC has almost a century of experience in utilizing the collaborative study as a means of determining the reliability of analytical methods for general purposes and, especially, for regulatory purposes. In fact, the AOAC's major contribution to analytical science has been to bring the collaborative study technique for the validation of analytical methods to a high degree of perfection. In such a study, laboratories analyze identical sample sets which cover the range of applicability of a method previously selected as being useful and practical. The purpose of the study is to establish the characteristics of the methods with respect to accuracy, precision, sensitivity, range, specificity, limit of detection, limit of reliable measurement, selectivity, practicality, and similar attributes, as required.

### Organization and Procedures for AOAC Collaborative Studies

The collaborative study is organized and directed by an analyst designated as the Associate Referee for the specific subject under investigation. Currently, some 600 Associate Referees appointed by the Association are responsible for as many topics. An Associate Referee is selected for his knowledge, interest, and experience in the subject matter field. He operates under the scientific guidance, support, and administrative supervision of a General Referee, who is in turn responsible for a product area. The Associate Referee reviews the literature and selects one or two of the better analytical methods available, modifying them as needed. Alternatively, he may develop or adapt a method used in his laboratory for the analyte and matrix under study, testing it thoroughly in his laboratory before designing a collaborative study. The General Referee is kept informed of such preliminary studies.

The samples analyzed in a collaborative study are normally prepared and distributed to the participants by the Associate Referee. The Association follows the recommendations of Youden (*2*) that not fewer than five laboratories participate and that a minimum of six sample materials be sent to each. These are minima and, in practice, both are usually exceeded. In addition, a reference or practice sample is included, where possible.

Laboratories with at least some experience in the general subject matter are selected as collaborators. Because the objective of the study is to standardize the method, as contrasted to standardizing the analyst (*3*), all analysts are instructed to follow the method exactly as written even though they may not concur with the Associate Referee's selection among possible alternatives. The level of the analyte in the samples is usually unknown to the participants.

All individual results obtained by the collaborators are reported to the Associate Referee, who compiles and evaluates them. Since statistical treat-

---

Prepared for the Joint International Symposium, "The Harmonisation of Collaborative Studies", in the Rooms of the Royal Society, 6 Carlton House Terrance, London SW1, England, 9–10 March 1978, by the AOAC Committee on Collaborative Studies: Elwyn D. Schall, Chairman, Charles W. Gehrke, William Horwitz, Anthony J. Malanoski, James P. Minyard, Jr., Forrest W. Quackenbush, and Ernest S. Windham. AOAC, Box 540, Benjamin Franklin Station, Washington, D.C. 20044

This article not subject to U.S. Copyright
Published 1978 American Chemical Society

CIRCLE 173 ON READER SERVICE CARD

***USA Exclusive***

**MACHEREY-NAGEL**
**HPLC Bulk Packings** for Adsorption
Partition • Reverse Phase Chromatography
Ion Exchange and Gel Permeation

In addition to stocking the full line of NUCLEOSIL® and other Macherey-Nagel high quality HPLC sorbents, Rainin also offers a full line of HPLC Packed Columns, other Packing Materials and Liquid Chromatography Equipment and Accessories. Our Technical Sales Department is prepared to help you specify the packings most suited for your specific applications.

*Full line catalog by return mail*

RAININ
INSTRUMENT CO INC
94 Lincoln Street, Brighton, Massachusetts 02135
1-800-225-4590 • Telex 94-0687

CIRCLE 181 ON READER SERVICE CARD

ment of the data is considered essential in a rigorous evaluation of the method for accuracy, precision, sensitivity, and specificity, it is now required for all studies. The Association considers this of such importance that it provides statistical assistance in all cases where it is otherwise unavailable to the Associate Referee. A statistical manual (*4*) is also provided.

The Associate Referee makes the initial judgment on the performance of the method. If he recommends approval, it passes to the General Referee and then to a committee of experts. If both recommend approval, the method is presented at the Association's annual business meeting for vote by the membership.

Approved methods and supporting data are published in the *Journal of the Association of Official Analytical Chemists*. They are subject to scrutiny and general testing by other analysts for at least a year before final adoption. They may be modified and restudied collaboratively as needed, should feedback from general use reveal flaws in the method or in its written set of directions. Approved methods are included in the Association's "Official Methods of Analysis", a book of some 1000 pages which is updated every 4–5 years.

The preceding summary of AOAC's modus operandi recognizes the need for healthy skepticism toward results obtained by analytical methods which have not undergone such rigorous scrutiny and interlaboratory testing of their accuracy, precision, dependability, specificity, and practicality.

### Selection of Methods for Study

A certain degree of variability is associated with all measurements. Much of the research on analytical chemistry is an attempt to minimize that variability. But there are many different types of variability in analytical work. We often find that when we attempt to minimize one kind, we must necessarily permit expansion in another kind. In practical analytical chemistry, the problem often comes down to which variability is to be minimized.

Some examples of this point may be helpful. In atomic weight determination, everything—especially *practicality*—is sacrificed for *accuracy*. A high degree of accuracy and practicality is required in the assay of precious metals, but the fire assay used is generally *applicable* to little else besides metals and minerals. In clinical chemistry, within-laboratory *precision* (repeatability) is critical, and often is of greater interest to clinical laboratories than absolute accuracy or agreement with the values of other laboratories (reproducibility). In drug analysis, a high degree of accuracy is required in

the therapeutic *range* because the analytical values determining the identity, strength, quality, and purity of pharmaceutical preparations, as laid down in pharmacopoeial specifications, are directly related to clinical value. With polynuclear hydrocarbons, *specificity* is important, since some of these compounds are carcinogenic while others are not. In applying the famous Delaney clause of the United States Federal Food, Drug, and Cosmetic Act, all attributes of the analytical methods are secondary to the detection of extremely small concentrations (*detectability*), or to exhibiting a high degree of response for small changes in concentration (*sensitivity*).

There is a very special case involving accuracy, where the "true value" is determined by the method of analysis. Many legal specifications and standards for food and agricultural products define ill-defined components such as moisture, fat, protein, and crude fiber in terms of reference methods. Therefore, the precision of these methods becomes the limiting factor for their performance. In fact, most analyses involved in commercial transactions require primarily that the buyer and seller agree on the same value (analytically and economically), regardless of where it stands on an absolute scale.

The point of these examples is that although methods of analysis are characterized by a number of attributes—accuracy, precision, specificity, sensitivity, detectability, dependability, and practicality—no method is so flawless that all these qualities can be maximized simultaneously. For any particular analysis, the analyst must determine, on the basis of the purpose of the analysis, which attributes are essential and which may be compromised.

Unfortunately, the literature is replete with examples indicating that an individual analyst, and especially the originator of a method of analysis, is not an unbiased judge of the relative merits of the methods of analysis which he develops and uses. In our experience, the collaborative study provides impartial data on the suitability of the method. The data, in many cases, speak for themselves.

The collaborative study, or ring test or round robin test, as it is called in other organizations, provides the basic information on the performance of analytical methods. The extent of the information will depend on the number of samples provided, the number of analyses performed, and the number of laboratories participating. The data should be unbiased because the composition of the samples is known only to the administrator of the study.

Some of the requirements of the study and their relationship to the characteristics and attributes of the method are as follows:

(1) *Accuracy.* Samples must be of defined composition (by spiking, by formulation, or by analytical consensus).

(2) *Specificity.* Samples should contain related analytes.

(3) *Sensitivity.* Samples should differ from each other or from negative samples by a known amount.

(4) *Applicability.* Samples should include the concentration range and matrix components of interest.

(5) *Blanks.* Samples should include different matrices with "none" of the component of interest.

(6) *Precision.* Instructions should request replicate analyses by the same or different analysts in the same laboratory, preferably on different days. By far a better procedure is to include "blind" (unknown to the analyst) replicate samples in the series.

(7) *Practicality.* Instructions should request information as to the actual and elapsed time required for the analyses; the availability of reagents, equipment, and standards; and any necessary substitutions. When practice samples are included, the number of analyses required to achieve the stated recovery and repeatability, should be reported.

### Procedural Details of Collaborative Study

As numerous beginners in this field have discovered, much preliminary work must be done before sending out samples:

(1) The method must be chosen and demonstrated to apply to the matrices and concentrations of interest.

(2) The critical variables in the method should have been determined and the need for their control emphasized [a ruggedness test (*5*) is useful for this purpose].

(3) The method should be written in detail by the Associate Referee and tested by an analyst not previously connected with its development.

(4) Unusual standards, reagents, and equipment must be available from usual commercial sources of supply, or sufficient quantities must be prepared or obtained to furnish to the participants.

(5) The samples must be identical and homogeneous so that the analytical sample error is only a negligible fraction of the expected analytical error.

(6) A sufficient number of samples must be prepared to cover typical matrices and the concentration range of interest (tolerance, maximum or minimum specifications, likely levels of occurrence, etc.).



At Corco, we make 132 standard solutions — and uncounted special or custom solutions. Volumetric. Percentage. For Aqueous and nonaqueous titrations. Special solutions to meet ACS and ASTM requirements. Indicators. Buffers. Clinical reagents. All within an accuracy to 0.05%.

As many companies come to Corco for normal solutions as those for special normalities. We make them just as easily and just as well. Because Corco makes only reagent-grade solutions. (Reagent acids, bases, and specialty chemicals, too.)

Corco has the solutions — special or standard — in pints, gallons, five-gallons and drums. Write or call for your copy of our booklet with that title. Or circle the number.


CORCO

**CORCO CHEMICAL CORPORATION**

*Manufacturers of*
*Reagent & Electronic Chemicals*
Tyburn Road & Cedar Lane • Fairless Hills, Pa. 19030
(215) 295-5006
CIRCLE 32 ON READER SERVICE CARD

# FACSS • V MEETS IN HISTORIC BOSTON


**Fifth Annual Meeting**
**Federation of Analytical Chemistry and Spectroscopy Societies**
**October 30 — November 3, 1978**
**Sheraton Boston Hotel**
**Hynes Auditorium**

## Call for Papers

Papers are invited in all areas of Analytical Chemistry and Spectroscopy. The deadline for titles and a 200–250 word abstract is May 1, 1978.
Send to:

**James F. Cosgrove**
**Program Chairman, FACSS-78**
**GTE Laboratories Inc.**
**40 Sylvan Road**
**Waltham, MA 02154**
(617) 890-8460

## General Information

**Contact**

**Arrangements Chairman**
Paul Lublin
GTE Laboratories Inc.
40 Sylvan Road
Waltham, MA 02154
(617) 890-8460

## Scientific Program

The scientific program will include papers in the following areas: Forensic Science; Thermoanalysis; Surface Analysis; Chromatography; GC/MS; Automation; Electron and Optical Microscopy; Electron and X-Ray Diffraction; Emission; X-Ray, Atomic and Acoustic Spectroscopy; Clinical; Chemical Institute Canada Symposium.

- Anachem Award
- Benedetti Pichler Award

## Instrument Exhibit

A large Laboratory Equipment Exposition in the Hynes Auditorium will feature displays of the latest developments in analytical instruments.

## Workshops

Infra-Red Spectroscopy
X-Ray Diffraction

## Short Courses

Modern Emission Spectroscopy
Fourier Transform Spectroscopy
Atomic Absorption Spectroscopy

## Special Events at FACSS — 1978

- **Mixer**
- **Clambake**
- **Spouses' Program**

CIRCLE 79 ON READER SERVICE CARD


(7) Samples must be stable and capable of surviving the rigors of commercial transportation.

(8) Reserve samples should be prepared and preserved to replace lost samples and to permit reanalysis of samples considered as outliers to attempt to discover the cause of abnormal results.

(9) The instructions must be clear. They should be reviewed by someone not connected with the study to uncover potential misunderstandings and ambiguities.

(10) If the analyte is subject to change (e.g., bacterial levels, nitroglycerin tablets), provision must be made for all participants to begin the analysis at the same time.

(11) Practice samples of a known and declared composition should be furnished with instructions not to analyze the unknowns until a specified degree of recovery and repeatability (or other attribute) has been achieved.

(12) Provision should be made when necessary for submission of standard curves, tracings of recorder charts, or photographs of thin-layer plates in order to assist in determining possible causes of error.

### Other Types of Interlaboratory Studies

This type of collaborative study, which is designed to determine the characteristics of a method, must be carefully distinguished from other types of interlaboratory studies which by design or through ignorance provide other kinds of information. The most important types of other studies are:

(1) Those studies which require the collaborators to investigate the variability of parts of methods or applicability to different types of samples. (An interlaboratory study is usually an inefficient way of obtaining this type of information.)

(2) Those studies which permit an analyst to use any method he desires. Such studies invariably produce such a wide scatter of results that the data are of little value for evaluation of methods. They may be useful in selecting a method from a number of apparently equivalent methods, provided the purpose is emphasized beforehand and the participants provide a description of the method used in order to permit a correlation of the details of the methods with apparent biases and variabilities.

(3) Those studies which are used for quality control purposes, whose participants are not permitted sufficient time to gain familiarity with the method, or who permit deviations to enter into the performance of the analyses on the grounds that the deviation is obviously an improvement which could not possibly affect the results of the analysis, or who claim to have a superior method.

With this background information, it is now appropriate to introduce the following definitions which were agreed upon as part of the guidelines for collaboration between the AOAC and the Collaborative International Pesticide Analytical Council Ltd. (CIPAC) (6).

*Collaborative study.* An analytical study involving a number of laboratories analyzing the same sample(s) by the same method(s) for the purpose of validating the performance of the method(s).

*Preliminary interlaboratory study.* An analytical study in which two or more laboratories evaluate a method to determine if it is ready for a collaborative study.

*Laboratory performance check.* The analysis of very carefully prepared and homogeneous samples, normally of known active ingredient content, to establish or verify the performance of a laboratory or analyst.

### Summary


The collaborative study is an experiment designed to evaluate the performance of a method of analysis through the analysis of a number of identical samples by a number of different laboratories. With proper design, it provides an unbiased evaluation of the performance of a method in the hands of those analysts who will use it. A collaborative study must be distinguished from those studies designed to choose a method or to determine laboratory or analyst performance.


### References


(1) AOAC, "Handbook of the AOAC", 4th ed., AOAC, Box 540, Benjamin Franklin Station, Washington, D.C. 20044, 1977.
(2) W. J. Youden, "Accuracy of Analytical Procedures", *J. Assoc. Off. Anal. Chem.*, **45**, 169–73 (1962).
(3) Harold Egan, "Methods of Analysis; An Analysis of Methods", *ibid.*, **60**, 260–7 (1977).
(4) W. J. Youden and E. H. Steiner, "Statistical Manual of the AOAC: Statistical Techniques for Collaborative Tests. Planning and Analysis of Results of Collaborative Tests", AOAC, Box 540, Benjamin Franklin Station, Washington, D.C. 20044, 1975.
(5) W. J. Youden, "The Collaborative Test", *J. Assoc. Off. Anal. Chem.*, **46**, 55–62 (1963).
(6) "Guidelines for Collaboration Between the Association of Official Analytical Chemists (AOAC) and the Collaborative International Pesticide Analytical Council Ltd. (CIPAC)", *ibid.*, **57**, 447–9 (1974).


### Bibliography


Daniel Banes, "The Collaborative Study as a Scientific Concept", *J. Assoc. Off. Anal. Chem.*, **52**, 203–06 (1969).
William Horwitz, "Problems of Sampling and Analytical Methods", *ibid.*, **59**, 1197–203 (1976).

# Lab-Crest® Low-Flow Rotameters

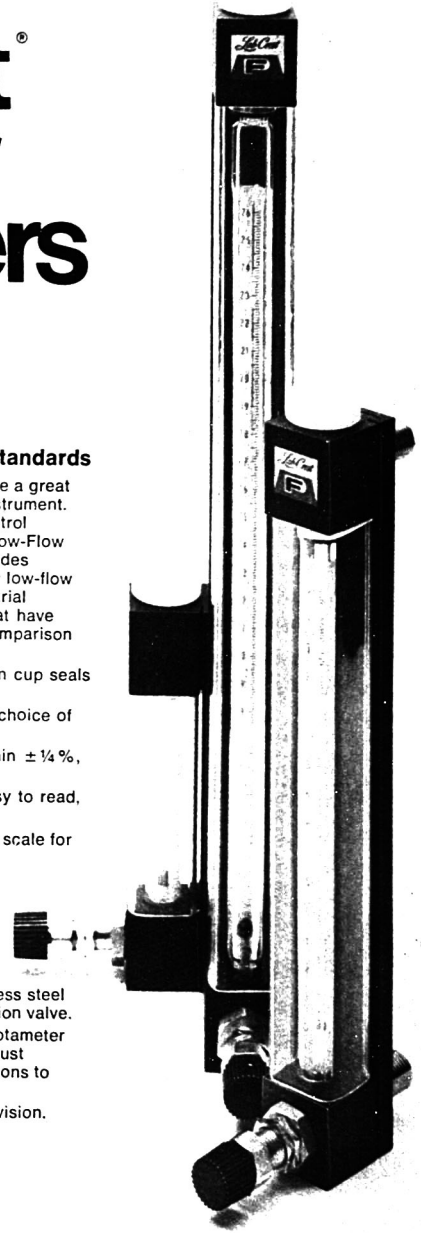

## The New Performance Leader . . . By All Standards

Now you can get all the features and options that make a great low-flow rotameter, combined in one and the same instrument. Built by the industry's most experienced team of control engineers and glass craftsmen, the new Lab-Crest Low-Flow Rotameter features a unique precision valve that provides linear control throughout the range of flows . . . a new low-flow tube with ⅛-inch float that operates reliably in industrial environments . . . plus all the time-tested features that have made Fischer & Porter rotameters the standard of comparison since the birth of the industry:

- **Convenience.** Quick-release metering tubes with Viton cup seals are easily interchanged without tools.
- **Rangeability.** Eight interchangeable tubes provide a choice of flow ranges from 50 cc/min to 148 SCFH (air).
- **Accuracy.** Instantaneous readings are repeatable within ± ¼%, a direct result of F&P's unsurpassed experience.
- **Visibility.** Ceramic scale with white background is easy to read, permanently fused into the borosilicate glass surface.
- **Versatility.** Choice of meter bodies with 3, 6 or 10-inch scale for in-line or panel-mounting . . . or with tripod mount.
- **Controllability.** Precision sixteen-turn valve with interchangeable stems and sleeves provides linear control at all flow rates, as well as positive shut-off; low-cost valve also available for less sensitive applications.
- **Corrosion Resistance.** Standard aluminum end fittings are also available with interchangeable brass or stainless steel inserts; stainless steel standard on models with precision valve.

More than ever, it makes sense to call us for all your rotameter needs, whether you are looking for OEM quantities or just one of a kind. We have the right type and the right options to meet your requirements exactly.

Call (215) 674-6000 and ask for Lab-Crest Scientific Division. Fischer & Porter Company, County Line Road, Warminster, Pa. 18974.

LAB-CREST SCIENTIFIC
A DIVISION OF FISCHER & PORTER

CIRCLE 78 ON READER SERVICE CARD

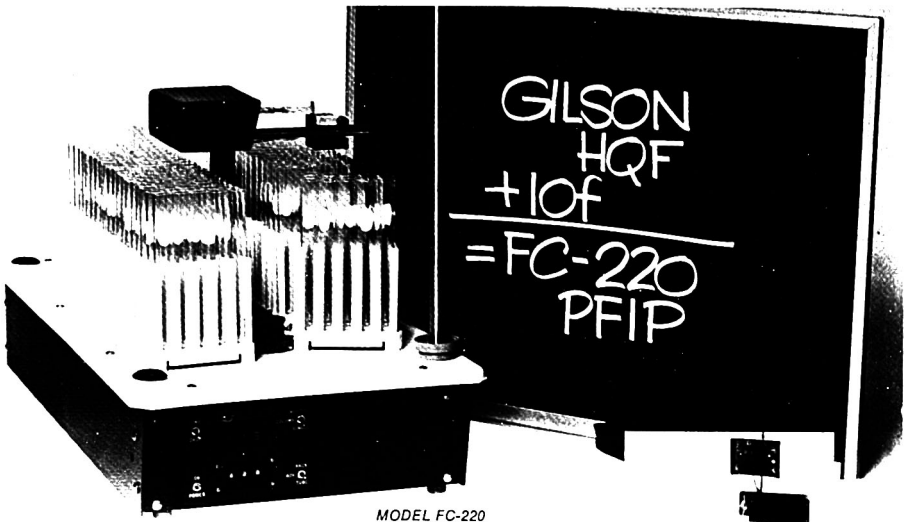


*MODEL FC-220*

**Translated, that means you can buy this High-Quality Fractionator (GILSON's FC-220) PREFERRED FOR ITS PERFORMANCE— with the 10 important features listed below. Why pay more when you can get the best for less?**

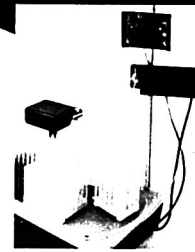

*MODEL FC-220 WITH CONTROL BOX AND SHUT-OFF VALVE MOUNTED ON MAST*

# THE GILSON RACE TRACK FRACTIONATOR FOR LIQUID CHROMATOGRAPHY

## Here are the COLD ROOM facts:

**1. Reliable cold-room operation down to 0 degree Celsius.** Includes self-contained heater, eliminating condensation problems. Components are selected to EXCEED requirements and will withstand hostile cold-room environment over extended use.

**2. 220 test tubes (18x150 mm or 13x100 mm).** Twenty-tube rack; block shape eliminates tipping of racks (separate rack carriers are not required).

**3. Drop counting or time method of collection** Can be set from 0.1 minute to 100 minutes per tube, in 0.1-minute increments; or from one drop per tube to the liquid capacity, in one-drop increments.

**4. Three-digit electronic display.**

**5. Optional flow-stop valve available.**

**6. Auxiliary power outlet** is included for turning off accessory equipment after the last tube is filled.

**7. Multiple-column collection** available for 2, 3, 4 or 5 columns (with separate adapter).

**8. Remote use of control unit is possible.**

**9. 220 tubes can be collected during unattended operation, or collection can be continued indefinitely** without interruption by periodically removing filled racks and adding empty racks.

**10. 21 U.S.A. Gilson sales and service locations** —one-year warranty.

**Size of the FC-220:** 36 cm wide and 69 cm deep (14"x27"). **Weight:** 13 kg (28 lbs.)

GILSON

Write or phone

**U.S.A. MANUFACTURING PLANT:**

**GILSON MEDICAL ELECTRONICS, INC.**

P.O. BOX 27, MIDDLETON, WIS. 53562
Telephone 608/836-1551 • TELEX 26-5478

**EUROPEAN MANUFACTURING PLANT:**

**GILSON MEDICAL ELECTRONICS (FRANCE) S.A.**

**69, 72 rue Gambetta • Boite Postale 5**
**VILLIERS-LE-BEL 95400 • ARNOUVILLE-LES-GONESSE, FRANCE**
**Telephone 990 54-41**

CIRCLE 85 ON READER SERVICE CARD


*The building in the background houses the Oak Ridge Isochronous Cyclotron Accelerator*

# Symposium on Advanced Analytical Concepts for the Clinical Laboratory

## Oak Ridge, Tenn. March 16–17, 1978

Oak Ridge National Laboratory (ORNL) will host the 10th Annual Symposium on Advanced Analytical Concepts for the Clinical Laboratory at Oak Ridge, Tenn., on March 16–17, 1978. The symposium is jointly sponsored by ORNL, the National Institute of General Medical Sciences, the Department of Energy, and the Academy of Clinical Laboratory Physicians and Scientists.

This symposium series, held annually at Oak Ridge National Laboratory, was established in 1969 to provide a forum for discussion of recent developments in the application of analytical concepts to clinical analysis. The technical program includes three sessions entitled Advanced Concepts, Analytical Systems, and Future Trends in Advanced Analytical Concepts. The nineteen papers scheduled at these sessions represent new ideas or new technology with a potential for application for the clinical laboratory. The highlight of the meeting will be the final session on Future Trends in Advanced Analytical Techniques. In this session a series of emerging analytical techniques will be analyzed and discussed, with predictions for future developments and ultimate utility in the clinical laboratory. All attendees are invited to a social hour and dinner on Thursday evening, March 16. The proceedings will be published as a single issue of *Clinical Chemistry*. The detailed program follows.

## PROGRAM

### Thursday Morning, Mar. 16

#### Session I: Advanced Concepts

*Chairman:* D. C. Cannon, U of Texas-Houston

**9:30 Introduction.** C. D. Scott, ORNL

**9:45 Cell Electrophoresis Applied to Immunologic Research.** P. Blume, A. Malley, R. J. Knox, G. V. F. Seaman, Good Samaritan Hospital

**10:10 Separation and Analysis of Arylsulfatase Isoenzymes in Body Fluids of Man.** W. D. Bostick, S. R. Dinsmore, J. E. Mrochek, ORNL

**10:35 Intermission**

**11:00 High-Performance Liquid Chromatographic Separation and Quantitation of Biogenic Amines in Plasma and Tissue.** T. P. Davis, C. W. Gehrke, T. D. Cunningham, K. O. Gerhardt, K. C. Kuo, C. W. Gehrke, Jr., U of Missouri-Columbia

**11:25 New Quantitative Ultramicro Immunoenzymatic Method: Measurement of Ig Antigenic Determinants at Single Cell Level.** P. Hösli, S. Avrameas, Institut Pasteur, France

**11:50 Melting Point of Gallium Apparatus for Thermometer Calibration.** P. Dudek, Yellow Springs Instruments Co.

### Thursday Afternoon, Mar. 16

**1:45 Multilayer Film Elements for Clinical Analysis: General Principles.** H. G. Curme, Eastman Kodak Co.

**2:10 Multilayer Film Elements for Clinical Analysis: Applications to Representative Chemistries.** R. W. Spayd, Eastman Kodak Co.

#### Session II: Analytical Systems

*Chairman:* J. C. Sternberg, Beckman Instruments

**2:40 Isoenzyme Analysis by HPLC.** T. D. Schlabach, A. Alpert, F. E. Regnier, Purdue U

**3:05 Automated System for Fractionation of Blood Samples.** N. E. Lee, R. K. Genung, J. E. Mrochek, C. D. Scott, ORNL

**3:30 Development and Evaluation of Glucose Analyzer for Glucose-Controlled Insulin Infusion System.** E. J. Fogt, L. M. Dodd, E. M. Jenning, A. H. Clemens, Miles Labs

### Friday Morning, Mar. 17

**9:00 Polychromatic Analysis: New Applications of an Old Technique.** B. Hahn, D. Vlastelica, L. Snyder, Technicon Instruments Corp.

**9:25 Rapid, Dual-Column Ion-Exchange Chromatography of β-AIBA and β-Ala in Physiological Fluids.** T. F. Cole, K. C. Kuo, C. W. Gehrke, U of Missouri-Columbia

**9:50 Improved Approach to Sequential Addition Immunoassay.** F. D. Lasky, A. Karmen, J. AlRazi, Albert Einstein College of Medicine

**10:15 Intermission**

**Session III: Future Trends in Advanced Analytical Concepts**

*Chairman:* W. H. C. Walker, McMaster U, Canada

**10:45 Determination of Psychoactive Drug Blood Levels by High-Performance Thin-Layer Chromatography.** D. C. Fenimore, C. J. Meyer, C. M. Davis, Texas Medical Center

**11:15 Coupled Reactions of Immobilized Enzymes and Immobilized Substrates: Clinical Applications.** M. H. Keyes, R. C. Barabino, D. N. Gray, Owens-Illinois

**11:45 Fluorescence and Enzyme Immunoassays for Enzyme and Bacterial Antigens in the Clinical Laboratory.** B. W. Papermaster, J. E. McEntire, P. D. Sandefur, U of Texas-Galveston

**Friday Afternoon, Mar. 17**

**1:45 Advances in Cytochemical Hormone Analysis.** L. Bitensky, Kennedy Institute of Rheumatology, UK

**2:15 New Liquid Chromatographic Techniques of Potential Interest to the Clinical Laboratory.** J. E. Mrochek, W. D. Bostick, S. R. Dinsmore, ORNL

**2:45 Applications of Calorimetry in the Clinical Laboratory.** N. N. Rehak, D. S. Young, NIH

**3:15 Closing Remarks.** R. S. Melville, National Institute of General Medical Sciences

## 1978 Benedetti-Pichler Award

For his outstanding contribution to microchemistry, Joseph Jordan of Pennsylvania State University has been named to receive the 1978 Benedetti-Pichler Award. The award will be presented at the 5th Annual Meeting of the Federation of Analytical Chemistry and Spectroscopy Societies, to be held in Boston, October 30–November 2, 1978. The award, sponsored by the American Microchemical Society, is given annually in recognition of services to microchemistry in its broadest meaning, which includes research, application, administration, teaching, or other means of promoting the advancement of microchemistry.

Professor Jordan was born in Rumania in 1919. He earned his doctorate degree in chemistry at the Hebrew University, Jerusalem, Israel, in 1945 and worked there until 1950. He came

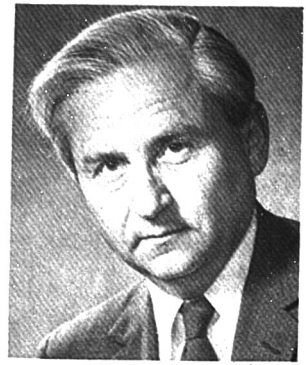

*Joseph Jordan*

to the U.S. in 1950 as a research fellow with J. J. Lingane at Harvard. From 1951 to 1954 he was associated with I. M. Kolthoff at the University of Minnesota. In the autumn of 1954, Professor Jordan joined the faculty of Pennsylvania State University as assistant professor. He was promoted to associate professor in 1957 and to full professor in 1960. He has over 100 publications including chapters and sections in treatises and reference books. His primary areas of interest are in electrochemistry and in thermochemistry. Dr. Jordan is a member of the Editorial Board of *Analytical Letters* and has also served on the Advisory Boards of ANALYTICAL CHEMISTRY and *Talanta*. He is a fellow of the American Association for the Advancement of Science and of the American Institute of Chemists, and a senior member of the Faraday Society.

## AOAC Invites Nominations for Harvey W. Wiley Award

The Association of Official Analytical Chemists (AOAC) invites nominations for the 22nd AOAC Harvey W. Wiley Award for outstanding contributions to analytical methodology important to government regulatory agencies.

AOAC established the $750 annual award in 1956 to honor Harvey W. Wiley, "Father of the Pure Food and Drug Act" and also a founder of the AOAC. The purpose of the award is to recognize an outstanding scientist or scientific team for contributions to analytical methodology in areas pertaining to agriculture and public health. Topics include foods, drugs, pesticides, cosmetics, feeds, fertilizers, beverages, colors, forensic science materials, hazardous substances, vita-

The fluorescent properties of many antitumor drugs make fluorescence spectrometric analysis particularly valuable in tracing the drugs from the distribution stage in the body, through the metabolic stage, to eventual elimination. As a part of the National Cancer Institute's $800-million-a-year cancer research program, the BioMolecular Sciences Section of Arthur D. Little Inc., is monitoring the metabolic distribution of anticancer drugs by fluorescence analyses. In the photo, a sample of antitumor drug metabolite is placed into the cell of a Perkin-Elmer fluorescence spectrophotometer by Marianne Callahann of Arthur D. Little Inc.

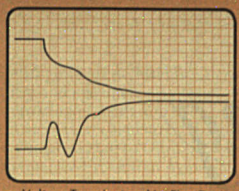

100 ms Voltage Transient and Its First Derivative

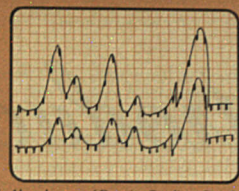

UV - Absorbance of Density Gradient Fractions

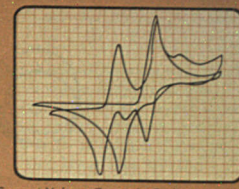

Current-Voltage Curves in Cyclic Voltammetry

# Introducing the Series 8000 Electronic Recorders with Data Processing and Storage

A major advance in recorders, the Bascom-Turner Series 8000 are new, electronic, multi-channel recorders with data processing and storage.

With the Series 8000 you can digitize, record, and process up to eight channels of analog data. Raw or processed data are graphed in real time on strip or X-Y chart paper and stored on flexible disk.

The Series 8000 lets you specify a wide variety of modes for data acquisition. You can record on preset triggering or on event triggering at speeds up to 10,000 points per second for a single channel. Alternatively, you can record at regular intervals as few as two points per day. In all cases, you have the advantages of superior accuracy offered by digital electronics and an input impedance of 100 megohms on all channels and all ranges.

A simple key sequence allows you to process data before plotting. For example, data from any channel can be integrated, differentiated, smoothed, normalized, converted to logarithms or reciprocals. Or, you can compare data from any two channels, or sequences of data from a single channel, and plot their difference, average, or quotient.

Storage is convenient, economical, and efficient. Each flexible disk is equivalent to 100 yards of chart paper. Yet, any sequence of data can be retrieved in graphical form in a few seconds.

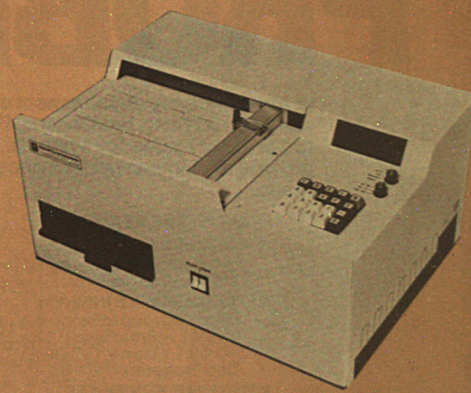

For all their versatility, Series 8000 recorders are priced from $3,700 to $4,900.

For more information, call Bob Sanford at (800) 225-3298

**Bascom-Turner Instruments**
A Division of EIC Corporation
111 Chapel Street Newton, Massachusetts 02158 U.S.A.

CIRCLE 25 ON READER SERVICE CARD

# *Introducing*

## the

# FX90Q

## featuring the

# OMNI PROBE

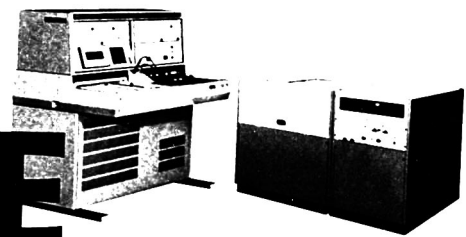

**In the continuing development of the FX series, JEOL now offers a compact, 90 MHz, broad-band, FT NMR System at a cost comparable to the lower frequency systems. The "OMNI PROBE" is designed to provide the highest performance throughout the entire observation range.**

**OMNI PROBE FEATURES:**

- **PERMA-BODY**
  Probe head is **fixed** in magnet for continuing optimum performance.
- **PLUG-IN SAMPLE INSERTS**
  10mm V.T. — BroadBand ($^{14}$N to $^{1}$H)
  5mm V.T. — BroadBand ($^{14}$N to $^{1}$H)
  Micro V.T. / 5mm V.T. / 10mm V.T.— Dual Frequency ($^{13}$C/$^{1}$H)
- **PLUG-IN R.F. MODULES**
  BroadBand ($^{14}$N to $^{1}$H)
  Dual Frequency ($^{13}$C/$^{1}$H)
- **IRRADIATION MODULES**
  Proton (standard)
- **LOCK**
  $^{2}$D/$^{7}$Li Dual Frequency internal/external system

**FX 90Q IS AVAILABLE WITH:**

- 90MHz Proton / 22.6 MHz Carbon observation
- Compact **Low Energy** magnet
- Digital Quadrature Detection
- Foreground/Background
- "SHIMPLEX" Auto Y/Curvature controller
- Computer based Multi-Pulse Generation
- $T_1$-rho/Spin Locking
- Digital Cassette/floppy disk/ moving head disk systems
- Light Pen Control System (LPCS)

JEOL

235 Birchwood Ave., Cranford, NJ 07016
201—272-8820

CIRCLE 108 ON READER SERVICE CARD

mins, water and air pollutants, microbiological and extraneous material contamination of foods and drugs, and general analytical chemistry. The 1977 award was presented to Gunter Zweig, Environmental Protection Agency, Washington, D.C., for his outstanding contributions to the analysis of pesticide residues.

For nomination forms and further information, contact Luther G. Ensminger, AOAC, Box 540, Benjamin Franklin Station, Washington, D.C. 20044. Nominations must be received by April 1, 1978.

## AOAC Membership Drive

"Are you a member of the AOAC? Can you prove it?" With this banner, the Association of Official Analytical Chemists (AOAC) has launched an unprecedented membership promotion campaign. Starting in 1978, membership in AOAC is no longer amorphous. Members were so informed by the president of the association, William W. Wright, at the general session of AOAC's 91st Annual Meeting held in Washington, D.C., October 17–20, 1977. In his President's Address, Mr. Wright outlined the new card-carrying membership plan in which all members are entitled to a subscription to the bimonthly AOAC newsletter, *The Referee*. Through the newsletter, members will have contact with the hundreds of other regulatory scientists working on methods validated through the AOAC process.

Exceptions to the mandatory dues ($10) are to be made, however, for General and Associate Referees, committee members, and other appointed officials. All potential members are asked to fill out a membership application, which is intended to supply contact information as well as to pinpoint areas of scientific interest.

## Oceanographers Study Oceanic Processes by On-Line Analyses

Oceanographers have unique problems in analytical areas. Sampling is a difficult problem both because of small sample size in relation to the ocean volume and because of possible contamination of samples—even changes in samples from possible adsorption of constituents on container walls. Not the least of the oceanographers' difficulties is connected with doing analyses at sea while moving, according to Alberto Zirino, Cesar Clavell, Jr., and Peter F. Seligman of the Naval Ocean Systems Center (NOSC) in San Diego, Calif.

Nevertheless, today's marine chemists are able to take advantage of some of the newer analytical methods to study oceanic processes. Researchers envision ocean-going vessels equipped with microprocessor-controlled and minicomputer-automated atomic absorption units and chromatographs, for instance.

A new level of sophistication in instrumentation permits real-time analyses. In sampling, tubular designed samplers can be placed "on-line" and tap into a continuous source of seawater. An example of underway sampling and automated instrumentation is afforded by an automated trace metal analyzer developed at NOSC. The unit measures Zn, Cu, Pb, and Cd in seawater by anodic stripping voltammetry.

This system has been used to measure trace metals from a small vessel in several locations including San Diego Bay. It was observed that Zn concentration fluctuated regularly with the tidal period. This was attributed to the fact that relatively metal-free open ocean water moved into the bay at flood tide, while relatively polluted bay water was sampled during low tide. Conventional single measurements might not have given this result.

Similarly, measurements while underway of surface pH, temperature, and chlorophyll-a fluorescence (an indicator of plants) near a discharge of a thermoelectric plant in the east loch of Pearl Harbor provided information that might have been missed with conventional sampling.

The higher acidity of discharged water is detectable in the pH, which decreases rapidly from an ambient 8.4 to 8.3. West of the discharge the fine structure in the pH profile clearly matches the detail in the chlorophyll-a profile. This occurs because plankton removes $CO_2$ from the water during photosynthesis and raises the ambient pH. Similarly, the absence of an increase in pH corresponding to the large phytoplankton patch east of the power plant suggests that photosynthesis may have been depressed by the extraneous warm water. With these systems and others, much can be learned about biologically active areas.

## Fluorocarbon-11 in Seawater

A team of researchers at the Naval Research Laboratory has been at work developing an analytical method for the determination of fluorocarbon-11 (trichlorofluoromethane, $CCl_3F$), a compound familiar to everyone. Their concern, however, was not with the depletion of the ozone layer, as one might expect. Their aim was to monitor the movement of water-mass by measuring the amount of fluorocarbon-11 that has settled into the world's oceans.

According to William Smith, the team's principal investigator, fluorocarbon-11 is an excellent tracer for the study of water-mass movements because the compound is essentially inert at the surface of the earth, has known sources, and can be measured at extremely low concentrations. And since the compound enters the ocean from the atmosphere, it is equally useful as a tracer of atmospheric mixing.

In the shipboard analytical method developed by the team, the fluorocarbon-11 gas dissolved in a 25-mL sample is stripped from the ocean water sample by a carrier gas and transported directly into a gas chromatograph. There, the $CCl_3F$ is separated from other gases and measured by an electron-capture detector. The small sample size and shipboard analysis of the $CCl_3F$ measurements permit multiple replication. The accuracy of these analyses depends on adequate calibration at extremely low concentrations of $CCl_3F$. Smith has developed a novel, two-stage gas-permeation technique for providing accurately known calibration mixtures in the concentration range of 2–200 parts per trillion by volume. They used the $CCl_3F$ method to trace the sinking and southward migration of cold water from arctic areas of the North Atlantic Ocean. Results were in agreement with those obtained by a much more elaborate radiochemical tracer method, used at other laboratories, which requires careful chemical purification and preconcentration for a period of three weeks prior to measurement of the tritium radioactivity.

## Meetings

- **ASTM Symposium on Computer Information Handling in Clinical Laboratories.** Mar. 8. Cleveland Convention Center, Cleveland, Ohio. *Contact: Robert Megargle, Dept. of Chemistry, Cleveland State University, Cleveland, Ohio 44115*
- **175th ACS National Meeting.** Mar. 12–17. Anaheim, Calif. *Contact: A. T. Winstead, ACS, 1155 16th St., N.W., Washington, D.C. 20036*
- **10th Annual Symposium on Advanced Analytical Concepts for**

**the Clinical Laboratory.** Mar. 16–17. Oak Ridge National Laboratory. *Contact: Charles D. Scott, Associate Director, Chemical Technology Div., Oak Ridge National Laboratory, P.O. Box X, Oak Ridge, Tenn. 37830. Page 1136 A, Nov.*

- **2nd Annual Workshop on Industrial Toxicology.** Mar. 28–31. Thomas Jefferson U., Philadelphia. *Contact: Dean R. C. Baldridge, College of Graduate Studies, Thomas Jefferson U., Philadelphia, Pa. 19107*
- **Technicon Symposia.** Mar. 29–31, Houston, Tex.; May 1–2, Montreal, Canada; May 4–5, Toronto, Canada; May 15–16, Vancouver, Canada. The symposia include presentations of papers discussing the latest techniques in automated laboratory procedures and an exhibit of Technicon's new instruments. *Contact: Technicon Corp., Tarrytown, N.Y. 10591*
- **1st European Conference on Optical Systems & Applications.** Apr. 4–6. Brighton, UK. *Contact: Institute of Physics, 47 Belgrave Sq., London SW1X 8QX, UK*
- **ACS 12th Middle Atlantic Regional Meeting.** Apr. 5–7. Hunt Valley Inn, Hunt Valley, Md. *Contact: F. Gornick, Dept. of Chemistry, U. of Maryland, Baltimore, Md. 21228*
- **8th Annual Symposium on the Analytical Chemistry of Pollutants.** Apr. 5–7. Geneva, Switzerland. *Contact: Congress Secretariat, P.O. Box 182, CH-4013, Basle, Switzerland. Page 708 A, July*
- **International Conference on Computers and Optimization in Analytical Chemistry.** Apr. 5–7. Amsterdam, The Netherlands. *Contact: Secretary, Computers and Optimization in Analytical Chemistry, Laboratory for Analytical Chemistry, Nieuwe Achtergracht 166, Amsterdam, The Netherlands*
- **9th Materials Research Symposium on Trace Organic Analysis: A New Frontier in Analytical Chemistry.** Apr. 10–13. Gaithersburg, Md. Sponsored by the National Bureau of Standards. *Contact: Stephen Chesler or Harry Hertz, Chemistry Bldg., Room A105, National Bureau of Standards, Washington, D.C. 20234. 301-921-2153. Page 708 A, July*
- **Symposium on HPLC with Application to the Pharmaceutical and Food Industries.** Apr. 10–14. Sunderland, England. *Contact: R. Dennis, School of Pharmacy, Sunderland Polytechnic, Chester Rd., Sunderland, Tyne & Wear, SR1 3SD, England*
- **7th International Geochemical Exploration Symposium.** Apr. 16–20. Golden, Colo. Sponsored by the Association of Exploration Geochemists. *Contact: M. A. Chaffee, Secretary, 7th IGES, U.S. Geological Survey, 5946 McIntyre St., Golden, Colo. 80401*
- **12th International Symposium on Remote Sensing of Environment.** Apr. 17–19. Philippines. *Contact: Environmental Research Institute of Michigan, P.O. Box 8616, Ann Arbor, Mich. 48107*
- **Scanning Electron Microscopy Symposium.** Apr. 17–21. Bonaventure Hotel, Los Angeles. *Contact: Om Johari, Director, SEM Symposia, 1420 B Volid Dr., Hoffman Estates, Ill. 60194*
- **Biennial Analytica 78 Exhibition.** Apr. 18–22. Munich. *Contact: Kallman Associates, Munich Fair Authority, 30 Journal Sq., Jersey City, N.J. 07306*
- **Electrophoresis '78.** Apr. 20–21. Cambridge, Mass. Sponsored by Massachusetts Institute of Technology. *Contact: N. Catsimpoolas, MIT, Room 56–307, Cambridge, Mass. 02139*
- **Canadian Chromatography Conference.** Apr. 27–28. Hotel Bonaventure, Montreal, Ontario. *Contact: V. M. Bhatnagar, P.O. Box 1779, Cornwall, Ont. K6H 5V7, Canada*
- **Computers in Activation Analysis and Gamma-Ray Spectroscopy.** Apr. 30–May 3. Mayaguez, Puerto Rico. Sponsored by Divisions of American Nuclear Society, American Chemical Society, and NBS; ERDA; and U. of Puerto Rico. *Contact: B. S. Carpenter, Reactor Bldg. 235, National Bureau of Standards, Washington, D.C. 20234*
- **3rd Annual Regional Spring Training Conference and Exhibition of AOAC.** May 1–3. Marriott Hotel, Atlanta. *Contact: Sol Cohen, Assistant Director for Research and Instrumentation, FDA, 60 Eighth St., N.E., Atlanta, Ga. 30309. 404-881-2131*
- **Seminar on Ionizing Radiation Measurement.** May 9–12. National Bureau of Standards, Washington, D.C. *Contact: E. H. Eisenhower, Center for Radiation Research, NBS, Washington, D.C. 20234*
- **69th Annual Meeting of American Oil Chemists' Society.** May 14–18. Chase Park Plaza Hotel, St. Louis. *Contact: George Willhite, JAOCS News, 508 S. Sixth St., Champaign, Ill. 61820*
- **9th International Symposium on Chromatography and Electrophoresis.** May 15–16. Riva Del Garda, Lake of Garda, Italy. *Contact: Alberto Frigerio, Istituto de Ricerche Farmacologiche, Mario Negri, Via Eritrea 62, 20157 Milan, Italy. Page 44 A, Jan.*
- **Analytical Methods for Safeguard and Accountability Measurements of Special Nuclear Materials.** May 15–17. Williamsburg, Va. Sponsored by Fuel Cycle Division and Virginia Section of American Nuclear Society, National Bureau of Standards, and Institute of Basic Standards. *Contact: Ron L. Hoffmann, Babcock & Wilcox, LRC, P.O. Box 1260, Lynchburg, Va. 24505. Page 1020 A, Oct.*
- **IMEKO Meeting on Application of Statistical Methods in Measurement.** May 17–19. Leningrad. *Contact: IMEKO Secretariat, H-1371 Budapest, POB 457, Hungary*
- **9th Annual Symposium and Short Courses on Applied Chromatography.** May 18–19. Hilton Inn, Kenner, La. Sponsored by the Louisiana Section of ACS. *Contact: Tom Pewitt, Shell Oil Co., P.O. Box 10, Norco, La. 70079*
- **6th International CODATA Conference.** May 22–25. Taormina, Italy. *Contact: CODATA Secretariat, 51 Blvd. de Montmorency, 75016 Paris, France*
- **International Symposium on Nuclear Activation Techniques in the Life Sciences.** May 22–26. Vienna, Austria. *Contact: John H. Kane, Energy Research & Development Administration, Washington, D.C. 20545*
- **ISA's Analysis Instrumentation Division Meeting.** May 23–25. Stouffer's Greenway Plaza Motel, Houston, Tex. *Contact: Thomas Puzniak, Gulf Science & Technology Co., P.O. Box 2038, Pittsburgh, Pa. 15230. 412-362-1600. Page 1136 A, Nov.*
- **International Symposium on the Analysis of Hydrocarbons and Halogenated Hydrocarbons in the Aquatic Environment.** May 23–25. McMaster U., Hamilton, Ont., Canada. Organized by the Canada Centre for Inland Waters, Burlington, Ontario, and the Institute for Environmental Studies, U. of Toronto. *Contact: Canada Centre for Inland Waters, P.O. Box 5050, Burlington, Ont., Canada L7R 4A6*
- **3rd International Conference on Stable Isotopes.** May 23–26. Oak Brook Hyatt House, Oak Brook, Ill Sponsored by Argonne National

# Gilford's Automatic Cuvette Programmer makes repositioning of microcuvettes a pushbutton routine.

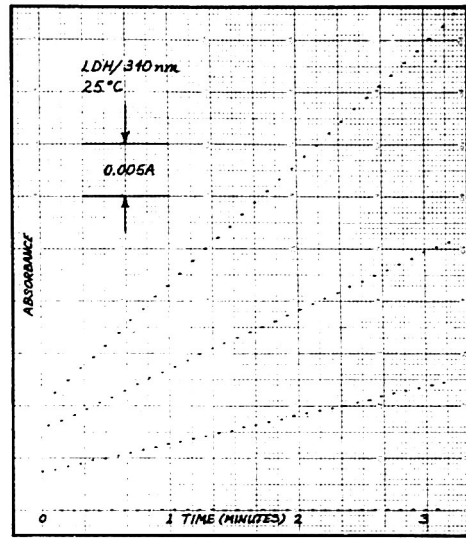


### Positioning Accuracy Helps Ensure Measurement Accuracy

For accurate, repeatable results, precise sample positioning is critical. Particularly if you want to use flow-through or microcuvettes. With such cuvettes and the associated microapertures, positioning inconsistencies would be translated into apparent absorbance errors on the recorder chart.

The four-cuvette Gilford system makes the necessary precision automatic, positioning cuvettes within 0.025mm time after time. No bother, no special (and expensive) optics required.

### Manual or Automatic, Positioning is Convenient and Fast

You can select a single cuvette position just by pushing a button, or choose a combination of positions for automatic operation. You can monitor any or all four cuvettes for precise dwell times of 2 to 99 seconds. And positioning itself is quick, just 1½ seconds between adjacent positions. Thus if you have all four cuvette positions selected, and have chosen a dwell time per cuvette of two seconds, you'll get a second reading on any given sample within 14 seconds. More readings per sample per unit time means that you can more accurately follow the progress of a reaction.

### Design of the Programmer Makes Recordings More Meaningful

Individual recorder offset controls for cuvette positions 2, 3, and 4 serve two functions: they let you separate overlapping traces for clarity in presentation; and they let you use the most sensitive recorder scale for the sample with the least activity. There's no need to adjust sample concentration so that all the samples you're measuring have similar absorbance characteristics.

Accessories to the Gilford Automatic Cuvette Programmer include an auxiliary timer for long-term assays and an analog multiplexer that allows you to monitor parameters like sample temperature in sequence with absorbance.

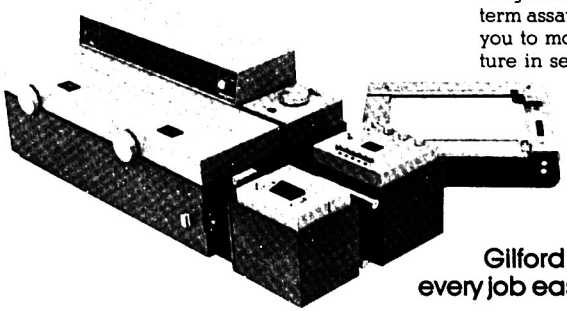

gilford INSTRUMENT

Oberlin, Ohio 44074
(216) 774-1041 Telex: 98-0456
Paris (Malakoff), France
Düsseldorf, W. Germany
Teddington, Middx., England
Toronto (Mississauga), Canada

**Gilford Research Spectrophotometers: every job easier, every result more accurate.**

CIRCLE 87 ON READER SERVICE CARD

Laboratory. *Contact: P. D. Klein, Div. of Biological and Medical Research, Argonne National Laboratory, Argonne, Ill. 60439*

- **ACS Joint 10th Central–12th Great Lakes Regional Meeting.** May 24–26. Butler U., Indianapolis. *Contact: R. T. Blickenstaff, Veterans Administration Hospital, 1481 W. 10th St., Indianapolis, Ind.*
- **26th Annual Conference on Mass Spectrometry and Allied Topics.** May 28–June 2. Stouffer's Riverfront Towers, St. Louis, Mo. Sponsored by American Society for Mass Spectrometry. *Contact: K. E. McCulloh, A145, Chemistry Bldg., National Bureau of Standards, Washington, D.C. 20234*
- **International Symposium on Instrumental Applications in Forensic Drug Chemistry.** May 29–30. Ramada Inn, Rosslyn, Va. Sponsored by the Drug Enforcement Administration, U.S. Department of Justice. Topics will include: application of advanced techniques in instrumentation, computer applications, chromatographic advances, special topics on forensic drug analysis. *Contact: Michael Klein, Special Testing & Research Laboratory, 7704 Old Springhouse Rd., McLean, Va. 22101*
- **61st Canadian Chemical Conference and Exhibition.** June 4–7. Convention Centre, Winnipeg, Man., Canada. *Contact: The Chemical Institute of Canada, 151 Slater St., Suite 906, Ottawa, Ont., Canada K1P 5H3*
- **4th ACS Rocky Mountain Regional Meeting.** June 6–8. U. of Colorado, Boulder. *Contact: C. Pierpont, Dept. of Chemistry, U. of Colorado, Boulder, Colo. 80309*
- **Microcomputer-Based Instrumentation Conference.** June 12–13. NBS, Gaithersburg, Md. Sponsored by NBS, IEEE Computer Society, IEE Group on Instrumentation and Measurement. *Contact: Bradford Smith, A130 Technology Bldg., National Bureau of Standards, Washington, D.C. 20234. 301-921-2381*
- **33rd Annual Symposium on Molecular Spectroscopy.** June 12–16. Ohio State U., Columbus, Ohio. *Contact: K. Narahari Rao, Dept. of Physics, Molecular Spectroscopy Symposium, Ohio State U., 174 West 18th Ave., Columbus, Ohio 43210*
- **2nd International Symposium on Quantitative Mass Spectrometry in Life Sciences.** June 13–16. Rijksuniversiteit Gent, Belgium. *Contact: A. De Leenheer, Symposium Chairman, Laboratoria voor Medische Biochemie en Klinische Analyse, de Pintelaan 135, B-9000 Gent, Belgium*
- **ACS 33rd Northwest Regional Meeting.** June 14–16. U. of Seattle. *Contact: D. Thorsell, Chemistry Dept., Seattle U., Seattle, Wash. 98122*
- **5th International Symposium on Mass Spectrometry in Biochemistry and Medicine.** June 19–21. Rimini, Italy. *Contact: Alberto Frigerio, Istituto de Ricerche Farmacologiche, Mario Negri, Via Eritrea 62, 20157 Milan, Italy. Page 44 A, Jan.*
- **13th Annual Microbeam Analysis Society Conference.** June 19–23. Ann Arbor Inn, Ann Arbor, Mich. *Contact: W. C. Bigelow, Dept. of Materials and Metallurgical Engr., U. of Michigan, Ann Arbor, Mich. 48104*
- **Symposium on Environmental Analytical Chemistry.** June 21–23. Brigham Young U., Provo, Utah. *Contact: Delbert J. Eatough, 271 FB, Thermochemical Institute, Brigham Young U., Provo, Utah 84602*
- **ACS 9th Northeast Regional Meeting.** June 25–28. Simmons College, Boston. *Contact: E. I. Becker, U. of Massachusetts, Harbor Campus, Boston, Mass. 02125*
- **ACS 31st Annual Summer Symposium.** June 26–28. Boulder, Colo. Sponsored by Analytical Chemistry Division. *Contact: R. E. Siever, Dept. of Chemistry, U. of Colorado, Boulder, Colo. 80302*
- **71st Annual Meeting of Air Pollution Control Association.** June 26–30. Houston, Tex. *Contact: Public Relations Dept., Air Pollution Control Assn., P.O. Box 2861, Pittsburgh, Pa. 15230. 412-621-1090*
- **ASTM Symposium on Some Impediments to Analysis.** June 27–28. Boston. *Contact: John E. Foster, Kawecki Berylco Industries, Inc., P.O. Box 567, Boyertown, Pa. 19512. Page 1022 A, Oct.*
- **World Chromatography Conference.** June 29–30. Sheraton Hotel, Stockholm, Sweden. *Contact: F. M. Bhatnagar, P.O. Box 1779, Cornwall, Ont. K6H 5V7, Canada*
- **Micro-78.** July 10–14. Bloomsbury Centre Hotel, London. *Contact: The Royal Microscopical Society, 37/38 St. Clements, Oxford, OX4 1AJ, England*
- **Gordon Research Conference on Electron Spectroscopy.** July 17–21. Wolfeboro, N.H. *Contact: Charles S. Fadley, Dept. of Chemistry, 2545 The Mall, U. of Hawaii, Honolulu, Hawaii 96822*
- **6th Discussion Conference on Macromolecules: Chromatography of Polymers and Polymers in Chromatography.** July 17–21. Prague. *Contact: P. M. M. Secretariat, c/o Institute of Macromolecular Chemistry, 162 06 Prague 616, Czechoslovakia*
- **30th National Meeting of American Association for Clinical Chemistry.** July 23–28. San Francisco. *Contact: William J. Campbell, AACC, 1725 K St., N.W., Washington, D.C. 20006*
- **Inter/Micro-78.** July 24–27. McCormick Inn, Chicago. Sponsored by McCrone Research Institute. Emphasis on new techniques in acoustic, infrared, interference microscopy; uses of laser Raman microprobe; techniques of modulation contrast, and combinations of microscopes and computers. *Contact: McCrone Research Institute, 2508 S. Michigan Ave., Chicago, Ill. 60616. 312-842-7105*
- **4th International Congress of Pesticide Chemistry.** July 24–28. Zürich, Switzerland. Sponsored by the International Union of Pure and Applied Chemistry. Includes sessions on pesticide residues. *Contact: M. Spindler, Congress Secretariat, 4th International Congress of Pesticide Chemistry, P.O. Box 182, CH-4013 Basle, Switzerland*
- **27th Denver Conference on Applications of X-ray Analysis.** Aug. 1–4. U. of Denver. Emphasis on x-ray powder diffraction. *Contact: Mildred Cain, Metallurgy and Materials Science Div., Denver Research Institute, U. of Denver, Denver, Colo. 80208. 303-753-2141*
- **20th Annual Rocky Mountain Conference on Analytical Chemistry.** Aug. 7–9. Denver, Colo. *Contact: Daniel A. Netzel, Conference Chairman, Laramie Energy Research Center, Box 3395, University Station, Laramie, Wyo. 82071. 307-721-2370. Page 1225 A, Dec.*
- **1978 Annual Symposium for Innovation in Measurement Science.** Aug. 20–25. Hobart and William Smith Colleges, Geneva, N.Y. Will include sessions on medical instrumentation, high precision measurement, petroleum industry, electronic innovations, chemical analysis, physical analysis, and environmental monitoring. *Contact: Peter Vestal, Instrument Society of America, 400 Stanwix St., Pittsburgh, Pa. 15222*
- **8th IMEKO Symposium on Photon Detectors.** Aug. 22–25. Prague.

# Plasma AtomComp III

## The instrument you asked Jarrell-Ash to make.

The newest Plasma AtomComp — **Mark III** — is the instrument hundreds of laboratories we surveyed asked us to produce.

It is a fully digital, easy-to-use system with an integral computer. A **PDP-11** computer.

This direct-reading plasma spectrometer actually matches AA in sensitivity. But to this sensitivity it adds a remarkable **capacity.** It can determine up to 48 elements simultaneously, in any combination, in any concentration, in a little over a minute.

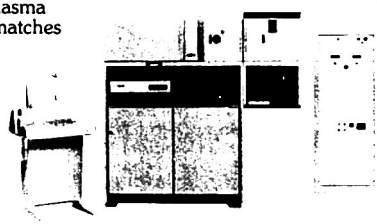

Just what the doctor ordered, when the problem is trace metals in solution, no matter what the field. Water, wastewater, air, soils, food, alloys, wear metals in petroleum, metabolites in biologicals — the Mark III will **expedite** your workloads.

### Not an add-on.

Unlike other systems on the market, the new third-generation Plasma AtomComp from Jarrell-Ash was designed **from the start** as a computer-controlled, computer data-managing instrument. This gives the Mark III a number of advantages over analog systems with a computer add-on.

**For example,** it has a significantly smaller number of parts — hence there's less possibility of downtime. It has self-diagnostic capability — hence there's no tedious check-out of electronics. It achieves a new level of speed — its 48 detectors can be read computer-fast, not one-at-a-time over a period of time. And it brings a new level of precision to the field — because its detectors are read with a sensitivity that is ultimately a **digital number,** not an analog approximation.

### Easy does it.

The system is as easy to operate as a typewriter. No computerese spoken here. You can tell your Mark III to erase all previous analytical results . . . run new samples in replicate . . . average the data . . . print out in % concentration, ppm, ppb, or any other units you need. You can even have different elements in the **same** sample print out in different units. You're boss.

You get automatic analysis over a dynamic concentration range of **100,000** — in a single sample — without changing a single parameter. And sequential analysis of widely differing concentrations from one calibration.

Mark III's integral PDP-11 gives it greater capabilities than ever — faster. Printout and subsequent runs can overlap, if you wish. You get outstanding storage **flexibility.** And you can expand into higher-level languages for data-handling when your needs change.

**Plasma AtomComp III** from Jarrell-Ash. In this age of crucial trace-metal and effluent analyses, can you settle for less?

To talk plasma spectrometry with an expert, call Dr. Arthur Ward at Jarrell-Ash headquarters. He knows the Mark III. The phone is **617-890-4300.** For product literature, use the reader-service number below.

**Jarrell-Ash**
A Division of Fisher Scientific Company
590 Lincoln Street Waltham MA 02154

CIRCLE 74 ON READER SERVICE CARD

*Contact: Dipl.-Ing. Jiri Král, House of Technics, Gorkého nám., 23, 11282 Praha 1, Czechoslovakia*

- **5th Biennial Conference of Australian and New Zealand Society for Mass Spectrometry.** Aug. 28–Sept. 1. U. of Queensland, Australia. *Contact: D. C. Green, Dept. of Geology & Mineralogy, U. of Queensland, St. Lucia, Queensland 4067, Australia*
- **6th International Conference on Raman Spectroscopy.** Sept. 4–9. Bangalore, India. *Contact: J. R. Durig, College of Science & Mathematics, U. of South Carolina, Columbia, S.C. 29208. 803-777-2505*
- **176th ACS National Meeting.** Sept. 10–15. Miami Beach, Fla. *Contact: A. T. Winstead, American Chemical Society, 1155 16th St., N.W., Washington, D.C. 20036*
- **8th International Conference on Magnetic Resonance in Biological Systems.** Sept. 11–14. Takayama, Japan. *Contact: S. Fujiwara, Dept. of Chemistry, U. of Tokyo, Hongo, Tokyo 113, Japan*
- **IMEKO Conference on Flow Measurement.** Sept. 12–15. Groningen. *Contact: FLOMEKO 1978, Groningen, POB 19, The Netherlands*
- **14th International Congress of the International Society for Fat Research.** Sept. 17–22. Brighton, England. Includes sessions on analysis and characterization of lipids. *Contact: ISF-78, Society of Chemical Industry, 14, Belgrave Square, London SW1X 8PS, England*
- **12th International Symposium on Chromatography.** Sept. 25–29. Baden-Baden, Federal Republic of Germany. Jointly organized by the Chromatography Discussion Group, the Groupment pour l'Avancement des Methodes Spectroscopique et Physicochimique d'Analyse, and the Arbeitskreis Chromatographie der Fachgruppe "Analytische Chemie" der Gesellschaft Deutscher Chemiker. *Contact: Geschäftsstelle der Gesellschaft Deutscher Chemiker, Abteilung Fachgruppen, Postfach 900440, 6000 Frankfurt/Main 90, Germany*
- **Biological/Biomedical Applications of Liquid Chromatography.** Oct. 5–6. Boston Park Plaza Hotel, Boston. 30 Papers and 40 poster presentations on use of liquid chromatography in peptides, amino acids, lipids, carbohydrates, drugs and drug metabolism, routine clinical applications and clinical research. *Contact: Gerald L. Hawk, Symposium Chairman, International Div., Waters Associates, Inc., Milford, Mass. 01757. 617-478-2000*
- **22nd Conference on Analytical Chemistry in Energy Technology.** Oct. 10–12. Gatlinburg, Tenn. *Contact: W. S. Lyon, Oak Ridge National Laboratory, P.O. Box X, Oak Ridge, Tenn. 37830*
- **8th Annual Conference of North American Thermal Analysis Society.** Oct. 15–18. Atlanta. *Contact: W. E. Clark, Delco Products Div., GMC, P.O. Box 230, Rochester, N.Y. 14601*
- **ISA/78.** Oct. 15–19. Philadelphia. *Contact: Instrument Society of America, 400 Stanwix St., Pittsburgh, Pa. 15222. Page 44 A, Jan.*
- **154th Meeting of the Electrochemical Society.** Oct. 15–20. Pittsburgh. *Contact: The Electrochemical Society, Inc., P.O. Box 2071, Princeton, N.J. 08540*
- **92nd Annual Meeting of Association of Official Analytical Chemists.** Oct. 16–19. Marriott Hotel, Twin Bridges, Washington, D.C. *Contact: Luther G. Ensminger, AOAC, Box 540, Benjamin Franklin Station, Washington, D.C. 20044*
- **13th International Symposium on Advances in Chromatography.** Oct. 16–19. Sheraton-St. Louis Hotel, St. Louis. *Contact: A. Zlatkis, Chemistry Dept., U. of Houston, Houston, Tex. 77004*
- **17th Annual Meeting of ASTM Committee E-19 on Practice of Chromatography.** Oct. 22–25. Atlanta, Ga. *Contact: Gerald Dupre, Bio/Dynamics, Inc., Box 43, Mettlers Rd., East Millstone, N.J. 08873*
- **3rd International Symposium on Polynuclear Aromatic Hydrocarbons.** Oct. 25–28. Battelle Columbus Labs, Ohio. *Contact: Peter W. Jones, Battelle Columbus Labs, 505 King Ave., Columbus, Ohio 43201*
- **ACS 14th Midwest Regional Meeting.** Oct. 26–27. U. of Arkansas, Fayetteville. *Contact T. D. Roberts, Dept. of Chemistry, U. of Arkansas, Fayetteville, Ark. 72701*
- **5th Annual Meeting of the Federation of Analytical Chemistry and Spectroscopy Societies.** Oct. 30–Nov. 3. Boston. *Contact: Paul Lublin, GTE Laboratories, 40 Sylvan Rd., Waltham, Mass. 02154. 617-890-8460. Page 44 A, Jan.*
- **ACS 30th Southeastern Regional Meeting.** Nov. 8–10. Savannah, Ga. *Contact: J. G. Brewer, Dept. of Chemistry & Physics, Armstrong State College, Savannah, Ga. 31406*
- **Symposium on Pulsed Nuclear Magnetic Resonance in Solids.** Dec. 18–19. Queen Elizabeth College, U. of London. *Contact: J.A.S. Smith, Dept. of Chemistry, Queen Elizabeth College, Campden Hill Rd., London, W8, UK*

## Short Courses

*ACS Courses. For more information, contact: Department of Educational Activities, American Chemical Society, 1155 Sixteenth St., N.W., Washington, D.C. 20036. 202-872-4508*

**Thin-Layer Chromatography**
Cleveland. Mar. 3–4. Victor W. Rodwell and Donald J. McNamara. $195, ACS members; $235, nonmembers

**Solving Problems with Modern Liquid Chromatography**
Cleveland. Mar. 3–5. J. J. Kirkland and Lloyd R. Snyder. $225, ACS members; $265, nonmembers

**Electroanalytical Chemistry**
Anaheim, Calif. Mar. 10–12. Dennis Evans and Paul Whitson. $225, ACS members; $305, nonmembers

**Carbon-13 NMR Spectroscopy**
Anaheim, Calif. Mar. 10–12. George Levy and Paul Ellis. $255, ACS members; $305, nonmembers

**Modern Techniques in Gas Chromatography**
Anaheim, Calif. Mar. 11–12. Harold McNair and Stuart Cram. $195, ACS members; $235, nonmembers

**Statistics for Experimental Design**
Anaheim, Calif. Mar. 11–12. John Hromi. $195, ACS members; $235, nonmembers

**Solving Problems with Modern Liquid Chromatography**
Anaheim, Calif. Mar. 11–12. J. Kirkland and Lloyd Snyder. $225, ACS members; $265, nonmembers

**Effective Writing for Scientists and Engineers**
Anaheim, Calif. Mar. 15–17. Henrietta Tichy and Sylvia Fourdrinier. $225, ACS members; $275, nonmembers

**Thin-Layer Chromatography**
Anaheim, Calif. Mar. 16–17. Victor Rodwell and Donald McNamara. $195, ACS members; $235, nonmembers

**Maintenance & Troubleshooting Chromatographic Systems Workshop**
Houston, Tex. Mar. 18–19, Apr. 21–22.

# New HP 1084B

The original Hewlett-Packard 1084A processor-controlled liquid chromotograph introduced new standards of precision, automation and reliability, and freed the chromatographer from a lot of tedious manual intervention.

The new 1084B liquid chromatograph combines all the original innovations with a new automatically controlled variable wavelength UV/visible detector and a new expanded software package.

These advances, together with the recently introduced automatic sampling system, provide new modes of operation which enable HPLC method development, routine analysis and trace analysis to be performed with far greater precision and efficiency.

**Pre-programmed variable wavelength detection.** Now you can have fast, pre-programmed wavelength changes during an analysis, allowing individual sample components to be detected at their optimum wavelength. A scanning capability aids your method development and helps to confirm qualitative identification.

**Pre-programmed parameter changes.** The new software package allows you to change separation parameters, wavelength sequences, calibration factors and calculation procedures between runs, automatically. An automatic sampling system holds up to 60 samples.

**HP 1084A can be upgraded.** If you already use an HP 1084A and wish to have these enhanced capabilities, rest assured your equipment can be quickly upgraded on site.

Why not write for details?

# HP: innovators in HPLC

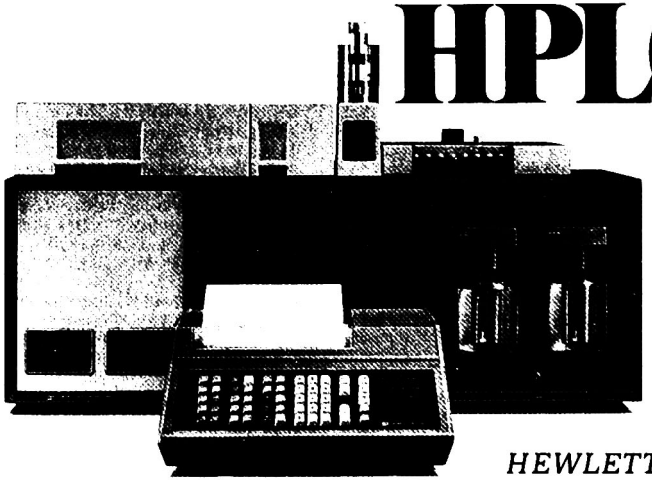

HEWLETT hp PACKARD

12801

Hewlett-Packard Co., Route 41, Avondale, Pennsylvania 19311, USA
Hewlett-Packard GmbH, Ohmstrasse 6, D-7500 Karlsruhe 41, Germany

CIRCLE 94 ON READER SERVICE CARD

John Q. Walker, M. T. Jackson, and M.P.T. Bradley. $225, ACS members; $265, nonmembers

**Microprocessors and Minicomputers**
Blacksburg, Va. Mar. 19–24, June 11–16. Raymond Dessy. $425, ACS members; $485, nonmembers

**Carbon-13 NMR Spectroscopy**
Philadelphia. Apr. 20–22. George C. Levy and Paul Ellis. $255, ACS members; $305, nonmembers

**Toxicology for Chemists**
Washington, D.C. May 2–4. Joseph Borzelleca and Frederick Sperling. $395, ACS members; $465, nonmembers

**Gas Chromatography–Mass Spectrometry**
New York City. May 18–19. J. Throck Watson and O. David Sparkman. $195, ACS members; $235, nonmembers

**Capillary Gas Chromatography**
Washington, D.C. May 19–20. Milos Novotny and Stuart Cram. $245, ACS members; $295, nonmembers

**Laboratory Safety—Recognition and Management of Hazards**
New York City. May 22–24. Norman Steere and Maurice Golden. $275, ACS members; $325, nonmembers

**Gas Chromatography, Theory and Practice**
Blacksburg, Va. June 6–9. Harold M. McNair. $395, ACS members; $455, nonmembers

**High-Pressure Liquid Chromatography Workshop**
Boston. June 24–25. David Freeman. $245, ACS members; $295, nonmembers

---

**High-Performance Liquid Chromatography**
California State U., Long Beach, Calif. Mar. 20–22. *Contact:* Van T. Lieu, Chemistry Dept., California State U., Long Beach, Calif. 90840. 213-498-4941

**Modern Concepts and Techniques in Analytical, Forensic, and Clinical Toxicology**
Houston, Tex. Apr. 3–6. *Contact:* Jack E. Wallace, Dept. of Pathology, U. of Texas Health Science Center, 7703 Floyd Curl Dr., San Antonio, Tex. 78284

**Thermal Analysis User Training Course**
Wilmington, Del. Apr. 5–7. Operating techniques for 990 Thermal Analyzer, 910 Differential Scanning Calorimeter, 951 Thermogravimetric Analyzer and 943 Thermomechanical Analyzer. $350. *Contact:* R. L. Blaine, Du Pont Instruments, Concord Plaza, Quillen, Wilmington, Del. 19898. 302-772-5733

**Microprocessor Interfacing**
Blacksburg, Va. Apr. 6–8. $295. *Contact:* Jonathan A. Titus, Course Director, Tychon, Inc., P.O. Box 242, Blacksburg, Va. 24060

**Introduction to Assembly Language Programming for 8080/8085 Processors**
Blacksburg, Va. Apr. 10–12. $295. *Contact:* Jonathan A. Titus, Course Director, Tychon, Inc., P.O. Box 242, Blacksburg, Va. 24060

**Intermediate Assembly Language Programming for 8080/8085 Processors**
Blacksburg, Va. Apr. 13–15. $295. *Contact:* Jonathan A. Titus, Course Director, Tychon, Inc., P.O. Box 242, Blacksburg, Va. 24060

**7th Gas Chromatography Short Course**
Villanova, Pa. May 10–12. Sponsored by the Chromatography Forum of the Delaware Valley. $90 if application received by April 1; after April 1st, $125. *Contact:* Robert L. Grob, Chemistry Dept., Villanova U., Villanova, Pa. 19085. 215-527-2100, ext. 496

**Applications of High-Performance Liquid Chromatography**
Chase-Park Plaza Hotel, St. Louis, Mo. May 19–20. Seven manufacturers will have equipment and representatives available for afternoon discussion sessions. $80, AOCS members; $125, nonmembers; $50, students. *Contact:* The American Oil Chemists' Society, 508 S. Sixth St., Champaign, Ill. 61820 (217-359-2344)

**Simplex Optimization in Research and Development**
Houston, Tex. May 22–23. Sponsored by Dept. of Chemistry, U. of Houston. S. N. Deming, S. L. Morgan, and M. R. Willcott. $250. *Contact:* S. N. Deming, Dept. of Chemistry, U. of Houston, Houston, Tex. 77004. 713-749-4809 or 713-749-2612

**Scanning Electron Microscopy and X-ray Microanalysis**
Bethlehem, Pa. June 12–16. J. I. Goldstein. $450. *Contact:* J. I. Goldstein, Metallurgy and Materials Engineering, Whitaker Lab #5, Lehigh U., Bethlehem, Pa. 18015 (215-691-7000, ext. 627)

## For Your Information

The National Science Foundation has announced plans to award a three-year $1.4 million grant to Oak Ridge National Laboratory, Oak Ridge, Tenn., to establish the country's first **National Research Facility for Small-Angle Neutron Scattering.** Scattering research—the bombardment of solids and liquids with electro-magnetic or particle radiation—is one of the most powerful tools available for obtaining basic information about the atomic structure of materials. The facility, to be in operation by mid-1979, will be accessible not only to experts in the techniques of neutron scattering but to researchers in a wide variety of disciplines.

A collection of **FORTRAN programs** generated in the course of research at the Organic Spectrochemistry Section of the Chemistry Division, the National Research Council, Canada, is now available. The set comes as a compilation of 50 FORTRAN programs in seven volumes, including descriptive text. The programs are also available on two 600-ft magnetic tape reels. Contact: R. Norman Jones, Division of Chemistry, National Research Council of Canada.

**Frost & Sullivan, Inc.,** 106 Fulton St., New York, N.Y. 10038 (Tel: 212-233-1080) announces the availability of a new market study on the clinical laboratory diagnostic reagent and test kit. The study shows the market will double to $1.3 billion over the next 10 years. Toxicology is included as a separate category. Other categories covered are clinical chemistry, hematology, radioimmunoassay (in vitro), and radioimmunoassay (in vivo). This market study costs $700.

**Labtest Equipment Co.,** manufacturer of emission spectrometers, computer-controlled analytical instrument systems, and industrial microcomputers, has opened a new Southwestern Regional Sales and Service office in Dallas, Tex., to cover the southwestern states of Texas, Oklahoma, Louisiana, Arkansas, Mississippi, Alabama, and Tennessee. The new office will be headed by W. C. MacPherson, who was previously employed by RCA, Bissett-Berman Corp., Display Devices, Inc., and Spectrocon Pty., Ltd.

A major **research complex for experimental ecology projects has recently been constructed at Battelle's Columbus Laboratories.** The facility, located at Battelle's West Jefferson site in suburban Columbus, Ohio, enables Battelle researchers to conduct intensive studies in the areas of environmental toxicology, ecological monitoring, forest and agricultural management, and ecosystems structure and function. The complex consists of 11 laboratories and 9 greenhouse bays in a 10 000-ft$^2$ renovated building. It also has experimental ponds, nurseries, agricultural plots, and surrounding natural ecosystems (woods, pasture, lake, and streams). The complex is operated by the Ecology and Ecosystems Analysis Section of Battelle's Department of Biological, Ecological, and Medical Sciences.

**The Ralston Purina Co. has announced the purchase of Warf Institute, Inc.,** through acquisition of all shares of its stock from the Wisconsin Alumni Research Foundation. The services of Warf Institute, a commercial research, testing, and consulting laboratory in Madison, Wis., complement those of the Ralston contract research laboratory, Research 900. The union of these two laboratories broadens the base of services available to customers, particularly the service capabilities in critical analytical areas. The expanded service capabilities include the industry compliance needs regarding the EPA Toxic Substances Act, analytical testing to support environmental impact statements, chemical toxicity studies, etc. The two laboratories will continue to operate at separate locations.

**American Ultraviolet Co.,** Chatham, N.J., has established a western sales and distribution affiliate, American Ultraviolet (West) Inc., at 20416 E. Walnut Dr., Suite B-23Z, Walnut, Calif. 91789. For current catalog or ultraviolet engineering assistance, call 714-598-2748 (no charge).

**"Chemical Executive Directory"** lists the names and titles of nearly 10 000 executives working for the leading chemical companies, oil companies, and manufacturers of paper, plastics, paints, drugs, etc. The names and titles of the executives are given under alphabetical listings of the companies with addresses for the parent company as well as addresses for the divisions and subsidiaries. Copies of the directory are available at $9.75 per copy from Executive Directories, Box 234, Kenilworth, Ill. 60043.


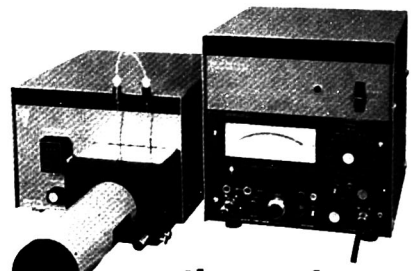

**Now... a continuously variable fluorescence detector for liquid chromatography**

UV/VIS excitation monochromator and readily adjustable emission wavelength in conjunction with a very accessible 5 ul flow through cuvette makes detection at picogram levels possible. The 970 Spectrofluro monitor can be attached and operated in conjunction with existing HPLC systems.

*Write today for complete technical literature.*

**Schoeffel Instrument Corporation** 24 Booker Street, Westwood, N. J. 07675 • 201-664-7263

SCHOEFFEL INSTRUMENT CORPORATION

CIRCLE 189 ON READER SERVICE CARD

**No other spectrophotometer gives you so much for so little.**

The Zeiss PM 2 with spectral range 290-850 nm; precision grating monochromator; digital readout for absorbance, concentration, transmission, and K-factor display; digital and analog outputs; and "lock-in" display. **$1485**

All the above, plus automatic blank reference and unique quartz funnel cell for rapid multiple determinations. **$1719**

All the above plus UV attachment (down to 200 nm). **$2327**

**Nationwide service.**

**Carl Zeiss, Inc.,** 444 5th Ave., New York, N.Y. 10018. (212) 730-4400.

ZEISS THE GREAT NAME IN OPTICS

CIRCLE 243 ON READER SERVICE CARD

# Analyze with it
# Acquire with it
# Teach with it
# Learn with it
# Experiment with it

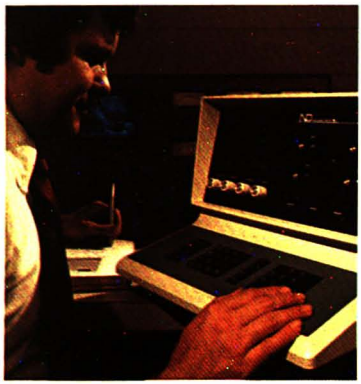

Photos Courtesy of Elmhurst College

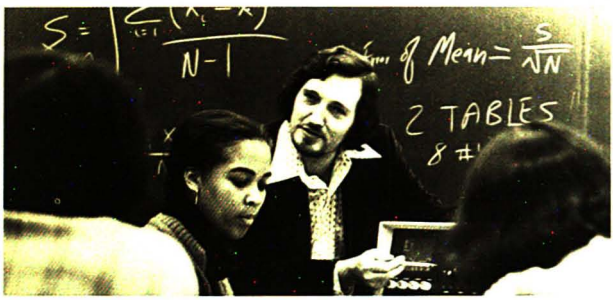


# Enjoy it.

The ND60 is no ordinary multi-channel analyzer.

It is the product of extensive input from scientists and educators who suggested each of its capabilities and features. It combines microprocessor technology with Nuclear Data's DataPlan Six design concepts in a sophisticated yet economical MCA system.

The ND60 is a flexible MCA system whose utility far exceeds any comparably priced measurement system. It is designed to operate like a computer terminal with comprehensive alphanumeric display of experiment and system parameters simultaneous with linear or logarithmic display or spectral data.

The ND60 is remarkably versatile with greater capabilities of data acquisition, display, manipulation and input/output flexibility than any MCA in its price range. It lends itself well to the demands of today's laboratory environment and requires a minimum of instruction to obtain clear and precise data.

ND60 Systems offer: large-screen, 8 by 10 cm display CRT; 2048 channel, solid state memory with selection of 4 subgroups; built-in preamplifier, amplifier and 50 MHz ADC; movable curser and dual markers for multiple region of interest selection; net area and background calculations; serial and parallel input/output interfaces; and auto analysis with selectable sequencing.

The ND60 is a lot of little analyzer from a lot of big ideas.

**Nuclear Data Inc**

Golf and Meacham Roads
Schaumburg, Illinois 60196
Tel: 312 884-3621

Bonameser Strasse 44
6000 Frankfurt/Main 50
Federal Republic of Germany
Tel: 529952

CIRCLE 148 ON READER SERVICE CARD

# NEW! PRECISION LIQUID DISPENSERS

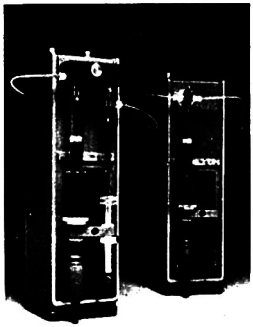

## Single and Dual Channel Dispensers

Now you can solve almost all of your liquid dispensing problems with Hamilton's new and improved, low-cost Precision Liquid Dispensers (PLD). Designed for industrial R&D, quality control, and filling operations, with accuracy and precision where strict tolerances are required.

Check these features:

- ☐ New, improved valve system.
- ☐ Longer valve life saves downtime.
- ☐ Easy cleaning and changing.
- ☐ Simple, trouble-free operation.
- ☐ Weight-balanced, rugged construction.
- ☐ Operates in any position or environment.
- ☐ Pneumatic (non-electric) operation.
- ☐ Ideal for operations where oxygen or flammables are present, or in most extremes of temperature or viscosity.
- ☐ Under standard conditions, precision is ±.05%, accuracy is ±1%.

If you have a liquid dispensing problem, call the experts. We'll send out a trained sales engineer or put you in touch with one of our dealers. Write for literature to John Nadolny, Hamilton Company, P.O. Box 10030, Reno, Nevada 89510, or call (702) 786-7077.

**HAMILTON**

CIRCLE 96 ON READER SERVICE CARD

# 99.9 - 99.99999% PURE INORGANICS

**SPEX HI PURE MATERIALS**

Over 500 high purity metals and compounds, each provided with a semiquantitative spectrographic determination of impurities. Accompanying each compound in addition is a wet chemical assay.

ELEMENT KITS—up to 2g quantities each of
49 Common Elements or 16 Rare Earths
or 10 Noble Metals

SPEX INDUSTRIES INC P O BOX 798 METUCHEN N J 08840 (201) 549 7144

CIRCLE 188 ON READER SERVICE CARD


FIRST CLASS
Permit No. 25682
Philadelphia, Pa.
19101

**BUSINESS REPLY CARD**
No postage stamp necessary if mailed in the United States

POSTAGE WILL BE PAID BY

**ANALYTICAL CHEMISTRY**
**P. O. Box #8660**
**Philadelphia, Pennsylvania 19101**

Analytical Chemistry — MARCH 1978 — Valid through July 1978

NEW PRODUCTS, CHEMICALS, LITERATURE: 401 402 403 404 405 406 407 408 409 410 411 412 413 414 415 416 417 418 419 420 421 422 423 424 425 426 427 428 429 430 431 432 433 434 435 436 437 438 439 440 441 442 443 444 445 446 447 448 449 450 451 452 453 454 455 456 457 458 459 460 461 462 463 464 465 466 467 468 469 470 471 472 473 474 475 476 477 478 479 480 481 482 483 484 485 486 487 488 489 490 491 492 493 494 495 496

ADVERTISED PRODUCTS: 1 2 3 4 5 6 7 8 9 10 11 12 13 14 15 16 17 18 19 20 21 22 23 24 25 26 27 28 29 30 31 32 33 34 35 36 37 38 39 40 41 42 43 44 45 46 47 48 49 50 51 52 53 54 55 56 57 58 59 60 61 62 63 64 65 66 67 68 69 70 71 72 73 74 75 76 77 78 79 80 81 82 83 84 85 86 87 88 89 90 91 92 93 94 95 96 97 98 99 100 101 102 103 104 105 106 107 108 109 110 111 112 113 114 115 116 117 118 119 120 121 122 123 124 125 126 127 128 129 130 131 132 133 134 135 136 137 138 139 140 141 142 143 144 145 146 147 148 149 150 151 152 153 154 155 156 157 158 159 160 161 162 163 164 165 166 167 168 169 170 171 172 173 174 175 176 177 178 179 180 181 182 183 184 185 186 187 188 189 190 191 192 193 194 195 196 197 198 199 200 201 202 203 204 205 206 207 208 209 210 211 212 213 214 215 216 217 218 219 220 221 222 223 224 225 226 227 228 229 230 231 232 233 234 235 236 237 238 239 240 241 242 243 244 245 246 247 248 249 250 251 252 253 254 255 256 257 258 259 260 261 262

READER SURVEY: 301 302 303 304 305 306 307 308 309 310 311 312 313 314 315 316 317 318 319 320 321 322 323 324 325 326 327 328 329 330 331 332 333 334 335 336 337 338 339 340 341 342 343 344 345 346

Name_____ Position_____

Company_____

Street_____ City_____

# USE . . .

these postage paid reply cards for free data

on all products advertised in this issue.

Analytical Chemistry — MARCH 1978 — Valid through July 1978

NEW PRODUCTS, CHEMICALS, LITERATURE: 401 402 403 404 405 406 407 408 409 410 411 412 413 414 415
416 417 418 419 420 421 422 423 424 425 426 427 428 429 430 431 432 433 434 435 436 437 438 439 440 441 442
443 444 445 446 447 448 449 450 451 452 453 454 455 456 457 458 459 460 461 462 463 464 465 466 467 468 469
470 471 472 473 474 475 476 477 478 479 480 481 482 483 484 485 486 487 488 489 490 491 492 493 494 495 496

ADVERTISED PRODUCTS: 1 2 3 4 5 6 7 8 9 10 11 12 13 14 15 16 17 18 19
20 21 22 23 24 25 26 27 28 29 30 31 32 33 34 35 36 37 38 39 40 41 42 43 44 45 46
47 48 49 50 51 52 53 54 55 56 57 58 59 60 61 62 63 64 65 66 67 68 69 70 71 72 73
74 75 76 77 78 79 80 81 82 83 84 85 86 87 88 89 90 91 92 93 94 95 96 97 98 99 100
101 102 103 104 105 106 107 108 109 110 111 112 113 114 115 116 117 118 119 120 121 122 123 124 125 126 127
128 129 130 131 132 133 134 135 136 137 138 139 140 141 142 143 144 145 146 147 148 149 150 151 152 153 154
155 156 157 158 159 160 161 162 163 164 165 166 167 168 169 170 171 172 173 174 175 176 177 178 179 180 181
182 183 184 185 186 187 188 189 190 191 192 193 194 195 196 197 198 199 200 201 202 203 204 205 206 207 208
209 210 211 212 213 214 215 216 217 218 219 220 221 222 223 224 225 226 227 228 229 230 231 232 233 234 235
236 237 238 239 240 241 242 243 244 245 246 247 248 249 250 251 252 253 254 255 256 257 258 259 260 261 262

READER SURVEY: 301 302 303 304 305 306 307 308 309 310 311 312 313 314 315 316 317 318 319 320 321 322 323
324 325 326 327 328 329 330 331 332 333 334 335 336 337 338 339 340 341 342 343 344 345 346

Name_____ Position_____

Company_____

Street_____ City_____

State_____ Telephone_____

FIRST CLASS
Permit No. 25682
Philadelphia, Pa.
19101

**BUSINESS REPLY CARD**
No postage stamp necessary if mailed in the United States

POSTAGE WILL BE PAID BY

**ANALYTICAL CHEMISTRY**
**P. O. Box #5000**
**Philadelphia, Pennsylvania 19101**


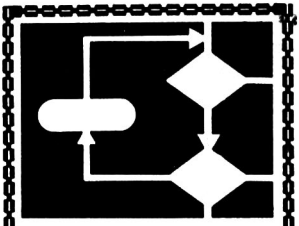

## Algorithms for Chemical Computations

ACS Symposium Series No. 46

Ralph E. Christoffersen, *Editor*
*The University of Kansas*

*A symposium sponsored by the Division of Computers in Chemistry of the American Chemical Society.*

This multidisciplinary collection of state-of-the-art papers assesses significant developments in algorithms for several important areas of chemistry and pinpoints places where currently available algorithms are inadequate.

Leading experts not only evaluate the tremendous opportunities for progress in chemical research that algorithms provide but also analyze the substantial difficulties that algorithms may present.

Topics covered include those of particular interest to scientists doing significant amounts of computing in the fields of quantum chemistry, scattering, computer handling of chemical information, and solid state theory.

CONTENTS

Graph Algorithms in Chemical Computation • Algorithm Design in Computational Quantum Chemistry • Rational Selection of Algorithms for Molecular Scattering Calculations • Molecular Dynamics and Transition State Theory • Newer Computing Techniques for Molecular Structure Studies by X-ray Crystallography • Algorithms in the Computer Handling of Chemical Information

151 pages (1977) Clothbound $12.75
LC 77-5030 ISBN 0-8412-0371-7

SIS/American Chemical Society
1155 16th St., N.W./Wash., D.C. 20036

Please send ____ copies of *SS 46 Algorithms for Chemical Computations* at $12.75 per copy.

☐ Check enclosed for $_____. ☐ Bill me. Postpaid in U.S. and Canada, plus 40 cents elsewhere.

Name

Address

City State Zip

# Just the Right Combination.


A delicate cheese with a fine, light wine. Each brings out the best in the other. And the same holds true for any great combination.

MC/B and EM have created a strong, diversified resource for the full range of laboratory chemicals. The result is just the right combination of sales and marketing, manufacturing, research and service.

MC/B, as an associate of E. Merck, Darmstadt, Germany, serves the market with reagents and specialties for laboratory testing and research, and intermediates for chemical processing. An innovative, new resource capable of responding quickly to your particular needs.

MC/B and EM. Just the right combination for you.

**MC/B® MANUFACTURING CHEMISTS, INC.**

Associate of E. Merck, Darmstadt, Germany

2909 Highland Avenue, Cincinnati, Ohio 45212 Telephone: (513) 631-0445

**REGIONAL SALES OFFICES**

**East**
Suite #16
4 Cornwall Drive
East Brunswick, N.J. 08816
(201) 257-7900

**Central**
Suite #404
9575 West Higgins Rd.
Rosemont, Ill. 60018
(312) 823-4778

**West**
P.O. Box 7203
2121 S. Leo Avenue
Los Angeles, Ca. 90022
(213) 685-5280

CIRCLE 143 ON READER SERVICE CARD


A new concept in carbon/sulfur determination.

More automatic
More accurate
More reliable
More rapid

Contact LECO today.

CIRCLE 127 ON READER SERVICE CARD

LECO™
LECO
LECO CORPORATION
3000 LAKEVIEW AVE
ST JOSEPH MICHIGAN 49085

PHONE (616) 983-5531
CABLE LECO
TELEX 72-9411

# LOOKING FOR THE BEST IN DIFFERENTIAL REFRACTOMETERS?

## Now you can get increased sensitivity, digital readout, switch-selectable cell temperatures, plus improved reproducibility and accuracy.

If you're looking for the best in differential refractometers, here's a new instrument that will be of interest to you. It's the Chromatix KMX-16 Laser Differential Refractometer and it has performance and features that put it way out in front of conventional instruments. Consider these:

**Increased Sensitivity.** The KMX-16 uses a coherent laser source that offers much greater beam collimation than the mercury or tungsten light sources used in conventional instruments. The optical design includes a telescope which increases the effective moment arm of the instrument. The result is a ten fold improvement in sensitivity to $2 \times 10^{-7}$ Refractive Index Units.

**Digital Readout.** A digital display on the front panel of the KMX-16 provides an unambiguous, easily read displacement value. Completely eliminated are the visual strain of using a magnifying eyepiece and the accompanying interpolation and estimation errors of superimposed images.


**Switch Selected Cell Temperatures.** The KMX-16 provides closed-loop cell temperature control over a −10 to +165°C operating range. Just set the desired cell temperature with the digital thumbswitch and the KMX-16 does the rest. For temperatures near ambient or below, external cooling may be required.

**Accuracy and Reproducibility.** The reproducibility of differential refractive index measurements is greatly improved with KMX-16 as compared to conventional instruments. This is due to the high energy laser source, digital displacement readout, mechanical and optical stability, and sample cell temperature control. The KMX-16 reproducibility is specified as $1 \times 10^{-6}$ R.I. Units. Accuracy of differential R.I. measurements is also improved with the KMX-16 because of its inherent wavelength accuracy, digital readout, and temperature control.

For full information on how you can make a significant increase in differential refractometer convenience, efficiency, and performance, contact Chromatix today. **Circle No. 37** for brochure. **Circle No. 38** for application information. **Circle No. 39** to have a technical representative call.

chromatix

560 Oakmead Parkway
Sunnyvale, CA 94086
Phone: (408) 736-0300
TWX: 910-339-9291

D6903 Neckargemünd 2
Unterestrasse 45a
West Germany
Phone: (06223) 7061/62
Telex: 461-691

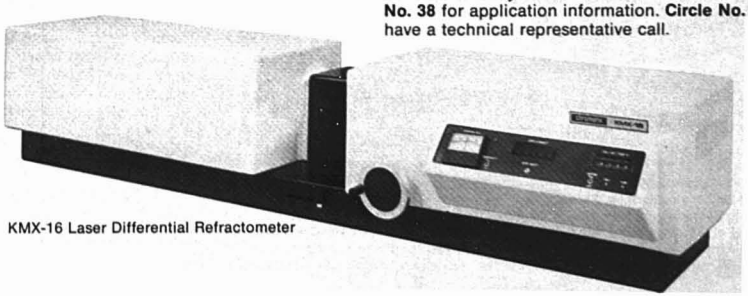

KMX-16 Laser Differential Refractometer

# New Products

## Enzyme Analyzer Spectrophotometer

The SEA Jr. spectrophotometer, designed primarily for the clinical laboratory, has an operating wavelength range of 330–710 nm. Absorbance and concentration measurements are digitally displayed and supplied to a printer output. The cuvette well accepts both cylindrical and square cuvettes. Major components of the instrument are a tungsten lamp, a narrow bandpass single-beam grating monochromator, and a vacuum photodiode detector. Accessories include an electronic printer and a flow-thru, temperature-controlled cuvette. Helena Laboratories **410**

## Mass Spectrometer Data System

The VG 2000DB series is specifically designed for use with double-beam organic mass spectrometers. In addition to all of the features of the VG 2000 series, the 2000DB range permits real time mass measurement accuracies of better than 15 ppm when operating in double-beam mode at 1000 resolving power. The system includes additional software for the real time determination of accurate mass at both low and high resolution in the single-beam mode. It is available in a wide range of configurations from simple stand alone systems through those operating in foreground/background mode to sophisticated multiple spectrometer systems that can operate in conjunction with all types of mass spectrometers. VG Data Systems Ltd. **426**

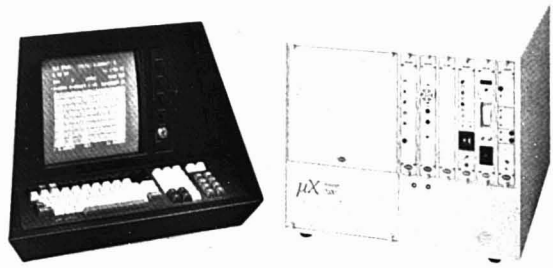

**The μX 7000 series analyzer for x-ray, Auger, and electron energy loss spectrometry** combines color-coded video display, 63-character ASCII keyboard, and dedicated single-function controls in a single interactive console. Four alternate data acquisition modes are keyboard selectable: x-ray energy spectrometry, pulse height analysis, sequential pulse counting or signal averaging, and simultaneous x-ray energy spectrometry and sequential analysis. Five data reduction functions are standard, and customized programs can be added. Floppy disk package is available for mass data and supplementary program storage. Kevex Corp. **403**

## Quadrupole Mass Analyzer

The IQ 200, with a range of 0–200 amu, features three video display modes. The tabular mode allows totally independent monitoring and precise calibration of up to 10 masses; the bar graph display mode permits broad spectra data display with Peak-Lock identification of mass number; and the conventional analog mode is used for display of peak shapes. Spectra manipulation is possible in all modes, permitting data storage, background subtraction, or inversion. Inficon Leybold-Heraeus Inc. **419**

## Photoionization Detector

Model PI 51 photoionization detector (PID) for gas chromatography can be used with column temperatures more than 100 °C higher than the previous version PID. The detector employs a sealed ultraviolet lamp adjacent to an ionization detector and uses ultraviolet photon energies of 9.5, 10.2, or 11.7 eV for ionization of the species. The dead volume has been reduced by a factor of three, making it ideal for capillary column analyses. Species that can be detected by this new PID include high molecular weight compounds such as drugs, pesticides, and polynuclear aromatics. HNU Systems, Inc. **412**

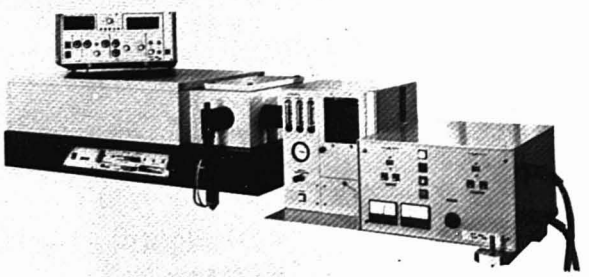

**JY-38 sequential plasma spectrometer** features an inductively coupled plasma source that permits the quantitative determination of trace elements in liquids. The instrument offers sensitivity down to the picogram level with an accuracy and repeatability in excess of 1%. The dynamic range of $10^6$ permits quantitative measurement over a wide concentration level. The instrument is computer compatible and is offered with a computer option including the software for automatic element search, background subtraction, and automatic calibration. Instruments SA, Inc. **401**

## GC/MS Data System

Model 29KS computerized data system features Stereospectrometry, the simultaneous acquisition and display of mass spectra acquired in two modes of spectrometer operation. The system can present EI/CI dual spectra, positive/negative ion CI spectra, or any other pair of spectra that the mass spectrometer is capable of acquiring. Data are displayed continuously on an interactive display monitor. Either spectra or ion currents can be monitored before and during acquisition. Other features include selected ion recording of ion chromatograms acquired in two simultaneous modes of operation, ratio calculation, and simultaneous recording of 12 ions. Teknivent Corp. **413**

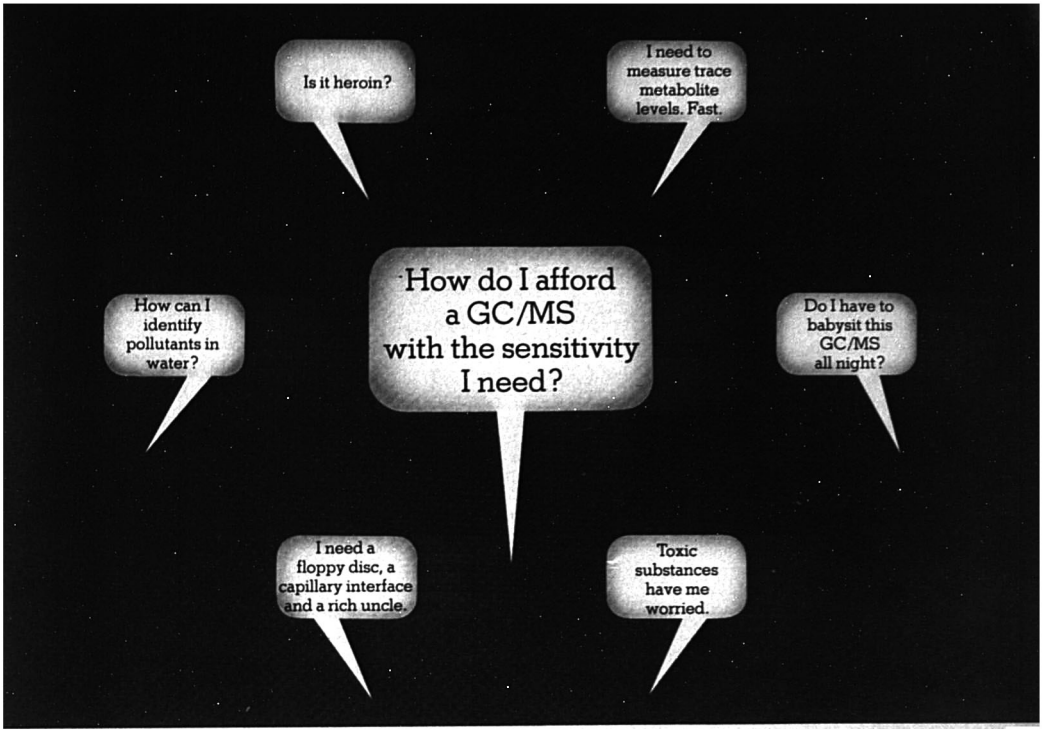


# We've got your problems covered.

We offer a comprehensive line of GC/MS instrumentation, including accessories and software. So you're almost sure to find an HP system that solves your problems, including budgetary ones. For details, call your local HP office, or write us at 1507 Page Mill Road, Palo Alto, California 94304.

## HP 5985A

- Mass range to 1,000 amu. Hyperbolic quadrupole.
- Dual EI/CI source optimizes results in both modes.
- HP 5840A microprocessor-controlled GC. HP's finest.
- Flexible GC/MS interface accommodates five different GC detectors.
- New generation computer (550 ns cycle time).
- Fully digital. Tunes itself to save time.

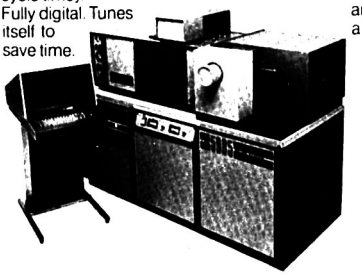

## HP 5993A

- Mass range to 800 amu.
- Powerful software includes batch processing, and much more.
- Fast new computer with 32K memory, dual disc.
- Compact GC/MS from the HP 5992A.
- Foreground/background operation.
- Neat combination of flexibility and simplicity at a neat price.

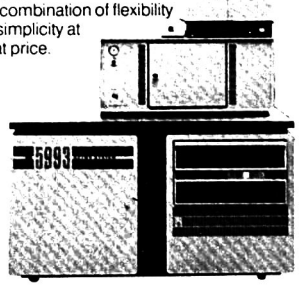


## HP 5992A

- Mass range to 800 amu.
- Hyperbolic quadrupole for excellent sensitivity.
- Friendly HP 9825A desktop computer (16K memory) for ease of use.
- Fits your lab bench as well as your budget.
- Tunes itself automatically.
- Software includes SIM and much more.

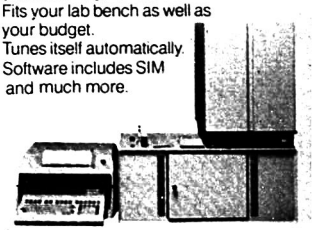

HEWLETT hp PACKARD

1507 Page Mill Road, Palo Alto, California 94304

For assistance call: Washington (301) 948-6370 Chicago (312) 255-9800 Atlanta (404) 955-1500 Los Angeles (213) 877-1282.

23704

CIRCLE 97 ON READER SERVICE CARD

# Another innovation from L/I:

# The REPIPET® II dispenser

## Virtually unbreakable!

**Better than any $85 plastic dispenser! But only $52.50!***

Here it is, the best value ever offered in reagent dispensers. The tough REPIPET II reflects more than 14 years of L/I's experience in liquid dispensing—your best assurance of quality and performance. All REPIPET II dispensers feature the use of fluorocarbon and extra-thick borosilicate glass for strength and durability. They're tough lab workhorses, virtually impossible to break.

Note the 100-division scales, printed where they should be—on the glass barrel, not on an elastic plastic! L/I's exclusive sturdy magnifying indicator is a further aid to precise volume settings.

L/I guarantees accuracy of 1.5% full scale and 0.2% reproducibility for all REPIPET II dispensers. They are suitable for use with all laboratory reagents (except HF).

(Although TEFZEL® plastic and TEFLON® plastic are chemically inert to all laboratory reagents, slight distortions may occur at autoclaving temperatures and with some strong solvents.)

REPIPET II dispensers are offered in three popular sizes, 5, 10, and 20 ml. Price of 5 and 10 ml units is $52.50; 20 ml, $58.50.

To order, contact your distributor. For literature, write, call or circle the reader service number below.

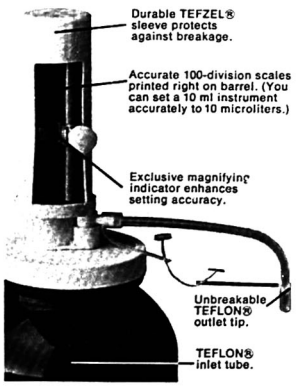


**LABINDUSTRIES**

620 Hearst Avenue, Berkeley, CA 94710
Phone (415) 843-0220

CIRCLE 128 ON READER SERVICE CARD


## New Products

### Mass Spectrometer

The Micromass 622 isotope enrichment mass spectrometer uses the technique of double-collector detection with ratio electronics to give the level of performance needed for the isotope tracer techniques now becoming more common with increased availability of stable isotopes. The 622 is primarily designed for N-15 determinations. Precision is 0.005 atom % N-15. VG-Isotopes Limited, The Kearns Group **414**

### Scanning Spectrometer

The RSS-C rapid ($10^{-3}$ s) or slow (minutes) scanning spectrometer has been developed using only two basic optical components in the monochromator, a low inertia grating mounted on the shaft of a galvanometer and a spherical mirror. This optical layout results in a number of improvements including increased throughput, resolution, and scan range. Although normally operated in the UV–VIS–NIR, the all reflective optics permits use of the instrument in the IR. Applications include study of kinetic reactions, spectroelectrochemistry, stopped flow, LC, GC, and routine measurements. $15 000. Harrick Scientific Corp. **415**

### HPLC Detector

The TL-5 thin-layer electrochemical cell, made from Kel-F, uses a "glassy carbon" electrode surface for increased solvent resistance and better electrode stability. It has been successfully used with reverse-phase systems containing a high percentage of acetonitrile and methanol in the mobile phase. In addition to its versatility in expanding the range of the electrochemical detection in HPLC, the new detector is easier to service and longer lasting than previous designs. Bioanalytical Systems, Inc. **409**

### Nitrous Oxide Capillary Burner

The 301 System is designed to allow safe burning of nitrous oxide–acetylene through the use of a specifically designed and fabricated capillary head that establishes a full Poiseville distribution of gases. This flow ensures a safe and stable flame. The Poiseville flow burner prevents flashback even with widely varying fuel oxidizing rates. The use of the 301 System will improve sensitivity for routine analysis and allows for determination of less volatile metals. The system is directly interchangeable with existing units and does not require any water cooling or special equipment. Cotronics Corp. **417**

**Model 150C liquid chromatograph/gel permeation chromatograph** is a high-speed, controlled-temperature instrument. Known as "The Hot One", the instrument provides rapid results, with separations in 7–15 min. Operation is microprocessor controlled. The Model 150C will analyze materials that dissolve only at elevated temperatures or require high temperatures to reduce viscosity. Waters Associates, Inc. **402**

### Si(Li) X-ray Detector

Model 7900 is designed exclusively for electron microscope applications. Major features include 149-eV FWHM resolution, 100-mm telescoping detector movement, peak-to-background ratio of 1500:1, 4-mm-diameter detector, an external collimator, and a dynamic charge restoring FET preamplifier. EG&G/Ortec **427**

### Argon Jet for Plasma Spectrometers

Spectrajet III, a new three-electrode argon jet for plasma emission spectrometers, features simplified operation, increased sample throughput, and improved sensitivity. It incorporates two graphite anodes and a tungsten cathode in an inverted 'Y' configuration. The three electrodes are moved into contact by argon-actuated pistons, and plasma ignition is initiated automatically without a high-voltage spark as the electrodes are withdrawn. The 'Y' configuration stabilizes the position of the plasma and sample excitation area. Operation is completely automatic. The Spectrajet II will be a standard feature on the Spectraspan III and IV spectrometers and can be retrofitted to all existing installations. Spectrametrics Inc. **418**

# LKB RediRac

## A new economy-priced fraction collector with the quality you have come to expect

### Every lab should have one, and can afford to have several

LKB

LKB Instruments Inc.
12221 Parklawn Drive, Rockville, Maryland 20852
Tel: (301) 881-2510

CIRCLE 126 ON READER SERVICE CARD

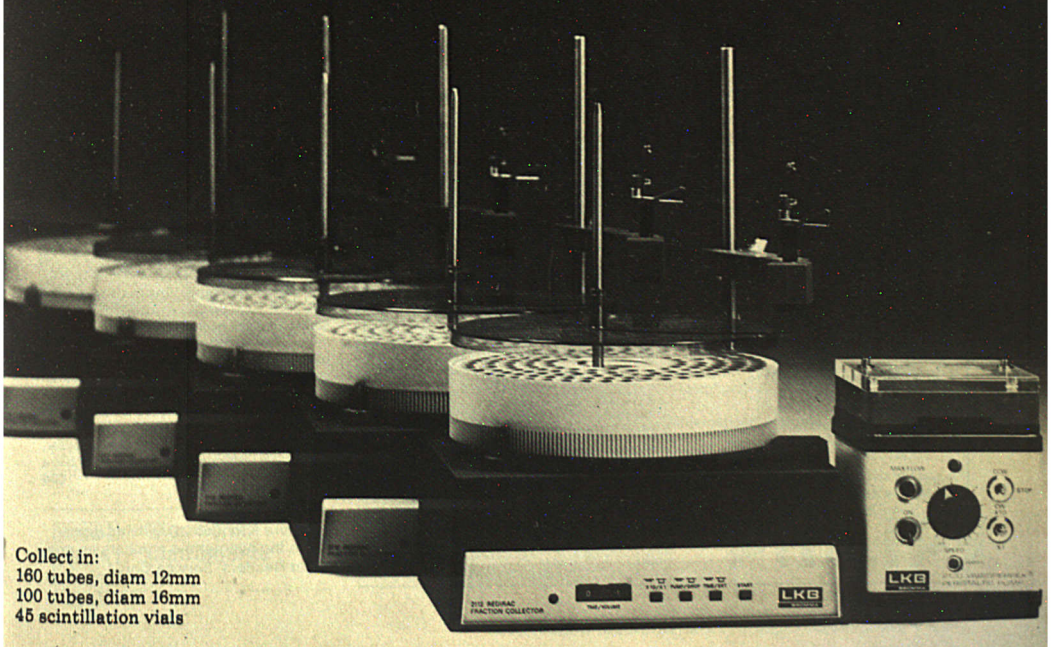


Collect in:
160 tubes, diam 12mm
100 tubes, diam 16mm
45 scintillation vials

# Calibrate your gas analyzer... objectively.

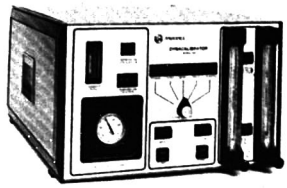

The Metronics Dynacalibrator gives you calibrations traceable to NBS standards for almost any gas analyzer or gas chromatograph, in the lab or in the field. That includes units you've rigged up yourself, and even instruments with suction rates up to *25 l*/min. And since calibration is our only business, you get an instrument that's coldly precise, easy-to-use and competitively priced. Key Dynacalibrator features include:

- Oven control within ±.05°C, NBS traceable
- Variable oven temperatures up to 50°C, 110°C optional
- Flow calibrated and stable to within 1% of each individual reading
- Our own calibrated permeation devices, certifications traceable to NBS standards
- Continuous, unattended automatic or remotely-controlled operation
- Optional "in-transit" maintenance of purge and temperature
- Dynamic gas concentration ranges of 60:1

The result? Calibration that's above suspicion—your best insurance against costly errors. Three models meet every requirement. For details and a demo, call or write: Metronics, 2991 Corvin Drive, Santa Clara, CA 95051
Phone: (408) 737-0550.
Telex: 35-2129.

Metronics
*Calibration you can count on.*

CIRCLE 139 ON READER SERVICE CARD



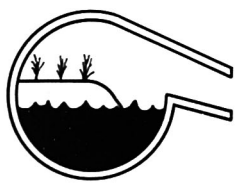

# Marine Chemistry in the Coastal Environment

ACS Symposium Series No. 18

Thomas M. Church, *Editor*

*A special symposium sponsored by the Middle Atlantic Region of the American Chemical Society.*

Now available—a comprehensive volume containing the most recent advances in this new and increasingly important field.

The collection represents an indispensable source of information for every marine scientist. Emphasis is not merely on describing coastal problems but on showing the potential in applying the tools of modern oceanography and chemistry to solve these problems.

***Forty-one chapters cover six major areas: physical, organic, and tracer marine chemistry; estuarine geochemistry; hydrocarbons and metals in the estuarine environment; ocean disposal forum; applications and resources in marine chemistry; and organic and biological marine chemistry.***

710 pages (1975) Clothbound $35.75
(ISBN 0-8412-0300-8) LC 75-28151

SIS/American Chemical Society
1155 16th St., N.W./Wash., D.C. 20036

**Please send _____ copies of *No. 18 Marine Chemistry in the Coastal Environment* at $35.75 per book.**

**☐ Check is enclosed for $_____. ☐ Bill me. Postpaid in U.S. and Canada, plus 40 cents elsewhere.**

**Name** _____

**Address** _____

**City** _____ **State** _____ **Zip** _____


## New Products

### GC/MS Data

The Riber 150 computer control and data acquisition system for quadrupole GC/MS instrumentation is a powerful and flexible approach to atuomating a GC/MS system. It permits the operator to set run conditions, specify maximum run time, and leave the system unattended to acquire all of the desired data. The Riber 150 will control multiple ion detection, handle up to eight different masses or mass ranges, and monitor an unlimited number of mass sets. Output can be a digital presentation of either GC or MS data on a CRT. The system can be easily tailored to meet specific laboratory requirements. Riber Data Systems, Inc. **416**

### Computing Data Acquisition Device

The Model 97S I/O calculator combines the HP-97 programmable printing calculator with BCD interfacing to provide data collection and computation from a wide range of instruments. The HP-97S manipulates the data according to user-designed programs and produces a printed hardcopy report. With the calculator, the user can take an instrument measurement and compare it to a standard or calibrate in data, do computation on each individual reading, or take multiple measurements and conduct computation and statistical analysis. Basic system is $1375. Hewlett-Packard Co. **420**

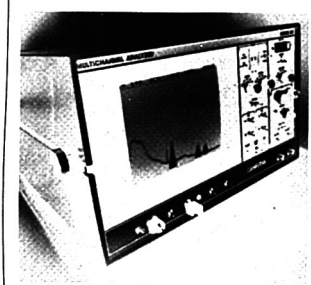

**Series 30 multichannel pulse height analyzer** features a 9-in. diagonal CRT, 1024 channel memory, and both PHA and MCS data acquisition modes. Digital integration, spectrum compare, and I/O interfacing for TTY, EIA devices and digital cassette are included in the basic unit. Plug-in options are available for a detector bias supply, high-resolution amplifier, and various additional I/O interfaces. Canberra Industries, Inc. **404**

**For more information on listed items, circle the appropriate numbers on one of our Readers' Service Cards**

# New from Philips: Atomic Absorption programmed for your applications.

**Introducing the Pye Unicam SP2900 double-beam AA spectrophotometer with powerful Data Center.**

This versatile Atomic Absorption system features a microprocessor-based Data Center offering the user unprecedented flexibility. With the program cards provided, you can easily tailor system performance to meet your own individual operating requirements.

Data Center's program cards offer a wide variety of different curve corrections and calibrations. The SP2900 provides simultaneous high accuracy background correction over a wider absorbance range. Data Center does the calculations, thus allowing you to do the chemistry!

You'll find that the SP2900 system offers a new level of precision, sensitivity and detection limits, all of which are backed up with fully-published specifications.

Beyond its pace-setting performance, there are many more reasons to see the SP2900 in action: Every Pye Unicam Atomic Absorption system is backed by comprehensive applications, sales and service assistance throughout North America and overseas.

Invest a few minutes of your time to request our Atomic Absorption information package, or see a demonstration of this powerful system. We think you'll find it programmed for *your* applications.


CIRCLE 167 ON READER SERVICE CARD

**Philips Electronic Instruments, Inc.**
A North American Philips Company

85 McKee Drive, Mahwah, N.J. 07430
Telephone (201) 529-3800

International — Contact Pye Unicam Ltd.
York Street, Cambridge, England CB1 2PX
Telephone, Cambridge (0223) 58866
Telex 817331

PHILIPS

**Electronic Instruments**

## X-ray Energy-Dispersive Analysis

EEDS-II is a low-priced energy dispersive x-ray analysis system. Major features include a flicker-free 11½-in. color TV display, a single, compact console, a 2048-channel multiported data storage memory, and convenient and simple controls. Additional features include a ratemeter, liquid-nitrogen monitor, smooth/strip capability, digital line scan, and multiple log displays. Ortec Inc. **421**

## Wheatstone Bridges

Models RN-1B and RN-3A effectively measure DC resistance values in ranges from 1 to 9 999 000 ohms. A self-contained power supply, which consists of three D-cells, is adequate for measurement in the lower portions of the ranges. An external power supply is available for increased sensitivity in the higher ranges. Model RN-3A also provides ratio settings used for Murray and Varley loop tests. Beckman Instruments, Inc. **424**

## Quartz Digital Thermometer

Model 2804A quartz thermometer with a range from −80 to 250 °C has a usable resolution of 0.0001 °C. It is more rugged and easier to use than standard grade platinum thermometers and also out performs industrial platinum, thermistor, and thermocouple thermometers in stability, repeatability, accuracy, and probe interchangeability. Two probe inputs and very high resolution make the 2804A ideal for differential measurements. Major features include selectable resolution, interchangeable probes, an analog output option, an IEEE-488 bus option, and simplified calibration. Hewlett-Packard Co. **422**

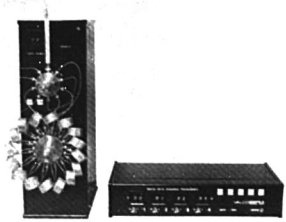

**Multiloop Autosampler, an automatic sampling system** for liquid chromatography, is designed for high reliability, ease of operation, and for applications where sample waste is critical. The sampler includes a low-pressure service 16-loop, 34-port automatic valve, a sample loading pump and digital timing system, and an automatic 7000 psi Universal HPLC injector. Operation may be in either normal mode or low sample waste modes. Valco Instruments Co. **405**

## Automatic Sampler

Model 420 auto sampler, designed for the completely automatic operation of the Series 2 and 3 liquid chromatographs, can also be used with almost any modern LC and integrator. Features include unattended analyses of up to 42 consecutive samples and operation in either the isocratic or gradient modes. Multiple input-output connection allows the auto sampler to be operated by either the LC systems or the timed event outputs of integrator computer systems. Conversely, the Model 420 can be used to control the LC and integrating instruments. Time delay settings are provided to accommodate programming or integration requirements. Perkin-Elmer Corp. **411**

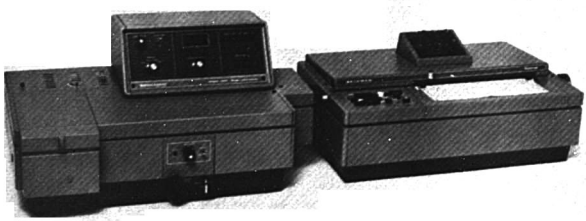

**Model 3600 recording UV/visible spectrophotometer** features holographic gratings and common optics. Holographic gratings assure higher optical uniformity and lower stray light, typically 0.05% at 220 nm. Common optics, the same mirrors in both sample and reference beam paths, provides flatter baselines and more precise absorbance measurements. The Model 3600 also offers both programmed and fixed slits. This choice enables the operator to record at constant signal/noise ratios with automatic programmed slits, or at a constant spectral bandpass by selecting any fixed slit width from 0.05 to 2.0 mm. Beckman Instruments, Inc. **406**

## Tunable Dye Laser

TFDL-1 high average power dye laser is a tunable instrument that can be adjusted to any color in the visible or near infrared spectrum (430–900 nm). Average power is 3–10 W. The laser provides low beam divergence and has a pulse-to-pulse repeatability of better than ±5%. It attains a rep rate of 30 Hz at 300-kW peak power and can achieve rep rates of 200 Hz at lower peak powers. It can be equipped for high average power in the ultraviolet range by frequency doubling. $25 000–$30 000. Candela Corp. **423**

## Preparative HPLC Columns

Chromegaprep columns are offered in 30- and 50-cm lengths and are packed with 10-μ particles of narrow particle size distribution. Column diameters are 9.6 mm i.d. (½ in. o.d.) and are equipped with ½–1/16-in. reducers on both ends. Columns of 1 and 2 in. diameters are available upon request. They are available in adsorbants as well as the following bonded phases: Chromegabond $C_{18}$, $C_8$, $C_2$, $C_1$, $NH_2$, CN, diol, cyclohexane, sulfonate, ether, WAX, and SCX. ES Industries **425**

# Chemicals

## Standard Solutions

Fourteen standard solutions for use in volumetric analysis and three buffer solutions (pH 4, pH 7, and pH 10) are now available. To assure quality and reliability, these solutions have been compared to NBS Standard Reference Materials. J. T. Baker Chemical Co. **430**

## Acids

Ultrahigh-purity Ultrex sulfuric, nitric, hydrochloric, and perchloric acids are available in 1-L sizes. Trace impurities are measured at the ppb level and lower. A Certificate of Analysis accompanying each bottle provides the detailed actual lot analysis. J. T. Baker Chemical Co. **431**

## Toxicity Control Gases

Certified standard gases on the NIOSH Priority Toxic Substances list are available. These gases are custom blended to any standards and to concentrations of less than 10 ppm to more than 1000 ppm and include ethylene oxide, propylene oxide, and styrene oxide. Liquid Carbonic Corp. **432**

# Manufacturers' Literature

**HPLC Columns.** Discusses the care and use of high-performance liquid chromatography columns packed with microparticle stationary phases. 20 pp. Whatman Inc. **435**

**Image Processing Newsletter.** The *Optronics Journal* is a quarterly newsletter devoted to the economic, scientific, and application sides of digital image enhancement, information extraction, and quantitative restoration techniques. The latest issue features an article on microdensitometry in crystallographic studies. 4 pp. Optronics International, Inc. **436**

**Process Control Programming System.** Describes the Model 7801 system of standard program control modules. Each system can be tailored to the demands of the process by a selected mix of standard module types, ranges, features, and options. 4 pp. Eurotherm Corp. **437**

**Hydrogen Sulfide Detection System.** Features the Colortec $H_2S$ detectors for simple, semiquantitative $H_2S$ measurements in applications ranging from personnel monitoring to area-wide transport studies. 4 pp. Metronics Associates, Inc. **438**

**Thermal Analysis Literature.** Lists 85 selected thermal analysis application studies, reprints, and newsletters. Topics covered include organic, inorganic, polymer, and pharmaceutical applications. 8 pp. Perkin-Elmer Corp. **439**

**Thin-Layer Chromatography.** Product guide includes information on Linear-K recoated plates, reversed-phase plates, high-performance TLC plates, classical silica gel plates, and supplies and accessories for TLC. 24 pp. Whatman Inc. **440**

**Recorders.** Describes the features, performances, specifications, and power requirements for complete line of strip chart recorders, recorder multiplexers, and recorder calibrators. 8 pp. Bailey Instruments **441**

**Infrared Analysis.** Bulletin IRB-56 describes the computed difference spectrum for latex occurring as an emulsion in water. Bulletin IRB-57 presents an analysis of shampoo in which the major constituents are separated by solvent extraction and column separation and identified by infrared spectroscopy. Perkin-Elmer Corp. **442**

**Gas Chromatography/Mass Spectrometry.** The November 1977 issue of *Pinnacle* features an article on the design concept and analytical advantages of simultaneous but separate chemical ionization and electron impact ionization, a feature of the Simulscan GC/MS system. 6 pp. Extranuclear Laboratories, Inc. **443**

**Gas Analyzers.** Describes the complete product line of quadrupole residual gas analyzers and mass spectrometer systems. 8 pp. CVC Products, Inc. **444**

**Strip Chart Recorders.** Describes the Models SDR 301 with single input span of 10 mV, SDR 302 with seven selectable input spans, and SDR 306 dual-channel recorder with independent multiple span switching. 1 p. Schoeffel Instrument Corp. **445**

**Immunochemistry System.** System combines advanced microprocessor control with state-of-the-art nephelometry to simplify and speed analysis of specific proteins. 12 pp. Beckman Instruments, Inc. **446**

**High-Performance Liquid Chromatography.** Product guide includes information on columns, media, adsorption chromatography products, reversed-phase chromatography products, ion-exchange chromatography products, and supplies and accessories for HPLC. 56 pp. Whatman Inc. **447**

**Environmental Laboratories.** Describes the Models DR-EL/1 and DR-EL/1a, portable kits containing all reagents and apparatus needed for 23 water tests. 5 pp. Hach Chemical Co. **448**

**Fluorescence Detectors for Liquid Chromatography.** Features Models LC-1000, 204S, 204A, MPF-43A, and MPF-44A fluorescence spectrophotometers especially adapted for detecting samples in LC fractions. 6 pp. Perkin-Elmer Corp. **449**

**Chromatography Data System.** Describes the features and applications of the SP4000 data system and illustrates the accuracy and speed of data processing from as many as 16 gas and/or liquid chromatographs. 16 pp. Spectra-Physics **450**

**Dipping Probe Colorimeters.** These colorimeters feature a fiber optic probe that is dipped directly into the solution to be tested for colorimetric and turbidimetric determinations. 20 pp. Brinkmann Instruments Inc. **451**

**Metals Chemistry.** Describes services available for the qualitative and quantitative determination of metals and their


KEVEX
SCORES THREE
XRF
FIRSTS!

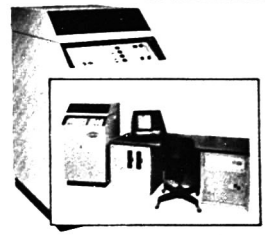

The new Kevex 0700 system is the second generation laboratory analysis XRF system, offering these important advances:

**1.** First commercial low wattage X-ray tube for both secondary target and direct sample excitation.
**Advantages:** Optimizes your ability to select the best sample analysis strategy. Eliminates the need for external cooling, 220 V power and expensive HV generator previously required for secondary target operation. Reduces system size and cost.

**2.** First quantitative software package providing your choice of either theoretical or empirical matrix correction.
**Advantages:** Simplifies and reduces the calibration and standardization requirements for quantitative analysis. Allows quantitation of thin films and irregular surfaces (chips and turnings). Features EXACT as a matrix correction system, flexible to your needs.

**3.** First completely automated XRF system.
**Advantages:** Computer (or manual) control of direct or secondary sample selection, filters, targets, excitation voltage and current are all standard on the 0700 system.

Call or write for literature. Better yet, visit us for a demonstration and analysis of your samples.

kevex

KEVEX CORPORATION
1101 Chess Drive • Foster City, CA 94404
Phone (415) 573-5866

CIRCLE 116 ON READER SERVICE CARD

purity. Techniques used include emission spectrometry, x-ray diffractometry, and x-ray fluorescence spectrometry. United States Testing Co., Inc. **452**

**Nitrogen Detection.** *Application Notes* features articles on the application of the Model 703 nitrogen detection system for the determination of morpholine preservative and for determining chemically bound nitrogen. 4 pp. Antek Instruments, Inc. **454**

**Infrared Spectrophotometers.** Features a wide range of IR supplies including liquid sampling cells, dies, KBr powder and hydraulic press for solid sampling, microsampling pelleting kits, gas sampling cells, and specular reflectance and multiple reflection accessories. 8 pp. Beckman Instruments, Inc. **455**

**Instrumentation Tape Recorder.** Describes the Model SE7000M, which combines the capacity and performance of laboratory installation with the versatility and operational simplicity of a fully portable general-purpose field recorder. 6 pp. EMI Technology Inc. **456**

**Liquid Chromatography.** A methods development guide is designed to aid the chromatographer in the selection of a suitable column and mobile phases for his purposes in the various modes of liquid chromatography: adsorption, partition, and ion exchange. Two other reports present column performance criteria and information on the Zorbax CN polar bonded phase packings. Du Pont Instruments **453**

## Catalogs

**Tools for Synthesis.** Lists compounds used in general laboratory and industrial synthesis, in polymer synthesis, and in the synthesis of organometallics. Also includes reagents for the determination of functional groups and lists of organometallics and complex salts. 22 pp. Publication No. JJ-195 available from Eastman Kodak Co., Department 412-L, Rochester, N.Y. 14650

**For more information on listed items, circle the appropriate numbers on one of our Readers' Service Cards**

**Chromatography Columns.** Describes new line of precision-designed columns made of high-quality borosilicate glass. Columns feature low dead space to minimize mixing of separated zones, allowing high resolution by ascending or descending flow. 5 pp. Amicon Corp. **458**

**Materials for Evaporation and Sputtering.** Includes full line of sputtering and evaporation equipment and over 300 metals, alloys, and nonmetallic materials up to 99.99+% purities. Materials Research Corp. **461**

**Stainless Steel Lab Products.** Lists a wide variety of items including portable pressure vessels, carboys, vacuum line fittings, Dewar flasks, reaction flasks, tanks, storage containers, and miscellaneous small utensils. 24 pp. Pope Scientific, Inc. **460**

**Optics and Optical Filters.** Features an expanded line of surplus items priced at 10–40% of list as well as the complete line of standard stock optical filters. 28 pp. Corion Corp. **463**

GCA CORPORATION

# 105nm TO 60μm

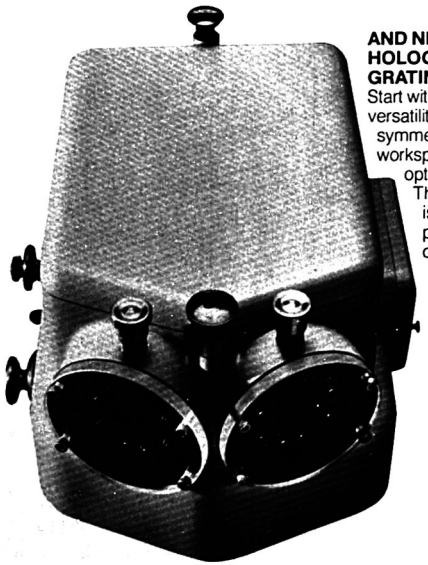

**AND NEW HOLOGRAPHIC GRATINGS**

Start with wavelength versatility. Add symmetrical profiles and plenty of workspace. Then add the new option of holographic gratings. The 0.3 meter McPherson 218 is destined to remain the most popular vacuum monochromator in the field.

Add the new McPherson 786 controller, and you scan digitally at 13 speeds from .05 to 500 nm/minute with TTL compatibility. The 786 retrofits any 218 and many other McPherson instruments.

Call (617) 263-7733, at our Acton, Mass., technical center for more information. Or write McPherson Instruments, **GCA/Precision Scientific Group,** 3737 West Cortland Street, Chicago, Ill. 60647

McPHERSON™
DOES IT WITH PRECISION

CIRCLE 88 ON READER SERVICE CARD

**Chemicals.** Chemalog 77/78 lists over 8000 biochemicals and organics including amino acids, t-BOC amino acids, peptides, peptide reagents, buffers, clinical chemicals, enzyme substrates, ion-exchange resins, molecular sieves, and nucleic acids and derivatives. Chemical Dynamics Corp. **459**

**Pressure Chemicals.** Features complete listings and prices of polystyrene sulfonate standards, metal carbonyls and their derivatives, liquid crystals and cholesteric esters, polymer standards, organophosphorus and organoarsenic compounds, and specialty chemicals. Catalog will be continually updated. To order send $1.00 each to Pressure Chemical Co., 3419 Smallman St., Pittsburgh, Pa. 15201

**Chart and Graph Papers.** Features comprehensive listing of chart and graph papers includingsquare-grid sheets, time-cycle sheets, data sheets, semi- and full-logarithmic sheets, rectangular-grid sheets, metric sheets, and other miscellaneous sheets. 36 pp. Codex Book Co. **462**

**Spectrophotometric Solvents.** Provides complete specifications for 38 spectrophotometric solvents. Also includes toxicity data, spill and disposal procedures, proper handling and storage conditions, effects of overexposure, and first-aid procedures. 52 pp. Eastman Kodak Co., Department 412-L, Rochester, N.Y. 14650

**Thin-Layer Chromatography.** Contains full line of products including equipment for TLC, paper chromatography, fraction collection, rotary flash evaporation, and viscosity determinations. Scientific Manufacturing Industries **467**

**Reagents for Acrylamide Gel Electrophoresis.** Includes information on gel-forming reagents, catalysts and initiators, buffers, dyes and stains, and miscellaneous reagents. Price list included. 12 pp. Eastman Kodak Co., Department 412-L, Rochester, N.Y. 14650

**Plastic Laboratory Products.** Features complete line of Lancer precision-molded polystyrene, polypropylene, and polyethylene products. 12 pp. P. J. Cobert Associates **468**

**Optical Mounts.** Includes over 1000 products including mounts, stages, laser application equipment, optics, vibration-stable platforms, and nondestructive testing systems. Introductory discussions provide the basics of lasers and holography. 100 pp. Newport Research Corp. **464**

**pH Meters.** Includes over 125 electrodes, pH meters with normal and expanded scale as well as digital readout, oxygen meters, conductivity meters, colorimeters, and tutorial data on pH and specific-ion electrodes. 24 pp. Chemtrix, Inc. **465**

**Safety Supplies.** Features complete line of safety supplies to assist in meeting OSHA regulations. Includes new reusable dust respirators and toxic gas monitoring equipment. 72 pp. Interex Corp. **471**

**Liquid Scintillation Chemicals and Solutions.** Features the complete line of high-efficiency liquid scintillation cocktails for aqueous and nonaqueous counting. 10 pp. National Diagnostics **472**


# 0.01nm RESOLUTION

**AND A NEW PROGRAMMER**

0.01 is for a regular 1200 G/mm grating. Results are equally impressive with other snap-in gratings, including holographic types. Model 2051 makes your work free of error from astigmatism, coma and spherical aberration, 185 nm to 78 $\mu$m.

Add the modestly priced new McPherson 786 controller, and you scan digitally at 13 speeds from .05 to 500 nm/minute with TTL compatibility.

Call (617) 263-7733, at our Acton, Mass., technical center for more information. Or write McPherson Instruments, **GCA/Precision Scientific Group,** 3737 West Cortland Street, Chicago, Ill. 60647

GCA CORPORATION

**McPHERSON.™**

DOES IT WITH PRECISION

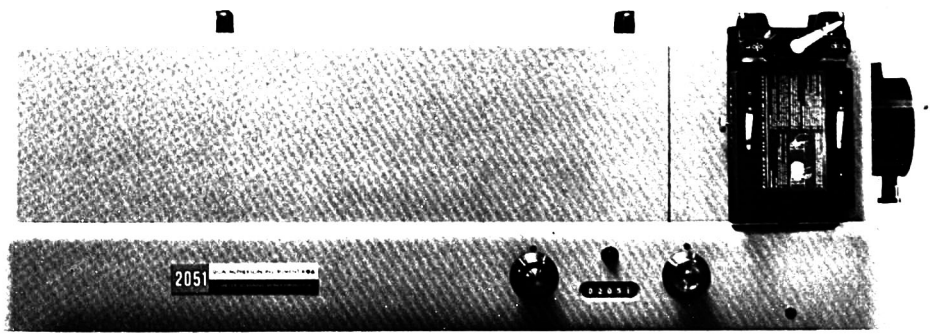


CIRCLE 89 ON READER SERVICE CARD

# Systematic Materials Analysis VOLUME 4

Edited by J. H. RICHARDSON and R. V. PETERSON

*A Volume in the MATERIALS SCIENCE AND TECHNOLOGY Series*

CONTENTS: *J. Ramirez-Muñoz*, Atomic-Absorption and Atomic-Fluorescence Flame Photometry. *T. A. Whatley and E. Davidson*, Ion Microprobe. *R. F. Skinner and E. Heron*, Mass Spectrometry. *R. V. Peterson*, Molecular Weight Determinations. *M. H. Mueller*, Neutron Diffractometry. *S. Kinsman*, Particulate Characterization. *J. H. Richardson*, Polarimetry. *P. Zuman*, Polarography and Related Methods. *S. K. Kurtz and J. P. Dougherty*, Methods for the Detection of Noncentrosymmetry in Solids. *E. M. Barrall, II and R. J. Gritter*, Technique of Materials Analysis—A Dynamic Thermal Approach to Materials Analysis. *J. C. Williams and N. Paton*, Transmission Electron Microscopy.

*1978, 512 pp., $49.50/£32.15; Subscription Price, $42.00*
*ISBN: 0-12-587804-4*

Subscription prices are valid only on orders for the complete set received before publication of the last volume. Subscription prices are not valid in the U.K., Australia, or New Zealand.

# Catalysis in Organic Syntheses 1977

Edited by GERARD V. SMITH

Covering practical and theoretical applications of catalysis in organic chemistry, this collection of papers offers the organic chemist a glimpse at some novel catalytic systems as well as an update of more traditional systems. A broad scope of topics are examined for both the casual catalysis reader and the specialist. The articles are at the research level and include both informative reviews and advanced research papers. The interdisciplinary nature of many articles makes them valuable to the practical organic chemist. The papers comprise the proceedings of the Sixth Conference on Catalysis in Organic Syntheses held by the Organic Reactions Catalysis Society in Boston on May 10-11, 1976.

SECTION HEADINGS: Hydrogenation. Special Topics. Unusual Catalysis and Special Preparations.

*1978, 296 pp., $15.00/£10.65 ISBN: 0-12-650550-0*

# Optoacoustic Spectroscopy and Detection

Edited by YOH-HAN PAO

CONTENTS: *L. B. Kreuzer*, The Physics of Signal Generation and Detection. *J. D. Stettler and N. M. Witriol*, Energy Transfer Mechanisms. *C. F. Dewey, Jr.*, Design of Optoacoustic Systems. *J. A. Gelbwachs*, Tunable Radiation Sources in the Ultraviolet and Visible Spectral Regions (0.1-1.0 μm). *P. L. Kelley*, Tunable Infrared Laser Sources for Optoacoustic Spectroscopy. *P. C. Claspy*, Infrared Optoacoustic Spectroscopy and Detection. *M. B. Robin*, Photoacoustic Spectroscopy of Gases in the Visible and Ultraviolet Spectral Regions. *A. Rosencwaig*, Solid State Photoacoustic Spectroscopy.

*1977, 256 pp., $19.00/£13.50 ISBN: 0-12-544150-9*

# Essays in Chemistry VOLUMES 6 and 7

Edited by J. N. BRADLEY, R. D. GILLARD and R. F. HUDSON

CONTENTS OF VOLUME 6: *L. D. Pettit and G. Brookes*, Why Stability Constants? *D. R. Williams*, Bio-Inorganic Calorimetry. *A. J. Lawson*, Thermal Homolytic Rearrangements. *J. H. P. Utley*, Electro-Organic Reactions.

*1977, 124 pp., $9.35/£4.80 ISBN: 0-12-124106-8*

CONTENTS OF VOLUME 7: *T. J. Kemp*, Problems in Photochemistry of Transition Metal Compounds. *A. J. McCaffery*, The Faraday Effect. *M. F. Pilbrow*, Chemical Transport Reactions. *J. Feeney*, Carbon-13 Nuclear-Magnetic Resonance Spectroscopy.

*1977, 108 pp., $9.35/£4.80 ISBN: 0-12-124107-6*

# Spectral Atlas of Nitrogen Dioxide 5530Å to 6480Å

By DONALD K. HSU, DAVID L. MONTS and RICHARD N. ZARE

*Spectral Atlas of Nitrogen Dioxide* makes available to the general scientific community high resolution spectra of the visible system of nitrogen dioxide in the wavelength region accessible to the most efficient of the dye lasers. The authors begin by introducing the spectroscopic nomenclature used throughout and by reviewing comprehensively the puzzling features of $NO_2$, about which more than two man-millenia of research has been spent, still without a full explanation as to $NO_2$'s anomalous behavior. The major portion of the book is a line atlas, presented in Chapter One, covering the region 5530Å to 6480Å and listing approximately 19,000 prominent lines. Chapter Two is a collection of all rotational analyses in the region from 5700Å to 6800Å. Also included are the unpublished laser excitation spectra of Smalley, Wharton, and Levy, obtained with a seeded beam of $NO_2$ rotationally cooled to a few degrees Kelvin by supersonic expansion. Chapter Three provides an annotated bibliography of nitrogen dioxide arranged according to a structural classification and containing over 500 references.

*1978, 646 pp., $39.50/£25.65 ISBN: 0-12-357950-3*

Send payment with order and save postage plus 50¢ handling charge.
Orders under $15.00 must be accompanied by payment.
*Prices are subject to change without notice.*

## ACADEMIC PRESS, INC.

*A Subsidiary of Harcourt Brace Jovanovich, Publishers*
111 FIFTH AVENUE, NEW YORK, N.Y. 10003
24-28 OVAL ROAD, LONDON NW1 7DX
CIRCLE 1 ON READER SERVICE CARD

# An Aid for the Practicing Chromatographer

**Chromatographic Systems—Maintenance and Troubleshooting.** 2nd Ed. J. Q. Walker, M. T. Jackson, Jr., and J. B. Maynard. xiii + 359 pages. Academic Press Inc., 111 Fifth Ave., New York, N.Y. 10003. 1977. $14.95

*Reviewed by R. E. Pecsar, Varian Assoc., 611 Hansen Way, Palo Alto, Calif. 94303*

Many texts exist on the principles of chromatography, but there has been a need for one devoted to the practicing chromatographer who wants to master his chromatograph. This book abounds with helpful operating hints and diagnostic techniques to optimize the instrument and nurse it back to health when troubles occur. The book also serves as an introduction to the techniques of liquid chromatography (LC) and gas chromatography (GC), as basic operating principles occupy about 50%. This may seem like undue emphasis, but if one does not appreciate what proper operation is, one will not recognize a problem. Understanding the basics also helps to direct one to the culprit more rapidly when troubleshooting a system.

The authors could have improved their cohesiveness by making one introductory theory chapter and including a single glossary for GC and LC. More attention to ASTM-approved nomenclature would also have been beneficial. The LC treatment of pumping systems and inlets is excellent. The detector chapter gives cursory treatment to variable wavelength UV/VIS detectors. These are the most rapidly growing type today.

The GC theory includes very beneficial parametric curves demonstrating the effect of operating variables on efficiency. Pneumatics are also well treated with practical discussions of all flow components. Inclusion of pyrolysis is worthwhile, but instead of treating the topic in the general format of the text, it is presented as an historical review, which is very much out of context. A good review of all significant types of GC detectors is included. The treatment of characteristic properties could use significant rewording. As the Coulson conductivity detector is used only limitedly, too much emphasis was given to this detector.

GC detector electronics and recorders are well done, but the discussion of data reduction devices is not representative of 1977 technology. Microprocessor-based systems with memory have captured the market, but the text treats this subject from a 1971 perspective.

GC and LC columns also suffer from a lack of currentness. In LC, pellicular packings are not the hope of the future, and liquid-liquid chromatography is nearly obsolete. Bonded phases on small totally porous supports are used by the majority of LC practitioners. In GC, stationary phase structures are very helpful, but squalane has not been seriously used since the advent of SE30. The OV series are currently the most popular.

Lest the reader of this review be misled, I heartily recommend this text overall. The comprehensive troubleshooting charts are very well done, and will be a savior for less experienced chromatographers. In addition, most chapters close with a question and answer format which practically applies the material covered on that topic.

The price of the text is reasonable, but unfortunately little or no attention is paid to proofreading. In reading the text, 162 errors were discovered. In spite of this, I expect to see this text in the lab working with the chromatographer, and not sitting on a library shelf.

**Vibrational Spectra of Organometallic Compounds.** Edward Maslowsky, Jr. xii + 528 pages. Wiley-Interscience, 605 Third Ave., New York, N.Y. 10016. 1976. $24.95

*Reviewed by James R. Durig, College of Science and Mathematics, University of South Carolina, Columbia, S.C. 29208*

The author has intended to provide a comprehensive review of the literature dealing with infrared and Raman spectra of organometallic compounds. He has included all compounds that contain a direct metal carbon interaction except those compounds that contain only carbonyl or cyano ligands or both unless other types of metal carbon interaction are found in the compounds. The definition used for a metal is rather broad in that the author has included the elements boron, silicon, germanium, phosphorus, arsenic, antimony, selenium, and tellurium, in addition to those elements more generally defined as metals. The literature reviewed includes work published up to the end of April 1976. In this reviewer's opinion, the author has admirably attained his goal of a comprehensive review in the area.

This comprehensive review of the literature is intended for vibrational spectroscopists and for inorganic chemists interested in characterizing the structures of organometallic compounds. Additionally, graduate or undergraduate students interested in organometallic or inorganic chemistry would find the book very useful. It is written at a level where the author has assumed that the reader has a fair knowledge of vibrational spectroscopy with an understanding of normal vibrations and character tables with their accompanying symmetry notation.

The book is divided into three sections. The first section is entitled "Alkyl Organometallic Derivatives". This section takes up approximately half of the book and includes 1014 references. The author discusses the vibrational assignments and lists most of the important group frequencies for representative compounds. Many of the assignments in comprehensive tables are summarized and the structural implications are discussed when appropriate. In the discussion of the structures, references have also been included on the application of other physical techniques such as single crystal x-ray, NMR, and electron diffraction studies to provide data relevant to the conclusions reached from vibrational studies. In most of the structural cases discussed, vibrational data are provided and the conclusions by the original workers are included. When controversy exists concerning the interpretations of the data, the author has presented both viewpoints. In many places he has indicated where there are inconsistencies in assignments and also where controversies exist in such assignments.

The second section of the book deals with "Non-Cyclic Unsaturated Organometallic Derivatives" and consists of 66 pages with 267 references. Again, the author has done an exceptionally good job in presenting the data and the various reasons for structural conclusions when appropriate.

The third section of the book is concerned with "Cyclic Unsaturated Or-

ganometallic Derivatives" and contains 205 pages with 852 references. This section includes data on three-, four-, five-, six-, seven-, eight- and nine-carbon rings. The activity of the normal modes is indicated, and many of the frequencies for the most important vibrations are listed. Conflicting assignments are reported, and reasons given for some of the problems. When data are sufficient for a structural determination, the author has so stated. In general, this section provides a comprehensive review of the infrared and Raman spectra of these compounds and includes supporting data whenever available.

In general, the book is very readable and contains few errors. A 21-page subject index is included. An exceptionally good job has been done in providing a comprehensive review of these organometallic compounds, and it is quite clear from reading the text that the author has carefully read the references he cites. One error appears on page seven in which the author has stated that "most vibrational studies have been in solution or in the liquid or vapor phases in which free rotation of the methyl groups is found". This statement appears in the section on methyl compounds, $(CH_3)_nM$ complexes, and the statement is not true with the possible exception for $(CH_3)_3B$ where, apparently, the barrier for internal rotation of the methyl groups in this compound is very small and can be considered as essentially free. For other molecules, such as the ones discussed in this chapter, the barriers are appreciable, irrespective of the physical state.

In conclusion, I believe most organometallic chemists and vibrational spectroscopists would find the book a welcome addition to their library. It is very reasonably priced, and although printed from a typewritten copy, it is very easily read and well illustrated.

**Analysis of Drugs of Abuse.** Eleanor Berman. x + 80 pages. Heyden & Son Inc., Kor-Center East, Bellmawr, N.J. 08030. 1977. $11

*Reviewed by Peter Jatlow, School of Medicine, Yale University, 333 Cedar St., New Haven, Conn. 06510*

Whether this book can be considered a success or failure depends upon a definition of the audience. As a "compact definitive book for the specialist" as stated by the publishers, it fails badly. As an overview for the neophyte, a goal expressed by the author in the introduction, it may be useful.

The title is misleading in that the book does not restrict itself to drugs of abuse. Granted that in the broad sense any inappropriately used drug is "abused", the toxicologist looks upon the analysis of drugs of abuse as the qualitative screening of urines for certain alkaloids, certain other bases, and barbiturates, in support of drug dependency treatment programs or for medical-legal purposes. Throughout the book, discussions of drug abuse and overdose are mixed, and indeed the case histories concern overdose. Actually, a chapter on therapeutic monitoring is also included although only seven pages are devoted to this complex field.

A considerable proportion of the limited space is spent on history and outdated techniques. This would be acceptable except that their evolution into modern day technology is never clarified. Also inappropriate are the detailed, but simplistic descriptions of the principles of the various forms of instrumentation. These descriptions are too superficial to be of use


# This Flame Ionization Gas Chromatograph Is Dedicated To Benzene Vapor Detection


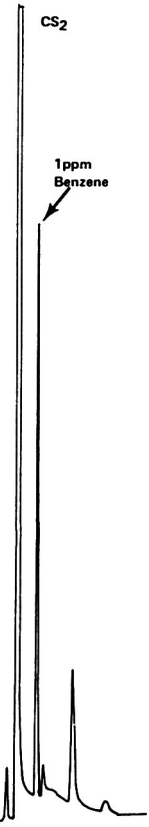


Attached is a routine chromatogram for benzene. It was run in less than three minutes. Sensitivity is at least comparable to more expensive FID Gas Chromatographs.

GOW-MAC's 750 FID Gas Chromatograph provides a precise and practical check for benzene vapors using the OSHA recommended method of collection of organic vapors on an adsorbent, desorption and analysis by gas chromatography.

OSHA's new emergency limit (and proposed permanent regulation) is 1 ppm exposure for benzene averaged over an 8 hour period.

A good reason why a dedicated FID should be in your lab is that it can keep your high priced GC more available by handling the routine work.

For prices, specs, applications, contact us or use the reader service number.

GOW MAC

**GOW-MAC INSTRUMENT CO.**
P.O. Box 32, Bound Brook, NJ 08805
Telephone: 201/560-0600
Shannon Free Airport, Co. Clare, Ireland
Telephone: 61632 Telex: 6254

CIRCLE 86 ON READER SERVICE CARD

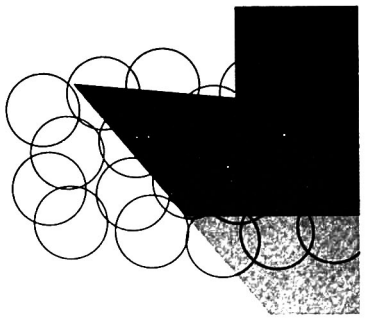

# Catalysts for the Control of Automotive Pollutants

Advances in Chemistry Series No. 143

James E. McEvoy, *Editor*

*A symposium sponsored by the Division of Industrial and Engineering Chemistry and co-sponsored by the Board-Council Committee on Chemistry and Public Affairs, the Division of Environmental Chemistry, the Division of Fuel Chemistry, and the Division of Petroleum Chemistry of the American Chemical Society.*

An up-to-date status report on the latest research by auto makers, catalyst companies, universities, and chemical and petroleum companies on all aspects of catalytic conversion to reduce automotive emissions.

The scope of coverage in this timely volume makes it an ideal reference text on analytical methods, mechanisms of catalytic removal, and catalysts themselves.

Specific topics examined in fourteen papers include:

- thermocatalytic detection of $NO_x$ and factors affecting catalyst activity
- thermodynamic interaction between catalyst and exhaust, degradation of control catalysts, and oxidation of CO and $C_2H_4$
- resistance of catalysts to thermal deactivation, variation of selectivity, catalyst poisoning, and the nature of the catalyst support.

199 pages (July 1975) $19.95 clothbound

SIS/American Chemical Society
1155 16th St., N.W., Wash., D.C. 20036

Please send _____ copies of *No. 143 Catalysts for the Control of Automotive Pollutants* at $19.95 per book.

☐ Check is enclosed for $_____. ☐ Bill me.
Postpaid in U.S. and Canada, plus 40 cents elsewhere.

Name _____

Address _____

City _____ State _____ Zip _____

---

S.G.E.

**gas chromatography mass spectrometry**

# accessories

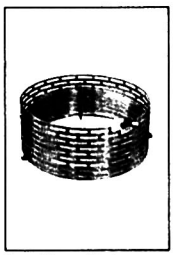

Capillary Columns and Support Cages

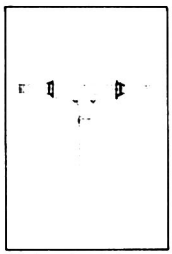

Molecular Jet Separator

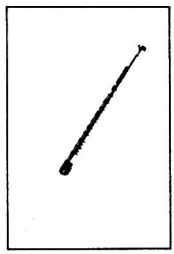

Syringes

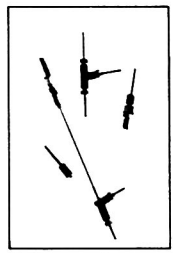

Valves and Low Hold-Up Unions

Glass Lined Tubing and Graphite Ferrules

**Head Office**
Scientific Glass Engineering Pty. Ltd.,
111 Arden Street
North Melbourne, Australia 3051
Tel: 329 6633

**U.S. Office**
Scientific Glass Engineering, Inc.
2800 Longhorn Blvd., Suite 104
Austin, Texas 78759
Tel: 512/837-7190

**European Office**
Scientific Glass Engineering (U.K.) Ltd.,
657 North Circular Road,
London NW2 7AY, Great Britain
Tel: 01-452-6244

CIRCLE 191 ON READER SERVICE CARD

to the specialist, and yet are not likely to be understood by the novice. A disproportionate emphasis is placed on infrared spectrometry, now used relatively little in drug analysis. There are also a number of errors, which, however, are not likely to bother the probable audience for this book. Acetaminophen and theophylline, which are listed as neutral drugs, are actually acids and in fact can be easily back-extracted from organic solvents into dilute base. High-pressure liquid chromatography does not necessarily use a liquid for both the stationary and mobile phases. The fluorometric and colorimetric methods referred to for analysis of procaineamide do not necessarily measure both parent and drug metabolite. In fact, this is one of their limitations. In the description of immunoassays, labeled and unlabeled drugs are referred to as "bound and unbound", respectively, which is an incorrect use of this terminology. The therapeutic ranges indicated for diphenylhydantoin and phenobarbital are wrong.

On the positive side, an enormous amount of material is covered in 66 pages. The book successfully conveys the complexity of this field, including the purposes of drug analyses, the types of compounds of concern, and the various techniques that can be used. It also successfully communicates the concept of specificity, and the problems of interfering endogenous compounds found in complex biological fluids. The latter problem is often a revelation to analytical chemists who have never worked with biological materials.

While this book is too superficial to be of value to the expert, or even the student of toxicology, it could provide a quick, but good introduction for the chemist or graduate student who is considering entering the field of analytical toxicology or who simply wishes to know something about it. The insights into the field of drug analysis provided by this book are more valuable and accurate than are the fine details.

**Analysis of Drugs and Metabolites by Gas Chromatography–Mass Spectrometry; Volume 1, Respiratory Gases, Volatile Anesthetics, Ethyl Alcohol and Related Toxicological Materials.** B. J. Gudzinowicz and M. J. Gudzinowicz. vii + 223 pages. Marcel Dekker, Inc., 270 Madison Ave., New York, N.Y. 10016. 1977. $23.75

*Reviewed by William C. Butts, Clinical Chemistry Laboratory, Group Health Hospital, Seattle, Wash. 98112*

The preface to this volume states its objectives to be threefold: 1) to compile the GC and GC–MS procedures available for the analysis of the title compounds; 2) to describe these procedures in detail; and 3) to indicate the applicability of these procedures to pharmacokinetic studies. Hopefully, potential readers will not be misled by the title. One need not possess a GC–MS to use the procedures presented in this book; in fact, MS is mentioned in only approximately 10 pages of the text in the entire book, the remainder being devoted to GC procedures.

The book is essentially presented as a chronological review through 1974. Most of the articles referenced are abstracted in great detail, and although the book's authors do not provide much critical comparison of methodologies, sufficient detail is provided for the reader to draw his own conclusions. Chapter 1 is devoted


The CIRA® 101
Chromatographic INFRARED Analyzer

Routine Separation & Identification of Drugs of Abuse

The CIRA 101 is a gc-IR accessory designed specifically for separating multi-component mixtures into their pure constituents for infrared analysis. The unit contains a proprietary gas chromatograph integrated with an infrared cell which together fit into the sample compartment of any standard infrared spectrometer.

The CIRA has been used to separate and identify a variety of drug mixtures, including *amphetamines, barbituates, cocaines, etc.*

**Here, for demonstration we present a mixture of benzocaine, xylocaine, procaine, and cocaine prepared in equal parts.**

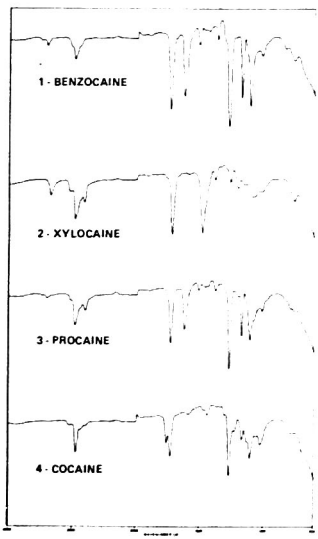


Infrared Spectra

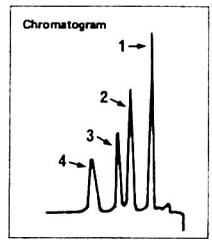


A 4 mg mixture of benzocaine, xylocaine, procaine, and cocaine was injected into the CIRA. The chromatogram of this mixture given by the CIRA is shown above. Each component was sequentially trapped as it eluted into the IR cell. The resultant IR spectra are shown.

Sadtler
Research Laboratories, Inc.
3316 Spring Garden St., Phila., Pa. 19104
(215) 382-7800

CIRCLE 192 ON READER SERVICE CARD

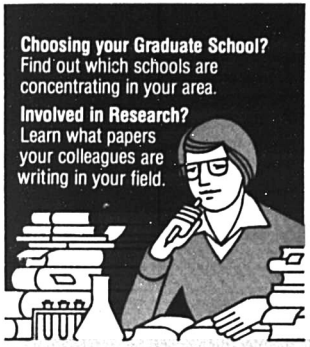


# The Directory of Graduate Research 1977

***Comprehensive listing of U. S. and Canadian Universities offering doctoral programs in chemistry, chemical engineering, biochemistry and pharmaceutical/medicinal chemistry including detailed information on research professors and their publications.***

Whether you are a recognized authority in your field, just about to start your graduate study, or concerned with research in chemical science, it is vital for you to know who is working in your area, what they are doing, and where they are doing it.

The Directory of Graduate Research lists complete information on universities—details on professors, the papers they have published, their areas of specialization. For added convenience, individual researchers are also listed alphabetically and individual telephone numbers are included in most cases.

Researcher or graduate student, you will find this comprehensive, 868-page, 8½ × 11 volume one of the best investments you can make. The cost is just $25.00.

To order your new 1977 copy, call: (202) 872-4364, write or mail the coupon below.

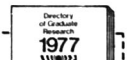


**Dept. 101**
**American Chemical Society**
**1155 16th Street, N.W.**
**Washington, D. C. 20036**

Please send me _____ copies of the Directory of Graduate Research, 1977 Edition @ $25.00 a copy.

Name _____

Affiliation (if any) _____

Address: ☐ Home ☐ Organization

_____

City _____ State _____

Zip _____ Phone _____

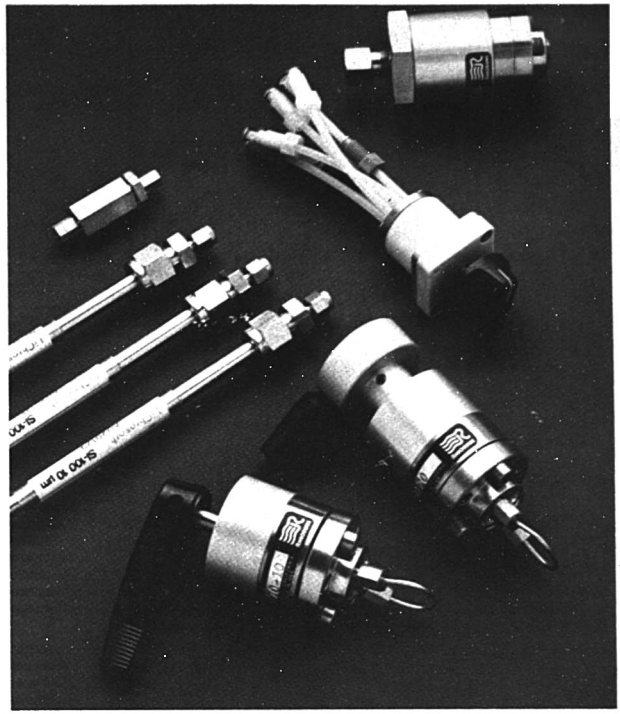

# You can't get a good chromotogram without a great beginning. We make it happen!

## VALVES, WELL PACKED HPLC COLUMNS AND FILTERS

In a way, we're sort of the front-end company in high pressure liquid chromatography. Almost everything you need to make better chromatograms in the beginning is on our shelf. Here's our line to you:

**The 70-10 Sample Injection Valve.** For just $290 you can get our 6-port sample injection valve with a removable sample loop and 7000 psi pressure rating. Size, 10 $\mu$1 to 2.0 ml.

**The 7120 Syringe Loading Sample Injector.** Fill loops conventionally or in the partial loop variable volume mode with only 0.5 $\mu$l sample loss.

**Teflon Rotary Valves.** For about half the cost you'd expecf to pay, we offer three, four and six way valves in 0.8 mm and 1.5 mm bores at $70 to $87. Features zero dead volume, chemical inertness and 300 psi rating.

**HPLC Columns.** Here are the columns with guaranteed peak symmetry and minimum plates per meter to doubly assure optimum column performance. Six columns currrently available priced from $180 to $240.

**The Column Inlet Filter.** It only costs a few dollars, but it can save you a boatload of trouble. Place this low dead volume filter between the injection valve and column to protect column inlet frits from plugging. Price, $40.

**The Model 7037 Pressure Relief Valve.** Protect your set-up against damage from over pressure (2000 to 7000 psi setting range).

**Write or call for more information.** Address Rheodyne, Inc. 2809 Tenth Street, Berkeley, CA 94710. Phone (415) 548-5374.

RHEODYNE
THE LC CONNECTION COMPANY
CIRCLE 178 ON READER SERVICE CARD

# The best GC/MS Data System just keeps getting better

When you look at the Riber 150 GC/MS Data System you may say it looks like the System Industries System 150.

Right and wrong.

The Riber 150 is based on the hardware and software of SI's System 150 first developed for use with quadrupole GC/MS in '69. It's now in use in hundreds of laboratories around the world.

But, we've already made a number of key hardware and software improvements to the system to increase it's capabilities for you. And, there are more in process.

Whether you're considering automating magnetic sector or quadrupole GC/MS, you won't find a data system that gives you better price/performance ... now or in the future.

That's because we've concentrated on developing a truly versatile data system that can easily be adapted to any GC/MS instrument. The Riber 150's modular flexibility lets you economically tailor a data system to meet your most exacting requirements.

In addition, we are carrying out an aggressive upgrade program with Ribermag, the number one GC/MS company in Europe, to insure the data system will keep pace with your state-of-the-art.

If you're considering automating your GC/MS instrumentation, find out more about the Riber 150, its proven price/performance and our plans to continually improve its value in your lab.

**RIBER DATA SYSTEMS**

1020 Corporation Way • Palo Alto, CA 94303 • (415) 961-2012
Telex 910-379-6474

In Europe contact:
RIBERMAG, Rueill
Malmaison, France,
Tel. 977.92.05

CIRCLE 179 ON READER SERVICE CARD


## Books

largely to analytical details for the analysis of respiratory gases, low-molecular-weight anesthetics, and a miscellaneous group comprised of sterilizing agents, organic solvents, and riot-control aerosol irritants. In addition to the articles referenced in the text, this chapter contains listings of general references under the categories: gas-liquid chromatography, mass spectrometry, integrated GC–MS, and pharmacology/pharmacokinetics. The highlight of the book is the extensive discussion of ethyl alcohol in Chapter 2 which includes a good discussion of the metabolism and pharmacokinetics of ethanol as well as analytical details. Chapter 2 concludes with a brief catch-all section on volatile constituents in human breath, fluids, and tissues. This section does not seem particularly pertinent to this volume other than to indicate some of the problems and techniques involved in handling volatile compounds.

As part of a multivolume series on GC–MS analysis of drugs, this book may find a place in many analytical and clinical libraries. As a single volume I feel its value is restricted to those involved specifically in the study of respiratory gases, volatile anesthetics, or ethyl alcohol.

**Fundamentals of RIA and Other Ligand Assays.** Jeffrey C. Travis. 168 pages. Scientific Newsletters, Inc., 2421 W. Broadway, P.O. Box 4546, Anaheim, Calif. 92803. 1977. $24

*Reviewed by W.H.C. Walker, Dept. of Pathology, McMaster University Medical Centre, 1200 Main Street West, Hamilton, Ont. L8S 4J9, Canada*

More than 50 million radioimmunoassays were performed in North America in the past year, but the quality of the results obtained continues too often to be inadequate. Interlaboratory comparisons demonstrate discrepancies of more than fourfold even when common reagents and standards are used. Errors introduced at the bench are passing unnoticed by the analyst. This lack of insight stems from the complexity of the procedure, the unpredictability of the standard curve which is inverse and nonlinear, and the failure of many protocols to identify critical steps in the operating procedures.

Dr. Travis has directed his text to the bench worker and succeeds in providing a clean uncluttered path through the maze of nomenclatural confusion. The common elements of all ligand assays are stressed, and the

artificial division between isotope and nonisotope assays, compounded by acronym abuse, has been removed.

There is a welcome absence of misuse of established terms such as "sensitivity", which has led to such confusion in the literature. As a further aid to comprehension, a glossary is provided that indicates those terms for which National Committee for Clinical Laboratory Standards definitions are available. The text lapses on page 42 by misusing the term "partition coefficient" where "response" or "dependent variable" is intended.

The author commendably manages to cover a range of basic concepts relating to antibody-ligand interaction such as titer, affinity, and binding capacity without demanding anything more than basic arithmetic skills. It is, however, essential that the mathematically unsophisticated reader shall not be misled, and both Figure 2 and Figure 11 contain calculation errors that demand early correction.

There is an error in question 10a (page 8), and question 23 (page 162) has the wrong answer. The section on reviews and suggested references strangely cites nothing after 1974 relating to radioimmunoassays although nonisotopic assay references are cited through 1977. The omission of several recent books must be corrected so that readers may progress to more practically oriented and advanced sources.

Despite the claim in the foreword, this book does not set out to be comprehensive. Its strength lies in presenting a complex and confusing subject in simple terms. It should be required reading for those involved in performing ligand assays. I am concerned only that its price will prevent the extensive use that it deserves.

## New Books

**Vibrational Spectroscopy—Modern Trends.** A. J. Barnes and W. J. Orville-Thomas, Eds. xiii + 442 pages. Elsevier Scientific Publishing Co., P.O. Box 211, Amsterdam, The Netherlands; 52 Vanderbilt Ave., New York, N.Y. 10017. 1977. $49.95, Dfl. 122

Twenty-six articles contributed by authors from the international community review recent advances in both infrared and Raman spectroscopy, with particular emphasis in the areas where these techniques have made the greatest contributions to studies of molecular structure and molecular behavior. The articles are divided into four major sections. The four articles in Section A on lasers and their applications in infrared spectroscopy re-


# Outstanding GC/MS performance from Europe's proven leader

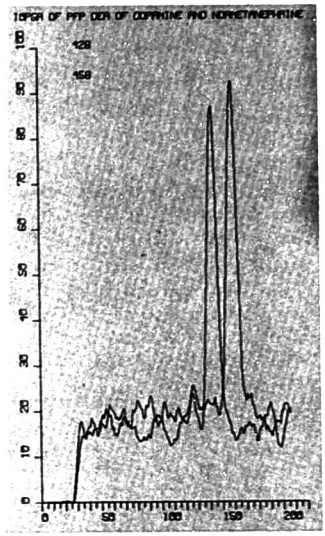


*A typical example of the picogram level detection for the PFP derivatives of two important biogenic compounds, dopamine and normetanephrine by Selected Ion Monitoring using RIBERMAG's advanced design ionization source. Chosen ions were m/e 428 for dopamine and m/e 458 for normetanephrine: up to 8 different ions may be selected simultaneously when the Riber Data System is being used.*

The highly versatile RIBERMAG GC/MS R 10-10 instruments offer such features as dual ionization switching from electron impact to chemical ionization mass spectrometry and back as well as two completely isolated diffusion pumping systems, 1000 L/sec for the ion source and 150 L/sec for the quadrupole filter.

A unique feature of the R 10-10 is the automatic protection provided by a modern pneumatic system which prevents an oil spill on the quadrupole probe in the event of power or vacuum failure.

Because of its large filter, the RIBERMAG R 10-10 demonstrates no mass discrimination even in the upper limit at mass 1000. It is by far the most stable quadrupole ever built.

No separator is used, even when GC carrier gas flow rates of 30 ml/min are used with 2mm 10-packed columns. The interface consistantly produces higher sensitivity with predictable repetition and insures perfect chromatographic resolution even in the most difficult cases.

If your work calls for consistantly high GC/MS performance, contact us today for more information on Europe's leading mass spectrometers.

**RIBERMAG**

49 Quai du Halage
92505 Rueil-Malmaison, France
(1) 977.92.05 Telex 692419

CIRCLE 180 ON READER SERVICE CARD

THE High Frequency Lock-in Amplifier from THE Leaders in Signal Processing Technology

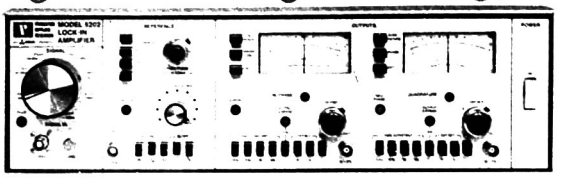

ONLY the 5202 can provide you with:

- 100 kHz-50 MHz operation
- 10 $\mu$V full-scale (FS) sensitivity
- 2000:1 dynamic reserve
- Two-phase operation
- Optional Vector/Phase output
- Optional A/B, log A or log
- A/B output

Find out now how the Model 5202 can simplify, solve or streamline your high frequency measurement problems.

Write or call today for more information. Princeton Applied Research Corporation, P.O. Box 2565, Princeton, New Jersey 08540; phone: 609/452-2111.

PRINCETON APPLIED RESEARCH
AN EG&G COMPANY

Circle 175 For Additional Information Only
Circle 176 To Have a Salesman Call

Thermolyne's Type 2200 Hot Plates can accommodate several vessels and deliver precisely controlled, uniform heat to each of them. Demand-type thermostat senses any change in plate temperature and responds with full power. Your best buy for big or multiple heating jobs.

Contact your Lab Supply Dealer or write to:

SYBRON | Thermolyne

Thermolyne Corp., a subsidiary of Sybron Corp., 2555 Kerper Blvd., Dubuque, IA 52001

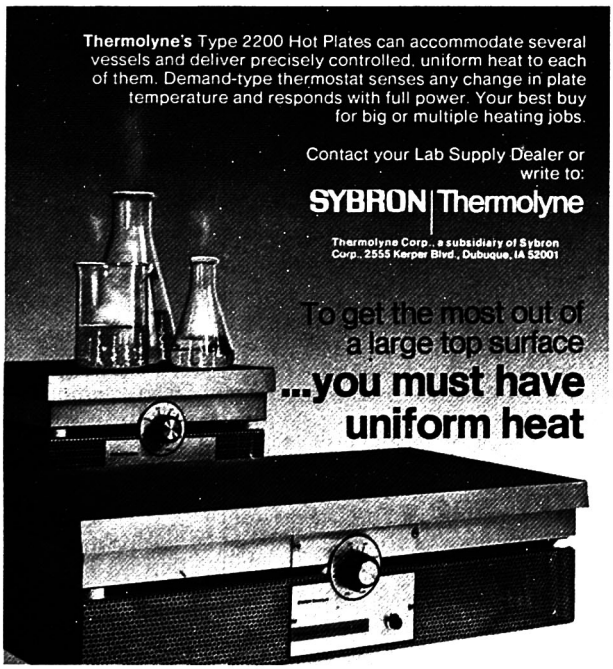


CIRCLE 204 ON READER SERVICE CARD

## Books

view the principles of lasers, nonlinear Raman effects, infrared fluorescence, and tunable infrared lasers. Section B contains six articles on experimental methods such as Fourier transform spectroscopy, matrix isolation, techniques for studying highly reactive species and high-temperature species, trace analysis by infrared spectroscopy, and resonance Raman spectroscopy. The seven articles in Section C on theoretical methods cover isotope substitution, analysis of infrared bands of different intensities and different contours, and force constant calculations. The last section on applications of infrared spectroscopy to solving problems in molecular structure contains eight articles devoted to a review of vibrational spectra of solids, transition metals, metal carbonyls, *n*-alkane and polyethylene compounds, polymers, nucleic acids and proteins, and some model compounds of heme proteins.

**Analytical and Quantitative Methods in Microscopy.** G. A. Meek and H. Y. Elder, Eds. 276 pages. Cambridge University Press, 32 East 57th St., New York, N.Y. 10022. 1977. $24.95, hardbound; $8.50, paperbound

This seminar series was initiated by the Society for Experimental Biology to aid research biologists. The aim is to acquaint the traditional biologists, accustomed to dealing only in qualitative aspects, with the recent analytical methods that can be applied to established techniques of microscopy to obtain accurate quantitative information. Topics of 13 chapters are: introduction, stereology, optical diffraction analysis of periodically repeating biological structures, quantitative fluorescence microscopy, quantitative image analysis, integrating microdensitometry, scanning microinterferometry, potential of the scanning transmission electron microscope in biology, scanning transmission electron microscopy at high resolution, microanalysis of biological material using electron energy loss spectrometry, energy dispersive x-ray microanalysis, wavelength dispersive x-ray microanalysis in biological research, and the use of ultrathin frozen sections for x-ray microanalysis of diffusible elements.

**Fate of Pesticides in Large Animals.** G. Wayne Ivie and H. Wyman Dorough, Eds. x + 270 pages. Academic Press, Inc., 111 Fifth Ave., New York, N.Y. 10003. 1977. $14.50

The contents of this volume are derived from a symposium on the fate of pesticides in large animals sponsored by the Pesticide Chemistry Division of

THINKING SERIOUSLY ABOUT LIGHT SCATTERING?

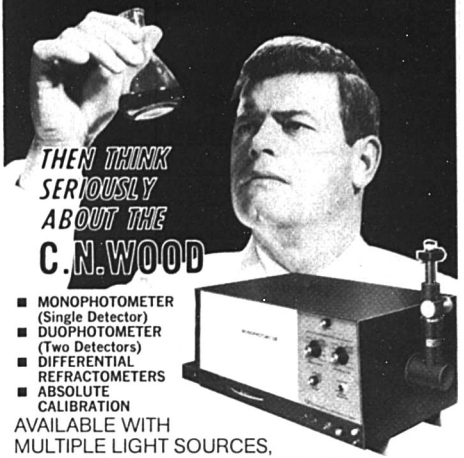

THEN THINK SERIOUSLY ABOUT THE C.N.WOOD

- MONOPHOTOMETER (Single Detector)
- DUOPHOTOMETER (Two Detectors)
- DIFFERENTIAL REFRACTOMETERS
- ABSOLUTE CALIBRATION

AVAILABLE WITH MULTIPLE LIGHT SOURCES, CONSTANT TEMPERATURE SYSTEM, AUTOMATIC SCANNING, MANY ACCESSORIES.

*Call (215) 968-4268 or send for literature and prices*

C.N.WOOD MFG. CO.
Newtown Industrial Commons
Route 332 ■ Newtown, Pa. 18940

CIRCLE 233 ON READER SERVICE CARD

"Thanks— definitely useful."

R. W. Dahlgren
Applied Automation
Bartlesville, Okla.


Use reader service number for your free copy.

CIRCLE 3 ON READER SERVICE CARD

ANNOUNCING . . .

A new solid state constant temperature circulator

**Specially designed for spectrophotometers**

**Model C-400** is a new system specially built to provide finely tempered water or oil for maintaining external baths, apparatus or instruments at closely controlled temperatures. The C-400 has all solid state controls, zero voltage switching, low liquid level and overheat protection and a powerful and positive pumping system. Control is ± 0.02°C, pumping rate 15 liters/minute, range −20 to 80°C. In addition to primary setting of temperature, fully variable over the whole range, a secondary preset temperature may also be selected at any point in the available temperature range.

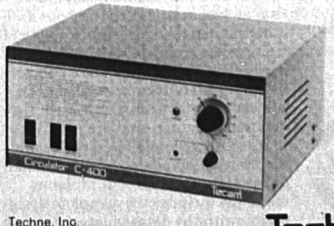


Techne, Inc.
3700 Brunswick Pike, Princeton, NJ 08540
Telephone (609) 452-9275 Telex 84 3319

Techne

CIRCLE 203 ON READER SERVICE CARD

Improved! Solvent Delivery Pumps for Liquid Chromatography


**REDUCES ANALYSIS TIME 15 TO 20 FOLD OVER HYDROSTATIC PRESSURE METHODS!**

- *FULL FLOW RANGE FROM 0 TO 1164 ML/HOUR.*
- *ACCURATE AT PRESSURES TO 100 P.S.I.G.*
- *REPEAT YOUR FLOW SETTINGS TO WITHIN 0.1%.*
- *DRIFT-FREE ACCURACY FOR LONG RUNS.*
- *REVERSIBLE WHILE RUNNING FOR QUICK COLUMN BACK FLUSH AND REGENERATION.*
- *SOLVENTS ONLY CONTACT HARD ALUMINA CERAMIC AND T.F.E.*
- *ABRASION-RESISTANT CERAMIC PISTON AND CYLINDER LINER.*
- *QUIET SYNCHRONOUS STEPPER MOTOR DRIVE.*
- *SMALL: ONLY 10.7" X 5" X 3.2" WIDE AND 8 POUNDS LIGHT.*
- *INEXPENSIVE:*

| | |
|---|---|
| #RP1SYCSC F.M.I. LAB PUMP | $450.00 |
| #R428 MICROMETER KIT | $ 40.00 |
| #R479 ¼-28 T.F.E. PORT ADAPTERS | NO CHARGE |
| COMPLETE F.O.B. PRICE | $490.00 |
| NOTE: FOR EXPLOSION-PROOF DRIVE, SPECIFY RP1SYXCSC, R428, AND R479 | ONLY $630.00 |

FMI FLUID METERING, INC.
P.O. BOX 507, OYSTER BAY, N.Y. 11771 • (516) 922-6050

CIRCLE 80 ON READER SERVICE CARD

the American Chemical Society at its Centennial Meeting in San Francisco, August 29–September 3, 1976. Why is the emphasis on the fate of pesticides in large animals, rather than just in animals generally? The answer to this question is an integral part of several papers. The symposium was divided into three sections. Papers presented in the first section were designed to delineate the rationale of the symposium and to discuss topics applicable to all facets of large animal metabolism. In the second section, presentations were somewhat more specific in that the comparative metabolism of selected groups of pesticides was examined. This section consisted of a general review of the specific subject, followed by the presentation of data from experiments recently conducted. The third section of the symposium consisted of papers dealing with specific compounds and/or specific large animal species. There is a total of 15 papers. The book is reproduced from typewritten text.

## Continuing Series

**Thermal Analysis.** H. Chihara, Ed. xxi + 573 pages. Heyden & Son Inc., Kor-Center East, Bellmawr, N.J. 08030. 1977. $65

The proceedings of the 5th International Conference on Thermal Analysis held in Tokyo, Japan, August 1–6, 1977, are presented. Unlike the previous volumes, which contained full texts, Volume 5 presents papers in the form of extended abstracts ranging in length from two to four pages. The organizers of the conference reason that publication in this format reduced publication time and also space. A total of 160 abstracts represents thermal analysis research papers in the areas of theory and instrumentation, inorganic chemistry, organic and macromolecular chemistry, earth sciences, applied sciences, and calorimetry. The abstracts are reproduced from author-furnished typewritten text.

**The Determination of Oxygen, Selenium, Chromium and Tungsten (Methods in Microanalysis, Volume 5).** J. A. Kuck, Ed. xxxi + 519 pages. Gordon and Breach Science Publishers, Inc., One Park Ave., New York, N.Y. 10016. 1977. $75

Microchemical research papers of exclusively European microanalysts (Italy, West Germany, Czechoslovakia, Hungary, Poland, Yugoslavia, and the Soviet Union) are collected in this volume. All papers were published previously either in the U.S. or in various European journals from 1956 to 1968. For this volume the papers have been translated into English by Kurt Gingold of American Cyanamid Co. Of the 36 articles, the first 24 are devoted to determination of oxygen by various microanalytical techniques, the following eight to selenium, and one each to chromium and tungsten. The last two articles review the progress in organic analysis in the Soviet Union and 50 years of organic analysis in the Soviet Union. The price seems rather high, particularly for a book reproduced from double-spaced typewritten text.

## U.S. Government Publications

*Order copies of the following PREPAID at the price shown and by SD Cat. No. from Superintendent of Documents, U.S. Government Printing Office, Washington, D.C. 20402. Foreign remittances must be in U.S. exchange and include an additional 25% of the publication price to cover mailing costs*

**Use of Monte Carlo Calculations in Electron Probe Microanalysis and Scanning Electron Microscopy.** K.F.J. Heinrich, D. E. Newbury, and H. Yakowitz, Eds. 169 pages. 1977. $2.35. SD Cat. No. 003-003-01737-0

This book is the formal report of the Workshop on the Use of Monte Carlo Calculations in Electron Probe Microanalysis and Scanning Electron Microscopy held at the National Bureau of Standards, October 1–3, 1975. The papers cover a wide range of topics within the field: the history and development of Monte Carlo methods for use in x-ray microanalysis; the study of the distribution of electron and x-ray signals by Monte Carlo techniques; the effect of the choice of scattering models on the calculations; techniques for considering the distribution of energies of the beam electrons propagating in the specimen; evaluation of ionization cross-section models; and applications of Monte Carlo techniques to the study of particles, thin films, and magnetic domain images.

**Lead in the Environment.** 272 pages. 1977. $4.00. SD Cat. No. 038-000-00338-1

This NSF publication is based on research sponsored by the Research Applied to National Needs program. Research on the occurrence, transport, distribution, and possible environmental effects of lead was carried out by Colorado State University, the University of Illinois at Urbana-Champaign, and the University of Missouri at Rolla. The report is divided into six parts entitled (1) Characteristics, Monitoring, and Analysis; (2) Transport and Distribution; (3) Effects of Lead; (4) Control Strategies; (5) Economic Aspects of Control; and (6) Summary and Conclusions.

**Publications of the National Bureau of Standards.** B. L. Burris, Ed. $8.25. SD Cat. No. 003-003-01743-4

Listed in this catalog are all scientific, technical, and consumer publications issued by the Commerce Department's National Bureau of Standards during 1976. The 1976 catalog is the first to include citations of patents given to NBS inventors and grantee-contract reports prepared by NBS contractors. These additions now join the list of research papers, applied mathematics series, interagency reports, national standard reference data series, building science series, monographs, handbooks, special publications, federal information processing standards publications, consumer information series, voluntary product standards and technical notes. Each publication is cited by title, authors, volume taken from, abstract, and key word. In addition, a special section categorizes all 1976 papers by major primary subject area.

## ASTM Publications

*The following is available from the American Society for Testing and Materials, 1916 Race St., Philadelphia, Pa. 19103 (US, Canada, and Mexico add 3% shipping charges. Other countries add 5%)*

**Part 48, Index to 1977 Annual Book of ASTM Standards.** 300 pages. 1977. $5.00

Part 48 is the combined index of all the 5600 ASTM standards and tentative, as well as proposed methods and other related material, appearing in all Parts of the Annual Book of Standards. The index comprises a subject index and an alphanumeric list. The subject index lists each standard under all headings that are pertinent to its contents; cross references enable the user to find all documents related to the area of search. The alphanumeric list includes the complete designation with the dates of latest revision and reapproval, and lists all current documents as well as those that have been discontinued or replaced.

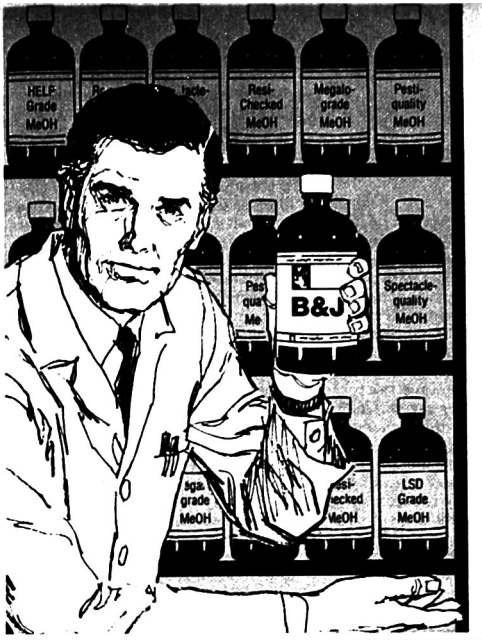


**Don't inventory all those grades of a solvent when ONE from B&J will do the job... better**

- Fewer bottles mean greater safety – fewer hazards.
- Fewer bottles mean less storage space – more lab space.
- Fewer bottles mean lower inventory costs.

You get the best when you order high purity solvents from Burdick & Jackson Laboratories, Inc. All solvents are available in either gallons or quarts.

Send for BJ-25.

BURDICK & JACKSON LABORATORIES, INC.
MUSKEGON, MICHIGAN 49442 (616) 726-3171

CIRCLE 23 ON READER SERVICE CARD

# ULTRAPURE chemicals

## When you simply can't tolerate impurities or uncertainties in your reagents

Over 100 of the purest reagents and chemicals available anywhere in the world. Every product is accompanied by a detailed **Certificate of Analysis** of the actual lot supplied. In terms of spectrochemically detectable impurities, **ULTREX** products are typically **99.995%** to **99.99995%** pure. And the extremely low content of all impurities (often at the parts per billion level) satisfies the most rigid use requirements.

Whenever your requirements for purity and product definition are stringent, ULTREX ultrapures can indeed insure against loss of time, effort, and other expenses.

Consider ULTREX when you just can't afford to gamble with impurities or uncertainties.

**ULTREX®**

Write for new ULTREX ultrapure Reagent brochure.

J. T. Baker Chemical Co.
Phillipsburg, N.J. 08865
201 859-5411

J.T.Baker® CHEMICALS

CIRCLE 24 ON READER SERVICE CARD

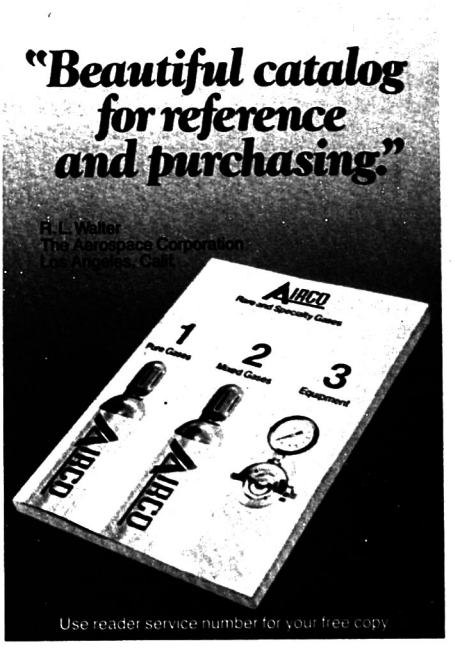


CIRCLE 4 ON READER SERVICE CARD

# Editors' Column

## Analytical Chemistry and Medicine

The recent publication of a study, "Chemistry in Medicine", by the American Chemical Society outlines the contributions of chemists in providing improved products and procedures for health care. The report, published by the Committee on Chemistry and Public Affairs, reviews past accomplishments, discusses the current state of knowledge, and suggests future potentials of chemistry in medical research. In one section on the contributions of basic research, "Chemistry in Medicine" discusses the value of developments in analytical chemistry. Increased sensitivity of analyses and sophisticated instrumentation now allow for the measurement of a chemical's presence or behavior in a complex system to a degree not possible before.

*Copies of "Chemistry in Medicine" are available at $7.50 each from Special Issues Sales, American Chemical Society, 1155 16th St., N.W., Washington, D.C. 20036.*

Basic analytical methodology plays an important role in chemistry's contributions to medical research. Contributions related to the development of drugs are some of the most widely known. Drugs available today radically alter the capabilities for treating illnesses. Most drugs are transformed in the body. The reactions involved must be studied to understand drug metabolism and to aid in the discovery of new drugs. Here very sensitive (parts-per-million) separation and detection techniques identify these reaction sequences and their importance.

Many of the sensitive methods and instruments widely used in pharmaceutical as well as other areas of medical research were originally developed for use in other fields. Mass spectrometry, for example, can detect minute quantities of drugs and their metabolites. Structures can be deduced from mass spectra by studying the ion fragments. Radioisotope techniques also provide highly sensitive and practical methods for quantitative drug metabolism studies.

In medical research, different forms of chromatography are used to separate small amounts of both natural and synthetic chemicals. Chromatography is important in the study of diseases caused by inborn errors of metabolism. In addition, the combination of gas chromatography with mass spectrometry produces a powerful tool for separating and identifying chemicals important in disease studies. Other forms of spectrometry, especially infrared and ultraviolet, are used in the study of steroid chemistry. Fluorescence spectrometry detects elements present in living tissues. Laser probe technology and x-ray emission spectrometry are two analytical techniques that also show promise in medical science. These techniques will allow the detection of trace elements in very small sample sizes, such as a single drop of blood.


# UNEXCELLED FLUORESCENCE, UNBEATABLE PRICE

Nothing tops the sensitivity of luminescence spectroscopy for measuring pico-to-nanograms of amino acids, hormones, enzymes, nucleic acids, proteins or phenols. And with the Perkin-Elmer MPF-44A fluorescence spectrophotometer, you get the high performance sources at a price you can afford.

**The MPF-44A handles practically any research situation.** It has a wavelength range from 200-1200 nm, resolution of 0.2 nm, and the sensitivity to detect picogram/ml concentrations of quinine sulfate. It's the newest addition to the line that made Perkin-Elmer the acknowledged leader in fluorescence performance.

**Two new microprocessor-based accessories.** One gives you corrected excitation and emission spectra. The other, the Differential Corrected Spectra Unit, adds differential (double-beam) operation without sacrificing sensitivity.

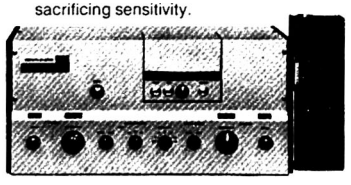

**A new ultra-micro flow cell accessory** with 20 µl sample capacity converts the MPF-44A into an extremely sensitive, versatile LC detector. Other accessories let you select TLC, low temperature luminescence (phosphorescence), polarization, and solid sampling (front surface viewing).

**If you have any questions** on a specific application for the MPF-44A, call us now at (203) 762-4379. Or for full details, write Perkin-Elmer Corp., Mail Station 12, Main Ave., Norwalk, CT 06856.

PERKIN-ELMER

CIRCLE 172 ON READER SERVICE CARD

# Two borosilicate glass flasks may often look as like as peas in a pod.

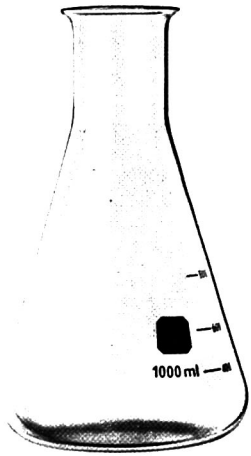


Brand X borosilicate glassware is superbly finished, has uniform wall thicknesses and doesn't lose its cool when the thermometer climbs to 500 °C. It conforms with the international standard ISO 3585.

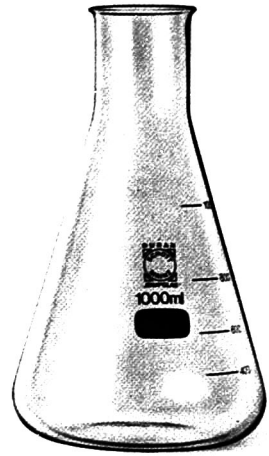


DURAN® borosilicate glassware is superbly finished, has uniform wall thicknesses and doesn't lose its cool when the thermometer climbs to 500 °C. It conforms with the international standard ISO 3585.

We don't know what trademark the glassware on your bench sports.

What we do know is that only one brand of laboratory glassware – DURAN® – is certain to have come from only one plant: the SCHOTT plant in Mainz. And not from a dozen or more scattered around the globe. That's why DURAN® flasks not only look as like as peas in a pod – they are, in dimensions and quality.

We have nine pernickety quality control inspections which put every piece of glassware through its paces before it goes out to you.

Into our DURAN® glassware goes all the experience of the inventors of borosilicate glass – SCHOTT's experience. And the finest of raw materials, which we import from five different countries. All part of the job of ensuring that DURAN® is free of heavy metals that could falsify analyses.

By the way: when we promise to deliver, we do deliver, right on the dot. A further advantage of concentrating production on one plant.

So you see, borosilicate glass is not just borosilicate glass, however it may look.

SCHOTT
JENA™ GLAS JENA™ GLASWERK SCHOTT & GEN.

Geschäftsbereich Chemie, Produktgruppe Laborglas,
Postfach 2480, D-6500 Mainz (West Germany),
Tel. (06131) 661, Telex 4187379 smz d

DURAN® – borosilicate glass
straight from the inventors' plant.

CIRCLE 110 ON READER SERVICE CARD

# The 204 Chromatograph expansion plan

The Pye Unicam Series 204 Gas Chromatograph – planned for exceptional versatility in setting up a system just right for your type of analysis – systems that start simple but that can be expanded when analytical requirements are changed or increased, anytime! The Series 204 plan is complete – from a choice of five detectors right down to a comprehensive range of columns and other ancillaries with a follow-up after sales service that includes for instance, application information that is direct between the Pye Unicam Application Laboratories and you. If you feel in an expansive mood get full information on the Pye Unicam Series 204 Gas Chromatograph now! Just 'phone, write or use the reader reply service.

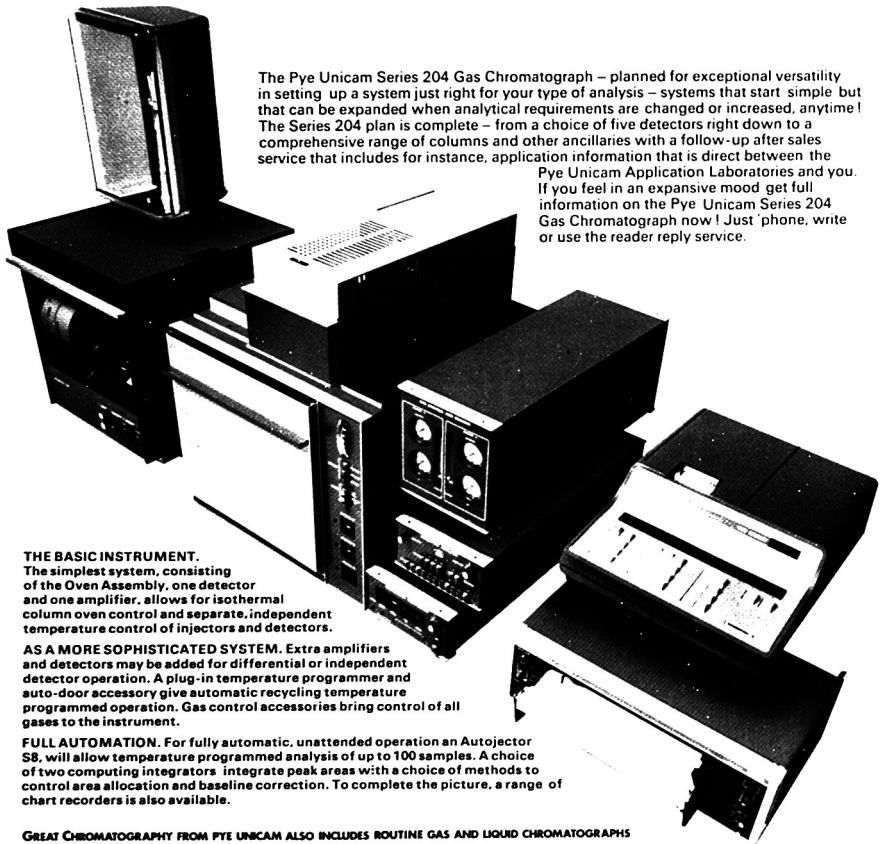

**THE BASIC INSTRUMENT.** The simplest system, consisting of the Oven Assembly, one detector and one amplifier, allows for isothermal column oven control and separate, independent temperature control of injectors and detectors.

**AS A MORE SOPHISTICATED SYSTEM.** Extra amplifiers and detectors may be added for differential or independent detector operation. A plug-in temperature programmer and auto-door accessory give automatic recycling temperature programmed operation. Gas control accessories bring control of all gases to the instrument.

**FULL AUTOMATION.** For fully automatic, unattended operation an Autoinjector S8, will allow temperature programmed analysis of up to 100 samples. A choice of two computing integrators integrate peak areas with a choice of methods to control area allocation and baseline correction. To complete the picture, a range of chart recorders is also available.

GREAT CHROMATOGRAPHY FROM PYE UNICAM ALSO INCLUDES ROUTINE GAS AND LIQUID CHROMATOGRAPHS

**Pye Unicam Ltd**

York Street, Cambridge, England CB1 2PX
Cambridge (0223) 58866. Telex: 817331

A member of the Pye of Cambridge Group

CIRCLE 168 ON READER SERVICE CARD

Many of these basic analytical methods also contribute to diagnostic testing. In the clinical laboratory many analyses are now run routinely and automatically on blood and tissue samples; the determination of cholesterol and fats, the determination of various ions such as sodium and potassium, and enzyme analyses are a few examples. The analytical methods involved must be refined to the point where accurate tests can be run continuously and automatically by relatively unskilled technicians.

As noted in "Chemistry in Medicine", perhaps one of the greatest analytical needs today is for methods that will permit biological processes to be studied in detail at the molecular and atomic levels. Detecting small changes in concentration and determining how molecules are functioning inside cells will assist in providing basic information about cell processes. A first move in this direction is ion-selective membrane electrodes. These electrodes are made small enough to permit direct measurement in the body. Membranes modified with a layer of an appropriate enzyme are used to measure body fluid constituents such as glucose, urea, and phenylalanine. Much research is needed to try and match body chemical reactions with ionic measurements and to expand the number of different ions that can be measured. Research in this area will lead to a better understanding of many body processes including nerve conduction, muscle contraction, bone formation, and blood coagulation.

Dr. Thomas P. Carney, president of Metatech Corp., headed the four-man subcommittee responsible for "Chemistry in Medicine". In the preface, Dr. Carney states: "Future historians may well view the late 1960's and early 1970's as one of those inflection points when major scientific findings raised health care to a new, higher level. The prospects offered by increasing knowledge of cellular function at the molecular level clearly presage impelling scientific gains. So does the growth in sophisticated analyses, instruments, and diagnostic techniques. We are thus in a period of great scientific promise."

Developments in analytical methodology are clearly playing a very important role in medical research. As shown in this brief overview, analytical chemists are contributing to the search for new drugs and diagnostic tools. These will aid the physician in treating and preventing many illnesses. In addition, the growth of sophisticated analyses and instruments will provide a better understanding of diseases and complex body processes.

*Deborah C. Stewart*


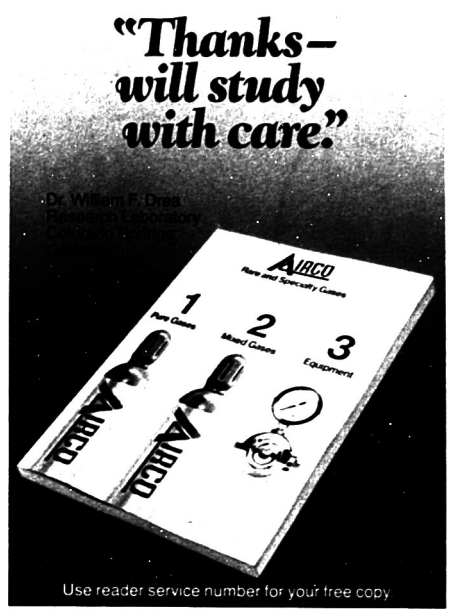


CIRCLE 5 ON READER SERVICE CARD

**INSTRUMENTATION RECYCLING**

**Do you need an analytical instrument but can't presently bear the expense of a new system?**

**We have the answer!**

Sixes and Sevens now offers a listing service for buyers and sellers of previously owned instrumentation with an original cost of $2000 or more. We've discovered that many labs and universities across the country own instrument systems that are not presently in use, but are still operational. Other systems, that have received heavy useage, are being refurbished to original specifications by reputable service engineering firms. In either case, our function is to locate instrumentation for you that's in **good working condition.** To begin, just let us know what's on your shopping list. There's no cost or obligation until a transaction is made as a result of our efforts.

**Please write, call collect, or circle our reader service number.**

**Sixes and Sevens**
**6032 197th Avenue East**
**Sumner, Washington 98390**
**206-863-1617**

CIRCLE 190 ON READER SERVICE CARD

# ADD TO THE SCOPE OF YOUR 'SCOPE WITH A 3M SIMS/SEM SYSTEM

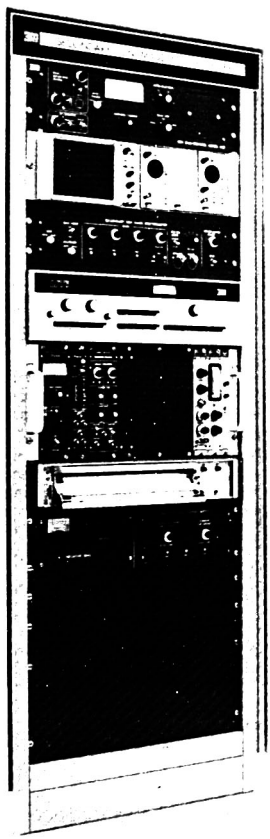

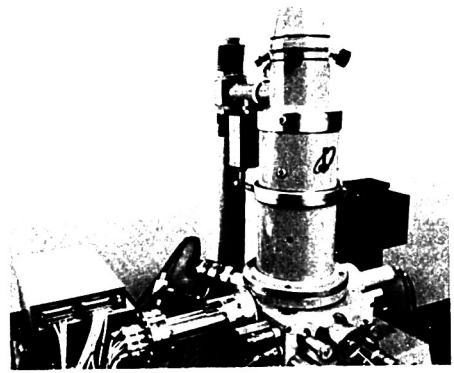

**Low Z detection, depth profiling and a surface sensitivity measured in Angstroms are only three benefits offered by a 3M SIMS System. There are more...**

Our extensive experience in the chemical analysis of surfaces with SIMS and our history of providing this capability as an attachment to existing instruments have resulted in a 3M SIMS System optimally designed for your SEM. That's why 3M Analytical Systems takes "turnkey" responsibility for the installation. When we say it's ready to go, you can be sure it's *really* ready to go.

And we've barely scratched the surface of our SIMS System here. The full scope of its capabilities must be seen to be appreciated. If you'd like a few more reasons for seeing a demonstration, call 612/733-3909, or write: Analytical Systems, 3M Company, 3M Center, Building 209, St. Paul, MN 55101 and ask for our latest SIMS/SEM brochure. In Europe: Cambridge Instruments, GmbH, Dortmund, Germany.

3M COMPANY

CIRCLE 206 ON READER SERVICE CARD

# TRACOR SPECTROSCOPY

## New instrumentation spanning the spectrum from X-rays to the near-IR.

**TN-2000 X-ray Elemental Analysis System** brings the full power of x-ray energy spectroscopy to your laboratory in an affordable, convenient, easy-to-operate system. System TN-2000 is easily expandable from qualitative to quantitative capability, with proven software capabilities to meet your analytical needs, *now and in the future.*

**TN-1710 Signal Averager,** a new microcomputer-based signal

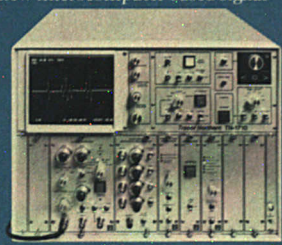

analysis system. Modular software and hardware allow you to precisely tailor the system to your analytical needs. Powerful data acquisition and processing are under convenient pushbutton *"firmware"* control, with features that include bipolar memory, versatile I/O interfaces, comprehensive alpha-numeric display information, a full repertoire of data processing operations, higher-level interactive programming, and support modules for fast pulse counting, four-input averaging, and parametric sweep averaging.

*Visit us at the Pittsburgh Conference, booths 1138, 1140, 1142.*

**Diode Array Rapid Scan Spectrometer** performs rapid

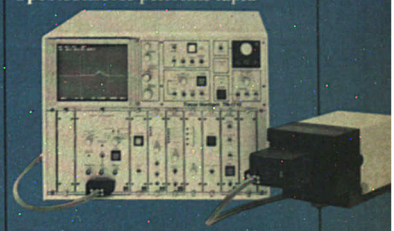

simultaneous measurement from 2000 to 1100 nm with the widest dynamic range and highest sensitivity available, enabling the spectroscopist to perform analyses that are difficult or impossible with conventional instrumentation.

*Applications include:*

**Detector lag-free UV-VIS absorption measurements for chemical kinetics studies.**

**Measurement of flame and DC arc emission spectra for simultaneous multielement analyses.**

**Fluorescence, chemiluminescence, and Raman spectral measurements.**

**UV-VIS absorption/fluorescence measurements for LC peak characterization.**


**Tracor Northern**

Tracor Europa B.V.
Schiphol Airport Amsterdam
Building 106, The Netherlands
Telephone (020) 41 1865
Telex 13695

2551 West Beltline Highway
Middleton, Wisconsin 53562
(608) 831-6511
TWX-910-280-2521

CIRCLE 200
CIRCLE 201
CIRCLE 202

# Reliable. Fast and Easy. MCI automatic analyzer.

Utilizes ASV method to simultaneously measure concentrations of 5 different trace heavy metals. Ultra-high sensitivity and automatic sample feed/discharge measuring cell assures fast, precise results. Reproducibility is 3-to-20%. Range: 0.1 PPB—10 PPM.

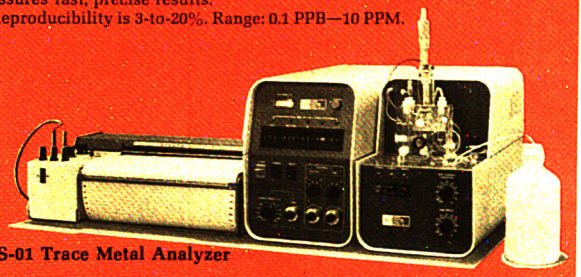

**AS-01 Trace Metal Analyzer**

MITSUBISHI CHEMICAL INDUSTRIES LIMITED

Instruments Dept., Mitsubishi Bldg., 5-2, Marunouchi 2-chome, Chiyoda-ku, Tokyo, 100 Japan Telex: J24901 Cable Address: KASEICO TOKYO

CIRCLE 144 ON READER SERVICE CARD



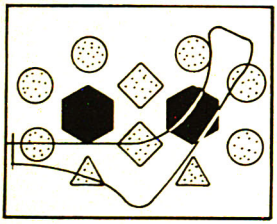

## Electrochemical Studies of Biological Systems

ACS Symposium Series No. 38

Donald T. Sawyer, *Editor*
*University of California*

*A symposium sponsored by the Division of Analytical Chemistry of the American Chemical Society.*

The twelve papers in this significant new collection provide a representative cross section of the kinds of electrochemical methods used to characterize biological systems, as well as the kinds of biological problems that are being studied by such methods.

**CONTENTS**

*vitamin $B_{12}$ and related cobalamins • bioelectrochemical modelling of cytochrome c • potentials of metal ion couples in complexes • metalloporphyrins in aprotic solvents • N-bridged dimer in nonaqueous media • reduction of nitrogenase substrates • manganese (II) and -(III) 8-quinolinol complexes • interfacial behavior of purines • coulometric titration of biocomponents • rotating ring disk enzyme electrode • left ventricle/aorta simulator • EDTA and NTA in phytoplankton media*

216 pages (1977) clothbound $15.50
LC 76-30831 ISBN 0-8412-0361-X

**SIS/American Chemical Society**
1155 16th St., N.W./Wash., D.C. 20036

Please send _____ copies of *SS 38 Electrochemical Studies of Biological Systems* at $15.50 per copy.

☐ Check enclosed for $ _____. ☐ Bill me. Postpaid in U.S. and Canada, plus 40 cents elsewhere.

Name

Address

City State Zip



# Special Tape Recordings

☐ **Milestones in Physical Chemistry**

8 Speakers — 315 Figures
Length: 5 Cassettes — 8 Hours
PRICE: $45 (postpaid)

The Speakers:
G. T. Seaborg
D. Hodgkin
G. Porter
P. J. Flory
W. O. Baker
L. C. Pauling
H. Eyring
J. H. Van Vleck

☐ **Evolution of Kinetics**

8 Speakers — 140 Figures
Length: 4 Cassettes — 6 Hours
PRICE: $35 (postpaid)

The Speakers:
B. S. Rabinovitch
W. A. Noyes, Jr.
R. A. Marcus
K. F. Freed
G. B. Kistiakowski
J. C. Polanyi
S. Claesson
J. Jortner

☐ **Structure & Quantum Chemistry**
**+**
**Evolution of Magnetic Resonance**

8 Speakers — 210 Figures
Length: 4 Cassettes — 6 Hours
PRICE: $35 (postpaid)

The Speakers:
J. A. Pople
H. G. Drickamer
F. H. Stillinger
R. Zwanzig
H. S. Gutowsky
J. S. Waugh
H. M. McConnell
F. A. Bovey

☐ **SPECIAL PRICE**

**ALL THREE SETS — $85 (postpaid) save $30!**

**Order From:**

**American Chemical Society**
1155 Sixteenth St., N.W.
Washington, D.C. 20036
ATTN: Dept. AP

Name

Address

City State Zip

(allow 4 to 6 weeks for delivery)


FOR THE CREATIVE CHEMIST:

# *EASTMAN* REAGENTS FOR GEL ELECTROPHORESIS.

Colorful currents soaring from the universe? No. It's actually a photomicrograph of EASTMAN Organic Chemical 8154, Phthalaldehyde, by John Delly, McCrone Research Institute. It demonstrates what can happen when you use your imagination and our chemicals.

For everyday applications, you'll appreciate the quality of our more than 120 Eastman gel-forming reagents, catalysts/initiators, buffers, dyes, stains, and other reagents for creative chemists working in acrylamide gel electrophoresis.

Dealers offering EASTMAN Organic Chemicals can also offer you thousands of other organics for electrophoresis; liquid scintillation counting; protein chemistry; dyes, stains, and indicators. See them for fast, reliable delivery and service, and a free reminder that chemistry is creative.

For a detailed description of Eastman reagents for gel electrophoresis, send for free technical literature. JJ-11. Write Eastman Organic Chemicals, Eastman Kodak Company, Dept. 412L, Rochester, N.Y. 14650.

**Take a close look at EASTMAN Organic Chemicals.** Dealers handling EASTMAN Organic Chemicals: American Scientific & Chemical, Bio Clinical Laboratories, Brand-Nu Laboratories, Inc., Bryant Laboratory, Inc., Custom Chemical Laboratories, Inc., Fisher Scientific, GAC Laboratories, Inc., Labproducts, Inc., Midland Scientific, Inc., North-Strong, Inc., Preiser Scientific, Sargent-Welch Scientific Products, Scientific & Industrial Sales & Service, Inc., VWR Scientific Inc., Ward's Natural Science Establishment, Inc.

CIRCLE 63 ON READER SERVICE CARD

# spectro-electro-chemistry

## Combination of Optical and Electrochemical Techniques for Studies of Redox Chemistry

**William R. Heineman**
Department of Chemistry
University of Cincinnati
Cincinnati, Ohio 45221

The combination of two quite different techniques, electrochemistry and spectroscopy, has proved to be an effective approach for studying the redox chemistry of inorganic, organic, and biological molecules. Oxidation states are changed electrochemically by addition or removal of electrons at an electrode. Spectral measurements on the solution adjacent to the electrode are made simultaneously with the electrogeneration process. Thus, spectroscopy is used as a probe to observe the consequences of electrochemical phenomena that occur in the solution undergoing electrolysis. Such "spectroelectrochemical" techniques are a convenient means for obtaining spectra and redox potentials and observing subsequent chemical reactions of electrogenerated species. This article describes several of the more commonly used spectroelectrochemical methods and presents illustrative examples of their application.

A variety of optical methods that have been coupled with electrochemistry are summarized in Figure 1. The most frequently used technique is absorption spectroscopy in the ultraviolet–visible–infrared region. Absorption spectroscopy can be implemented by any of three methods. Transmission spectroscopy (Figure 1A, 1B) involves passing the optical beam directly through a transparent electrode and the adjacent solution (*1–3*). In specular reflectance spectroscopy (Figure 1C) the beam is passed through solution and reflected from the electrode surface back through the solution (*4, 5*). Internal reflectance spectroscopy (Figure 1D) involves introducing the optical beam through the back side of a transparent electrode at an angle greater than the critical angle so that the beam is totally reflected (*1–3, 6*). Spectral changes near the electrode are observable due to the small penetration of the electric field vector into the solution. Sensitivity for both types of reflectance spectroscopies can be enhanced by multiple reflections.

Luminescence and scattering spectroscopic techniques have been coupled with electrochemistry. In Raman and resonance Raman spectroelectrochemistry (Figure 1E) the excitation is by a laser beam directed through solution at an electrode and the Raman back-scattering is observed (*7*). A particularly important aspect of Raman spectroelectrochemistry is the structural information about electrogenerated species which is contained in a Raman spectrum. A beam of excitation light can be passed through an electrochemical cell, and the resulting fluorescence of electrogenerated species observed (*8*). A variety of electrode reactions are accompanied by the emission of light. Such electrogen-



0003-2700/78/0350-390A$01.00/0
© 1978 American Chemical Society

Figure 1.
**Spectroelectrochemical techniques**

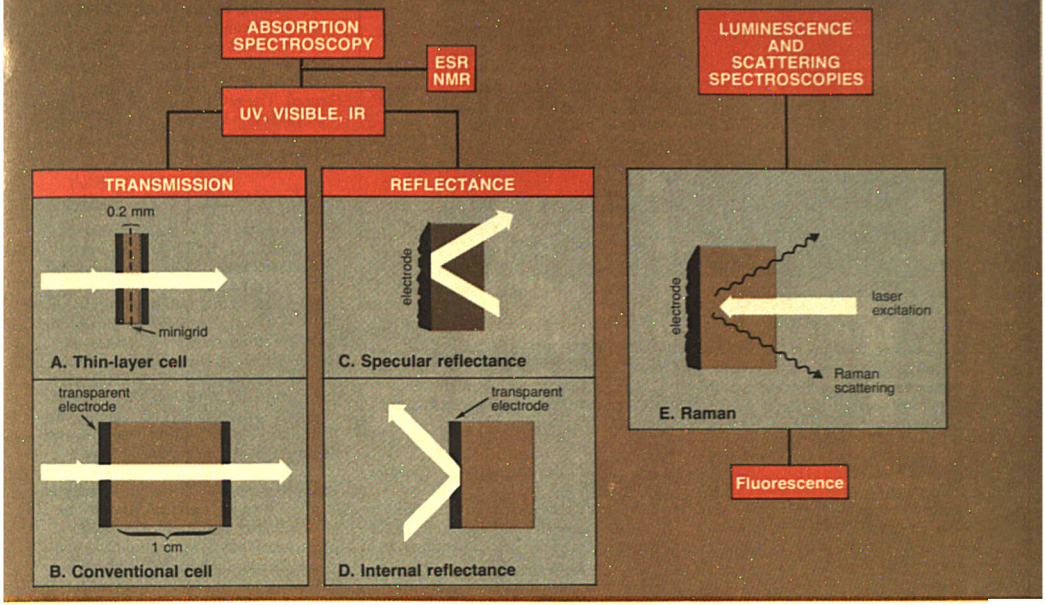


erated chemiluminescence results from decay of an excited state formed by the solution reaction of electrogenerated cations and anions (*9*).

Electrochemical cells have been placed in the sample cavities of ESR and NMR spectrometers to record the absorption spectra of electrogenerated species (*10, 11*). Recently, mass spectroscopy has been coupled to an electrochemical cell (*12*).

Two types of solution geometries are commonly used in conjunction with the above optical techniques. The usual cell (Figures 1B, 1C, 1D) is analogous to a conventional electrochemical cell in that the electrode is in contact with an electrolyte solution much thicker than the diffusion layer adjacent to the electrode (*1–3*). By contrast, the thin-layer cell (Figure 1A) confines a thin (<0.2 mm) solution layer adjacent to the electrode (*13*). The most significant virtue of thin-layer cells is the rapidity with which electroactive species within this layer can be completely electrolyzed (typically 20–120 s).

**Optically Transparent Electrodes.** Progress in the methodology of spectroelectrochemistry has been stimulated by the development of suitable optically transparent electrodes that enable the light beam to be passed directly through the electrode and adjacent solution. Although reflectance, luminescence, and scattering techniques can be implemented with conventional electrodes, transparency is necessary for transmission and internal reflectance spectroelectrochemistry.

One type of transparent electrode consists of a very thin film of conductive material such as platinum, gold, tin oxide, or carbon that is deposited on a transparent substrate such as glass (visible), quartz (UV–visible), or germanium (infrared), depending on the spectral region of interest. The transparency (20–85%) of these electrodes is due to the thinness (100–5000 A) of the conducting film.

A second type of transparent electrode is the minigrid electrode which consists of a metal (Au, Ni, Ag, or Cu) micromesh of 100–2000 wires per inch. In this case, the transparency (20–80%) is due to the physical holes in the minigrid structure. The minigrid has been used primarily in the thin-layer cell configuration in conjunction with transmission spectroscopy as shown in Figure 1A.

"Mercury" transparent electrodes have been prepared by electrodepositing a thin film of Hg onto Pt and carbon film electrodes and Au and Ni minigrids. This imparts some of the excellent negative potential range of mercury. A good review of transparent electrodes is given in ref. *1*.

**Thin-Layer Spectroelectrochemistry.** One of the most generally useful spectroelectrochemical experiments involves observation of a thin layer of solution confined next to a transparent electrode as shown in Figure 1A. The optical beam of the spectrometer is passed directly through the transparent electrode and the solution.

The Schiff base complex of $Co^{II}$, bis(salicylaldehyde)ethylenediimine cobalt (II), provides a typical example of a thin-layer spectroelectrochemical study (*14*).

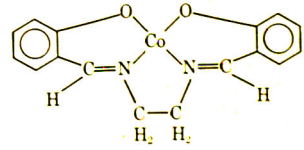

$Co^{II}(sal_2en)$

A cyclic voltammogram (Figure 2), in which the potential applied to the working electrode is scanned and the current measured, shows two potential regions in which current is observed due to electrolysis of the cobalt complex. A positive scan initiated at −0.3 V results in oxidation of $Co^{II}$ to $Co^{III}$ as indicated by the anodic current. The rapid drop in current after the peak signifies complete conversion to

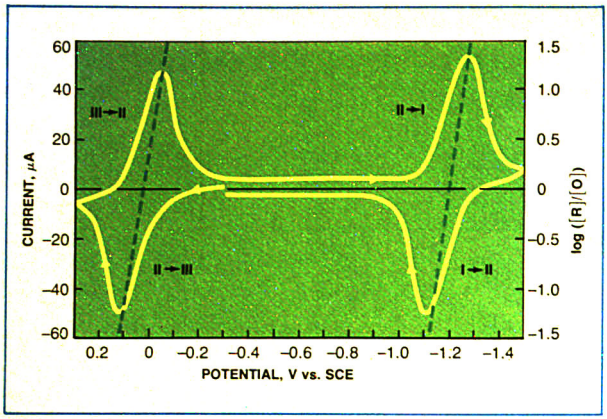


**Figure 2.** —, left axis. Cyclic voltammogram of 1.3 m*M* $Co^{II}(sal_2en)$ in 0.5 M tetraethylammonium perchlorate-dimethylformamide. Optically transparent thin-layer electrode with gold minigrid. Scan rate 2 mV $s^{-1}$. - - -, right axis. Nernstian plots of log ([red]/[ox]) vs. $E_{applied}$ for $Co^{III}$, $Co^{II}$ and $Co^{II}$, $Co^{I}$ couples

the $Co^{III}$ oxidation state within the thin solution layer. A reversal of the potential scan at +0.3 V to the negative direction results in reduction of the $Co^{III}$ back to the original $Co^{II}$ complex and finally to the $Co^{I}$ oxidation state at a potential of about −1.2 V. Another reversal at −1.5 V to scan in the positive direction causes oxidation of $Co^{I}$ back to the $Co^{II}$ complex. The complex can be cycled repeatedly among the three oxidation states, indicating stability of the electrogenerated $Co^{III}$ and $Co^{I}$.

Figure 3 shows visible absorption spectra recorded at a series of increasingly negative potentials applied to the cell. Each potential was maintained until electrolysis ceased (ca. 2 min) so that the solution was in equilibrium with the electrode potential before the corresponding spectrum was recorded. As the potential was made more negative, the complex was converted to the $Co^{I}$ form as evidenced by the appearance of the absorbance peak at 710 nm. In addition to obtaining the spectrum of the complex in its completely reduced form (curve j), this experiment enables a precise value of the formal reduction potential $E^{\circ\prime}$ ($Co^{II}$, $Co^{I}$) to be measured. The ratio of $[Co^{I}]/[Co^{II}]$ in the thin solution layer is controlled by the applied potential as defined by the Nernst equation.

$$E_{applied} = E^{\circ\prime} - \frac{0.059}{n} \log \frac{[Co^{I}]}{[Co^{II}]}$$

For each value of $E_{applied}$, the corresponding ratio of $[Co^{I}]/[Co^{II}]$ can be calculated from the absorbance at 710 nm in Figure 3. A Nernstian plot of the data from Figure 3 is shown by the dotted line in Figure 2. The plot is linear as predicted by the Nernst equation with an $n$ of 1.0 calculated from the slope and an $E^{\circ\prime}$ of −1.193 V vs. SCE from the intercept. The one-electron nature of the $Co^{II}$, $Co^{I}$ couple can be confirmed by thin-layer coulometry (*14*). An analogous experiment performed by recording spectra during conversion to $Co^{III}$ gives the spectrum for $Co^{III}(sal_2en)$ and the data for the $Co^{III}$, $Co^{II}$ Nernstian plot shown in Figure 2. Thus, spectra, reduction potentials, and the number of electrons involved can be obtained in a single experiment.

The thin-layer spectroelectrochemical technique has also been used effectively in the study of biological molecules which are difficult to investigate

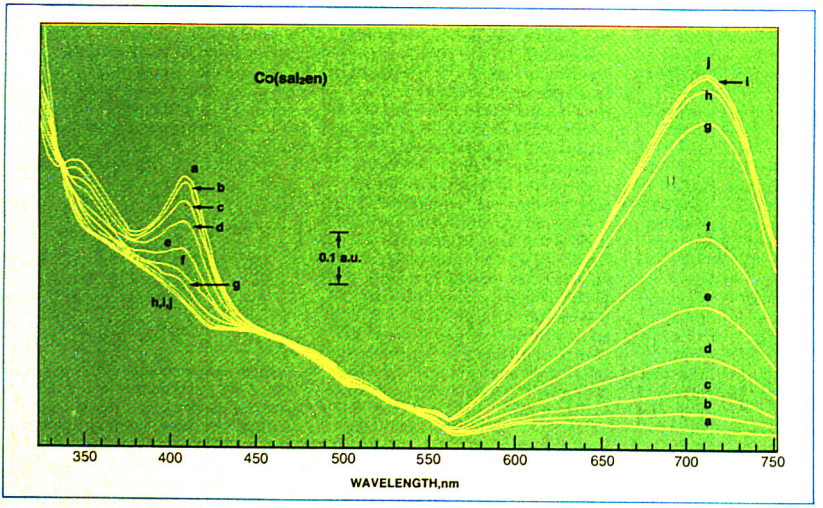


**Figure 3.** Spectra of $Co(sal_2en)$ in optically transparent thin-layer electrode for series of potentials
$E_{applied}$: (a) −0.900, (b) −1.120, (c) −1.140, (d) −1.160, (e) −1.180, (f) −1.200, (g) −1.250, (h) −1.300, (i) −1.400, (j) −1.450 V vs. SCE
Reproduced from ref. *14*, courtesy of Plenum Press

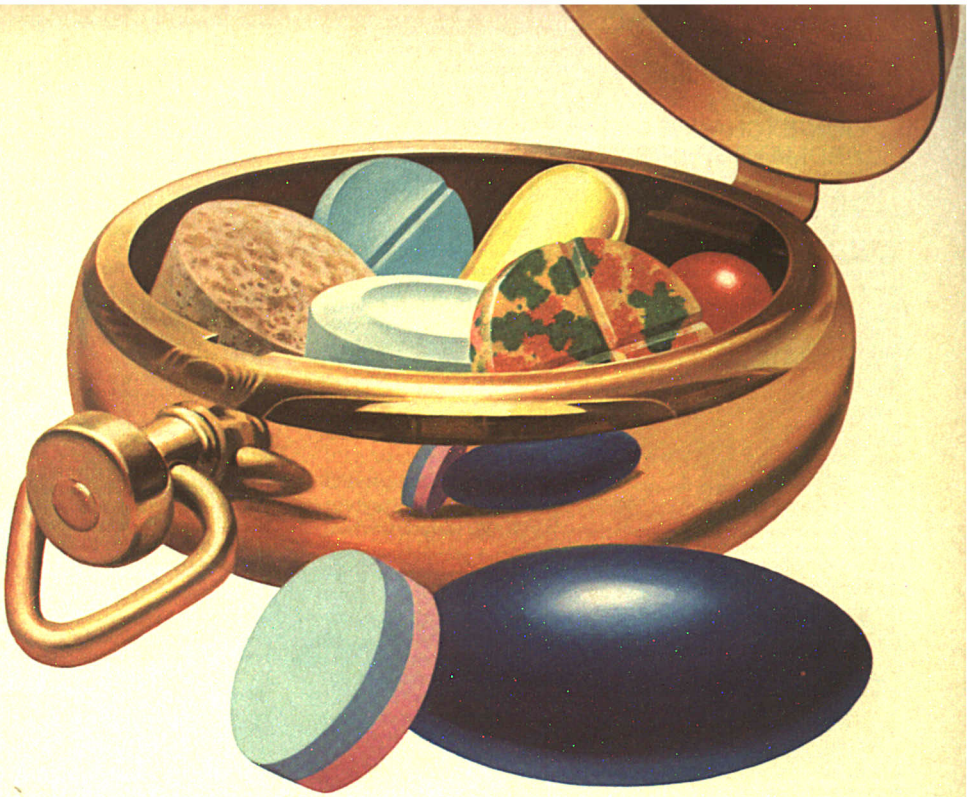

# How potent is the pill?

Mettler automatic titration systems help pharmaceutical manufacturers synthesize new products. Drug potency is tested by breaking down the substance according to functional groups. If each group performs effectively, a methods development is prepared for quality assurance purposes. Production runs of the drug must then adhere to these strict potency standards. – Mettler helps solve problems

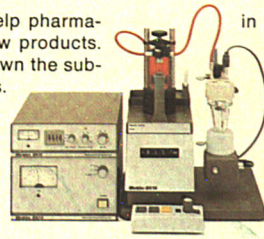

in analytical laboratories and on the production floors of industry. We market a variety of weighing and measuring instruments. All of them made with world-renowned Mettler craftsmanship. All of them backed by a worldwide team of service specialists who can be there when you need them. Mettler – instruments and people you can depend on.

## Depend on Mettler for the answer.

Mettler

Electronic balances and weighing systems · Thermoanalytical instruments · Automatic titration systems · Laboratory automation

Mettler Instrumente AG, CH-8606 Greifensee-Zürich, Switzerland · Mettler-Waagen GmbH, D-63 Giessen 2, Postfach 2840, BRD
Mettler Instrumenten B. V., Postbus 68, Arnhem, Holland · Mettler Instrument Corporation, Box 100, Princeton, N. J. 08540, USA

CIRCLE 142 ON READER SERVICE CARD

# Benchmark® Papers in Analytical Chemistry

## VOLUME 1
## ION-EXCHANGE CHROMATOGRAPHY

Edited by HAROLD F. WALTON

"Clearly, this volume is a very good vehicle for gaining an informed perspective on the subject of column, ion-exchange chromatography."—*Journal of the American Chemical Society*

Forty-eight landmark papers, along with Professor Walton's expert commentary, trace the most significant advances in this increasingly useful field.

Papers by such noted pioneers and innovators as K. A. Kraus and F. Nelson, S. Moore and W. H. Stein, F. H. Spedding, and L. C. Brown, G. M. Begun, and G. E. Boyd, cover applications of ion-exchange chromatography to inorganic chemical analysis as well as to organic and biochemical analysis. Modern developments in liquid chromatography are also included. A 1939 paper by O. Samuelson, which perhaps marks the earliest use of an ion-exchange resin in chemical analysis, introduces the work. The remaining papers are arranged by topic in twelve parts. Many of these documents are otherwise difficult to obtain, and several appear here in English for the first time. Partial translations are provided for papers printed in other languages.

*1976, 464 pp., $33.00/£23.45*
*ISBN: 0-12-787725-8*

## VOLUME 2
## THERMAL ANALYSIS

Edited by
W. W. WENDLANDT and L. W. COLLINS

The thirty-six important papers included in this volume are concerned with the development of two major thermal analysis techniques—differential thermal analysis (DTA) and thermogravimetry (TG).

Highlighting the collection are papers by H. Le Chatelier (Concerning the Action of Heat on Clays); W. C. Roberts-Austen (Fifth Report to the Alloys Research Committee); G. K. Burgess (On Methods of Obtaining Cooling Curves); K. Honda (On a Thermobalance); and C. Duval (Continuous Weighing in Analytical Chemistry).

CONTENTS: Part I. Commentary on Differential Thermal Analysis and Differential Scanning Calorimetry. Part II. Commentary on Thermogravimetry.

*1976, 352 pp., $35.00/£24.85*
*ISBN: 0-12-787750-9*

***Published by Dowden, Hutchinson & Ross, Inc. Distributed Worldwide by Academic Press, Inc.***

*N.B.* These series are now available on a continuation order basis. Your continuation order authorizes us to ship and bill each volume automatically, immediately upon publication. This order will remain in effect until cancelled. Please specify volume with which your order is to begin.

Send payment with order and save postage plus 50¢ handling charge.

*Prices are subject to change without notice.*

# Academic Press

*A Subsidiary of*
*Harcourt Brace Jovanovich, Publishers*
111 FIFTH AVENUE, N.Y., N.Y. 10003
24-28 OVAL ROAD, LONDON NW1 7DX

CIRCLE 2 ON READER SERVICE CARD


by conventional electrochemical methods (*15*). An example is cytochrome *c* in which the redox center is a heme iron surrounded by a protein matrix, giving a molecular weight of about 12 000. Molecules of this type often exchange electrons poorly with an electrode, presumably due to insulation of the redox center from the electrode by the surrounding protein. For example, a thin-layer cyclic voltammogram is essentially featureless for cytochrome *c*. However, spectroelectrochemical measurements of the type described above for $Co(sal_2en)$ can be made on cytochrome *c* by adding to the solution a small amount of another redox species [a mediator-titrant (*16*)] which transports electrons between the electrode and cytochrome *c*. Thus, the cytochrome redox couple is indirectly coupled to the electrode potential by the mediator-titrant, M, as depicted below.

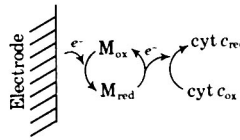


When the electrode potential is changed, the electrode reduces/oxidizes the mediator-titrant which in turn reduces/oxidizes the cytochrome. The $E^{o\prime}$ and *n* values for the $[Fe^{II}]/[Fe^{III}]$ couple of the heme in the cytochrome can be measured spectroelectrochemically by recording spectra of the cytochrome as the potential is stepped.

In addition to the absorption spectroscopy techniques described above, thin-layer cells have been used for fluorescence yield changes, circular dichroism (*8*), ESR measurements (*10*), and specular reflectance (*17*). Thin-layer spectroelectrochemical measurements have been made on organic molecules and inorganic metal complexes in aqueous and nonaqueous solvents (*1*) and on biological materials such as cytochromes (*15*), photosynthetic electron-transport components (*8*), and vitamin $B_{12}$ (*18*).

The forte of thin-layer spectroelectrochemistry is its experimental simplicity and versatility. One type of spectroelectrochemical cell is easily fabricated by sandwiching a small piece of commercially available gold minigrid between two optically transparent plates (ordinary microscope slides will suffice for the visible region) which are separated about 0.2 mm by Teflon strips placed along the periphery (*13, 15*). Such a cell can be assembled in about 30 min at a cost of less than $5.00. Spectroelectrochemical measurements can be performed by positioning the cell in the light beam of any conventional ultraviolet–visible spectrometer with a sufficiently large cell compartment. Adequate potentiostats for thin-layer electrochemistry are available for $300.

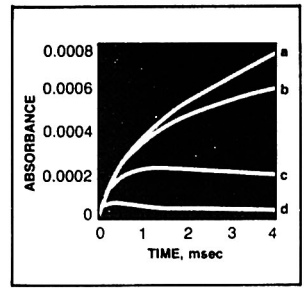


**Figure 4.** Absorbance-time curves for *k* values of (a) 0, (b) $10^5$, (c) $10^6$, and (d) $10^7$ $M^{-1}$ $s^{-1}$

*R* monitored optically, $D_O = 10^6$ cm$^2$ s$^{-1}$, $\epsilon_R = 10^4$ L mol$^{-1}$ cm$^{-1}$, concentrations of *A* and *Z* = 1.0 m*M*

**Reaction Kinetics.** Electrochemistry is a convenient way for generating reactive oxidation states of molecules. Subsequent homogeneous chemical reactions of the electrogenerated species can be monitored optically to probe the mechanism and rate of reaction (*1–3*). Consider the situation in which species *O* is present in an unstirred solution that is contacting an optically transparent electrode through which a light beam is passed as shown in Figure 1B. Species *R* is electrogenerated from *O* by a potential applied to the transparent electrode.

$$\text{Electrode:} \quad O + e^- \rightarrow R \qquad (1)$$

If the wavelength is such that *R* absorbs light, an absorbance-time response of the type shown by curve a in Figure 4 is obtained. The increase in absorbance reflects the generation of *R* at a rate determined by the diffusion of *O* to the electrode surface. This absorbance-time behavior is described by the following equation

$$A = \frac{2}{\pi^{1/2}} \epsilon_R C_O^* D_O^{1/2} t^{1/2} \qquad (2)$$

where $\epsilon_R$ is the molar absorptivity of the optically monitored species *R*, and $C_O^*$ and $D_O$ are the solution concentration and diffusion coefficient, respectively, of the species from which *R* is being electrogenerated, *O*. Consider now the situation in which another species *Z* is added to the solution. Species *Z* is capable of rapid homogeneous chemical reaction with *R* at a rate characterized by the second order rate constant *k* to form product *P*.

$$\text{Solution:} \quad R + Z \xrightarrow{k} P \qquad (3)$$

# "With Graphics I can see at a glance what used to take hours to uncover."

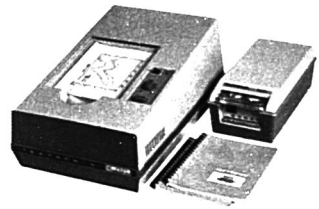

You can get clean, sharp, hard copies from the 4631 Hard Copy unit; local storage with the 4923 Digital Cartridge Tape Recorder; and multicolor plots from the 4662 Interactive Digital Plotter, shown left.

**Problem: Data reduction can be the weakest link in your analytical chain.**

Every time you have to analyze spectral data from lists of numbers, you not only lose a world of time, you risk not recognizing important spectral patterns.

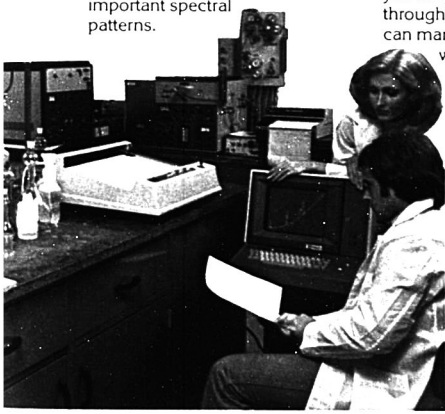

**Solution: Tektronix Interactive Graphics can replace manual operations with precise, instant visual displays.**

Tektronix Graphics Terminals let you keep to waveform display throughout your processing. You can manipulate data at will—without tedious and time-consuming manual translation. **You can see Graphic results immediately.** You can integrate and scale, correct baselines, perform mathematical transforms, and command camera-ready hard copy all with unequalled interactivity and simplicity.

**Keeping your eyes on the display keeps your mind on the solution.** Tektronix Graphics is priced right to begin with, and more than pays for itself in performance. And because it's from Tektronix, you know it's got the reliability that's been respected by research for years.

To get the whole Graphics story, talk to your Tektronix Sales Engineer, or write Tektronix.

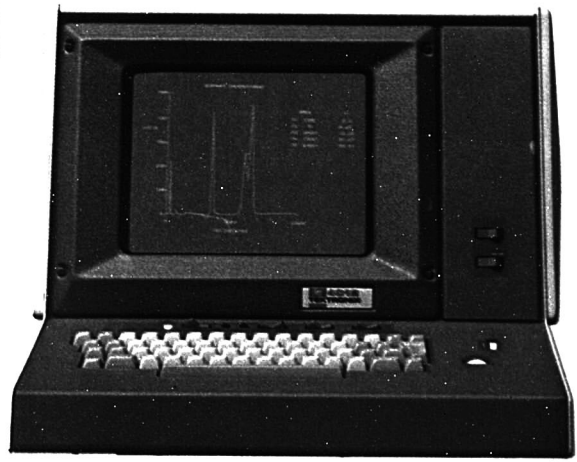

**Tektronix, Inc.**
Information Display Group
P.O. Box 500
Beaverton, OR 97077
**Tektronix Datatek N.V.**
P.O. Box 159, Badhoevedorp,
The Netherlands

Copyright © 1977, Tektronix, Inc.
All rights reserved.
OEM Information Available

CIRCLE 205 ON READER SERVICE CARD

**Tektronix**
COMMITTED TO EXCELLENCE

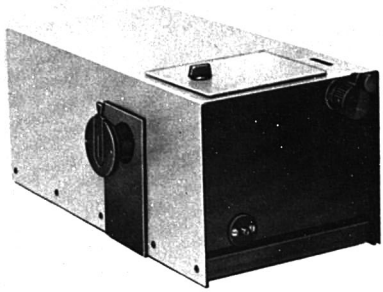

**Who put all those wonderful specifications in one little monochromator?**

Who but **Jarrell-Ash,** for over half-a-century a leader in monochromator engineering. J-A's newest ¼-meter, the Mark X, brings you more great features than ever:

■ Dramatically improved focal-plane accessibility. Lets you use the latest **multi-element arrays** (Vidicon, Pyrocon, charge-coupled devices, etc.) as well as photomultipliers. Incomparably versatile!

■ New optical design that **intrinsically** eliminates re-entry spectra at all wavelengths.

■ Superb infrared as well as visible and UV capability.

■ Choice of **10** quick-change pre-aligned gratings — a 175nm-40$\mu$ range. With remarkable dispersion (e.g., 3.0nm/mm with our 1200g/mm grating).

■ Finest resolution in its field. Better than 0.6nm with 1200 g/mm grating). On our parabolic-mirror model Mark X, it's **0.3nm!**

■ Minimal scattered light. At 500nm, it's less than **0.05%!**

■ A beautiful selection of accessories to make your lab life easier. Like digital Omni-Drive (1-200nm/minute) . . . quantum photometer . . . filter wheels to expedite fluorescence, phosphorescence, luminescence, polarization and photometry studies . . . **and much more.**

Use Mark X as a heavy-duty monochromator or as a spectrograph. In instruction **or** research. It's all in a handsome little package with a handsome little price. Not $2500, not $2000, but — thanks to volume production — a little over $1000.

Incidentally, we **call** it a quarter-meter. Actually we've made it 275mm for greater dispersion, improved focal plane. The extra 25mm are on the house.

***The monochromator people***

**Jarrell-Ash**

590 Lincoln St
Waltham MA 02154
(617) 890-4300

**A Division of Fisher Scientific Company**

CIRCLE 75 ON READER SERVICE CARD

The complete mechanism now consists of generation of $R$ at the electrode (Equation 1) with reaction of $R$ as it diffuses away from the electrode and encounters $Z$ (Equation 3). When the potential-step experiment is repeated, the absorbance response caused by generation of $R$ is less, due to its reaction with $Z$. Curves b–d show how the absorbance due to $R$ is diminished as the rate constant increases. The value for $k$ can be calculated from the magnitude by which the absorbance is decreased by the reaction. The appropriate diffusion equations must be solved or simulated to calculate rate constants (*2, 3*). Since the shape of the absorbance-time response varies depending upon the mechanism of the reaction, mechanistic information can also be obtained.

Although this discussion has focused on optical observation of the reaction by a light beam passing through an OTE and the solution, specular reflectance (*4*), internal reflectance (*1–3*), and resonance Raman (*7*) spectroscopies have also been used. These techniques are capable of monitoring extremely fast reactions with rates up to the diffusion-controlled limit. Consequently, instrumentation requirements are more stringent. Fast potentiostats and spectrometers interfaced with a computer for signal-averaging of repetitive pulses are necessary to realize the full capabilities of the technique. Rapid scanning spectrometers that can record several hundred complete spectra per second are utilized for obtaining spectra of short-lived intermediates in more complicated reaction mechanisms (*19*).

The thin-layer electrode is also useful for studying reaction mechanisms (*20, 21*). In this case, a potential is applied to the cell for about 30 s to completely convert all of $O$ in the thin solution layer to $R$. The reaction of $R$ is then monitored optically by light passing through electrode and solution. This approach is analogous to conventional kinetic methods such as stopped-flow. Consequently, the absorbance-time response can be mathematically treated with conventional kinetic equations. Since about 30 s is required to completely convert $O$ to $R$, this technique is used for slower reactions. As such, it complements the faster technique described above.

A variety of chemical reactions have been studied by the various spectroelectrochemical techniques. A few representative examples are listed in Table I.

**Indirect Coulometric Titration with Optical Monitoring.** The titration of molecules by reductant or oxidant quantitatively generated at an electrode is known as coulometry.

HPLC news:

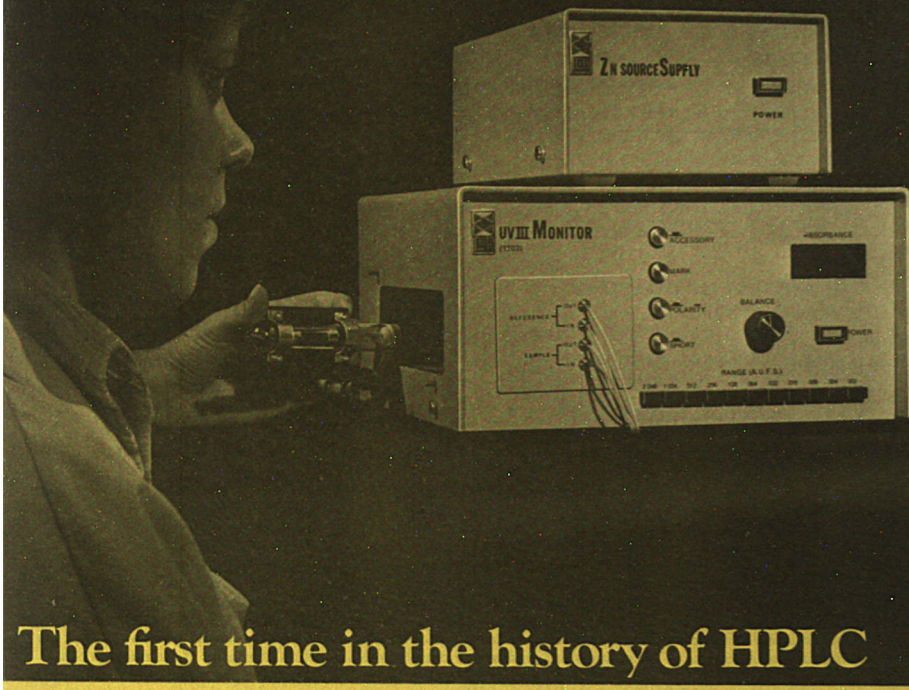


# The first time in the history of HPLC

# A fixed wavelength UV detector at 214 nm.

LDC announces a fixed wavelength UV Monitor with a 214 nm excitation source. This range has previously been available only in the more expensive variable wavelength detectors.

Among the many features of the new LDC UV III:

It's the most sensitive detector on the market at 254 nm and now 214 nm.

New long lifetime (up to 1,000 hours) zinc excitation source provides high sensitivity in new applications.

Digital display of differential absorbance.

Detection capability of 0.002 AUFS sensitivity.

Model 1203, 254 nm: $1800.

Model 1203, 214 nm: $2250.

In addition, a kit is available to convert existing Model 1203 UV Monitors to 214 wavelength. Send for brochure today.

Liquid chromatography by

**LABORATORY DATA CONTROL**
Division of Milton Roy Co.
P.O. Box 10235, Riviera Beach, Fl. 33404
305/844-5241. Telex 513479

European Office:
1 Newcastle St. Staffordshire,
ST15 - 8JU England
Telephone: 0785 83 4028 • Telex: 36623

CIRCLE 125 ON READER SERVICE CARD

**Table I. Reactions Studied by Spectroelectrochemistry**

| Electrogenerated species | Chemical reaction | Rate constant | Spectroelectrochemical technique |
|---|---|---|---|
| $MV^{\cdot}$ | $MV^{\cdot} + cyt\ c(III) \longrightarrow MV^{2+} + cyt\ c(II)$ | $> 2 \times 10^{8}\ M^{-1}\ s^{-1}$ | Transmission (*22*) |
| $Fe(CN)_6^{3-}$ | $2Fe(CN)_6^{3-} +$  $\longrightarrow 2Fe(CN_6)^{2-} +$  $+ 2H^{+}$ | $25\ M^{-1}\ s^{-1}$ | Transmission (*23*) |
| $TAA^{\cdot}$ | $TAA^{\cdot} + CN^{-} \longrightarrow TAA + CN\cdot$ | $2 \times 10^{5}\ M^{-1}\ s^{-1}$ | Transmission (*23*) |
| $Ta_6Br_{12}^{4+}$ | $Ta_6Br_{12}^{2+} + Ta_6Br_{12}^{4+} \longrightarrow 2Ta_6Br_{12}^{3+}$ | $7 \times 10^{7}\ M^{-1}\ s^{-1}$ | Internal reflection (*24*) |
| $TAA^{\cdot}$ | $TAA^{\cdot}$ ferrocene $\longrightarrow$ TAA + ferricinium | $1 \times 10^{9}\ M^{-1}\ s^{-1}$ | Internal reflection (*25*) |
| $DPA^{\cdot}$ | $DPA^{\cdot} + py \longrightarrow DPA(py)^{\cdot}$ | $2 \times 10^{4}\ M^{-1}\ s^{-1}$ | Transmission (*26*) |
| $\phi_2C{=}C\phi_2^{\cdot}$ | $2\phi_2C{=}C\phi_2^{\cdot} \rightleftharpoons \phi_2C{=}C\phi_2 + \phi_2C{=}C\phi_2^{2+}$<br>$\phi_2C{=}C\phi_2^{2+} \xrightarrow{k}$ cyclization | $1.5 \times 10^{-3}\ s^{-1}$ | Transmission (*27*) |
| | 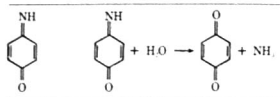 | $7 \times 10^{-3}\ s^{-1}$ | Transmission thin-layer (*20*) |
| | $\phi$–N(H)–N(H)–$\phi$ + $2H^{+} \longrightarrow H_2N$–$\phi$–$\phi$–$NH_2$ | $3 \times 10^{-2}\ s^{-1}$ | Transmission thin-layer (*21*) |

$MV^{\cdot}$: methyl viologen cation radical, $CH_3$–N⁺(C₅H₄)–C₆H₄–N⁺(C₅H₄)–$CH_3$ cyt *c*: cytochrome *c*

TAA: tri-*p*-anysilamine, $(CH_3O$–C₆H₄–$)_3$–N DPA: 9,10-diphenylanthracene

When the generating electrode is optically transparent, the course of the titration can be monitored optically by light passing through the electrode and the stirred solution (Figure 1B). A titration curve is obtained by plotting the absorbance at the monitored wavelength as a function of charge passed through the cell, the charge being proportional to the amount of titrant generated. The shape of the titration curve is determined by the optical properties, redox potentials, and *n* values of both the molecule being titrated and the electrogenerated titrant. Redox potentials of complex biological molecules can be obtained by careful measurement of the shape of titration curves (*1, 16, 28*).

An example of the capabilities of this technique is the titration of cytochrome *c* oxidase in the presence of cytochrome *c* (*29*). As the terminal component in the oxidative phosphorylation chain, cytochrome *c* oxidase transfers electrons from cytochrome *c* to oxygen, reducing the latter to water. It is a complex molecule containing two heme irons and two coppers (for a total of four redox centers) imbedded in a lipoprotein matrix. By contrast, cytochrome *c* is a relatively simple molecule with only a single heme iron as the redox center.

Figure 5 shows spectra recorded during the reductive titration of a mixture of cytochrome *c* oxidase and cytochrome *c*. The biocomponents were initially in their fully oxidized state. Each spectrum was recorded after the coulometric addition of 5.0 nequiv of the reductant methyl viologen radical cation, $MV_{\cdot}^{+}$, which was generated at a tin oxide transparent electrode by the following reaction:

$SnO_2$ electrode:

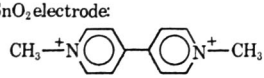

$$+ e^{-} \longrightarrow MV^{+}_{\cdot}$$

Solution: $xMV^{+}_{\cdot} + cyt_{ox}$

$$\longrightarrow xMV^{2+} + cyt_{red}$$

The absorbance increase at 605 nm corresponds to the reduction of the two heme components of cytochrome *c* oxidase; the increase at 550 nm corresponds to the reduction of the heme in cytochrome *c*. The inset figure shows the absorbance changes at 605 and 550 nm as a function of the amount of $MV_{\cdot}^{+}$ generated in terms of charge passed through the cell. Evaluation of the relative shapes of the two titration curves indicates the sequence of titration: one heme of cytochrome *c* oxidase is reduced first, followed by the heme in cytochrome *c* and then the second heme in cytochrome *c* oxidase. Overlap occurs as a result of the close proximity of the redox potentials. Comparison between such experimental titration curves and computer-simulated curves for various values of redox potentials enables the exact redox potentials of the hemes and coppers in cytochrome *c* oxidase to be evaluated. The total amount of charge required for complete reduction of the two cytochromes corresponds to a five-electron stoichiometry: one electron for cytochrome *c* and four electrons for the two hemes and two coppers in cytochrome *c* oxidase.

Cytochrome *c*, myoglobin, cytochrome *c* oxidase, blue copper laccases, and spinach ferredoxin have been studied by indirect coulometric titration. The technique exhibits several advantageous features. Nanoequivalent aliquots of oxidant or reductant can be accurately and precisely generated. Small-volume (one mL and less) cells require only small amounts of expensive biocomponents for measurements. The biocomponent can be repetitively reduced and oxidized.

# The Intelligent Approach to LC.

Intelligence adds a critical new dimension to today's most dynamic analytical problem solver—Liquid Chromatography.

Waters, building on its proven base of leadership in LC instrumentation, has developed a new generation of "Intelligent" LC modules.

This Intelligent Approach incorporates microprocessor-based Intelligence in every module that does more than just automate specific fixed functions. These modules can stand alone, perform independently, and communicate with each other. The user can now tailor his LC instrumentation to meet specific problem-solving needs.

This is all possible because of a unique system architecture called Intelink™. Intelink permits Distributed Chromatographic Processing (DCP™)—total system coordination without inflexible central control. Intelligent LC instrumentation has the capacity to evolve—new modules can be added anytime.

Advanced equipment design is just one aspect of The Intelligent Approach to LC. Our application support, training programs, specialized technical representatives, and worldwide seminars ensure unrivaled levels of customer success. Our position as world leader in LC is the result of our total commitment to provide you with advanced products and successful solutions.

Find out what Waters' Intelligent Approach means to you. Write for complete information.

**Waters Associates**
Milford, Massachusetts 01757

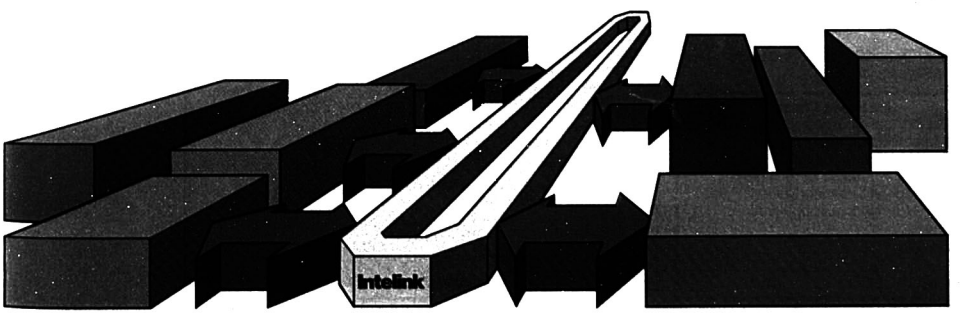


CIRCLE 240 ON READER SERVICE CARD

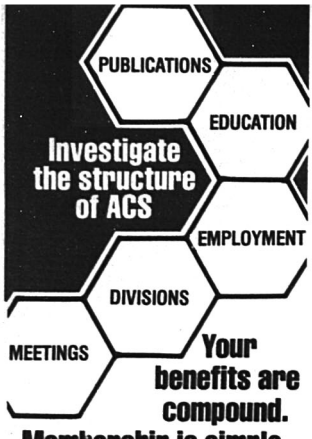


American Chemical Society members receive *Chemical and Engineering News* each week. *C&E News* brings you the up-to-date happenings in the chemical world plus official ACS news.

**AND THERE ARE MANY OTHER BENEFITS:**

**Publications**—Members enjoy substantial savings on world renowned ACS publications.

**Meetings**—Two national meetings each year plus a host of regional and local meetings are held for your benefit.

**Local Sections**—provide you with activities of local interest and an opportunity to participate in Society affairs.

**Divisions**—28 subject divisions help you keep up with your special chemical interest.

**Educational Activities**—short courses, audio courses and interaction courses help you expand as a professional.

**Employment Aids**—give you a helping hand in today's tight job market.

But most important, your membership helps support the scientific and educational society that represents *you* as a professional.

110,000 Chemists and Chemical Engineers know the value of ACS membership.

Send coupon below today for an application.

**American Chemical Society**
Office of Member Services
1155 Sixteenth Street, N.W.
Washington, D. C. 20036

Yes, I am interested in membership in the American Chemical Society. Please send information and application.

Name _____
Address _____
City _____
State _____ Zip _____


Redox potentials can be measured for optically nonabsorbing redox components (*30*). No volume changes occur during titrations, eliminating dilution corrections for spectral data. Solutions are easily rendered and maintained anaerobic by vacuum degassing procedures (*28*).

**Surface Studies.** The importance of surface studies stems from the influence of the surface condition on the rate and mechanism of an electrode reaction. The nature of the electrode surface itself can be probed by reflectance, internal reflection, transmission, Raman, and ellipsometric spectroscopies (*1–3, 5, 6, 31, 32*). The formation of oxide layers on metal electrodes and the absorption of ions, organic molecules, and proteins on the electrode surface have been observed optically. Techniques such as ESCA and Auger spectroscopy have yielded valuable information about the surfaces of electrodes after their removal from the electrochemical cell (*33, 34*).

## Conclusion

The precision with which oxidation states can be controlled, coupled with the capability for obtaining spectral information, is stimulating the adoption of spectroelectrochemical techniques for the study of inorganic, organic, and biological redox species.

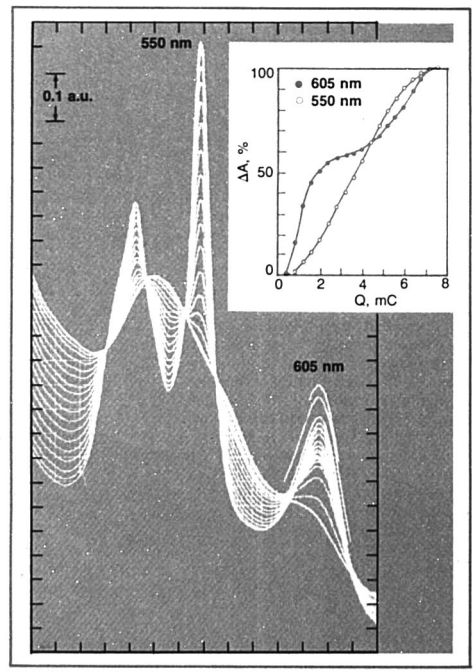


**Figure 5.** Indirect coulometric titration of cytochrome *c* (17.5 $\mu M$) and cytochrome *c* oxidase (6.3 $\mu M$) by reduction with $MV^{+\cdot}$ electrogenerated at $SnO_2$ optically transparent electrode

Each spectrum recorded after generation of $5 \times 10^{-9}$ equiv (0.5 millicoulombs) of $MV^{+\cdot}$. Inset shows titration curves recorded at 550 and 605 nm (*29*)

## References


(1) T. Kuwana and W. R. Heineman, *Acc. Chem. Res.*, **9**, 241 (1976).
(2) N. Winograd and T. Kuwana, "Spectroelectrochemistry at Optically Transparent Electrodes", in "Electroanalytical Chemistry", Vol 7, A. J. Bard, Ed., Marcel Dekker, New York, N.Y., 1974.
(3) T. Kuwana, *Ber. Bunsenges. Phys. Chem.*, **77**, 858 (1973).
(4) A.W.B. Aylmer-Kelly, A. Bewick, P. R. Cantrill, and A. M. Tuxford, *Faraday Discuss. Chem. Soc.*, No. 56, 96 (1973).
(5) J.D.E. McIntyre, "Specular Reflection Spectroscopy of the Electrode-Solution Interphase", in "Advances in Electrochemistry and Electrochemical Engineering", Vol 9, R. H. Muller, Ed., Wiley-Interscience, New York, N.Y., 1973.
(6) W. N. Hansen, "Internal Reflection Spectroscopy in Electrochemistry", *ibid.*
(7) D. L. Jeanmaire, M. R. Suchanski, and R. P. Van Duyne, *J. Am. Chem. Soc.*, **97**, 1699 (1975).
(8) F. M. Hawkridge and B. Ke, *Anal. Biochem.*, **78**, 76 (1977).
(9) L. F. Faulkner and A. J. Bard, in "Electroanalytical Chemistry", Vol 10, A. J. Bard, Ed., Marcel Dekker, New York, N.Y., 1977.
(10) T. M. McKinney, "Electron Spin Resonance in Electrochemistry", in "Electroanalytical Chemistry", Vol 10, A. J. Bard, Ed., Marcel Dekker, New York, N.Y., 1977.
(11) J. A. Richards and D. H. Evans, *Anal. Chem.*, **47**, 964 (1975).
(12) M. Petek and S. Bruckenstein, *J. Electroanal. Chem.*, **47**, 329 (1973).
(13) R. W. Murray, W. R. Heineman, and G. W. O'Dom, *Anal. Chem.*, **39**, 1666 (1967).

# THE WHOLE IS GREATER THAN THE SUM OF THE PARTS.

When you buy a Hamilton 1800 Syringe you're really buying a dozen parts assembled together as a precision syringe.

All the parts are replaceable and interchangeable, so if you break or bend any part, you can replace it and put everything back together again as good as new...and for a lot less money than a new syringe.

You can even stock a few spare parts for quick repairs to eliminate any down time if something happens to your syringe.

But there are several other good reasons the 1800 syringe may be the best one you'll ever buy. It was designed for high pressure chromatography, at working pressures of over 400 atmospheres (6000 psi).

It is available in 10 µl, 25 µl, 50 µl and 100 µl capacities ...with a Teflon tip on the plunger, making it both gas and liquid tight.

The special finger grip makes it comfortable and handy to use. You can adjust the handle to apply varying degrees of friction on the plunger to avoid slippage at high pressures. There's also a stop for the prevention of plunger blow-out.

You can adjust the needle to scale zero on the glass barrel...and lock it there... by a simple finger adjustment.

The metal holder acts as a guide, making it almost impossible to bend plungers.

Put it all together and you have the "most modern syringe available for chromatography." Let us tell you all about it, write for literature to John Nadolny, Hamilton Company, Post Office Box 10030, Reno, Nevada 89510.

**HAMILTON**



CIRCLE 95 ON READER SERVICE CARD

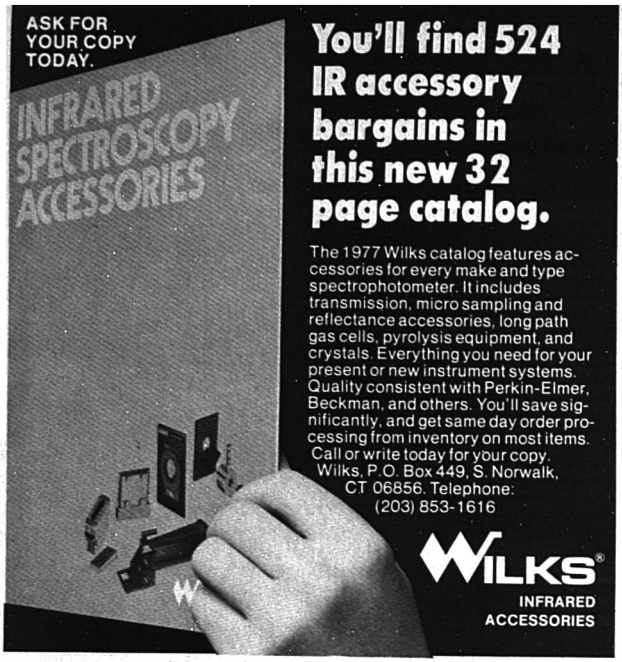


CIRCLE 235 ON READER SERVICE CARD

*Worried About The Accuracy Of Your Lab's Data?*

Stop worrying! Evaluate your lab confidentially with certified reference samples — — PesTicidS™, PotableWatR™ and WasteWatr™ samples are available.


UNCONDITIONALLY GUARANTEED!

FREE *"Guide to Quality Control Practices.."* to all new customers.

**environmental resource associates**
120 east sauk trail
south chicago heights, illinois 60411
(312) 755-6060

CIRCLE 64 ON READER SERVICE CARD

(14) D. F. Rohrbach, E. Deutsch, and W. R. Heineman, "Thin Layer Spectroelectrochemical Studies of Cobalt and Copper Schiff Base Complexes in *N,N*-Dimethylformamide", in "Characterization of Solutes in Nonaqueous Solvents", G. Mamantov, Ed., Plenum, New York, N.Y., 1978.
(15) W. R. Heineman, B. J. Norris, and J. F. Goelz, *Anal. Chem.*, **47**, 79 (1975).
(16) R. Szentrimay, P. Yeh, and T. Kuwana, "Evaluation of Mediator-Titrants for the Indirect Coulometric Titration of Biocomponents", in "Electrochemical Studies of Biological Systems", D. T. Sawyer, Ed., American Chemical Society, Washington, D.C., 1977.
(17) P. T. Kissinger and C. N. Reilley, *Anal. Chem.*, **42**, 12 (1970).
(18) T. M. Kenyhercz, T. P. DeAngelis, B. J. Norris, W. R. Heineman, and H. B. Mark, Jr., *J. Am. Chem. Soc.*, **98**, 2469 (1976).
(19) J. W. Strojek, G. A. Gruver, and T. Kuwana, *Anal. Chem.*, **41**, 481 (1969); E. Steckhan and D. A. Yates, *Ber. Bunsenges. Phys. Chem.*, **81**, 369 (1977).
(20) R. L. McCreery, *Anal. Chem.*, **49**, 206 (1977).
(21) E. A. Blubaugh, A. M. Yacynych, and W. R. Heineman, unpublished data.
(22) L. N. Mackey and T. Kuwana, *Bioelectrochem. Bioenerg.*, **3**, 596 (1976).
(23) H. N. Blount, N. Winograd, and T. Kuwana, *J. Phys. Chem.*, **74**, 3231 (1970).
(24) N. Winograd and T. Kuwana, *J. Am. Chem. Soc.*, **92**, 224 (1970).
(25) N. Winograd and T. Kuwana, *ibid.*, **93**, 4343 (1971).
(26) H. N. Blount, *J. Electroanal. Chem.*, **42**, 271 (1973).
(27) E. Steckhan, *Electrochim. Acta*, **22**, 395 (1977).
(28) F. M. Hawkridge and T. Kuwana, *Anal. Chem.*, **45**, 1021 (1973).
(29) W. R. Heineman, T. Kuwana, and C. R. Hartzell, *Biochem. Biophys. Res. Commun.*, **50**, 892 (1973).
(30) J. L. Anderson, T. Kuwana, and C. R. Hartzell, *Biochemistry*, **15**, 3847 (1976).
(31) R. H. Muller, "Principles of Ellipsometry", in "Advances in Electrochemistry and Electrochemical Engineering", Vol 9, R. H. Muller, Ed., Wiley-Interscience, New York, N.Y., 1973.
(32) D. L. Jeanmaire and R. P. Van Duyne, *J. Electroanal. Chem.*, **84**, 1 (1977).
(33) K. S. Kim, A. F. Grossman, and N. Winograd, *Anal. Chem.*, **46**, 197 (1974).
(34) C. M. Elliott and R. W. Murray, *ibid.*, **48**, 1247 (1976).

*William R. Heineman is an associate professor of chemistry and chairman of the analytical division at the University of Cincinnati. His current research interests include bioelectrochemistry, electroanalysis with thin-layer cells, and the development and application of optically transparent electrodes and thin-layer spectroelectrochemical techniques.*

# WHO DID WHAT WITH FLORISIL IN CHROMATOGRAPHY. FREE.

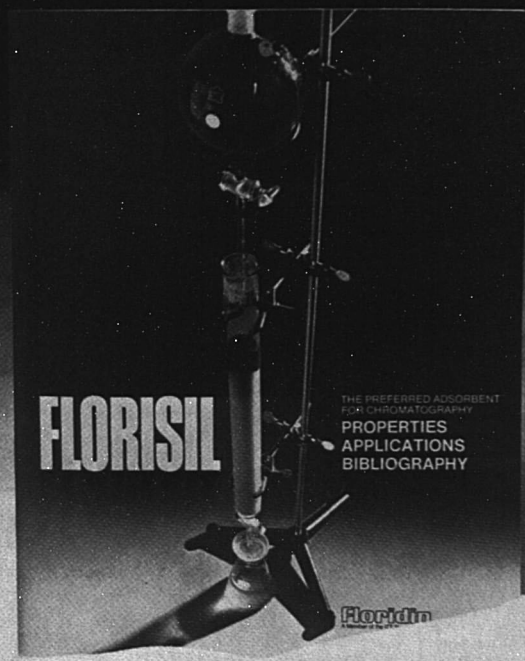


You can get this 60-page chromatography bibliography free for the asking from Floridin. It'll tell you exactly why Florisil® is widely used to solve tough separation problems in column and thin layer chromatography.

The bibliography includes Florisil's chemical composition, physical properties and adsorptivity data. And a listing of who did what in chromatography with Florisil. Everything from Alkaloids to Thiosteroids.

Free for all. Floridin's Chromatography Bibliography. Contact Floridin Company, Dept. A-4, Three Penn Center, Pittsburgh, PA 15235. Phone: (412) 243-7500.

Floridin
A Member of the ITT System

CIRCLE 165 ON READER SERVICE CARD PG-700

# Bio-Rad AG® resins

## unparalleled after more than 2 decades for purity and uniformity.

The purity and sizing of ion exchange resins play the key roles in reliability and reproducibility of results. Bio-Rad AG resins are purified by several steps to very low levels of heavy metals. And we size our resins until microscopic examination shows that 95% of the resin beads are within the specified range. The photomicrograph clearly shows the difference painstaking sizing makes.

Oddly enough, you pay little or nothing more for these superior resins! Why not get the best?

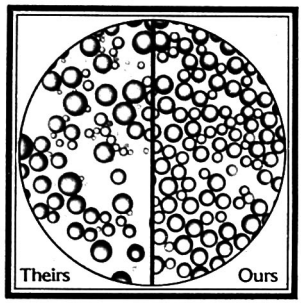


**Our massive wall chart**

To help you select the proper AG resin for the application, Bio-Rad has prepared a massive (70x100 cm) full color wall chart that is both useful and attractive. Your inquiry will speed a copy to you.


BIO-RAD *Laboratories*

2200 Wright Avenue, Richmond, CA 94804
Phone (415) 234-4130
Also in: Rockville Centre, N.Y. Toronto, Ontario, London, Milan, Munich, Sao Paulo, Vienna

CIRCLE 28 ON READER SERVICE CARD

# New PPM and Percent Photometric Analyzer for continuous monitoring

The Model 514 is a continuous-duty photometric analyzer suitable for monitoring parts-per-million (ppm) and percentage concentrations of water in a variety of compounds — acids, alcohols, aromatics, chlorinated hydrocarbons, oils, ammonia, ethylene dichloride, and many other liquid and gas applications. Use is primarily for process control, quality assurance and corrosion prevention. The system can replace time-consuming laboratory analysis with real time monitoring. The method of analysis — measuring the radiation absorbed in a selected band of the near-infrared portion of the spectrum — features a single sample cell, chopped beam, dual wavelength electro-optical design for maximum stability, high sensitivity and automatic turbidity compensation.

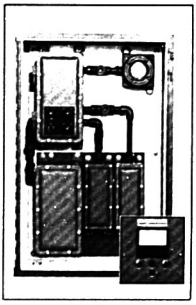

For added reliability, the new analyzer incorporates modular, integrated-circuit electronics — including direct meter readout, analog output signals and electronic alarms. An automatic zero can be supplied as an option. For more information contact TAI.

*A HIGH TECHNOLOGY COMPANY*

TELEDYNE ANALYTICAL INSTRUMENTS
333 West Mission Drive, San Gabriel, California 91776
Phone: (213) 283-7181 Telex: 910 589 1605

CIRCLE 207 ON READER SERVICE CARD

# Drug Metabolism Concepts

ACS Symposium Series No. 44

Donald M. Jerina, *Editor*
*The National Institutes of Health*

*A symposium co-sponsored by the Division of Medicinal Chemistry and the Division of Analytical Chemistry of the American Chemical Society.*

**SIS/American Chemical Society**
1155 16th St., N.W.
Wash., D.C. 20036

Written by leading authorities in the field, this new interdisciplinary collection will make a valuable contribution to the literature of scientists working in medicinal chemistry, pharmacology, biochemistry, and toxicology.

Eight chapters present in-depth research reports on the role of enzyme systems, especially cytochrome P-450, in drug activation and detoxification. This timely study on drug metabolic pathways is vital because of the possibilities of toxic or carcinogenic intermediates caused by the action of enzymes on drugs and anesthetics.

**CONTENTS**

Cytochrome P-450 in Oxygen Activation for Drug Metabolism • Synthetic Models for the Reaction Stages of Cytochrome P-450 • Isolation of Multiple Forms of Liver Microsomal Cytochrome P-450 • Resolution of Multiple Forms of Rabbit Liver Cytochrome P-450 • Enantiomeric Selectivity and Perturbation of Product Ratios as Methods for Studying the Multiplicity of Microsomal Enzymes • Purified Cytochrome P-448 and Epoxide Hydrase in the Activation and Detoxification of Benzo[a]pyrene • In vitro Reactions of the Diastereomeric 9,10-Epoxides of (+) and (−)-*trans*-7,8-Dihydroxy-7,8-dihydrobenzo[a]pyrene with Polyguanylic Acid • Metabolic Activation in Chemical-Induced Tissue Injury

196 pages (1977) clothbound $15.50
LC 77-2279 ISBN 0-8412-0370-9

# Now You can shake Separatory Funnels as big as 2000ml.

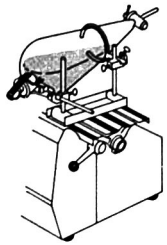

Rest your wrist! Get this new separatory funnel support for your Burrell Wrist-Action™ Shaker and shake any separatory funnel . . . from 500 to 2000 ml capacity. Replicable results because you set the height and angle of the vessel and control the time and amplitude of the Shaker. The new Burrell Separatory Funnel Supports fit any Burrell Shaker equipped with a platform.

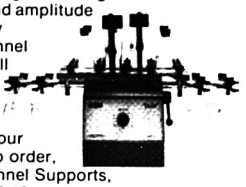

For more information, write for our product data sheet. To order, ask for Separatory Funnel Supports, CATALOG NO. 75-777-12.

BURRELL

**BURRELL** CORPORATION
2223 Fifth Avenue Pittsburgh Pa 15219
Telephone 412-471-2527

CIRCLE 29 ON READER SERVICE CARD

# FLUORESCENCE SIMPLIFIED

Compact and sturdy, the JY-3 Spectrofluorometer is adaptable to suit your analytical needs. Design is fully modular; an extensive line of accessories is available. Fine spectral purity achieved via holographic concave gratings.

☐ 5 cell turret sample chamber
☐ Transmission capability ☐ Ratio reference cell
☐ Interchangeable slits: 0.2 to 10 nm

For real time fluorescence studies, ask about our JY-4 Video Spectrofluorometer.

Instruments SA, Inc., J-Y Optical Systems Division, 173 Essex Avenue, Metuchen, N.J. 08840. (201) 494-8660. Telex 844-516. In Europe, Jobin Yvon, Division d'Instruments SA, 16-18 Rue du Canal, 91160 Longjumeau, France. Tel. 909.34.93 Telex JOBYVON 842-692882.

JOBIN YVON **Instruments SA, Inc.**
**J-Y Optical Systems Division**

CIRCLE 103 ON READER SERVICE CARD

# OVENS

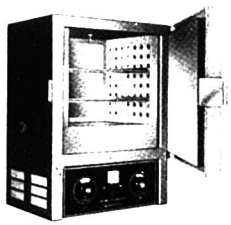

**AMERICA'S PREFERRED LINE— 1078 MODELS IN ALL!**

Bench type gravity ovens to 96 cu. ft. mechanical ovens. Temperatures to +1300°F. Advanced engineering, including FRICTION-AIRE™ — patented heaterless chambers which heat by moving air. Exclusive Blue M controls on most models — all applied by Blue M trained personnel, not reps. For data, contact: Blue M Electric Company; Corporate Headquarters: Blue Island, Illinois 60406.

BLUE M

CIRCLE 30 ON READER SERVICE CARD

Unprecedented performance in...

# CIRCULAR DICHROISM

ISA's Mark III Dichrograph remains the outstanding system in circular dichroism. Offering sensitivity as much as 10 times greater ($10^{-6}$ $\Delta A$/mm, or 0.03 m°/mm), spectral range 180 - 800 nm or 180 - 1000 nm, high resolution, system stability and measurement repeatability, the Mark III's excellence is the result of highest quality optics and a sophisticated total system design. It is entirely computer compatible.

For actual tests on your samples or further information, call or write: Instruments SA, Inc., J-Y Optical Systems Division, 173 Essex Avenue, Metuchen, N.J. 08840 (201) 494-8660, Telex 844 516. In Europe, Jobin Yvon, Division d'Instruments SA, 16-18 Rue du Canal, 91160 Longjumeau, France, Tel. 909.34.93 Telex JOBYVON 842-692882.

JOBIN YVON **Instruments SA, Inc.**
**J-Y Optical Systems Division**
DIVISION D'INSTRUMENTS SA

CIRCLE 104 ON READER SERVICE CARD

# LABORATORY SERVICE CENTER


2-Amino-5-chlorobenzophenone • 4-Aminoantipyrine • Bromoacetal
p-Bromoaniline • 1-Bromonaphthalene • 2-Chloro-4-nitrobenzoic Acid
Dimethyl Acetal • Disodium Phenylphosphate • Dodecyl Gallate
Ethyl Lactate • Ethyl Thiourea • 2-Furildioxime • L-Lysine MonoHCl
6-Methoxy-1-tetralone • Methyl Acetate • α-Naphtholphthalein
Neutral Red • Nitroso-R-Salt • Oxamide • K & Na Rhodizonates
Pyruvic Acid • Reinecke Salt • Sarcosine • Silver Diethyldithiocarbamate
Sodium Dithionate • Sodium Tetraphenylboron • Succinimide • Xanthone

*Write for our Products List of over 3,000 chemicals*

Tel.: 516-273-0900 TWX: 510-227-6230

**EASTERN CHEMICAL**
Division of GUARDIAN CHEMICAL CORP.
BOX 2500 N
HAUPPAUGE, N. Y. 11787

**Nitrogen 15**
15 years' experience in synthesising
LABELLED COMPOUNDS
Prochem
19 Ox Bow Lane
Summit, N.J. 07901
201-273-0440
NEW CATALOG AVAILABLE

**Microparticle Standards**
Large assortment of well-characterized microspheres and micropowders for analytical, research, and testing applications. Range of diameters from .05 to 500 microns (μm). Size and other physical properties are listed for each product. Materials include polystyrene, glass, pollens, minerals, many others. Write or telephone for Data File 45.
Duke Scientific Corporation
445 Sherman Avenue
Palo Alto, CA 94306
Phone (415) 328-2400

**Laboratory Service Center** (Equipment, Materials, Services, Instruments for Leasing), Maximum space — 4 inches per advertisement. Column width, 2-3/16"; two-column width, 4-9/16". Artwork accepted. No combination of directory rates with ROP advertising. Rates based on number of inches used within 12 months from date of first insertion. Per inch: 1" — $58; 12" — $57; 24" — $56; 36" — $55; 48" — $54.

*CALL OR WRITE BARBARA AUFDERHEIDE*

**ANALYTICAL CHEMISTRY**
**25 Sylvan Road, So.**
**Westport, Ct. 06880**
**203-226-7131**

**LAB SAFETY**
*Send for 1978 Catalog*
LAB SAFETY SUPPLY CO.
P.O.Box 1422, Janesville, WI 53545

**USE LABORATORY SERVICE CENTER**


## INDEX TO ADVERTISERS IN THIS ISSUE

# INDEX TO ADVERTISERS IN THIS ISSUE



** Company so marked has advertisement in the foreign regional edition only*

*Advertising Management for the American Chemical Society Publications*

**CENTCOM, LTD.**

Thomas N. J. Koerwer, President; James A. Byrne, Vice President; Clay S. Holden, Vice President; Benjamin W. Jones, Vice President; Robert L. Voepel, Vice President; C. Douglas Wallach, Vice President, 25 Sylvan Rd. South, Westport, Connecticut 08880 (Area Code 203) 226-7131

ADVERTISING SALES MANAGER
**James A. Byrne**

SALES REPRESENTATIVES

**Atlanta, GA . . . Robert E. Kelchner, CENTCOM, Ltd. Telephone: 203-226-7131**

**Boston, MA . . . Don Davis, CENTCOM, LTD. Telephone 203-226-7131**

**Chicago . . . Thomas Hanley, CENTCOM, LTD., 540 Frontage Rd., Northfield, Ill. 60093. 312-441-6383.**

**Cleveland . . . James Pecoy, CENTCOM, LTD., Suite 205, 18615 Detroit Ave., Lakewood, Ohio 44107. 216 228-8050.**

**Houston . . . Robert LaPointe, CENTCOM, LTD., 415-692-0949.**

**Denver . . . Clay S. Holden, CENTCOM LTD., 213-776-0552.**

**Los Angeles 90045 . . . Clay S. Holden, CENTCOM, LTD., Newton Pacific Center, 3142 Pacific Coast Highway, Suite 200, Torrance, CA 90505, 213-325-1903**

**New York 10017 . . . Don Davis, Richard L. Going, CENTCOM LTD., 60 East 42nd St., 212-972-9660**

**Philadelphia . . . Richard L. Going, CENTCOM LTD., GSB Building, Suite 510 1 Belmont Avenue Bala Cynwyd, Pa. 19004. Telephone: 215-667-9666**

**San Francisco, CA . . . Robert LaPointe, CENTCOM, LTD., Room 235, 1499 Bayshore Highway, Burlingame, CA 94010. Telephone: (415) 692-0949**

**Westport 06880 . . . Don Davis, CENTCOM, LTD., 25 Sylvan Rd. So., 203-226-7131.**

**Manchester, England . . . Jill E. Loney, Technomedia Ltd., 216, Longhurst Lane, Mellor, Stockport, SK6 5PW, Telephone: 061-427-5660**

**Reading, England . . . Malcolm Thiele, Technomedia Ltd., Wood Cottage, Shurlock Row, Reading, RG10 OOE. Telephone 073-581-302**

**Paris, France . . . Patric B. Hale, Technomedia Ltd., 18 Rue Gounod, 92 Saint-Cloud, Paris. Telephone: 602-24-79**

**Tokyo, Japan . . . Haruo Moribayashi, International Media Representatives Ltd., 1, Shibe-Kotohiracho, Minato-ku Tokyo. Telephone: 502-0656**

PRODUCTION DEPARTMENT

*Production Director*
**Joseph P. Stenza**

*Advertising Production Assistant*
**Barbara Aufderheide**

## We're kind of a chromatographic hardware store . . . if you don't see it, ask us.

Over recent years, we've developed what is probably the broadest line of chromatographic apparatus and supplies available from one company.

Being candid about it, we didn't do it ourselves.

Many of the developments that we've added to our Chromaflex® line came from users—researchers and leaders in the field of chromatography. We paid attention to needs and worked with researchers to solve peculiar problems they had.

Then we had a new piece of apparatus to offer researchers with similar needs.

Some of these items were unique, such as the first separable column with removable fritted disc; the first all-glass ground TLC plates; the first conical bottom Microflex® storage tubes for valuable samples; and recently, the first practical disposable column.

What's meaningful to you now is that many of these firsts have grown into complete lines, and we no doubt have what you need in chromatographic apparatus ready for off-the-shelf delivery.

But unlike a hardware store, we carry only one brand—the Kontes crown—which says quality, no matter what you ask for from us.

Ask your Kontes salesman for our new Chromaflex® Catalog CA-3, or contact the home store.

® Trademark of Kontes Glass Company

**KONTES**

Vineland, N.J. 08360

Exclusive Distributors: **KONTES OF ILLINOIS,** Evanston, Illinois • **KONTES OF CALIFORNIA,** San Leandro, California
**KONTES (U.K.) LTD.,** Carnforth, England

CIRCLE 115 ON READER SERVICE CARD

Use this card to receive *your own* monthly copy of 1978

# ANALYTICAL CHEMISTRY

Start my subscription as follows:

| | U.S. | Can.** | Foreign** |
|---|---|---|---|
| ACS Members* | ☐ $10.00 | ☐ $19.00 | ☐ $19.00 |
| Nonmembers (Personal) | ☐ $14.00 | ☐ $23.00 | ☐ $23.00 |
| Institutional | ☐ $14.00 | ☐ $23.00 | ☐ $29.00 |

☐ Bill me ☐ Bill Company ☐ Payment enclosed

(Make payable: American Chemical Society)

Name_____

Position_____

Your Employer_____

☐ Home

Address ☐ Business_____

City_____ State_____ ZIP_____

Employer's business ☐ Manufacturing ☐ Academic ☐ Government ☐ Other_____

If manufacturer, type of products produced_____

_____

*Subscriptions at ACS member rates are for personal use only.

**Payment must be made in U.S. Currency, by international money order, UNESCO coupons, U.S. bank draft; or through your book dealer.

*Allow 60 days for your first copy to be put in the mail.*

9998-G

***Mail this postage-free card today***

Use this card to receive *your own* monthly copy of 1978

ANALYTICAL CHEMISTRY

Start my subscription as follows:

| | U.S. | Can.** | Foreign** |
|---|---|---|---|
| ACS Members* | ☐ $10.00 | ☐ $19.00 | ☐ $19.00 |
| Nonmembers (Personal) | ☐ $14.00 | ☐ $23.00 | ☐ $23.00 |
| Institutional | ☐ $14.00 | ☐ $23.00 | ☐ $29.00 |

☐ Bill me ☐ Bill Company ☐ Payment enclosed

(Make payable: American Chemical Society)

Name_____

Position_____

Your Employer_____

☐ Home

Address ☐ Business_____

City_____ State_____ ZIP_____

Employer's business ☐ Manufacturing ☐ Academic ☐ Government ☐ Other_____

If manufacturer, type of products produced_____

_____

*Subscriptions at ACS member rates are for personal use only.

**Payment must be made in U.S. Currency, by international money order, UNESCO coupons, U.S. bank draft; or through your book dealer.

*Allow 60 days for your first copy to be put in the mail.*

9998-G

***Mail this postage-free card today***

FIRST CLASS
Permit No. 1411-R
Washington, D.C.

**BUSINESS REPLY MAIL**
No postage stamp necessary if mailed in the United States

Postage will be paid by

**AMERICAN CHEMICAL SOCIETY**
**1155 Sixteenth Street, N. W.**
**Washington, D.C. 20036**

*ATTN: G. HEBRON*

FIRST CLASS
Permit No. 1411-R
Washington, D.C.

**BUSINESS REPLY MAIL**
No postage stamp necessary if mailed in the United States

Postage will be paid by

**AMERICAN CHEMICAL SOCIETY**
**1155 Sixteenth Street, N. W.**
**Washington, D.C. 20036**

*ATTN: G. HEBRON*

analytical chemistry

*Editor:* **Herbert A. Laitinen**

EDITORIAL HEADQUARTERS
1155 Sixteenth St., N.W.
Washington, D.C. 20036
Phone: 202-872-4570 Teletype: 710-8220151

*Managing Editor:* Josephine M. Petruzzi
*Associate Editor:* Andrew A. Husovsky
*Associate Editor, Easton:* Elizabeth R. Rufe
*Assistant Editors:* Barbara Cassatt, Nancy J. Oddenino, Deborah C. Stewart
*Production Manager:* Leroy L. Corcoran
*Art Director:* John V. Sinnett
*Designer:* Alan Kahan
*Artist:* Diane Reich

**Advisory Board:** Donald H. Anderson, Peter Carr, Velmer Fassel, David Firestone, Kurt F. J. Heinrich, Philip F. Kane, Barry L. Karger, J. Jack Kirkland, Lynn L. Lewis, Marvin Margoshes, Harry B. Mark; Jr., J. W. Mitchell, Harry L. Pardue, Garry A. Rechnitz, W. D. Shults

**Instrumentation Advisory Panel:** Gary D. Christian, Catherine Fenselau, Nathan Gochman, Gary M. Hieftje, Gary Horlick, Peter J. Kissinger, James N. Little, C. David Miller, Sidney L. Phillips.

*Contributing Editor:* Claude A. Lucchesi
Department of Chemistry, Northwestern University, Evanston, Ill. 60201

*Published by the*
**AMERICAN CHEMICAL SOCIETY**
1155 16th Street, N.W.
Washington, D.C. 20036

**Books and Journals Division**
*Director:* D. H. Michael Bowen
*Editorial:* Charles R. Bertsch
*Magazine and Production:* Bacil Guiley
*Research and Development:* Seldon W. Terrant
*Circulation Development:* Marion Gurfein

Manuscript requirements are published in the January 1978 issue, page 189. Manuscripts for publication (4 copies) should be submitted to ANALYTICAL CHEMISTRY at the ACS Washington address.

The American Chemical Society and its editors assume no responsibility for the statements and opinions advanced by contributors. Views expressed in the editorials are those of the editors and do not necessarily represent the official position of the American Chemical Society.

# The Toy Theory of Modern Analysis

In an article entitled "The Toy Theory of Western History", [*CHEMTECH.*, **7**, 595 (1977)], M. E. D. Koenig described the evolution of military weapons in terms of the desire for man to play with toys of an ever-increasing power and complexity. Even though the article has nothing to do with analytical chemistry, the concept of gadgetry seeming to feed upon itself to reach truly awesome proportions of complexity must on occasion haunt laboratory managers and research directors. This thought evidently was the main justification for publishing the article, for in the table of contents checklist was the query "Will that double overhead, quadriphonic, Fourier transform, gazzeloping hustang really solve The problem or do you just want to play with it?"

Looking at the past several decades of analytical instrumentation, one gets the impression that the trend toward complexity is not a linear but an exponential function of time. It is not difficult to recall examples of compounded intricacy that seem to support the idea of the toy theory. By and large, however, there is a close coupling between the complexity of equipment and the degree of sophistication of the information obtained. There seems to be no end to the demand for more and more detail of analytical information when it becomes possible to attain it. This is true both for complex systems in which components are being detected and measured at higher and higher sensitivity and resolution, and also for relatively simple systems in which nontraditional analytical information is being sought higher and higher levels of detail and complexity.

Up to a point, this is all to the good, for it stimulates analytical research which in turn pays dividends in useful output. The question at some point arises as to whether this more detailed information is worth the investment in instrumentation and personnel. There is no absolute answer to this question. Rather, each specific situation needs to be examined in terms of the problems that need solution. If a problem can be adequately solved by a test tube observation, there is no justification for elaborate instrumental measurements; but if the problem involves intricate information about complex systems, there is no alternative to a correspondingly sophisticated measurement. We all need occasionally to sidestep the temptation to play with our toys unnecessarily, and to get on with the task of solving the problem.

# Wavelength-Modulated Continuum Source Atomic Fluorescence Spectrometer

**F. Lipari and F. W. Plankey***

*Department of Chemistry, University of Pittsburgh, Pittsburgh, Pennsylvania 15260*

**The wavelength-modulation capability of an oscillating narrow bandpass interference filter has been combined with the versatility of an atomic fluorescence flame spectrometer with continuum source. The operating characteristics of this device are described for solutions of Cu and Mg in the presence of interfering elements Na, Li, and Pb. Detection limits are within an order of magnitude of other flame spectroscopic techniques and the background correction feature of wavelength modulation is effective in reducing spectral interferences. The system was applied, with good results, to a pooled blood serum sample. Because of the large throughput of the filter, the major noise was due to flame background flicker.**

This paper describes a simple atomic fluorescence spectrometer employing a continuum source, interference filters, and wavelength modulation as the method of reducing scatter, spectral, and flame background interferences. The applicability to a real analysis of Cu and Mg levels in blood serum is also described.

Wavelength modulation involves the rapid scanning of a small wavelength interval at some modulation frequency ($f_0$) while the subsequent photodetector signal is then measured at two times the modulation frequency ($2f_0$) with a phase and frequency selective amplifier (i.e., a lock-in-amplifier).

This type of modulation ordinarily has been accomplished in atomic spectrometry by vibrating a quartz refractor plate just before the exit slit of a monochromator (*1–3*). The modulation has proved effective in reducing low frequency additive noises, spectral interference, scatter, and broadband molecular absorption which has resulted in improved detection limits for flame emission (*1*) and continuum source atomic absorption spectrometry (AAS) (*3, 4*). Double modulation (i.e., source and wavelength modulation) has also been applied to continuum source atomic fluorescence spectrometry with fair success owing to the elimination of analyte emission by source modulation and the elimination of scatter and thermal flame emission by wavelength modulation (*5*). More recently, wavelength modulation in continuum source AAS with an echelle monochromator has resulted in detection limits better than or comparable to the best detection limits by AAS with a line source (*4*).

Wavelength modulation can also be accomplished with an oscillating or vibrating interference filter. The generally low cost and greater spectral throughout (Jacquinot's advantage) of interference filters compared to monochromators are two potential advantages for their use in atomic fluorescence spectrometry (AFS). Hieftje (*6*) has recently designed and demonstrated the use of a wavelength modulated filter photometer in correcting for interferences and applied it to a real analysis.

The potential advantages of nondispersive atomic fluorescence spectrometry have been discussed by Vickers (*7*). These advantages include increased spectral throughput and simultaneous collection of multiple fluorescence lines with simple and rugged instrumentation. Since no monochromator is employed, the ideal flame should be one of low background emission within the spectral response range of the detector. As a consequence, interference filters and solar blind photomultiplier tubes have been used to obtain increased collection of source radiation and increased spectral throughput (Jacquinot's advantage) (*8–10*).

Vickers (*11*) in a recent review has shown that there are some drawbacks to the use of a nondispersive system. Among these include the relatively low transmission of interference filters below 300 nm and the relatively low sensitivity of the R166 solar-blind photomultiplier tube compared to the more commonly used 1P28 photomultiplier tube. Also, since most nondispersive systems are flicker noise limited (*11*) due to flame background emission or fluorescence (*12*), the S/N ratio may decrease in comparison to dispersive systems for elements which have resonance lines in a region of high flame background (e.g., Fe). At extremely low wavelengths (near 200 nm) where both flame background and monochromator efficiency are low, the S/N ratio may increase for a nondispersive system. However, photomultiplier tube dark current (detector shot noise) may be the limiting factor in these regions. Scatter of incident radiation can pose a serious problem to a nondispersive system but the effect can be minimized through the use of an efficient atomization system such as an air–acetylene flame and appropriate matrix-matched calibrating solutions (*13*).

A wavelength modulated nondispersive atomic fluorescence system with a continuum source can offer some distinct advantages for practical analyses. The feasibility of using only one source instead of several line sources and of using interference filters instead of a monochromator can result in considerable savings in analysis time and cost. Also, the relative freedom from physical interferences of wavelength modulation can eliminate the need for carefully matched matrices and calibrating or blank solutions.

**Wavelength Modulation Using Interference Filters.** The basic operation of a wavelength modulated filter system depends on the fact that the central or peak wavelength of transmission of an interference filter shifts to shorter wavelengths as the angle of incidence of radiation changes from the normal angle. Ordinarily, the central wavelength of an interference filter is specified for collimated radiation normal to the filter surface. If the incident angle changes, the filter's central wavelength is shifted to shorter wavelengths, and in effect a certain wavelength region is scanned by varying the angle of incidence. The variation in angle of incidence can be achieved by oscillating or rotating the filter about a vertical axis at a fixed frequency, $f_0$. Interference filters can be purchased with their central wavelength coincident with an atomic resonance line. Therefore, if the filters are made to oscillate equally on both sides of normal, the analyte line will be coincident with the bandpass maximum or central wavelength twice for each cyclic scan of the filter. The modulated photodetector signal due to the analyte can be measured at two times the modulation frequency ($2f_0$) with a lock-in amplifier. The extent of modulation can be chosen such that the analyte line will be shifted out of the bandpass

0003-2700/78/0350-0386$01.00/0 © 1978 American Chemical Society

Table I. Experimental Apparatus and Manufacturers

| Component | Description | Manufacturer |
|---|---|---|
| Xenon Illuminator | Model VIX-150 150 W, collimated, high pressure short-arc, xenon illuminator | Varian, Eimac Div., San Carlos, Calif. 94070 |
| Illuminator Power Supply | Model P-150S-72 | Varian, Eimac Div., San Carlos, Calif. 94070 |
| Burner | Perkin-Elmer Model 303 premix burner/nebulizer equipped with (a laboratory constructed) 1.1-cm circular capillary burner head | Perkin-Elmer Corp., Norwalk, Conn. 06856 |
| Photomultiplier | E.M.I. Model 9738B | E.M.I.-Gencon Inc., Plainview, N.Y. 11803 |
| Photomultiplier Power Supply | Keithley 240 Regulated High Voltage Supply | Keithley Instruments, Inc., Cleveland, Ohio 44139 |
| Current Amplifier | Keithley Model 427 Current Amplifier | Keithley Instruments, Inc., Cleveland, Ohio 44139 |
| Lock-In Amplifier | Keithley Model 840 Autoloc Amplifier | Keithley Instruments Inc., Cleveland, Ohio 44139 |
| Filter Modulator System | Laboratory constructed | |
| Interference filters | Cu and Mg atomic absorption line interference filters | Corion Corp., Holliston, Mass. 01746 |
| Torque motor | Model S4-075B | MFE Corp., Salem, N.H. 03079 |
| Oscilloscope | Tektronix Model T935 35 MHz Oscilloscope | Tektronix, Inc., P.O. Box 500, Beaverton, Ore. 97077 |
| Strip Chart Recorder | Omniscribe Model A5123-5I | Houston Instrument, Austin, Texas 78753 |
| Function generator | Heath-Schumberger Model EU-81A | Heath Company Benton Harbor, Mich. 49022 |

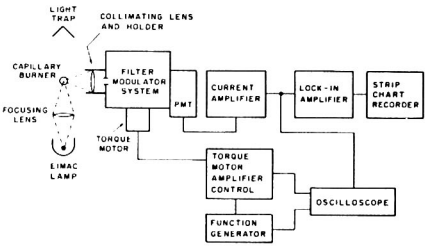


Figure 1. Block diagram of experimental apparatus

of the filter at the extreme end of the filter oscillation cycle.

The effect of rotating an interference filter causes its effective peak transmittance to be reduced and at high modulation amplitudes considerable bandpass distortion results. Therefore, continuum spectral features (i.e., flame background) are also modulated at two times the modulation frequency, $2f_0$.

## EXPERIMENTAL

A block diagram of the experimental arrangement which was used is given in Figure 1, along with a summary of the major instrumental components and manufacturers (Table I).

The heart of the experimental system is the filter modulator system which consists of a $2^3/_4$-inch cubic block aluminum enclosure. The interference filters are mounted onto custom made machined aluminum holders which in turn are mounted onto the shaft of a limited rotation torque motor whose shaft protrudes through the base of the system. Incident radiation is limited to a $^1/_4$-inch circular entrance port on the front of the system. The inside of the modulator system contains appropriate baffles and light traps to minimize stray radiation. The photomultiplier tube (PMT) is mounted on the rear of the system with a $^1/_4$-inch circular aperture concentric with the entrance port. The top of the modulator system contains a demountable plate or shutter which can be lowered in front of the PMT when removing or replacing interference filters to avoid shutdown of the PMT power supply.

The operation of the modulator system was as follows: A Perkin-Elmer model 303 burner/nebulizer was fitted with a laboratory constructed circular capillary-type burner and

Table II. Experimental Conditions

| | |
|---|---|
| Xenon lamp power supply | 12 A |
| Flame conditions | Air 9.7 L/min<br>$C_2H_2$ 1.5 L/min<br>Argon 15.5 L/min |
| Aspiration rate | 4.0 mL/min |
| Viewing height in flame | ~16 mm above burner top |
| Photomultiplier voltage | −725 V |
| Current amplifier | $10^6$ gain (volts per ampere)<br>0.01-ms risetime |
| Lock-in amplifier | sensitivity as required<br>3-s time constant |
| Modulation frequency ($f_0$) | 40 Hz |

provisions for inert gas sheathing. Source radiation from a 150-W Eimac lamp was focused by a 2-inch diameter $2^1/_2$-inch focal length lens to about a $^1/_4$-inch spot onto the top of the burner. Fluorescent radiation was then collimated by a 1-inch diameter, 2-inch focal length lens onto the entrance port of the modulator system. The filter was made to oscillate an equal distance on both sides of the radiation normal by applying a 40-Hz sine wave from the function generator to the torque motor amplifier control. The amplitude of rotation was controlled by varying the amplitude of the sine wave voltage or by adjusting the gain on the torque motor amplifier control. The rest position of the filter was determined by turning the position control on the torque motor amplifier control until an output of zero volts was observed on the oscilloscope. The amplitude of oscillation was chosen so that the analyte line which was almost coincident with the central wavelength of the filter would be shifted out of the bandpass of the filter. The subsequent photosignal was fed into a current amplifier and then to a lock-in amplifier tuned to twice the frequency of oscillation. The photosignal from the current amplifier was also monitored on the oscilloscope to ensure that a maximum $2f_0$ component of the signal was observed at the modulation amplitude chosen. A maximum $2f_0$ component of the signal was observed by shining light from Cu and Mg hollow cathode lamps directly onto the respective filters and varying the amplitude of oscillation so as to obtain a maximum $2f_0$ component. Once the proper modulation amplitude was chosen, the air, acetylene, argon, and aspiration flow rates were adjusted along with the viewing height in the flame so as to give a maximum S/N at the modulation frequency. For experimental conditions, see Table II.

The filter transmission characteristics (Table III) were determined in another series of experiments in which light from an

Table III. Interference Filter Transmission Characteristics

| Element | Central wavelength, nm | Transmission at normal incidence, %[a] | Bandpass, nm |
|---|---|---|---|
| Cu | 324.5 | 13 | 2.15 |
| Mg | 285.2 | 10 | 2.34 |

[a] Measured with Shimadzu Double-beam Spectrophotometer UV-200 (Shimadzu Seisakusho Ltd., Japan).

Eimac lamp was directed onto the surface of the interference filters placed in front of the entrance slit of a GCA/McPherson EU-700 scanning monochromator. The effects of bandpass, transmission, and central wavelength changes were determined as a function of incidence angle of the light. A calibration plot of modulation amplitude with output voltage of the sine wave generator was made and therefore the exact position of the analyte line with respect to possible interfering lines and with respect to its position in the filter's bandpass was known as a function of modulation amplitude.

The dc mode of operation of the system was also investigated. The dc method involved only locating the normal position of the filter, turning off the sine wave generator, and disconnecting the current amplifier to lock-in amplifier input.

**Reagents and Solution Preparation.** Certified (1000 μg/mL) copper, magnesium, and lead atomic absorption standards were purchased from Fisher Scientific Co., Pittsburgh, Pa. 15219. Pooled blood serum samples were generously supplied by Presbyterian-University Hospital of Pittsburgh, Pa. 15261.

Standard Li, 1000 μg/mL and standard NaCl, 2500 μg/mL, solutions were prepared by dissolving the appropriate amounts of dried $Li_2CO_3$ (J. T. Baker Chemical Co.) and NaCl (Fisher Scientific) salts in HCl and water respectively and diluting to 1 L with deionized water. Standard solutions for the analytical curves were prepared by serial dilutions of the copper and magnesium stock solutions. Blood serum solutions were prepared by a 1 to 5 dilution of serum with deionized water in a 2-dram vial for the copper analyses and a 1 to 100 dilution of serum with deionized water for the magnesium analyses. For the copper and magnesium analyses of blood serum by the standard additions method, known quantities of Cu and Mg standards were added to the serum and then diluted accordingly with deionized water.

**Waveform Figure Preparation** Flame background, analyte, and interferent waveform figures were prepared with the aid of a PDP 11/10 computer (Digital Equipment Corp.) interfaced to the filter modulator system. The subsequent current amplifier signals were signal averaged by the computer through the use of SPARTA (Signal Processing and Real Time Analysis) Software supplied by Digital Equipment Corp. and the averaged signal displayed on a storage oscilloscope (Tektronix Model 603, Tektronix Inc.) Fourier transform spectra were also prepared with the SPARTA software.

## RESULTS AND DISCUSSION

**Correction for Scatter and Flame Background Interferences.** In order to investigate the utility of this system, solutions of varying concentrations of Cu and Mg were made up in 1000 μg/mL Na. The solutions were run in the wavelength modulation (WM) mode with the subsequent results compared to those obtained by their analyses via atomic absorption spectrometry (AAS). The modulation amplitude was chosen as described earlier. Modulation amplitudes of approximately 9.2° and 13° were chosen for Cu and Mg, respectively. The phase control of the lock-in amplifier was set with a standard solution of Cu or Mg, respectively.

The effect of 1000 μg/mL Na does not change the slope of the analytical curve but only the intercept of the curve (additive interference) and can usually be corrected for by a suitable blank correction. The signal due to the 1000 μg/mL Na solution is probably stray light for it shows up as a positive

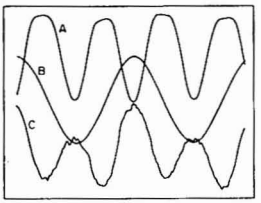


Figure 2. Signal averaged waveforms of current amplifier photocurrent during wavelength modulation with the Mg interference filter. (A) Modulated signal due to 1 μg/mL Mg being aspirated. (B) Sine wave driving waveform from the function generator to the torque motor amplifier control. (C) Modulated signal due to flame background with deionized water being aspirated

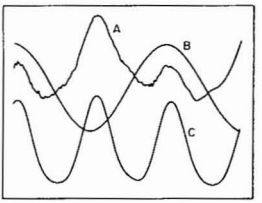


Figure 3. Signal averaged waveforms utilizing the Mg interference filter for (A) Flame background signal due to 1000 μg/mL Na being aspirated. (B) Sine wave driving waveform. (C) 1 μg/mL Mg solution being aspirated. Sensitivity 200-fold less than A

signal on the recorder and not as a negative signal as would be observed for an interfering line. As stated earlier, rotation of the filter causes the overall integrated transmittance of the filter to decrease, thereby modulating any continuous spectral features at two times the modulating frequency as shown in Figure 2. A 1000 μg/mL Na solution (Figure 3) produces a small $2f_0$ component in phase with the $2f_0$ component of Mg and therefore a 1000 μg/mL Na signal shows up as a positive deflection on the lock-in. However, the magnitude of the 1000 μg/mL Na stray light signal corresponds to an equivalent signal produced by 0.05 μg/mL and 0.1 μg/mL Mg and Cu solutions, respectively. The apparent sensitivity of the analytical curve is not affected by Na and its effect can be minimized by a suitable blank correction. However, even with a blank correction, a small but noticeable intercept occurs and thus may affect the accuracy of determinations near the detection limit. Background does not appear to be a major problem at concentration levels removed from the detection limit.

As pointed out by Vickers (*11*), flame background emission or fluorescence can be a serious limitation in nondispersive AFS. A sloping or changing background in the modulation interval will produce both $f_0$ and $2f_0$ signal components. This effect can be attributed to the derivative nature of the modulation which senses changes in intensity with wavelength such as that near an absorption line or curving background (*14*). Normally, the modulation interval with wavelength modulation by oscillating refractor plates was chosen so that the modulation interval was approximately equal to or two times the spectral slit width of the monochromator (*4*, *15*). Consequently, the modulation interval, $\Delta\lambda$, was on the order of a few angstroms. The background over such a small region was essentially constant and did not contribute to the signal. A wavelength modulation interval with interference filters corresponds to a much larger modulation interval due to the much larger bandpass of an interference filter compared to the spectral slit width of a monochromator. Therefore, if the background changes over that interval, then a small $2f_0$

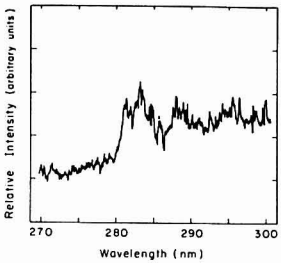


**Figure 4.** Selected portion of flame background molecular fluorescence spectrum obtained in the dc mode with a 150-W Eimac lamp, a GCA/McPearson EU-700 scanning monochromator, and stoichiometric air/$C_2H_2$ flame

component will result. An examination of the flame background of an air–acetylene flame (Figure 4), obtained in the dc mode with a scanning monochromator reveals the presence of a small slope or change in intensity with wavelength. Therefore, at reasonably high modulation amplitudes a small $2f_0$ component due to flame background can be seen (Figure 2). Also, as described earlier, the effective change in transmittance and bandpass shape of the filter induces a small $2f_0$ component. Similarly, unequal tilting of the filter can lead to non-uniform background modulation and can result in a small fundamental ($f_0$) signal as in Figure 2.

It appears that because of the increased spectral throughput of interference filters as compared to monochromators, flame flicker is the major source of noise in the present system. This fact along with the various other factors just described ultimately affects the S/N ratio and detection limit for most elements.

**Correction for Spectral Interferences.** Correction for spectral interferences can normally be accomplished by the use of the zero-crossing technique introduced by Epstein and O'Haver (*15*). The technique is based upon the fact that the second harmonic response function of a wavelength modulated system resembles a second derivative curve with two zero crossings (i.e., points where the intensity goes through zero) on either side of the central maximum (*16*). The assumption that the wavelength positions of the inflection points (zero crossings) are independent of interfering species concentration is valid up to a point where at high concentrations self-absorption broadening of the analyte line approaches the instrumental slit function. However, with the present system, the bandpass of the filter is so large compared to the absorption line width that self-absorption broadening is not a limiting factor. The unique aspect of wavelength modulation is that the positions of the zero crossings are adjustable parameters and not a property of the analyte or interferent. The adjustment is usually made by aspirating a concentrated solution of the interferent and adjusting the modulation interval so that the point of zero crossing (or zero intensity) of the interfering line lies under the analyte maximum or 90° out of phase with the analyte, thereby resulting in a zero output from the lock-in amplifier. In a similar manner, it has been shown by Hieftje and Sydor (*6*) that wavelength modulation by interference filters results in a modulation pattern for the interfering line that differs from the analyte on the basis of phase and frequency.

In order to test the effectiveness of our system from spectral interferences, the effect of the Li line at 323.3 nm on the Cu 324.7 nm resonance line and the effect of the Pb line at 283.3 nm on the Mg 285.2 nm resonance line were investigated. Both of these interfering lines fell within the bandpass of their respective filters. Solutions of Cu and Mg were made up with

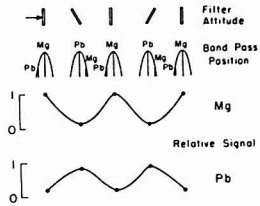


**Figure 5.** Schematic diagram illustrating the effect of Pb and Mg on the resulting signal waveform at low modulation amplitudes (see text for explanation)

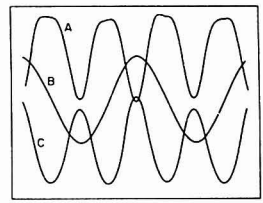


**Figure 6.** Signal averaged waveforms utilizing the Mg interference filter for (A) 1 μg/mL Mg solution being aspirated. (B) Sine wave driving waveform. (C) 200 μg/mL Pb solution being aspirated. Sensitivity is the same as in C as in A

varying concentrations of Li and Pb, respectively, and investigated in both the dc fluorescence and wavelength modulation modes. Ideally, the modulation interval should be chosen so that the interferent line would be shifted out of the filter bandpass and at the same time the analyte line will be a maximum (zero-crossing techniques). However, this was impossible in our case, since the central wavelength maximum of the filter was approximately coincident with the analyte line and both interfering lines lie at shorter wavelengths than the analyte line. Upon rotation, the shift to shorter wavelengths of the filter wavelength maximum would cause the analyte line to be out of the bandpass and the interferent line to be at a maximum. Therefore, it was decided to adjust the modulation interval such that both analyte and interferent lines were shifted out of the bandpass and discrimination could be achieved on the basis of the differing phase and frequency composition of the interferent peaks.

The interference of Pb on Mg was investigated by comparing the lock-in amplifier signals from 0.5 μg/mL Mg and 0.5 μg/mL Mg with 50 μg/mL Pb added as a function of modulation amplitude. At low modulation amplitudes, a 50 μg/mL Pb solution gave a negative lock-in signal, indicative of a 180° phase shift with respect to the Mg signal. The signal due to 0.5 μg/mL Mg with 50 μg/mL Pb was much smaller than the 0.5 μg/mL Mg signal. However, the sums of the 0.5 μg/mL Mg plus 50 μg Pb and the 50 μg/mL Pb signals were approximately equal to the amplitude of the 0.5 μg/mL Mg signal. At higher modulation amplitudes, the Pb signal became progressively smaller and the amplitude of the 0.5 μg/mL Mg plus 50 μg/mL Pb signal approached that of the 0.5 μg/mL Mg signal. At a modulation amplitude of about 21.4°, 50 μg/mL Pb produces about a 2.5% interference (or signal reduction) on 0.5 μg/mL Mg. These results are shown in Figure 5 and Figure 6.

At higher modulation amplitude (~15°) such that the Mg lines shifts out of the bandpass and the Pb line remains in the bandpass but with greatly reduced intensity (Figure 7), the Mg line again appears at $2f_0$ but the Pb line now begins to show noticeable $4f_0$ components superimposed on its main $2f_0$ waveform. This is because at that modulation amplitude

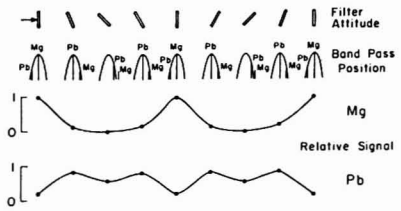


**Figure 7.** Schematic diagram illustrating the effect of Pb and Mg on the resulting signal waveform at high modulation amplitudes (~15°) (see text for explanation)

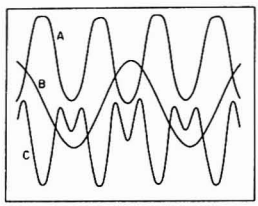


**Figure 8.** Signal averaged waveforms utilizing the Mg interference filter at high modulation amplitudes (~15°) for (A) 1 μg/mL Mg solution being aspirated. (B) Sine wave driving waveform. (C) 200 μg/mL Pb solution being aspirated. Sensitivity is the same in C as in A

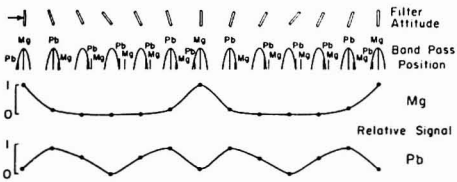


**Figure 9.** Schematic diagram illustrating the effect of Pb and Mg on the resulting signal waveform at very high modulation amplitudes (~21.4°) (see text for explanation)

the Mg line shifts out of the filter bandpass and appears at essentially zero intensity (Figure 8) while the Pb line remains in the bandpass and appears at a finite but somewhat reduced intensity than when Pb is at maximum intensity. At normal incidence, the Mg line is at maximum intensity while the Pb line is at minimum intensity (but not zero). Upon rotation, the Pb line approaches a maximum and Mg approaches a minimum, further rotation causes the Pb line intensity to be reduced slightly and the Mg line intensity to be essentially zero and therefore, a $4f_0$ component appears for Pb. At much higher modulation amplitudes (~21.4°) both the Mg and Pb lines are shifted out of the bandpass (Figure 9). As a consequence Pb appears essentially at $4f_0$ and Mg at $2f_0$ (Figure 10). From Figure 10, it is evident that when Mg is at a maximum, Pb is at a minimum and when Mg is shifted out of the bandpass (zero intensity), Pb also appears with essentially zero intensity. The broadened base of the Mg $2f_0$ components is indicative of the fact that the Mg line stays out of the bandpass for a much longer time period than the Pb line. Since Pb appears at $4f_0$ and Mg at $2f_0$, discrimination by the lock-in can be achieved on the basis of frequency of the interferent peaks. The fact that the Pb interference is not reduced to zero at this modulation amplitude is probably due to the extensive modulation of the flame background at such large amplitudes that distortion of the bandpass shape may result inducing $2f_0$ signal components (180° out of phase

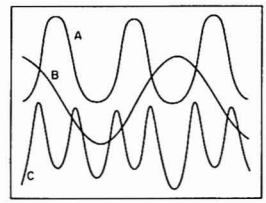


**Figure 10.** Signal averaged waveform utilizing the Mg interference filter at very high modulation amplitudes (~21.4°) for (A) 1 μg/mL Mg solution being aspirated. (B) Sine wave driving waveform. (C) 200 μg/mL Pb being aspirated. Sensitivity is the same in C as in A

with respect to Mg) due to flame background (Figure 2). As a consequence, zero suppression is needed for the Mg analysis. The Fourier transform power spectrum of intensity vs. frequency for 200 μg/mL Pb at a modulation amplitude of 21.4° shows a rather large $4f_0$ component due to Pb and a much smaller $2f_0$ component.

A similar investigation for the Li interference on the Cu signal was also conducted and it was found that at a modulation amplitude of approximately 14.5°, 100 μg/mL Li produces about a 5% interference on 0.1 μg/mL Cu. The somewhat higher interference due to Li is due to the fact that 100 μg/mL Li produces a fairly intense emission signal which is modulated by the filter resulting in a negative deflection (180° quadrature) of the lock-in amplifier.

In the dc mode of operation, both the Li and Pb effect on Cu and Mg, respectively, were more pronounced along with a great deal more interference from scatter due to Na and flame background.

It is apparent that wavelength modulation can correct for spectral interferences. However, the magnitude of the correction is based on the differing frequency composition of the interferent peaks with respect to the analyte peaks and thus dependent on the modulation amplitude chosen. Therefore, very narrow bandpass interference filters should be used to limit the bandpass distortion that results at high modulation amplitudes and help eliminate foreign lines that might fall in the filter bandpass. It should be cautioned, however, that high modulation amplitudes increase the likelihood of foreign lines falling in the filter bandpass and bandpass distortion which induce $2f_0$ signal components due to flame background modulation; both interferences limit the magnitude of the correction.

**Linearity and Detection Limits.** The extent of linearity for Cu and Mg by WMAFC is about the same as that obtained by AAS. Cu appears to be linear up to 7.5 μg/mL and Mg up to 1.0 μg/mL. The value for Mg appears a little low; however, this may be due to appreciable self-absorption of fluorescence and the range may be extended by focusing the source radiation onto the portion of the burner nearest the detector. The detection limits are within an order of magnitude of the best reported detection limits by AAL, AFL, AFC (Table IV) and comparable to those obtained by high resolution wavelength AAC with an echelle monochromator. The average S/N for a particular Cu concentration was found to be relatively independent of modulation amplitude, probably owing to the essentially constant flame and source background in that region (*12*). The average S/N for Mg, however, was found to increase with increasing modulation amplitude to a maximum near an amplitude of 15° and remain essentially constant at higher amplitude. This effect can be explained by the fact that the Mg line was shifted completely out of bandpass at that modulation amplitude. However, noticeable $2f_0$ components of the flame background are present at high modulation amplitude (Figure 2).

Table IV. Comparative Detection Limits[a,b] for Cu and Mg

| Element | WM AFC[c] | DC AFC[d] | AAL[e] | AAC[f] | AFL[g] | AFC[h] |
|---|---|---|---|---|---|---|
| Cu | 0.02 | 0.08 | 0.004[i] | 0.018[i] | 0.001[k] | 0.0015[k] |
| Mg | 0.0025 | 0.01 | 0.0003[k] | 0.002[i] | 0.0003[k] | 0.0003[k] |

[a] Detection limits are defined as that concentration which gives a signal 2 × rms noise level. [b] Detection limits are in μg/mL. [c] WMAFC denotes wavelength modulation atomic fluorescence flame spectrometry with a continuum source (present work). [d] DCAFC denotes dc atomic fluorescence flame spectrometry with the radiation normal to the filter surface with the dc mode of detection and no modulation (present work). [e] AAL = atomic absorption flame spectrometry with a line source. [f] AAC = atomic absorption flame spectrometry with a continuum source and a wavelength modulated echelle monochromator. [g] AFL = atomic fluorescence flame spectrometry with a line source. [h] AFC = atomic fluorescence flame spectrometry with a continuum source. [i] Reference 17. [k] Reference 18. [l] Reference 4.

Table V. Comparitive Determinations of Cu and Mg Levels in Pooled Blood Serum in μg/mL.

| Element | WMAFC standard addtions | WMAFC analytical curve | AAL[a] standard additions | AFC (*19*) |
|---|---|---|---|---|
| Cu | 1.28 | 1.34 | 1.30 | 1.31 ± 0.35 |
| Mg | 23.5 | 25.1 | 22.3 | 24.6 ± 6.1 |

[a] = Perkin-Elmer Model 305 Atomic Absorption Spectrophotometer equipped with Cu and Mg Hollow Cathode Lamps.

The detection limits for the dc mode of operation are about an order of magnitude worse than the WMAFC. Flame background, scatter, and spectral interferences are more pronounced in the dc mode.

In order to ascertain the relative accuracy of our system in a real analysis, a sample of pooled blood serum was analyzed for Cu and Mg levels (Table V). Human blood serum affords a fairly complex background matrix to test the effectiveness of our system. The analysis was performed utilizing both the standard additions and analytical curve methods with the results compared to the results obtained by the standard additions method and atomic absorption spectrometry. The results obtained by the WMAFC standard addition and AAS standard additions differ by about 1.5% and 5.5% for Cu and Mg, respectively. The values obtained by the WMAFC analytical curve and AAS differ by about 3.1% and 5.1% for Cu and Mg, respectively. The values obtained by WMAFC and AAS standard addition methods are in complete agreement with the mean values obtained for Cu and Mg serum levels in our laboratory (*19*). The values obtained by the WMAFC analytical curve method and WMAFC standard additions method differ by about 4.7% and 6.7% for Cu and Mg, respectively, and are within the experimental error of the technique. This is probably due to the difference between the water standards and the serum matrix and can be eliminated by dilution of both serum and standards with a 10% glycerol solution (*19*). As can be seen by the accuracy of our results, the WMAFC approach does not necessitate the use of complex blank solutions or matched matrices, and accurate results can be obtained with the analytical curve method and simple water standards.

## CONCLUSION

A wavelength modulated continuum source atomic fluorescence spectrometer shows considerable promise as a dedicated instrument for the analysis of several trace elements in diverse matrices. The wavelength modulation feature has proved effective in reducing scatter, flame background, and spectral interference. It has resulted in reasonably good detection limits and accurate analyses for Cu and Mg levels in such complicated matrices as human blood serum without the need for complicated blank solutions. The fact that the wavelength modulation can be accomplished with interference filters is important for it allows the filter to act as both the spectral isolation device and the background correction device eliminating the need for a monochromator. Also, since a continuum source can be used instead of several line sources, it allows for a low cost, simple, dedicated system to be built for several elements. As a consequence of the high spectral throughput of interference filters, flame flicker appears to be the major noise source and an atomization system of low background, e.g., a graphite furnace cell, may prove most effective. Also, the use of very narrow bandpass interference filters is recommended to reduce any modulated $2f_0$ background signal components and eliminate the likelihood of foreign spectral lines falling in the filter bandpass.

The system is currently being improved and its applicability to the analysis of several trace elements in diverse matrices with a graphite atomizer is being investigated.

## LITERATURE CITED


(1) W. Snelleman, *Spectrochim. Acta, Part B*, **23**, 403 (1968).
(2) W. Snelleman, T. C. Rains, K. W. Yee, H. D. Cook, and O. Menis, *Anal. Chem.*, **42**, 394 (1970).
(3) R. C. Elser and J. D. Winefordner, *Anal. Chem.*, **44**, 698 (1972).
(4) A. T. Zander, T. C. O'Haver, and P. N. Keliher, *Anal. Chem.*, **48**, 1166 (1976).
(5) W. K. Fowler, D. O. Knapp, and J. D. Winefordner, *Anal. Chem.*, **46**, 601 (1974).
(6) R. J. Sydor and G. M. Hieftje, *Anal. Chem.*, **48**, 535 (1976).
(7) T. J. Vickers, P. J. Slevin, V. I. Muscat, and L. T. Farias, *Anal. Chem.*, **44**, 930 (1972).
(8) D. G. Mitchell and A. Johanasson, *Spectrochim. Acta, Part B*, **25**, 175 (1970).
(9) P. D. Warr, *Talanta*, **17**, 543 (1970).
(10) R. C. Elser and J. D. Winefordner, *Appl. Spectrosc.*, **25**, 345 (1971).
(11) V. I. Muscat, T. J. Vickers, W. E. Rippetoe, and E. R. Johnson, *Appl. Spectrosc.*, **29**, 52 (1975).
(12) W. K. Fowler and J. D. Winefordner, *Anal. Chem.*, **49**, 944 (1977).
(13) P. L. Larkins and J. B. Willis, *Spectrochim. Acta, Part B*, **29**, 319 (1974).
(14) R. N. Hager, *Anal. Chem.*, **45**, 1131A (1973).
(15) M. S. Epstein and T. C. O'Haver, *Spectrochim. Acta, Part B*, **30**, 135 (1975).
(16) A. T. Zander, T. C. O'Haver, and P. N. Keliher, *Anal. Chem.*, **49**, 838 (1977).
(17) F. S. Chuang and J. D. Winefordner, *Appl. Spectrosc.*, **29**, 412 (1975).
(18) D. J. Johnson, F. W. Plankey, and J. D. Winefordner, *Anal. Chem.*, **47**, 1739 (1975).
(19) R. D. Dresser and F. W. Plankey, unpublished work, this laboratory.


RECEIVED for review August 1, 1977. Accepted December 14, 1977. Acknowledgement is made to the Donors of The Petroleum Research Fund, administered by the American Chemical Society, for the support of this research.

# Selective Excitation Fluorometry for the Determination of Chlorophylls and Pheophytins

**Kevin G. Boto* and John S. Bunt**

*Australian Institute of Marine Science, Cape Ferguson, P.M.B. No. 3, Townsville M.S.O., Q. 4810, Australia*

**A modified fluorometric method for the determination of chlorophylls a, b, and c and their corresponding pheophytins is presented. The use of selected monochromatic excitation and emission wavelengths enables each component to be determined with greater selectivity than with previous spectrophotometric or fluorometric methods. The factors limiting the accuracy of determination of each pigment in the usual multicomponent mixtures encountered are discussed.**

Estimates of chlorophyll concentrations in natural waters are frequently required in studies related to primary production. Probably the most widely used analytical technique depends upon spectrophotometric measurements of extinctions of 90% acetone extracts at three different wavelengths. Solution of appropriate simultaneous equations (trichromatic) provides estimates of chlorophylls a, b, and c (*1*). Pheophytin a can also be estimated by this method after acidification of the extract solution. Various improvements to the trichromatic equations have been published by a number of authors; for example, new data for the extinction coefficients of the chlorophylls, including $c_1$ and $c_2$, based on highly purified samples of each pigment (*2*).

Fluorometric methods, most of which give crude estimates of chlorophyll a only, have also been used (*3*). Loftus and Carpenter (*4*) have refined the fluorometric method for the analysis of chlorophylls using the Turner Fluorometer, employing a series of emission filters to improve the selectivity between the emission spectra of each chlorophyll. Their method involves the measurement of the emission through three separate filter combinations and again requires the solution of simultaneous equations to yield the concentrations of each pigment. Acidification of the extract, followed by a further three measurements through the filter combinations yields, in theory, the concentration of the corresponding pheophytins. However, only pheophytin a can be estimated with any degree of certainty, and then only if chlorophyll b is not present as a significant component of the mixture. Improved accuracy of chlorophyll b and c determinations compared with spectrophotometric methods is claimed.

The most obvious advantage of a fluorometric technique is the greatly increased sensitivity compared with spectrophotometry. An increase in sensitivity of two orders of magnitude is easily achieved and, provided that no loss of accuracy is incurred, fluorometric techniques should provide a much faster method than conventional spectrophotometry for performing chlorophyll analyses in natural water samples. In addition, fluorometry eliminates any possible interference by the absorption of nonchlorophyllous pigments in the 600+ region of the spectrum.

This paper describes a new approach to the usual fluorometric method. Variable monochromatic excitation is used to greatly improve selectivity between chlorophylls a, b, and c and their corresponding pheophytins. Thus, appropriate selection of excitation and emission wavelengths reduces the overlap between the emission spectra of each pigment to a greater extent than is possible with broad band excitation and the use of relatively broad band filters for emission.

Table I. Chlorophyll a, b, and c Spectral Properties in 90% Acetone

| Chloro-phyll | $\lambda_{max}$, nm I | II | III | Ratios $A_I/A_{II}$ | $A_I/A_{III}$ | $A_{II}/A_{III}$ |
|---|---|---|---|---|---|---|
| a | 432 | 664 | | 1.11 | | |
| b | 459 | 647 | | 2.67 | | |
| c | 444 | 580 | 631 | | 7.22 | 0.63 |

## EXPERIMENTAL

Chlorophylls a and b were extracted from local land plants (e.g., *Melaleuca alba*) methanol or acetone. The crude pigment extract was purified by thin-layer chromatography (*3*) using Merck Silica Gel 0.2-mm plates with dioxane (30%) in hexane as the solvent. Chlorophyll c was similarly isolated from locally available *Sargassum* sp. All solvents were of analytical reagent grade. The purified pigments were stored at −20 °C until used although samples were not kept for more than 24 h.

The purity of each pigment was checked by UV-visible spectrophotometry with an Aminco DW-2 spectrophotometer. No significant decomposition products or xanthophyll impurities were detected although some chlorophyll a samples contained a small amount (<3%) of pheophytin a.

Table I shows the wavelength of maximum absorption for the major "blue" and "red" peaks for each chlorophyll and the ratios of their absorption values in 90% acetone. The chlorophyll c obtained from some batches of algae contained small amounts of what appeared to be chlorophyllide a due to the presence of an active chlorophyllase in some of the species extracted. Barrett and Jeffrey (*5*) have described this product. The presence of the impurity did not appear to affect the chlorophyll c fluorescence properties and the chlorophyllide in fact behaved fluorometrically very similarly to chlorophyll a. This indicates that the fluorometric method would not distinguish between chlorophyll a and chlorophyllide a.

The concentration of each purified pigment solution was spectrophotometrically determined, using the extinction coefficients according to Jeffrey and Humphrey (*2*), which appeared to be the most reliable available. To calculate the chlorophyll c concentration, it was assumed that $(c_1):(c_2)$ was 1:1. This will introduce some small errors in the subsequent determination of chlorophyll c if the $(c_1):(c_2)$ is greatly different. Jeffrey (*6*) has listed the absorption and fluorescence spectral properties of chlorophylls $c_1$ and $c_2$ and hence the appropriate correction can be made if desired. Solutions for fluorescence studies were prepared by diluting the concentrated (usually 5–15 $\mu g\ mL^{-1}$) purified solution with 90% acetone. Primary dilutions were made with a calibrated (by weight) 1-mL bulb pipet and 100-mL volumetric flasks to maximize precision. Solutions so prepared were then used as secondary stock solutions from which further dilutions were made to prepare calibration curves for each pigment. Solutions of the pheophytins were prepared by the addition of 1 or 2 drops of 0.1 M HCl solution to the chlorophyll.

The fluorescence studies were performed with an Aminco-Bowman spectrofluorometer (J4-8203G Model). Special attention must be given to the slit combinations in the optical system of this instrument. For the degree of resolution considered acceptable and for good sensitivity, the slit combination used was as follows: Xenon lamp emission: 1 mm (i.e., 5-nm bandpass); slit slide 1, fully open; excitation monochromator, 2 mm; slit slide

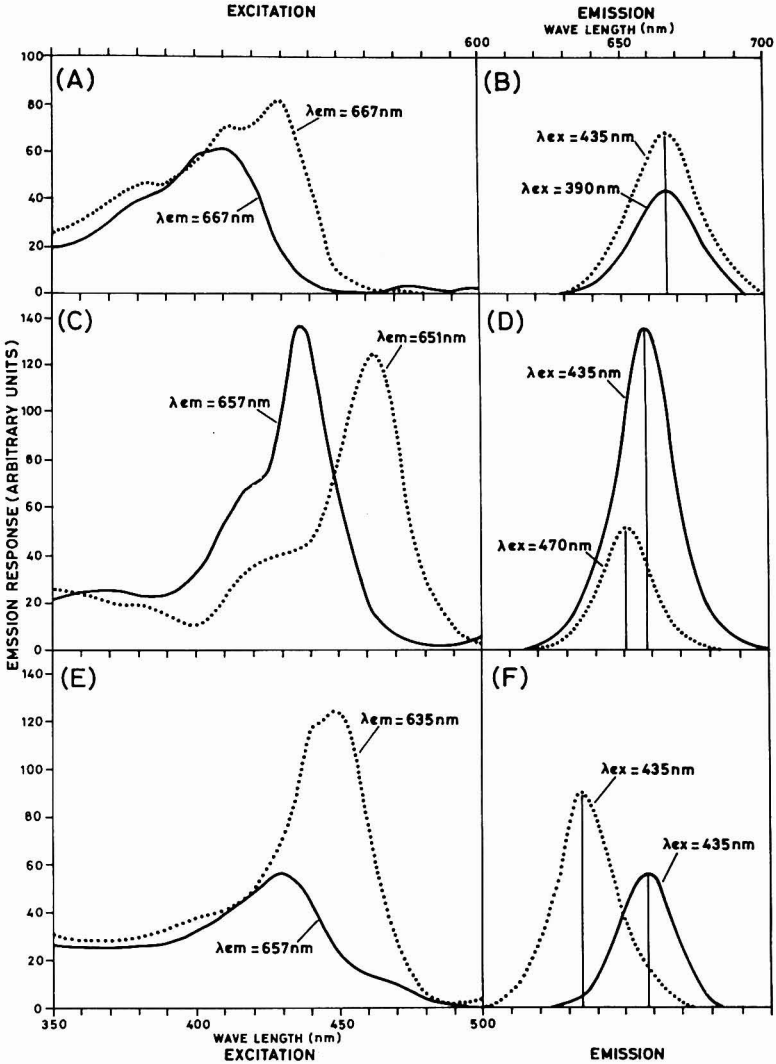


**Figure 1.** Excitation and emission spectra of: (A and B) Chlorophyll a (---) and pheophytin a (—), concn of both = 0.134 $\mu$g mL$^{-1}$. (C and D) Chlorophyll b (---) and pheophytin b (—), concn of both = 0.172 $\mu$g mL$^{-1}$. (E and F) Chlorophyll c (---) and pheophytin c (—), concn of both = 0.042 $\mu$g mL$^{-1}$. Note that the pheophytin c curves are shown on a tenfold higher sensitivity scale to the others. All solutions are in 90% acetone

2, fully open; photomultiplier, 2 mm. The calibration and linearity of the instrument were checked at frequent intervals with standard 1.0 and 0.01 $\mu$g mL$^{-1}$ quinine/0.1 N $H_2SO_4$ solutions. Also, after every five measurements, the emission response for the 0.01 $\mu$g mL$^{-1}$ standard was checked and adjusted if necessary, as a short term drift of ±5% was sometimes noted. Wavelength calibration for emission and excitation were also checked regularly, although no variation was ever observed.

## RESULTS

Figure 1 shows the excitation and emission spectra for chlorophylls a, b, and c and their respective pheophytins. The excitation spectra were obtained by holding the emission wavelength at the emission maximum and slowly scanning the excitation wavelength over the required range. The emission spectra shown have not been corrected for changes in photomultiplier response with wavelength. These spectra show that with suitable choice of excitation wavelengths, good selectivity can be achieved. Assuming that a given mixture contains all three chlorophylls and their pheophytins, a detailed set of equations can be derived for the emission responses at the usual emission maxima of each pigment when the mixture is excited at various chosen wavelengths. After

acidification of the mixture to pheophytins alone, further information can be obtained as indicated below.

In the following equations, $H$ ($\lambda_{ex}$, $\lambda_{em}$) denotes the height of the emission measured at $\lambda_{em}$ following excitation of $\lambda_{ex}$, and $K$ ($\lambda_{ex}$, $\lambda_{em}$, $x$) denotes the coefficient of emission response vs. concentration (of species $x$) at the same $\lambda_{ex}$ and $\lambda_{em}$. $C_x$ is the concentration of chlorophyll $x$ in the mixture while $C_{px}$ refers to the concentration of pheophytin $x$. All concentrations are in $\mu g\ mL^{-1}$ in the actual extract solution. After acidification $C'_{px} = C_{px} + C_x$, i.e., the new pheophytin $x$ concentration is now equal to that originally present ($C_{px}$) plus the amount formed from the chlorophyll ($C_x$). The equations are:

(a) Before acidification of the solution,

$$H(435, 667) = \underline{K(435, 667, a)C_a} + K(435, 667, b)C_b + K(435, 667, c)C_c + K(435, 667, P_a)C_{pa} + K(435, 667, pb)C_{pb} + K(435, 667, pc)C_{pc} \quad (1)$$

$$H(470, 651) = \underline{K(470, 651, b)C_b} + \underline{K(470, 651, c)C_c} + K(470, 651, a)C_a + K(470, 651, pa)C_{pa} + K(470, 651, pb)C_{pb} + K(470, 651, pc)C_{pc} \quad (2)$$

$$H(435, 635) = \underline{K(435, 635, c)C_c} + K(435, 635, b)C_b + K(435, 635, a)C_a + K(435, 635, pa)C_{pa} + K(435, 635, pb)C_{pb} + K(435, 635, pc)C_{pc} \quad (3)$$

(b) After acidification,

$$H(390, 667) = \underline{K(390, 667, pa)C'_{pa}} + K(390, 667, pb)C'_{pb} + K(390, 667, pc)C'_{pc} \quad (4)$$

$$H(435, 657) = \underline{K(435, 657, pb)C'_{pb}} + K(435, 657, pc)C'_{pc} + K(435, 657, pa)C'_{pa} \quad (5)$$

The terms underlined are the major terms in each equation. Note that in Equation 5, as the excitation and emission spectra of pheophytins b and c overlap greatly, only one equation is obtainable and the concentrations of pheophytins b and c must be estimated by a reiterative procedure (below). Although the equations appear complex, it must be remembered that, in most cases, the $K$ values in the minor terms are such that many can be neglected at the 2% error level. Further simplification is often possible when one considers that, in most offshore seawater samples, the only primary pigments found are chlorophylls a and c along with pheophytin a. Chlorophyll b and pheophytins b and c are either absent or present in minor amounts. Pheophorbides also are commonly found. However, these would probably have very similar fluorometric properties to the pheophytins and, hence, could not be separately determined by any fluorometric method.

Table II shows a full listing of all the $K$ values required for Equations 1 to 5. $H$ values were measured as the number of recorder divisions obtained with the photomultiplier set on the most sensitive setting, i.e., the 0.1 multiplier scale on this instrument. For purposes of cross calibration with other instruments, emission peak height ($H$350ex, 448em) of the 0.01 $\mu g\ mL^{-1}$ quinine standard was 2100 divisions on the 0.1 multiplier scale. The response for the standard was always set to this value as noted above. The $K$ values were then

**Table II. The $K(\lambda_{em}, \lambda_{em}, x)$ Coefficients Required for Solution of Equations 1 to 5 (see text)**

| | |
|---|---|
| $K(435, 667, a) = 5013$ | $K(435, 635, c) = 22966$ |
| $K(435, 667, b) = 731$ | $K(435, 635, a) = 401$ |
| $K(435, 667, c) = 850$ | $K(435, 635, b) = 731$ |
| $K(435, 667, pa) = 308$ | $K(435, 635, pa) = 25$ |
| $K(435, 667, pb) = 3893$ | $K(435, 635, pb) = 892$ |
| $K(435, 667, pc) = 629$ | $K(435, 635, pc) = 115$ |
| $K(470, 651, b) = 5800$ | $K(390, 667, pa) = 3464$ |
| $K(470, 651, a) = 47$ | $K(390, 667, pb) = 561$ |
| $K(470, 651, c) = 1469$ | $K(390, 667, pc) = 262$ |
| $K(470, 651, pa) = 76$ | $K(435, 657, pb) = 8111$ |
| $K(470, 651, pb) = 282$ | $K(435, 657, pc) = 1048$ |
| $K(470, 651, pc) = 76$ | $K(435, 657, pa) = 185$ |

calculated ($K(\text{ex, em}, x) = H(\text{ex, em})/C_x$) either by the slope of $H$(ex, em) vs. $C_x$ calibration graphs for each pigment, or, in some cases where $K$ was small, by direct calculation from the excitation and emission spectra for each pure pigment in a solution of known concentration. The $H$ vs. $C$ calibration graphs were linear, in all cases, in the concentration range 0.003 to 0.2 $\mu g\ mL^{-1}$ with never more than a 2% deviation from linearity for any individual point.

It should be noted that, while the $K$ values are listed for completeness, the purpose of this paper is to demonstrate the *principle* of the method only. It is strongly recommended that any laboratory wishing to consider this modified fluorometric technique carry out individual calibrations as described above.

Using the $K$ values listed in Table II, and taking into account the most likely pigment compositions of the phytoplankton in most seawater samples, a simplified set of equations was obtained as shown below. As the quantum efficiency of chlorophyll c appears to be very high (large $K$ value), its emission spectrum is very little affected by interference from the emissions of other pigments. Therefore, its concentration can be quite accurately calculated and this value then used to give accurate estimates of the others, viz:

(a) Before acidification,

$$H(435, 635) = K(435, 635, c)C_c \quad (6)$$

$$H(435, 667) = K(435, 667, a)C_a + K(435, 667, c)C_c \quad (7)$$

$$H(470, 651) = K(470, 651, b)C_b + K(470, 651, c)C_c + K(470, 651, a)C_a \quad (8)$$

(b) After acidification,

$$H(390, 667) = K(390, 667, pa)C'_{pa} \quad (9)$$

$$H(435, 657) = K(435, 657, pb)C'_{pb} + K(435, 657, pc)C'_{pc} \quad (10)$$

To solve Equation 10, initially put $C'_{pc} = C_c$ and solve for $C'_{pb}$ and then use this value to give a better estimate of $C'_{pc}$ and so on. Usually only two or three iterations are required for convergence. This procedure is, of course, subject to substantial error when one considers the likely errors involved in reading the actual $H$ values. Hence the final estimates of $C_{pb}$ or $C_{pc}$ originally present probably will only represent order-of-magnitude estimates unless either pb or pc is present in relatively large amounts. Note that in all analyses and calibrations, the $H$ values must be corrected for the usually small, but nonneglible solvent fluorescence at the particular wavelength investigated.

Using Equations 6 to 10, calculations can be performed reasonably quickly by manual methods; however, use of a simple computer program enables greater refinement of the estimates using Equations 1 to 6 with reiterative procedures

Table III. Results of Analyses Using the Proposed Fluorometric Method for Artificial Mixtures and Actual Seawater Extracts (in 90% Acetone)

| Sample type | Actual concentrations[a] | | | Measured concn[a] (errors in parentheses) | | | | | |
|---|---|---|---|---|---|---|---|---|---|
| | $C_a$ | $C_b$ | $C_c$ | $C_a$ | $C_b$ | $C_c$ | $C'_{pa}$ | $C'_{pb}$ | $C'_{pc}$ |
| Prepared mixture | 0.176 | 0.0954 | | 0.171 (−2.8%) | 0.0935 (−2.0%) | | 0.178 (+0.9%) | 0.0943 (−1.1%) | |
| Prepared mixture | 0.0176 | 0.00954 | | 0.0185 (+5.1%) | 0.00968 (+1.5%) | | 0.0172 (−2.4%) | 0.0091 (−5.0%) | |
| Prepared mixture | 0.161 | 0.054 | 0.0595 | 0.155 (−3.7%) | 0.049 (−9.3%) | 0.057 (−4.2%) | | | |
| Prepared mixture | 0.094 | 0.014 | 0.0595 | 0.087 (−7.4%) | 0.0135 (−3.6%) | 0.059 (−0.8%) | | | |
| Prepared mixture | 0.021 | 0.007 | 0.00774 | 0.020 (−3.8%) | 0.0053 (−2.4%) | 0.0076 (−1.8%) | | | |
| Prepared mixture | 0.115 | | 0.563 | 0.120 (+4.3%) | 0.006 | 0.057 (+1.2%) | 0.110 (−4.3%) | 0.0003 | 0.050 (−11.1%) |
| Local seawater extract[b] | | | | 0.059 | 0.001 | 0.0087 | 0.086 | 0.0018 | 0.0327 |
| Similar collected near same spot[b] | | | | 0.046 | 0.0002 | 0.0088 | 0.090 | 0.0012 | 0.0458 |

[a] Concentrations in $\mu g\ mL^{-1}$ of the *actual extract*. [b] Results shown here are averages of duplicates for each seawater sample.

to apply the small corrections needed. In applying these procedures to pigment analyses from samples of local seawater, it was found that this refinement is usually unnecessary at a 5% level although it became necessary for some artificial mixtures (see later) where the concentration ratios of each pigment were deliberately adjusted to give analytically unfavorable conditions.

A number of samples containing mixtures of (a) chlorophylls a and b only, (b) chlorophylls a, b, and c, and (c) chlorophylls a and c only were prepared and analyzed, with the results shown in Table III. Also, two actual analyses of 10-mL extracts from local seawater are shown in Table III.

## DISCUSSION

From the results shown in Table III it can be seen that for mixtures containing only chlorophylls a and b, very good estimates were obtained, the worst error of +5% for $C_a$ obtained with a solution containing only 0.0176 $\mu g\ mL^{-1}$ of a and 0.00954 $\mu g\ mL^{-1}$ of b. The $C_b/C_a$ ratio of ca. 0.5 in these analyses represented an unfavorable case where correction of $C_a$ for the $C_b$, term is necessary. On acidification, the estimates of $C'_{pa}$ and $C'_{pb}$ (= $C_a$ and $C_b$, respectively in these solutions as no extra pa or pb is present), were also very good although it should be noted that, in mixtures containing a, b, and c, the pheophytin b estimations would be expected to be less accurate. Analysis of a, b, and c mixtures showed that the estimates of a and c were within ±7% or better while the estimate of b could be subject to fairly large errors (up to 30%) when $C_b$ was very small or if $C_c$:$C_b$ was 5:1 or greater. Theoretical calculations using Equations 1 to 3, with estimates of the inaccuracies involved in the readings of the emission responses, showed that the estimation of $C_b$ was subject to errors in agreement with those actually found. Also, similar calculations showed that, if only a and c were present, and if $C_c$ and/or $C_a$ were of the order of 0.1 $\mu g\ mL^{-1}$, then $C_b$ could be estimated as being 0.006 $\mu g\ mL^{-1}$ when *none* was actually present. Actual analysis of such a mixture (Table III) confirmed this possibility. Thus such levels of chlorophyll b, if found in real samples, would need to be treated with suspicion.

The local seawater sample analysis (Table III) showed an unusually high concentration of pheophytin c. In this situation, it could be demonstrated by use of Equations 1 to 5 that the expected order of accuracy would be 10–20%. Therefore the proposed method at least gives a reasonably reliable estimate of pheophytin c if present at these levels. This is certainly an improvement on previous techniques where pheophytin b or c was not obtainable.

In general, as the method gives good selectivity and avoids the use of equations with *large* correction terms (except perhaps for chlorophyll b), it is felt that the concentrations of chlorophylls and their pheophytins can be estimated with a greater degree of confidence than with previously available methods.

## ACKNOWLEDGMENT

The authors acknowledge the assistance of Phillip Edwards with the experimental work presented in this paper. Also the very helpful comments and criticisms of the manuscript by Shirley Jeffrey (CSIRO Division of Fisheries and Oceanography, Cronulla, N.S.W.) are gratefully acknowledged.

## LITERATURE CITED

(1) J. D. H. Strickland and T. R. Parsons, *Bull. Fish. Res. Board Can.*, **167** (2nd ed.), (1972).
(2) S. W. Jeffrey and G. F. Humphrey, *Biochem. Physiol. Pflanz.*, **167**, 191–194 (1975).
(3) O. Holm-Hansen, C. J. Lorenzen, R. W. Holmes, and J. D. H. Strickland, *J. Cons., Cons. Int. Explor. Mer.*, **30**, 3–15 (1965).
(4) M. E. Loftus and J. H. Carpenter, *J. Mar. Res.*, **29**, 319–338 (1971).
(5) J. Barrett and S. W. Jeffrey, *J. Exp. Mar. Biol. Ecol.*, **7**, 255–262 (1971).
(6) S. W. Jeffrey, *Biochem. Biophys. Acta*, **270**, 15–33 (1972).
(7) S. W. Jeffrey, *Biochem. J.*, **86**, 313–318 (1963).

RECEIVED for review August 22, 1977. Accepted November 14, 1977.

# Multicomponent Analysis by Synchronous Luminescence Spectrometry

**Tuan Vo-Dinh**

*Health and Safety Research Division, Oak Ridge National Laboratory, Oak Ridge, Tennessee 37830*

**A methodology for the synchronous excitation technique is developed to improve the selectivity of luminescence spectrometry. This approach offers several advantages, including narrowing of spectral bands, an enhancement in selectivity by spectral simplification, and a decrease of measurement time in multicomponent analysis.**

Luminescence spectrometry with its excellent sensitivity has provided a useful analytical tool for monitoring trace organic compounds. Nevertheless, despite the ability to select both the excitation and the emission wavelengths, the conventional luminescence methods have limited applicability since most spectra of complex mixtures often cannot be resolved satisfactorily. The present awareness of the large variety of pollutants in our environment has increased the necessity to have instruments and methods for monitoring complex samples. Our present approach to this need for multicomponent analysis is to develop and extend the applicability of simple methods which can be used on a routine basis without resorting to techniques that are expensive or excessively time consuming.

In this work, an attempt will be made to evaluate the applicability of simultaneous analysis of multicomponent mixtures by the so-called synchronous excitation technique. The idea of synchronous excitation luminescence was first suggested by Lloyd (*1*). Although forensic researchers and oil-spill analysts have often employed this technique in an empirical manner (*2, 3*), the effective use of this technique in the general field of analytical luminescence spectrometry has been limited somewhat. This might be partly due to a lack of specific information and methodology which makes it difficult for analysts who are not familiar with spectroscopic techniques to exploit fully the possibilities offered by this simple approach. Practical applications have been limited so far only to providing fingerprints of complex samples such as crude oils of various origins (*3*). The intention of this paper is to develop and present a simple method for organic trace analysis and to investigate how the technique of synchronous excitation can be applied to obtain not only spectral signatures from complex samples but also specific information of analytical interest. A methodology for multicomponent analysis is suggested. Specific examples of the fluorometric characterization of various representatives of the important class of polynuclear aromatic hydrocarbons (PAH) are presented. The results illustrate that this technique has a great potential to offer an effective, rapid, and simple "screening type" method of analysis.

## BASIC PRINCIPLE

In conventional luminescence spectrometry, an emission spectrum can be monitored by scanning the emission wavelength $\lambda_{em}$ while the luminescent compound is excited at fixed excitation wavelength $\lambda_{exc}$. On the other hand, an excitation spectrum can be obtained by scanning $\lambda_{exc}$ while the emission is monitored at a given $\lambda_{em}$. It was suggested that a third possibility consists of varying simultaneously (or "synchronously") both $\lambda_{exc}$ and $\lambda_{em}$ while keeping a constant wavelength interval $\Delta\lambda$ between them (*1, 2*). At first glance, the use of a constantly changing excitation energy may seem undesirable for spectrometric applications. This continuous variation of the excitation would not allow it to be used as a light source to record emission spectra in the usual manner (constant excitation energy) that spectrometrists employ. This feature however can be a distinct advantage. In order to assess the figures of merit of the synchronous technique, it is necessary to discuss the corresponding luminescence expressions.

Consider a luminescent substance excited at a given wavelength $\lambda'$. $E_M(\lambda)$ is defined as the intensity distribution pattern of the emission (also referred to as an emission spectrum). The recorded luminescence signal at a given emission wavelength $\lambda$, $I_\lambda$, which depends on the value of $E_M$ at $\lambda$, is also proportional to the spectral radiance of luminescence $R_{\lambda'}$ emitted by the compound excited at $\lambda'$:

$$I(\lambda) = kR_{\lambda'}E_M(\lambda) \tag{1}$$

where $k$ = a constant factor.

In the above expression and in further development, $\lambda(\lambda')$ denotes the wavelength variable that corresponds to the actual wavelength position of the emission (excitation, respectively) monochromator. The effect of instrumental factors (spectrometer profile function, detection system response, transmission factor of all optics, etc.) not essential to our discussion is neglected. Assuming the validity of the well-known Lambert law for dilute solutions, $R_{\lambda'}$ can also be expressed as:

$$R_{\lambda'} = k'Y_L(\lambda')I_0(\lambda')\epsilon(\lambda')cd \tag{2}$$

where $Y_L$ = the luminescence quantum yield, $I_0$ = the incident exciting light intensity, $\epsilon$ = the molar extinction coefficient, $c$ = the concentration of the analyte, $d$ = the thickness of the sample, $k'$ = an experimental constant factor.

The product, $Y_L I_0 \epsilon$, which depends exclusively on $\lambda'$ can be related to the excitation function. It is proportional to the excitation spectrum $E_X(\lambda')$ which is experimentally measured when the excitation wavelength is scanned:

$$E_X(\lambda') = k''Y_L(\lambda')I_0(\lambda')\epsilon(\lambda') \tag{3}$$

where $k''$ = constant factor.

By combining Equations 1, 2, and 3, we can obtain the synchronous luminescence intensity ($I_s$) expression as a function of $\lambda$ and $\lambda'$:

$$I_s(\lambda',\lambda) = KcdE_X(\lambda')E_M(\lambda) \tag{4}$$

with $K = kk'k''^{-1}$. One specific condition of the synchronous technique is

$$\lambda - \lambda' = \Delta\lambda \ (= \text{constant})$$

or

$$\lambda = \lambda' + \Delta\lambda \tag{5}$$

0003-2700/78/0350-0396$01.00/0 © 1978 American Chemical Society

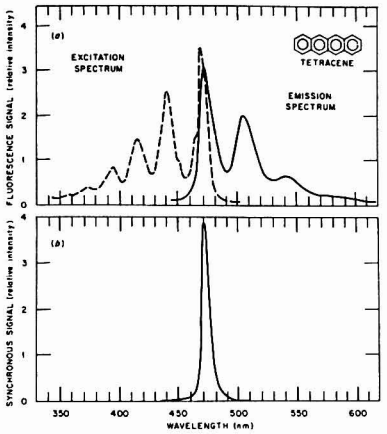


**Figure 1.** (a) Fluorescence emission and excitation spectra of tetracene. (b) Synchronous fluorescence signal of tetracene

In order to introduce explicitly the parameter $\Delta\lambda$, Equation 4 can be expressed as

$$I_s = KcdE_X(\lambda - \Delta\lambda)E_M(\lambda) \qquad (6)$$

This relation represents the basic equation of synchronous spectrometry. In conventional luminescence, the intensity of the emission spectrum depends upon the excitation wavelength. This dependence, however, is restricted solely to the intensity factor of the spectrum but the spectral features remain generally unchanged. In other words, the excitation wavelength acts only as a multiplicative parameter in the emission expressions of conventional luminescence spectrometry. On the other hand, in the synchronous technique, as shown in Equation 4, the luminescence intensity expression is an explicit function of $\lambda$ as well as $\lambda'$. The improvement in sensitivity of this technique is indeed reflected in Equation 6 which involves two functions instead of only one in the conventional luminescence method. In addition a new degree of selectivity is introduced by the parameter $\Delta\lambda$ which can be selected by the experimenter.

## EXPERIMENTAL

**Apparatus.** In this work, a Perkin-Elmer spectrofluorimeter (Model 43A, Perkin Elmer, Norwalk, Conn.) was used for spectrometric measurements. Both excitation and emission wavelengths can be locked together and scanned synchronously: this possibility was primarily designed in the commercial instrument for absorption measurements. A 150-W xenon arc lamp was used as an excitation light source. The detection device was a R508 photomultiplier (Hamamatsu Co., Middlesex, N.J.) that has a spectral response from 200 to 750 nm. Spectral resolution less than 2 nm was used. No correction for instrumental response was applied. All spectra were recorded on a strip-chart recorder (Perkin-Elmer, Model 023).

**Reagents.** All compounds investigated were commercially available and used without further purification.

## RESULTS AND DISCUSSION

**The Synchronous Signal.** The basic performance of the synchronous technique is illustrated in Figure 1. The conventional excitation and emission spectra of tetracene in a solution of ethanol is shown in Figure 1a. The fluorescence spectrum (with $\lambda_{exc}$ = 442 nm), showing three distinct emission bands at 473 nm, 507 nm, and 546 nm, covers the spectral range from 460 nm up to 600 nm under our experimental conditions. The excitation spectrum (with $\lambda_{em}$ = 507 nm) ranges from 480 nm to 350 nm, revealing absorption bands at 470 nm, 442 nm, 416 nm, and 397 nm. There is a small wavelength difference of 3 nm, often called the "Stokes shift," between the peaks of the 0–0 band in the emission and in the excitation spectra. With a wavelength interval $\Delta\lambda$ = 3 nm, matching the Stokes shift, the synchronous spectrum of tetracene is shown in Figure 1b. Instead of a spectrum covering several hundreds of nanometers, the synchronous signal consists simply of one single peak located at 473 nm. This unique feature is the consequence of the restrictive character of the product of the two nearly mirror-symmetric functions $E_M(\lambda)$ and $E_X(\lambda')$. Since $E_M(\lambda)$ is a function which is limited on the short wavelength range and $E_X(\lambda')$ is a function limited on the long wavelength range, the corresponding synchronous signal, resulting from their product, must necessarily have a limited spectral band width.

Note that what is usually called a "synchronously excited emission spectrum" is referred to here as simply a "synchronous signal" or "synchronous spectrum" since it can be considered either as an emission or as an excitation spectrum. Effectively, it can be noticed that Equation 4 does not give priority to the emission wavelength $\lambda$ or to the excitation wavelength $\lambda'$. Expressed explicitly in function of $\lambda'$, Equation 6 could also be written as:

$$I_s(\lambda,\lambda') = KcdE_X(\lambda')E_M(\lambda' + \Delta\lambda) \qquad (7)$$

Relation 7 shows that the synchronous signal could also be considered as an excitation spectrum with a synchronously scanned emission wavelength.

**Narrowing of Spectral Bands.** There are various causes for diffuseness in the spectrum of complex mixtures. One trivial reason is that the emission bands of each individual spectrum are intrinsically broad. Severe overlapping of various spectra are often another cause for diffuseness. It will be shown that the synchronous technique can decrease the adverse effect of these two sources of diffuseness.

In conventional luminescence spectrometry, the spectrum can show a resolved structure only when the monitored luminescence function consists of narrow bands. But with the synchronous technique, it is sufficient, in order to observe a narrow peak, that either one of the two functions $E_M(\lambda)$ or $E_X(\lambda')$ has resolved structure in a given spectral range. This increases the chance of obtaining spectra having resolved structure. The synchronous signal fails to show a resolved peak only when both functions $E_X(\lambda')$ and $E_M(\lambda)$ are featureless. We consider the example shown in Figure 2, where $E_M(\lambda)$ and $E_X(\lambda')$ represent two bands belonging to an emission and an excitation spectrum. In this case, the optimal condition is achieved when $\Delta\lambda$ is chosen to match the wavelength interval between the maxima of these two peaks. This situation provides the most intense synchronous signal with narrowest half-width. In Figure 2a, the hypothetical emission $E_M(\lambda)$ and excitation $E_X(\lambda')$ bands were represented for the sake of simplicity, with Gaussian shapes and identical intensities. If the sample is excited monochromatically at $\lambda_1'$ ($\lambda_2'$ or $\lambda_3'$, respectively), the observed emission spectrum $I_L$ would show an intensity represented by $I_{L_1}$ ($I_{L_2}$, $I_{L_3}$, respectively). As shown in Figure 2b, the intensity is increased proportionally with the excitation (absorption) intensity but the band width of the observed emission remains unchanged. However, as depicted in Figure 2c, if the emission is monitored while the exciting radiation is varied (synchronous method) the signal would show a more narrow peak having the intensity that corresponds to the maximum value $I_{L_1}$ obtained with fixed $\lambda_{exc}$. This band-narrowing effect is essentially a consequence of the multiplication of two functions increasing and/or decreasing simultaneously. This process is illustrated in Figure 3. The dashed curve shows a portion of the fluorescence

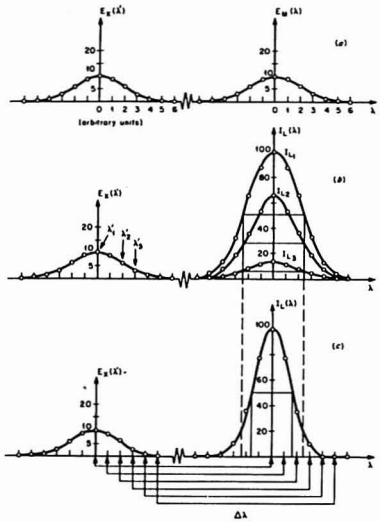

Figure 2. Schematic representation of the band narrowing effect

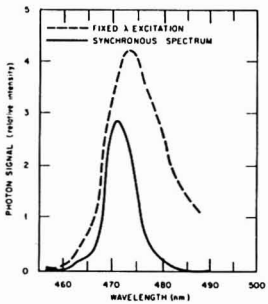


Figure 3. Band width of conventional and synchronous fluorescence signal of tetracene

spectrum of tetracene using fixed excitation at 440 nm. The solid line curve shows the significantly narrower synchronous signal (with $\Delta\lambda$ = 3 nm) of the same sample.

**Simplification of Emission Spectra.** In some cases, the synchronous technique can greatly simplify complex quasi-linear spectra. In order to bring out the situation more clearly, two graphical examples are given in Figure 4. A signal is observed only when $\Delta\lambda$ matches the interval between one absorption band and one emission band. If it is possible to select and use one particular $\Delta\lambda$ which matches one unique pair of absorption and emission bands, the synchronous spectrum will show only one single peak. This situation is shown in Figure 4a, where $\Delta\lambda$ ($= \lambda_1 - \lambda_0'$) is assumed to be the wavelength interval which matches only the absorption band at $\lambda_0'$ and the emission peak at $\lambda_1$. As can be observed, instead of a complex emission spectrum, only one peak at $\lambda_1$ should be observed. In multicomponent mixtures, the spectra of various compounds will be consequently simplified and interferences resulting from spectral superposition will be greatly reduced. An interesting feature is the possibility to analyze a specific compound in a mixture by selecting an

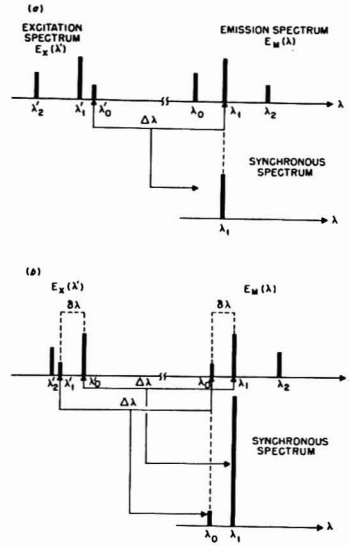


Figure 4. Spectral simplification effect. $E_M(\lambda)$ = emission spectrum; $E_X(\lambda')$ = excitation spectrum

appropriate $\Delta\lambda$ value among the numerous combinations of wavelength intervals. This would offer another opportunity to study selectively a certain component in a mixture in the case where the traditional approach with fixed excitation would be unsuccessful.

In order to have a situation where an interval $\Delta\lambda$ can be found to match solely one pair of excitation and emission bands, it is necessary that the emission and the excitation spectra consist of bands which are not separated by similar wavelength intervals. The situation where, by accidental coincidence, two (or several) pairs of bands in the emission and excitation spectra show identical intervals ($= \delta\lambda$) is illustrated in Figure 4b. Even in this case, if $\Delta\lambda$ is chosen to match the two strong bands (in Figure 4b, at $\lambda_0'$ and $\lambda_1$), the intense peak at $\lambda_1$ is enhanced more strongly than the weak peak at $\lambda_0$. It is important to emphasize here again that, whereas in conventional spectrometry with fixed $\lambda_{exc}$ one can only increase the intensity of all the emission bands at the same time, the synchronous technique can increase selectively the stronger peaks when a proper $\Delta\lambda$ is used. The situations discussed above show how the synchronous technique, if applied properly, can enhance the selectivity: characteristic intense peaks are increased strongly while, on the other hand, the interfering effect of weak bands can be reduced.

**Reduction of the Spectral Range.** For the spectrometrist involved in fundamental research, the detailed structure of the entire emission spectrum is of crucial importance since it reflects directly the physical properties in which he is interested. For the analytical chemist, however, the details of the whole spectrum might not be of vital importance: usually he selects only one or several spectral bands useful for his analysis, provided these spectrometric data are suitable for his needs (for example, direct correlation with the amount of analytes). Most of the other spectrometric details are generally not considered and their presence serves only to confuse the total spectrum by interfering with the emission of other components in the mixture. The previous discussions show the various processes by which the synchronous tech-

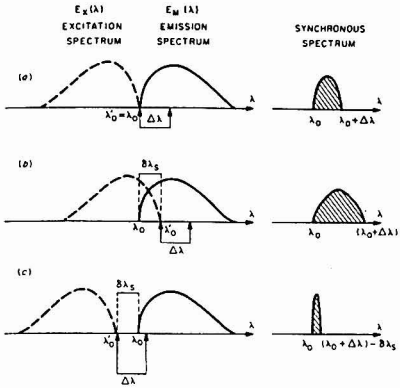


**Figure 5.** Influence of the Stokes shift and the wavelength interval on the synchronous signal

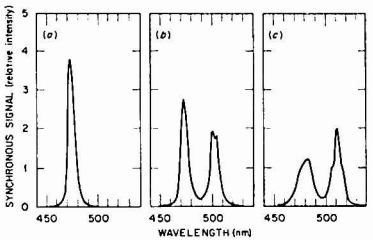


**Figure 6.** Effect of the wavelength interval on the synchronous fluorescence signal of tetracene: (a) $\Delta\lambda$ = 3 nm, (b) $\Delta\lambda$ = 30 nm, (c) $\Delta\lambda$ = 45 nm

nique can simplify the emission signal and reduce spectral interference; this section will describe how the choice of $\Delta\lambda$ can affect the spectral range of the synchronous signal. The influence of the Stokes shift is also discussed.

The emission and excitation spectra with various spectral overlaps are schematically shown in Figure 5. The shortest wavelength of the emission spectrum is depicted as $\lambda_0$ and the longest wavelength of the excitation spectrum is $\lambda_0'$. In Figure 5a, the spectral overlap is assumed to have zero value ($\lambda_0' = \lambda_0$). If a given wavelength interval $\Delta\lambda$ is used, the synchronous signal would have a band width of $\Delta\lambda$, covering from $\lambda_0$ (where the compound starts its emission) to $\lambda_0' + \Delta\lambda$ (where the compound no longer absorbs the excitation radiation). Figure 5b illustrates the situation where the emission and the excitation spectra overlap each other ($\lambda_0 < \lambda_0'$); in this case the synchronous spectrum covers from $\lambda_0$ to $\lambda_0 + \Delta\lambda + \delta\lambda_s$, having therefore a band width of $\Delta\lambda + \delta\lambda_s$, $\delta\lambda_s$ being the spectral overlap. In Figure 5c, the situation involving a Stokes shift of $\delta\lambda_s$ is illustrated: in this case ($\lambda_0' < \lambda_0$), the spectral band width of the synchronous signal is equal to $\Delta\lambda - \delta\lambda_s$ (from $\lambda_0$ to $\lambda_0 + \Delta\lambda - \delta\lambda_s$). It is therefore experimentally possible to modify the spectral band width of the synchronous signal by varying $\delta\lambda_s$ and $\Delta\lambda$. The Stokes shift can be varied by changing the solvent environment. But of most interest, the width of the synchronous spectrum can be directly compressed or expanded just by decreasing or increasing the experimental parameter $\Delta\lambda$. Whenever it is experimentally possible, the decrease of the band width of the synchronous signal would be advantageous since spectral overlap could be greatly reduced. This possibility to modify the spectral band width of

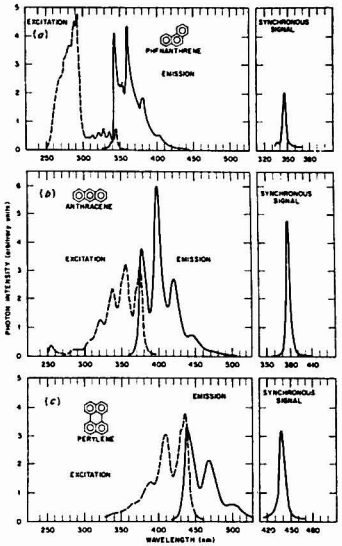


**Figure 7.** (a) Fluorescence excitation, emission, and synchronous spectra of phenanthrene. (b) Fluorescence excitation, emission, and synchronous spectra of anthracene. (c) Fluorescence excitation, emission, and synchronous spectra of perylene

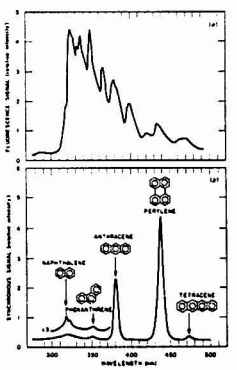


**Figure 8.** (a) Conventional fluorescence spectrum of a mixture of naphthalene, phenanthrene, anthracene, perylene, and tetracene. (b) Synchronous spectrum of the mixture

the emission signal of each individual component in a mixture is the most outstanding feature offered by the synchronous technique. Figure 6 shows the effect of various $\Delta\lambda$ values upon the synchronous fluorescence spectra of tetracene: the $\Delta\lambda$ values were 3 nm (Figure 6a), 30 nm (Figure 6b) and 45 nm (Figure 6c).

**Multicomponent Analysis.** One illustration of the methodology developed in this paper is given in Figures 7 and 8. Figure 7 shows the fluorescence excitation and emission spectra as well as the synchronous luminescence (SL) signal of several compounds such as phenanthrene, anthracene, and perylene. The conventional fluorescence spectrum shows several typical vibronic bands of the compound that covers a large spectral range of several hundreds of nanometers. In

the synchronous spectrum (using $\Delta\lambda$ = 3 nm, which is close to most Stokes shifts), only one single band, having approximately 10 to 15 nm in halfwidth, appears at the 0-0 band positions: 347 nm for phenanthrene, 381 nm for anthracene, and 440 nm for perylene.

The conventional fluorescence spectrum of a mixture of five PAHs of various sizes and configurations in a solution of ethanol is shown in Figure 8a: naphthalene, phenanthrene, anthracene, perylene, and tetracene. The excitation wavelength was at 258 nm. Although the total spectrum reveals several peaks, the analysis of such a mixture is not simple and straightforward. On the other hand, if the synchronous technique is used, the resulting spectrum, illustrated in Figure 8b, consists of a series of exceptionally well-resolved peaks. Each band (or group of bands for naphthalene) corresponds unequivocally to one component is the mixture and can be correlated perfectly with its synchronous signal in each individual spectrum (compare with Figure 7).

**Correlation of the Synchronous Signal with the Structure of the PAH Compound.** The first correlation between the structure of a PAH compound and its fluorescence spectrum is reflected by the dependence of the energy of the 0-0 band with the ring size of the compound. The information provided by the vibronic structure is less typical because, for most PAHs, the fluorescence spectra usually consist of a principal series of vibronic bands of diminishing intensity which are evenly spaced at intervals of equal frequency, 1400 $cm^{-1}$, due to the dominant C–C vibrational modes (*4*). On the other hand, the spectrum of a higher ring number linear cyclic compound occurs generally at a longer wavelength than a lower ring number compound. Nonlinear PAHs also follow, to a certain extent, this basic rule. With conventional spectrometry, because of severe spectral overlap, this simple rule cannot be efficiently applied, especially when a large number of components in a mixture have to be analyzed. With the synchronous technique, however, the effect of limiting each individual spectrum to a definite spectral band provides the most useful feature to locate the presence of specific compounds in a mixture. The method is most suitable to give information about the presence of a given compound or group of compounds. Its simplicity makes it very suitable as a rapid "screening method". As shown in Figure 8a and 8b, the synchronous technique can achieve some sort of "spectral confinement" or "spectral separation" into individual components without requiring any actual physical separation process.

**Data Chart for Synchronous Spectra.** Because of the simplicity of the signal which shows generally one or a limited number of emission bands within a definite spectral range, one can construct some type of graphical classification. The spectral location of the synchronous signal can be determined from spectrometric data already available in the literature. An example of such a chart for a variety of polyaromatic hydrocarbons is given in Figure 9; most of the spectral information used to construct this chart was deduced from data in Berlman's Handbook (*5*). The synchronous signal of each compound is limited by $\lambda_0$, the shortest wavelength of the emission, and by $\lambda_0' + \Delta\lambda$ ($\lambda_0'$ being the longest wavelength of the absorption and $\Delta\lambda$ the assumed wavelength interval); $\Delta\lambda$ used for the chart in Figure 9 was taken to be 3 nm. It is clear from Figure 9 that such a chart is useful in the analysis of mixtures. Note the shaded areas in Figure 9 which should theoretically represent the synchronous signals of naphthalene, phenathrene, anthracene, perylene, and tetracene. These bands are in excellent agreement with the experimental data in Figure 8.

**Analytical Considerations.** As expressed in Equation 4, the linear relationship between the measured synchronous signal $I_s$ and the concentration of the luminescent compound is preserved in the same way as with conventional spectrometry. Quantitative analysis is therefore straightforward. Synchronous spectrometry should offer the same possibilities and have the same limitations as those that are encountered in conventional spectrometry. The figures of merit of luminescence spectrometry such as linear and dynamic range of analytical curves, accuracy of experimental data, etc., are well documented and, so, are not discussed here. The general applicability of luminescence analysis has been amply presented in a large number of works (*6*, *7*). The possibility of quantitative analysis by synchronous spectrometry is demonstrated in a study of shale oil processed water (*8*). Conversely, synchronous spectrometry has also the limitations inherent to the luminescence technique, such as spectral distortions caused by intermolecular interactions and by static, as well as dynamic, quenching processes. Especially at high concentrations, energy transfer processes can become quite effective; in these cases, it is expected that the intensities of the emission from compounds with high excited state energies should decrease whereas those from compounds with lower energies should increase. These observations have been reported by John and Soutar in their studies of crude oil (*3*).

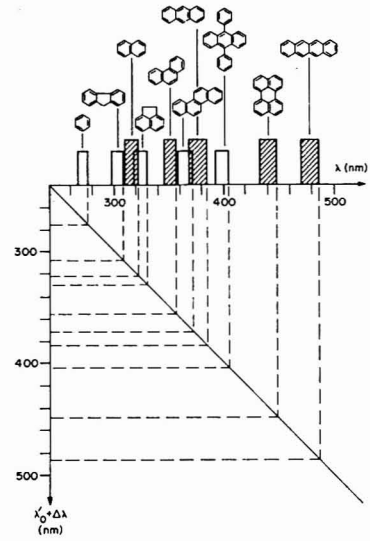


Figure 9. Data chart for synchronous spectra

**Sensitivity.** One important factor in any analytical technique is the sensitivity of the method. The synchronous spectra shown in the previous examples were measured with relatively narrow slit widths (1–2 nm). Because of the small value of the wavelength interval $\Delta\lambda$ (3 nm) employed, the use of larger slits would create undesired scattering and stray light interferences. One might think, therefore, that the synchronous method would be limited by the use of such narrow slits and consequently by low sensitivity. Nevertheless, the tradeoff between spectral resolution and sensitivity must be considered. In Figures 7 and 8, the vibronic band widths are of the order of 4 nm. In low temperature studies which use special solvents such as the Shpolskii matrices (*9*), the quasilinear structure can even have emission band widths of the order of 0.1 nm. The use of broad slit widths would increase the radiance throughput but at the same time would

alter the spectral structure. The same tradeoff consideration applies also for excitation: an excitation covering a large spectral band would increase the limit of detection but also remove the selectivity of the excitation since several compounds would also be excited simultaneously. There is another factor the analyst should keep in mind: for a mixture, the method with the lowest detection limit is not necessarily the one which provides the strongest signal because only the signal-to-noise ratio determines the detection limit. This feature favors the synchronous technique since a synchronous signal, as previously discussed, shows less contribution from emission of other components in the mixture. The photon noise associated with the emission from other compounds would decrease the signal-to-noise ratio. Finally, the simplicity of this technique makes it particularly attractive as a monitoring method for organic pollutants on a routine basis. It can easily be applied to fluorimetry as well as phosphorimetry, which are two complementary luminescence tools. No additional equipment is required and synchronous measurement can be performed directly using any commercial spectrometer in which excitation and emission monochromators can be interlocked.

**Selectivity and Multicomponent Analysis Approach.** It is noteworthy to emphasize again the multicomponent excitation approach of the synchronous technique in contrast with the fixed wavelength excitation method. Even if in those situations where it is possible to excite selectively each component present in a mixture, several measurements have to be performed, each using a different excitation most suitable for one specific component. In contrast, it was shown in Figure 8 that for compounds of a given group (such as the PAHs), it is possible with the synchronous method to obtain in the same measurement all the information specific to each compound. This would result in a shorter measurement time. It could be argued that the information obtained by this "multicomponent excitation approach" has to be traded against the loss of spectral information that would have been contained in the complete spectrum obtained with the conventional fixed excitation method. Fortunately this loss of spectral information that is contained in the other part of the spectrum does not have any adverse effect on the analysis but, on the contrary, can reduce interfering spectral overlap. It is interesting to note that the multicomponent feature offered by the synchronous approach is provided by the simultaneous scanning of both excitation and emission wavelengths, which allows each component to be excited and measured at a specific spectral range most suitable to them.

This simple method of analysis using synchronous excitation and detection opens up a host of possibilities for monitoring organic pollutants by luminescence spectrometry. Some recent practical applications include the characterization of polynuclear aromatic compounds (PNA) in by-product water from the Synthane gasifier and the multicomponent analysis by room temperature phosphorimetry of organic compounds absorbed on filter paper (*8*).

## LITERATURE CITED


(1) J. B. F. Lloyd, *Nature (London)*, **231**, 64 (1971).
(2) J. B. F. Lloyd, *J. Forensic Sci. Soc.*, **12**, 83 (1972); **11**, 153 (1971); **11**, 235 (1971).
(3) P. John and I. Soutar, *Anal. Chem.*, **48**, 520 (1976).
(4) J. B. Birks, "Photophysics of Aromatic Molecles", J. Wiley, London, 1970.
(5) I. B. Berlman, "Handbook of Fluorescence Spectra of Aromatic Molecules", Academic Press, New York, N.Y., 1965.
(6) C. A. Parker, "Photoluminescence of Solutions with Applications to Photochemistry and Analytical Chemistry", American Elsevier, New York, N.Y., 1968.
(7) G. G. Guilbault, "Practical Fluorescence: Theory, Methods and Techniques", Marcel Dekker, New York, N.Y., 1973.
(8) T. Vo-Dinh, R. B. Gammage, J. Thorngate, and A. Hawthorne, to be published.
(9) E. V. Shpolskii, *Sov. Phys.-Usp. (Engl. Transl.)*, **5**, 522 (1962).


RECEIVED for review October 11, 1977. Accepted December 19, 1977. Research sponsored by the Department of Energy under contract with Union Carbide Corporation.

# Experimental and Theoretical Considerations of Flow Cell Design in Analytical Chemiluminescence

**Scott Stieg and Timothy A. Nieman***

*School of Chemical Sciences, University of Illinois, Urbana, Illinois 61801*

**A modular flow cell has been designed for chemiluminescence (CL) analysis. The cell features inert construction, detection of light not front emitted, and ability to vary cell geometry to optimize for a particular chemical system. A mathematical model was developed to predict observed CL intensity as a function of solution absorbance ($\epsilon c$), cell depth ($l$), and degree of reflectance at the back wall of the cell ($r$). The cell and theory were tested with several geometries including cell depths between 0.2 cm and 1.0 cm (volumes between 0.25 mL and 4.50 mL). The chemical systems employed were luminol, which has no significant absorption of the CL emission, and gallic acid, which has significant absorption. Theory and experimental observation show excellent agreement. A practical limit on cell depths is such that $\epsilon cl$ is less than about 0.65.**

For our studies of the analytical applications of chemiluminescent (CL) systems (*1*), we have found it necessary to develop a flow cell suited particularly for CL measurements rather than the more common measurements of solution absorbance or fluorescence. This cell was designed with four goals in mind. The geometry of the cell should be easily variable in order to see the effect of changes in cell dimensions on the observed CL. The cell should collect light which is not emitted in the direction of the detector. (This approach has been suggested, but not systematically investigated, in discussions of other CL measurement systems (*2–4*), and is presently employed in certain commerical fluorescence cells (*5*).) Flow characteristics must ensure an even, well-rinsing flow through the cell. Finally, the cell must be chemically inert, since many of the CL reactions studied are sensitive to trace concentrations of metal ions and are performed in strongly alkaline $H_2O_2$. Because the first goals are related to the absorbance of the resident emitting solution, we have chosen two CL reactions, luminol and gallic acid, to evaluate the flow cell. In the gallic acid system, the products are strongly absorbing (*1, 6*); however, in the luminol system, neither the reactants nor products absorb significantly over

0003-2700/78/0350-0401$01.00/0 © 1978 American Chemical Society

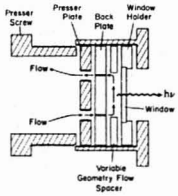


**Figure 1.** Diagram of CL flow cell

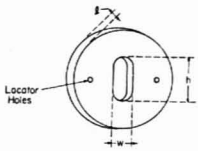


**Figure 2.** Diagram of flow spacer

**Table I. Dimensions of Flow Spacers (cm)**

| Sets | $h$ | $w$ | $l$ |
|---|---|---|---|
| A | 4.5 | 1.0 | {0.2, 0.3, 0.4, 0.5, 1.0} |
| B | 2.5 | 1.0 | {0.2, 0.4, 0.6, 0.8, 1.0} |
| C | 2.5 | 0.5 | {0.2, 0.4, 0.6, 0.8, 1.0} |

the region of maximum CL intensity (*7*).

## EXPERIMENTAL

**Cell Design.** Our flow cell consists of several TFE plates stacked into a threaded tube and pressed tightly together by means of a large presser screw and a stainless steel presser plate (Figure 1). The front TFE plate holds the Pyrex window (21 mm in diameter, 3 mm thick) flush against the flow spacers. The back plate has two 1.5-mm holes which carry the flow of solution into (and out of) the chamber created by the flow spacer. Thus, the flow enters from a small hole and makes two right angles before exiting: a path favorable to turbulent flow and efficient rinsing. In some of the experiments, the back plate was white TFE (highly reflective (*8*)) and in others it was dark brown Delrin (nonreflective); we were, therefore, able to compare the observed CL from cells in which only the light emitted towards the detector is detected with cells in which the detector receives both the light emitted towards the front and the light reflected off the back wall. To facilitate leak-tight seals with the 80 lb $in.^{-2}$ used in the stopped-flow system, a small amount of silicone grease was applied to the TFE plates. The cell is easily connected to our delivery system (*1*) using commercially available inert fittings which screw through the steel presser plate rather than into the soft TFE in which threads are easily stripped. The width, $w$, height, $h$, and depth, $l$, of the cell (Figure 2) can be varied by placing flow spacers having desired dimensions between the window holder and the back plate. The cells used in this study (Table I) have volumes between 0.25 and 4.50 mL. The cell is easily disassembled for cleaning, changing flow spacers, or replacing the window, should it break or become scratched.

**Reagents.** Luminol (Pfaltz and Bauer) and gallic acid (Mallinckrodt, reagent grade) were used without further purification. Solutions of $H_2O_2$ were made from an unstabilized 30% solution. $Co(NO_3)_2{\cdot}6H_2O$ was used to prepare all solutions of Co(II).

**Procedure.** The total CL was measured as previously described (*1*) without wavelength discrimination. Absorbance was measured as a function of time in a 1-cm path length flow cell (Precision Cells) with a GCA/McPherson Model 721 Spectrophotometer; the measurements were made at 425 nm for luminol and at 643 nm for the gallic acid system, the wavelengths of maximum CL intensity (*1, 3, 4*). The reactant concentrations (moles/liter, before mixing) used were (a) luminol system: $[luminol] = 1.0 \times 10^{-4}$, $[OH^-] = 1.0$, $[H_2O_2] = 0.01$, and $[Co(II)] = 1.0 \times 10^{-6}$, and (b) gallic acid system: $[gallic\ acid] = 2.6 \times 10^{-3}$, $[OH^-] = 0.10$, $[H_2O_2] = 0.40$, and $[Co(II)] = 1.0 \times 10^{-5}$. Co(II) is present to enhance the CL emission.

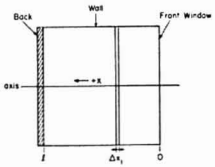


**Figure 3.** Schematic of CL solution within cell

## RESULTS AND DISCUSSION

The CL from the two systems was measured for three sets of flow spacers (dimensions given in Table I). Data from each set was taken using both the TFE (from now on called the "white" cell) and the Delrin (from now on called the "black" cell) back plates. We then constructed, from mathematical considerations of CL emission and solution absorption, a model for the relative intensity of CL observed as $l$ (cell depth) was varied.

Consider the CL solution in the flow cell as a series of $n$ thin plates of area = $A$ (the cell aperture) and depth $\Delta x$. Thus $l = n\Delta x$. The first plate, at $x = 0$ is closest to the photocathode of the PMT, and the last plate, at $x = l$, is adjacent to the white or black back (Figure 3). Initially, the light emitted from the plate towards the PMT is $P_{f,0}$ and the light emitted from the plate towards the back of the cell is $P_{b,0}$; that is, only light in the $\pm x$ direction is considered. This simplification can be rationalized by considering that for each plate an average luminescence is detected by the PMT directly from photons emitted along the $x$ direction and from photons emitted up to about 10° above and below the $x$ axis for a PMT 5 cm away from $x = 0$. Emission at angles greater than this is not detected directly, but is scattered by the TFE walls and a portion of it eventually detected. This light integrating effect tends to equalize the light contribution of each plate. We can, therefore, speak of the average luminescence per plate if we are interested only in the effect of increasing the distance of a given plate from $x = 0$, and as if the luminescence ($P_{f,0}$ and $P_{b,0}$) were absorbed by a pathlength, $b$, determined by the plate's position, $x$. Since the emission from a plate is isotropic with respect to the $x$ direction,

$$P_{f,0} = P_{b,0} = P_0 \tag{1}$$

$P_0$ is proportional to the thickness of the emitting plate. Hence,

$$P_0 = S\Delta x \tag{2}$$

where $S$ is a function of the particular CL system, the concentrations of reagents, the aperture, the distance of the PMT from the first plate, CL emission efficiency, and time. In this study since the first five are constant for a given set of spacers and CL system, and the measurement of CL and absorption are at one given time, $t_{obs}$, $S$ is a constant for a given CL system and cell aperture.

The pathlength, $b$, for $P_{f,0}$ is simply:

$$b = x \tag{3}$$

and for $P_{b,0}$ reflected at the back of the cell,

$$b = 2l - x \tag{4}$$

Thus,

$$P_f = P_0 10^{-\epsilon c x} \tag{5}$$

and

$$P_b = rP_0 10^{-\epsilon c(2l-x)} \tag{6}$$

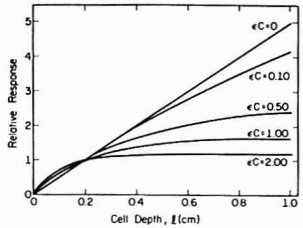


**Figure 4.** Predicted relative response (Equation 10) for various values of $\epsilon c$. ($r = 1$)

where $P_f$ and $P_b$ are the light intensities of monochromatic light seen at the PMT after absorption of $P_{f,0}$ and $P_{b,0}$ by the solution resident at $t_{obs}$, $r$ is the fraction of $P_{b,0}$ reflected at the back of the cell, $\epsilon$ is the molar absorptivity and $c$ is the molar concentration of the absorbing species. Adding Equations 5 and 6, and substituting Equation 2, all light seen at the PMT from one plate, then is

$$P_f + P_b = S\Delta x(10^{-\epsilon cx} + r10^{-\epsilon c(2l-x)}) \quad (7)$$

$P_{tot}$, then is the sum over $n$ of these emitting plates:

$$P_{tot} = \sum_{i=0}^{n} S\Delta x_i(10^{-\epsilon cx} + r10^{-\epsilon c(2l-x)}) \quad (8)$$

If $n = l/\Delta x$ and $\Delta x \to dx$, then $n \to \infty$ and

$$P_{tot} = \int_0^l S(10^{-\epsilon cx} + r10^{-\epsilon c(2l-x)})dx \quad (9)$$

Solving Equation 9,

$$P_{tot} = S(2.3\epsilon c)^{-1}(1 - r10^{-2\epsilon cl} + (r-1)10^{-\epsilon cl}) \quad (10)$$

To illustrate the relative CL responses ($P_{tot}$) predicted, Equation 10 is plotted for $r = 1$ (total reflectance at the back wall) for various values of $\epsilon c$, the absorbance through a 1-cm path of the resident solution; $P_{tot}$ for $l = 0.2$ cm is defined to be unity (Figure 4). Note that when Equation 10 is taken to a limit of $\epsilon c = 0$, a straight line occurs, indicating simply the additive process of endless depths of solution giving endless amounts of CL. Since all real cases can only approach $\epsilon c = 0$, all real solutions will eventually show a leveling of response, at some upper limit of $l$, and the higher the value of $\epsilon c$ is for a solution, the shallower the cell need be for this leveling off to occur. Eventually, at the limit of a completely opaque solution ($\epsilon c \to \infty$), we can see that the relative response would be independent of any variation in cell depth. Our two real cases, luminol and gallic acid, lie between these two extremes.

The data for each CL system for each of the three spacer sets were plotted along with the predicted response curve. Each data set was normalized (the parameter $S$ adjusted) such that the predicted value of $P_{tot}$ was unity for the white cell back with $l = 0.2$ cm. Only one parameter was adjusted. The same value of $S$ was used with data from both the white and black cells. The normalized data appears in Figure 5 (luminol) and Figure 6 (gallic acid); the individual data points for each spacer set (15 points on each curve, one point for each flow spacer listed in Table I) are shown in graph A and the average of the three spacer sets is shown in graph B. For luminol, the predicted curves were drawn using the limit $\epsilon c = 0$, and for gallic acid the curves were drawn for $\epsilon c = 1.6$. For both the luminol and gallic acid systems, $\epsilon$ is fairly constant over the detected emission band. The values of $\epsilon c$, used to draw the theoretical lines, were experimentally obtained from absorbance measurements at the maxima of the emission bands. In each graph, the upper curve and points correspond to $r = 1$, or a white cell back, and the lower curve and points correspond to $r = 0$, or a black cell back. It is interesting to note that, within the uncertainty of our data, the reflectivities of TFE and Delrin are indeed 1 and 0, respectively. There is good agreement between the results for the three different cell geometries and between the experimental observations and the model predictions; no systematic difference is observed between data from the three different sets of flow spacers.

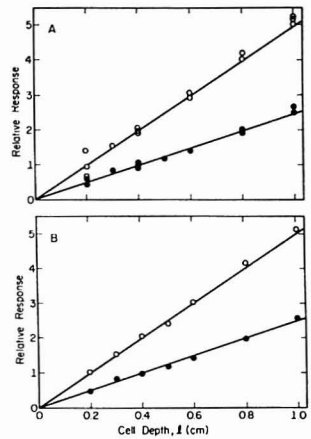


**Figure 5.** Luminol. Experimental results with white back (O); experimental results with black back (●); theoretical calculations (——), $\epsilon c = 0$. (A) Individual data for three spacer sets. (B) Average response for the three spacer sets

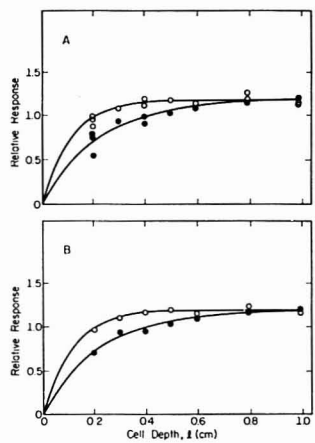


**Figure 6.** Gallic acid. Experimental results with white back (O); experimental results with black back (●); theoretical calculations (——), $\epsilon c = 1.6$. (A) Individual data for three spacer sets. (B) Average response for the three spacer sets

## CONCLUSIONS

Within the geometrical variation achieved by spacer sets used, we found that the *relative* CL response (as cell depth is increased) is independent of the aperature, $A$, as shown by Figures 5 and 6. The relative CL response is shown to be a simple function of $\epsilon c$ at $t_{obs}$, and cell depth, $l$ (if $\epsilon c$ is constant

over the wavelength range of observed emission). This result implies the validity of the "average plate luminescence" assumption made earlier. However, the *absolute* CL response, which depends on $S$, is not independent of the aperture and increases as the aperture does, as expected. It would be desirable, then, to increase $A$ as much as possible to achieve better sensitivity and lower detection limits. However, a fourth set of spacers constructed to this end, and having $w = 1.5$ cm and $h = 2.5$ cm, did not rinse efficiently enough for analytical use. Thus, the requirement for efficient rinsing places an upper limit on the cell width. For our flow system, this limit is at about 1 cm. Presumably, a limit is placed on cell depth in the same way; however, we did not use any cells with depths greater than 1 cm. Obviously, need for a reasonable sample size and reactant volume will also limit the cell dimensions.

Use of a CL system which has a large value of $\epsilon c$ will also place a definite upper limit on cell depth; in the case of gallic acid, use of cell depths greater than about 0.4 cm is a waste of reacting solution. From Equation 10, if $r = 1$, and $P_\infty = S(2.3\ \epsilon c)^{-1}$ which is the response observed for a cell of infinite depth, then $P_{tot} = P_\infty\ (1 - 10^{-2\epsilon cl})$. For gallic acid $\epsilon c = 1.6$, and at the practical maximum value of $l$ which is 0.4 cm, $P_{tot} = 0.95\ P_\infty$. By the time $\epsilon cl$ has increased to 0.65, about 95% of the maximum response is obtained.

As $\epsilon cl$ becomes very large, then, the reflectance of the rear wall has no effect on the CL observed. This is seen experimentally and theoretically in Figure 6. For gallic acid, beyond about 0.4-cm cell depth, only light which is front emitted ($P_{f,0}$) is detected and the responses of cells having $r = 0$ and $r = 1$ become identical. Thus, the desirability of a CL flow cell to collect light that is not front emitted ($P_{b,0}$) is dependent on the absorbance of the resident solution.

All of the work reported in this paper was done with a stopped flow delivery system (*1*), but the results and conclusions are applicable to both stopped flow and continuous flow systems. We routinely use cells based on this modular design for measurements in both stopped flow and continuous flow systems. Results dealing with the effect of $\epsilon c$, $l$, and $r$ on the observed signal are also applicable to CL measurements which are not done in flowing streams.


## ACKNOWLEDGMENT

We thank Richard Geiger for helpful discussions concerning the mathematical model.


## LITERATURE CITED


(1) S. Stieg and T. A. Nieman, *Anal. Chem.*, **49**, 1322 (1977).
(2) E. W. Cottman, R. B. Moffett, and S. M. Moffett, *Proc. Indiana Acad. Sci.*, **47**, 124 (1937).
(3) U. Isacsson and G. Wettermark, *Anal. Chim. Acta*, **83**, 227 (1976).
(4) W. R. Seitz and M. P. Neary in "Methods of Biochemical Analysis", Vol. 23, D. Glick, Ed., John Wiley and Sons, New York, N.Y., 1976, p 169.
(5) Model FSA 980, $2\pi$ stearadian flow-through cuvette, Schoeffel Instrument Corp., Westwood, N.J.
(6) D. Slawinska and J. Slawinski, *Anal. Chem.*, **47**, 2101 (1975).
(7) J. Lee and H. Seliger, *Photochem. Photobiol.*, **11**, 247 (1970).
(8) *NBS, Opt. Rad. News*, Sept. 1975.


RECEIVED for review September 27, 1977. Accepted December 19, 1977. This work was supported, in part, by a grant from Research Corporation.

# Flow Photometric Monitor for Uranium in Carbonate Solutions


**B. B. Jablonski and D. E. Leyden***

*Department of Chemistry, University of Denver, Denver, Colorado 80208*



**The reaction between U(VI) and 2,3-dihydroxynaphthalene-6-sulfonic acid is the basis of a continuous flow photometric monitor for uranium in carbonate solution. Linearity in the 0–100 ppm range has been observed with relative standard deviation of 1.1% at 60 ppm uranium and a lower detection limit of 3.5 ppm. The applicability of the method has been tested by analyzing process samples from a solution mining operation. Very few interferences have been observed.**


Uranium can be effectively recovered from low grade deposits through the use of a solution mining technique which has only recently been applied to uranium mining. The process relies on the solubilization and complexation of uranium in the ore deposit by ammonium carbonate solutions. Carbonate forms a strong complex with the uranyl cation, facilitating its solubilization. When the uranium is in solution, it can be removed from the deposit. The next step in the process is to recover the uranium as $UO_2(CO_3)_3^{4-}$ or $UO_2[(CO_3)_2{\cdot}2H_2O]^{2-}$ on an ion-exchange bed. Because the anionic complex is recovered, quaternary ammonium ion exchangers are used.

The removal of uranium from solution can be improved by cycling the carbonate host through the bed. Once the uranium concentration in the bed effluent drops below several parts per million, further cycling no longer improves the recovery of uranium and, for economic reasons, the cycling process is stopped. At present, it can take considerable time to obtain a sample of the bed effluent, transport the sample to the laboratory, and determine the amount of uranium in the sample. A simple on-line monitor for uranium would improve the efficiency of uranium processing by reducing the time spent waiting for analytical results.

Numerous methods for determination of trace amounts of uranium exist. An early review of methods for uranium determination covers a wide range of techniques (*1*). Colorimetric methods have enjoyed wide popularity. Rodden (*2*) lists at least 40 different colorimetric procedures for uranium. The most widely used photometric procedure involves extraction of the sample with trioctylphosphine oxide (TOPO) and the use of either dibenzoyl methane or 4-(2-pyridylazo)resorcinol as the colorimetric reagent (*3*). Other instrumental methods of analysis have been applied to the problem of uranium quantitation. A partial listing of techniques includes neutron activation analysis (*4*), UV fluorescence (*2*), x-ray fluorescence (*5*), polarography (*6*) and spectrophotometry (*2*).

Despite the abundance of methods for uranium analysis, very few applications of these methods to automated analysis have been found. In 1958, Bertram et al. (*7*) published the design of a flow system for a polarographic monitor for

0003-2700/78/0350-0404$01.00/0 © 1978 American Chemical Society

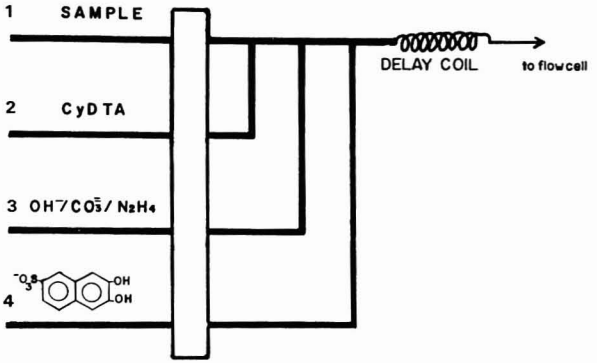


**Figure 1.** Flow system design

uranium in process solutions. The system is critically dependent on accurate dilution of the sample with supporting electrolyte and requires close control of temperature. Recently, a continuous flow method designed for a Technicon AutoAnalyzer has been proposed (*8*). The method is a colorimetric procedure employing 2-(2-pyridylazo)-5-diethylaminophenol (PADAP) as the colorimetric reagent. The reported relative standard deviation is 2–3%. The technique which is intended to be used with acid digested ore samples is not totally automated and involves an extraction of the ore sample or leach solution into TOPO. The extraction is performed manually and the organic phase is manually placed in the Technicon sampler.

The complexities of existing instrumental methods and the requirement of an acid pH for most colorimetric procedures make it difficult to automate uranium analysis. We have developed an unsegmented, continuous flow monitor for uranium based on the colorimetric reaction between uranium and 2,3-dihydroxynaphthalene-6-sulfonic acid at alkaline pH. The reagent was chosen on the basis of its selectivity for uranium and that color development takes place in alkaline solution (*9*, *10*).

## EXPERIMENTAL

**Reagents.** All reagents employed were reagent grade. A stock solution of 1000 ppm uranium (as U) was prepared by dissolving 1.7819 g of uranyl acetate (Baker) in 1 L of deionized water. Solutions for the standard curves were made by dilution of the uranium stock solution with appropriate amounts of either deionized water or ammonium carbonate. Stock solutions of 10 M NaOH, 20% $(NH_4)_2CO_3$ and 5% cyclohexanediaminetetraacetic acid (CyDTA, Aldrich) were also prepared. A 64% solution of hydrazine (Eastman) was used as received from the manufacturer. The mixture of reagents indicated in Figure 1 (pump channel No. 3) was prepared by mixing 20 mL of the hydrazine solution with 200 mL each of the sodium hydroxide and ammonium carbonate solutions. A 3% solution of 2,3-dihydroxynaphthalene-6-sulfonic acid, sodium salt (Pfaltz and Bauer) was prepared daily since the reagent oxidizes upon exposure to atmospheric oxygen for long periods of time. Oxidation of the reagent increased the blank by 0.002 absorbance unit over a period of 18 h. This change in absorbance is equivalent to 0.8 ppm uranium.

**Apparatus.** The flow system employed a 4-channel peristaltic pump (Polystatic) as shown in Figure 1. Latex tubing ($^1/_{32}$ inch) was used in all four pump channels. Tygon tubing ($^1/_{32}$ inch) served as transmission tubing. All connections were made with Technicon AutoAnalyzer glass connectors. The delay coil was made from 40 inches of $^3/_{32}$ inch Tygon tubing mounted on a glass support.

A Perkin-Elmer model 200 double beam spectrophotometer was used for detection. A Savant Precision Cell (Savant Instruments, Inc.) with 250-$\mu$L volume and 10-mm path length was used in the sample beam. A cuvette filled with deionized water was placed in the reference beam.

**Procedure.** In laboratory studies the uranium solution was manually placed in the sample channel of the flow system (channel No. 1, Figure 1). For on-line analysis, this channel can be connected to the process stream. Enriched process samples were analyzed after dilution by an appropriate amount to bring the concentration into the linear range. Once steady state was achieved, a percent transmittance measurement was made from the digital readout of the spectrophotometer. Both the uranium stock solution and concentrated process samples were also analyzed by oxidimetry as described by Main (*11*). The titration procedure involved pre-reduction of the sample with $SnCl_2$ and titration against standard 0.02 N $K_2Cr_2O_7$ to a diphenylaminesulfonate endpoint.

## RESULTS AND DISCUSSION

The success of the carbonate solution mining process is dependent on the large overall formation constant for uranyl–carbonate complexes (*12*).

$$UO_2^{2+} + 2CO_3^{2-} \rightleftarrows [UO_2(CO_3)_2 \cdot 2H_2O]^{2-} \qquad \beta_2 = 4 \times 10^{14} \tag{1}$$

$$UO_2^{2+} + 3CO_3^{2-} \rightleftarrows UO_2(CO_3)_3^{4-} \qquad \beta_3 = 2 \times 10^{18} \tag{2}$$

Unfortunately, the stability of the complexes limits the possibility of a quantitative reaction between uranium and any known colorimetric reagent. To free uranium from carbonate so that the colorimetric reaction may take place, concentrated NaOH is added to induce the formation of a diuranate anion (*13*):

$$2UO_2(CO_3)_3^{4-} + 6OH^- \rightleftarrows U_2O_7^{2-} + 6CO_3^{2-} + 3H_2O \tag{3}$$

The reaction takes place above pH 11. Because the uranium is liberated from the carbonate complex, it is then able to undergo the reaction with the colorimetric reagent more quantitatively. Compared to acidic leaching, the presence of carbonate in the solution mining process streams is an asset as far as possible interferants are concerned. In solutions with a moderate to high carbonate content very few ions are soluble, thus reducing the number of interferants in the analysis. Unfortunately, in practice the carbonate concentrations have been observed to vary as much as a factor of a thousand (0.01% to 10%) creating interference problems in solutions with a low carbonate content. $Ca^{2+}$ and $Fe^{2+}$ may be present in such solutions. To prevent precipitation of $Ca(OH)_2$ and $Fe(OH)_2$ upon addition of the NaOH, CyDTA is employed as a masking agent. CyDTA was chosen rather than EDTA

Table I. Statistics of Results[a]

| Trial No. | Uranium found, ppm | Trial No. | Uranium found, ppm |
|---|---|---|---|
| 1 | 8.25 | 1 | 60.6 |
| 2 | 9.40 | 2 | 59.4 |
| 3 | 8.25 | 3 | 59.4 |
| 4 | 7.09 | 4 | 60.6 |
| 5 | 8.25 | 5 | 59.4 |
| Mean | 8.25 | Mean | 59.9 |
| Std dev | 0.817 | Std dev | 0.658 |
| RSD, % | 9.89 | RSD, % | 1.1 |
| Lower limit of detection, ppm | | | 3.5 |

[a] Samples are in 1% carbonate solutions.

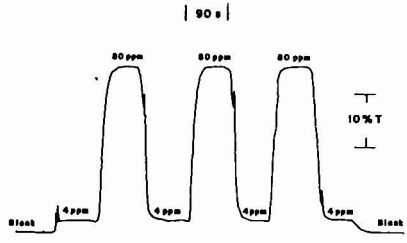


**Figure 2.** Response of flow cell

because CyDTA depressed color intensity to a lesser degree than other complexans of this type (*14*).

A second problem associated with varying carbonate concentration is that for a given concentration of uranium, the absorbance of sample solutions will decrease with increasing carbonate. To avoid the problem of carbonate dependence, a sufficient amount of 20% $(NH_4)_2CO_3$ is added to bring the carbonate concentration of all samples above 10%, at which point the absorbance is no longer dependent on the carbonate concentration.

At the high pH involved in the analysis scheme, 2,3-dihydroxynaphthalene-6-sulfonic acid is susceptible to oxidation. In the presence of hydrazine, no time dependence is observed and oxidation is effectively prevented.

The colorimetric reagent forms a *tris* complex with uranium above pH 10. The complex obeys Beer's law up to 100 ppm uranium. Above 100 ppm, a negative deviation from linearity is observed. A least squares fit of the data for the calibration curve evaluated the equation of the line to be Abs = $1.6 \times 10^{-4}$(ppm U)$-1.1 \times 10^{-3}$. The correlation coefficient was calculated to be 0.999 with Student's $t = 140$. Standards for the calibration curve were 1% in $(NH_4)_2CO_3$.

The precision of the analysis was evaluated at 8 ppm and 60 ppm uranium. The precision at low concentration of uranium (8 ppm) was found to be 9.9%, improving to 1.1% at 60 ppm. Data relating to precision of the analysis are presented in Table I. A lower limit of detection, taken as the concentration of uranium necessary to give an absorbance equal to three times the standard deviation of the blank determination, was calculated to be 3.5 ppm.

In designing the flow system, the philosophy was to keep the device as simple as possible. Therefore, no bubble segmentation is used. In order to minimize the number of pump channels required to deliver the reagents, a mixture of reagents is used in the pump channel No. 3 (Figure 1). A pump rate of 18 mL/min was employed throughout this study. As can be seen in Figure 2, washout time for the flow cell is approximately 0.5 min. An analysis time of approximately 1.5 min per sample was observed at the flow rate employed. A total reagent volume of 20 mL is consumed per analysis of 6 mL of sample. Since the system has been designed for on-line analysis, there is no shortage of sample and sample consumption as high as 6 mL is not prohibitive. Since the reagents are inexpensive and readily available, reagent consumption does not preclude the utility of the system. Reduction of both sample and reagent volumes by 50% can be reasonably expected in an on-line application. In acquiring the data presented here, the system was allowed to achieve steady state before a new sample was introduced to the flow system. No memory effect has been observed in the tubing. Figure 2 is a recorder trace of the Perkin-Elmer instrument showing the response (as %$T$) of the system to alternate injections of 4-ppm and 80-ppm samples. If memory were indeed a problem, analysis of the lower concentration sample after a sample of high uranium content should displace the measurement of the 4-ppm sample to a higher absorbance (lower %$T$) reading. In fact, no such effect is observed.

Table II. Interference Study

| Uranium taken, ppm | Interferant | Concn, ppm | Uranium found, ppm |
|---|---|---|---|
| 100 | $VO_3^-$ | 100 | 100 |
| | | 1000 | 99.8 |
| | | 10000 | 102.2 |
| | $MoO_4^{2-}$ | 100 | 100.1 |
| | | 1000 | 99.6 |
| | | 10000 | 106 |
| 50 | Fe(II) | 2 | 69 |
| | | 5 | 95 |
| | | 10 | 97 |
| | | 10[a] | 31 |
| | Ca | 50 | 50.1 |
| | | 100 | 49.9 |
| | | 1000 | 49.8 |
| | | 2000 | 47.5 |

[a] Cation exchange column used to remove Fe(II).

As mentioned previously, very few interfering metal ions are anticipated because of the presence of carbonate. The major contaminants in solution mining process streams are low levels (<20 ppm) of $MoO_4^-$ and $VO_3^-$. Six process samples were analyzed for the presence of interferants by energy dispersive x-ray fluorescence spectrometry. The samples were pre-concentrated by evaporating a 20-mL aliquot of each sample to circa 1 mL. The remaining solution was deposited and evaporated onto filter paper. In all six cases, less than 2 ppm of Mo and V was detected. Additionally a slight amount (less than 1 ppm) of Ca and Fe was detected in only one sample. The degree of interference by molybdate and vanadate was investigated using solutions which were 100 ppm in uranium. The effects of the presence of Ca and Fe were examined using 50 ppm solutions of uranium. Results of the interference study are given in Table II. Interference is a significant problem only at concentrations of interferant much higher than normally found in process samples. Fe(II) interferes to a greater extent than any of the other species investigated. The carbonate concentration of all samples was 0.1%.

The flow method was evaluated by comparing it to two other colorimetric methods using actual process samples. The colorimetric method employing 4-(2-pyridyl)azoresorcinol as described by Florence and Farrar (*14*) was used in the comparison study. The second method involved extraction of the uranium sample into trioctyl phosphine oxide with dibenzoyl methane as a colorimetric agent. The DBM-TOPO data were acquired by the laboratory supplying the process samples. Table III contains the data for the three methods

Table III. Comparison of Methods Using Process Samples, ppm $U_3O_8$

| Sample No. | This method | PAR | DBM-TOPO |
|---|---|---|---|
| 1 | 84.5 | 85.8 | 87.0 |
| 2 | 11.4 | 11.4 | 10.8 |
| 3 | 85.2 | 85.2 | 83.0 |
| 4 | 39.1 | 39.1 | 36.0 |
| 5 | 27.4 | 27.4 | 20.0 |
| 6 | 4.2 | 4.2 | ... |
| 7 | 25.2 | 25.2 | 25.4 |

Table IV. Statistics of Results, No Carbonate Present

| Trial No. | Uranium found, ppm | Trial No. | Uranium found, ppm |
|---|---|---|---|
| 1 | 4.40 | 1 | 82.7 |
| 2 | 4.40 | 2 | 82.7 |
| 3 | 4.17 | 3 | 83.0 |
| 4 | 4.85 | 4 | 83.0 |
| 5 | 4.85 | 5 | 82.4 |
| Mean | 4.58 | Mean | 82.8 |
| Std dev | 0.286 | Std dev | 0.273 |
| RSD, % | 6.2 | RSD, % | 0.3 |
| Lower limit of detection, ppm | | | 0.59 |

and agreement is quite good. A statistical test (pair data experiment) was applied to the data set to see if the methods give statistically equivalent results. At a 95% confidence level, the data can be said to belong to the same population.

The applicability of the flow method to the analysis of uranium in natural waters was examined by performing the analysis on synthetic uranium samples in the absence of carbonate. Since carbonate is not present at the high levels associated with solution mining, there is no need to add NaOH or $(NH_4)_2CO_3$. As a result, improved sensitivity and detection limit are anticipated. The pump manifold was altered by eliminating pump channel No. 3, that is, the mixture of NaOH, $(NH_4)_2CO_3$, and $N_2H_4$ was not employed. The detection limit improved to 0.59 ppm uranium as indicated in Table IV. The sensitivity improved by a similar amount. Unfortunately, the linear region for this method extends only to 60 ppm. The equation of the least-squares fit of the calibration curve is Abs = $2.03 \times 10^{-3}$ (ppm U) + $1.84 \times 10^{-2}$. The correlation coefficient is 0.993 and Student's $t$ (5 degrees of freedom) is 18.7. Precision was evaluated to be 6.2% at 4.5 ppm and 0.3% at 83 ppm uranium. Data pertaining to the precision of the method in the absence of carbonate are included in Table IV.

The proposed flow method gives rapid and precise analyses for uranium in the presence of large amounts of carbonate. The method is simple and does not require that the carbonate be destroyed by lowering the pH to the acid range, nor does the method require extraction of the uranium sample into an organic solvent.


## ACKNOWLEDGMENT

The authors express their gratitude to P. W. Carr for the use of the flow cell, to Perkin-Elmer Corporation for the use of a spectrometer, and to W. Lemons for his assistance.


## LITERATURE CITED


(1) C. J. Rodden, *Anal. Chem.*, **25**, 1958 (1953).
(2) C. J. Rodden, Ed., "Analytical Chemistry of the Manhattan Project", McGraw-Hill, New York, N.Y., 1950 pp 3–159.
(3) R. Pribil, "Analytical Applications of EDTA and Related Compounds", Pergamon, New York, N.Y., 1972, pp 263–279.
(4) R. J. N. Brits and M. C. B. Smit, *Anal. Chem.*, **49**, 67 (1977).
(5) L. R. Hathaway and C. W. Jones, *Anal. Chem.*, **47**, 2035 (1975).
(6) M. A. Flashka and A. J. Barnard, "Chelates in Analytical Chemistry", Vol. 1, Marcel Dekker, New York, N.Y., 1967, pp 251–255.
(7) H. W. Bertram, M. W. Lerner, G. J. Petretic, E. S. Roszcowski, and C. J. Rodden, *Anal. Chem.*, **30**, 354 (1958).
(8) T. V. Iorn, paper presented at 7th Technicon International Congress, New York, N.Y., 13 December 1976.
(9) L. Sommer, *Z. Anal. Chem.*, **187**, 263 (1962).
(10) L. Sommer, *Collect. Czech. Chem. Commun.*, **30**, 3426 (1965).
(11) A. R. Main, *Anal. Chem.*, **26**, 1507 (1954).
(12) L. A. Maclaine, "The Carbonate Chemistry of Uranium; Theory and Applications", in *Proc. Int. Conf. Peaceful Uses At. Energy*, **8**, 26–27 (1956).
(13) Fathi Habashi, "Principles of Hydrometallurgy", Vol. 2, Gordon and Breach, New York, N.Y., 1970, p 217.
(14) T. M. Florence and Y. Farrar, *Anal. Chem.*, **35**, 1913 (1963).


RECEIVED for review May 13, 1977. Accepted December 12, 1977. This work was supported in part by Research Grant CHE-7618385 from the National Science Foundation.

# Pulsed Radiofrequency-Excited Electrodeless Discharge Lamps for Analytical Atomic Spectrometry


**John W. Novak, Jr. and Richard F. Browner***

*School of Chemistry, Georgia Institute of Technology, Atlanta, Georgia 30332*



**Novel behavior of rf excited electrodeless discharge lamps is observed when these sources are operated in a pulsed mode. The radiant output of the EDLs is found to increase rapidly when short (<0.8 ms) pulses are used, at incident powers where CW operation of the lamps often results in decreased radiant output, thus indicating different excitation processes. The behavior of rf excited Ar, Hg, Cd, and Zn EDLs is compared with microwave excited lamps for the same elements. An intensity comparison of the metal EDLs gives Hg: rf > microwave; Cd: rf ≡ microwave; Zn: rf < microwave.**


The search for new and improved radiation sources for analytical atomic spectrometry, particularly atomic fluorescence spectrometry, has recently received a great deal of attention (*1–6*). In particular, much recent work has been with pulsed sources, and the potential advantage of pulsed source operation in AFS has been thoroughly described by Omenetto et al. (*3, 6, 7*). However, experimental detection limits obtained for many elements using pulsed sources, including pulsed HCls (*4, 5, 8*), pulsed tunable dye lasers (*2, 6*) and pulsed continuum sources (*1*), have been disappointing (*7*). As a consequence of the problems observed with the previously mentioned sources, a study of the spectral properties of electrodeless discharge lamps (EDLs) when operated under high power pulsed conditions was initiated. While CW or modulated operation of metal EDLs (both microwave (*9–14*) and rf excited (*15–17*) has been thoroughly examined, we know of no previous studies involving the high

0003-2700/78/0350-0407$01.00/0 © 1978 American Chemical Society

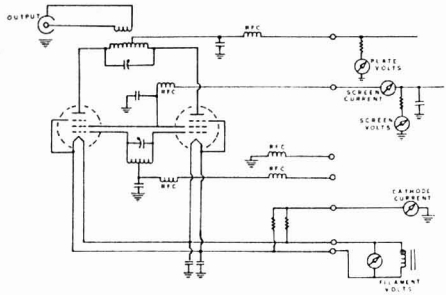


**Figure 1.** Circuit diagram of rf generator

power pulsed operation of these lamps, other than for wavelength assignments (*18–21*), although recently the high power CW operation of sealed rf excited lamps has been described (*22*).

## EXPERIMENTAL

**Optical System and Electronics.** All source radiance measurements were made on a 0.5-m Ebert monochromator (Jarrell-Ash model 82-020) using an 1180 grove/mm grating, blazed at 190.0 nm with a Varian model EMI 9783 B photomultiplier. Supply voltage to the PMT (-700 V) was from a Keithley Instruments model 244 High Voltage supply. Source emission signals were displayed on a Tektronix model 561A oscilloscope or, in a few instances, on a Keithley model 4145 Picoammeter connected to a Sargent-Welch model S26 recorder.

Focusing lenses were of fused quartz with diameter = 5 cm, focal length = 12.5 cm.

**Electrodeless Discharge Lamps.** Lamps were made from Vitreosil transparent quartz tubing 8 cm in length and 8–30 mm internal diameter. Lamps with an internal diameter between 13 and 20 mm proved most satisfactory. Tubes of 16-mm i.d. were found to be optimum, and were used primarily in this study. All lamps were single element (or element plus $I_2$), prepared as described by Dagnall and West (*12*). The pure metal was used for most Zn, Cd, and Hg lamps, but the iodides of Zn and Cd were also investigated. Argon was used as the fill gas with pressures varying from 0.3 to 3.0 Torr. No other fill gas was studied, as Ar has been previously demonstrated to provided an optimum combination of long lamp lifetime and high output intensity (*13*, *23*).

**RF Generator and Pulsing Unit.** A circuit diagram of the generator is shown in Figure 1. The generator was operated at a frequency of 13.5 MHz. The plate voltage was variable from 0 to 3000 V. During pulsing, the cathode current rarely exceeded 700 mA. In the pulsed mode the range of the generator was between 100 and 1600 W peak power.

The excitation coil was made from 12 turns of 4-mm o.d. copper tube and the lamp was positioned axially along the coil. The coil (6.4-cm i.d., 14 cm long) was widely spaced and radiation was measured at right angles to the tube axis along a cross-sectional diameter. An open plate capacitor was used in tuning the cavity, the optimum tuning criteria being a combination of maximum lamp emission intensity and minimum screen current.

The pulsing unit (circuit diagram available on request) gave pulse repetition rates variable from about 1 $s^{-1}$ to 1.5 × $10^{-3}$ $s^{-1}$. Pulse width was variable from 10 to 0.2 ms. The total power coupled to the discharge was limited by the low $Q$ of the system. It is unlikely that more than 20% of the rf energy coupled to the EDL although accurate coupling efficiency measurements were not attempted. The coupling efficiency could be improved by use of more carefully designed energy couplers (*24*, *25*), but in order to be effective these require a highly frequency stable rf source. The frequency stability of the rf generator was not adequate to take advantage of the higher $Q$ possible with these couplers.

The microwave generator used for comparison purposes was a 2.45-GHz Microtron 200 MK III unit (Electromedical Supplies, Wantage, U.K.) with variable frequency source modulation. A 3/4 λ Broida cavity was used for lamp coupling. Microwave excited lamps were optimized for temperature by operation in a thermostated mode.

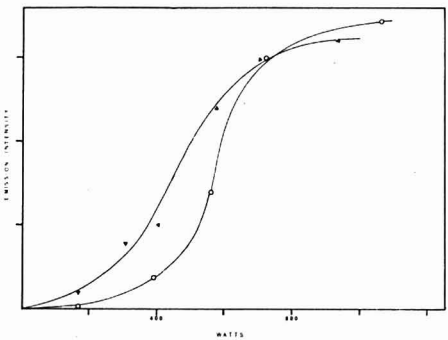


**Figure 2.** Comparison of radiant output of pulsed and CW operated Ar EDLs as a function of incident rf power. (O) pulsed operation, (Δ) CW operation. In the pulsed mode, the signals recorded are peak values

**EDL Temperature Control.** The lamp temperature was optimized for each measurement by controlling the temperature of the air from a fan/heater-coil arrangement. Air temperature was variable from 20 to 400 °C. Individual temperature optimization of the lamps was necessary at each power setting in the CW mode in order to compensate for the considerable inductive rf heating which occurred, particularly at high powers. However, in the pulsed mode one temperature setting of the heater was usually sufficient. At most, there was a need for only two temperature settings, one for high power and one for low power operation.

## RESULTS AND DISCUSSION

The first study of pulsed EDLs consisted of a comparison of UV resonance line intensities, with the lamps operated first in a pulsed mode, then CW. The lines monitored were those commonly used for AFS: namely Zn, 213.8 nm; Cd, 228.8 nm; and Hg, 253.6 nm. Ar was monitored both at its 420.1 nm and 337.1 nm resonance lines and also at the 247.9 nm ion line. There were no noticeable differences in behavior between the resonance and ion lines and only curves for the 247.9 nm line are presented here. All lines measured were integrated over the entire line profile by the use of instrumental spectral band widths of ≥0.1 nm. Line profile effects would not, therefore, be observed from these data.

**Ar Electrodeless Discharge Lamps. (Influence of Power on Emission Intensity).** The variation in Ar emission intensity as a function of incident rf power was first studied for a low pressure (~1 Torr) Ar lamp with both pulsed and CW operation (Figure 2). The S-type curves in Figure 2 are explained as follows: (i) when the lamp first ignites, the discharge is concentrated along the inner axis of the tube. (ii) As the power increases, the lamp suddenly develops a "fireball" type of emission, with a very intense area occupying about a third of the tube length. (iii) As the power is raised further, the intense discharge spreads more evenly over the entire tube. (iv) After the intense discharge fills the tube, an increase in power creates a much more moderate increase in lamp intensity. Heating effects of the inner plasma probably become significant when the rf power is increased further, resulting in decreasing intensity, especially in the CW mode, even when the lamp is cooled.

From the two curves, one can see that at lower wattages the CW mode results in a higher source intensity. Also the intense glow occurs at a lower power. However, as the power

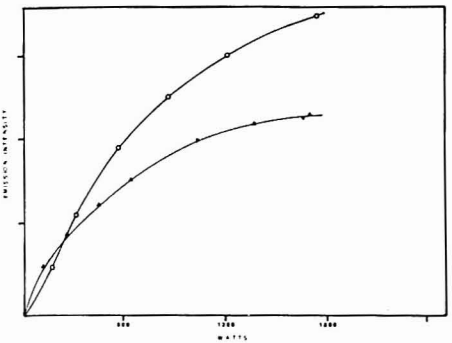

Figure 3. Comparison of radiant output of pulsed and CW operated Ar EDLs as a function of incident rf power; no high intensity mode occurring. (O) pulsed operation, (▲) CW operation. In the pulsed mode, the signals recorded are peak values

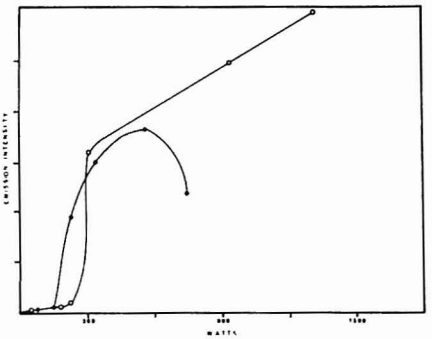

Figure 4. Comparison of radiant output of pulsed and CW operated Hg EDLs as a function of incident rf power. (O) pulsed operation, (◊) CW operation. In the pulsed mode, signals recorded are peak values

is increased, the output of the pulsed lamps continues to rise while the CW lamp output levels off. The slope is not very steep, even for the pulsed lamps. A disadvantage with the rf generator used in these studies was the lack of peak power output advantage in the pulsed mode compared to the CW mode of operation. As a consequence of this, and the lack of our ability to couple rf energy more efficiently with the EDLs (see Experimental section), it proved impossible to determine the form of these curves at higher powers. Consequently, it is not known whether the curve for pulsed source operation will ultimately reach a peak or a plateau region.

Lamps made with argon at fill pressures greater than approximately 3 Torr failed to make the transition to the "fireball" state and, consquently, radiant output at the Ar lines was much lower in both CW and pulsed modes of operation than with the 1-Torr lamps. However, the difference in intensity between the two modes was more marked than for 1-Torr lamps (Figure 3). In this case the pulsed lamp intensity at maximum rf power was about a third brighter than for the CW lamp, and was still rising sharply, whereas the CW operated lamp intensity became asymptotic to the power axis.

**Tube Diameter and Fill Gas Pressure.** The effect of tube diameter and fill gas pressure was investigated for Ar and Hg EDLs. The optimum fill pressures for all the lamp diameters investigated (i.e., 8–30 mm i.d.) was found to be in the range 0.3–3 Torr. There was little difference between the maximum intensities at the different pressures, but the transition from diffuse glow to "fireball" emission occurred at lower powers with lower fill gas pressure. It was also found that the "fireball" emission occurred at lower powers in the larger diameter tubes.

**Hg Electrodeless Discharge Lamps.** A comparison of pulsed vs. CW operation for a typical Hg lamp (~1 Torr Ar fill gas) showed a similar pattern to the Ar lamp (Figure 4). Initially, the glow was concentrated along the tube axis. Under these conditions there was probably strong self-reversal of the source output, resulting from reabsorption of radiation in the nonemitting outer layers of the lamp. Again, there was a clear transition between a region of low slope at powers below about 300 W, followed by a region of high slope. The CW operated lamp again went into its high intensity glow at lower power than the pulsed lamp. However, at higher powers the pulsed Hg EDL continued to increase in intensity while the CW operated lamp reached a maximum intensity, followed by a rapid drop in output with further increase of rf power. A likely explanation for this behavior is that adequate cooling of the CW operated lamp, which is necessary in order to maintain

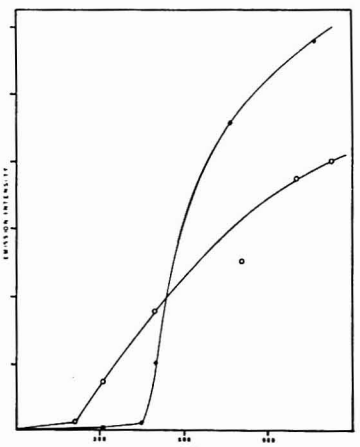

Figure 5. Comparison of radiant output of pulsed and CW operated CD EDLs as a function of incident rf power. (♦) pulsed operation, (O) CW operation. In the pulsed mode, signals recorded are peak values

an optimum vapor pressure of the Hg in the lamp, becomes impossible at such high powers. The resulting high Hg vapor pressure probably results in severe self-reversal of the emitted radiation, producing a net drop in intensity. However, other mechanisms may also play a part in influencing this behavior.

**Cd Electrodeless Discharge Lamps.** Cd EDLs showed similar behavior to the Hg lamps. Figure 5 shows a comparison of pulsed vs. CW operation for a typical cadmium EDL (2-Torr fill pressure). As before, the emission was more intense at lower rf powers in the CW mode; however, once the "fireball" emission took place, the pulsed EDLs surpassed the CW EDLs in intensity. As maximum generator power was approached, the slope of the CW Cd emission curve was less than that of the pulsed emission curve.

One interesting aspect of pulsed mode operation is that it proved possible to dispense with the external thermostating recommended by Browner and Winefordner (*13*), and control the lamp temperature by varying the duty cycle (pulse width × pulse rate). However, this would be feasible only with lamps containing volatile elements or compounds, and for most of the studies external thermostating was necessary.

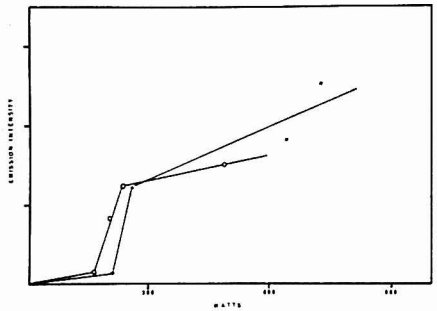

**Figure 6.** Comparison of radiant output of pulsed and CW operated Zn EDLs as a function of incident rf power. (X) pulsed operation. (O) CW operation. In the pulsed mode signals recorded are peak values

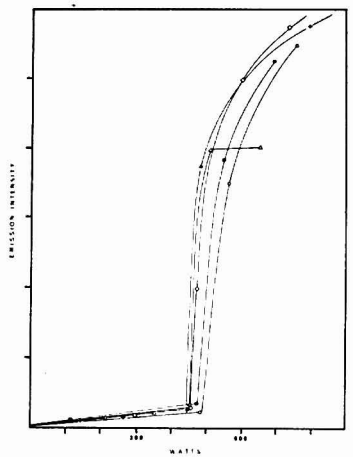

**Figure 7.** Comparison of radiant output of pulsed Hg EDLs at varying pulse rates as a function of incident rf power (Pulse width constant at 1 ms). (◊) 100 Hz, (X) 50 Hz, (■) 250 Hz, (O) 10 Hz, (Δ) 500 Hz. Signals recorded are peak values

**Zn Electrodeless Discharge Lamps.** The Zn lamps (2.8-Torr fill pressure) (Figure 6) did not show quite as marked a change as the Ar, Hg, or Cd lamps and the initial appearance of the "fireball" emission was less intense. Further increase in incident rf power produced a progressive increase in emission intensity up to the output limit of the rf generator. The slopes of these lines showed no great difference between pulsed and CW operation.

**Duty Cycle.** The effect of duty cycle (pulse width × pulse rate) on the emission intensity was observed for the metal lamps by varying pulse width and pulse rate independently. The effect of varying the pulsing rate (at a fixed pulse width) for a Hg lamp is shown in Figure 7. Very little difference in emission resulted, except differences which could be attributed to heating effects. As a consequence, more rapid pulsing was found to diminish the Hg emission slightly, probably from overheating, in spite of the use of cooling air, as the dimensions of the lamps (16-mm i.d.) make effective uniform cooling impossible at high powers. A similar lack of any significant relationship between emission intensity and pulse rate was found for Zn and Cd.

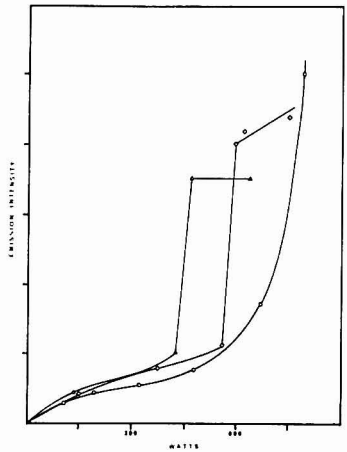

**Figure 8.** Comparison of radiant output of pulsed Hg EDLs at varying pulse widths as a function of incident rf power (Pulse rate constant at 225 Hz). (O) 0.5-ms width, (◊)0.8-ms width, (Δ) 1.6-ms width. Signals recorded are peak values

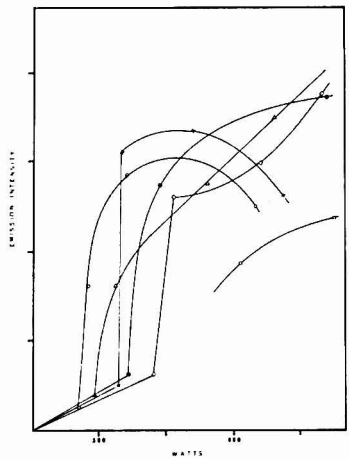

**Figure 9.** Comparison of radiant output of pulsed Cd EDLs at varying pulse widths as a function of incident rf power. (◊) 1.0-ms width, 240 Hz = rate; (●) 2.0-ms width, 240 Hz = rate; (X) 3.0-ms width, 240 Hz = rate; (Δ) 0.5-ms width, 625 Hz = rate; (O) 1.2-ms width; 625 Hz = rate; (□) 0.3-ms width; 240 Hz = rate. Signals recorded are peak values

The pulse width, by contrast, was found to exert a significant effect on lamp emission. Maximum emission intensity for Hg EDLs occurred at about 0.5 ms, and decreased with increasing pulse width to 1.6 ms. At pulse widths below ca. 0.4 ms, there was a drop in intensity, but source instability precluded recording accurate data in this region. The curves for Hg are shown in Figure 8.

Cd lamps followed the same general pattern as the Hg EDLs. Figure 9 shows the effect of duty cycle on the emission intensity. Again, pulse repetition rate had very little effect on the emission intensity, except for a reduction in intensity at high repetition rates, due possibly to overheating problems.

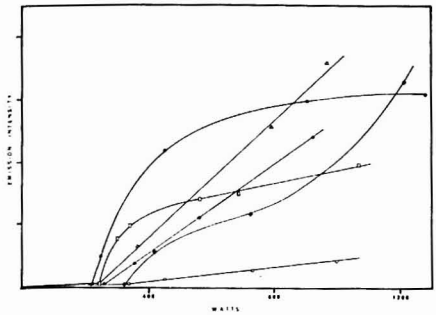

Figure 10. Comparison of radiant output of pulsed Zn EDLs at varying pulse widths as a function of incident rf power. (Δ) 0.8-ms width, 285 Hz = rate; (●) 1.2-ms width, 285 Hz = rate; (×) 0.6-msec width, 285 Hz = rate; (○) 0.4-ms width, 285 Hz = rate; (♦) 0.6-ms width, 625 Hz = rate; (□) 2.0-ms width, 625 Hz = rate. Signals recorded are peak values

The major point of interest is that maximum signals and highest slopes of these curves resulted from pulse widths below 1 ms. The clear difference between the behavior of lamps excited with narrow (≤1 ms) and broad >1 ms) pulses is most significant and would indicate differences in excitation mechanism. Pulse widths below 0.4 ms resulted in lower emission intensity, as with the Hg EDLs.

Zn EDLs (Figure 10) followed a slightly different pattern. Initially there was an increase in intensity with pulse width, but source intensity then dropped off much more slowly than with either Cd or Hg as the pulse width was increased. Maximum intensity and slope was found for a pulse width of approximately 0.8 ms, which is about the same value found for Cd EDLs, but slightly longer than that found for Hg EDLs. Again pulse rate appeared to have a negligible effect, provided adequate thermostating was available. Without proper temperature control, problems arise with lamp stability and intensity, especially at the lower duty cycles.

**Comparison between RF and Microwave Excited EDLs.** Lamp intensity comparisons were made between rf and microwave excited EDLs. The microwave excited EDLs were conventional 8-mm i.d., 35-mm long lamps with ~1 Torr Ar fill gas, prepared in our laboratory. It was found that with the present apparatus, peak pulsed intensities for rf lamps were approximately the same as maximum CW intensities for the microwave excited lamps. The Hg rf excited EDLs were more intense than the microwave excited EDLs, CD EDLs were about the same for both systems, and the Zn EDLs were slightly more intense with microwave excitation than with rf excitation.

Modulation of the microwave generator was also examined but, with the current apparatus, this was not analogous to rf pulsed operation. The microwave system can at best produce 75% modulation over a constant level of 25% power. This is necessary to keep the lamps from extinguishing. The rf lamps in the pulsed mode are totally self-initiating whether hot or cold, which allows easy pulsing of the system from a true zero level, unlike the microwave system.

**Source Drifts and Noise.** Source drift was rarely a problem with the rf system. The drift was primarily sinusoidal in nature, the amplitude seldom exceeded 5% of the total signal. The microwave sources operated in the 3/4 λ Broida cavity required more care to prevent drifting source intensity. Thermostating the lamps improved the situation for both rf and microwave excitation (*13*). Source noise was comparable for both systems, i.e., ≤1% total signal.

**Lamp Lifetimes.** Lifetimes of the rf and microwave excited EDLs were also compared. No Hg, Zn, or Cd microwave excited lamps had failed after approximately 100 hours running time, as expected. The rf excited Hg and Cd lamps also behaved stably for the same running time, and the clean-up on their inner surface appeared no worse than that of the microwave excited lamps. However, the rf excited Zn lamps have shown signs of failure after approximately 50 hours running. At present, there appears to be no obvious explanation for this behavior. Ar lamps also showed a drop in intensity after about 25 hours running time.

## CONCLUSIONS

In order for high power pulsed rf EDLs to offer a major advantage over either CW-rf or CW-microwave excited EDLs as sources for atomic fluorescence spectrometry, it is necessary that the pulsed rf lamps should produce peak intensities of atomic resonance lines far in excess of the intensities produced by either of the CW sources (rf or microwave). So far, current studies with pulsed rf EDLs have not achieved this looked-for gain in intensity. However, it is clear from the plots of resonance line emission intensity vs. rf power input that maximum intensity has not been reached for any of the EDLs studied. Furthermore, with the Hg and Cd lamps, the curves were still of very high slope at the rf power limit (for Zn, the slope was less steep). While it is dangerous to speculate on the form of the continuation of these curves at higher rf powers, there is reason to hope that the maximum emission intensity for pulsed operation might be well above that for CW operation, as the curves for CW operation of the Hg and Cd lamps had already reached a maximum value at the rf powers used in these studies. By contrast, the curves for pulsed operation of Hg and Cd lamps were still of steep slope at the same powers where CW operation had produced a maximum value.

In addition, the pulse width studies have indicated a strong inverse dependence between pulse width and peak intensity. Output intensity of the EDLs is greater for short (≤0.8 ms) pulses than for longer (>1 ms) pulses or for CW operation. Furthermore, the slopes of the curves of peak intensity vs. rf power are steepest for the short pulses, and output intensity is again limited primarily by the power available from the present rf generator.

The need for further studies with pulsed rf EDLs is clear, in order to establish fully their potential as sources for AFS. Primarily, power must be coupled more efficiently with the EDLs in order to investigate their behavior at higher input powers. In addition, mechanistic studies should be made in order to clarify differences between pulsed and CW excitation modes, and line profile studies should also be made in order to examine possible broadening processes. With these developments, it is hoped that pulsed rf excited EDLs may fulfill a valuable role as sources for AFS. A preliminary examination of their properties as sources for AFS and AAS will be presented in a later paper.

## ACKNOWLEDGMENT

Thanks are due to G. O'Brien for the design of electronic components and to K. Williams for machine shop work with optics.

## LITERATURE CITED

(1) D. J. Johnson, W. F. Fowler, and J. D. Winefordner, *Talanta*, **24**, 227 (1977).
(2) H. L. Brod and E. S. Yeung, *Anal. Chem.*, **48**, 344 (1976).
(3) N. Omenetto, *Anal. Chem.*, **48**, 75A (1976).
(4) H. G. C. Human, *Spectrosc. Lett.*, **6** (12), 719 (1973).
(5) J. O. Weide and M. L. Parsons, *Anal. Lett.* **5**, 363 (1972).
(6) N. Omenetto, L. M. Fraser, and J. D. Winefordner, *Appl. Spectrosc. Rev.*, **8**, 428 (1973).
(7) N. Omenetto, G. D. Boutilier, S. J. Weeks, B. W. Smith, and J. D. Winefordner, *Anal. Chem.*, **48**, 1076 (1977).
(8) J. B. Dawson and D. J. Ellis, *Spectrochim. Acta, Part A*, **23**, 565 (1967).

(9) K. L. Smith, *Rev. Sci. Instrum.*, **44**, 1108 (1973).
(10) R. F. Browner, R. M. Dagnall, and T. S. West, *Anal. Chim. Acta*, **45**, 163 (1969).
(11) D. O. Knapp, K. E. Zacha, and J. D. Winefordner, *Spectrochim. Acta, Part B*, **23**, 389 (1968).
(12) R. M. Dagnall and T. S. West, *Appl. Opt.*, **7**, 1287 (1968).
(13) R. F. Browner and J. D. Winefordner, *Spectrochim. Acta, Part B*, **28**, 263 (1973).
(14) R. M. Dagnall, M. D. Silvester, and T. S. West, *Talanta*, **18**, 1103 (1971).
(15) W. E. Bell, A. L. Bloom, and J. Lynch, *Rev. Sci. Instrum.*, **32**, 688 (1961).
(16) R. G. Brewer, *Rev. Sci. Instrum.*, **32**, 1356 (1961).
(17) N. P. Ivanov, L. V. Minervina, S. V. Baranov, L. G. Pofralidi, and I. I. Olikov, *Zh. Anal. Khim.*, **21**, 1129 (1966).
(18) J. Reader, *J. Opt. Soc. Am.*, **65**, 988 (1975).
(19) J. Reader, *J. Opt. Soc. Am.*, **65**, 286 (1975).
(20) L. Minnhagen and L. Stigmark, *Ark. Fys.*, **13** (2), 27 (1957).
(21) L. Minnhagen, B. Peterson, and L. Stigmark, *Ark. Fys.*, **16** (45), 571 (1960).
(22) H. U. Eckert, Report No. ATR-77(9472)-2 (1977), Aerospace Corporation, El Segundo, Calif.
(23) J. P. S. Haarsma, G. J. DeJong, and J. Agterdenbos, *Spectrochim. Acta, Part B*, **29**, 1 (1974).
(24) W. W. Macalpine and R. O. Schildknecht, *Electronics*, **33**, 140 (1960).
(25) F. C. Gabriel, *Rev. Sci. Instrum.*, **47**, 484 (1976).

RECEIVED for review October 17, 1977. Accepted December 12, 1977.

# Stationary Cold-Vapor Atomic Absorption Spectrometric Method for Mercury Determination

**Soo-Loong Tong**

*Department of Chemistry, University of Malaya, Kuala Lumpur, Malaysia*

**A new stationary cold-vapor atomic absorption method using an ordinary 4-cm UV-cell for mercury determination is proposed. Mercury(II) is reduced and then partitioned between an aqueous and a gas phase in a stoppered UV-cell. Direct atomic absorption measurement is taken by allowing the mercury resonant light beam to pass through the vapor phase of the system while non-atomic absorption is corrected using an automatic background corrector. The calibration graph obtained for Hg(II) in 4 M $H_2SO_4$ is linear from 0 to 30 ppb and absorbance at concentrations up to 50 ppb shows only slight deviation from linearity. The slope of the linear region is 0.0253 $ppb^{-1}$ and the detection limit is 0.02 ppb or 0.1 ng. The absorbance was found to be dependent on the concentration of the common acids used. The partition constant of elemental mercury between the two phases was also determined employing a radiotracer technique. The value obtained was 0.66 ± 0.04 for Hg(II) in 2 M $H_2SO_4$.**

Most determinations of mercury by atomic absorption spectrophotometry at ppb and sub-ppb levels are based on the cold-vapor method reported by Poluektov et al. (*1*) and Hatch and Ott (*2*). There are many modifications and improvements on this principle which have become standard in many laboratories (*3*). Practically all of these involved measurements of transient atomic absorption of reduced mercury. In one approach, mercury reduced by stannous ion is bubbled and swept with a carrier gas through the absorption cell or, alternatively, the carrier gas is continuously recirculated so that more steady absorbance readings can be obtained. In another method, the reduced mercury is partitioned between the liquid and a fixed volume of air by agitation, after which the mercury-laden air is blown directly through the absorption cell.

In principle, the reduction and partition of mercury may be carried out in a closed vessel with UV-transparent windows followed by direct stationary atomic absorption measurement if accurate non-atomic absorption correction can be made easily. Such a system with a minimum dead volume for the air phase would then provide better detection sensitivity, further simplification in operation and be subject to less analytical variables. In this report, a detailed study on the use of an ordinary rectangular 4-cm UV-cell for this purpose is described. In addition, the partition constant of reduced mercury between the solution and air phase determined by a radiotracer technique is also reported.

## EXPERIMENTAL

**Apparatus.** All atomic absorption measurements were made on an Instrumentation Laboratory IL-251 double beam spectrophotometer equipped with an automatic background corrector. The burner in the atomization compartment was replaced by a specially designed holder (Figure 1) for a 4-cm UV-cell (Spectrosil, dimensions: 10 × 32 × 40 mm, Thermal Syndicate Limited, England) which allows for proper alignment with the atomic light beam. A Varian mercury hollow-cathode lamp and a hydrogen continuum lamp for background correction were used.

Gamma activity for $^{203}Hg$ was measured using a 50 × 50 mm well-type NaI(Tl) detector in conjunction with an ORTEC single channel analyzer.

**Reagents.** Reagent grade chemicals and deionized-distilled water were used for all the preparation of solutions. Stock mercury solution (1000 μg/mL) was prepared by dissolving 1.354 g mercury(II) chloride in 50 mL of concentrated hydrochloric acid and then dilute to 1 L. Working standards (0.2–1.0 μg/mL) were prepared weekly by appropriate dilution from this solution with 5% $HNO_3$–0.01% $K_2Cr_2O_7$ solution. The reductant consisted of 10% (w/v) $SnCl_2$, 5% (w/v) NaCl, and 10 mL $H_2SO_4$ in 100 mL solution.

Radioactive $^{203}Hg$ was purchased as mercuric chloride in 0.1 N HCl solution (Radiochemical Centre Ltd., Amersham) with specific activity of 0.68 mCi/mg.

**Procedure.** A pair of 4-cm UV-cells, of volumes 12.9 mL and 13.0 mL each have been used alternatively for the reduction-partition and subsequent cold-vapor atomic absorption measurement. To obtain the calibration graphs, 5.0 mL of acid solutions were pipetted into the cell followed by the addition of appropriate volumes (0.020–0.50 mL) of the working standards of Hg(II) and 0.20 mL of the reducing agent and the cell was tightly stoppered. After shaking for 2 min, the cell was placed in the holder fixed to the atomic absorption spectrophotometer. The holder has been previously aligned to allow the atomic light beam to pass through the upper gas phase of the cell with maximum intensity. Lamp currents applied to the mercury hollow-cathode lamp and hydrogen continuum lamp were 4 mA and 15 mA, respectively. The mercury 253.7-nm resonant line was used with slit width of 320 nm and photomultiplier high

0003-2700/78/0350-0412$01.00/0 © 1978 American Chemical Society

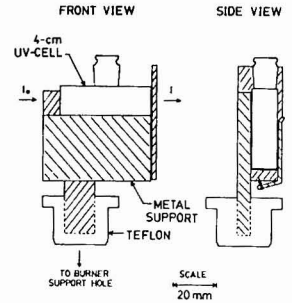


**Figure 1.** Cell holder attachment for stationary cold-vapor atomic absorption measurements

voltage of 460 volts. Atomic absorption of the mercury vapor was taken using double-beam and simultaneous background correction mode with 1-s integration time. After the measurement, the cell was washed with dilute nitric acid–dichromate solution in a fume cupboard and thoroughly rinsed with deionized water and shaken dry.

Experimental conditions for the determination in hydrochloric, nitric, and sulfuric acids of various concentrations have been studied. Linear and working ranges of the mercury solution of the proposed procedure, and the possible effect due to room temperature fluctuation during an analysis, were investigated.

Direct determination of the partition constant of elemental mercury between the solution and gaseous phases has been carried out using varying concentrations of $^{203}$Hg-labeled standards ranging from 1.2–59.6 ppb in 2 M $H_2SO_4$. After carrying out the reduction and partition equilibration in the cell as described above, exactly 4 mL of the solution were pipetted cautiously into a 4.5-mL vial. The vial was stoppered tightly and counted immediately with the single-channel $\gamma$-ray counter. The concentrations of mercury remaining in the solution phase at equilibrium were determined by comparing the counting data with the count-rate of a $^{203}$Hg-labeled standard.

## RESULTS AND DISCUSSION

The optimum volume of the sample solution to be used in the system described here was found to be not more than 6 mL, in order to give a minimum dead volume possible for the gas phase upon which the atomic light beam is being passed through. Larger solution volume would cause partial absorption interference which cannot be corrected by simultaneous background correction. Sample solution of 5.0 mL with 0.20–0.40 mL of the reducing agent was found to be satisfactory for Hg(II) concentration ranging from 0–50 ppb.

Partition equilibrium of reduced mercury between the two phases was established in less than 1 min by applying moderate shaking; normally each solution was shaken for 2 min before absorbance was taken. Cell positioning with respect to the beam path is quite critical and cell-in cell-out reproducibility has to be observed carefully to achieve optimum precision. The absorbance reading usually became stabilized within 30 s after insertion of the cell into the holder. Initial fluctuations observed are suspected to be due to the thin film of liquid adhered on the cell windows. From repetitive measurements of a 5.0 ppb Hg(II) solution, relative precision of 2% was obtained. Temperature effect on the partition equilibrium has been investigated although no strict temperature regulation of the present system is possible. No noticeable changes were found in the absorbance readings, however, when room temperature fluctuated between 22–26 °C.

The calibration graph for Hg(II) in 4 M $H_2SO_4$ solution is linear from 0 to 30 ppb and absorbance at concentrations up

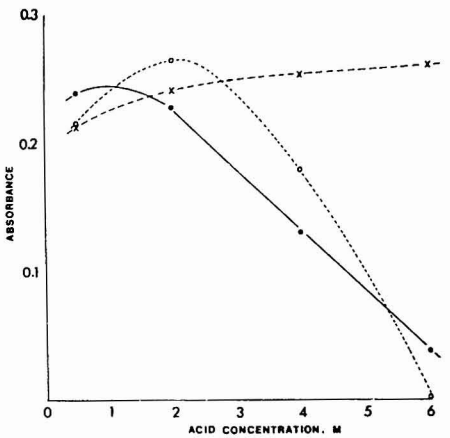


**Figure 2.** Cold-vapor absorbance of 10 ppb Hg(II) in $H_2SO_4$ (X), in HCl (●), and in $HNO_3$ (O)

to 50 ppb (1.230 absorbance) shows only slight deviation from linearity. The sensitivity in terms of the slope of the calibration graph in the linear region is 0.0253 ppb$^{-1}$. The detection limit, defined as the concentration which yields an absorbance twice that of the standard deviation of the absorbance of a blank, is 0.02 ppb or 0.1 ng under the present instrumental conditions. These results compare favorably even with the best detection limits for the transient cold-vapor absorption method as reported by Hawley and Ingle, Jr. (*4*). The slopes of the atomic absorption calibration and the detection limits obtained by them were 0.0219 ppb$^{-1}$ and 3 ppt Hg(II), respectively, for a 20-cm cell, and 0.0636 ppb$^{-1}$ and 1 ppt Hg(II), respectively, using a 60-cm cell. These results were achieved through the reduction of dead volume of the reducing apparatus, increasing the efficiency of diffusion of elemental mercury into the carrier gas, and by modifying the instrument light source and detector. Our method, being simpler in operation, can be further improved in sensitivity with the use of a similar UV-cell of longer pathlength (such as 10 or 20 cm).

As shown in Figure 2, the absorbance measured is strongly dependent on the concentration of the acid medium. The gradual increase observed in the absorbance of 10 ppb Hg(II) solutions in $H_2SO_4$ of increasing concentration is qualitatively consistent with the observation of Koirtyohann and Khalil (*5*) who have found a more rapid change. The absorbance was found to decrease rapidly in hydrochloric acid of more than 2 M and nitric acid of more than 3.5 M concentration. Contrary to these trends, the latter authors found practically no variations for both acids three to four times more concentrated. In the system we employed, the volatility of these acids possibly causes not only reduction in the amount of elemental mercury distributed in the gas phase but also errors in the automatic background correction.

As a test of feasibility for real sample analysis, the method described has been used for the analysis of fish samples digested according to the procedure of Ramirez-Munoz (*6*). The digested solution was filtered after the oxidation but before the addition of hydroxylamine sulfate for the reduction of excess permanganate. Results based on the standard addition method are shown in Figure 3. Linear regressions carried out for each set of the known addition data gives correlation coefficients of 0.993–0.998. It is therefore con-

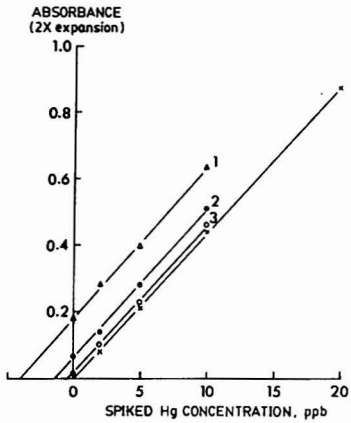


**Figure 3.** Known addition determination of mercury in digested fish sample solutions. Concentrations of Hg(II) found in solution 1: 3.9 ppb; solution 2: 1.4 ppb; and solution 3: 0.3 ppb. Blank solution: -x-x-

cluded that ions commonly present in digested fish solution do not interfere with the determination. However, incomplete digestion often encountered for fish tissues of high fat content have been found to render the method inapplicable because of foaming problems.

The system is expected to be generally useful for monitoring mercury in natural and polluted water as well as mercury in other digested samples. Common oxidants normally required for sample treatments such as potassium dichromate, potassium permanganate, hydrogen peroxide, and bromine, do not interfere with the determination.

The partition constant of the reduced mercury between the liquid and vapor phases is of fundamental interest for the cold-vapor methods. However, few studies concerning this have appeared in the literature. A rough estimate based on the results of Ure and Shand (7) yields a partition constant value of 0.25, which is defined as

$$K = \frac{\text{Concentration of Hg in air}}{\text{Concentration of Hg in liquid}}$$

This value is significantly lower than the values reported by Koirtyohann and Khalil (5). The latters found $K$ values of 0.40 for mercury in hydrochloric and nitric acids, and from 0.40–0.70 for mercury in 0–6 M $H_2SO_4$. Our results from using radioactive $^{203}Hg$ tracer and the system described above are presented in Table I. The mean partition constant is 0.66 ± 0.04 for Hg(II) in 2 M $H_2SO_4$ ranging from 1.2–59.6 ppb, as compared with the value of approximately 0.50 obtained by Koirtyohann and Khalil (5) under the same acid condition. As shown previously in Figure 2, variations of the partition constant as a function of the concentration of some common acids are prominent for our system.

**Table I. Partition Constant of Reduced Mercury between the Liquid and Gas Phase**

| Hg(II) concn, ppb | Partition constant, $K$[a] |
|---|---|
| 1.2 | 0.61 |
| 2.4 | 0.70 |
| 7.2 | 0.63 |
| 14.4 | 0.68 |
| 28.8 | 0.66 |
| 59.6 | 0.69 |
| Mean ± std. dev | 0.66 ± 0.04 |

[a] Average of triplicate determinations.

In conclusion, transient peak atomic absorption and peak area integration measurements for the cold-vapor method can be replaced by a steady-state atomic absorption method. Although simultaneous background correction is essential while employing the technique, it is basically simpler in operation than many other techniques for rapid mercury determinations. With the use of a set of 4 reduction-absorption cells, an average of 20 determinations can be carried out per hour.

## ACKNOWLEDGMENT

The author thanks M. C. Lim and C. K. Chu for many helpful suggestions related to this work.

## LITERATURE CITED

(1) N. S. Poluektov, R. A. Vitkun, and T. V. Zelyukova, *Zh. Anal. Khim.*, **19**, 937 (1964).
(2) W. R. Hatch and W. L. Ott, *Anal. Chem.*, **40**, 2085 (1968).
(3) A. M. Ure, *Anal. Chim. Acta*, **76**, 1 (1975).
(4) J. E. Hawley and J. D. Ingle, Jr., *Anal. Chem.*, **47**, 719 (1975).
(5) S. R. Koirtyohann and M. Khalil, *Anal. Chem.*, **48**, 136 (1976).
(6) J. Ramirez-Munoz, Beckman Instruments Inc., *Appl. Res. Tech. Rep.*, No. 556, (1971).
(7) A. M. Ure and C. A. Shand, *Anal. Chim. Acta*, **72**, 63 (1974).

RECEIVED for review August 30, 1977. Accepted October 17, 1977.

# Discrimination of Monostereoisomers in Asymmetric Solvents by Fourier Transform Infrared Spectrometry

**David L. Grieble and Peter R. Griffiths***

*Department of Chemistry, Ohio University, Athens, Ohio 45701*

**Tomas Hirschfeld**

*Block Engineering, Inc., 19 Blackstone Street, Cambridge, Massachusetts 02139*

**In principle, both members of an enantiomeric pair have identical physical properties except to polarized radiation, and thus cannot be distinguished by conventional spectrometric methods. To resolve both compounds, diastereoisomeric derivatives may be prepared by combining them with an asymmetric reagent ("resolving agent"). The resulting change in molecular symmetry then makes both molecules distinguishable. The same effect may be used for analytical purposes through the measurement of spectral perturbations caused by dissolving the enantiomers in an asymmetric solvent. The "virtual diastereoisomers" produced by the solute–solvent interactions will then produce different solvent-induced band shifts which could be used analytically. The procedure is demonstrated by measurements on all the permutations of both stereoisomers of malic acid dissolved in both stereoisomers of 2-octanol.**

The analytical differentiation of monostereoisomers is an important aspect of the analysis of natural products, biochemicals, and pharmaceuticals. Such isomers are indistinguishable, in principle, by any physical measurement except those employing polarized radiation. The most common method of distinguishing between monostereoisomers is to determine the optical rotatory activity of a solution in an optically inactive solvent (*1*). This measurement is generally performed using ultraviolet or visible radiation, since the optical components necessary for these measurements (achromatic quarter wave plates, rotators, etc.) are not available for infrared radiation. Thus the infrared equivalent of the highly successful ultraviolet–visible optical rotatory dispersion or circular dichroism techniques has not been achieved even though it should have great value in structural analysis.

In several analytical and preparative techniques, otherwise identical monostereoisomers are distinguished by combining them with a second monostereoisomer (the "resolving agent"). The resulting diastereoisomeric derivative now shows gross differences in physical properties depending on which initial compound it was obtained from.

It should be possible for analytical purposes to dispense with the synthetic step described above, and to study the properties of the different "virtual diastereoisomers" formed by solute–solvent interactions between an asymmetric sample and an asymmetric solvent. Fourier transform infrared (FT-IR) spectrometry has been used to distinguish between the spectra of closely related isomers (*2*) and to detect weak solute–solvent interactions (*3*) through the application of absorbance subtraction routines. A logical extension of these studies was to investigate whether the absorbance subtraction technique could be used to show specific interactions between asymmetric solutes and asymmetric solvents. In this work we have used the two optical isomers of malic acid for the solute and those of 2-octanol for the solvent.

## EXPERIMENTAL

Samples of the enantiomers of malic acid, designated +M and −M, (Fluka AG, Puriss Grade) and of 2-octanol, designated +O and −O, (Fluka AG, Purum Grade) were obtained from Tridom Chemical, Inc. (Hauppage, N.Y.). The octanol samples had been determined as better than 99% pure by gas chromatography, and had specific rotations, $[\alpha]_{546}^{20}$ of $\pm 11 \pm 1°$. The malic acid samples had quite different physical properties. Whereas the sample of +M was white and apparently quite pure [mp = 98-102 °C, cf. the literature value (*4*) of 100–103 °C] and dissolved readily in octanol, the sample of −M was discolored, had a melting range of 92–103 °C, and did not completely dissolve in octanol. The sample of −M was purified by dissolving it in the minimum amount of a heated 1:1 mixture of acetone and chloroform, filtering the solution after most of the sample had dissolved, and cooling the filtrate in ice to recover the malic acid. After three such treatments a white product was obtained whose melting range was 100–102 °C and whose dissolution properties in octanol were identical to those of +M. The specific rotations of the malic acid samples measured as 10% (w/w) solutions in water were −1.7° and +1.6°, respectively.

All spectra were measured using a Model FTS-14 FT-IR spectrometer (Digilab, Inc., Cambridge, Mass.) at a resolution of 4 $cm^{-1}$ using double precision (32 bits per word) signal-averaging, FFT, and arithmetic routines. Solutions with 0.100 mole fraction of malic acid in 2-octanol were prepared and held in a precision sealed cell (Wilks Scientific Corp., South Norwalk, Conn.). This cell was the thinnest we could obtain commercially, but even though its pathlength was specified as 15 μm, it was measured as 25 μm. At this pathlength, one band in the spectrum of malic acid and three bands due to 2-octanol had peak absorbances greater than 2.5. The absorbance of all the other bands in the spectra of the solutions studied were of the correct magnitude to allow spectral subtraction techniques to be used to differentiate the spectra. All measurements were made without dismantling the cell holder, and we believe the pathlength to be constant to within 1%.

## RESULTS AND DISCUSSION

The spectra of all four solutions (−M in +O, +M in +O, −M in −O, and +M in −O) showed appreciable differences in overall intensity as shown in Figure 1. All bands in the spectrum of −M in +O were substantially weaker than the corresponding bands in the spectra of any of the other solutions, and the spectrum of +M in −O was somewhat more intense than that of the other two solutions. No obvious spectral shifts are seen from these spectra before spectral subtraction routines are applied, but the relative intensities of several bands can be seen to have changed. The most obvious region where this effect can be observed is between 1100 and 1000 $cm^{-1}$ (see Figure 2), where the intensity of the band at 1040 $cm^{-1}$ relative to the intensity of the band at 1070 $cm^{-1}$ can be seen to change markedly.

Before the result of applying spectral subtraction routines is discussed, it should be recognized that for these routines

0003-2700/78/0350-0415$01.00/0 © 1978 American Chemical Society

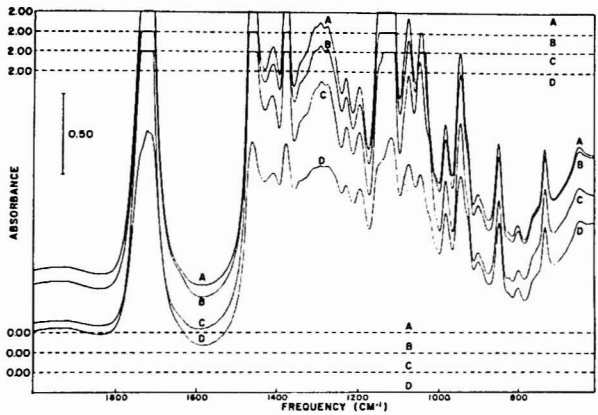


**Figure 1.** Absorbance spectra of the malic acid/2-octanol solutions. (A) (+M in −O); (B) (−M in −O); (C) (+M in +O); (D) (−M in +O)

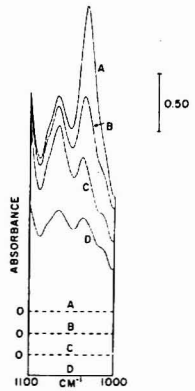


**Figure 2.** Scale-expanded absorbance spectra of malic acid/2-octanol solutions between 1100 and 1000 $cm^{-1}$. (A) (+M in +O); (B) (−M in −O); (C) (+M in −O); (D) (−M in +O)

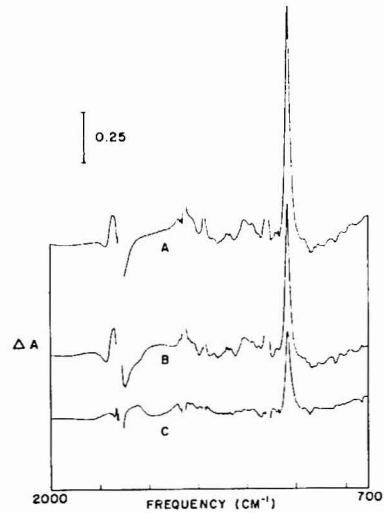


**Figure 3.** Unscaled difference spectra of malic acid/2-octanol solutions. (A) (+M in +O) − (+M in −O); (B) (+M in +O) − (−M in −O); (C) (−M in −O) − (+M in −O). Note evidence of a shift in the carbonyl band of (+M in +O) and (+M in −O) (spectrum A), but the similarity between the spectra of (−M in −O) and (+M in −O) (spectrum C). The variation in intensity of the 1035 $cm^{-1}$ band is very apparent from these spectra. Frequency regions where the absorbance of either spectrum exceeds 2.5 are left blank

to be effectively used, the peak absorbance of all bands in the spectrum should be small, preferably less than 0.7 (*5–8*). However both malic acid and octanol are such strong infrared absorbers that we were unable to keep the peak absorbance of the strongest bands in the solution spectra (at 1715, 1455, 1375 and 1110 $cm^{-1}$) below 2.5 with the IR cells available to us at the moment. If absorbance spectra containing such intense bands as these require multiplication by a large scaling factor before subtraction, it is known that artifacts will be introduced into the difference spectrum due to the effect of "resolution errors" (*5*). Thus all difference spectra are plotted only at frequencies where the absorbance is less than a certain value, which was arbitrarily selected as 2.5. In addition no difference plots involving strong bands in the spectrum of −M in +O are shown, since the scaling factor would have to be so great that enormous resolution errors are incurred and meaningful conclusions cannot be drawn from the data.

The three difference spectra showing the result of subtracting each combination of two of the other three spectra are shown in Figure 3. Two features, centered at 1715 $cm^{-1}$ and 1035 $cm^{-1}$, are prominent in these spectra. The band at 1715 $cm^{-1}$ may be unequivocally assigned to the carbonyl stretching vibration of malic acid, while the 1035 $cm^{-1}$ band is present at medium intensity in the spectrum of octanol and weakly in the spectrum of malic acid. Since octanol is the major component, it is most likely that perturbations to this band indicate an interaction with the octanol molecule. However, we are not certain of the vibrational mode to which this band can be assigned; initially we believed it to be due to the C–O stretching vibration, but the strong band at 1110 $cm^{-1}$ is better assigned to this mode for a secondary alcohol (*9*). Small shifts and intensity changes associated with other bands are evident from the difference spectra, but the effects

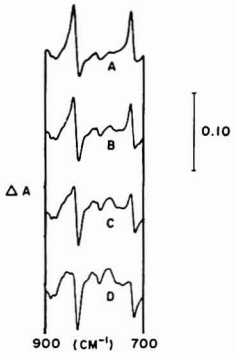


**Figure 4.** Scaled difference spectra, (+M in –O) – $x$(–M in +O), between 900 and 700 $cm^{-1}$. (A) $x$ = 1.15; (B) $x$ = 1.20; (C) $x$ = 1.25; (D) $x$ = 1.30

of these changes are generally of much smaller magnitude than the effect of the band shift on the carbonyl band of malic acid and the intensity change in the 1035 $cm^{-1}$ band of 2-octanol. Therefore it appears that infrared difference spectrometry can indeed detect spectral changes due to interactions near the chiral center, and thus differentiate between monostereoisomers for analytical purposes. It is also apparent that much more work is needed for a theoretical interpretation of these perturbations in terms of sample structure.

An interesting question is raised by the intensity difference between the spectrum of –M in +O and that of +M in –O. This anomaly, which occurs for the bands due to *both* components of the solutions, could not be traced to air bubbles, cell thickness variations, sample preparation, or other such trivial causes.

It is also of interest that whereas some bands in the spectra of the other three solutions were as much as twice as intense as the corresponding bands in the spectrum of –M in +O, other bands are only slightly stronger. For example, in the region between 900 and 700 $cm^{-1}$, there are two bands of medium intensity (at 840 $cm^{-1}$ and 722 $cm^{-1}$). Each of these bands in the spectrum of –M in +O is apparently slightly shifted from the corresponding bands in the spectra of the other three solutions, while also exhibiting a relatively small intensity change. Figure 4 shows the result of multiplying the spectrum of –M in +O by various scaling factors and subtracting the result from the spectrum of +M in –O. The intensity of the 840 $cm^{-1}$ band is equalized by applying a scaling factor of 1.20, as evidenced by the most symmetrical feature in the series of difference spectra, while the intensity of the 722 $cm^{-1}$ band is equalized by applying a scaling factor of 1.25. Other bands in the spectrum require scaling factors of 2.0 or more to minimize the difference band, although it should be stressed that the effect of resolution errors is very noticeable when such large scaling factors are applied.

The explanation of these phenomena seems to lie in the nature of the residual polarization in Michelson interferometers. It has been shown that the beamsplitter acts differently on both polarizations, so that a weak residual polarization develops in the output beam (*10*). However, since at all scan locations except the center fringe there is a phase delay between the interfering beams, this residual polarization will be not linear but elliptical (*11*).

The spectral degeneracy between monostereoisomers will, of course, break down in elliptically polarized light. The effect has not yet been calculated quantitatively because of the multicyclic nature of the delay and the mathematical consequences of the Fourier transformation, which lead to fairly complex equations. The complementary output emerging from the interferometer will show a residual ellipticity of the opposite sense, raising the possibility of infrared circular dichroism measurements using a dual-beam (optical subtraction) FT-IR system of the type described recently (*12*), and an attempt to build a spectrometer for this purpose is now under way.

In summary it can be stated that the solute–solvent interactions between a monostereoisomeric solute and a chiral solvent lead to the formation of a virtual diastereoisomer capable of breaking the degeneracy between the spectra of the enantiomers. These interactions, picked up by absorbance subtraction FT-IR spectrometry allow analytical differentiation of monostereoisomers. The behavior of different bands can be used to study molecular structure and behavior, although much work will have to be done to clarify these phenomena.

## ACKNOWLEDGMENT

We gratefully acknowledge the advice for the purification of malic acid given to us by William Huntsman of Ohio University.

## LITERATURE CITED

(1) C. Djerassi, "Optical Rotatory Dispersion", McGraw-Hill, New York, N.Y., 1960.
(2) R. M. Gendreau and P. R. Griffiths, *Anal. Chem.*, **48**, 1910 (1976).
(3) T. Hirschfeld and K. Kizer, *Appl. Spectrosc.*, **29**, 345 (1975).
(4) "CRC Handbook of Chemistry and Physics", 48th ed., The Chemical Rubber Co., Cleveland, Ohio, 1967.
(5) R. J. Anderson and P. R. Griffiths, *Anal. Chem.*, submitted for publication (1977).
(6) T. Hirschfeld, *Appl. Spectrosc.*, **29**, 523 (1975).
(7) T. Hirschfeld, *Appl. Spectrosc.*, **30**, 550 (1976).
(8) T. Hirschfeld, *Anal. Chem.*, submitted for publication (1977).
(9) K. Nakanishi, "Infrared Absorption Spectroscopy—Practical", Holden-Day, San Francisco, Calif., 1962.
(10) T. Hirschfeld, *Appl. Spectrosc.*, **29**, 192 (1975).
(11) M. J. Block, *J. Opt. Soc. Am.*, (advertisement), April 1960.
(12) D. Kuehl and P. R. Griffiths, *Anal. Chem.*, **50**, this issue.

RECEIVED for review August 22, 1977. Accepted December 2, 1977.

# Dual-Beam Fourier Transform Infrared Spectrometer

**Donald Kuehl and Peter R. Griffiths***

*Department of Chemistry, Ohio University, Athens, Ohio 45701*

**A system is described for increasing the sensitivity of absorption spectrometry using a Fourier transform infrared (FT-IR) spectrometer in which both exit beams from a Michelson interferometer are passed onto the same detector. With this system the detector may be changed from the conventional triglycine sulfate (TGS) pyroelectric bolometer to the more sensitive mercury cadmium telluride (MCT) photoconductive detector without limiting the sensitivity by digitization noise. The sensitivity of the system is about ten times greater than that of a conventional FT-IR spectrometer and would be a factor of a least five greater than this were it not for the fact that the response of the MCT detector becomes nonlinear at high levels of incident radiation.**

General purpose mid-infrared Fourier transform spectrometers have the rather unusual design criterion that the scan speed of the moving mirror must be fast enough to ensure that the signal-to-noise ratio (S/N) of spectra is always limited by the infrared detector and not by the analog-to-digital converter (ADC) or the data system of the spectrometer. In order to obtain absorption spectra with the very low noise levels of which Fourier spectrometry is capable, rapidly scanned interferograms are signal-averaged before the Fourier transform. For the measurement of medium or low resolution (2 $cm^{-1}$ or lower) mid-infrared spectra on a 2-inch aperture interferometer operating at its throughput limit using conventional continuous sources (Nernst glower, globar, nichrome wire), a triglycine sulfate (TGS) detector, and a 15-bit ADC, the scan speed of the moving mirror must be at least 2 mm $s^{-1}$.

To substantially increase the sensitivity of rapid-scanning Fourier spectrometers while maintaining a reasonable measurement time, one would like to replace the somewhat insensitive TGS detector ($D^*$ $\sim 2 \times 10^8$ W $Hz^{-1/2}$) by a more sensitive detector such as the mercury cadmium telluride (MCT) photodetector, the average $D^*$ of which is *at least* ten times greater than that of TGS. If the average transmittance of the sample and sampling accessory is less than approximately 0.07, it can be shown that a TGS detector may be directly replaced by an MCT detector without limiting the sensitivity of the measurement by digitization noise (*1*). However if the average transmittance of the sample approaches 1.00, the S/N of interferograms measured with an MCT detector near the point of stationary phase will exceed the dynamic range of a 15-bit ADC if the scan speed of the interferometer is not changed. Of course, the S/N of the interferogram may be reduced by increasing the scan speed. However to decrease the S/N by a factor of $(0.07)^{-1}$, the scan speed has to be increased by a factor of $(0.07)^{-2}$, or about 200. In practice the scan speed has to be increased by an even greater amount than 200, since the $D^*$ of the MCT detector increases with modulation frequency.

The sampling frequency of a He-Ne laser referenced interferometer for mid-infrared measurements between 400 and 4000 $cm^{-1}$ when the scan speed of the interferometer is 1.6 mm $s^{-1}$ is 5 kHz. Increasing the scan speed of the moving mirror by a factor of 200 implies that the sampling frequency must be increased to about 1 MHz, a value which is far greater than the maximum allowed sampling frequency of state-of-the-art 15-bit ADC's and disk data systems.

Another method of eliminating the dynamic range problem includes the use of a gain-ranging amplifier (*2*); but we have found that the S/N of spectra measured on our system with and without a gain-ranging amplifier are little different. Two other techniques which have been suggested are blanking or clipping the interferogram near the point of stationary phase (*3*); however, with either technique the photometric accuracy of the computed spectra is very low and it is very unlikely that weakly absorbing bands could be measured in either case. Finally the use of chirped interferograms (*4*) has also been suggested for this purpose, but there are two arguments against the use of chirping. The beamsplitters of most commerical interferometers are not designed to chirp the interferogram, and the calculation of the FFT of a highly chirped interferogram takes much longer than the corresponding calculations for a relatively unchirped signal.

In this paper, a technique will be described which is designed to reduce the S/N of the interferogram without reducing the amplitude of modulations due to sample absorption bands. The system is based on the optical subtraction method first suggested by Bar-Lev (*5*) and applied to GC-IR measurements using an early low resolution interferometer by Low (*6*). In this dual-beam Fourier transform infrared (DB-FT-IR) system, both beams from a conventional Michelson interferometer, see Figure 1, are measured using a single detector. If a sample of transmittance $T_\nu$ is placed in beam $B$, the resultant ac interferogram, $I(\delta)$, is theoretically given by (*7*):

$$I(\delta) = {}^1/_2 \int_{-\infty}^{+\infty} B(\nu)[1 - T_\nu] \cos(2\pi\nu\delta + \theta_\nu)\mathrm{d}\nu$$

where $B(\nu)$ is the relative spectral energy of the source at wavenumber, $\nu$ $cm^{-1}$; $\delta$ is the optical retardation, in cm; and $\theta_\nu$ is a frequency-dependent phase angle. The greater is $T_\nu$, the smaller is the amplitude of the interferogram at all values of $\delta$, so that interferograms of weakly absorbing samples may be measured using intense continuous sources and sensitive detectors without limiting the spectral S/N by digitization noise.

## INSTRUMENTATION

The optical layout was built around an FTS-14 spectrophotometer (Digilab, Inc., Cambridge, Mass.) as shown in Figure 2. The radiation from a modified Nernst glower source (Perkin-Elmer Corp., Norwalk, Conn.) is collimated by a 3-inch focal length off-axis paraboloid (Special Optics, Little Falls, N.J.) and enters the interferometer at an angle, relative to the beamsplitter, of 49.5°. The two exit beams (A and B in Figure 1) are picked off by two plane mirrors and reflected to two 3-inch focal length paraboloids (Special Optics) which focus the beams in the sample compartment. The beams are picked up by two off-axis ellipsoids (Special Optics) and focused onto the detector. The diameter of the beams at the sample focus is 3 mm and at the detector it is 2 mm. The detectors used in this study were the Barnes Engineering (Stamford, Conn.) TGS detector which is a component of the FTS-14 spectrometer, and an MCT detector (Texas Instruments, Dallas, Texas) which was interfaced to the spectrometer using a Perry Amplifiers (Brookline, Mass.) Model 601 amplifier.

0003-2700/78/0350-0418$01.00/0 © 1978 American Chemical Society

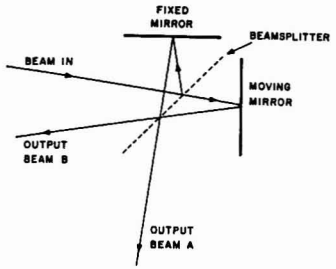


**Figure 1.** The two output beams (A and B) from a Michelson interferometer when the input beam is slightly skewed

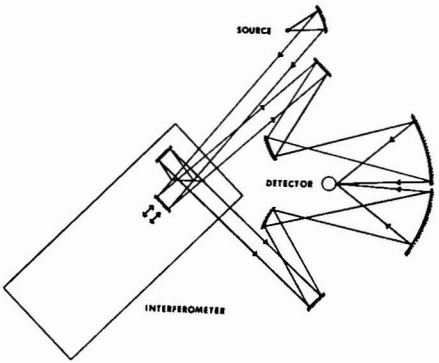


**Figure 2.** Optical diagram of the dual-beam Fourier transform spectrometer used in this work

The geometry of the interferometer does not quite allow the full 2-inch diameter collimated beam from the source to reach the detector. However, the S/N of spectra measured on a standard FTS-14 spectrometer were almost identical to those measured on our system using the same source and TSG detector with one beam blocked.

The optics were designed in a modular fashion to accommodate either conventional infrared cells, flow through cells for on-line identification of HPLC peaks, or parallel GC-IR light-pipes. In the latter mode, the two off-axis ellipsoids and the detector are moved back as a unit to allow the light-pipes to be mounted.

## RESULTS AND DISCUSSION

**Measurement of Transmittance Spectra.** As was discussed earlier, the result of the Fourier transform of a dual-beam interferogram is $B(\nu)\ [1 - T_\nu]$. For the calculation of $T_\nu$, therefore, this spectrum must be divided by the single-beam background spectrum, $B(\nu)$, and the resultant spectrum must be subtracted from unity. In practice it is found that a perfect optical subtraction is never achieved on DB-FT-IR systems (*8*, *9*), and we have found two broad residual bands centered at 840 and 550 $cm^{-1}$. This observation differs from the previous reports, where a third band, at 1225 $cm^{-1}$, was reported. The maximum value of $I(\delta)$ for the system with one beam blocked and no sample present is about 30 times greater than the maximum value in the dual-beam configuration, so that the system could be used for the measurement of the spectra of weakly absorbing samples using the MCT detector without encountering digitization noise.

If a very flat spectral baseline is desirable (which is always necessary if $T_\nu$ is large), the dual-beam background must be subtracted before division by $B(\nu)$. For certain measurements we have found it preferable to subtract a dual-beam background interferogram from the sample interferogram before the FFT, while for others better results were found by first performing the transform on the spectrum as measured and then subtracting a dual-beam background spectrum. We were not able to find any way of forecasting whether subtraction of interferograms or spectra would provide superior results for a given experiment. The steps in the calculation of the transmittance spectrum of a film of polyethylene are illustrated in Figure 3 with subtraction of the background spectrum. A comparison of the spectrum measured in this way and a transmittance spectrum of polyethylene measured using the conventional ratio-recording technique shows little apparent difference between the spectra, each of which was measured with a TGS detector.

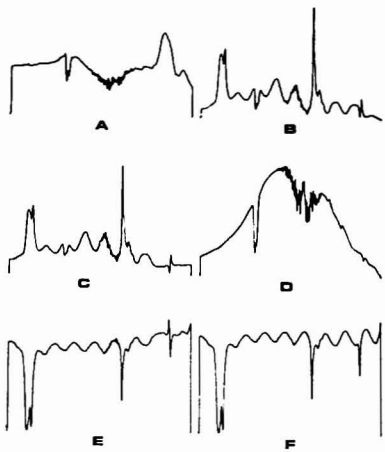


**Figure 3.** Steps in the calculation of transmittance spectra in a dual-beam FT-IR spectrometer, using the spectrum of polyethylene from 3200 to 400 $cm^{-1}$ for illustration. (A) Dual-beam background with no sample in either beam; (B) Uncorrected dual-beam spectrum of polyethylene; (C) Result of subtracting A from B; (D) Single-beam background spectrum; (E) Result of dividing C by D, subtracting the resulting spectrum from unity, and multiplying by −1; (F) Transmittance spectrum of polyethylene measuring using a conventional single-beam FT-IR spectrometer. Comparison of E and F shows the result of poor phase correction for the sharp band at 720 $cm^{-1}$ but otherwise good photometric accuracy

**Practical Comparison of Sensitivity.** A direct comparison of the S/N advantage of the dual-beam system with an MCT detector over the conventional single-beam measurements with a TGS detector was made using a series of successively more dilute solutions of anisole in $CCl_4$ in a 90-$\mu$m fixed pathlength cell. A variable pathlength cell (Wilks Scientific Corp., S. Norwalk, Conn.), whose pathlength was adjusted to give the best optical null in the dual-beam configuration when the sample cell was filled with pure $CCl_4$, was placed in the reference beam.

The dual-beam measurement was made by subtracting the dual-beam background interferogram from the corresponding sample interferogram, and the single-beam transmittance measurement was made by ratioing the sample spectrum by the reference spectrum. All spectra were measured at 8 $cm^{-1}$ resolution, signal-averaged over 10 scans, and computed using double-precision (32 bits per word) software. The measured spectra are shown in Figure 4.

The S/N of the dual-beam system was a factor of 9 better than that of the single-beam system in the fingerprint region

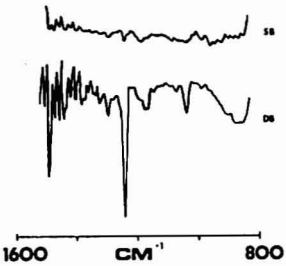


**Figure 4.** Direct comparison of a single-beam (SB) spectrum measured using a TGS detector and a dual-beam (DB) spectrum measured using an MCT detector. The sample is a 0.01% solution of anisole in $CCl_4$ in a 90-$\mu$m cell (with a reference cell of equal pathlength). The spectra were both measured at 8 $cm^{-1}$ resolution after averaging ten interferograms. The absorbance of the 1240 $cm^{-1}$ band is $1.7 \times 10^{-4}$

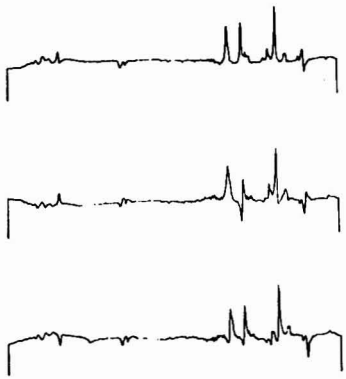

**Figure 5.** Three successive single-scan spectra from 3200–800 $cm^{-1}$ of a 0.1% solution of anisole in $CCl_4$ (90-$\mu$m pathlength) with a cell of equal thickness filled with pure $CCl_4$ in the reference beam, showing the difficulty in phase correction

of the spectrum. In the dual-beam spectra, the stronger bands of a 0.005% (v/v) solution could be easily identified and could still be seen at concentrations as low as 0.001%. With extensive signal-averaging, absorption bands from solutions containing less than 1 ppm of anisole in the 90-$\mu$m cell could be observed.

**Phase Errors.** When dual-beam interferograms were transformed, the effect of poor phase correction was often observed in the resulting spectra, especially for weakly absorbing samples. Improving the optical alignment occasionally improves the phase correction, but by no means completely solves the problem, since scan-to-scan variations in spectral baseline and band shapes were noticed even on a well aligned system, see Figure 5. This effect is apparently caused by a short-term optical instability, the source of which was very hard to track down.

Changes in band shapes were often noticed when the size of the short double-sided interferogram used in the Mertz method of phase correction (*10*) was increased. However, changing the number of points in the phase array rarely led to correct overall phase correction. It is well known that the Mertz method of phase correction works best for single-beam interferograms when $B(\nu)$ is non-zero at all wavenumbers, and does not give good results for the computation of discrete emission spectra (or FT-NMR spectra for which similar problems are found). The DB-FT-IR spectra are similar in

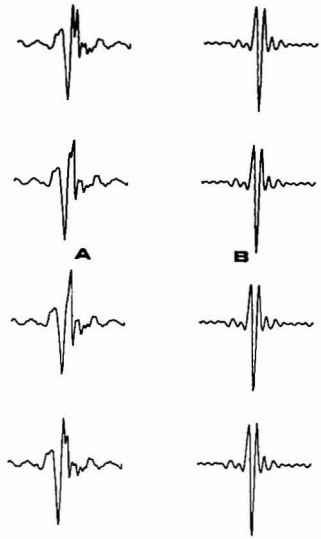


**Figure 6.** Four successive single-scan interferograms in the region of zero retardation, (A) measured dual-beam and (B) measured single-beam; both sets of data were measured using a TGS detector

appearance to emission spectra, but we believed that if a "good" stored phase spectrum could be computed using the dual-beam system with a spectrally uniform screen of high transmittance, this spectrum could be used for all subsequent calculations of discrete absorption spectra. Unfortunately, this approach also failed to yield satisfactory results, presumably due to the variations in $I(\delta)$ from scan to scan.

We finally discovered the cause of this short term instability was to be found in the interferometer itself. The largest intensity variations are near the point of stationary phase, see Figure 6, and since it is this region from which the phase information is extracted, it is easily seen why such poor phase correction is observed. When a new (1976) Digilab Model 396 interferometer was tested with our optical system, the scan-to-scan variations in the dual-beam interferograms disappeared almost completely. It is probable that this difference is caused by the new "fast break" mechanism installed in recent Digilab interferometers to increase their duty cycle efficiency at low resolution. On interferometers fitted with the fast break device, a steep ramp voltage across the drive transducer coil rapidly retards and stops the moving mirror at the end of its retrace; on older systems a foam rubber stop was used for this purpose. By eliminating the vibrations caused on impact with the rubber stop, the newer interferometers appear to be much more stable for dual-beam measurements.

**Linearity of the MCT Detector.** The measured increase in sensitivity of DB-FT-IR measurements made with an MCT detector compared with the corresponding single-beam or dual-beam measurements made with a TGS detector is less than the ratio of the published $D^*$ values of the two detectors. The probable reason for this effect is that the photoconductive MCT detector is driven towards saturation by the very high level of incident radiation from the source. To illustrate the magnitude of this effect, the peak intensity of the polyethylene band at 2875 $cm^{-1}$ measured in the dual-beam configuration was plotted against the percentage of the total radiation reflected from the paraboloidal mirror in the source unit and

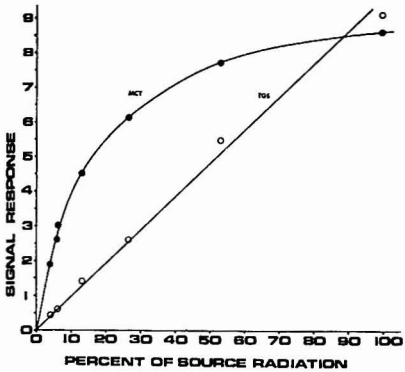


Figure 7. Maximum intensity of the 2875 $cm^{-1}$ polyethylene band measured using the dual-beam optics as a function of the percentage of the radiation from a modified Nernst glower source using the MCT detector (●) and TGS detector (○). The nonlinearity of the response of the MCT detector is evident. (The ordinate scale for the MCT detector is ten times larger than that for the TGS detector)

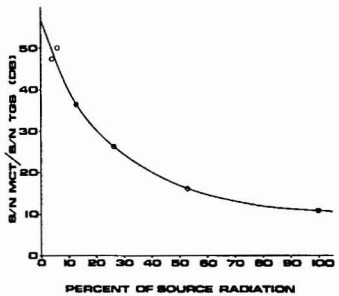


Figure 8. The relative S/N for the 2875 $cm^{-1}$ polyethylene band measured with the dual-beam optics using the MCT and TGS detectors, as a function of the percentage of the source radiation entering the interferometer

transmitted through calibrated wire mesh screens, see Figure 7. The resulting nonlinear plot suggests the approach of detector saturation. No spectroscopic evidence of nonlinearity (such as the presence of high frequency overtones of sharp bands) was observed. Very recently Borrello et al. (*11*) have reported that the $D^*$ of the MCT detector should vary approximately with the square root of the background flux above a certain threshold, and our results agree quantitatively with their calculations. Hirschfeld (*12*) has also suggested that part of the reduction in S/N at high photon flux is caused by the increase in photon shot noise. However the noise level measured at the detector with both beams incident was the same as the noise level with both beams blocked so that, for our system at least, the contribution of photon shot noise is negligible.

The linear region of the detector response is found at radiation levels below 5% of the maximum allowed throughput from the source, and it is at such low levels of radiation density that the MCT detector is most commonly used in single-beam systems. On the other hand, the TGS detector shows good linear response over the full range of radiation intensity from our source, see Figure 7. A plot of the ratio of the S/N of the 2875 $cm^{-1}$ polyethylene band measured using the MCT and the TGS detectors against the transmittance of the screens,

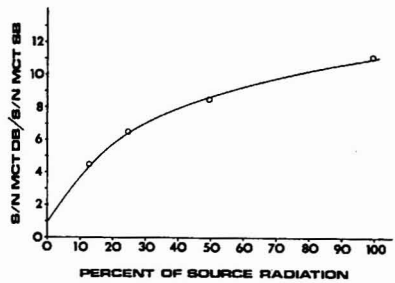


Figure 9. Calculated ratio of the relative S/N of the 2875-$cm^{-1}$ polyethylene band measured using an MCT detector in the dual-beam and single-beam configurations, as a function of the source radiation entering the interferometer

see Figure 8, reveals the sensitivity advantage of the MCT detector as a function of source intensity for our spectrometer. To obtain these measurements the TGS detector was also placed in the dual-beam optics, so that the only difference between the two sets of measurements was the detector.

At low incident energy it may be seen that our MCT detector is a factor of about 70 more sensitive than the TGS detector at 2875 $cm^{-1}$. However the advantage drops for the high source intensities which the dual-beam system was designed to measure. For most measurements of high incident source energies, the dual-beam technique affords an improvement in sensitivity of a little better than a factor of ten over the corresponding measurements made using a TGS detector.

Most commercially available FT-IR spectrometers using a TGS detector in the single-beam mode operate close to the digitization noise limit. Under these conditions a change to a more sensitive detector would result in little or no net gain in sensitivity. A plot of the calculated S/N advantage of the dual-beam system using an MCT detector over a single-beam system also using an MCT detector against the percentage of the maximum allowed energy from a typical infrared source is shown in Figure 9. It can be seen from this plot that the maximum advantage for the dual-beam system in this case is found when a high proportion of the source radiation is incident on the detector.

## CONCLUSION

The dual beam system offers about an order of magnitude gain in sensitivity over conventional single-beam FT-IR spectrometers. This approach is most useful where trace quantities of materials are to be identified under conditions where the sampling technique gives radiation losses of less than 90%. Thus the DB-FT-IR technique is readily applicable to the on-line identification of compounds separated by gas and high performance liquid chromatography. Our system was designed with such measurements in mind, and papers describing GC-IR and HPLC-IR measurements using the dual-beam approach are in preparation.

The problem of phase correction is apparently characteristic of our instrument as the newer interferometers do not exhibit this problem. The nonlinearity of the MCT detector response reduces the overall sensitivity of the technique. The solution to this problem is not apparent to us, and is the limiting factor in obtaining the maximum sensitivity from dual-beam FT-IR.

## LITERATURE CITED

(1) P. R. Griffiths unpublished work, 1975.
(2) P. R. Griffiths, "Chemical Infrared Fourier Transform Spectroscopy", Wiley-Interscience, New York, N.Y., 1975, Chap. 2.
(3) H. Mark and M. J. D. Low, *Appl. Spectrosc.*, **25**, 605 (1971).

(4) L. Mertz, "Transformations in Optics", John Wiley, New York, N.Y. 1965.
(5) H. Bar-Lev, *Infrared Phys.*, **7**, 93 (1967).
(6) M. J. D. Low, *Anal. Lett.*, **1**, 819 (1968).
(7) P. R. Griffiths, "Chemical Infrared Fourier Transform Spectroscopy", Wiley-Interscience, New York, N.Y., 1975, Chap. 7.
(8) M. J. D. Low and H. Mark, *J. Paint Technol.*, **43** (533), 31 (1971).
(9) P. R. Griffiths and J. O. Lephardt, paper presented at the 20th Pittsburgh Conference on Analytical Chemistry and Applied Spectroscopy, Cleveland, Ohio, 1969.
(10) L. Mertz, *Infrared Phys.*, **7**, 17 (1967).
(11) S. Borrello, M. Kinch, and D. LaMont, *Infrared Phys.*, **17**, 121 (1977).
(12) T. Hirschfeld, personal communication, 1977.

RECEIVED for review June 13, 1977. Accepted November 9, 1977. This work was supported by the U.S. Environmental Protection Agency under grant number R804333-01.

# On-Line Identification of Gas Chromatographic Effluents by Dual-Beam Fourier Transform Infrared Spectrometry

**Maria M. Gomez-Taylor and Peter R. Griffiths***

*Department of Chemistry, Ohio University, Athens, Ohio 45701*

**An infrared optical system was built around a commercial Fourier transform spectrometer primarily for the on-the-fly analysis of organic compounds eluting from a gas chromatograph. This system is based on the dual-beam or optical subtraction technique, whereby the dynamic range of the interferogram is reduced without decreasing the total energy flux reaching the detector. Therefore a more sensitive detector may be used without encountering digitization noise problems that occur when the signal-to-noise ratio of the interferogram exceeds the dynamic range of the analog-to-digital converter of the data system. The use of a mercury cadmium telluride photoconductive detector, a high temperature source and light-pipe gas-cells of high optical transmission contributed to the high sensitivity achieved by the system. Identifiable spectra of 100 ng or less of strong absorbers have been obtained with this dual-beam GC-IR system.**

One factor limiting the sensitivity of conventional infrared Fourier transform spectrometers is the dynamic range of the analog-to-digital converter (ADC). For example, the signal-to-noise ratio (S/N) of an interferogram of an unattenuated incandescent source generated by a rapid-scanning interferometer and measured with a pyroelectric bolometer can be as high as $10^4$:1, so that if the signal were digitized with a 15-bit ADC, the noise level would be less than two bits. If the S/N of the interferogram were much larger, the noise level would fall below the least significant bit of the ADC, and the noise level on the spectrum would be determined by the ADC (digitization noise) rather than by the detector (detector noise). In order to avoid inaccurate sampling of the interferogram, at least one bit should be used to sample detector noise. Under these circumstances, the full benefits of replacing the relatively insensitive triglycine sulfate (TGS) pyroelectric bolometer normally used for FT-IR spectrometers with the liquid nitrogen-cooled mercury cadmium telluride (MCT) photoconductive detector are not attained even though this detector is at least 20 times more sensitive than the TGS detector.

Several methods can be used to keep the S/N of the interferogram from exceeding the dynamic range of the ADC when the MCT detector is used for GC-IR measurements. The temperature of the infrared source could be reduced; however, the S/N of the spectrum would be significantly degraded at high frequencies. The dynamic range of the interferogram could be reduced by scanning the moving mirror faster. However to reduce the S/N of the interferogram by a factor of $X$, the velocity must be increased by a factor of $X^2$. As a result of this, the data rate may well be increased beyond the maximum allowed by the ADC or the disk-based data system. In addition, the duty cycle efficiency of the interferometer is usually lowered as the scan speed is increased. Azarraga (*1*) developed a technique to eliminate the dynamic range problem which involves the use of long and narrow light-pipes where reflection losses attenuate the signal across the complete spectrum. The decrease in sensitivity due to a smaller energy flux at the detector is partially compensated by the increase in the absorbing pathlength of the cell. However, Griffiths (*2*) recently made some calculations showing that the S/N gained using Azarraga's method with an MCT detector is only about a factor of four better than the optimum value obtainable using a TGS detector.

A technique that has been used to get around the dynamic range problem without decreasing the total energy flux reaching the detector involves dual-beam (DB) or optical subtraction FT-IR, the theory of which is discussed elsewhere (*3–5*). The dual-beam technique has been used in the past for gas analysis by several authors with limited success. Bar-Lev (*6*) described a dual-beam interference spectrometer incorporating one source, two detectors, and a long pathlength cell. This system was used for the detection of gases at low concentration. A nulling ratio (*7*) of 40:1 was attained with this system. Low (*8*) described an experimental arrangement designed for the infrared identification of GC effluents, which consisted of one detector and two sources. A nulling ratio of 30:1 was obtained with both gas cells at room temperature and the nulling ratio decreased to 20:1 after the cells were heated. Several years later, Low and Mark (*9*) described a system consisting of one source and two detectors, using which a nulling ratio of 100:1 was achieved. Griffiths and Lephardt (*10*) designed an arrangement using a single source and a single detector for the purpose of measuring the infrared spectra of GC peaks. They attained a nulling ratio of 100:1 even when the gas cells were hot. The main advantage of this system was that no pick-off mirrors were present in the beam path, thus increasing the optical throughput of the spectrometer. Surprisingly enough, the dual-beam technique has rarely been used under conditions when the single-beam spectrum would have been digitization noise limited (which is really the only time that this method is useful). As pointed out previously

0003-2700/78/0350-0422$01.00/0 © 1978 American Chemical Society

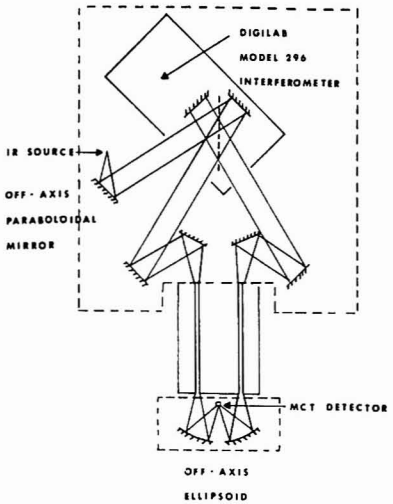


**Figure 1.** Optical layout of the dual-beam system for the on-line measurement of GC peaks

(5), the application of the DB-FT-IR technique should allow a definite improvement in the sensitivity of GC-IR measurements now that the sensitive MCT detector is readily available.

This paper describes a system designed around a Digilab Model FTS-14 Fourier Transform spectrometer for DB-FT-IR work using an MCT detector. The system has been applied to the on-the-fly measurement of infrared spectra of GC peaks. This system has both a high optical transmission and a high optical throughput and, consequently, a very high sensitivity should be achieved.

## EXPERIMENTAL

**Instrumentation.** The optical layout of the dual-beam GC-IR system is shown diagrammatically in Figure 1. The source is a modified Nernst glower (137 type from Perkin-Elmer Corp., Norwalk, Conn.). A 3-inch focal length 45° off axis paraboloidal mirror (Special Optics Corp., Little Falls, N.J.) was used to produce a beam of radiation 2 inches in diameter with a solid angle of $3.43 \times 10^{-3}$ steradians as input into a Model 296 interferometer (Digilab Inc., Cambridge, Mass.). The input beam to the interferometer is slightly skewed allowing both output beams to be collected by two plane mirrors which direct the radiation towards two off-axis paraboloids identical to the one mounted in the source unit. Each output beam is brought to a 3-mm diameter focus at the entrance to the light-pipes. Two light-pipes 30 cm in length and 4 mm × 4 mm in cross-section enclosed in an oven assembly (Norcon Instruments, Inc., S. Norwalk, Conn.) were used in this study. The two emerging beams from the light-pipes are focused onto a 2-mm square MCT detector (Texas Instruments, Dallas, Texas) by two off-axis ellipsoidal mirrors cut from a 12.5-inch diameter section with focal lengths of 4.3 and 10.3 inches (Special Optics Corp.).

**Chromatography.** The gas chromatography was performed using a Perkin-Elmer Model 3920 gas chromatograph equipped with a thermal conductivity detector. For observing sample quantities of less than 1 μg, a Gow-Mac Model 40-700 flame ionization detector (FID)/electrometer unit was adapted to the chromatograph. This detector was used in conjunction with an effluent stream splitter whose measured split ratio was about 14:1. The temperature of the transfer line between the chromatograph and the light-pipes was monitored in several places to ensure that no cold spots were present.

**Procedure.** Interferograms were signal-averaged during the time that each peak was present in the light-pipe, and interferograms from successive GC peaks were stored in sequential arrays in the data system of the FTS-14 spectrometer. A 100-scan optically subtracted reference interferogram of the empty cells was subtracted digitally from each sample interferogram and the subtracted interferogram was then transformed using double-precision software (32 bits per word) to give the infrared spectrum. All spectra were measured at 8 $cm^{-1}$ resolution.

## RESULTS AND DISCUSSION

The dual-beam system for GC-IR work achieved a nulling ratio of 15:1 when the light-pipes were heated. Even with this rather poor nulling, the reduction of the modulated signal of the interferometer was sufficient to reduce the S/N at zero path difference below the dynamic range of the ADC.

The different variables affecting the sensitivity of any GC-FT-IR system have been discussed in detail previously (*11*). These include the chromatographic conditions, the dimensions of the light-pipe gas-cell, the type of source, the type of detector, and the scan speed of the interferometer. The dual-beam FT-IR configuration for GC-IR measurements was designed with these variables taken into consideration. The improvement in sensitivity achieved by the system over an earlier GC-IR system based on the FTS-14 spectrometer (*12*) was derived from three main modifications: (1) the replacement of the nichrome wire source normally used with the FTS-14 spectrometer with a modified Nernst glower, (2) the installation of light-pipe gas-cells of dimensions 30 cm × 4 mm × 4 mm, and (3) the replacement of the standard TGS detector with an MCT detector.

The replacement of the nichrome wire source with a modified Nernst glower permits operation at higher temperatures, thus increasing the infrared energy reaching the detector especially in the fingerprint region, below 2000 $cm^{-1}$. It was found that the use of a Nernst glower source allowed spectra to be measured at about two to three times greater sensitivity than that attainable with the nichrome wire source in this region. The S/N advantage decreases at higher frequencies since above 2000 $cm^{-1}$ the emissivity of the Nernst glower falls off quite rapidly.

In order to obtain the maximum sensitivity in GC-IR, as much sample as possible should be present in the light-pipe during the measurement time. Griffiths (*13*) has made some theoretical calculations for the optimum dimensions of light-pipe gas-cells according to the chromatographic conditions and found that the optimum volume for a flow-through gas-cell is equal to the volume of the carrier gas between the half-width points of the GC peak. Sharp peaks are desired to obtain a greater S/N and the cell volume must be limited in order to avoid the possibility of having two different GC peaks in the cell simultaneously. The half-width of a *sharp* peak eluting from a gas chromatograph with a $^1/_8$-inch o.d. packed column is typically about 5 mL, so that the volume of the light-pipes used, 4.8 mL, is therefore very nearly ideal for GC-IR work utilizing packed columns. The pathlength and cross-sectional area for this cell are close to the optimum calculated dimensions, although the measured transmittance of the tubes (20–25%) was only about half of the calculated value (~50%).

An experimental comparison with respect to the relative sensitivities of the MCT and TGS detectors is complicated by the nonlinearity of the MCT detector response. Kuehl and Griffiths (*14*) have found that a high d.c. level of radiation on the MCT detector caused the sensitivity advantage of an MCT detector to be smaller than expected. At high radiation levels the detector is apparently driven to saturation which causes the nonlinearity in the observed response. As the energy reaching the detector is attenuated, the relative advantage of using an MCT detector over a TGS detector in-

**Table I. Experimental Detection Limits for a Group of Organic Compounds in the Dual-Beam System. The Experimental Detection Limits Obtained with a Single-Beam System Using Both a TGS and an MCT Detector Are Included for Comparison**

| | Detection limits, μg | | |
|---|---|---|---|
| | Single-beam | | |
| Compound | TGS | MCT | Dual-beam |
| Anisole | 0.8 | 0.20 | 0.050 |
| Chlorobenzene | 1 | 0.25 | 0.075 |
| Diethyl malonate | 2 | 0.45 | 0.100 |
| Acetonitrile | 5 | 1.5 | 0.400 |
| Benzonitrile | 10 | 2.5 | 0.750 |
| Aldrin | 5 | 1.5 | 0.400 |
| Perthane | 10 | 2.5 | 0.750 |
| *p,p'*-DDT | 6 | 1.5 | 0.400 |
| Heptachlor | 8 | 2.0 | 0.600 |

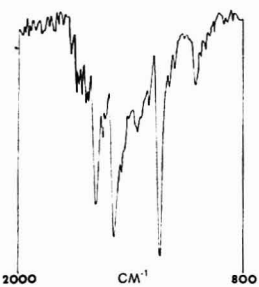


**Figure 2.** Ordinate expanded spectrum of 100 ng of anisole between 2000 and 800 $cm^{-1}$

creases and, at low radiation levels, the MCT detector response becomes linear. The S/N obtained with the dual-beam system for GC-IR measurements agrees well with the detector response calculations under conditions when the source signal is attenuated to 20–25%.

Tabel I shows the detection limits obtained for several organic compounds measured on-the-fly using the dual-beam GC-IR system. Some sensitivity results obtained with a single-beam GC-IR system designed in our laboratory using the same source, interferometer, and light-pipes are included for comparison. The replacement of the TGS detector with an MCT detector in the single-beam system led to an improvement in sensitivity of approximately a factor of four. The radiation from the source had to be attenuated somewhat to avoid digitization noise problems in this system. The dual-beam system gave an improvement in sensitivity of a factor of three compared to the single-beam system with identical optics. Consequently, this system is at least an order of magnitude more sensitive than the corresponding system utilizing a pyroelectric bolometer for infrared detection. Less than 100 ng of strong absorbers gave identifiable spectra for on-the-fly measurements with the dual-beam GC-IR system. Figure 2 shows a scale expanded spectrum of anisole obtained from 100 ng of injected sample between 2000 and 800 $cm^{-1}$. All the strong bands in this region are still apparent in the spectrum.

For all infrared measurements a dual-beam interferogram of the empty cells was subtracted digitally from the dual-beam sample interferogram to eliminate the residual background due both to the imperfect matching of the optics and to the presence of surface species on the beamsplitter. Figure 3 shows a spectrum of 100 ng of chlorobenzene between 2000 and 800 $cm^{-1}$ contrasting the effect of subtracting the sample


**Figure 3.** Ordinate expanded spectra of 100 ng chlorobenzene between 2000 and 800 $cm^{-1}$ (a) subtracting interferograms, (b) subtracting spectra

and reference interferograms before performing the FFT on the resultant interferogram and subtracting the spectra after performing the FFT on each individual interferogram. A fairly flat baseline was obtained when the interferograms were subtracted but a less flat baseline was obtained when spectra were subtracted. This result is the opposite of the result that was found for longer measurements using condensed phase samples, and is presumably related to the lack of repeatability of the dual-beam interferograms from scan to scan. It may be noted that the water vapor absorption is also better compensated when interferograms are subtracted, resulting in a slightly higher S/N between 1900 and 1300 $cm^{-1}$. The detrimental effects of uncompensated water vapor was one of the main problems during the measurements, although it may be noted that all results were found using an unpurged spectrometer.

It is possible that the width of the GC peaks may become broadened during the transit time from the GC column to the light-pipes. Such an effect would result in undesirable degradation of GC resolution. As a check on the amount of peak broadening in our system, cyclohexanone was injected into the chromatograph and the IR absorption profile was determined from the variation of the absorbance of the carbonyl stretching mode during consecutive scans; the IR absorption profile was then compared with the GC profile (see Figure 4). With a helium gas flow rate of 30 mL/min, the half-width of the GC peak was 10 s which corresponds to a peak volume of 5 mL, while the IR profile shows a half-width of approximately 14 s. Peak broadening due to the integration of the sample in the light-pipe will always occur, and it has been shown (*13*) that for a peak volume approximately equal to the light-pipe volume (as is the case here), the IR profile should be 1.5 times broader than the GC profile. These results therefore suggest that there is little peak diffusion occurring in the transfer line. The profile was also monitored by placing

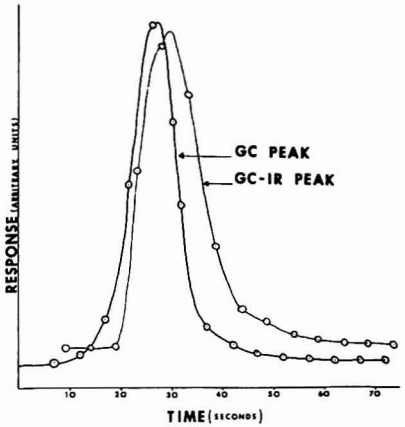


**Figure 4.** IR absorption profile vs. GC profile. Carrier flow rate: 30 mL/min

a flame ionization detector at the exit of the light-pipe. A peak broadening of about 25% was observed at this point but this value is relatively insignificant if the GC peaks are resolved in the chromatogram.

The feasibility of performing quantitative GC-IR analysis has also been investigated, using the chlorobenzene band located at 1080 $cm^{-1}$ (away from the water vapor region). Different amounts of chlorobenzene were injected on the chromatograph and the GC-IR spectra were measured on-the-fly. A plot of the S/N obtained for the 1080 $cm^{-1}$ band vs. the amount of injected sample is linear except at very low sample concentration indicating that the technique can be used for quantitative analysis. At very low concentrations the S/N observed is slightly less than that expected from the results at higher concentrations, which may indicate a small amount of error in the data collection timing due to the "hit-or-miss" nature of the measurements. This effect may also be due to sample loss somewhere in the system but we were unable to detect any cold spots between the detector and the light-pipes.

It is likely that the detection limits observed in these studies will be further reduced if the chromatographic conditions are optimized, for example through the use of support-coated open-tubular columns. It should also be noted that these measurements were taken on a three-year-old spectrometer and the performance of commercial FT-IR instrumentation has been improved over the past three years. If all chromatographic and spectroscopic parameters were optimized, it is very likely that the detection limits of GC-IR measurements will be reduced below 10 ng for strong absorbers.

## LITERATURE CITED

(1) L. V. Azarraga, paper presented at the 5th Annual Conference on the Analytical Chemistry of Pollutants, Jekyll Island, Ga., 1975.
(2) P. R. Griffiths, Chapter 10 in "Fourier Transform IR: Applications to Chemical Systems", J. R. Ferraro and L. J. Basile, Ed., Academic Press, New York, N.Y., in press, 1977.
(3) W. J. Burroughs and J. Chamberlain, *Infrared Phys.*, **11**, 1 (1971).
(4) J. O. Lephardt, Ph.D. Dissertation, University of Maryland, 1972.
(5) P. R. Griffiths, "Chemical Infrared Fourier Transform Spectroscopy", Wiley-Interscience, New York, N.Y., 1975, Chapter 7.
(6) H. Bar-Lev, *Infrared Phys.*, **7**, 93 (1967).
(7) P. R. Griffiths, Ref. 5, p. 175.
(8) M. J. D. Low, *Anal. Lett.*, **1**, 819 (1968).
(9) M. J. D. Low and H. Mark, *J. Paint Technol.*, **43** (No. 553), 31 (1971).
(10) P. R. Griffiths and J. O. Lephardt, paper presented at the Pittsburgh Conference on Analytical Chemistry and Applied Spectroscopy, 1969.
(11) P. R. Griffiths, Ref. 5, Chapter 10.
(12) K. L. Kizer, *Am. Lab.*, **5** (6), 40 (1973).
(13) P. R. Griffiths, *Appl. Spectrosc.*, **31**, 284 (1977).
(14) D. Kuehl and P. R. Griffiths, *Anal. Chem.*, this issue.

RECEIVED for review June 13, 1977. Accepted August 22, 1977. This work was supported by the U.S. Environmental Protection Agency under grant number R804333-01.

# Determination of Fluorine in Organic and Inorganic Pharmaceutical Compounds by High Resolution Nuclear Magnetic Resonance Spectrometry Interfaced with a Computer System

**Richard J. Warren,* A. Douglas Bender, David B. Staiger, and John E. Zarembo**

*Smith Kline & French Laboratories, 1500 Spring Garden Street, P.O. Box 7929, Philadelphia, Pennsylvania 19101*

**A commerical computer has been interfaced with a high resolution nuclear magnetic resonance spectrometer equipped with a fluorine accessory and has been used successfully to quantitatively determine the fluorine content of organic and inorganic compounds. Organically bonded fluorine may be determined by previous combustion or run directly without prior treatment. Inorganic compounds may be analyzed directly by dissolving them in appropriate solvents. We have demonstrated that after selecting appropriate tuning parameters, the integration of the nuclear magnetic resonance signal by the above-mentioned computer system is accurate and reproducible. The method can be used without signal enhancement techniques for samples containing approximately 5% fluorine by weight.**

On the past several years $^{19}F$ nuclear magnetic resonance spectrometry (NMR) has been used extensively in structural analysis and assignment of molecular configuration (*1–4*). There have also been reports of the use of $^{19}F$ NMR for quantitative analysis of certain functional groups and enantiomers (*5, 6*). These analyses have involved derivatization techniques followed by NMR analysis of the fluorinated products. This paper reports the direct quantitative analysis of fluorine-containing pharmaceuticals and pharmaceutical intermediates by an $^{19}F$ NMR interfaced with a computer. The method is rapid, accurate, and specific for fluorine. It has the added advantage of having no interferences from other ions. The method can be used without signal enhancement techniques for samples containing approximately 5% fluorine by weight and uses as little as 25 mg of sample.

## EXPERIMENTAL

**Apparatus.** All experiments were controlled and monitored via an interface of a Perkin-Elmer Model R32 90-MHZ spectrometer to an Electronics Associates Industries PACE III computer system.

**Reagents.** The trifluoroacetanilide used in this study was NBS material. The sodium fluoride was analytical grade material and used without further purification. The DMSO-$d_6$ was obtained from Merck & Co. The following standard samples were obtained in these laboratories and were shown by other methods to be of the highest purity: Bendroflumethiazide, Triflupromazine and Trifluoperazine.

**Procedure.** The fluorine-containing material, 25–50 mg, is weighed into a small vial. An accurate weight of trifluoroacetanilide is added and the combined sample is dissolved in approximately 0.8 mL of DMSO-$d_6$. The solution is then transferred to a standard 5-mm o.d. NMR tube. The fluorine spectrum is then obtained on a Perkin-Elmer Model R32 NMR spectrometer equipped with a fluorine accessory package operating at 84.6 MHZ. The $^{19}F$ spectrum is integrated five times. The integration ratio of sample to standard is obtained and the average of the five ratios is then used to calculate the amount of fluorine in the sample. The fluorine can be reported as milligrams per unit weight or milligrams per unit dosage form (tablet, ampule, etc.).

The same procedure with modifications is followed for inorganic samples. The most significant change is occasional use of a different internal standard. For most inorganics, sodium fluoride has been found to be satisfactory. In cases where TFAA can be used, this is the standard of choice.

Table I. Tuning Parameters for Computer System

| Parameter | Value/units | Function |
|---|---|---|
| Peak opening slope | 0.79 mV/min | Peak detection |
| Opening duration counter | 0.3 s | Peak detection |
| Filter time constant | 0.7 s | Signal smoothing noise rejection |
| Inflection point sensitivity | 0.1 + 5 mV/-min² | Shoulder detection |
| Inflection point duration counter | 19 s | Shoulder detection |
| Baseline slope drift | 1.0 mV/min | Allowance for baseline drift |

Table II. Computer Print-out of Fluorine Analysis by NMR

Analysis: 13 General Run

| Name | Time | Percent | Raw area |
|---|---|---|---|
| UNK NWN | 7 | .85481 | .1148E−2 |
| UNK NWN | 9 | .10772 | .1447E−3 |
| UNK NWN | 13 | 39.184 | .5266E−1 |
| UNK NWN | 28 | 00.000 | .0000E+0 |
| UNK NWN | 31 | .07931 | .1065E−3 |
| UNK NWN | 34 | .11035 | .1483E−3 |
| UNK NWM | 36 | .09236 | .1241E−3 |
| UNK NWM | 37 | .01120 | .1505E−4 |
| UNK NWN | 40 | .01760 | .2366E−4 |
| UNK NWN | 43 | .19726 | .2651E−3 |
| UNK NWN | 47 | .10389 | .1382E−3 |
| UNK NWN | 49 | .14922 | .2005E−3 |
| UNK NWN | 56 | 59.094 | .7942E−1 |

Sum .1344E+0
Stop Time 69

## RESULTS AND DISCUSSION

The NMR method as described is quite straightforward and depends on the integration of the $^{19}F$ signal from the sample relative to the integrated signal of a reference material added as an internal standard. For organically bound fluorine, we have found that trifluoroacetanilide (NBS material) is satisfactory. It is readily available, soluble in most NMR solvents, and gives a single NMR signal. The internal standard (TFAA) signal is found at 0.2 ppm upfield from trifluoracetic acid which is used as a zero reference for chemical shift assignments. The organic fluorine-containing samples studied by this method appeared at approximately 18 ppm downfield from trifluoroacetic acid.

0003-2700/78/0350-0426$01.00/0 © 1978 American Chemical Society

Table III. Results of Analysis of Fluorine-Containing Compounds by $^{19}F$ NMR

| Compound | % F, Theory | $^{19}F$ NMR method | | | |
|---|---|---|---|---|---|
| | | Computer integration | Δ | Recorder integration | Δ |
| Triflupromazine $C_{18}H_{19}N_2SF_3$ | 14.66 | 14.65 | 0.01 | 14.89 | 0.23 |
| Trifluoperazine $C_{21}H_{24}F_3N_3S \cdot 2HCl$ | 11.87 | 11.70 | 0.17 | 11.89 | 0.02 |
| Bendroflumethiazide $C_{15}H_{14}F_3N_3O_4S_2$ | 13.52 | 13.55 | 0.03 | 13.73 | 0.21 |

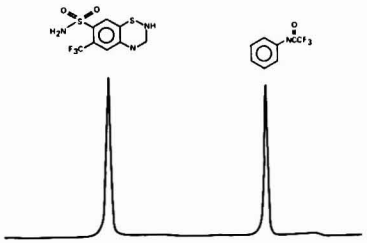

Figure 1. Typical spectrum of fluorine organic and internal standard

The PACE III computer system interfaced to the NMR was a computer system used for handling chromatographic data. One channel of the computer was reserved for NMR data processing. The PACE III is a fully programmed digital computer-based system designed to automate data acquisition, data reduction, interpretation, and report generation operations. An ASR Model teletype is the primary means of entering information into, and receiving messages and reports out of the system. The PACE III digital computer has 16384 words of core storage for instructions, standard data tables, and data input. The tuning parameters were calculated based on 150-mV recorder response for the P–E Model R32. Values for these parameters are given in Table I.

PACE III is connected directly into the output section of the NMR spectrometer. On the Perkin-Elmer R32 the connection is made at the auxiliary signal output. From this point, the computer system takes over the data processing functions all the way through to production of a complete sample report.

Certain computer parameters must be adjusted for a specific analysis such as fluorine or proton NMR. The parameter values vary from one type of analysis to another but once established they remain constant. The parameters which must be established for $^{19}F$ analyses are those involving peak shape, scan speed, recorder response in millivolts, and computer points.

Adjustments are made so that the peaks are Gaussian and de-tuned to eliminate ringing—if not the computer will read each of the sharp, ringing peaks as individual signals.

Spectra are phased and baseline drift is corrected for prior to integration. Note that once these adjustments are made for the first sample, subsequent analysis of the same kind (same sample and solvent) requires no adjustments or very minor adustments at most. Our observation has been that analogue integration of a detuned signal is as reliable as a well tuned signal providing sweep rate is sufficient to prevent saturation.

The scan speed must be optimized. If the speed is too slow, saturation results; if too fast, there will be computer integration of an insufficient number of points.

Figures 1 and 2 show the typical NMR spectra of organic and inorganic fluorine-containing compounds. A typical print-out from the computer using a general run (area normalization) is shown in Table II. The sample appeared 13

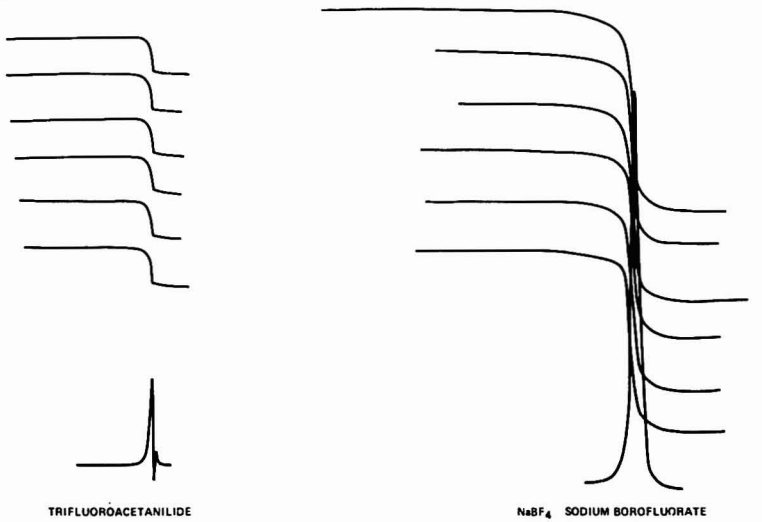


Figure 2. Analysis of inorganic F compounds by $^{19}F$ NMR

seconds into the run and the internal standard is shown at 56 seconds. Both the raw areas of the signals and the percents (normalized) are given.

Table III shows the results of analyses obtained by the computer method and compares these with results obtained by recorder integration and hand calculation. The computer system is able to read weaker signals more accurately and, of course, has the added advantage of rapid calculations for repetitive samples.

The procedure for analysis of dosage forms is as follows. Grind a tablet or contents of a spansule in a mortar and pestle. Slurry with DMSO-$d_6$. Add an accurately weighed quantity of internal standard, mix, and transfer to a small vial. Centrifuge, draw off the supernatant with a Pasteur pipet, and filter through a cotton plug into an NMR tube. Obtain the NMR spectrum and integrate the spectrum five times. Average the five integrations and calculate the fluorine content.

The advantage of speed, accuracy, the nondestructive nature of the method, and the absence of common interferences such as phosphorous, halogens, and certain metallic impurities, all recommended this method.

## LITERATURE CITED

(1) F. L. Ho, *Anal. Chem.*, **45**, 603–605 (1973).
(2) F. L. Ho and R. R. Kohler, *Anal. Chem.*, **46**, 1302–1304 (1974).
(3) "High Resolution Nuclear Magnetic Resonance Spectroscopy", Vol. 2, Emsley, Feeney, and Sutcliffe, Pergamon Press, Elmsford, N.Y., 1966.
(4) "An Introduction to $^{19}$F NMR Spectroscopy", E. F. Mooney, Heyden/Sadtler, London, 1970.
(5) K. Konishi, Y. Mori, and N. Taniguchi, *Analyst (London)*, **94**, 1002–1005 (1969).
(6) Ref. 5, pp 1006–1009.

RECEIVED for review August 25, 1977. Accepted December 12, 1977. Presented in part at the 29th Pittsburgh Conference on Analytical Chemistry and Applied Spectroscopy, Cleveland, Ohio, March 1977.

# Curie-Point Pyrolysis and Field Ionization Mass Spectrometry of Polysaccharides

**H.-R. Schulten* and W. Görtz**

*Institut für Physikalische Chemie, Universität Bonn, Wegelerstr. 12, 5300 Bonn, West Germany*

**A technique for controlled thermal degradation of technical and biological polymers by Curie-point pyrolysis *inside* the mass spectrometer and the analysis of the pyrolysis products by field ionization mass spectrometry is introduced. Integrated ion recording by photographic detection gave reproducible fingerprints of the macromolecular substances. High resolution and accurate mass measurements revealed that the spectra contained almost exclusively molecular ions of the pyrolysis products, which could be correlated with chemical species found in previous chemical and pyrolytic studies. The method appears as an useful tool for differentiation, characterization, and identification of micrograms of biopolymers and contributes to a better understanding of the mechanisms in the pyrolysis of macromolecules.**

Pyrolysis techniques, in combination with gas chromatography (GC), mass spectrometry (MS), or gas chromatography combined with mass spectrometry (GC-MS), have been used extensively to identify synthetic polymers (*1–6*) and complex biological material (*7–9*). Using these techniques, high molecular weight materials have been characterized by their typical pyrograms or by specific pyrolysis products which could be correlated with their chemical structures. Polymeric substances analyzed include proteins (*10*), nucleic acids (*11–13*), lignins (*14, 15*), and in addition complex organic matter such as humic acids (*16, 17*), and even whole bacteria or microorganisms (*18–23*).

The thermal degradation of polysaccharides has been investigated thoroughly by GC (*24, 25*), other chromatographic techniques (*26, 27*) and GC-MS (*28*). However, to date only a few studies on direct vacuum pyrolysis of these biopolymers in combination with the mass spectrometric analysis of the pyrolysis products have been reported (*29, 30*). This fact and the improvements in the techniques for pyrolysis as well as in mass spectrometry prompted our study in this field. In particular, the development of Curie-point pyrolysis (*31, 32*) using rapid heating rates (>1 °C/ms), reproducible time/temperature profiles, and small sample amounts appeared promising for studies in conjunction with the mass spectrometer. In order to identify individual chemical species in the complex mixtures produced in the pyrolysis of biological material, it is desirable to reduce the ionization-induced fragmentation in the mass spectrometer as far as possible. Therefore, once a reproducible and significant pyrolytic fragmentation has been obtained, the use of MS with low voltage electron impact (EI) ionization (*33*) or better by mild ionization modes such as chemical ionization (CI) (*34*), field ionization (FI) (*35*), and field desorption (FD) (*36, 37*), is advantageous.

It is the purpose of this paper to report the first pyrolysis MS experiments involving vacuum Curie-point pyrolysis in the ion source of a high resolution FI mass spectrometer in order to explore the potential of this combination for the differentiation, characterization, and identification of small amounts of biopolymers and for the elucidation of the chemical composition and structure of the pyrolysis products of biological material.

## METHODS

**Field Ionization Mass Spectrometry.** The FI mass spectra were produced on a modified CEC 21-110B instrument (*38*), using the photographic detection system with Ilford Q2 plates. The resolution obtained was better than 10 000 (at half peak width), and the average accuracy in the mass determination was ±2.5 mmu for all peaks. For accurate mass measurements (in the text the theoretical masses are given), reference masses were taken from the FI mass spectrum of perfluorotributylamine. The emitters used in all experiments were prepared by high temperature

0003-2700/78/0350-0428$01.00/0 © 1978 American Chemical Society

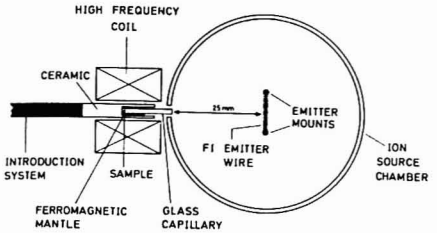


**Figure 1.** Schematic drawing of the instrumental setup for Curie-point pyrolysis in combination with field ionization mass spectrometry. The pyrolyzer and the FI ion source chamber are mounted in the source-housing of the CEC 21-110B mass spectrometer

activation of 7-$\mu$m diameter tungsten wires (*39, 40*). The distribution and morphology of the carbon microneedles was different from those of the usually employed field desorption anodes (*39*). The typical FI emitter was a tungsten wire with small-toothed needles (like a fine comb) having an average length of 3 to 5 $\mu$m. As standards we used emitters which gave a total emission of $3 \times 10^{-7}$ A and a signal for the molecular ion ($m/e$ 58) of 2 V (amplification factor of the multiplier $1 \times 10^6$; output resistance of the multiplier $10^8$ Ω; ion source and emitter temperature ~50 °C) when checked using acetone at a source pressure of $5 \times 10^{-4}$ Torr.

**Curie-Point Pyrolysis.** The pyrolysis mass spectrometry system shown schematically in Figure 1 was designed in our laboratory. Basically, this system consists of a special Curie-point pyrolysis inlet with a high frequency coil (Fischer, Labortechnik 1.5 kW, 1-MHz hf power supply) fixed close to the FI ion source. The sample is transferred in a glass capillary into the source housing via the conventional direct introduction system of the mass spectrometer (vacuum lock). The capillary is mounted exactly in the center of a cylinder of ferromagnetic metal which is adjusted in the middle of the high frequency coil by the introduction rod. When the high frequency pulse is applied (usually between 2 and 4 s), the metal mantle reaches its Curie-point (change from ferromagnetism to paramagnetism) within a fraction of a second and keeps a precise temperature specific to the metal used, e.g., for iron 770 °C, nickel 358 °C, cobalt 1128 °C. The sample is pyrolyzed almost simultaneously and the products diffuse into the high vacuum of the ion source chamber (glass cylinder) and are field-ionized.

**Curie-Point Pyrolysis in Combination with High Resolution FI Mass Spectrometry.** D(+)-Glycogen (MW 270 000 to 3 500 000, Fluka AG., Buchs, Switzerland) and a series of dextrans with MW between 32 000 and 40 000 000 (Serva, Heidelberg, West Germany) were pyrolyzed at the Curie-point of a cylindric iron mantle (Figure 1). The ionization (and exposure) time of the pyrolysates was regulated with an automated emitter heating device (*41, 42*). The time program for the emitter heating current and the observed total emission measured between the field anode and the slotted cathode plate at 2-mm distance and at +10/−2 kV accelerating voltage are shown in Figure 2. Before the start of the pyrolysis pulse, a background emission of about $5 \times 10^{-9}$ A was observed due to ionization of residual gas ($5 \times 10^{-7}$ Torr) in the ion source chamber (a). As depicted, pyrolysis starts at (b) and gives momentarily an intense ion current which drops after about 10 s. At this point (c), the emitter heating programmer raises the heating current (dashed line in Figure 3) linearly from 0 to 10 mA and is subsequently turned off. During this procedure, those products are desorbed which have been adsorbed onto the emitter surface after pyrolysis of the polymeric material. This field desorption is clearly indicated by a slight rise in the total emission (d) and contributes to the detection of substances of lower volatility which survived for the time required to travel between the place of pyrolysis and the emitter. Figure 2 shows that the total emission due to FI of the gaseous pyrolysis products by the cleaned, low temperature surface of the emitter is at first enhanced, but within 5 min falls close to the value observed at the beginning (a), although a second heating interval was applied after 4 min. Prior to the evaluation of the high resolution data from the photoplate, the characteristic profiles of the heating current and total emission gave an indication of the thermostability and thus the best pyrolysis temperature of the material under investigation.

The time consumed for one analysis is approximately 10 min for sample loading, probe introduction, pyrolysis, and recording of the FI mass spectrum. However, processing of the photoplate and data acquisition (up to 32 spectra are stored) takes a few hours. Obviously the main obstacles to making the proposed technique available for routine work are the considerable costs of the Herzog–Mauttauch geometry instrument, the data system, and the necessary comparator.

## RESULTS AND DISCUSSION

Figure 3 shows the FI mass spectrum of the thermal degradation products of glycogen, a branched polymer of amylose chains joined through $\alpha$ 1 → 6 links. When Curie-point pyrolysis was performed in the ion source of the mass spectrometer (Figure 2), the photographically recorded mass spectrum gives a fingerprint for this polysaccharide. Repeated measurements under the same experimental conditions revealed that the characteristic pattern of the pyrolysis products is reproducible and allows the recognition of the biopolymer.

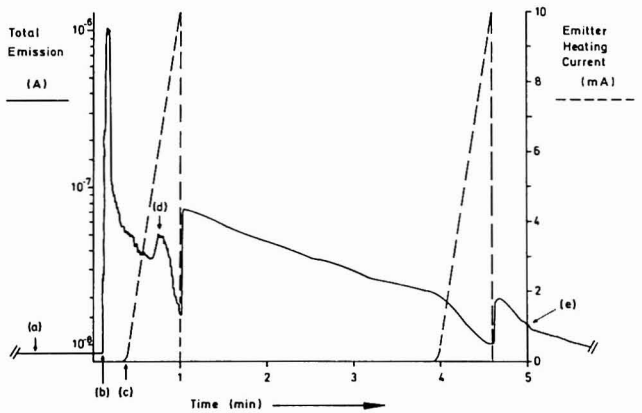


**Figure 2.** Total emission (solid line) and emitter heating current (dashed line) plotted vs. the time used for the pyrolysis of the glycogen sample (see FI spectrum in Figure 3)

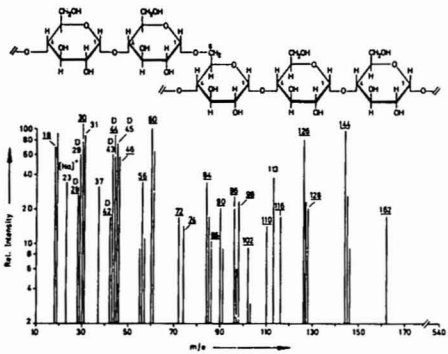

**Figure 3.** FI mass spectrum of the pyrolysis products of Curie-point pyrolysis of glycogen (pyrolysis program in Figure 2)

Reproducibility here means that qualitatively the same ionized products are always found and that the pattern of the signal intensities differed significantly from that of other polysaccharides. The variation in the relative intensities of the ions for repetitive pyrolysis was about ±5% for peaks between 10 and 80% logarithmic blackening. However, in view of the considerable inner variance of the technique due to the field ionization process itself and the recording system used, the advantage of Curie-point pyrolysis/FI-MS is not its reproducibility. Clearly, the differences in the quality of the photographic emulsion, the developing procedure, and the small dynamic range of the photoplate for the recording of large, organic ions contribute intrinsically to the deviations in the signal intensities. In this respect, the method for fingerprinting of polymers and micro-organisms described by Meuzelaar and co-workers (*33*), using Curie-point pyrolysis in combination with electron impact ionization in a low resolution quadrupole mass spectrometer and registration of the spectra in a time averaging computer is superior. But as far as specificity of the pyrolysis data, that is the production and identification of primary, thermal degradation products is concerned, the results of this high resolution FI investigation make our method attractive for the following reasons.

1. The soft ionization mode produces almost exclusively molecular ions and thus *mass spectrometric fragmentation* does not obscure the recognition of the chemical substances in the complex mixture which is created in the rapid thermal degradation of a macromolecule.

2. The resolving power achieved enables accurate mass measurements and gives a reliable indication of the elemental composition of the individual chemical species.

3. As described in the Methods part (see Figure 1), in this first approach to performing Curie-point pyrolysis in the ion source of the mass spectrometer, the distance between the places of pyrolysis and ionization was considerably smaller than the free pathway of the pyrolysis products after release from the direct pyrolysis zone. Therefore intermolecular and wall collisions are strongly reduced and the escaping products should enable a direct correlation with the structure of the macromolecule investigated.

4. Even the strongly fluctuating currents of a wide variety of different ions generated in the pyrolysis pulse are registered by integration and simultaneously as the photoplate is employed as a recording device.

Indeed, as may be inferred from Table I for the peaks shown in Figure 3, an elemental composition was found and a chemical structure for these pyrolysis products was tentatively assigned. With the exception of $m/e$ 146, 144, 116, 102, and

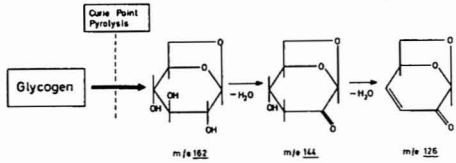


**Figure 4.** Proposed pathway for the formation of the larger pyrolysis products (> $m/e$ 100), e.g. levoglucosenone by dehydration of levoglucosan

84 all substances listed in this table have been identified previously in other pyrolysis experiments of carbohydrates. Since only pyrolysis products with a maximal number of six carbon atoms were observed, it was assumed that splitting of the polymer into monomer subunits followed the mechanisms suggested by Shafizadeh et al. (*43*) for other 1 → 4 linked polysaccharides such as cellulose. In order to explain the formation of the observed ions and in order to correlate their occurrence with the structure of the biopolymer, three basic chemical reaction mechanisms were employed. Dehydration, retroaldolization, and decarbonylation were taken to be the essential processes for generating the smaller pyrolysis products, in particular after the cleavage of the polymer into $C_6$ subunits.

In vacuum pyrolysis of 1,4 linked polysaccharides, one of the main products is 1,6-anhydro-β-D-glucopyranoside (levoglucosan) (*26*). The formation of levoglucosan as a primary product of the thermal fragmentation explains the appearance of $m/e$ 162 in the FI spectrum of glycogen (Figure 3). Levoglucosan, which is thought to be a key compound for further pyrolysis reactions in the thermal degradation of cellulose (*26, 43, 44*) can yield products that contribute to the ions at $m/e$ 144 and $m/e$ 126 by dehydration as depicted in Figure 4. One possible structure for the ion at $m/e$ 126 is 1,6-anhydro-3,4-dideoxy-β-D-glycero-hex-3-enopyranos-2-ulose (levoglucosenone) which was found by other authors in acid-catalized pyrolysis of cellulose and related carbohydrates (*45, 46*). In addition, this compound was identified by Ohnishi et al. as the prevailing volatile product in Curie-point pyrolysis-GC investigations of cellulose (*47*). A probable structure for the pyrolysis product which gives a prominent ion at $m/e$ 144 in FI-MS is proposed in Figure 4. This compound, 1,6-anhydro-3-deoxy-β-D-threo-hexopyranos-2-ulose was not found previously, but appears to be a reasonable intermediate in the reaction pathway involving water elimination.

At present, an assignment of a certain structure to the ions at $m/e$ 146, 116, and 113 on the basis of the high resolution data alone is difficult and requires the analysis by other techniques such as collisional activation MS (*48*).

As may be inferred from Figure 5, the formation of the smaller thermal degradation products of the polymer originates from the proposed $C_6$ subunit and follows the three dominant pyrolysis mechanisms: dehydration, retroaldolization, and decarbonylation. Moreover, this pyrolysis pattern is strongly supported by the thorough investigations of the substances generated by thermal decomposition of levoglucosan (*44*) which is thought to be a principal and important intermediate in the pyrolysis of 1 → 4 linked polysaccharides (*26*). Furthermore, the pyrolysis products of glycogen which are represented by the FI ions at $m/e$ 102.031 ($C_4H_6O_3$) and $m/e$ 84.020 ($C_4H_4O_2$) can be explained by dehydration of erythrose and fit into the pyrolysis pathway of glycogen described in Figure 5.

Under the same experimental conditions, other polysaccharides give a different pattern of pyrolysis products. For instance, a dextran with a molecular weight of 2 000 000 shows

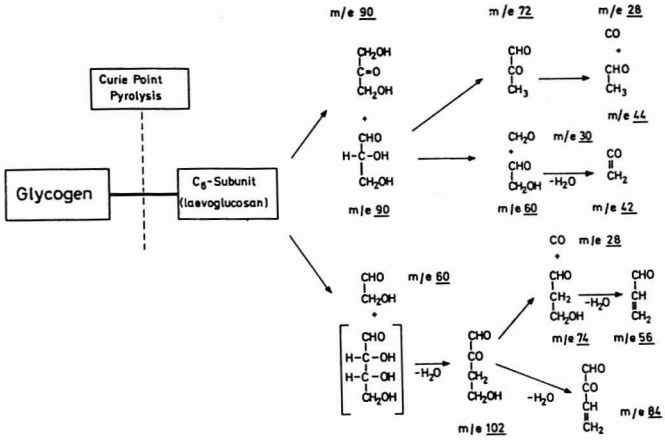


**Figure 5.** Rationalization of the origin of the smaller pyrolysis products (< *m/e* 100) by dehydration, retroaldolization, and decarbonylation. One intermediate, erythrose (in brackets) was not found in the FI mass spectrum because of its lower volatility. However, this compound was identified in other pyrolysis studies of carbohydrates (*44*). Furthermore, an ion at *m/e* 120.042 ($C_4H_8O_4$) was found in the field desorption pyrolysis of glycogen (*29*) and recently by FD-MS in extracts of pyrolysis residues in glass capillaries after Curie-point pyrolysis of glycogen

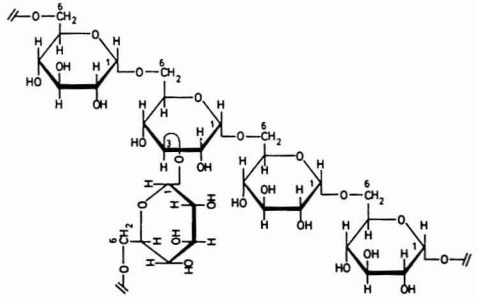

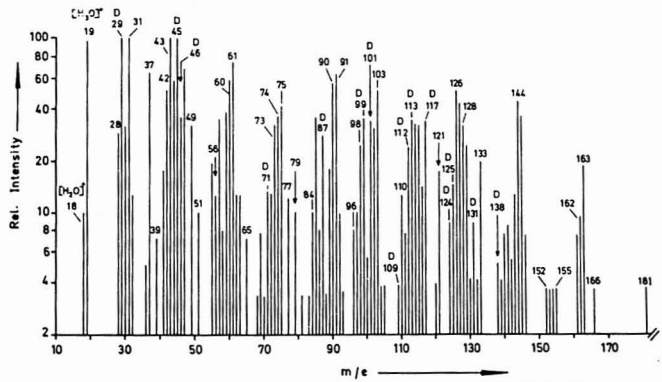


**Figure 6.** FI mass spectrum of the pyrolysis products of Curie-point pyrolysis of a dextran (MW 2 000 000)

a spectrum (Figure 6) which can be distinguished from the Curie-point FI mass spectra of glycogen by three general facts. First, this polysaccharide yields more gaseous pyrolysis products (and a higher total emission) under the same experimental conditions. Second, proton transfer reactions are more pronounced as may be inferred from the intensities of the signals at *m/e* 18/19; *m/e* 60/61; *m/e* 90/91 for example. Third, accurate mass measurements reveal intense FI ions in

Table I. High Resolution Data and Proposed Chemical Identity of the Observed Molecular Ions in the Curie-Point Pyrolysis/Field Ionization Mass Spectrum of Glycogen

| Theoretical mass | Error, mmu | Probable elemental composition | Ion type | Proposed compounds |
|---|---|---|---|---|
| 18.011 | +2 | $H_2O$ | M | Water |
| 19.018 | 0 | $H_3O$ | M + 1 | |
| 22.989 | −2 | Na | | Sodium[a] |
| 27.997 | +3 | CO | M | Carbon monoxide |
| 28.031 | −3 | $C_2H_4$ | M | Ethene (*28*) |
| 29.003 | +4 | CHO | f | |
| 29.039 | +2 | $C_2H_5$ | f | |
| 30.011 | −4 | $CH_2O$ | M | Formaldehyde (*25, 26*) |
| 31.018 | −2 | $CH_3O$ | M + 1 | |
| 37.029 | −2 | $H_4O_2$ | | |
| 42.010 | +3 | $C_2H_2O$ | M | Ketene (*26*) |
| 42.047 | +2 | $C_3H_6$ | M | Propene (*28*) |
| 43.018 | +4 | $C_2H_3O$ | M + 1 | |
| 43.055 | −2 | $C_3H_7$ | f | |
| 43.990 | −4 | $CO_2$ | M | Carbon dioxide |
| 44.026 | −3 | $C_2H_4O$ | M | Acetaldehyde (*25, 26, 28, 44*) |
| 44.997 | +4 | $CHO_2$ | f | |
| 45.034 | 0 | $C_2H_5O$ | M + 1 | |
| 46.005 | 0 | $CH_2O_2$ | M | Formic acid (*26*) |
| 55.018 | +3 | $C_3H_3O$ | f | |
| 56.026 | −5 | $C_3H_4O$ | M | Acrolein (*25, 28, 44*) |
| 57.070 | −3 | $C_4H_7$ | f | |
| 60.021 | +2 | $C_2H_4O_2$ | M | Hydroxyacetaldehyde (*26, 43, 49*) |
| 61.029 | −2 | $C_2H_5O_2$ | M + 1 | |
| 72.021 | 0 | $C_3H_4O_2$ | M | Pyruvaldehyde (*26, 43, 44*) |
| 74.036 | −1 | $C_3H_6O_2$ | M | Hydroxypropanone (*26, 43, 44*) |
| 84.021 | +4 | $C_4H_4O_2$ | M | *b* |
| 85.029 | −2 | $C_4H_5O_2$ | M + 1 | |
| 86.037 | −4 | $C_4H_6O_2$ | M | 2,3-Butanedione (*26, 28, 43, 44*) |
| 90.032 | −2 | $C_3H_6O_3$ | M | Glyceraldehyde (*26, 43, 49*)<br>Dihydroxypropane (*49*) |
| 91.040 | 0 | $C_3H_7O_3$ | M + 1 | |
| 96.021 | +3 | $C_5H_4O_2$ | M | 2-Furaldehyde (*25, 26, 43, 44, 46, 47*) |
| 97.029 | +2 | $C_5H_5O_2$ | M + 1 | |
| 98.036 | 0 | $C_5H_6O_2$ | M | Furfurylalcohol (*28*)<br>1,5-Anhydro-2,3-dideoxy-β-D-(pent-2-enofuranose (*45,46*) |
| 102.032 | −1 | $C_4H_6O_3$ | M | *b* |
| 103.040 | +3 | $C_4H_7O_3$ | M + 1 | |
| 110.037 | +3 | $C_6H_6O_2$ | M | 5-Methyl-2-furaldehyde (*26, 28*) |
| 113.024 | −1 | $C_5H_5O_3$ | M + 1 | *b* |
| 116.047 | −1 | $C_5H_8O_3$ | M | |
| 126.032 | −3 | $C_6H_6O_3$ | M | Levoglucosenone (*45-47*)<br>5-Hydroxymethyl-2-furaldehyde (*26, 43, 44, 46, 47, 49*) |
| 127.039 | −4 | $C_6H_7O_3$ | M + 1 | |
| 128.047 | −2 | $C_6H_8O_3$ | M | 1,6-Anhydro-3-deoxy-β-D-threo-hex-3-enopyranose (*47,*) |
| 144.042 | +2 | $C_6H_8O_4$ | M | *b* |
| 145.050 | +3 | $C_6H_9O_4$ | M + 1 | |
| 146.058 | −2 | $C_6H_{10}O_4$ | M | *b* |
| 162.052 | −3 | $C_6H_{10}O_5$ | M | Levoglucosan (*26, 43, 49*)<br>1,6-Anhydro-β-D-glucofuranose (*43, 49, 50*) |

[a] Impurity. [b] Molecular ion or protonated molecules not previously found.

the higher mass range which contain more than six carbon atoms (see Figure 6).

## CONCLUSION

The results described above clearly demonstrate three basic features of the Curie-point pyrolysis FI-MS combination. First, large primary products are generated, predominantly by *thermal* cleavage of the macromolecule. Second, the analytical procedure to identify these substances involves high resolution and accurate mass measurements. Third, as consecutive *mass spectrometric* fragmentation does not obscure the spectral lines due to the thermal fragmentation and an elemental composition of the molecular ions can be assigned, a direct correlation between the pyrolysis products and the structure of the polymer can be established.

The main reasons for the potential of this technique are: High vacuum pyrolysis, the short distance between the position of pyrolysis and of ionization, and a soft ionization mode. FI is a particularly suitable mode because of the small electronic excitation energy transferred in the ionization process (only a few tenth of an electron volt) and due to the fact that ionization at the emitter surface offers the possibility of energy relaxation of the thermally excited pyrolysis products.

## ACKNOWLEDGMENT

The authors are grateful to O. Chizhov, Zelinsky Institute, Moscow, U.S.S.R., for helpful discussions and critical comments.

## LITERATURE CITED

(1) W. H. T. Davison, S. Slaney, and A. L. Wragg, *Chem. Ind. (London)*, 1356 (1954).
(2) M. T. Jackson and J. Q. Walker, *Anal. Chem.*, **43**, 74 (1971).
(3) A. Zeman, *Angew. Makromol. Chem.*, **31**, 1 (1973).
(4) D. O. Hummel, in "Analytical Pyrolysis", C. E. Roland-Jones and C. A. Cramers, Ed., Elsevier, Amsterdam, 1977, pp 117 ff.
(5) I. Lüderwald and Urrutia, in "Analytical Pyrolysis", C. E. Roland Jones and C. A. Cramers, Ed., Elsevier, Amsterdam, 1977, pp 139 ff.
(6) H. D. Beckey and H.-R. Schulten, in "Applied Spectroscopy Series", C. McEwen and C. Merritt, Ed., Marcel Dekker, New York, N.Y., in press.
(7) J. Janak, *Collect. Czech. Chem. Commun.*, **25**, 1780 (1960).
(8) E. Reiner, *Nature (London)*, **206**, 1272 (1965).
(9) H. L. C. Meuzelaar, P. G. Kistemaker, and M. A. Posthumus, *Biomed. Mass Spectrom.*, **1**, 312 (1974).
(10) P. D. Zemany, *Anal. Chem.*, **24**, 1709 (1952).
(11) H.-R. Schulten, H. D. Beckey, A. J. H. Boerboom, and H. L. C. Meuzelaar, *Anal. Chem.*, **45**, 2358 (1973).
(12) H.-R. Schulten and H. D. Beckey, *Adv. Mass Spectrom.*, **6**, 499–507 (1974).
(13) M. A. Posthumus, N. N. M. Nibbering, A. J. H. Boerboom, and H.-R. Schulten, *Biomed. Mass Spectrom.* **1**, 352 (1974).
(14) E. Stahl, F. Karig, U. Brögmann, H. Nimz, and H. Becker, *Holzforschung*, **27**, 89 (1973).
(15) L. Stieglitz and W. Leger, *Vom Wasser*, **45**, 233 (1975).
(16) B. R. Nagar, E. S. Waight, H. L. C. Meuzelaar, and P. G. Kistemaker, *Plant Soil*, **43**, 681 (1975).
(17) H. L. C. Meuzelaar, K. Halder, B. R. Nagar, and J. P. Martin, *Geoderma*, **17**, 239 (1977).
(18) E. Reiner, (1967) *J. Gas Chromatogr.*, **5**, 65 (1967).
(19) P. G. Simmonds, *Appl. Microbiol.*, **20**, 567 (1970).
(20) H. L. C. Meuzelaar and R. A. In't Veld, *J. Chromatogr. Sci.*, **10**, 213 (1972).
(21) H.-R. Schulten, H. D. Beckey, H. L. C. Meuzelaar, and A. J. H. Boerboom, *Anal. Chem.*, **45**, 191 (1973).
(22) H. L. C. Meuzelaar and P. G. Kistemaker, *Anal. Chem.*, **45**, 587 (1973).
(23) J. P. Anhalt and C. Fenselau, *Anal. Chem.*, **47**, 219 (1975).
(24) D. J. Bryce and C. T. Greenwood, *Staerke*, **15**, 285 (1963).
(25) S. Glassner and A. R. Pierce, *Anal. Chem.*, **37**, 525 (1965).
(26) F. Shafizadeh, *Adv. Carbohydr. Chem.*, **23**, 417 (1968).
(27) E. Stahl and T. Herting, *Chromatographia*, **7**, 637 (1974).
(28) K. Heyns and M. Klier, *Carbohydr. Res.*, **6**, 436 (1968).
(29) H.-R. Schulten, in "New Approaches to the Identification of Microorganisms", C. G. Heden and T. Illeni, Ed., John Wiley & Sons, New York, N.Y., 1975, Part A, pp 155–164.
(30) H.-R. Schulten, in "Analytical Pyrolysis", C. E. Roland-Jones and C. A. Cramers, Ed., Elsevier, Amsterdam, 1977 pp 17 ff.
(31) J. Voellmin, P. Kriemler, I. Omura, J. Seibl, and W. Simon, *Microchem. J.*, **11**, 73 (1966).
(32) C. Bühler and W. Simon, *J. Chromatogr. Sci.*, **8**, 323 (1970).
(33) H. L. C. Meuzelaar, M. A. Posthumus, P. G. Kistemaker, and J. Kistemaker, *Anal. Chem.*, **45**, 1546 (1973).
(34) G. W. A. Milne and M. J. Lacey *Crit. Rev. Anal. Chem.*, **5**, 45 (1974).
(35) H. D. Beckey, (in "Field Ionization Mass Spectrometry", Pergamon Press, Oxford, 1971); in "Principles of Field Ionization and Field Desorption Mass Spectrometry", Pergamon Press, Oxford, in press.
(36) H. D. Beckey and H.-R. Schulten, *Angew. Chem.*, **87**, 425 (1975); *Angew. Chem. Int. Ed. Engl.*, **14**, 403 (1975).
(37) H.-R. Schulten, in "Methods of Biochemical Analysis", D. Glick, Ed., Interscience Wiley, New York, N.Y., Vol. 24, 1977, pp 313–448.
(38) H.-R. Schulten and H. D. Beckey, *Org. Mass Spectrom.*, **7**, 861 (1973).
(39) H.-R. Schulten and H. D. Beckey, *Org. Mass Spectrom.*, **6**, 885 (1972).
(40) H. D. Beckey, E. Hilt, and H.-R. Schulten, *J. Phys. E.* **6**, 1043 (1973).
(41) H.-R. Schulten, *Cancer Treat. Rep.* **60**, 501 (1976).
(42) H.-R. Schulten and N. N. M. Nibbering, *Biomed. Mass Spectrom.*, **4**, 55 (1977).
(43) F. Shafizadeh and Y. L. Fu, *Carbohyd. Res.*, **29**, 110 (1973).
(44) F. Shafizadeh and Y. Z. Lai, *J. Org. Chem.*, **37**, 278 (1972).
(45) Y. Halpern, R. Riffer, and A. Broido, *J. Org. Chem.*, **38**, 204 (1973).
(46) F. Shafizadeh and P. S. Chin, *Carbohyd. Res.*, **46**, 149 (1976).
(47) A. Ohnishi, K. Kato, and E. Takagi, (1975) *Polymer J.*, **7**, 431 (1975).
(48) K. Levsen and H.-R. Schulten, (1976) *Biomed. Mass Spectrom.*, **3**, 147 (1976).
(49) D. Gardiner, (1966) *J. Chem. Soc.*, 1473 (1966).
(50) A. Broido, M. Evett, and C. C. Hodges, *Carbohyd. Res.*; **44**, 267 (1975).

RECEIVED for review August 23, 1977. Accepted November 18, 1977. This work was supported by grants from the Deutsche Forschungsgemeinschaft, Ministerium für Wissenschaft und Forschung des Landes Nordrhein-Westfalen and Fonds der Deutschen Chemischen Industrie.

# Automated Simultaneous Qualitative and Quantitative Analysis of Complex Organic Mixtures with a Gas Chromatography–Mass Spectrometry–Computer System

**S. C. Gates,[1] M. J. Smisko,[2] C. L. Ashendel,[3] N. D. Young,[4] J. F. Holland, and C. C. Sweeley***

*Department of Biochemistry, Michigan State University, East Lansing, Michigan 48824*

**A system has been developed which uses retention indices in performing an off-line reverse library search of selected mass chromatograms from the repetitive scanning GC-MS analysis of complex mixtures. More than 100 components in a typical mixture of organic acids from urine are automatically identified and quantitated at a rate of one compound each 6 s. Typical of the analytical results obtained in this study are an observed precision of retention index determination of 0.2%, a lower limit of detection of 10 ng injected, a GC-MS precision of 8% upon duplicate determinations of the same sample, and a 1000-fold linear range of quantitative analysis.**

Analysis of multicomponent organic mixtures is of interest in a number of specialities within the field of analytical chemistry. Classically, analytical procedures have been designed for the analysis of one or a very small number of compounds in these mixtures, but a more recent trend has been to develop a means of measuring the complete "profile", or analyte pattern. The utility of such systems is particularly apparent to forensic, atmospheric, and clinical chemists, all of whom occasionally analyze multicomponent mixtures when it is not known in advance what compounds will be of most importance.

A common feature of most such profiles is the relative lack of qualitative variation from sample to sample, despite the considerable complexity of the samples. Thus, for example, the clinical chemist analyzing urine samples encounters virtually the same set of compounds in each sample, with relatively minor variations. The two features of interest, then, are quantitative differences in one profile compared to a profile from another source or the same source at a different time, and the appearance of one or more highly unusual constituents in a particular sample. The task of analyzing the profile is therefore greatly simplified because a massive library search

[1] Present address, Department of Chemistry, University of Michigan, Ann Arbor, Mich. 48104.
[2] Present address, Aeroquip Corp. 300 S.E. Ave. Jackson, Mich. 49203.
[3] Present address, McArdle Laboratory, University of Wisconsin, Madison, Wis. 53715.
[4] Present address, Upjohn Company, Kalamazoo, Mich. 49001.

0003-2700/78/0350-0433$01.00/0 © 1978 American Chemical Society

of comparison features (spectra or other physical properties) need not be undertaken to identify every compound in each such sample. A "local" library of features that are particularly pertinent to the type of sample being analyzed can thus be maintained and referenced conveniently on a conventional laboratory minicomputer system.

A typical approach in the determination of profiles has been a chromatographic separation of the components, followed by spectroscopic analysis of the separated sample. When 100 or more components are present in a given sample or fraction, the method of choice has most frequently been gas chromatographic separation followed by mass spectrometric identification of individual GC peaks (*1–4*). Some use has also been made of liquid chromatographic separations to obtain profiles (*5, 6*), but such efforts have been hampered by the lack of a detection system capable of uniquely distinguishing a wide variety of closely eluting substances in a liquid medium.

Two problems associated with profile analysis by gas chromatography–mass spectrometry (GC-MS), however, have been the lack of a means of identifying substances that are incompletely resolved, and an inability to quantitate the large number of minor components typically present in biological mixtures. Traditional library search techniques, even on small data bases, are poorly suited to the identification of individual components when a mass spectrum may contain contributions from as many as five or more compounds. Furthermore, selected ion monitoring, usually the method of choice for quantitative analysis by GC-MS, cannot be used for analyses of more than a dozen or so compounds, at least with presently available instruments.

Hence, most published GC and GC-MS profiles of biological fluids have not identified or quantitated more than the major components in the mixture (*1–4, 7, 8*). An approach taken by some laboratories to circumvent this problem has been to group compounds together and quantitate clusters of unresolved compounds by GC peak area (*7, 8*). A more satisfactory solution has been the use of capillary GC columns (*9–11*); these have been especially effective when used with suitable data processing techniques to allow compound identification (*12*). However, even capillary columns do not fully resolve all components, nor do they provide completely unambiguous identification of substances without the use of a mass spectrometer.

Hence, the goal of this laboratory has been to develop a low resolution GC–low resolution MS–computer system which would provide automated quantitative and qualitative analysis of 100 or more components in a complex organic mixture. The system that was developed to meet this goal is described in this paper.

## EXPERIMENTAL

**Urine Separation.** Organic acids are separated from human urine by a modified version (*13*) of the procedure of Thompson and Markey (*7*). In brief, this procedure consists of precipitation of polybasic inorganic salts from 1 to 2 mL urine with barium hydroxide, oxime formation with hydroxylamine hydrochloride (J. T. Baker Chemical Co.), and separation of the neutralized urine on a column of DEAE-Sephadex (Pharmacia) in the acetate form. After an aqueous wash of the column (50 mL), acids are eluted with 40 mL of 1.5 M pyridinium acetate and the eluate is lyophilized to dryness. The residues are treated with 250 $\mu$L of bis(trimethylsilyl)trifluoroacetamide (BSTFA), containing 1% trimethylchlorosilane (TMCS) (Pierce), in dry, redistilled pyridine (4:1, v/v). Trimethylsilylation is carried out at 80 °C for 1 h, after which the samples are stored in sealed, silanized glass capillaries at 4 °C.

**Gas Chromatography.** Gas chromatography is performed on a Varian 2100 GC equipped with dual flame ionization detectors and Varian A-25 recorders. Aliquots (2 $\mu$L) of the trimethylsilylation reaction mixture are chromatographed on 12 ft by 2 mm i.d. glass columns containing 5% OV-17 on 80/100 mesh Supelcoport (Supelco). Conditions of analysis include injector and detector temperatures of 300 °C, amplifier gain of $10^{-10}$ A/V, attenuation at 2, and recorders at 1-mV full scale. The column oven is temperature programmed from 60 to 290 °C at 4°/min, with no initial isothermal period. Gases used are helium as carrier at 40 mL/min, hydrogen at 30 mL/min and air at approximately 300 mL/min.

**Mass Spectrometry.** Mass spectral data are obtained on an LKB-9000 gas chromatograph–mass spectrometer (LKB Produktur) with a Digital Equipment PDP 8/e-based data system (*14*). The gas chromatograph of the LKB contains a 10 ft by 2 mm i.d. coiled glass column packed with 5% OV-17 on 80/100 mesh Supelcoport. During normal operation, the column is temperature programmed from 50 to 260 °C at 4°/min; the sample (2–8 $\mu$L) of the silylated organic acids fraction (described above) is injected when the column reaches 60 °C and data collection begins approximately 7 min later. Other conditions are: ion source temperature, 290 °C; GC injection port, 150 °C; gain 8 on the multiplier; scans at constant 4-s intervals at scan speed 8 over the range $m/z$ 49 to $m/z$ 550; accelerating voltage, 3.5 kV; trap current, 65 $\mu$A; filament current, approximately 4A; and ionizing voltage, 70 eV. Calibration of nominal mass against perfluorokerosene masses and checking of system noise levels are performed once each day. A test sample of urinary organic acids is also injected at the beginning of each day to check the performance of the entire GC–MS–computer system.

When the system has met the test specifications, the GC column of the LKB is pre-treated by two injections of the BSTFA–TMCS silylating mixture and the column cooled to room temperature. An aliquot (0.5 $\mu$L) of a mixture of 8 straight-chain hydrocarbons (with 10, 11, 12, 14, 16, 18, 20, and 24 carbon atoms) in hexane is withdrawn into a 10-$\mu$L syringe, followed by a 0.5-$\mu$L air "spacer" and 2 to 8 $\mu$L of the derivatized urine sample. The sample capillary is discarded immediately, even if sample remains. The sample is analyzed on the LKB under the above conditions, after which the run is validated by brief manual inspection of a few mass chromatograms, and the data are then transferred to a PDP 11/40 computer (Digital Equipment) for subsequent processing. During the transfer, which takes 6 to 10 min, the data are converted to the standard mass spectral data format used on the PDP 11/40 in this laboratory (*15*). The PDP 11/40 system consists of a 16-bit, 56000-word core memory minicomputer with two 1.2-million word removable disks, a 7-track magnetic tape drive, DECwriter, Tektronix 4010 scope display unit, and a Tektronix 4610 hard copy unit. All programs on the PDP 11/40 are designed to be used with the Digital Equipment time-sharing system, RSX-11D (Version 6B). Programs are written in assembly language, Fortran IV, or a mixture of both. MSSMET (described later) occupies approximately 8100 words of core memory in the PDP 11/40, exclusive of a 12000-word library of general purpose system and Fortran subroutines.

## ANALYSIS OF GC-MS DATA

Once the GC–MS data are collected and transferred, they can be processed at any later time by the mass spectral metabolite program (MSSMET), copies and details of which are available from the authors. This program is used to convert GC–MS data to analyte identities and relative or absolute concentrations. In brief, it does this by using a reverse library search of individual ion profiles (mass chromatograms (*16*)) in the region of the expected gas chromatographic retention index (*17*) of each compound of interest. If a small set of 2 to 8 pre-selected differentiating ions are all found to apex at the same location and in the proper ratio, as specified by the library entry for that compound, the substance is considered positively identified. Each compound is quantitated by calculating the ratio of an ion peak area and peak height of the compound relative to the ion peak area and peak height of a quantitative internal standard. This search of $m/z$ intensities is performed automatically by the computer for each library entry and the results are printed or stored for further statistical analysis.

Program operation is flow-charted in Figure 1; details are published elsewhere (*18*). In general, MSSMET is designed to

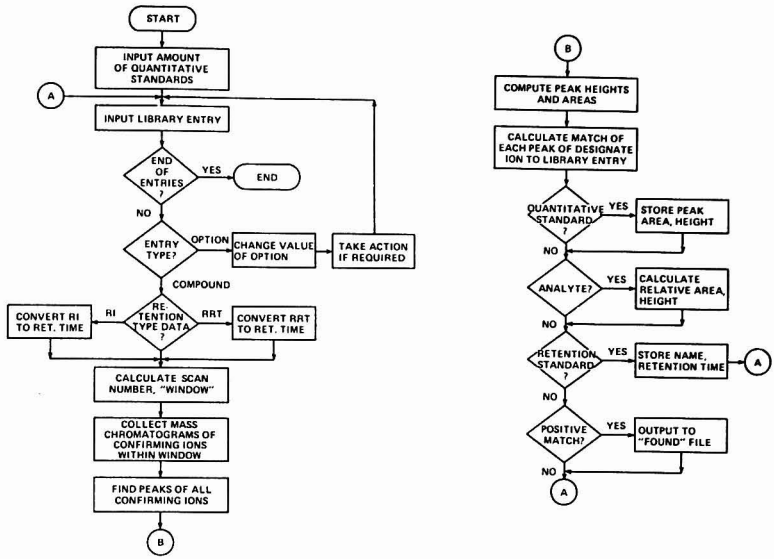


**Figure 1.** MSSMET flowchart

be completely automatic; hence, all but the initial set of commands are entered from a library file which resides permanently on the disk and which is read sequentially by the computer. All entries in the library are of one of two forms: either a command to change the value of a particular program variable ("option") or a set of information about a particular compound. Each of these types of entries may also be entered manually from the teletype during the program execution, if desired.

A typical analysis by MSSMET begins with the operator specifying the names of the two disk files containing the library entries and the mass spectral data. In addition, the operator is prompted to provide information about the amount of internal standard added to the original sample, the volume of sample (urine) extracted, and the amount of any other normalizing factor to be used in quantitation (e.g., creatinine concentration). Once these data are entered, the first entry in the library file is read. Usually, the first several entries provide the initial numerical values of the 34 program options. The information on the first compound in the library is then read in the library file. This four-line entry includes the compound's identifying number and name, if known; its nominal (expected) retention time; the $m/z$ of the "designate" ion and a quantitation factor, and the set of "confirming" ions and their expected relative intensities. The designate ion is that ion which is expected, based on previous experience, to be most differentiating of the compound at its anticipated elution position. The ratio of the area of the designate ion of the compound to the area of the designate ion of the internal standard is converted to actual concentration using the quantitation factor and the following formula:

$$C = k \frac{A_x}{A_{is}} \frac{W}{V} \tag{1}$$

where $C$ is concentration in mg/mL, $A$ is the area of the designate ion, $W$ is the weight (mg) of the internal standard added to the sample, and $V$ is the volume (mL) of sample extracted.

The quantitation factor, $k$, is determined experimentally utilizing a pure reference compound. The accuracy of concentration ($C$) obtained from Equation 1 depends on the reproducibility of the designate ion intensity, relative to total ionization. The confirming ion set includes those ions that must peak at the same time as the designate ion, each paired with its intensity relative to the other confirming ions. By definition, the designate ion must be included in the set of confirming ions.

Once a library entry for a compound is read into core memory, the computer calculates an expected retention time for the substance. Library retention data may be expressed as retention time in minutes and seconds, relative retention time, or retention index; regardless of the form, it is converted to the scan number in the GC-MS data. A time "window" is then calculated within which the substance is expected to elute. The width of the window is based on the value of a library option; it is typically 120 to 200 s wide in our system, and is centered at the expected retention time. Mass chromatograms are collected of all of the confirming ions within the window, and the computer finds any peaks of the individual ions.

After the mass chromatogram peaks are located, an area and height are calculated for each. The ratios of the areas (or heights) of all of the confirming ions are calculated and compared to the library ratios using a slightly modified version of a formula by Grotch (*19*):

$$MC = \left\{ 1 - \left[ \frac{\sum_{j=1}^{N} |I_j^F - I_j^D|}{\sum_{j=1}^{N} (I_j^F + I_j^D)} \right] \right\} 100 \tag{2}$$

where $MC$ = match coefficient, $N$ = number of confirming ions, $I_j^F$ = intensity of $j$th ion in library entry, $I_j^D$ = intensity of $j$th ion in data.

The "match coefficient" calculated by this method is used

as one measure of the match between the library entry and the spectra from the GC-MS analysis. The other measure is the deviation of the retention index (or other measure of retention behavior) observed experimentally from that predicted by the library entry. The match coefficient and the retention index deviation must both be within certain limits, set by library options, for a positive identification ("+" match category). Marginal matches between library and sample data are noted ("?" match category), as are negative matches ("-" match category), and a file containing only compounds considered to be positive matches is established; it is this "found" file which is generally retained for manual or statistical evaluation. Both types of files contain the name of the compound; the match coefficient and the match category (+, ?, or -); peak area and height; uncorrected relative concentration; retention time; retention index; deviation in time and retention index units of the compound from its nominal value; and the scan numbers where the peak was found. Match coefficients and relative concentrations are computed from both peak heights and peak areas. Any or all of this information may be suppressed using the appropriate value of the "print" option.

**Peak and Baseline Determination.** Two critical parts of the program deal with the detection and quantitation of peaks in the individual mass chromatograms. Peak detection consists of a series of decisions based upon the critical parameter values provided by the library. The program consecutively detects three regions of each peak. Initially, the intensity at each succeeding scan within the window is examined until a pre-set number of increasing points, or a critical slope value, is surpassed. Then, in the second region, the program examines points until a maximum has been detected and the peak intensity falls below a predetermined threshold, which may be either a fixed intensity value or, more usually, a fraction of the height of the peak. In the last region, each point is examined to see if the intensity has begun increasing again; if it has, or if the end of the window is encountered, the peak is considered ended.

When all peaks of the confirming ions within the window have been located, a second pass through the data is used to select up to 20 points for a baseline. All data points within the window are examined as potential candidates for the baseline. They are discarded from consideration if they meet any of the following criteria: occurrence before the beginning of the first peak; occurrence after the end of the last peak; occurrence within the boundaries of a peak, except for the first and last points of the peak; occurrence at a point common to two unresolved peaks, unless that point is lower than the previous baseline point; occurrence at the first point of the window, unless lower than the next baseline point; or occurrence at the last point of the window, unless lower than the previous baseline point.

The baseline points selected by this process are used to determine an unweighted least-squares fit to an $n$th order curve, where $n$ is set by the library to a value between 1 and 5, inclusive. A complete baseline is then interpolated from these data and the baseline subtracted areas of all peaks are determined. Unresolved peak areas are divided at the minimum between the two peaks. No further attempt is made to deconvolute the peaks.

**Retention Index Determination.** Although gas chromatographic retention behavior may be expressed in terms of elapsed time, relative retention time, or retention index, the last measure has been most commonly used with MSSMET. Two similar methods for computing retention indices have been tried. The first relies exclusively on the retention data of the straight-chain hydrocarbons co-injected with the sample. In this method, one of the hydrocarbons is located using an estimated retention time and a very wide search window. All other hydrocarbons are located using estimated retention times relative to the first hydrocarbon located. Retention indices of components of the mixture are then calculated by linear interpolation between the appropriate pair of flanking hydrocarbons.

The second approach is to locate a hydrocarbon standard by estimated retention time, then locate two neighboring sample components (not hydrocarbons) by relative retention time. These two are then used as retention index standards to locate, by linear extrapolation, several other sample components, which are, in turn, added to the list of retention index standards. Retention indices of other compounds are then calculated by linear interpolation between flanking retention index standards, exactly as when using hydrocarbon standards.

**Selection of Library.** The library is built using the standard text editor on the PDP 11/40. Each library entry is based on studies of the mass spectra of reference compounds, or mass spectra from the type of sample to be analyzed. Retention indices are determined empirically and periodically updated as more samples are analyzed.

Two methods have been used to select designate and confirming ion sets for use in the library. One of these is strictly intuitive, based on knowledge of the general types of spectra involved. The second, and more recent, approach is to use an algorithm (MSSDSG) which compares the complete library spectrum to spectra taken from a sample of the type to be analyzed. The key feature of this comparison is that the library spectrum is compared to spectra taken from the region of the sample where it would be expected to occur, based on the retention index of the library spectrum. Thus, for example, a mass spectrum of the trimethylsilyl derivative of lactic acid might be compared to 16 mass spectra taken during GC separation of a urine extract in the region around the nominal retention index of the TMSi derivative of lactic acid (1101 on 5% OV-17). Based on this comparison, ratios are computed which compare each ion of the normalized library spectrum to the corresponding ion in the normalized sum of the sample spectra:

$$R_m = \frac{L_m{}^q}{S_m} \tag{3}$$

where $R_m$ is the ratio for ion mass $m$, $L_m$ is the normalized intensity of ion of mass $m$ in the library spectrum, $S_m$ is the normalized intensity of the ion mass $m$ in the summed sample spectra, and $q$ is a factor (typically 1.05) used to weight intense ions more heavily.

The ratios are calculated for as many as 10 different samples and the ratios computed for each sample are then ranked by another program (MSSCHS) and summed. The highest set of ranked ratios are selected and the ion with the highest ratio is chosen to be the designate ion. Up to 7 other ions are selected to complete the confirming ion set. Only one ion from each isotope cluster is chosen.

Once library entries have been selected by either method, they are tested against several samples. Using the "debug" option to examine the actual ratios of the confirming ions, the library entry is modified until it adequately functions in finding the library compound in several biological samples. The library determined by this method for organic acids in human urine is available from the authors and is included as an appendix in Ref. 18.

## RESULTS AND CONCLUSIONS

**Baseline and Peak Area Determination.** The performance of MSSMET was evaluated in part by comparing the results obtained by this method with data calculated from manually determined baselines and areas. As illustrated in

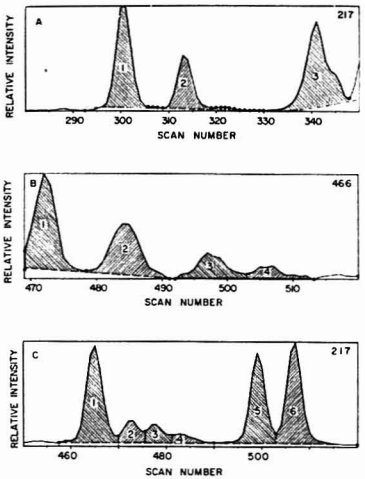


**Figure 2.** Peak and baseline determination by MSSMET. Each black circle represents a baseline point which would be selected by MSSMET. The dotted line represents a second-order least squares fit of the baseline points

Figure 2, the MSSMET algorithms are capable of resolving complex peaks, detecting changing or nonlinear baselines, and integrating even small peak areas. Unlike other peak resolving algorithms (*20*), there is no limit to the number of components which can be resolved in a cluster of peaks, as long as the confirming ions of each compound are at least partially resolved from one another. The determination of baseline can use up to a fifth-order least-squares fit, but a second-order fit is generally most satisfactory for a window width of 30 scans (120 s). The typical mass chromatogram peak of a designate ion detected by MSSMET is 15 scans, although peaks from 4 to 28 scans are routinely detected within the 30-scan window.

**Match Coefficient.** Previous studies by us with pure compounds have indicated that the match coefficient is sensitive and reliable down to the limit of detection of the designate ion (*21*). Since the limit of detection varies with the substance and the intensity of the ion chosen, as well as with the sensitivity of the GC-MS at the time of analysis, no definite detection limit can be established. However, for most samples, about 10 ng must be injected before match coefficients above 80 are observed. When program options are set so that either the peak height or the peak area match coefficient must exceed 80 to permit a positive match, the 157 compounds found in a series of urine samples had a mean match coefficient of approximately 93, as shown in Figure 3. Experience with the system has shown that retention behavior and peak areas for compounds with mean match coefficients below 86 are unreliable; these low match coefficients are observed with substances that are present in very small amounts, and with substances for which an optimal library entry has not yet been obtained.

**Retention Index.** As noted by Nau and Biemann (*22*) and independently by our work with metabolic profiling (*21, 23–25*), retention indices are an extremely precise measure of compound identity, despite the fact that GC-MS data points are recorded for each mass only once every scan (4 s in our system). Pure compounds are found with the most precision; the mean standard deviation for multiple determinations of several pure compounds was 2.20 ($n$ = 156). Compounds in

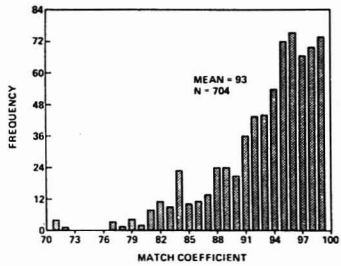


**Figure 3.** Distribution of individual match coefficients. Peak height and peak area match coefficients were calculated for compounds found in 4 urinary organic acid samples by MSSMET

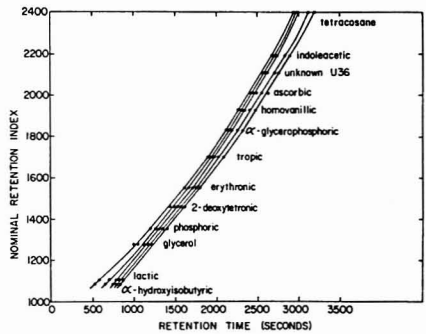


**Figure 4.** Variability of retention times of retention index standards. Retention times were found by MSSMET for each of the retention index standards in 5 samples of urinary organic acids analyzed on the LKB-9000 over a 1-year period

a highly complex biological sample such as urine are found somewhat less precisely (mean standard deviation was 2.79 for 652 determinations). If substances in the sample are used instead of hydrocarbons as retention index standards, precision improves considerably (mean standard deviation was 2.38 for 784 determinations). Retention times and relative retention times are less precise than retention indices. As shown in Figure 4, retention times, even when they are reasonably reproducible over short time periods, can vary markedly over longer periods of time (1 year in Figure 4), with some variations as well in the shape of the retention time vs. nominal retention index curves.

**Quantitative Analysis.** MSSMET has been tested on a variety of pure samples to evaluate quantitative precision and accuracy (*24, 25*). Subsequent studies on urine samples have confirmed that the repetitive scanning technique provides linear results over approximately a 1000-fold range. In complex mixtures such as the urinary organic acid fraction, the technique therefore yields reliable quantitative data even for substances representing 0.01% or less of the dry weight of the total mixture. The reproducibility of relative peak area determinations with the organic acids fraction from urine samples is illustrated in Figure 5. MSSMET was used to quantitate the relative peak areas of 106 urinary organic acids found in two injections of the same sample. Individual data are plotted in order of increasing retention index. The sample marked with triangles was analyzed on the GC-MS one week after the sample marked with circles; data from both samples are plotted as the percent each is of the mean value of the

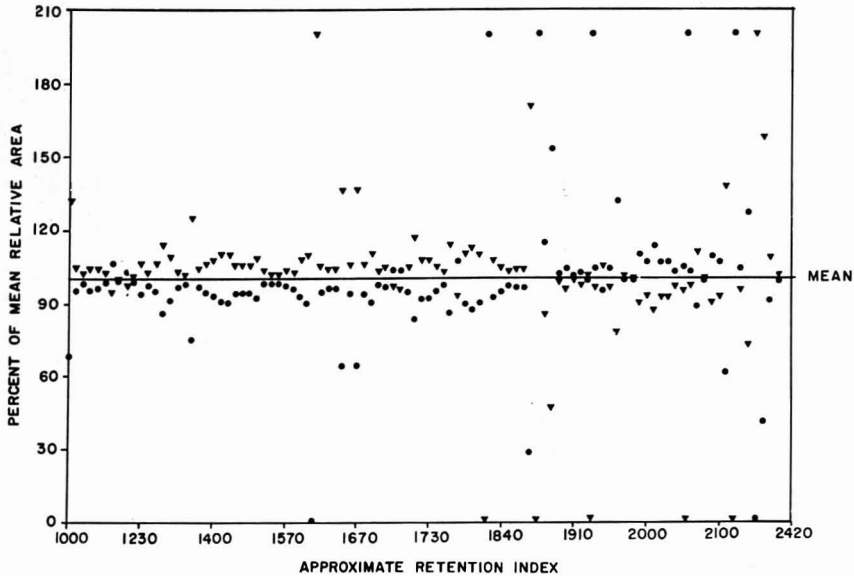


**Figure 5.** Reproducibility of repetitive scanning GC-MS on urine samples

two samples. Of the 14 compounds with a relative standard deviation greater than 35%, one is an artifact peak, 2 are substances just above their limits of detection, 3 have a retention index more than 6 retention index units from the library value (and 2 of these also have one of their match coefficients below 80), and 4 show evidence that the designate ion peak is poorly resolved. The problems with the remaining four substances are not explainable on the basis of the data contained in the MSSMET outputs. Analysis of the data suggests that use of multiple quantitative standards would help improve quantitative precision.

**Analysis of Urine Samples.** Routine MSSMET analysis of the acidic fraction of urine samples has indicated that approximately 100 ± 30 components are reliably detected and quantitated by MSSMET with a version of the library that does not contain some 40 unidentified substances for which library data are presently being obtained. As shown in Figure 6, many of the substances are incompletely resolved by the GC. The analysis is therefore dependent on the use of differentiating ion mass chromatograms. It should be noted that many of the substances in Figure 6 are compounds for which pure standards are not yet available; these substances are treated no differently by MSSMET. Provisional identities in some cases are based on spectra in the literature (*26*, *27*).

## DISCUSSION

MSSMET is a reliable method for both quantitative and qualitative analysis of complex mixtures by GC-MS techniques. Once a suitable library has been assembled and tested, MSSMET operates rapidly and requires little or no decision-making by the analyst. Typically, with the 157-compound library, less than 6 s is required for the computer to identify and quantitate each compound. Excluding the time required to set up files and locate the retention index and quantitation standards, the time required is approximately 4 s per compound. Most of this time is required to transfer data from the disk to core memory.

Occasionally, one or more of the retention time standards is not found properly because it deviates too far from its expected retention time. In these cases, it is a simple matter for the operator to change the expected retention time and have the computer reprocess the library entry for the standard. Generally, once the retention standard is properly located, no further difficulties are encountered. After the quantitative internal standard is located, no further operator intervention is required. About 4 min per sample is required at the teletype for overall supervision of the process.

**Reverse Library Search Using Retention Indices.** The use of retention indices and a reverse library search with a small set of differentiating ions has resulted in a much higher degree of precision of identification than most conventional library searches that are based solely on forward searches of mass spectral data. Retention indices often provide more precise information about compound identity than do mass spectral fragmentation patterns, especially when dealing with large numbers of relatively similar mixtures. In our system, retention index precision is such that the compound can be assumed to occur within a region of 4 to 5 scans (about 9 RI units) on either side of its nominal retention index; hence, the use of the retention index narrows the search for a compound to a region representing less than 2% of the total GC-MS run. Even including the somewhat larger "window" needed to integrate the peak area adequately, less than 4% of the spectra are examined to find a particular compound.

Abramson has pointed out (*28*) that reverse search procedures, even without using retention indices, avoid the problem of supression of important ions from one compound by the presence of ions from a large, overlapping compound. McLafferty has also advocated the use of the reverse search method (*29*) and has provided a means for selecting appropriate ions to use in such searches (*30*). Nau and Biemann originally developed a method for assigning retention indices to GC-MS data (*22*), which they used to help interpret results from GC-MS analyses (*31*). Reimendal and Sjovall (*32*) used

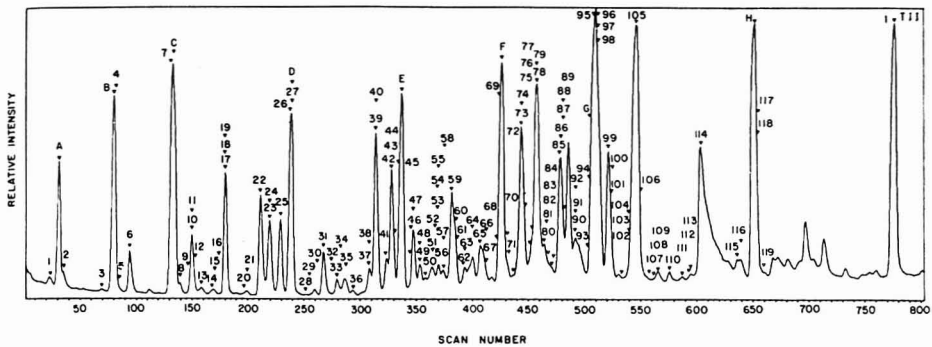


**Figure 6.** Urinary acids identified by MSSMET in urine sample from a "healthy" adult subject. Substances labeled A through I are straight-chain hydrocarbons with 10, 11, 12, 14, 16, 18, 20, 24, and 28 carbon atoms per molecule, respectively. The other substances are: (1) U-1, (2) U-50 (3) α-hydroxyisobutyric, (4) lactic, (5) U-2, (6) glycolic, (7) β-hydroxybutyric, (8) U-4 (pyruvic oxime), (9) U-79, (10) U-5 (cresol), (11) oxalic, (12) U-6, (13) U-51, (14) U-7, (15) glycerol, (16) levulinic, (17) malonic, (18) methylmalonic, (19) U-RA 183, (20) U-OXB1, (21) U-9 (2-methylglyceric), (22) phosphoric, (23) U-10 (deoxyerythronic), (24) benzoic, (25) U-11 (deoxythreonic), (26) succinic, (27) fumaric, (28) phenylacetic, (29) nicotinic, (30) U-54 (deoxytetronic), (31) U-14 (deoxytetronic), (32) U-56 (deoxythreonic), (33) U-57 (threonolactone), (34) glutaric, (35) 3,3-dimethylglutaric, (36) citramalic, (37) malic, (38) U-58 (3-methyl glutaconic-peak 1), (39) U-16 (erythronic), (40) U-80 (3-methylglutaconic-peak 2), (41) U-59 (threonolactone), (42) U-17 (threonic), (43) mandelic, (44) adipic, (45) 3-methyladipic, (46) *o*-hydroxybenzoic, (47) U-60, (48) α-hydroxyglutaric, (49) U-61, (50) β-hydroxy-β-methylglutaric, (51) U-21, (52) U-82, (53) *m*-hydroxybenzoic, (54) pyroglutamic, (55) U-83 (hydroxymethylfuroic), (56) U-22, (57) *o*-hydroxyphenylacetic, (58) U-84, (59) tropic (internal standard), (60) arabonolactone, (61) α-ketoglutaric oxime, (62) *p*-hydroxybenzoic, (63) *m*-hydroxyphenylacetic, (64) U-24, (65) *p*-hydroxyphenylacetic, (66) ribonolactone, (67) arabonic, (68) suberic, (69) β-glycerophosphoric, (70) U-64, (71) U-87, (72) U-65, (73) α-glycerophosphoric, (74) U-26, (75) *cis*-aconitic, (76) U-66, (77) U-67, (78) U-68, (79) citric, (80) azelaic, (81) terephthalic, (82) vanillic, (83) U-89, (84) U-29, (85) homovanillic, (86) galactono-1,4-lactone, (87) *m*-hydroxyphenylhydracrylic, (88) veratric, (89) U-30, (90) *o*-coumaric, (91) hexuronic, (92) gluconic, (93) *p*-hydroxyphenyllactic, (94) U-72, (95) vanilmandelic, (96) ascorbic, (97) U-91, (98) hexuronic, (99) hexuronic, (100) hydrocaffeic, (101) U-74, (102) U-2071, (103) palmitic, (104) U-75, (105) hippuric, (106) caffeic-peak 1, (107) U-76 (hydroxydecanedioic), (108) U-77, (109) U-37, (110) indoleacetic, (111) U-NE8, (112) caffeic-peak 2, (113) urocanic, (114) uric, (115) U-41, (116) *m*-hydroxyhippuric, (117) U-42, (118) 3,4,5-trimethoxycinnamic, (119) 5-hydroxyindoleacetic

mass chromatograms in a semi-automated reverse search procedure which later included some quantitative analysis (*33*). However, it has been the combination of retention indices and reverse library search, developed in this laboratory (*21*, *23–25*) and later used elsewhere (*20*, *34*), which has proved to be the most precise means of identifying multiple components in complex mixtures.

Retention indices also allow a considerable extension of the type of technique used by McLafferty (*30*) to select appropriate ions and weighting factors for computer decisions about whether a spectrum from a particular sample represents a sufficient match to a given library spectrum. As shown in Figure 7, the intensities of ions at a given area of the GC-MS run may vary markedly from the overall distribution of ions in the sample analyzed. This variation frequently can be observed even on a scan-to-scan basis, so that the quality of the reverse library search is improved considerably by knowing, in advance, the approximate set of "interfering" substances which may be present at the same set of scans as the compound of interest. Thus, selection procedures such as MSSDSG and MSSCHS can be used with retention indices to identify the region where the compound is expected to elute in any sample; the reference spectrum can then be compared to the spectra of exactly the milieu in which it must elute, if it exists in the sample.

**Baseline and Peak Area Determination.** Originally, the peak area within a mass chromatogram was determined by integrating the designate ion intensity from the starting point of a peak to its end, with the baseline determined by linear interpolation between the two points. Comparison to manually chosen integration limits and baseline values indicated that this approach was inaccurate in many cases. Hence, a series of increasingly sophisticated algorithms was tested, each one being modified as anomalous results were detected.

The principal limitation to accurate peak area determination appears to be the narrow width of the window. Most of the special provisions within the baseline determination algorithm are a consequence of the difficulty in processing peaks which either begin prior to the start of the window or finish after the end of the window. Frequently, a baseline value must be extrapolated for such peaks, as shown in Figure 2. Fortunately, if the window is properly centered, the peak of interest occurs at the center of the window, and integration is much more accurate.

It is important to note that the proper choice of designate and confirming ions plays a critical role in peak area determination. If these ions are chosen so that they are the most well-resolved ions for that compound, the integration will be correspondingly accurate. The need for well-resolved mass chromatograms peaks is not unique to MSSMET; the Stanford group's "cleanup" procedure (*20*) is equally dependent upon the detection of such peaks. It may be possible to devise methods that are capable of functioning without the need for well-resolved ion sets; one such method has been developed in this laboratory and will be published elsewhere (*35*).

In our experience, it is almost always possible to find at least 2 ions of reasonable intensity that are well resolved (unique for a particular compound). Cases such as the one illustrated in Figure 8, where a number of compounds elute at almost the same time, are extremely common; qualitative and quantitative analysis are thus both dependent on the correct selection of designate ions. Practically the only exceptions are those in which two isomeric substances elute very near each other. In these cases, confirming ions of one substance may be partially obscured by the ions of the other. Depending upon the degree of overlap of the two substances, MSSMET either groups the two substances together (if overlap is severe) or computes separate areas for each.

**Quantitation.** In addition to providing rapid qualitative

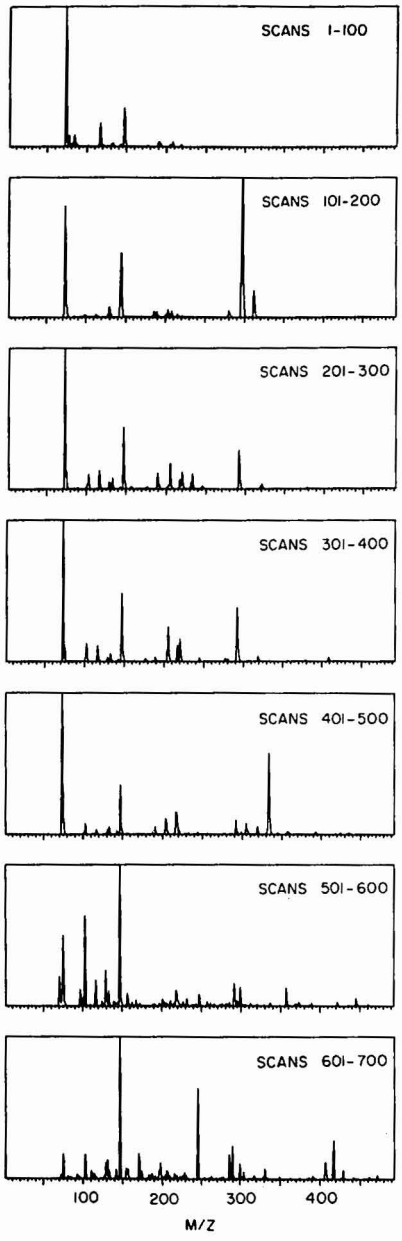


**Figure 7.** Dependence of ion distribution upon the region of the GC-MS analysis of trimethylsilyl organic acids of human urine. Ion intensities have been summed for selected scans within the scan range marked on each plot

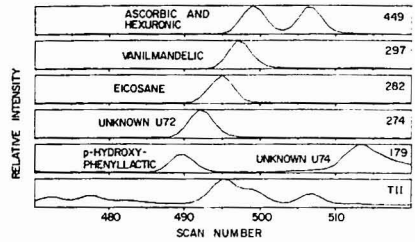


**Figure 8.** Identification of closely-eluting substances by MSSMET

analyses, MSSMET routinely calculates the areas of designate ions, relative to an internal standard designate ion, of each of the 100 or more substances present in a typical sample of organic acids in urine. Since $k$ factors have not yet been determined for most of the library compounds, a value of 1.00 is usually used for $k$ in Equation 1. Hence, the values reported are uncorrected for percents of ionization or recovery during the extraction procedure. The uncorrected concentrations suffice for most profiling purposes, but inter-laboratory or inter-method comparisons of data would require absolute values.

An alternate method has been described by Smith et al. (*36*) for qualitative and quantitative analysis of complex mixtures. It utilizes techniques similar to MSSMET, in that a reverse library search is made with specific regions of mass chromatograms, and identifications are based on both gas chromatographic retention indices and mass spectral patterns. However, this technique differs from MSSMET in that all of the ions belonging to a single compound are used for the quantitation, after spectra are "cleaned up" of contributions from background and other interfering peaks. Quantitation is not corrected for incomplete recoveries in the pre-purification process or for differences in total ion intensities among compounds, since it is relative to an external standard.

Direct comparison of the results obtained by Smith et al. (*36*) with data obtained by MSSMET is not possible, since different sample extraction techniques were used, and because accuracy, precision, sensitivity, and linear range of the method of Smith et al. have not yet been reported (*36*). However, their system can resolve doublets but not multiple overlapped mixtures of substances, whereas MSSMET has successfully and routinely handled peak envelopes containing contributions from 5 or more substances (Figure 8). Since multiply overlapped peaks can be quite common in some complex mixtures (Figure 6), this can be a significant problem. To our knowledge, no other automated system is currently capable of resolving all of the components shown in Figure 6 by GC-MS. In addition, methods that base quantitation upon an estimate of total ion intensity (called "areal total ion current" in Ref. 36) are very dependent upon accurate resolution of the most intense ions; however, in the case of trimethylsilyl derivatives, the most intense ions are frequently those produced by the derivatizing group, and hence mass chromatograms of these ions are usually the least well-resolved by the GC. Dependence upon approximate methods for resolving such ions may result in significant inaccuracies during quantitation. In contrast, MSSMET uses designate ions which are selected specifically because they are well-resolved and unique; hence, quantitation is based almost exclusively on ions for which there is minimal inaccuracy. If several ions for a given compound are well-resolved, precision (not accuracy) may be improved by using all such ions during quantitation; however, the more complex the mixture, the smaller the number of well-resolved ions will be.

In general, the results obtained with MSSMET over a period of more than two years lead us to believe that it has a very good potential for metabolic profiling studies. While our experience has been limited to analyses of the organic acids and steroid fractions of human urine, it appears that MSSMET can easily be adapted to a variety of other fractions and sample types. We have begun to use MSSMET "found" files as the basis for statistical analysis of urine samples (*13*) and to develop other methods for increasing the size of the MSSMET library (*35, 37*). Preliminary results on these projects suggest that at least 140, and perhaps more, organic acids can be monitored routinely in urine, and that the challenge for users of MSSMET and related systems will be the interpretation of the wealth of new data provided by these techniques.

## ACKNOWLEDGMENT

The authors gratefully acknowledge the technical assistance of J. Harten and N. Dendramis, and D. Byrne for typing the manuscript.

## LITERATURE CITED

(1) E. C. Horning and M. G. Horning, *J. Chromatogr. Sci.*, **9**, 129 (1971).
(2) F. Hutterer, J. Roboz, L. Sarkozi, A. Ruhig, and R. Bacchin, *Clin. Chem. (Winston-Salem, N.C.)*, **17**, 789 (1971).
(3) E. Jellum, O. Stokke, and L. Eldjarn, *Scand. J. Clin. Lab. Invest.*, **27**, 273 (1971).
(4) J. C. Crawhall, O. Mamer, S. Tjoa, and J. C. Claveau, *Clin. Chim. Acta*, **34**, 47 (1971).
(5) D. S. Young, *Am. J. Clin. Pathol.*, **53**, 803 (1970).
(6) W. W. Pitt, Jr., C. D. Scott, W. F. Johnson, and G. Jones, Jr., *Clin. Chem. (Winston-Salem, N.C.)*, **16**, 637 (1970).
(7) J. A. Thompson and S. P. Markey, *Anal. Chem.*, **47**, 1313 (1975).
(8) A. M. Lawson, R. A. Chalmers, and R. W. E. Watts, *Clin. Chem. (Winston-Salem, N.C)*, **22**, 1283 (1976).
(9) B. J. Kimble, R. E. Cox, R. V. McPherron, R. W. Olsen, E. Roitman, F. C. Walls, and A. L. Burlingame, *J. Chromatogr. Sci.*, **12**, 647 (1974).
(10) W. Bertsch, R. A. Chang, and A. Zlatkis, *J. Chromatogr. Sci.*, **12**, 175 (1974).
(11) J. A. Luyten and G. A. F. M. Rutten, *J. Chromatogr.*, **91**, 393 (1974).
(12) A. B. Robinson and L. Pauling, *Clin. Chem., (Winston-Salem, N.C.)*, **20**, 961 (1974).
(13) S. C. Gates, N. Dendramis, and C. C. Sweeley, unpublished results.
(14) N. D. Young, J. F. Holland, and C. C. Sweeley, unpublished results.
(15) C. Ashendel, N. Young, J. F. Holland, and C. C. Sweeley, unpublished results.
(16) R. A. Hites and K. Biemann, *Anal. Chem.*, **42**, 855 (1970).
(17) E. Kovats, *Helv. Chim. Acta*, **41**, 1915 (1958).
(18) S. C. Gates, "Automated Metablic Profiling of Organic Acids in Human Urine by Gas Chromatography-Mass Spectrometry", Ph.D. Dissertation, Michigan State University, East Lansing, Mich., 1977.
(19) S. L. Grotch, *Anal. Chem.*, **45**, 2 (1973).
(20) R. G. Dromey, M. J. Stefik, T. C. Rindfleisch, and A. M. Duffield, *Anal. Chem.*, **48**, 1368 (1976).
(21) S. C. Gates, N. D. Young, J. F. Holland, and C. C. Sweeley, "Advances in Mass Spectrometry in Biochemistry and Medicine, Vol. II", A. Frigerio, Ed., Spectrum Publications, New York, N.Y., 1976, p 171.
(22) H. Nau and K. Biemann, *Anal. Lett.*, **6**, 1071 (1973).
(23) C. C. Sweeley, N. D. Young, J. F. Holland, and S. C. Gates, *J. Chromatogr.*, **99**, 507 (1974).
(24) S. C. Gates, N. D. Young, J. F. Holland, and C. C. Sweeley, "Advances in Mass Spectrometry in Biochemistry and Medicine, Vol. I", A. Frigerio and N. Castagnoli, Ed., Spectrum Publications, New York, N.Y., 1976, p 483.
(25) C. C. Sweeley, S. C. Gates, R. H. Thompson, J. Harten, N. Dendramis, and J. F. Holland, "Quantitative Mass Spectrometry in Life Sciences", Elsevier, Amsterdam, 1977, p 29.
(26) S. P. Markey, W. G. Urban, and S. P. Levine, "Mass Spectra of Compounds of Biological Interest", National Technical Information Service, U.S. Department of Commerce, Springfield, Va., 1974.
(27) G. Lancaster, P. Lamm, C. R. Scriver, S. S. Tjoa, and O. A. Mamer, *Clin. Chim. Acta*, **48**, 279 (1973).
(28) F. P. Abramson, *Anal. Chem.*, **47**, 45 (1975).
(29) F. W. McLafferty, R. H. Hertel, and R. D. Villivock, *Org. Mass Spectrom.*, **9**, 690 (1974).
(30) G. M. Peysna, F. W. McLafferty, R. Venkataraghavan, and H. E. Dayringer, *Anal. Chem.*, **47**, 1161 (1975).
(31) H. Nau, H.-J. Förster, J. A. Kelley, and K. Biemann, *Biomed. Mass Spectrom.*, **2**, 326 (1975).
(32) R. Reimendal and J. B. Sjövall, *Anal. Chem.*, **45**, 1083 (1973).
(33) M. Axelson, T. Cronholm, T. Curstedt, R. Reimendal, and J. Sjövall, *Chromatographia*, **7**, 502 (1974).
(34) B. E. Blaisdell, *Anal. Chem.*, **49**, 180 (1977).
(35) B. E. Blaisdell and C. C. Sweeley, unpublished results.
(36) D. R. Smith, M. Achenbach, W. J. Yeager, P. J. Anderson, W. L. Fitch, and T. C. Rindfleisch, *Anal. Chem.*, **49**, 1623 (1977).
(37) S. C. Gates and C. C. Sweeley, unpublished results.

RECEIVED for review August 8, 1977. Accepted December 6, 1977. This investigation was supported by Grant RR-00480 from the Biotechnology Resources Branch of the National Institutes of Health. All figures are taken from the Ph.D. Dissertation of S.C.G. (Ref 18).

# Magnetic Fields to Eliminate Beta-Ray Interference in Measurement of X-rays Following Neutron Activation

**M. Mantel,* Z. B. Alfassi,[1] and S. Amiel**

*Nuclear Chemistry Department, Soreq Nuclear Research Centre, Yavne, Israel*

**Magnetic deflection is used for the elimination of beta interference with the measurement of x-rays obtained following neutron activation. Theoretical calculations and experimental results show that permanent magnets of 3.5–4 kG greatly improve the accuracy of the measurements of x-rays of low and medium *Z* elements in the presence of strong $\beta$ emitters by lowering the background. This effect increases with increasing intensity of the magnetic field and for a 50 $\mu$Ci $^{32}$O source reaches 99% and 95% for 4.5 and 14 keV, respectively.**

[1] Permanent address, Nuclear Engineering Department, Ben-Gurion University of the Negev, Beer-Sheeba, Israel.

The simultaneous nondestructive determination of many elements in the same irradiated sample has been achieved by applying x-ray spectrometry to activation analysis (*1–3*). One of the problems associated with this method is the interference of $\beta$ particles emitted from the irradiated sample. These $\beta$ particles may increase the dead-time of the Si(Li) detector upsetting its resolution, which causes inaccurate integration of the x-ray peaks. Furthermore the $\beta$ particles produce a high background which may completely obscure the x-ray peaks obtained from trace amounts of low and medium *Z* elements. The elimination of this interference is especially important for matrices such as biological materials and seawater, since their major components—sodium, potassium, chlorine, and phosphorus—are strong $\beta$ emitters, following irradiation.

The principle of this technique has been briefly explained previously (*4*). The present work shows a detailed study of

0003-2700/78/0350-0441$01.00/0 © 1978 American Chemical Society

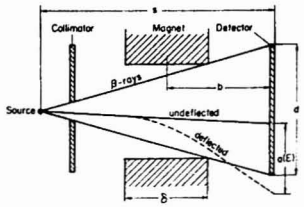


**Figure 1.** Schematic diagram of the experimental setup

the possible use of magnetic deflection of $\beta$ rays in neutron activation followed by x-ray spectrometry. Theoretical calculations were carried out, their principle was explained, and the results were compared to those obtained experimentally. Several practical examples which illustrate the usefulness of the technique are described.

## EXPERIMENTAL

**Apparatus.** The experimental setup used is shown schematically in Figure 1. A 100-mm$^2$ area and 4-mm depth Si(Li) detector (manufactured by Seforad Israel) was used. The output signals from the detector were passed through an Ortec 118A preamplifier and an Ortec 410 amplifier, Ortec 408 biased amplifier, and Ortec 411 pulse stretcher. The resulting pulses were analyzed by a T.M.C. 400-channel analyzer. The resolution of the system for the 6.4-keV Fe K$\alpha$ x-rays (obtained from $^{57}$Co) was 450 eV (FWHM).

A magnet of 3.4 kG manufactured by AEI for a MINIMASS Massspectrometer PPG-2, was used in most experiments.

**Standard Sources.** The standard sources used were: a 10-$\mu$Ci $^{57}$Co source obtained from Amersham, England, and 50-$\mu$Ci $^{32}$P source prepared by evaporation of a calibrated solution of $^{32}$P obtained from the Nuclear Research Center, Negev, Israel.

**Samples.** Thin and uniformly distributed samples were prepared as described before (*2, 3*), by introducing the smallest possible quantity of the material to be analyzed into small polyethylene cups.

**Irradiation.** The irradiations were carried out in the pneumatic tube of the IRR-1 reactor.

## RESULTS AND DISCUSSION

**Theoretical Calculations.** The purpose of the calculations was to determine the fraction of $\beta$ particles in a $\beta$-particle beam moving perpendicular to the detector, which will be deflected by a given magnetic field, according to its intensity and the source–detector distance, and thus prevented from reaching the detector.

A magnetic field applied perpendicular to the direction of the $\beta$ particles will deflect them in a circular path. The radius of the deflection is given by the equation (*5*):

$$r(E) = \frac{17033.10^3}{H}[(E/0.5198 + 1)^2 - 1]^{1/2} \qquad (1)$$

where $r(E)$ is the radius of deflection (cm), $E$ the kinetic energy of the $\beta$ particle (MeV), and $H$ the magnetic field intensity (Gauss). As an example, in order to obtain $r$ = 2 cm which is a practical radius of deflection, the required magnetic field is 3.05 kG for $E$ = 1.39 MeV ($E_{max}$ of $^{24}$Na $\beta$ rays).

The fraction of $\beta$ particles which are deflected from the detector by a given magnet can be calculated from geometrical considerations, the radius of deflection $r(E)$, and the spectrum of the $\beta$ particles. The calculations are based on the experimental setup shown schematically in Figure 1.

The collimator, C, is used to prevent those $\beta$ particles which would not ordinarily collide with the detector, from hitting it because of deflection by the magnet.

If the radius of deflection $r(E)$ is smaller than the width of the magnetic poles ($r(E) < \delta$), the $\beta$ particles move in a circle in the area between the source and the detector and will never reach the plane of the surface of the detector.

For $r(E) > \delta$, the distance $a(E)$ by which the $\beta$ particles are deflected on the plane of the surface of the detector (see Figure 1) can be shown by geometrical consideration to be given by the equation:

$$a(E) = (b\delta + \delta^2/2 - r^2 + r\sqrt{r^2 - \delta^2})/\sqrt{r^2 - \delta^2} \qquad (2)$$

where $r$ is $r(E)$ from Equation 1.

If $a(E)$ is larger than the diameter of the detector, $d$, none of the $\beta$ particles with energy $E$ will hit the surface of the detector. For $a(E) < d$ only a fraction of the $\beta$ particles will hit the detector. This fraction $f(E)$ of $\beta$ particles with kinetic energy $E$ which hit the detector is the segment of the area of a circle with diameter $d$ overlapped by the same circle with its diameter shifted, by the distance $a(E)$, along the line of the centers.

The fraction of $\beta$ particles removed by the magnet, $k(E)$, is given by

$$k(E) = \frac{2}{\pi}[X(E)\sqrt{1 - X^2(E)} - \arcsin X(E)] \qquad (3)$$

where $X(E) = a(E)/d$.

Since the $\beta$ particles are not monoenergetic, the deflected fraction $k(E)$ has to be averaged over the whole spectrum of the $\beta$ particles. Thus the fraction of $\beta$ particles which are removed by the magnetic field is given by the equation:

$$\Delta = \frac{\int_0^{E_m} k(E)p(E)dE}{\int_0^{E_m} p(E)dE} \qquad (4)$$

where $p(E)dE$ is the number of $\beta$ particles having a kinetic energy between $E$ and $E + dE$, and $E_m$ is the maximum energy of the $\beta$ particles.

The main sources of $\beta$ particles obtained from irradiated biological and seawater samples are $^{24}$Na, $^{32}$P, and $^{38}$Cl. These nuclides are all low $Z$ elements and hence their $\beta$ particle energy spectra can be described quite accurately by the expression (*6*):

$$p(E)dE = C(E + 0.511)(E^2 + 1.022E)^{1/2}(E - E_m)^2dE \qquad (5)$$

where $C$ is a normalization constant. $E$ and $E_m$ are in MeV. From this equation and Equation 4 the fraction of $\beta$ particles removed by a magnetic field was calculated by integration using Simpson's rule, for the particular case in which the width of the magnetic poles ($\delta$) is equal to the source detector distance ($b = \delta/2$). For each value of the maximum energy of $\beta$ particles, the fraction removed was calculated as a function of the intensity of the magnetic field and the source–detector distance. Table I shows the calculated fraction removed for 1.71 MeV ($^{32}$P) and 4.92 MeV ($^{38}$Cl) $\beta$ particles. As may be seen, in the case of $^{32}$P $\beta$ rays, a magnet of 3 kG is necessary for the removal of 98% of the $\beta$ particles at a source–detector distance of 2 cm, and a 2-kG magnet for the same percentage at a distance of 3 cm. On the other hand for the $^{38}$Cl $\beta$ particles, it will be necessary to use a very strong magnet ($H$ = 5 kG) to achieve 98% removal at 2 cm, or to increase the distance to 4.5 cm for a 3-kG magnet.

Due to the physical size of the magnet, the counts of both x rays and $\beta$ particles are reduced by the geometric factor $(s + l)/l^2$ where $l$ is the distance between the surface of the detector and its detecting layer and $s$ is the source–detector distance (see Figure 1). This factor is given in the second column of Table I for $l$ = 0.5 mm, for a source–detector distance ranging from 1 to 5.5 cm and represents the percent of x rays reaching the detector. Thus it is possible using Table I to calculate the feasibility of the method in every case, i.e.,

Table I. Fraction of $\beta$ Particles Deflected by a Magnetic Field

| $\beta$ particle energy, MeV | Source detector distance, cm | Geometric factor, % | Magnetic field, kG | | | | |
|---|---|---|---|---|---|---|---|
| | | | 1 | 2 | 3 | 4 | 5 |
| 1.71 | 1.00 | 11.11 | 0.07 | 0.21 | 0.42 | 0.66 | 0.86 |
| $^{32}$P | 1.50 | 6.25 | 0.16 | 0.47 | 0.79 | 0.98 | 1.00 |
| | 2.00 | 4.00 | 0.30 | 0.73 | 0.98 | 1.00 | 1.00 |
| | 2.50 | 2.78 | 0.45 | 0.91 | 1.00 | 1.00 | 1.00 |
| | 3.00 | 2.04 | 0.60 | 0.99 | 1.00 | 1.00 | 1.00 |
| | 3.50 | 1.56 | 0.74 | 0.99 | 1.00 | 1.00 | 1.00 |
| | 4.00 | 1.23 | 0.86 | 1.00 | 1.00 | 1.00 | 1.00 |
| | 4.50 | 1.00 | 0.93 | 1.00 | 1.00 | 1.00 | 1.00 |
| | 5.00 | 0.83 | 0.98 | 1.00 | 1.00 | 1.00 | 1.00 |
| | 5.50 | 0.69 | 0.99 | 1.00 | 1.00 | 1.00 | 1.00 |
| 4.92 | 1.00 | 11.11 | 0.02 | 0.05 | 0.10 | 0.15 | 0.22 |
| $^{38}$Cl | 1.50 | 6.25 | 0.05 | 0.13 | 0.22 | 0.35 | 0.48 |
| | 2.00 | 4.00 | 0.10 | 0.23 | 0.39 | 0.57 | 0.74 |
| | 2.50 | 2.78 | 0.15 | 0.35 | 0.57 | 0.77 | 0.91 |
| | 3.00 | 2.04 | 0.22 | 0.48 | 0.73 | 0.91 | 0.99 |
| | 3.50 | 1.56 | 0.29 | 0.61 | 0.86 | 0.98 | 1.00 |
| | 4.00 | 1.23 | 0.38 | 0.73 | 0.94 | 1.00 | 1.00 |
| | 4.50 | 1.00 | 0.46 | 0.83 | 0.98 | 1.00 | 1.00 |
| | 5.00 | 0.83 | 0.55 | 0.91 | 1.00 | 1.00 | 1.00 |
| | 5.50 | 0.69 | 0.64 | 0.96 | 1.00 | 1.00 | 1.00 |

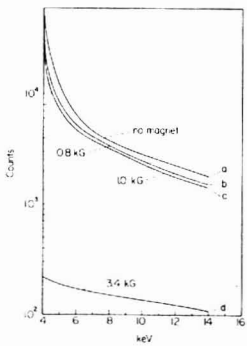


Figure 2. Influence of magnetic fields of different intensities on the spectrum of 50-$\mu$Ci $^{32}$P

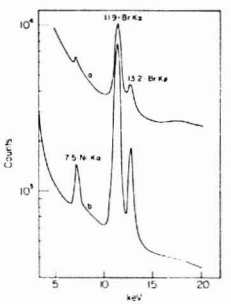


Figure 3. X-ray spectra of neutron irradiated hair. 90 mg hair, irradiated for 30 min in the reactor core, counted for 40 min. (a) without a magnetic field; (b) with a magnetic field

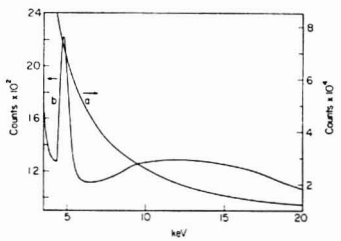


Figure 4. Spectra obtained for 1 mg Cr and 50 mg phosphate irradiated for 30 min in the reactor core, counted for 10 h. (a) without magnet; (b) with magnet

the theoretical limits of detection for different elements in the presence of strong $\beta$ emitters as a function of the magnetic field.

**Experimental Results.** *Effect of Magnetic Deflection.* The effect of magnetic deflection on the high background produced by $\beta$ rays was studied by measuring a 50-$\mu$Ci $^{32}$P source with magnetic fields of different intensities (0.8, 1.0 and 3.4 kG). The spectra were compared with that obtained for the same source without a magnet. As may be seen in Figure 2, the use of a magnet results in the drastic lowering of the background. This reduction increases with the increasing intensity of the magnetic field and reaches 99% and 95% for 4.5 and 14 keV, respectively. The influence of this effect on the measurement of x rays may be seen from the examples given below.

*Examples of Practical Applications.* (1) Determination of Copper and Bromine in Hair. A sample of 90 mg of hair was prepared as described before (*1*), irradiated for 30 min in the core of the IRR-1 reactor and the x-ray spectrum measured with and without the 3.4-kG magnet. The results given in Figure 3, show that the 7.5-keV Ni K$\alpha$ x rays obtained from Cu following neutron irradiation are completely obscured by the background and cannot be measured without the use of a magnetic field (spectrum a). From spectrum b, obtained with a magnetic field, the amount of Cu in hair could be calculated by comparison with a pure Cu standard to be about 20 ppm. For bromine, the 11.9-keV Br K$\alpha$ x rays may be measured without a magnetic field (spectrum a), but the peak-to-background ratio increases with the use of a magnet from 3.5 to 13 making the integration of the peak more accurate. Preliminary results obtained for Br are 250 ppm.

(2) Determination of Cr in the Presence of Phosphates. A sample containing phosphate and chromium in the ratio of 100:1 was prepared and irradiated for 30 min in the core of the reactor as described previously (*1*). The sample was

counted for 10 h with and without a magnetic field. Figure 4 shows the results obtained. In this case also, without a magnetic field the 4.8-keV V x rays, obtained from Cr after irradiation are completely obscured by the background produced by the $\beta$ particles emitted from the irradiated phosphate. By applying a magnetic field, the V K$\alpha$ x rays may be accurately integrated and measured.

This experiment is of special importance for the analysis of biological materials by nondestructive activation analysis. The other $\beta$ emitters contained in these matrices (Na, K, Cl) produce isotopes with much shorter half-lives than $^{32}$P (14 d) and Cr (27 d) after neutron activation. Thus, after an appropriate waiting period, the $^{32}$P will remain the only serious source of interference with the nondestructive determination of Cr in these matrices.

**Comparison of Experimental and Calculated Results.** A magnet of 3.4 kG with circular poles of about 2.5-cm diameter was used in the experiments. Because of the shape of the magnet, the source-detector distance was about 5 cm. Thus one of the conditions on which the calculations were based, that the magnet should fill the entire source-detector distance, was not fulfilled. As a result, the fraction of $\beta$ particles removed from the surface of the detector cannot be obtained exactly from Table I. However, this table indicated that for our setup, at least 99% of $^{32}$P $\beta$ particles (1.71 meV) will be removed by the magnet compared with the experimental value of 95–97% (calculated from Figure 2).

There are several possible factors which could contribute to the slight discrepancy between the experimental and calculated results. (i) In the calculations, it was assumed that we have a radioactive point source and a collimator which prevents all the $\beta$ particles which do not hit the detector in the absence of a magnet from hitting it after deflection. On the other hand, in the experiments a 6-mm diameter source was used without a collimator to get enough activity.

(ii) The deflected $\beta$ particles could collide with different materials which as a result will emit bremsstrahlung. The latter are detected by the detector but have not been considered in the calculation.

(iii) Equation 1 is valid only in vacuum. It does not consider the possible collision of $\beta$ particles with air molecules and the resulting change in their momentum. However, experiments were also carried out at lower pressures down to 1 Torr without any further reduction in the background, indicating that the presence of air probably does not contribute to the discrepancy.

(iv) The calculations yield the fraction of $\beta$ particles removed by the magnetic field, but do not take into account that, as a result, the spectra of the $\beta$ particles which reach the detector are changed as compared to the initial spectra. This change of spectra has to be calculated in order to evaluate the changes in the detector background. To this purpose, the response functions of the detector to monoenergetic electrons of various energies, will have to be studied.

(v) The whole area of the detector was considered to have the same efficiency whereas it was found (*7*) that for x-ray measurement, there are radial gradients in the efficiency of Si(Li) detectors.

## ACKNOWLEDGMENT

The authors thank Raia Nothman for her help and initiative in carrying out the experiments.

## LITERATURE CITED

(1) M. Mantel and S. Amiel, *Anal. Chem.*, **44**, 548 (1972).
(2) M. Mantel and S. Amiel, *J. Radioanal. Chem.*, **16**, 127 (1973).
(3) M. Mantel and S. Amiel, *Anal. Chem.*, **45**, 2393 (1973).
(4) S. Amiel, M. Mantel, and Z. B. Alfassi, *J. Radioanal. Chem.*, **37**, 189 (1977).
(5) E. Segre, "Experimental Nuclear Physics", Vol 3, Pergamon Press, London, 1952, p 428.
(6) I. Kaplan, "Nuclear Physics", Addison-Wesley, New York, N.Y., 1962, p 363.
(7) Z. B. Alfassi and R. Nothman, *Nucl. Instrum. Methods*, **143**, 57 (1977).

RECEIVED for review June 8, 1977. Accepted November 11, 1977. This work was supported by the U.S.-Israel Binational Foundation.

# Preservation of Some Trace Metals in Samples of Natural Waters

**K. S. Subramanian, C. L. Chakrabarti,* J. E. Sueiras,[1] and I. S. Maines**

*Metal Ions Group, Department of Chemistry, Carleton University, Ottawa, Ontario, Canada K1S 5B6*

**The loss of 11 trace metals on storage of both synthetic water samples and natural water samples in Pyrex glass, Nalgene linear polyethylene, and Teflon containers has been studied using graphite furnace atomic absorption spectrometry. The amount of each trace metal lost has been studied as a function of time in the pH range from 1.5 to 8.0. Acidification to pH < 1.5 with nitric acid and storage in Nalgene containers are found to be the most effective ways of preventing the loss of trace metals from natural waters.**

Several workers have reported significant loss of trace metals from aqueous solutions upon storage—the extent varied, among other things, with the type of container, contact time, pH, and the initial concentration of the metal. Eichholz et al. (*1*) reported loss of trace metals from hard water stored in polyethylene and borosilicate glass containers. Robertson (*2*) reported significant losses of Ag, Co, Fe, In, Sc, and U on storage of seawater in Pyrex and polyethylene containers. Durst and Duhart (*3*) could find no suitable containers for storage of dilute aqueous solutions of Ag. Posselt and Weber (*4*) and King et al. (*5*) observed that at pH > 7, cadmium in distilled water was adsorbed more by glass than plastic containers; however, at pH < 2, adsorption of cadmium by either of these containers was negligible. Other workers (*6–9*) reported the need of acidifying the samples with $HNO_3$ to pH < 1 in order to prevent precipitation and adsorption of trace metals by container walls. It was reported that the amount of trace metal lost was directly related to the length of storage time and inversely related to the concentration of the trace metal (*10–12*).

[1] On leave from the Department of Chemistry, Santiago de Compostela University, Santiago de Compostela, Spain.

0003-2700/78/0350-0444$01.00/0 © 1978 American Chemical Society

Most of the published literature to date is on the loss of trace metals from synthetic samples of dilute aqueous solutions. Little has been reported about the magnitude and the rate of loss of trace metals on storage of natural water samples in glass or plastic containers. However, the above studies indicate that there is a problem of severe loss of trace metals from natural waters. In view of the above, it was thought advisable to study the effect of pH and container material on the stability of natural water samples under routine conditions of sample collection and storage, and to find out the most suitable container that prevents or at least decreases the extent of the loss. The metals studied were Al, Cd, Co, Cr, Cu, Fe, Mn, Ni, Pb, Sr, and Zn.

## EXPERIMENTAL

**Apparatus.** The amounts of trace metals were determined using a Perkin-Elmer atomic absorption spectrophotometer, model 503, equipped with a Heated Graphite Atomizer 2000 (HGA-2000), single-element hollow cathode lamps as narrow line sources, and a Perkin-Elmer Deuterium Background Corrector.

**Container for Water Samples.** Pyrex glass (borosilicate glass—100-mL volumetric flasks with ground-glass stoppers) and Nalgene (linear polyethylene, 250-mL and 1000-mL screw-cap bottles) were used as containers for water samples. Teflon beakers (fitted with tight-fitting lids) were used for zinc because of the severe contamination found with Pyrex and Nalgene containers.

**Reagents.** (a) Ultrapure water of resistivity 18.3 megohm-cm was obtained from a Milli-Q2 System (Millipore Corporation).

(b) Stock solutions of Al, Cu, Fe, Ni, and Zn were prepared by dissolving pure metals in a minimum amount of ultrapure $HNO_3$, evaporating off the excess acid and making it up with ultrapure water—the final solution contained 1% (v/v) $HNO_3$. Stock solutions of Cd, Co, Cr, Mn, Pb, and Sr were prepared by dissolving a suitable oven-dried AnalaR salt of each metal separately in ultrapure water and acidifying the solutions to pH 2.0. All stock solutions were stored in clean polyethylene bottles (with the exception of zinc, which was stored in a Teflon bottle) and contained 1000 μg/mL of metal. Appropriate standard solutions were prepared by serial dilution of the stock solutions with ultrapure water immediately prior to analysis.

(c) Humic acid (Technical Grade, Aldrich Chemical Company, Milwaukee, Wis.) was purified by leaching it for 3 days with 0.1 M $HNO_3$ (stirring continuously with a magnetic stirrer) to remove heavy metals. The leached acid was washed with ultrapure water and dried at 180 °C. A stock solution containing 100 μg/mL of humic acid was prepared by dissolving 5.0 mg of the purified acid in 5.0 mL of 2 M $Na_2CO_3$ (which had been purified by electrolysis), and then diluting the solution to 500 mL with ultrapure water.

(d) Synthetic water samples and Rideau River (Carleton University site, Ottawa, Ontario) water samples studied are described below. The bulk composition of the synthetic water samples was as follows (*13*): (i) Inorganic bulk matrix (in μg/mL): $Ca^{2+}$, 40; $Na^+$, 12; $HCO_3^-$, 115; $Cl^-$, 25; and $SO_4^{2-}$, 25; Organic bulk matrix: humic acid, 5 μg/mL; (ii) Trace metals: the values selected were based on the results of analysis of a Rideau River water sample by graphite furnace atomic absorption spectrometry (GFAAS). The values selected are presented in Table I.

**Procedure.** Immediately prior to use, all containers were cleaned sequentially as follows: a detergent wash, tap water rinse, soaking in 2% $HNO_3$ for 24 h, distilled water rinse (6 times), and ultrapure water rinse (6 times). After the cleaning operation, any containers found to give blanks (with ultrapure water acidified to pH 1.0 with nitric acid) having detectable concentrations of the trace metals were rejected.

Stability of water samples was studied using both synthetic water samples and Rideau River water samples at pH's: 1.5, 2.5, 4.0, 6.0, and 8.0. The pH values were adjusted with ultrapure $HNO_3$. Unacidified natural water samples were found to have a pH of about 8.0 and were used as the water samples at pH 8.0. The samples were stored in two containers of each material (Pyrex glass and Nalgene linear polyethylene for all metals except zinc for which Teflon was used) at each of the above pH values at 23–24 °C. (Before adjustment of pH and storage, the river water samples were filtered through a 0.45-μm membrane filter). The amount of each trace metal lost was determined by GFAAS on days: 1, 2, 3, 4, 5, 10, 20, and 30. The GFAAS technique was chosen because it has the extremely high sensitivity required for determining, without pre-concentration, the low concentration levels (0–50 ng/mL) at which trace metals are present in natural waters, and also because it has the high selectivity, precision, and day-to-day reproducibility required for reliable analytical results.

**Table I. Analytical Lines and Operating Conditions for Graphite Furnace Atomic Absorption Spectrometry**

| | | | Atomization parameters | | |
|---|---|---|---|---|---|
| Element | line, nm | Charring temp[a], °C | Temp[a], °C | Time s | Sensitivity,[b] 1 × $10^{-12}$ g |
| Ag | 328.1 | 300 | 2400 | 5 | 10 |
| Al | 309.2 | 1200 | 2400 | 6 | 35 |
| Cd | 228.8 | 250 | 1500 | 4 | 3 |
| Co | 240.7 | 800 | 2500 | 6 | 80 |
| Cr | 357.9 | 900 | 2500 | 6 | 40 |
| Cu | 324.8 | 700 | 2500 | 6 | 70 |
| Fe | 248.3 | 900 | 2500 | 6 | 50 |
| Mn | 279.5 | 900 | 2500 | 6 | 25 |
| Mo | 313.3 | 1200 | 2500 | 8 | 120 |
| Ni | 232.0 | 800 | 2500 | 8 | 220 |
| Pb | 283.3 | 500 | 2100 | 4 | 30 |
| Sr | 460.7 | 600 | 2500 | 8 | 80 |
| V | 318.4 | 1300 | 2500 | 8 | 600 |
| Zn | 213.9 | 400 | 2000 | 5 | 1.3 |

[a] Temperatures represent the meter settings on the control panel of the power supply. [b] Mass for 0.0044 absorbance with the purge gas flow in the normal mode excepting for Al, Cd, Pb, and Zn for which the interrupt mode was used. Except for Al when argon was used as the purge gas, for all other elements nitrogen was used as the purge gas.

For the determination of a particular metal, 5-, 50-, or 100-μL volumes (depending on the sensitivity of the metal) of samples were introduced into the graphite furnace with an Eppendorf syringe fitted with disposable plastic tips. Prior to use, the tips were decontaminated from traces of metals by soaking them for 24 h in 5% nitric acid (Baker Ultrex), followed by four rinses with Ultrapure water. The sequential "dry", "char", and "atomize" program of the HGA-2000 was followed, and the peak absorbance noted. The results of five replicate analyses of each test solution per container were averaged. The cumulative averages from the two containers for each metal at each pH were then used to draw the plots of % loss of metal vs. time. These plots obtained for each metal in the natural water sample were then compared with those in the synthetic water samples to determine the change in loss, if any, due to difference in the composition between the natural water and the synthetic water samples.

The amount of each trace metal in the river water sample immediately after collection, and at time intervals of 1, 2, 3, 4, 5, 10, 20, and 30 days were obtained by reference to linear working curves prepared using a series of standard aqueous solutions of each metal, acidified to pH 1.0 using $HNO_3$ (Baker Ultrex). At this pH, the standard solutions were found to be stable at least for one day. Nevertheless, compensation for small changes in the working curve due to conditions beyond the control of the analyst was made by running the standards at pH 1.0 at about 30-min intervals during the analytical run. Also, on the days when the water samples were tested, a fresh calibration curve was prepared using a series of fresh (aqueous) standard solutions at pH 1.0. The relative standard deviation of each point in the calibration curve was 2–3%.

The concentrations of the trace metals in the synthetic water samples immediately after spiking and at the above time intervals were determined. The calibration curve obtained with aqueous standards was used for determining the concentration of the trace metals in synthetic water samples because it was found that the aqueous samples and synthetic water samples with the same analyte concentration gave the same instrumental response within the limits of experimental error, i.e., no interference was observed

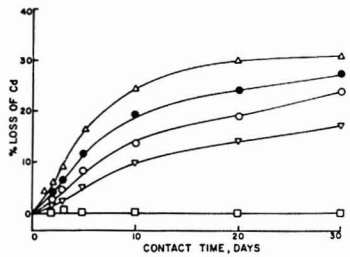


**Figure 1.** Loss of cadmium from Pyrex glass and Nalgene containers. Rideau River water sample (0.12 μg/L Cd); Pyrex glass: (□) pH 1.6, 2.5, 4.0; (●) pH 6.0; (△) pH 8.0. Nalgene: (□) pH 1.6, 2.5, 4.0, 6.0, 8.0. Synthetic water sample (0.10 μg/L Cd); Pyrex glass: (□) pH 1.6, 2.5, 4.0; (▽) pH 6.0; (○) pH 8.0. Nalgene: (□) pH 1.6, 2.5, 4.0, 6.0, 8.0

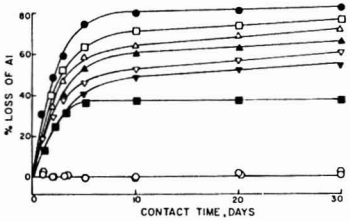


**Figure 2.** Loss of aluminum from Pyrex glass and Nalgene containers. Rideau River sample (230 μg/L Al); Pyrex glass: (○) pH 1.6, 2.5; (▽) pH 4.0; (□) pH 6.0; (●) pH 8.0 Nalgene: (○) pH 1.6, 2.5; (■) pH 4.0, 6.0, 8.0. Synthetic water sample (200 μg/L Al) Pyrex glass: (○) pH 1.6, 2.5; (▼) pH 4.0; (▲) 6.0; (△) pH 8.0. Nalgene: (○) pH 1.6, 2.5; (■) pH 4.0, 6.0, 8.0

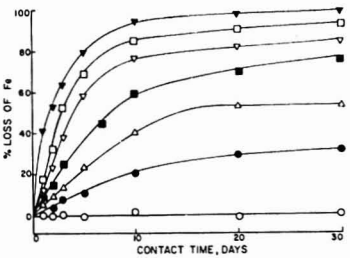


**Figure 3.** Loss of iron from Pyrex glass container. Rideau River water sample (170 μg/L Fe): (○) pH 1.6; (●) pH 2.5; (■) pH 4.0; (□) pH 6.0; (▼) pH 8.0. Synthetic water sample (150 μg/L Fe): (○) pH 1.6; (●) pH 2.5; (△) pH 4.0; (▽) pH 6.0, 8.0

with the synthetic water samples. No such tests could be made with the natural water samples since an accepted standard natural water sample was not available. However, the values obtained for the trace metals in natural water samples using the above calibration curve method and the standard addition method are in good agreement. Therefore, the day-to-day concentrations of the trace metals in the natural water samples were also determined by reference to the calibration curve obtained using aqueous standard solutions.

## RESULTS AND DISCUSSION

Table I presents analytical lines and operating conditions used for graphite furnace atomic absorption spectrometry. Table II presents results of analysis of water samples by graphite furnace atomic absorption spectrometry. Figures 1–7

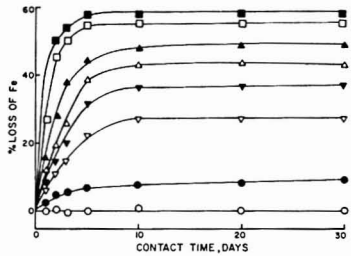


**Figure 4.** Loss of iron from Nalgene container. Rideau River water sample (170 μg/L Fe): (○) pH 1.6; (●) pH 2.5; (▼) pH 4.0; (▲) pH 6.0; (■) pH 8.0. Synthetic water sample (150 μg/L Fe): (○) pH 1.6; (●) pH 2.5; (▽) pH 4.0; (△) pH 6.0; (□) pH 8.0

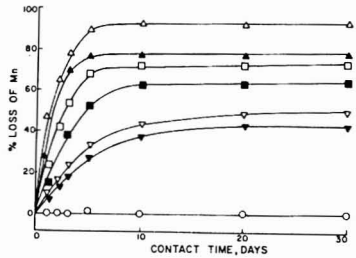


**Figure 5.** Loss of manganese from Pyrex container. Rideau River water sample (30 μg/L Mn): (○) pH 1.6, 2.5; (▽) pH 4.0; (□) pH 6.0; (△) pH 8.0. Synthetic water sample (25 μg/L Mn): (○) pH 1.6, 2.5; (▼) pH 4.0; (□) pH 6.0; (▲) pH 8.0

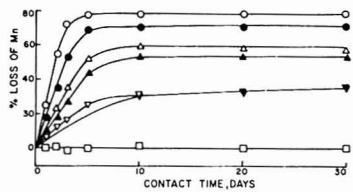


**Figure 6.** Loss of manganese from Nalgene container. Rideau River water sample (30 μg/L Mn): (□) pH 1.6, 2.5; (▽) pH 4.0; (△) pH 6.0; (○) pH 8.0. Synthetic water sample (25 μg/L Mn): (□) pH 1.6, 2.5; (▼) pH 4.0; (▲) pH 6.0; (●) pH 8.0

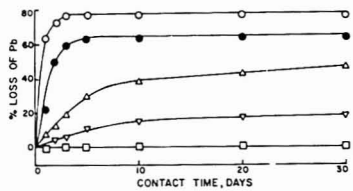


**Figure 7.** Loss of lead from Pyrex glass and Nalgene containers. Rideau River water sample (4 μg/L Pb); Pyrex glass and Nalgene containers: (□) pH 1.6; (△) pH 2.5, 4.0; (○) pH 6.0, 8.0. Synthetic water sample (5 μg/1 Pb); Pyrex glass and Nalgene containers: (□) pH 1.6; (▽) pH 2.5, 4.0; (●) pH 6.0, 8.0

show the percent loss of Cd, Al, Fe, Mn, and Pb from synthetic and river water samples stored in Pyrex glass and Nalgene linear polyethylene containers at various pH values as a

Table II. Results of Analysis of Water Samples by Graphite Furnace Atomic Absorption Spectrometry

| Element | Rideau river sample,[a] concn found, μg/L[b] | Synthetic water sample: Concn added, μg/L | Synthetic water sample: Concn found, μg/L[b] |
|---|---|---|---|
| Ag | not detectable | ... | ... |
| Al | 230 (229) | 200 | 198 (196) |
| Cd | 0.12 (0.15) | 0.1 | 0.1 (0.1) |
| Co | 1.6 (1.5) | 2 | 2 (2) |
| Cr | 0.5 (0.6) | 1 | 1 (1) |
| Cu | 1.4 (2.0) | 2 | 2 (2) |
| Fe | 170 (168) | 150 | 148 (149) |
| Mn | 30 (32) | 25 | 26 (26) |
| Mo | not detectable | ... | ... |
| Ni | 7 (6) | 5 | 6 (5) |
| Pb | 4.3 (4) | 5 | 5 (5) |
| Sr | 42.5 (44.0) | 50 | 48 (47) |
| V | not detectable[c] | ... | ... |
| Zn | 2.8 (3.0) | 5 | 5 (5) |

[a] Samples collected on October 18, 1974. [b] Concentrations given in parentheses were obtained by the method of standard additions. All other values were obtained by the calibration curve method using metal standards in aqueous solutions acidified to pH 1.0. The average of the values obtained by the calibration curve method and standard addition methods is taken to represent the initial concentration of each analyte. The % loss reported in Figures 1-8 for each element was obtained by reference to these initial concentrations. The relative standard deviation is 2-3%. [c] No signal from 200-μL samples.

function of time. The percent loss of each element was determined with reference to the initial measured concentration of each element given in Table II. As can be seen from these Figures, storage of synthetic and river water samples in Pyrex and Nalgene containers resulted in no loss for Al, Fe, and Pb at pH <1.5, for Mn at pH <2.5, for Cd, and Cu (no Figure) at pH <4.0, and for Cr, Ni, and Sr (no Figure) at pH <8.0. The stability of these metals in solution may be due to the absence of any biological transformation or lack of formation of any colloidal or ion-exchangeable species likely to be adsorbed by the container surface (*14*). Calculations based on stability constant values (*15*) show that Al, Cu, Cd, Fe, Mn, and Pb exist in solution as aquo ion, and Cr, Ni, and Sr remain in solution in complexed or anionic form (*16*) at the pH's stated above.

As can be seen from Figures 2-7, losses were observed for Al, Fe, and Pb at pH > 1.5, for Mn at pH > 2.5, and for Cu (no Figure) at pH > 4.0, when both synthetic and river water samples were stored in Nalgene or Pyrex glass containers. The following features of Figures 2-7 are worth noting; explanation of some of these features is offered below.

(i) Most of the losses for the above metals (except copper) occurred within 5 days of storage. Virtually no further loss occurred up to 30 days of storage. In the case of copper, most of the loss (35% at pH 6.0, and 50% at pH 8.0) occurred in one day, and no further loss was observed up to 30 days.

(ii) The amount lost increased with increasing pH irrespective of the composition of the water samples, and the nature of the container. Thus, in Pyrex glass containers, the percent loss in 30 days from river water samples at pH 4.0, 6.0, and 8.0 was: for aluminum—53, 70, and 81, respectively (Figure 2); for iron—54, 78, and 85 (Figure 3); for manganese—43, 72, and 90 (Figure 5); and for lead—48, 62, and 76 (Figure 7). The corresponding loss from synthetic samples was: for aluminum—49, 60, 65 (Figure 2); for iron—37, 70, and 70 (Figure 3); for manganese—35, 62, and 77 (Figure 5); and for lead—same as for river water samples (Figure 7). In Nalgene containers, the percent loss in 30 days at pH 4.0, 6.0, and 8.0 was: for iron—32, 44, and 58 (river water samples), and 22, 39, and 55 (synthetic water samples), respectively (Figure 4); for manganese—32, 60, and 78 (river water samples), and 32, 53, and 70 (synthetic water samples), respectively (Figure 6). Since the amount of adsorption generally increases with increasing pH (*17*), it is probable that the increasing loss of the metals with the increasing pH is due to adsorption by the container surface of hydroxo or carbonato complexes of metals which predominate with increasing pH. Based on stability constant values (*15*), the various species may be identified as: colloidal hydrated aluminum oxide in the case of aluminum; $CuHCO_3^+$ and $CuCO_3$ at pH 6.0, and $Cu(CO_3)_2^{2-}$ at pH 8.0 in the case of copper; and $CdHCO_3^+$ at pH 6.0, and $CdCO_3$ at pH 8.0 in the case of cadmium. Benes and Smetana (*18*), who observed significant loss of iron ($10^{-7}$ to $10^{-5}$ M) above pH 3.0 (e.g., ~98% at pH > 6.6) attributed the loss to chemisorption of $FeOH^{2+}$ and $Fe(OH)_2^+$ in the pH range from 2 to 5, and of colloidal hydrous ferric oxide above pH 5. The loss of iron observed in the present study may be explained similarly. Jenne (*19*) has reported that hydrous manganese oxides are to remain coated on silicate surfaces. It is probable that the loss of manganese in the present study may be due to adsorption of the hydrous oxide on the container surface, especially the glass surface.

(iii) At a given pH, loss of metals from river water samples was always higher than from synthetic water samples (Figures 1-6). This is probably due to the greater biological activity of the river water samples. Additionally, in the case of iron, the organic acids (e.g., humic acids) in river waters have been reported (*20*) to hold the iron as peptized sols above pH 5; the rate of adsorption of these iron-organic colloids by the container walls may be greater than that of the inorganic iron sols. Similarly, the smaller concentration of cadmium in the river water samples (0.12 μg/L) than in the synthetic water samples (1.00 μg/L) may be responsible for the greater loss of cadmium from the river water samples (26% at pH 6.0, and 31% at pH 8.0 in 30 days) than from the synthetic water samples (17% at pH 6.0, and 24% at pH 8.0 in 30 days) (*21*).

(iv) Loss of metals from the Pyrex glass containers was higher than from the Nalgene linear polyethylene containers (Figures 1-6). For example, cadmium showed no loss on storage of synthetic water samples, and river water samples in Nalgene linear polyethylene containers at pH < 8.0 (Figure 1). King et al. (*5*) also observed no loss for two weeks on storing an aqueous solution of 25 ng/mL of cadmium in polyethylene, polypropylene, and poly(vinyl chloride) containers in the pH range from 3 to 10. There was considerable loss on storage of samples in Pyrex glass containers (Figure 1). Struempler (*22*) also found that an aqueous solution containing 1 ng/mL cadmium stored in borosilicate glass containers showed a 20% loss in 20 days of storage. The maximum loss of aluminum from river water samples and synthetic water samples stored in Nalgene linear polyethylene containers for 30 days was 35% in the pH range from 4.0 to 8.0 (Figure 2). The loss on storage in Pyrex glass was 81% from river water samples, and 65% from synthetic water samples, at pH 8.0 in 30 days. As discussed in section ii, similar results were obtained for iron and manganese. The difference in the nature of surface of the Pyrex glass and the Nalgene linear polyethylene may be responsible for the difference in the amount of metal species adsorbed.

Synthetic and river water samples containing zinc could not be stored in Pyrex glass or Nalgene linear polyethylene containers because of the continuous increase in the concentration of zinc in the sample solution on storage in these containers. Pyrex glass and Nalgene linear polyethylene containers have been reported to contain 730 ng/mL and 28 ng/mL zinc, respectively (*23*). Also, Struempler (*22*) could

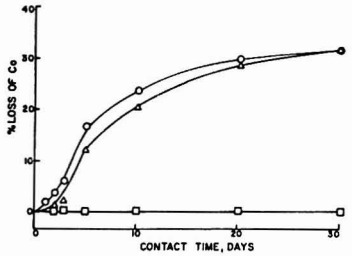


**Figure 8.** Loss of cobalt from Pyrex glass and Nalgene containers. Rideau River water sample (1.6 μg/L Co); Pyrex glass: (□) pH 1.6; (○) pH 8.0. Nalgene: (□) pH 1.6, 8.0. Synthetic water sample (2.0 μg/L Co); Pyrex glass: (□) pH 1.6; (△) pH 8.0. Nalgene: (□) pH 1.6, 8.0

not preserve dilute aqueous solutions containing 100 ng/mL zinc in polypropylene containers because of severe contaminations by zinc. Since Teflon containers were found to be free of contamination from zinc (*24*), they were used in the present study. Samples stored in these containers showed no loss of zinc in the pH range from 1.5 to 8.0 for at least 30 days. It seems that the various species of zinc (based on stability constant values (*15*)), which predominate in various pH's, viz., Zn(II) aquo ion at pH < 4.0, $ZnHCO_3^+$ and $ZnCO_3$ at pH 6.0, and $ZnCO_3$ at pH 8.0, are not adsorbed by the surface of Teflon.

Figure 8 presents the loss of Co from Pyrex glass and Nalgene linear polyethylene containers. Like Cd, Co showed no loss on storage of synthetic and river water samples in Nalgene linear polyethylene containers in the pH range from 1.5 to 8.0. Results were, however, different when synthetic and river water samples containing Co were stored in Pyrex glass containers. As seen in Figure 8, no loss of Co was observed at pH 1.5. However, at pH 8.0, the loss of Co was initially linear, reaching values of 12% and 16% in 5 days for synthetic and river water samples, respectively. Beyond 5 days, the rate of loss was much smaller—29% in 20 days and 32% in 30 days for both synthetic and river water samples. As in the case of cadmium, the loss of cobalt was probably due to adsorption of some cobalt species, e.g., hydroxo or carbonato species formed by Co(III) (after oxidation of Co(II) to Co(III)).

## CONCLUSIONS

Since appreciable amounts of trace metals can be lost from unpreserved samples of natural waters, caution should be exercised in interpreting the results of analysis of such samples. The best method of preservation seems to be acidification of the samples with nitric acid to a pH ≤ 1.5, and storage in Pyrex glass or Nalgene linear polyethylene containers (except in the case of zinc, for which Teflon is the only suitable container). However, since Nalgene linear polyethylene is less expensive, lighter, more durable, and easier to handle than Pyrex glass, it is the preferred material for containers for natural water samples.

## LITERATURE CITED

(1) G. G. Eichholz, A. E. Nagel, and R. B. Hughes, *Anal. Chem.*, **37**, 863 (1965).
(2) D. E. Robertson, *Anal. Chim. Acta*, **42**, 533 (1968).
(3) R. A. Durst and B. T. Duhart, *Anal. Chem.*, **42**, 1002 (1970).
(4) H. S. Posselt and W. J. Webber, "Environmental Chemistry of Cadmium in Aqueous Systems", *Tech. Rep.*, T-71-1, University of Michigan, Ann Arbor, Mich., 1971.
(5) W. G. King, J. M. Rodriguez, and C. M. Wai, *Anal. Chem.*, **46**, 771 (1974).
(6) E. F. McFarren and R. J. Lishkar, *Adv. Chem. Ser.*, **73**, 253 (1968).
(7) A. O. Rathje, *Am. Ind. Hyg. Assoc. J.*, **30**, 126 (1969).
(8) M. R. Greenwood and T. W. Clarkson, *Am. Ind. Hyg. Assoc. J.*, **31**, 250 (1970).
(9) R. D. Edgar, *At. Absorpt. Newsl.*, **12**, 151 (1973).
(10) R. V. Coyne and J. A. Collins, *Anal. Chem.*, **44**, 1093 (1972).
(11) C. Feldman, *Anal. Chem.*, **46**, 99 (1974).
(12) R. M. Rosain and C. M. Wai, *Anal. Chim. Acta*, **65**, 279 (1973).
(13) H. H. Dobson, "Principle Ions and Dissolved Oxygen in Lake Ontario", Reprint Series No. 32, Department of Energy, Mines and Resources, Ottawa, Canada, 1967.
(14) L. J. Stryker and E. Matijevic, *Adv. Chem. Ser.*, **79**, 44 (1968).
(15) W. Stumm and J. J. Morgan, "Aquatic Chemistry", Wiley-Interscience New York, N.Y., 1970, pp 167–221.
(16) P. Beneš and E. Steinnes, *Water Res.*, **9**, 741 (1975).
(17) P. Beneš and I. Rajman, *Collect. Czech. Chem. Commun.*, **34**, 1375 (1969).
(18) P. Beneš and J. Smetana, *Collect. Czech. Chem. Commun.*, **34**, 1360 (1969).
(19) E. A. Jenne, *Adv. Chem. Ser.*, **73**, 337 (1968).
(20) J. Shapiro, *J. Am. Water Works Assoc.*, **56**, 1062 (1964).
(21) G. Tölg, *Talanta*, **19**, 1489 (1972).
(22) A. W. Struempler, *Anal. Chem.*, **45**, 2251 (1973).
(23) D. C. Burrell, "Atomic Spectrometric Analysis of Heavy-metal Pollutants in Water", Ann Arbor Press, Ann Arbor, Mich., 1974, p 97.
(24) D. E. Robertson, in "Ultrapurity", M. Zief and R. Speights, Ed., Marcel Dekker, New York, N.Y., 1972, pp 208-250.

RECEIVED for review May 17, 1977. Accepted November 18, 1977. The authors are grateful to Environment Canada for a three-year research agreement in support of this study. One of the authors (J.E.S) is indebted to the Ministry of Education, Government of Spain, for a postdoctoral fellowship.

# Radioimmunoassay of Calcitonin in Normal Human Urine

**Richard H. Snider,* Charles F. Moore, Omega L. Silva, and Kenneth L. Becker**

*Metabolic Research Laboratory (688/151J), Veterans Administration Hospital, 50 Irving Street, NW, Washington, D.C. 20422*

**Direct radioimmunoassay of calcitonin in human urines containing ≤3 ng/mL is complicated by interference from substances most probably structurally similar to the methylated xanthines. A simple, reproducible procedure is described for the removal of the interfering substances prior to radioimmunoassay. Utilizing this procedure and a sensitive antiserum specific for the carboxyl terminal region of calcitonin, it has been possible to obtain precise estimates of calcitonin concentrations in the urine over the range, 0.02–3.0 ng/mL within which calcitonin is found in normal urine. The intra- and interassay $s/\bar{X}$ were 5 and 15%, respectively. The urine calcitonin values apparently reflect serum calcitonin concentrations (e.g., urine/serum $r = 0.9873$ for 40 hypercalcitonemic patients); but urine calcitonin determination has two important advantages: greater reproducibility because of decreased heterogeneity and greater differentiation of patient populations. In view of these results, the assay of urine calcitonin may prove to be a very useful clinical tool.**

Since the discovery of the hypocalcemic, hypophosphatemic polypeptide hormone calcitonin (CT), by Copp (*1*) in 1961, much effort has been directed toward the development of techniques for its measurement in biologic fluids. Much of the uncertainty over serum concentrations in normals as determined by radioimmunoassay (RIA) appears to emanate from size- and immuno-heterogeneity of the hormone as well as the presence of interfering substances (*2*).

In 1971 Voelkel and Tashjian (*3*) reported finding hypocalcemic activity in the urine of patients with medullary thyroid cancer (MTC). Later Melvin and co-workers (*4*) found that the hypocalcemic activity in the urine was immunochemically similar to human CT and co-eluted with the synthetic hormone on short G-75 Sephadex columns.

We have developed a simple, reproducible technique for the assay of CT in human urine which should yield consistent interlaboratory results provided that the same standards and assay conditions are utilized. Urinary CT concentrations appear to reflect CT concentrations in the serum (particulary for patients with hypercalcitonemia) and they afford an earlier indication of an increased production rate or metabolic clearance of the hormone, and permit the study of physiologic changes which may not be detected in the serum.

## EXPERIMENTAL

**Collection and Storage of Samples.** Serum from fasting patients was collected in 13 × 100 mm non-siliconized glass tubes (Venoject; Kimble-Terumo, Elkton, Md. 21921) and stored at −20 °C until assayed.

Urine from fasting patients was collected in polyethylene or flint glass receptacles containing sufficient $NH_4HCO_3$ to maintain a pH ≥ 7.5. Usually the first morning urine was discarded, and the urine for assay was collected over a fixed period of time (1–2 h). One-mL aliquots of the urine are stored at −20 °C until assayed.

**Radioimmunoassay of Serum CT.** Synthetic human CT (see Acknowledgment) was labeled to a specific activity of 150–250 μCi/μg utilizing a modification of the Hunter–Greenwood chloramine-T method (*5*). Non-equilibrium and equilibrium assays were performed with carboxyl terminal antiserum Ab-IV and midportion antisera Ab-II and Ab-III as previously described (*2*). A new midportion antiserum Ab-IIIb very similar to Ab-III, but 2–3 times more sensitive (based on 50% $[B/B_0]$ in a logit–log plot of the standard curve) than Ab-IV was also utilized. Calculated from Scatchard plots (*6*), the dissociation constants ($K_{Diss}$) were $\sim 3.2 \times 10^{-11}$ M for Ab-IV and $\sim 1.0 \times 10^{-11}$ for Ab-IIIb, and the binding site concentrations were $\sim 2.3 \times 10^{-11}$ M for Ab-IV and $\sim 7.6 \times 10^{-12}$ M for Ab-IIIb. Serum aliquots of ≤50 μL were used for most assays. Beckman CT (according to Beckman, their 0.5-mg vial (lot #B0903) contains 0.58 mg human CT) was utilized to generate the data in this paper. This standard yields slightly lower concentrations (~20%) than we have reported in earlier papers using Organon CT standards.

**Purification of Urine Samples.** The 1-mL aliquot for RIA was boiled for 3 min and dextran blue (B-2000, 2 000 000 daltons; Sigma Chemical Co., 3500 DeKalb Street, St. Louis, Mo. 63118) added. The boiled urine was passed through a 6 × 220 mm glass column containing 5 mL polyacrylamide gel (Bio-Gel P-2; 100–200 mesh; Bio-Rad Laboratories, 32nd and Griffin, Richmond, Calif. 94804) suspended in 0.1 M $NH_4HCO_3$ at pH 7.5. The blue void volume was collected in a 7-mL non-siliconized glass tube, lyophilized, and reconstituted in 2 mL of 1% (w/v) human serum albumin (Cutter Labs, Inc. Berkeley, Calif. 94710) in buffer containing 0.15 M NaCl and 0.13 M $H_3BO_3$ at pH 7.5. Columns were rinsed with 1 M HCl and repacked before use. Urines containing ≥10 ng/mL were not purified.

**Radioimmunoassay of Urine CT.** The assay was carried out as described for serum except for the addition of 10% guinea pig or hypocalcitonin human serum. The addition of guinea pig serum accomplished two functions: assay sensitivity was increased (*2*) and the occasional non-parallelism of dilution curves for urine CT component U-2 as compared to the standard curve was eliminated.

The boiled and gel filtered urine which was reconstituted to 2 mL is assayed in aliquots of 10–200 μL. Urine column fractions were assayed as described for serum fractions.

**Permeation Gel Chromatography.** Urine samples were chromatographed on 3 × 110 cm glass columns containing 800 mL G-75 superfine Sephadex suspended in 0.1 M $NH_4HCO_3$ at pH 7.5 or 0.1 M $NH_4O_2CH$ at pH 4.7. The sample was eluted in 6.4-mL aliquots (7–8 aliquots/0.1 $K_d$) which were assayed and the concentrations were plotted graphically as described previously for serum (*2*).

**Concentration of Urine CT for Permeation Gel Chromatography on G-75 Sephadex Columns.** Concentration of the CT in urine samples containing more than 200 pg/mL was unnecessary; however, the following procedures were utilized on some high CT as well as low CT samples to determine recoveries.

*Trichloroacetic Acid Precipitation of Protein.* Urine CT was co-precipitated with urine proteins by the addition of 10% trichloroacetic acid as described by L. Constan and co-workers for proinsulin and insulin (*7*).

*Petroleum Ether Emulsion.* Alkaline urine was added to 300 mL petroleum ether (ACS grade), (bp 35–60 °C, Fisher Scientific Co., Silver Spring, Md. 20910) in a 2-L separatory funnel. The funnel was shaken vigorously for 2 min and the two phases were allowed to separate. An emulsion formed at the interface. The ether and aqueous phases were removed and the emulsion was dried by flash evaporation. The dried emulsion, which contained 20–30% of the total CT, was dissolved in 10 mL 0.1 M $NH_4HCO_3$ buffer, pH 7.5, and freeze dried. A modification of the above procedure utilized for urine from some MTC patients was to add 1 mL normal human serum and to reextract following emulsion formation with three more 300-mL portions of petroleum ether.

This paper not subject to U.S. Copyright. Published 1978 by the American Chemical Society

Table I. Serum iCT Compared to Urine iCT for MTC Patients

| Sample | Serum iCT, ng/mL | Urine iCT ng/mL (A) | Urine iCT ng/mg Creatinine (B) | Ratio (A)/serum | Ratio (B)/serum |
|---|---|---|---|---|---|
| 1 | 0.19 | 3.5 | 2.3 | 18 | 15 |
| 2 | 0.62 | 36 | 15 | 58 | 24 |
| 3 | 0.62 | 2.2 | 14 | 3.5 | 23 |
| 4 | 1.2 | 78 | 38 | 65 | 32 |
| 5 | 1.3 | 46 | 26 | 35 | 20 |
| 6 | 1.4 | 35 | 26 | 25 | 19 |
| 7 | 9.0 | 250 | 95 | 28 | 11 |
| 8 | 14 | 210 | 480 | 15 | 34 |
| 9 | 19 | 380 | 360 | 20 | 19 |
| 10 | 50 | 1230 | 830 | 25 | 17 |
| 11 | 50 | 1940 | 1020 | 39 | 20 |
| 12 | 150 | 3650 | 3950 | 24 | 26 |
| Mean | | | | 28 | 22 |
| (± S.D.) | | | | ±18 | ±7 |
| Correlation ($r$) | | | | 0.9815 | 0.9897 |

This procedure recovered 55% of the urine CT.

**Creatinine Determinations.** Creatinine was assayed in aliquots of urine as described by Henry (*8*).

**Isoelectric Focusing.** Sucrose density gradient isoelectric focusing was carried out in various pH ranges at ~20 °C on a 110-mL LKB 8101 column (LKB-Produkter AB, Bromma 1, Sweden) essentially as described by Haglund (*9*).

## RESULTS AND DISCUSSION

**Radioimmunoassay of CT in Urine.** Initially, Melvin and co-workers (*4*) indicated that ≤25 μL of urine could be radioimmunoassayed directly. In our laboratory, urine samples from MTC and other hypercalcitonemic patients containing ≥3 ng/mL CT did yield results by direct RIA (in aliquots ≤5 μL) which were consistent with results obtained following gel filtration of the urine on our long G-75 Sephadex columns (Figure 1, a and b). The principal fraction of immunoreactive calcitonin (iCT) in most MTC urines, U-2, had an apparent molecular size of 5400 daltons on pH 7.5 columns and 4500 daltons on pH 4.7 columns and was best recognized by carboxyl terminal antisera (3–5 times better than midportion recognizing antisera). The apparent molecular size of U-2 on the pH 7.5 columns is altered following pretreatment with acid or base. Pretreatment of the 5400 dalton fraction with acid yielded the 4500 dalton fraction. Pretreatment of the 4500 dalton fraction with 1 N $NH_4OH$ at 55 °C for 1 h yielded a 5400 dalton fraction. Guanidine hydrochloride, 5 M, at pH 4.7, had no effect on the apparent molecular size of U-2 except the effect described above for low pH. It should be noted that synthetic $^{125}$I-HCT added to urine eluted with apparent molecular size of 3500 daltons and its $K_d$ was unaffected by the pH of the columns or pretreatment with acid or base. Salmon CT (excreted by patients receiving salmon CT therapy for hypercalcemia) eluted with a $K_d$ much closer to that of synthetic salmon CT monomer. Fraction U-1 (~8000 daltons) was recognized as well or better by midportion antisera as by carboxyl terminal antisera. Because of the greater recognition of the principal MTC urine fraction, U-2, by carboxyl terminal antisera, Ab-IV, a carboxyl terminal antiserum was chosen for most of our urine studies. Although most normal urines tested in our laboratory produced only 5–10% damage of $^{125}$I-HCT in 24 h (as determined by binding to excess antibody), $NH_4HCO_3$ was added to all urines in order to prevent the degradation of urine CT which occurs at low pH (*3*). Basal and post stimulation concentrations of urine CT were correlated better with serum CT concentrations when the urine CT was expressed as ng CT/mg creatinine (Table I). The correlation, $r$, for 40 basal urine/serum concentrations for MTC patients was 0.9873.

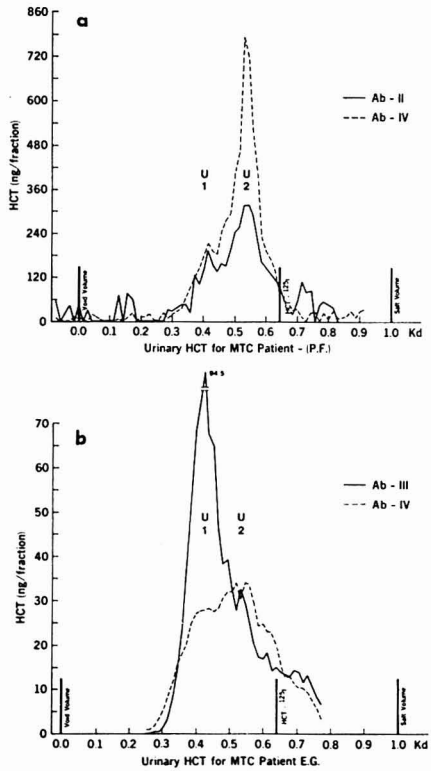


Figure 1. (a) Urine from MTC patient having mostly U-2 fraction of calcitonin. (b) Urine from MTC patient having mostly U-1 fraction of calcitonin

Despite the good results obtained for direct RIA of CT in the urine of patients with hypercalcitonemia, difficulties were encountered in trying to determine the CT concentrations in the urine of normals and patients who had had thyroidectomy (Thx). Direct RIA of urines from these patients in aliquots

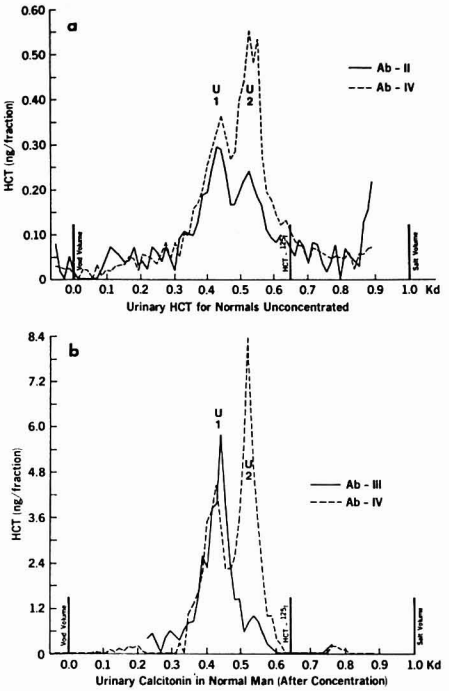


**Figure 2.** (a) Unconcentrated urine of a normal person. (b) Concentrated urine calcitonin (trichloroacetic acid) of a normal person from urine utilized for 2a

Table II. Compounds Interfering with RIA of iCT with Carboxyl Terminal Antisera

| Interfering compound | Apparent iCT in ng iCT/mg interfering compound |
|---|---|
| Caffeine (1,3,7-trimethylxanthine) | 2.9 |
| Paraxanthine (1,7-dimethylxanthine) | 2.1 |
| Theophylline (1,3-dimethylxanthine) | 1.5 |
| Theobromine (3,7-dimethylxanthine) | 0.9 |
| 7-Methylxanthosine | 0.9 |
| Guanosine | 0.3 |
| Creatinine | 0.1 |
| DNA | 0.1 |
| Deoxyadenosine | 0.06 |
| Thymidine | 0.05 |
| Urea | Does not interfere at $<50$ $\mu$L urine |
| Xanthine | Mostly insoluble; interferes slightly |
| Uric acid | Mostly insoluble; interferes slightly |
| Bilirubin | Mostly insoluble; binds label |
| Proline | 0 |
| Histidine | 0 |
| Creatine | 0 |
| Hemocyanin (Keyhole Limpet) | 0 |

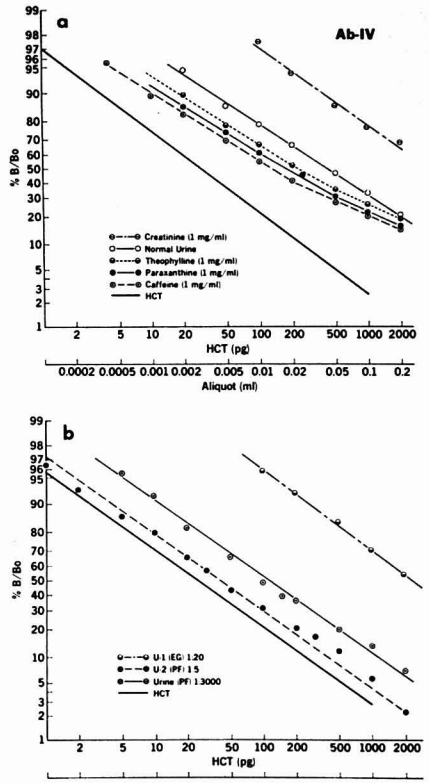


**Figure 3.** (a) Dilution curves for interfering substances compared to the standard curve in the radioimmunoassay. (b) Dilution curves for U-1, U-2 (without hypocalcitonin serum), and a diluted urine (PF) which had high concentration of iCT compared to the standard curve

of 10–20 $\mu$L did not correlate well with results for gel filtration of the unconcentrated urine on our long G-75 Sephadex columns. As shown in Figure 2, a and b, two fractions of CT were found in the urine of normals which corresponded both in apparent molecular size and antibody recognition to those found in MTC patients; however, the total amount obtained for the gel filtration fractions from normals did not correspond to the amount found by direct RIA. The average displacement of $^{125}$I-HCT from antibody for 20-$\mu$L aliquots of urine from 23 normals was 25.2% (% $B/B_0 = 74.8 \pm 8.4$), which would correspond to a mean CT of 0.44 ng/mL. The average displacement of $^{125}$I-HCT from excess antibody added at the end of the routine RIA incubation period was 2.9% (% $B/B_0 = 97.1 \pm 2.2$) indicating that damage to label did not account for much of the observed displacement. Dextran-coated charcoal (*10*) extracted urine, in 20-$\mu$L aliquots, displaced only 8.6% (% $B/B_0 = 91.4 \pm 7.2$) $^{125}$I-HCT from antibody in routine RIA; therefore, most of whatever interfered in the RIA as well as the CT was extracted. Chromatography on the long G-75 Sephadex columns revealed that the source of interference was of small molecular size (eluting in the salt fraction). A series of known constituents of the urine as well as analogues were tested in the RIA system with the results shown in Figure 3a and Table II. It should be noted that the

urine in Figure 3a was found to contain only 0.035 ng/mL of actual CT. Interestingly, the methylated xanthine, caffeine, was the most potent interfering substance producing significant displacement of $^{125}$I-HCT from antibody even at the 500-ng level. Since caffeine and other methylated xanthines are contained in many food and beverage products and are excreted with their metabolites in the urine (*11*), these compounds may account for much of the interference. Chloroform removed some, but not all, of the interfering substances from the urine. The interference produced by the methylated xanthines is region specific, affecting carboxyl terminal but not midportion recognizing antisera. The methylated xanthines and creatinine interfered in equilibrium as well as non-equilibrium assays. Figure 3b gives dilution curves for U-1, U-2 (without hypocalcitonin serum), and MTC urine as compared to the standard curve.

**Radioimmunoassay of CT in Gel Filtered Urine.** In order to assay small amounts (≤3 ng/mL) of CT in the urine by RIA, a method for separating CT from the interfering substances was developed which satisfied 4 objectives: (1) the method was rapid and simple; (2) the recovery was ≥90%; (3) replicate samples and identical antisera yielded reproducible results; (4) and the levels determined on purified samples corresponded to the amounts found in CT fractions for the same urine samples on long Sephadex columns.

Simkin (*12*) had previously reported using the affinity of purines for polyacrylamide gel to separate serum uric acid on Bio-Gel P-2 columns. Because the interfering substances were of small molecular size and were likely to be structurally similar to the purines, the gel filtration procedure described in the Experimental section was devised. When $^{14}$C-labeled caffeine was added to urine <0.2% appeared in the void volume when filtered through a Bio-Gel P-2 column. Furthermore, coffee drinking was not found to have any significant effect on the assay results when the urine was gel filtered. One additional modification in assay procedures was required. Although fraction U-1 diluted parallel to the standard curve in our standard assay buffer, fraction U-2 diluted slightly nonparallel to the standard curve. All fractions of urine CT could be made to dilute parallel to the standard curve by the inclusion of hypocalcitonin or guinea pig serum at a final concentration of 10% v/v. Although the reasons for this last observation are unknown, it is noteworthy that the effects of the interfering substances in the urine and of the methylated xanthines were significantly reduced by the inclusion of such serum; therefore, the serum was included in all urine assays to ensure consistent results over the usable dilution range of the assay. Boiling the urine was included as a step in the procedure because some (<5%) of the urines studied contained sufficient enzymes to degrade both the urine CT and the labeled CT during the assay. Boiling did not alter the concentrations of CT determined following filtration of the urine. For example, three 1-mL aliquots of urine from one normal patient contained 0.148 ± 0.017 (mean ± S.D.) ng/mL CT without boiling and 0.150 ± 0.031 ng/mL following boiling.

**Rapidity.** Ten or more of the Bio-Gel P-2 columns may be run simultaneously requiring 20 min for elution of the CT in the void volume; the 1-h total turnover time includes rinsing the columns with 1 N HCl and repacking with fresh polyacrylamide gel. The void volumes containing CT may be assayed directly or lyophilized and reconstituted in 2 mL of standard assay buffer for RIA.

**Recovery.** Two kinds of recovery experiments were done: high CT samples were assayed before and after passage through the polyacrylamide gel columns; and low CT samples with and without added amounts of synthetic CT and U-2 were assayed subsequent to filtration on polyacrylamide gel. Results for 11 MTC urines are shown in Table III. The average recovery for these urines was 96 ± 10%. Recoveries of added CT were similar. For example, a urine containing 0.149 ± 0.022 ng/mL (6 determinations) contained 0.201 ± 0.014 ng/mL (10 determinations) following the addition of 0.05 ng/mL to the urine. No detectable losses of urine CT were observed for alkaline urines from normal or MTC patients allowed to stand at room temperature for 24 h.

**Reproducibility.** Table IVa compares individual urine CT concentrations determined with two different carboxyl terminal antisera after gel filtration. The correlation, *r*, for the CT concentrations compared in Table IVa is 0.9999; while the correlations for the various categories of CT concentrations compared for the two antisera to date are given in Table IVb. When eight 1-mL aliquots of the same normal urine were filtered and assayed on two separate occasions the means ± S.D. were: 0.154 ± 0.008 and 0.154 ± 0.008 ng/mL, respectively. Thus the within assay relative standard deviation ($s/\bar{X}$) was only 5.2%. Similarly the interassay ($s/\bar{X}$) was 14.8% for 19 consecutive assays with Ab-IV. These results indicate that good interlaboratory reproducibility should be obtained using the techniques we have described, the same

**Table III. Recovery of iCT from Urine after Gel Filtration through Polyacrylamide (Bio-Gel P-2) Columns**

| Sample | Urine iCT, ng/mL: Unchromatographed | Urine iCT, ng/mL: Chromatographed | Recovery, % |
|---|---|---|---|
| 1 | 4.32 | 4.24 | 98 |
| 2 | 38.1 | 35.3 | 93 |
| 3 | 337 | 324 | 96 |
| 4 | 219 | 178 | 81 |
| 5 | 401 | 357 | 89 |
| 6 | 63 | 59 | 94 |
| 7 | 648 | 671 | 104 |
| 8 | 340 | 400 | 118 |
| 9 | 67 | 71 | 106 |
| 10 | 15.7 | 15.6 | 99 |
| 11 | 383 | 317 | 83 |

Av recovery = 96 ± 10%

**Table IVa. Comparison of Urine iCT Levels Determined with Two Different Carboxyl Terminal Antisera**

| Sample | Antiserum-A (Ab-IV) urine iCT, ng/mL | Antiserum-B urine iCT, ng/mL |
|---|---|---|
| 1 | 0.037 | 0.060 |
| 2 | 0.043 | 0.060 |
| 3 | 0.070 | 0.090 |
| 4 | 0.11 | 0.12 |
| 5 | 0.13 | 0.14 |
| 6 | 0.14 | 0.14 |
| 7 | 0.34 | 0.33 |
| 8 | 0.42 | 0.44 |
| 9 | 0.22 | 0.19 |
| 10 | 1.09 | 1.04 |
| 11 | 1.13 | 1.02 |
| 12 | 2.2 | 1.8 |
| 13 | 30 | 23 |
| 14 | 36 | 36 |
| 15 | 180 | 175 |
| 16 | 1950 | 1900 |

**Table IVb. Correlation of iCT Levels Determined with Two Different Carboxyl Terminal Antisera**

| Patients | No. | *r* | Slope | Intercept |
|---|---|---|---|---|
| Normal | 19 | 0.9894 | 0.8591 | 0.022 |
| MTC | 9 | 0.9987 | 0.9691 | 3.21 |
| All | 28 | 0.9988 | 0.9745 | 11.50 |

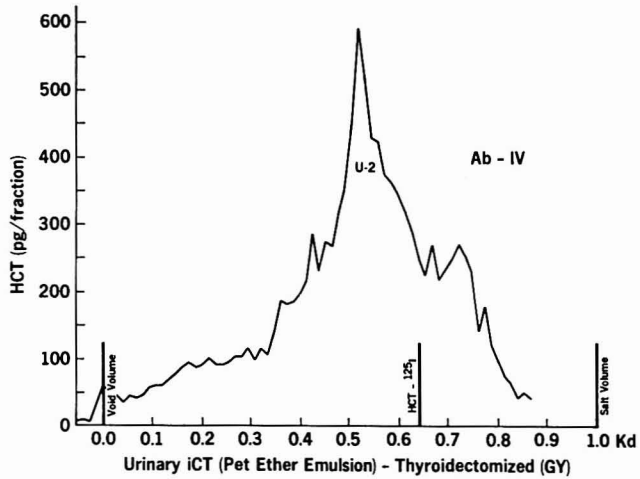


**Figure 4.** Concentrated urine calcitonin (Petroleum Ether Emulsion) of thyroidectomized patient

standards, and similar antisera. The correlations between urine CT concentrations determined with Ab-IV and those determined with Ab-IIIb were not as good as those obtained for the two carboxyl terminal antisera. The correlations were $r = 0.4078$ for 17 normals, $r = 0.8032$ for 24 MTC patients, and $r = 0.8765$ for all 44 patients studied. The very poor results for normals appears to result from the relatively greater proportion of CT recognized by midportion antiserum in their urines as compared to MTC urines.

**Validation of Post-Filtration Calcitonin Levels.** As shown in Table V for 10 Thx patients (9 male, 1 female) the concentrations of CT determined for filtered urines is lower than for unfiltered urines demonstrating that the interference from non-CT constituents in the urine is considerable. Although it was possible to demonstrate that the CT levels determined for some normal males who had ≥0.15 ng/mL of urine CT did correspond to the CT content of the iCT fractions obtained after the gel filtration of the unconcentrated urines of these individuals on our long Sephadex columns (e.g., Figure 2a), it was not possible to detect the low concentrations found in the unconcentrated urines of most Thx patients following gel filtration on the long Sephadex columns. Since it was necessary to determine whether the low levels determined for Thx following filtration of the urine were real or artifactual, the urine CT was concentrated in order to determine whether the apparent CT in Thx urine did correspond to the appropriate gel filtration fractions on the long Sephadex columns. The method first tried was extraction of CT from the urine with 10 mg/mL Quso G-32 (micro fine precipitated silica, Philadelphia Quartz Co., Valley Forge Executive Mall, Valley Forge, Pa. 19482) by mixing it with urine for 1 h followed by elution of CT with 20% acetone, 1% acetic acid in water (v/v). Although this procedure has been used successfully to purify labeled CT (*13*), the recovery of urine CT by this method was 5 ± 2%. Recovery of purified urine CT added to 1% HSA was slightly better: 10 ± 2%. Ultrafiltration with an UM-2 filter on an Amicon thin channel ultrafiltration cell TCF10 (Amicon, 21 Hartwell Ave., Lexington, Mass., 02173) followed by filtration on the long G-75 Sephadex columns gave ≤10% recoveries with severe degradation of the hormone. Trichloroacetic acid precipitation and subsequent elution of urine proteins, a method which has been very successful for the extraction of insulin from the urine (*6*), gave only 10–25% yields of urine CT (e.g., Figure 2b). Finally, it was found that formation of petroleum ether emulsions followed by filtration on the long Sephadex column yielded ≥25% of the urine CT. When this latter method was applied to two different urines of Thx patients, it was found that both contained "apparent" iCT which eluted on the long Sephadex columns with the peak fraction having the same $K_d$ as fraction U-2 in normal and MTC patients (e.g., Figure 4). Furthermore, assay of aliquots of these extracts filtered on the short polyacrylamide columns corresponds to the amounts determined for the CT fraction found on the long Sephadex columns. Thus although we are not able at this time to be certain that all the "apparent" CT in the gel filtered urine of Thx patients is real, it is highly likely that much of it is. It should be noted that the evidence that what is being assayed in MTC urine is derived from serum CT is substantial: urine/serum CT concentrations correlate extremely well both before ($r = 0.9873$ for 40 basal samples and $r = 0.8973$ for 30 post stimulation samples) and after thyroidectomy for MTC. Presently, the best available evidence that what is assayed in normal and Thx urine is derived from CT is experimental data which demonstrates the identity of the assayed material in the different urines. Urines from all three groups, MTC,

**Table V. Estimate of Artifactual iCT in Urine of Thyroidectomized Patients**

| Sample | Urine iCT, ng/mg Creatinine | | Artifactual iCT, ng/mg creatinine |
|---|---|---|---|
| | Unchromatographed | Chromatographed | |
| 1 | 0.23 | 0.027 | 0.20 |
| 2 | 0.33 | 0.017 | 0.32 |
| 3 | 0.43 | 0.058 | 0.37 |
| 4 | 0.26 | 0.032 | 0.23 |
| 5 | 0.28 | 0.028 | 0.25 |
| 6 | 0.45 | 0.023 | 0.43 |
| 7 | 0.26 | 0.024 | 0.23 |
| 8 | 0.25 | 0.033 | 0.22 |
| 9 | 0.25 | 0.031 | 0.22 |
| 10 | 0.52 | 0.061 | 0.46 |
| Mean ± S.D. | 0.33 ± 0.10 | 0.034 ± 0.029 | 0.29 ± 0.10 |

normal, and Thx patients, have a fraction which elutes from G-75 Sephadex columns with the same $K_d$. Furthermore, isoelectric focusing over the pH range 3.5–10 has resolved two major bands at pI = 4.9 ± 0.2 and pI = 6.3 ± 0.2 (synthetic human CT has pI = 8.0 ± 0.2) as well as immunoreactivity with pI < 3.5 in concentrates of both MTC and normal urine.

Present evidence indicates spot urines may be utilized for assay of CT if the concentrations are expressed as a ratio of CT to creatinine (volume and collection times do not have to be measured). Sequential 2-h urine samples throughout the day have shown no significant variation with the exception that the first morning urine had less CT than samples taken the rest of the day (e.g., for one patient 8 continuous 2-h samples gave 0.25 ± 0.04 ng/mg creatinine; whereas, the first morning sample contained 0.19 ng CT/mg creatinine). This decreased concentration of first morning urine CT may be due to enzymatic destruction of CT in the acid media of the bladder.

**Application of Urine Calcitonin Measurements.** To date, concentrations of urine CT have been lowest for Thx patients (mean ± S.D. = 0.034 ± 0.015 ng iCT/mg creatinine and concentrations for women (0.059 ± 0.019 ng iCT/mg creatinine) have been significantly higher than for Thx patients ($p < 0.002$) but significantly lower ($p < 0.02$) than men (0.11 ± 0.067 ng iCT/mg creatinine). Preliminary results indicate that urine CT increases appropriately following stimulation (*14*) and may serve to better discriminate patients having hypercalcitonemia from normal patients (*15*), probably because of the smaller amount of heterogeneity, ability to remove interfering substances, and relatively greater increments in the urine relative to the serum. Although urine CT concentrations reflect serum CT concentrations for different population groups (e.g., Thx patients compared to women and women compared to men), for various stimulation tests (e.g., calcium infusion), and for individual hypercalcitonemic patients; no significant urine/serum CT concentrations correlation has been found for normal individuals.

## CONCLUSION

Direct RIA of urine CT is possible for urines containing ≥3 ng/mL; however, RIA of CT in urines containing less CT is complicated by interfering substances most probably structurally similar to creatinine and the methylated xanthines.

We have described a simple, reproducible method for the removal of these interfering substances from urine and subsequent RIA of CT in human urine which reflects the concentrations of CT in the serum. Because RIA of serum CT is more difficult to interpret because of substantial size- and immuno-heterogeneity, protein effects, and perhaps interference from substituted purines, it would appear that RIA of urine CT utilizing our procedures provides a greater index of discrimination between patient groups and allows study of conditions in which the production rate and metabolic clearance are altered prior to manifest changes in the serum.

## ACKNOWLEDGMENT

We thank H. M. Greven, Organon Laboratories, Oss, The Netherlands, for his gifts of synthetic human calcitonin and peptide fragments; J. Bastion and P. Alfred, Armour Pharmaceutical Co., Kankahee, Ill., for their gifts of synthetic human calcitonin; W. Rittel, Ciba-Geigy Corporation, Basal, Switzerland, for his gift of peptide fragments; and the British Medical Research Council, Mill Hill, London, N.W. 7, for human calcitonin MRC standards.

## LITERATURE CITED

(1) D. H. Copp, A. G. F. Davidson, and B. A. Cheney, *Fed. Biol. Soc.*, **4**, 17 (1961).
(2) R. H. Snider, O. L. Silva, C. F. Moore, and K. L. Becker, *Clin. Chim. Acta*, **76**, 1 (1977).
(3) E. F. Voelkel and A. H. Tashjian, Jr., *J. Clin. Endocrinol. Metab.*, **32**, 102 (1971).
(4) K. E. W. Melvin, H. H. Miller, and A. H. Tashjian, Jr., *N. Eng. J. Med.*, **285**, 1115 (1971).
(5) O. L. Silva, R. H. Snider, and K. L. Becker, *Clin. Chem.*, (*Winston-Salem, N.C.*), **20**, 337(1974).
(6) G. Scatchard, *Ann. N.Y. Acad. Sci.*, **51**, 660 (1949).
(7) L. Constan, M. Mako, D. Juhn, and A. H. Rubenstein, *Diabetologia*, **11**, 119 (1975).
(8) R. J. Henry, in "Clinical Chemistry: Principles and Technics", Harper and Roe, New York, N.Y., 1964, p 294.
(9) H. Haglund in "Methods of Biochemical Analysis," Vol. 19, C. Glick, Ed., Interscience Publishers, New York, N.Y., 1971 pp 1–104.
(10) V. Herbert, K. S. Lau, C. W. Gottlieb, and S. J. Bleicher, *J. Clin. Endocrinol. Metab.*, **25**, 1375 (1965).
(11) M. J. Arnaud, *Biochem. Med.*, **16**, 67 (1976).
(12) P. A. Simkin, *Clin. Chem.* (*Winston-Salem, N.C.*), **16**, 191 (1970).
(13) A. H. Tashjian, Jr., *Endocrinology*, **84**, 140 (1969).
(14) K. L. Becker, O. L. Silva, R. H. Snider, and C. F. Moore, *Clin. Res.* **25** (3), 534A (1977).
(15) O. L. Silva, R. H. Snider, S. B. Baylin, C. F. Moore, and K. L. Becker, Program of the American College of Physicians Fifty-Eighth Annual Session, Dallas, Texas, Abst. 36 (1977).

RECEIVED for review August 25, 1977. Accepted December 8, 1977. This work has been supported by Veterans' Administration Medical Research Funds at the Veterans' Administration Hospital in Washington, D.C. 20422. A preliminary report of this work was presented at the 28th Pittsburgh Conference on Analytical Chemistry and Applied Spectroscopy Cleveland, Ohio, March 3, 1977 (paper #357).

# Kinetic Determination of Borate at the Parts per Million Level

**J. C. Gijsbers and J. G. Kloosterboer***

*Philips Research Laboratories, Eindhoven, The Netherlands*

**The hydrolysis of *N*-nitrosohydroxylamine-*N*-sulfonate is catalyzed by protons, boric acid, and certain metal ions. At a constant pH and in the presence of a complexing agent, the reaction can be used for the kinetic determination of boric acid in solution. The hydrolysis is followed by monitoring of the sulfonate absorbance at 258 nm. Optimum reaction conditions have been established. Interfering metal ions have to be complexed. No interference by anions has been observed. Borofluoride, however, does not catalyze the hydrolysis of the sulfonate. Result for the determination of borate in NBS glass No 93: 12.7% $B_2O_3$ with an absolute standard deviation of 0.2%; certified content 12.76% $B_2O_3$.**

Several suitable titrimetric methods exist for the macrodetermination of boric acid, e.g., direct titration with alkali in an aqueous mannitol solution, iodometric titration of mannitoboric acid, or indirect complexometric titration after precipitation of boron as barium borotartrate (*1*, *2*). Micro and trace analysis is usually done by spectrophotometry.

A large number of organic reagents, e.g., $\alpha$-hydro- and $\alpha$-aminoanthraquinones, azo compounds, and reagents such as quercetin and curcumin, yield intensely colored complexes with boron. Curcumin in concentrated sulfuric acid is one of the most widely used reagents. It is extremely sensitive: the boron complex has a molar absorptivity of 180 000 at 555 nm. However, because of this sensitivity, a very careful purification of all reagents is required. Since many other elements form colored complexes with the organic reagents which react with borate, preliminary separation of borate by distillation of its trimethyl ester is necessary. The boric acid-catalyzed decomposition of *N*-nitrosohydroxylamine-*N*-sulfonate, described by Switkes, Dasch, and Ackermann (*3*) prompted us to explore the utility of this reaction for micro and trace analytical purposes.

Since the strong UV absorption band of the sulfonate disappears completely upon decomposition, the course of the reaction can be followed by aid of spectrophotometry. After proper calibration, the observed rate of decomposition may be used as a measure for the quantity of borate present in a sample solution.

## EXPERIMENTAL

**Chemicals.** Dipotassium *N*-nitrosohydroxylamine-*N*-sulfonate, $K_2N_2O_2SO_3$, was prepared by the procedure of Nyholm and Rannitt (*4*) with the following alterations: (i) upon the addition of KOH to the $SO_2$ saturated solution of potassium hydroxide, the pH was adjusted to a value of 11.5, using thymol blue as indicator. This required more KOH than prescribed in the original publication. At the lower pH values used originally, the final product was found to be readily decomposed, resulting in an extremely low yield.

Before the introduction of NO, the solution was flushed with nitrogen in order to remove dissolved oxygen.

(ii) The introduction of NO was stopped as soon as the indicator turned yellow again (pH 8).

In aqueous solution the molar absorptivity of the product had a value of 7860 $M^{-1}$ $cm^{-1}$ at 258 nm and at pH 12. Ackermann and Powell found 7140 at 258 nm and unspecified pH (*5*).

All other chemicals were of reagent grade.

**Reagent Solutions.** A $10^{-3}$ M stock solution of the sulfonate was prepared by dissolving approximately 20 mg in 100 mL dilute alkali (pH 11) which was made from KOH and quartz-distilled water. Oxygen was removed by bubbling of nitrogen through the solution. The reagent solution was stored in ice. It proved to be stable for more than one month. A phosphate buffer solution of pH 6.80 contained 1.695 g $KH_2PO_4$ and 1.765 g $Na_2HPO_4$ in 250 mL quartz-distilled water. The pH was adjusted with $H_3PO_4$. The buffer solution was made $3 \times 10^{-4}$ M in CDTA to prevent catalysis by metal ions. A borate standard solution containing 400 $\mu$g B/mL was made by dissolving 228.4 mg $H_3BO_3$ in 100 mL quartz-distilled water. Suitable dilutions were made from this solution.

**Apparatus.** The decomposition of the *N*-nitrosohydroxylamine-*N*-sulfonate solution was followed spectrophotometrically by monitoring of the absorbance at 258 nm using a Cary 16 spectrophotometer and thermostated optical cells with a path length of 1 cm.

**Procedure.** The uncatalyzed reaction was started by pipetting 1.00 mL sulfonate solution, 2.00 mL buffer solution, and 0.50 mL water into the cuvette. In calibration and analysis runs, the water was replaced by standard and sample solution, respectively.

The absorbance at 258 nm was recorded as a function of time. Pseudo-first-order reactions were followed for one or two half-lives. Conditions were chosen to obtain half-lives of 5–15 minutes.

## RESULTS AND DISCUSSION

**Rate Equation.** Below a pH of 10 the following mechanism has been proposed for the acid-catalyzed hydrolysis of the sulfonate (*3*, *6*):

$$ON(SO_3^-)NO^- + H^+ \overset{K}{\rightleftharpoons} ON(SO_3^-)NOH \quad (1)$$

$$ON(SO_3^-)NOH + H_2O \xrightarrow{k_1} \text{cis-}HONNO^- + SO_4^{2-} + 2H^+ \quad (2)$$

$$\text{cis-}HONNO^- \xrightarrow{k_2} N_2O + OH^- \text{ with } k_2 >> k_1 \quad (3)$$

The rate equation for the disappearance of the sulfonate ion can then be written as

$$\frac{-d[ON(SO_3^-)NO^-]}{dt} = k_1K[H^+][ON(SO_3^-)NO^-] = k_a[ON(SO_3^-)NO^-] \quad (4)$$

The rate constant $k_a$ is the pseudo-first-order rate constant which is observed at a constant pH in the absence of other catalyzing species than the proton.

In the presence of borate at pH $\leq$8, where the borate is present as boric acid an additional reaction (*5*) occurs:

$$ON(SO_3^-)NOH + H_3BO_3 \xrightarrow{k_3} N_2O + SO_4^{2-} + H^+ + H_3BO_3 \quad (5)$$

The rate of the borate-catalyzed disappearance of the sulfonate ion can be written as

$$\frac{-d[ON(SO_3^-)NO^-]}{dt} = k_3[H_3BO_3]K[H^+][ON(SO_3^-)NO^-] = k_b[H_3BO_3][ON(SO_3^-)NO^-] \quad (6)$$

In Equation 6, $k_b$ represents the second-order rate constant that would be observed at a constant pH if only the borate-catalyzed reaction occurred. If the proton- and bo-

0003-2700/78/0350-0455$01.00/0 © 1978 American Chemical Society

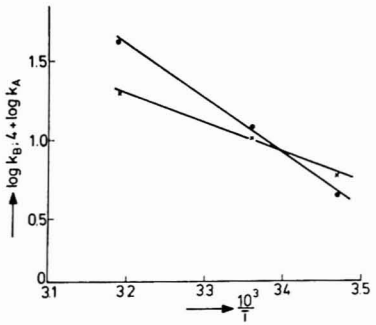


**Figure 1.** Rate constants $k_a$ of the uncatalyzed and $k_b$ of the borate-catalyzed decomposition of *N*-nitrosohydroxylamine-*N*-sulfonate as a function of temperature. pH 7.0. (●) $k_a$ ($s^{-1}$). (×) $k_b$ ($M^{-1}$ $s^{-1}$)

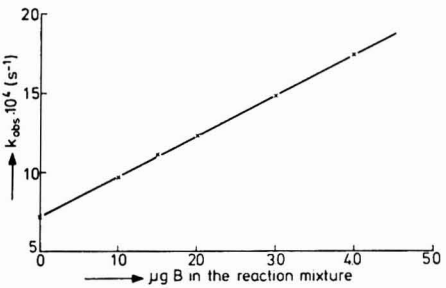


**Figure 2.** Calibration curve of the kinetic determination of borate. Temperature: 15 °C. pH 6.80. $k_a = 7.2 \times 10^{-4}$ $s^{-1}$; $k_b = 9.6$ $M^{-1}$ $s^{-1}$

rate-catalyzed reaction take place simultaneously, the overall rate of disappearance of the sulfonate may be described by the empirical rate equation

$$\frac{-d[ON(SO_3^-)NO]}{dt} = (k_a + k_b[H_3BO_3]_T)[ON(SO_3^-)NO^-] = k_{obsd}[ON(SO_3^-)NO^-] \quad (7)$$

if the pH is kept constant. $[H_3BO_3]_T$ represents the total concentration of borate, irrespective of its actual form in the solution (*3*) and $k_{obsd}$ is the observed pseudo-first-order rate constant.

In the presence of other catalysts, additional terms have to be added to Equation 7.

**Choice of Reaction Conditions.** For a sensitive detection of borate, it is desirable that the ratio $k_b/k_a$ be as high as possible. Determination of the rate constants at three different temperatures shows that this ratio increases with decreasing temperature (Figure 1).

A reaction temperature of 15 °C was chosen. Lower temperatures proved impractical because of the condensation of moisture on the cell windows. The pH was lowered from 7.0 to 6.8 to bring the observed rate constants into the desired range (half-lives between 5 and 15 minutes).

In Figure 2, a calibration curve is shown. It has been drawn for a limited range of concentrations. We have extended the range of borate concentrations up to 12 μg B but no deviations from linearity have been observed. However, the use of an extended range of concentrations is impractical since at high concentrations the rate of the reaction increases considerably.

**Table I. Kinetic Determination of Borate Obtained from Various Calibration Curves**

| | | Calibration | | Analysis | |
|---|---|---|---|---|---|
| Sample No. | Type of sample | $10^4 \cdot k_a$ ($s^{-1}$) | $k_b$ ($M^{-1}$ $s^{-1}$) | $10^4 \cdot k_{obsd}$ ($s^{-1}$) | μg B found |
| 1 | $La_2O_3$-$Al_2O_3$-$B_2O_3$ glass no. 1 | 7.4<br>7.6 | 10.2<br>10.5 | 15.3<br>15.6 | 2.92<br>2.88 |
| 2 | $La_2O_3$-$Al_2O_3$-$B_2O_3$ glass no. 2 | 7.4<br>6.3 | 10.2<br>8.9 | 16.9<br>14.5 | 3.52<br>3.46 |
| 3 | Aqueous solution of $H_3BO_3$ | 7.3<br>6.9 | 9.7<br>9.6 | 12.5<br>12.1 | 2.03<br>2.02 |

This makes an accurate determination of the rate constant very difficult. For accurate rate measurements, proper mixing and stabilization of temperature is absolutely necessary. Reaction rates at high concentrations may be reduced by decreasing $[H^+]$ but then the measurement of the blank solution will require impractical long times of reaction.

With 0 and 4 μg B, the reaction half-lives were approximately 15 and 7 min, respectively. The inclusion of long reaction times for the blank requires more time than needed for a proper dilution.

When the sulfonate solution was stored overnight in a refrigerator at 6 °C both slope and intercept of the calibration curve varied considerably from day to day. Such variations, however, did not seriously affect the analytical results if calibrations were made daily: straight plots were always obtained. In Table I, a few results are given which were obtained from different calibration curves. The last sample was treated with a sulfonate solution which was kept in ice and in a nitrogen atmosphere. Under these conditions $k_b$ was nearly constant over a period of a month but $k_a$ was not. In order to facilitate comparison of results, the calibration curves used in the following have been shifted vertically to match the curve of Figure 2 at the point [B] = 0.

The stability of the reagent solution and the reproducibility of the calibration graph seem to be affected by temperature and oxygen concentration. The slow, thermal oxidation of alkaline solutions of the sulfonate has been reported by Ackermann and Powell (*5*) and, at temperatures above 40 °C, a hydroxide-dependent decomposition has been observed in the absence of oxygen (*3*). Since the proton- and borate-catalyzed reaction are first-order in the sulfonate concentration, a small reduction of the latter would not be expected to have a large influence on the observed rate constant unless the oxidation products catalyze the decomposition of the sulfonate.

**Some Interferences and Their Removal.** *Metal Ions.* Heavy metal ions, e.g., $Cu^{2+}$, are known to catalyze the decomposition of the sulfonate ion (*7*). This interference may be overcome by complexation of the metal ions, e.g., with EDTA.

We found that aluminum also interfered with the determination of boron. EDTA reacts only very slowly with aluminum (*8*). The rate of complexation may be enhanced by boiling. CDTA (1,2-cyclohexylene dinitrilotetraacetic acid) reacts immediately with aluminum at room temperature. Therefore the use of this compound was preferred for the determination of boron in aluminum–lanthanum alloys. Results are given in Table II. Monovalent metal ions which were present in excess as $K^+$ and $Na^+$ ions from the buffer solution did not interfere.

*Silicate and Fluoride.* For the determination of boron in glass, the interference of fluoride and silicate was investigated separately and in combination. The presence of an excess of either or both anions has hardly any effect on the borate content found (Table III). However, if glass is dissolved in hydrofluoric acid, $BF_4^-$ anions are formed, and these do not

Table II. Determination of Boron in the Presence of Aluminum and Lanthanum

| B taken, μg | La added, μg | Al added, μg | EDTA added, μmol | CDTA added, μmol | $10^4$ $k_{obsd}$ $s^{-1}$ | B found μg |
|---|---|---|---|---|---|---|
| 0 | ··· | ··· | ··· | ··· | 7.2 | 0 |
| 2.00 | ··· | ··· | ··· | ··· | 12.3 | 2.00 |
| 2.00 | 25 | 25 | 6 | ··· | 15.4 | 3.24 |
| 2.00 | 25 | 25 | 6[a] | ··· | 12.1 | 1.94 |
| 2.00 | ··· | ··· | ··· | 10 | 12.3 | 2.00 |
| 2.00 | ··· | ··· | ··· | 10 | 12.3 | 2.00 |
| 2.00 | ··· | ··· | ··· | 10 | 12.3 | 2.00 |
| 2.00 | 25 | 25 | ··· | 10 | 12.7 | 2.14 |
| 2.00 | 25 | 25 | ··· | 10 | 12.4 | 2.08 |
| 2.00 | 25 | 25 | ··· | 10 | 11.9 | 1.86 |

[a] Solution boiled for 5 minutes.

Table III. Determination of Boron in the Presence of Silicate and Fluoride

| B added as $H_3BO_3$, μg | B added as $NaBF_4$, μg | Si added as $Na_2SiO_3 \cdot 9H_2O$, μg | F added as NaF, μg | $10^4$ $k_{obsd}$ $s^{-1}$ | B found, μg |
|---|---|---|---|---|---|
| 0 | ··· | ··· | ··· | 7.1 | 0 |
| 4.00 | ··· | ··· | ··· | 17.3 | 4.00 |
| 4.00 | ··· | 20 | ··· | 17.3 | 4.00 |
| 4.00 | ··· | 100 | ··· | 17.3 | 4.00 |
| 4.00 | ··· | ··· | 250 | 17.5 | 4.08 |
| 4.00 | ··· | ··· | 500 | 17.3 | 4.00 |
| 4.00 | ··· | 100 | 250 | 17.3 | 4.00 |
| ··· | 4.00 | ··· | ··· | 7.0 | 0.0 |
| ··· | 4.00[a] | ··· | ··· | 17.4 | 4.04 |

[a] After treatment of the $NaBF_4$ solution with $AlBr_3$.

catalyze the decomposition of *N*-nitrosohydroxylamine-*N*-sulfonate.

Though $BF_4^-$ ions may be converted to borate by the addition of aluminum bromide (fluoride ions are complexed more strongly by aluminum than by boron (*9*)), this method is not very useful for the determination of boron in glass; silicate, brought into solution as $H_2SiF_6$, is also deprived of its fluoride ions and then precipitation of $SiO_2 \cdot nH_2O$ occurs.

*Other Anions.* The specific catalytic effect of boric acid on the rate of decomposition of the sulfonate was discovered by Seel and Winkler (7), who studied the acid-catalyzed decomposition of the sulfonate using different buffer solutions and salts for ionic strength control.

Phosphate, carbonate, sulfate, and perchlorate were found to give rise to no interference at a concentration level between $10^{-2}$ and $10^{-1}$ M. We observed that neither chloride nor bromide nor fluoride interfered. However, a negative primary salt effect has been reported for the acid-catalyzed decomposition of the sulfonate (7). The ionic strength should therefore be kept approximately constant.

*Check for Other Sources of Interference.* One of the difficulties of kinetic analysis is that samples may contain unexpected catalysts. A useful check for their presence is to analyze an aliquot of the sample solution after the addition of a known amount of a borate standard solution. If the rate constant measured after standard addition fits the calibration graph, no interference is to be expected. If not, a careful investigation of the cause of interference may be necessary. In cases where the composition of the matrix is known, the preparation of a calibration curve with the same matrix solution can be useful. However, in view of the causes of interferences studied, the reaction seems to be fairly specific in the presence of a strong complexing agent for heavy metal ions.

Table IV. Analysis of Boron in NBS Glass No. 93 (Certified Content: 12.76% $B_2O_3$)

| weight of glass, mg | $B_2O_3$ found, % |
|---|---|
| 50.9 | 12.5 |
| 98.2[a] | 12.9 |
| 99.0 | 12.7 |
| 99.5 | 12.8 |
| 101.8 | 12.7 |
| Average ± σ | 12.7 ± 0.2 |

[a] After digestion, the melt was heated in the platinum crucible for an additional 10 min at 850–900 °C in order to check for any loss of boron.

**Determination of Boron in Borosilicate Glass.** Since dissolution in hydrofluoric acid proved to be inadequate, recourse was had to dissolution after fusion of the glass with alkali carbonate. We first checked for interference from carbonate ions or from possibly dissolved platinum ions from the crucible, but no interference was observed.

To 100 mg of glass, 700 mg of a mixture of sodium and potassium carbonate were added (60 wt% of $Na_2CO_3$) and the glass was digested by heating to 850–900 °C (*10*). After cooling to room temperature, the mixture was dissolved in 50 mL $10^{-2}$ M hydrochloric acid. The solution was transferred to a volumetric flask of 100 mL and made up to the mark with quartz-distilled water.

To a portion of 10.00 mL of this solution, 100 mg CDTA were added and the pH was raised with KOH to a value of 11–12 in order to dissolve the CDTA. The solution was diluted to 45 mL in a 50-mL volumetric flask, the pH was reduced to 6.80 by means of hydrochloric acid, and the volume was made up to the mark. From this solution 0.50 mL was pipetted into the cuvette and borate was determined as described under Experimental.

Results are shown in Table IV. The usefulness of the kinetic method is obvious from the results shown in this Table.

## LITERATURE CITED


(1) L. Meites, "Handbook of Analytical Chemistry", McGraw-Hill, New York, N.Y., 1963.
(2) A. A. Nemodruk and Z. K. Karakova, "Analytical Chemistry of Boron", Ann Arbor Humphry Science Publishers, Ann Arbor, Mich., 1969.
(3) E. G. Switkes, G. A. Dasch, and M. N. Ackermann, *Inorg. Chem.*, **12**, 1120 (1973).
(4) S. Nyholm and L. Rannitt, *Inorg. Synth.*, **5**, 117 (1957).
(5) M. N. Ackermann and R. E. Powell, *Inorg. Chem.*, **6**, 1718 (1967).
(6) K. Clusius and H. Schumacher, *Helv. Chim. Acta*, **40**, 1137, (1957).
(7) F. Seel and R. Winkler, *Z. Naturforsch. A*, **18**, 155 (1963).
(8) R. Přibil, "Analytical Applications of EDTA and Related Compounds", Pergamon Press, Oxford, 1972, p 330.
(9) L. G. Sillen and A. E. Martell, *Chem. Soc. Spec. Publ.* **No. 17 and 25** (1964 and 1971).
(10) R. Bock, "Aufschlussmethoden in der anorganischen und organischen Chemie", Verlag Chemie, Weinheim, 1972, p 81.


RECEIVED for review September 20, 1977. Accepted December 2, 1977.

# Interlaboratory Comparison of Determinations of Trace Level Petroleum Hydrocarbons in Marine Sediments

**L. R. Hilpert, W. E. May, S. A. Wise, S. N. Chesler, and H. S. Hertz***

*Analytical Chemistry Division, National Bureau of Standards, Washington, D.C. 20234*

**Results of the determination of petroleum hydrocarbons at the μg/kg (ppb) level in marine sediments have been compared among eight laboratories. Values for concentrations of total extractable hydrocarbons scattered between 9 to 500 μg/kg and 49 to 6625 μg/kg for the two sites examined. Scatter of results for hydrocarbons in the gas chromatographic elution range, the most abundant aliphatic and aromatic hydrocarbons, and total polynuclear aromatic hydrocarbons (four rings and larger) were similar. Results for percent water and pristane/phytane ratio were somewhat more consistent. Sample inhomogeneity and analysis uncertainty contributed to an observed intralaboratory precision (1σ) of ±25% for nine replicate analyses of one sediment sample. The data are discussed with regard to the reliability and comparability of current methods for environmental baseline measurements.**

Analytical methodology for the determination of petroleum hydrocarbons in sediments is evolving at a rapid rate. Studies on the fate of hydrocarbons that enter the marine environment from natural sources such as seeps or that are introduced through man's activity in the form of pollution with fossil fuels have recently been reviewed (*1, 2*). Uptake by intertidal and benthic sediments is one such fate. Since the oil may then persist for years, resulting in continuous exposure of the marine ecosystem, measurement of petroleum hydrocarbon content in sediments must be an integral part of oil pollution studies. Intensified research efforts arising from environmental and public health questions have resulted in numerous methods for the measurement of hydrocarbons in sediments (*3-8*). The toxicity of petroleum is well documented for a number of different compound classes and specific compounds such as naphthalene, benzo[*a*]pyrene, and toluidine (*9*). Polynuclear aromatic hydrocarbons (PAH) have been studied extensively in recent years because of reported mutagenic and carcinogenic properties (*10*). Environmental PAH concentrations must be monitored in order to assess potential human exposure.

Analyses of environmentally significant molecules present at trace levels are currently being performed in many laboratories, and the environmental analytical chemist is being called upon to report narrower confidence limits at lower levels of petroleum pollution. Ultimately, he must seek to extend the range of analysis to the sub-ppb level for accurate measurement and assessment of the hydrocarbon burden.

For many of the environmental analyses, there is little or no knowledge of comparability of data from different laboratories and, in most cases, probably little knowledge of intralaboratory precision. In order that the data from diverse methods be meaningful and reliable, there must be a basis for intercomparability. Furthermore, unless the data can be put on an equivalent basis, environmental standards can be neither set nor enforced.

Farrington et al. have intercalibrated gas chromatographic analyses for hydrocarbons in spiked cod liver lipid extracts and tuna meal samples and found good agreement among three laboratories (*11*). Results of an initial feasibility study consisting of an intercalibration of sediment analysis between two laboratories have recently been published (*12*). The results of an eight laboratory intercomparison exercise for the determination of hydrocarbons in two intertidal sediment samples from the Northeastern Gulf of Alkaska are described below. It was decided to intercalibrate on "real world" samples (i.e., samples containing hydrocarbons from natural sources and not "spiked"), recognizing that the mixture of chemicals in petroleum is highly complex and that the products of weathering and microbial degradation compound this complexity. It is also true that sample inhomogeneity may complicate intercalibration studies of a natural sample. If these problems can be controlled effectively, these data could be uniquely valuable in assessing the variability and reliability of current sediment hydrocarbon analyses from sample work-up through measurement and interpretation.

## EXPERIMENTAL

The intercalibration material consisted of two intertidal sediment samples from the Prince William Sound and Northeastern Gulf of Alaska. Two sites were selected for sampling:

Hinchinbrook Island: 146° 41′ W, 60° 21′ N; this site is at the ocean entrance to the Prince William Sound and is constantly being washed with water from the Gulf of Alaska.

Katalla River: 144° 35′ W, 60° 11′ N; this site is downstream from a known oil seep and provides samples with hydrocarbons known to be of petroleum origin.

All samples were collected during low tide and stored in precleaned 1-gal. tin-plated steel cans. Samples were frozen immediately with dry ice and maintained in that state except for a brief period when the sediments were homogenized. The bulk sediment from each site was homogenized by mixing for 3 h in a specially modified cement mixer which had been cleaned with pentane prior to use. Subsamples (~350 g) of each sediment were removed from the rotating mixer with a stainless steel trowel and placed in 16-oz, acid-washed, glass bottles. The bottles were sealed with plastic screw caps containing aluminum foil cap liners. These samples were refrozen immediately after packaging.

Two bottles each of the Katalla and Hinchinbrook sediment samples were shipped frozen to each participating laboratory. The following data were to be obtained for each sample:

1. Total hydrocarbons in GC elution range (approximately $C_{10}$–$C_{30}$).
2. Total extractable hydrocarbons.
3. Pristane/Phytane ratio and the amount of each of these present.
4. Percent water.
5. Identities and amounts of the three most abundant aliphatic and three most abundant aromatic hydrocarbons.
6. Total polynuclear aromatic hydrocarbon (PAH) concentration (4 rings and larger).
7. Identity and amount of the most abundant PAH (4 rings or larger).

The analytical methods employed by each of the participating laboratories are summarized briefly in Table I.

## RESULTS AND DISCUSSION

The importance of establishing environmental baselines for hydrocarbon levels in sediments is well accepted; however, these baselines are meaningful only if one can assess the accuracy and precision of the data. This intercalibration

This paper not subject to U.S. Copyright. Published 1978 by the American Chemical Society

**Table I. Methods of Sediment Analysis**

| Lab | Extraction | Separation | Gas Chromatography: Column | Gas Chromatography: Standard |
|---|---|---|---|---|
| NBS | (a) Dynamic headspace extraction of 100 g sediment in 500 mL pure $H_2O$. Volatiles trapped on Tenax GC adsorbent. | | 100 m SE-30 SCOT 80 °C for 4 min → 275° at 4°/min. | Aliphatic and aromatic internal standard added prior to sample work-up at start of analysis. |
| | (b) Diethyl ether and methylene chloride Soxhlet extraction of 100 g wet sediment. | Liquid chromatography on μBondapak $NH_2$ to remove polar biogenic compounds. | Same as above. | Squalene internal standard added at start of analysis. |
| 2 | Diethyl ether extraction of 100 g wet, acidified sediment on ball-mill tumbler for 18 h. | Column chromatography on activated silica gel. Aliphatics eluted with petroleum ether. Aromatics eluted with methylene chloride in petroleum ether. | 20–30 m SE-30 SCOT 60 °C for 10 min → 250° at either 2 or 4°/min. | Hexamethylbenzene standard added prior to GC analysis. |
| 3 | 300 g wet sediment dried by washing with methanol. Reflux extraction with benzene–methanol (3:2) for 14 h. Saponification with 0.5 N KOH in methanol; extraction into benzene and taken to dryness. Residue taken up in hexane. | Column chromatography on alumina:silica gel (1:3). Aliphatics eluted with hexane. Aromatics eluted with benzene. Polar fraction eluted with methanol. | 6 ft 4% FFAP on Gas Chrom Z. 80 °C → 225° at 4°/min. or 6 ft 3% SP 2100 on Supelcoport 100 °C → 325° at 4°/min. | External standard containing several aliphatic, aromatic, and olefinic hydrocarbons. |
| 4 | 250 g wet sediment extracted with methanol and benzene: methanol azeotrope. Reduced volume and extracted with hexane and methylene chloride. Reduced volume. | Organic extract partitioned in nitromethane:cyclohexane to give polycyclic fraction. Column chromatography on silica gel; eluted with hexane. | 3% OV-17. 70 °C → 300° at 8°/min. | External standard containing polynuclear aromatic hydrocarbon. |
| 5 | 150 g dried sediment extracted with heptane on ball-mill tumbler for 4 h. | Column chromatography on alumina:silica gel (1:1) aliphatics eluted with heptane; aromatics eluted with benzene. | 20 ft 5% eutectic ($LiNO_3$, $NaNO_3$, $KNO_3$) on Chromosorb G 150 °C → 280 °C at 20°/min. | Spiked blanks: $C_{18}$, $C_{20}$, phytane, anthracene, pyrene. |
| 6 | Freeze-dried sediment reflux extracted with toluene:methanol (3:7) for 14 h; sediment reextracted with hexane. Combined extracts saponified with KOH in methanol and toluene. Extracted nonsaponifiables into hexane. | Column chromatography on alumina:silica gel (1:2) aliphatics eluted with hexane; aromatics eluted with benzene. | 5% FFAP on Gas Chrom Q 70 °C → 270 °C at 6°/min. | External standard *n*-$C_{16}$, $C_{18}$, $C_{21}$, $C_{24}$, $C_{28}$, $C_{32}$, pristane, phytane. |
| 7 | 80 g wet sediment saponified in KOH: methanol under reflux for 24 h. Extracted into hexane. | Column chromatography on alumina:silica gel (1:1) aliphatics eluted with hexane; aromatics eluted with benzene. | OV-101 80 °C for 2 min → 280° at 8°/min. | Spiked blank and *n*-alkane external standard. |
| 8 | 100 g freeze-dried sediment reflux extracted with toluene:methanol (3:7). Extract saponified in 6N KOH:methanol:water; extraction into hexane. | Column chromatography on alumina:silica gel aliphatics eluted with heptane; aromatics eluted with benzene. | 152 m stainless steel capillary coated with 10% Apiezon L. 155 °C for 8 min → 280° at 2°/min. | External standard |

Table II. Homogeneity Studies on Intercalibration Materials, Results of Replicate Analyses

| Hinchinbrook Sediment | | Katalla Sediment | |
|---|---|---|---|
| Bottle | Hydrocarbons in GC range, μg/kg | Bottle | Hydrocarbons in GC range, μg/kg |
| H-4 | 437 | K-21 | 709 |
| | 318 | | 816 |
| | 290 | | 767 |
| H-23 | 564 | K-36 | 1071 |
| | 470 | | 728 |
| H-39 | 399 | K-1 | 1226 |
| | 352 | | 1093 |
| | | | 1175 |
| H-30 + H-31 homogenized | 282 | K-15 | 602 |
| | 723 | | |
| | 394 | | |
| | 386 | | |
| | 408 | | |
| Average[a] | 418 ± 124 (30%) ($n$ = 12)[b] | Average | 910 ± 231 (25%) ($n$ = 9)[b] |

[a] Precision expressed as the standard deviation (1σ). [b] $n$ indicates number of analyses.

Table III. Analyses of Hinchinbrook and Katalla Sediments[a]

| | Water, % | | Total extractable hydrocarbons, μg/g | |
|---|---|---|---|---|
| Laboratory | Hinchinbrook | Katalla | Hinchinbrook | Katalla |
| NBS | 4.4 ± 0.1 | 22.5 ± 0.2 | 0.22 | 2.5 |
| 2 | 4.7 | 23.5 | 4.4 | 12.8 |
| | 4.4 | 22.6 | 6.2 | 11.0 |
| 3 | 5.0 | 23.5 | 24.3[b] | 65.8 |
| | 5.8 | 22.8 | 7.9 | 57.6 |
| 4 | - | - | - | - |
| 5 | 4.3 | 22.4 | - | - |
| | 4.3 | 22.2 | - | - |
| 6 | 4.79 | 26.3 | 3.12 | 109 |
| | - | 21.3 | 7.92 | 10.7 |
| 7 | 15.4 ± 5.7 | 36.5 ± 6 | 2.9 | 5.4 |
| | 14.3 ± 2.1 | 34.3 ± 2.1 | 0.64 | 3.9 |
| 8 | - | - | - | - |
| Range | 4.3 – 15.4 | 21.3 – 36.5 | 0.22 – 7.92 | 2.5 – 109 |

[a] Some laboratories supplied results of duplicate analyses. In such cases both results are presented in the Table. Where presented, precision is expressed as the standard deviation (1σ). [b] Laboratory 3 reported that this result is probably in error.

exercise was conducted to determine the adequacy of analytical procedures for hydrocarbon determinations in sediments and to indicate the uncertainty with which results from different laboratories may be compared. The current, most commonly used analytical approach for determining hydrocarbons in sediments involves an organic solvent extraction, saponification, and column or thin-layer chromatography to isolate the hydrocarbons (*1, 13*). Within this general scheme, however, there exists a variety of analytical methods. Since the "true" or "actual" values cannot be verified with current state-of-the-art methodology, one cannot conclude which is the "best" method or result. It is imperative, however, that one be cognizant of the limitations of each method; knowledge of how a procedure compares with others is extremely important when environmental decisions with far reaching economic and social consequences are to be made.

Examination of the Hinchinbrook and Katalla sediments showed both to be predominantly fine to medium grain sand. Homogeneity studies on the two sediments were conducted by the National Bureau of Standards utilizing the dynamic headspace sampling technique previously described (*8*). The results of these studies are summarized in Table II. The relative standard deviation for the Katalla sediment (910 μg/kg ± 25%, $n$ = 9) is slightly better than that for the Hinchinbrook sediment (420 μg/kg ± 30%, $n$ = 12). An internal standard of phenanthrene was added to both sediments at the 20 μg/kg concentration level; an average of 83% was recovered from the Karalla sediment, while only 41% was recovered from the Hinchinbrook sediment. Mesitylene, naphthalene, and trimethylnaphthalene also exhibited similar recovery behavior from the two sediments. The Hinchinbrook sediment thus appears to have greater affinity for hydrocarbons than the Katalla sediment.

**Intercomparison Results.** Table III contains the results of percent water analyses for the two sediments. The agreement is generally good with the exception of high results from lab No. 7, which accounts for the large standard deviations (Hinchinbrook = 6.7 ± 4.3% $H_2O$, Katalla = 25.3 ± 5.2% $H_2O$). However, this uncertainty or even larger uncertainties have no significant effect on the remaining data, which are reported on a dry weight basis.

The amount of extractable hydrocarbons obtained for the sediments is reported in Table III. Laboratories 5, 6, and 8 dried the samples (freeze dried or otherwise) prior to extraction. The drying process results in some loss of hydrocarbons (up to $C_{20}$, depending on the procedure, temperature, etc.) from the mixture of hydrocarbons to be measured. Farrington (*14*) has suggested an alternative method to circumvent this loss which employs a headspace analysis of the sediment, followed by freeze drying and solvent extraction.

Table IV. Hinchinbrook Sediment[a,b]

| Laboratory | Hydrocarbons in GC range, μg/kg: Aliphatic | Unsat./aromatic | Total | Pristane/phytane ratio | Most abundant hydrocarbons, μg/kg: Aliphatic | | Aromatic | |
|---|---|---|---|---|---|---|---|---|
| NBS (headspace) | | | 420 ± 120 | 0.9 ± 0.2 | $C_{19}$ 16 ± 12<br>$C_{18}$ 15 ± 8<br>$C_{17}$ 12 ± 1 | | Me-Naph 2 ± 1<br>$C_2$-Naph 1<br>$C_2$-Naph 1 | |
| NBS (extraction) | | | 250 | 0.8 | $C_{25}$ 7<br>$C_{24}$ 7<br>$C_{23}$ 6 | | -<br>-<br>- | |
| 2 | 140 | 4 | 144 | 2.59 | $C_{25}$ 40 | $C_{23}$ 30 | $C_3$-Naph 1.3 | $C_3$-Naph 2.7 |
| | 93 | 10 | 103 | - | $C_{26}$ 20<br>$C_{24}$ 19 | $C_{24}$ 12<br>$C_{26}$ 12 | Phen 0.7<br>$C_2$-Fluor 0.2 | Phen 0.7<br>2-Me-Naph 0.3 |
| 3 | 54 | 21 | 75 | 2.05 | Prist 4 | $C_{17}$ 5 | unk 7 | unk 3 |
| | 57 | 23 | 80 | 2.78 | $C_{18}$ 4<br>$C_{19}$ 4<br>$C_{27}$ 4 | $C_{18}$ 5<br>$C_{19}$ 5 | unk 3<br>unk 3 | unk 3<br>unk 3 |
| 4 | - | - | - | - | | - | | - |
| 5 | 9 | 35 | 44 | - | | - | unk 6 | unk 3 |
| | 26 | 12 | 38 | - | | - | - | unk 2 |
| | | | | | | - | - | unk 1 |
| 6 | | | 15.9 | - | $C_{18}$ 1.4 | $C_{21}$ 4.7 | unk 1.8 | unk 0.6 |
| | | | 34.1 | 1.67 | $C_{20}$ 1.3<br>$C_{19}$ 1.1 | $C_{22}$ 4.5<br>$C_{20}$ 3.3 | unk 1.5<br>unk 1.2 | unk 0.5<br>unk 0.4 |
| 7 | 100 ± 50 | 40 ± 30 | 140 | - | | - | | - |
| | 500 ± 600 | 400 ± 100 | 900 | - | | - | | - |
| 8 | - | - | - | 2.71 | $C_{17}$ 0.39 | $C_{17}$ 2.9 | | - |
| | | | | 3.6 | Prist 0.38<br>$C_{18}$ 0.32 | $C_{18}$ 1.9<br>$C_{19}$ 1.8<br>Prist 1.6 | | |
| Range | 9-500 | 4-400 | 15.9-900 | 0.8-3.6 | | | | |

[a] Some laboratories supplied results of duplicate analyses. In such cases both results are presented in the Table. Laboratory 7 submitted a summary of multiple analyses on each bottle of sediment. All precision data is expressed as the standard deviation (1σ). [b] In the Table, unk is used as an abbreviation for unknown; $C_x$ represents *n*-alkane containing *x* carbons; Prist is pristane; Me is methyl; Naph, Phen, and Fluor are naphthalene, phenanthrene, and fluoranthene, respectively. A dash (—) is used when results were not supplied by a participating laboratory.

Losses of volatile hydrocarbons would be minimized with such a procedure and a broader molecular weight range of compounds could be analyzed.

Data obtained for the Hinchinbrook sediment, including hydrocarbons in the GC range, pristane/phytane ratio, and the most abundant aliphatic and aromatic hydrocarbons are presented in Table IV; analogous data for the Katalla sediment are shown in Table V. The results of measurement of hydrocarbons in the GC range vary widely among the eight laboratories; the agreement is better for the Katalla sediment than for the Hinchinbrook sediment. This variability, which exists even for laboratories employing similar extraction and/or work-up procedures, may be partially a result of the different manner in which the gas chromatographic quantification was carried out. GC analysis of the saturated or aliphatic fraction of the sediment extract usually produces a chromatogram with an unresolved complex mixture of alkanes and cycloalkanes with a wide range of molecular weights. Quantitative data based solely on resolved chromatographic peaks differs from that in which a contribution from the unresolved "envelope" is considered. Studies were conducted at NBS in which a sediment sample was headspace-extracted and analyzed by capillary column gas chromatography. The resulting chromatogram was quantified both on the basis of resolved peaks only, and resolved peaks plus a contribution from the unresolved envelope. Values for the hydrocarbon concentration showed a variability as high as 300%.

In cases where quantitation was based on an external standard, the percent recovery for each component of the standard must be known. Warner (*15*) has shown that diethyl ether extraction recoveries for naphthalene, dimethylnaphthalene, and biphenyl from spiked marine organisms may be as low as 40% for concentrations below 0.1 μg/g. The addition of an internal standard prior to any analysis step would seem logical in order to correct for such losses. The internal standard should contain both aliphatic and aromatic components characteristic of the molecular weight range and concentration of compounds to be analyzed in the samples. Losses during sample work-up are compensated for by a similar loss of the internal standard. The sample must be analyzed with and without the internal standard, however, to ensure that components in the standard are not also present in the sample; or if they are present, their contribution can be taken into account. The underlying assumption in methods involving an internal standard is that the standard is incorporated into, and equilibrated with, the sample matrix. This may or may not be the case, however, and errors may result. Values for the most abundant aliphatic hydrocarbons in the Katalla sediment (Table V) show that the headspace extraction recovered the volatile, lower molecular weight components, $C_9$-$C_{11}$, which may be lost during the sample drying step or the solvent concentration step required in methods employing an organic extraction.

Sample extracts were saponified to reduce the problem of separating hydrocarbons from lipids coextracted from the sediments by laboratories 3, 6, 7, and 8. These compounds may co-elute or overlap with peaks of interest on certain chromatographic systems (*14*). Methods which do not remove these polar compounds may be expected to give results for hydrocarbon content which are high. Even when saponification is carried out, there is a potential problem of transesterification with the potassium hydroxide–methanol extraction usually used. Methyl esters of fatty acids may be produced at concentrations which are significant when analyzing for hydrocarbons at the ppm level (*16*). Farrington has noted that saponification in the presence of 25% water will reduce transesterification considerably (*3*). Laboratory

Table V. Katalla Sediment[a,b]

| Laboratory | Hydrocarbons in GC range μg/kg: Aliphatic | Unsat./aromatic | Total | Pristane/phytane ratio | Most abundant hydrocarbons, μg/kg: Aliphatic | Aromatic |
|---|---|---|---|---|---|---|
| NBS (headspace) | | | 910 ± 230 | 1.9 ± 0.02 | $C_{10}$ 32 ± 11<br>$C_{11}$ 25 ± 7<br>$C_9$ 23 ± 13 | Me-Naph 16 ± 5<br>$C_2$-Naph 15 ± 3<br>$C_3$-Naph 14 ± 4 |
| NBS (extraction) | | | 2700 | 1.7 | $C_{11}$ 66<br>$C_{14}$ 66<br>Prist 58 | $C_2$-Naph 54<br>$C_2$-Naph 27<br>Me-Naph 24 |
| 2 | 610 | 120 | 730 | 3.27 | $C_{25}$ 42 $C_{23}$ 98<br>$C_{19}$ 24 $C_{24}$ 60<br>Prist 23 $C_{26}$ 57 | Phen 9.7 Phen 9.1<br>$C_2$-Naph 7.1 $C_3$-Naph 7.4<br>2-Me-Naph 5.3 2-Me-Naph 5.7 |
| | 880 | 130 | 1010 | 3.27 | | |
| 3 | 1940 | 530 | 2470 | 3.55 | $C_{17}$ 180 Prist 110<br>$C_{18}$ 180 $C_{19}$ 100<br>Prist 140 unk 90 | unk 50 unk 72<br>unk 50 unk 58<br>unk 40 unk 29 |
| | 1420 | 710 | 2130 | 6.32 | | |
| 4 | – | – | – | – | – | – |
| 5 | 3454 | 401 | 3855 | 2.81 | $C_{24}$ 75 $C_{23}$ 194<br>$C_{22}$ 57 $C_{24}$ 179<br>$C_{21}$ 53 $C_{25}$ 138 | unk 19 unk 14<br>unk 14 unk 13<br>unk 8 unk 5 |
| | 6625 | 417 | 7042 | 2.69 | | |
| 6 | 196 | 14 | 210 | 3.71 | $C_{21}$ 19.9 $C_{22}$ 4.3<br>$C_{22}$ 18.7 $C_{21}$ 4.1<br>$C_{20}$ 13.7 $C_{20}$ 3.9 | unk 2.9 unk 0.8<br>unk 2.5 unk 0.7<br>unk 2.1 unk 0.7 |
| | 49.4 | 4.2 | 53.6 | 2.38 | | |
| 7 | 200 ± 200 | 300 ± 300 | 500 | – | $C_{17}$ + Prist 47 | – |
| | 400 ± 200 | 80 ± 10 | 480 | – | $C_{16}$ 36<br>$C_{18}$ + Phyt 21 | –<br>– |
| 8 | – | – | – | 3.25 | Prist 28.8 Prist 19.9 | – |
| | | | | 3.10 | $C_{19}$ 22.7 $C_{27}$ 16.2<br>$C_{20}$ 22.7 $C_{17}$ 15.5 | –<br>– |
| Range | 49.4-6625 | 4.2-710 | 53.6-7042 | 1.7-6.32 | | |

[a] Some laboratories supplied results of duplicate analyses. In such cases both results are presented in the Table. Laboratory 7 submitted a summary of multiple analyses on each bottle of sediment. All precision data is expressed as the standard deviation (1σ). [b] Abbreviations are the same as in Table IV, in addition Phyt is phytane. A dash (—) is used when results were not supplied by a participating laboratory.

Table VI. Polynuclear Aromatic Hydrocarbons in Sediments[a,b]

| Laboratory | Hinchinbrook Sediment: Total PAH, μg/kg, 4 rings and larger | Most abundant PAH, μg/kg | Katalla Sediment: Total PAH, μg/kg, 4 rings and larger | Most abundant PAH, μg/kg |
|---|---|---|---|---|
| NBS | 5 ± 0.5 | chrysene 0.3 | 40 ± 2 | Me-chrysene 3 |
| 2 | – | pyrene 0.08 | 10 | Me-pyrene 3.9 |
| | | pyrene 0.1 | 8.6 | Me-pyrene 3.2 |
| 4 | 3.8 | chrysene 1<br>Me-pyrenes and Me-fluoranthenes 1 | 74 | Me-pyrenes and Me-fluoranthenes 28 |
| Average | 4.4 ± 0.85 ($n$ = 2)[c] | | 33.2 ± 31 ($n$ = 4) | |

[a] Results of duplicate analyses are presented for Laboratory 2. All precision data is expressed as the standard deviation (1σ). [b] A dash (—) indicates no results were supplied. [c] $n$ indicates the number of values averaged.

1 (NBS) employed high-performance liquid chromatography (HPLC) to remove the polar biogenic compounds in the extraction procedure, but not in the headspace procedure (see Table I). It was found that an HPLC clean-up of headspace sampled sediment resulted in no change in the results of the GC analysis. This result indicates that these interfering compounds were removed from the sample matrix during solvent extraction only and not during headspace sampling.

Values for relative amounts of pristane and phytane are sometimes used to differentiate natural sources of hydrocarbons such as biogenic hydrocarbons from petroleum-based pollutants (5). Experimental values for the pristane/phytane ratio (Tables IV and V) are in sufficient agreement to answer this question.

Results for the polynuclear aromatic hydrocarbon (PAH) content of the samples are presented in Table VI. Only three of the eight laboratories involved in the intercomparison submitted results for PAH concentrations. It seems clear from this limited response that this higher molecular weight fraction, which may be the most critical in terms of toxicity, carcinogenicity, and persistence, cannot be easily determined by gas chromatography alone. Laboratories 2 and 4 both found the methylpyrenes to be the most abundant PAH (4 rings and larger) in the Katalla sediment. Laboratory 4 identified methyl-substituted pyrenes and fluoranthenes, and chrysene in the Katalla sediment by comparison of their mass spectra with known standards. NBS used HPLC and fluorescence emission spectroscopy to identify methylchrysene as the most abundant PAH in the Katalla sediment.

## CONCLUSIONS

The results of this study indicate the high variability of state-of-the-art hydrocarbon analyses on "real world" sediment samples. Unlike intercalibration on spiked samples where a substrate is added to a matrix at a suitable concentration and assumed to be incorporated into and equilibrated with the matrix, intercalibration on real samples requires no such assumption. In setting environmental baselines, use of inaccurate and imprecise consensus values is always a danger; we feel the intercomparison data for a common (homogeneous) sediment sample are a necessary addition to such baseline data. We hope other laboratories will be encouraged to

undertake such interlaboratory comparisons with sediment samples in the future, especially as new methods are developed and applied to environmental analyses. Such studies are needed to determine when different numbers generated by different laboratories using different methods are environmentally significant.

If nothing else, the results of this intercomparison study should serve as a warning against overinterpretation of currently generated trace-level hydrocarbon determinations. The results should *not* be used as an argument against further intercomparison exercises, but should be used as encouragement for the continued development of the state-of-the-art of trace organic analysis. Ultimately, the goal of the National Bureau of Standards is to produce a Standard Reference Material with certified trace-level concentrations of environmentally significant organic compounds in a "real" matrix. Unfortunately, methods for preparing and certifying such a material have not yet been developed. Problems associated with sample homogeneity, stability, matrix effects, etc. must also be resolved before any such standard can become available. The low concentration of hydrocarbons anticipated in many pollution baseline studies necessitates the development of sensitive analytical techniques. Finally, some form of information exchange or intercomparison must exist among laboratories in order to assess the uncertainty of the data from these new analytical techniques.

## ACKNOWLEDGMENT

The authors thank P. D. LaFleur for his critical reading of this manuscript. The following laboratories and scientists participated with NBS in the intercomparison study: John A. Calder, Florida State University; Ronald A. Hites, M.I.T.; John L. Laseter, University of New Orleans; William MacLeod, NOAA-Seattle; Steven J. Martin, Geochem Laboratories; Patrick L. Parker, University of Texas; and David Shaw, University of Alaska.

## LITERATURE CITED

(1) National Academy of Sciences, "Inputs, Fate, and Effects of Petroleum in the Marine Environment", A Report of the Ocean Affairs Board, National Academy of Sciences, Washington, D.C., 1975.
(2) "Baseline Studies of Pollutants in the Marine Environment and Research Recommendations", Office of the International Decade of Ocean Exploration, National Science Foundation, Washington, D.C., 1972.
(3) J. W. Farrington, and B. W. Tripp, *ACS Symp. Ser.*, **18**, 267–284 (1975).
(4) D. G. Shaw, *Environ. Sci. Technol.*, **7**, 740–742 (1973).
(5) M. Blumer, and W. D. Snyder, *Science*, **150**, 1588 (1965).
(6) W. W. Youngblood, and M. Blumer, *Geochim. Cosmochim. Acta*, **39**, 1303–1314 (1975).
(7) J. W. Farrington, and J. G. Quinn, *Geochim. Cosmochim. Acta*, **35**, 735–741 (1971).
(8) W. E. May, S. N. Chesler, S. P. Cram, B. H. Gump, H. S. Hertz, D. P. Enagonio, and S. M. Dyszel, *J. Chromatogr. Sci.*, **13**, 535 (1975).
(9) K. Winters, R. O'Donnell, J. C. Batterton, and C. VanBaalen, *Mar. Biol.*, **38**, 269–276 (1976).
(10) L. Fishbein, W. G. Flamm, and H. L. Falk, "Chemical Mutagens", Academic Press, New York, N.Y., 1972.
(11) J. W. Farrington, J. M. Teal, G. C. Medeiros, K. A. Burns, E. A. Robinson, Jr., J. G. Quinn, and T. L. Wade, *Anal. Chem.*, **48**, 1711 (1976).
(12) S. A. Wise, S. N. Chesler, B. H. Gump, H. S. Hertz, and W. E. May, in "Fate and Effects of Petroleum Hydrocarbons in Marine Ecosystems and Organisms", D. A. Wolfe, Ed., Pergamon Press, New York, N.Y., 1976, pp 345–350.
(13) J. W. Farrington, and P. A. Meyers, in "Environmental Chemistry", Vol. 1, G. Eglinton, Ed., The Chemical Society, Burlington House, London, 1975.
(14) J. W. Farrington, personal communication.
(15) J. S. Warner, *Anal. Chem.*, **48**, 578 (1976).
(16) R. L. Glass, *Lipids*, **6**, 919–925 (1971).

RECEIVED for review August 30, 1977. Accepted November 21, 1977. The authors acknowledge partial financial support from the Office of Energy, Minerals, and Industry within the Office of Research and Development of the U.S. Environmental Protection Agency under the Interagency Energy/Environment Research and Development Program and the Bureau of Land Management through interagency agreement with the National Oceanic and Atmospheric Administration, under which a multiyear program responding to needs of petroleum development of the Alaskan continental shelf is managed by the Outer Continental Shelf Environmental Assessment Program (OCSEAP) Office. In order to specify procedures adequately, it has been necessary to identify commercial materials in this report. In no case does such identification imply recommendation or endorsement by the National Bureau of Standards, nor does it imply that the material identified is necesarily the best available for the purpose.

# Indirect Determination of Selenium in Sodium Selenate

**Wladyslaw Reichel* and Meyer Lallouz**

*Canadian Copper Refiners Limited, Montreal East, Quebec, Canada H2Y 3H2*

**A method for the determination of $Se^{6+}$ in sodium selenate, based on the stoichiometric reduction of hexavalent selenium to the tetravalent state with hydrochloric acid, has been developed. A calculated excess of $As^{3+}$ is added to the dissolved sample. Liberated chlorine oxidizes $As^{3+}$ to $As^{5+}$ and the excess $As^{3+}$ is titrated with standard potassium bromate. $Se^{4+}$ does not interfere. The accuracy of the method was evaluated using high purity sodium selenate to which calculated amounts of $Se^{4+}$ were added. Average recovery of $Se^{6+}$ was 99.98%. The standard deviation was 0.023% at 41.38% $Se^{6+}$ concentration.**

An increasing demand for purer sodium selenate, particularly by drug manufacturers, has become apparent in recent years. Therefore the precise and accurate determination of $Se^{6+}$ has become imperative. Gravimetric analysis (*1*) is not sufficiently accurate, since moisture retained by selenium causes high results. Common volumetric methods (*2, 3*) are subject to interferences and unacceptable errors. These procedures are not specific for $Se^{6+}$ and require corrections for interfering ions, including $Se^{4+}$. Barabas and Bennett (*4*) developed a differential potentiometric method for the determination of selenium in refined selenium with acceptable precision. However, a correction for $Se^{4+}$ is mandatory, a step which introduces an error. The same limitation can be observed in the differential AAS procedure of Reichel (*5*).

Kolthoff and Elving (*2*) suggest a reaction in which hexavalent selenium is quantitatively reduced to the tetravalent state on reaction with hydrochloric acid:

$$H_2SeO_4 + 2HCl \rightarrow H_2SeO_3 + Cl_2 + H_2O \quad (1)$$

0003-2700/78/0350-0463$01.00/0 © 1978 American Chemical Society

Table I. Recovery of Selenium$^{6+}$ from Synthetic Standards

| Sodium selenate, g[a] | Equivalent $Se^{6+}$, g | Added sodium selenite, g | Equivalent $Se^{4+}$ | $Se^{6+}$ found, g | Recovery, % |
|---|---|---|---|---|---|
| 1.7000 | 0.7103 | 0.3000 | 0.1370 | 0.7102 | 99.99 |
| 1.8000 | 0.7521 | 0.2000 | 0.0913 | 0.7523 | 100.02 |
| 1.9000 | 0.7939 | 0.1000 | 0.0457 | 0.7938 | 99.99 |
| 1.9800 | 0.8189 | 0.0200 | 0.0091 | 0.8186 | 99.96 |
| 1.9900 | 0.8272 | 0.0100 | 0.0046 | 0.8273 | 100.01 |
| 1.9960 | 0.8323 | 0.0040 | 0.0018 | 0.8321 | 99.97 |

[a] Sodium selenate used was 99.98% pure.

On the basis of this reaction a single vessel technique has been devised in which a calculated excess of trivalent arsenic (as $As_2O_3$) is oxidized to the pentavalent state by chlorine liberated upon the reduction of selenium.

$$AsCl_3 + Cl_2 \rightarrow AsCl_5 \quad (2)$$

The reaction is carried out under reflux and is completed within one hour. The optimum excess $As^{3+}$ established by preliminary analysis is then titrated with standard potassium bromate. High accuracy is achieved since only a small portion of the originally added arsenic is titrated.

## EXPERIMENTAL

**Apparatus.** A 500-mL conical flask with a ground joint, attached to a 50-cm water-cooled condenser and a combination hot plate–magnetic stirrer were used.

**Reagents.** All reagents should be of analytical grade. Distilled or deionized water should be used. The reagents used were: Potassium bromide solution, 2% w/v; Sodium hydroxide solution, 2.5 M; Methyl orange solution, aqueous, 0.1% w/v (free of sediment); Arsenic trioxide, powder form; and Potassium bromate solution, 0.02 N.

**Procedure.** Weigh 2 ± 0.0002 g of the sample in triplicate into the 500-mL flasks, each containing 1.0470 g arsenic trioxide. Carry a reagent blank throughout the procedure in which sodium selenate and arsenic trioxide are omitted. Add 10 mL of 2.5 M sodium hydroxide solution and mix. Heat gently with frequent agitation until the arsenic trioxide is completely dissolved. Cool and add 50 mL concd HCl. Connect immediately to the water condenser and reflux for 1 h on the hot plate at a temperature of 89 ± 4 °C. When reflux is completed, wash down the condenser with 50 mL of distilled water into the flask. Disconnect the flask, introduce a magnetic stirring bar into the solution, add 2 drops of KBr solution and 2 drops methyl orange. Be consistent in the addition of methyl orange. Add the same number of drops to the blank. Raise the temperature to 85 ± 5 °C and maintain it throughout the titration. Use one of the triplicate samples to determine the approximate volume of potassium bromate titrant needed to reach the end point. Titrate the remaining two samples to within 2 to 3 mL of the end point. Complete the titration dropwise until the color of methyl orange is discharged. Correct the result with that obtained on the reagent blank.

**Calculations.** The selenium concentration is given by

$$\%Se^{4+} = \frac{(A - B) \times 1.0539 \times 100}{C}$$

where $A$ is the mass in grams, of $As^{3+}$ added; $B$ is the mass in grams, of $As^{3+}$ found, and $C$ is the mass in grams, of the sample. The ratio of the atomic weights of selenium to arsenic is 1.0539.

## RESULTS AND DISCUSSION

Several samples of commercial grade sodium selenate were analyzed and found to contain between 40.65 and 41.68% $Se^{6+}$. The amount of $As^{3+}$ added varied with the purity of the sample, such that excess arsenic ranged between 10 and 15 mg. Greater excesses of arsenic resulted in higher titrations and decreased accuracy.

**Interferences.** Strong oxidants such as nitric acid, permanganate, and chromate, or strong reductants such as organic matter and stannous chloride seriously interfere. $Te^{6+}$ reacts in the same manner as $Se^{6+}$ and also interferes; $Te^{4+}$, $Ag^+$, $Zn^{2+}$, $Sb^{5+}$, $Pb^{2+}$, $Na^+$, $Cr^{3+}$, $Cu^{2+}$, $Fe^{3+}$, $V^{4+}$, $Sn^{4+}$, and $Ni^{+2}$ did not interfere up to 0.01%. The presence of $Cr^{3+}$, $Cu^{2+}$, $Fe^{3+}$, $V^{4+}$, and $Ni^{2+}$ in higher concentration than 0.01% results in highly colored solutions, obscuring the detection of the end point. This interference study was performed on synthetic samples of sodium selenate spiked with the above elements at their various oxidation states. It is, however, most unlikely that the interfering ions will be present in high purity sodium selenate, particularly those in their lower oxidation state.

Table II. Precision Study Data

| % $Se^{6+}$ | | |
|---|---|---|
| 41.39 | 41.39 | |
| 41.39 | 41.34 | |
| 41.41 | 41.35 | |
| 41.36 | 41.34 | |
| 41.34 | 41.37 | |
| 41.36 | 41.37 | $n$ = 18 |
| 41.39 | 41.39 | Av, 41.38% |
| 41.39 | 41.40 | Std dev, 0.023% |
| 41.40 | 41.38 | Rel std dev 0.054% |

**Effect of Hydrochloric Acid Concentration.** Optimum conditions were reached by addition of concentrated HCl to the dissolved sample to result in a final 10 M HCl solution. In more dilute solutions the reduction of selenium was slow and required longer refluxing time.

**Effect of Temperature and Reflux.** Arsenic losses occurred over a wide range of temperatures. Volatilization of arsenic chloride resulted at temperatures as low as 50 °C.

The use of a water cooled condenser prevented losses of arsenic at temperatures of up to 95–100 °C. At higher temperatures, severe losses occured even under reflux. Although losses appeared to be minimized at lower temperatures, the reaction was found to be complete only at or above 85 °C.

**Accuracy and Precision.** The accuracy of the procedure was evaluated by recovery experiments on synthetic samples of pure sodium selenate to which calculated amounts of $Se^{4+}$ were added. Near-theoretical recoveries were obtained (Table I). The precision was evaluated on a sodium selenate sample with a mean $Se^{6+}$ concentration of 41.38%. The standard deviation for a set of 18 results was 0.023% with relative standard deviation of 0.054% (Table II).

**Other Applications.** The method with slight modification was successfully applied to the determination of selenium in sodium selenite. In a preliminary step, $Se^{4+}$ is oxidized to $Se^{6+}$ with hydrogen peroxide in the presence of excess sodium hydroxide. The indirect bromate procedure is then followed.

## LITERATURE CITED

(1) N. Howell Furman, "Standard Method of Chemical Analysis", Sixth ed., Volume I, Robert E. Krieger Publishing Company, Huntington, N.Y., 1975, p 928.
(2) I. M. Kolthoff and P. J. Elving, "Treatise on Analytical Chemistry", Part II, Volume 7, Interscience Publishers, New York, N.Y., 1961, pp 175–179.
(3) Silvio Barabas and W. Charles Cooper, *Anal. Chem.*, **28**, 129 (1956).
(4) Silvio Barabas and Peter W. Bennett, *Anal. Chem.*, **35**, 135 (1963).
(5) Wladyslaw Reichel, *Anal. Chem.*, **43**, 1501 (1971).

RECEIVED for review September 5, 1977. Accepted December 5, 1977.

# Determination of Residual Chlorine in Water with Computer Automation and a Residual-Chlorine Electrode

**Lester P. Rigdon,* Gwilym J. Moody,[1] and Jack W. Frazer**

*Lawrence Livermore Laboratory, University of California, Livermore, California 94550*

**A method of determining active chlorine in water in the concentration range 3 to 100 ppb with an accuracy of 2 ppb has been developed. The method uses the Orion model 97-70 residual-chlorine electrode and the known standard-addition potentiometric technique to measure the potential difference between iodide and iodine that is generated by active chlorine. The assay is computer-automated to carry out the multiple addition of a standard; measure the potentials; plot the potentiometric curve, its Gran version, and an error function; and calculate the concentration of active chlorine in the assay solution. The electrode, the chemical reactions that occur during the assay, the preparation and storage of standards, and the procedure are discussed. Data obtained from the assay of standards prepared from deionized water, two sources of public water supply, and one swimming pool are presented.**

The Orion Research Inc. model 97-70 residual-chlorine electrode has been used to develop a procedure for determining active chlorine in water in the concentration range 3 to 100 parts per billion (ppb). Although the lower concentration limit of the linear calibration curve for the electrode is quoted at about 50 ppb, our procedure, using two such electrodes, consistently yields linear calibrations beginning at about 3.5 ppb. This combination electrode offers a simple, rapid and more sensitive alternative to the established American Society for Testing and Materials (ASTM) procedures for total residual chlorine (*1*, *2*). This dual sensor comprises a platinum redox element that develops a potential $E_1$ based on the relative levels of iodine and iodide ion in solution:

$$E_1 = E_0 + \frac{S}{2} \log [I_2] - S \log [I^-] \quad (1)$$

where $S$ represents the Nernstian factor, 2.303 $RT/nF$. The iodide sensing element develops a potential $E_2$ that depends on only the iodide level in solution;

$$E_2 = E_0' - S \log [I^-] \quad (2)$$

The difference $\Delta E$ between the individual potentials that is developed by the sensors is simply related to the iodine in solution by

$$\Delta E = \text{constant} + S/2 \log [I_2] \quad (3)$$

Thus the residual-chlorine electrode can be used to indirectly determine active chlorine after in situ stoichometric conversion of iodide to iodine by such chlorine species in a pH 4 acetate-buffered solution (*1*). The reactions pertinent to the success of the assay, using hypochlorite to represent active chlorine, are:

$$OCl^- + 2I^- + 2H^+ \rightarrow I_2 + Cl^- + H_2O \quad (4)$$

$$O_2 + 4I^- + 4H^+ \rightarrow 2I_2 + 2H_2O \quad (5)$$

$$I_2(\text{solution}) \rightarrow I_2(\text{gas}) \uparrow \quad (6)$$

Thus oxidizing agents, including bromine, iodate, cupric ion, and manganese dioxide, that convert iodide to iodine will interfere with the assay (*3*). Oxygen dissolved in the sample or absorbed from the atmosphere during the assay can oxidize the iodide, giving significantly high results in the low-ppb range samples. Loss of gaseous iodine may also occur, resulting in erroneously low results. It is desirable to minimize the effect of these latter two reactions and operate under conditions where their magnitudes are comparable.

In the method described below, the assay technique of known standard-addition was employed. Also, we used computer automation to add a standard, measure the potential; plot the potentiometric curve, its Gran version, an error function (*4*, *5*); and calculate the amount of chlorine in the assay solution. The error function locates the region of a potentiometric titration curve where the electrochemical cell is most nearly Nernstian.

## EXPERIMENTAL

**Apparatus.** Two Orion Research Inc. model 97-70 residual-chlorine electrodes were used in this work. For a few preliminary manual electrode calibrations, the potentials were measured with a Fisher Scientific Co. model 520 pH/ion meter with digital readout to 0.1 mV. For the computerized measurements, the electrode potentials were amplified, filtered, and interfaced to the computer through an analog-to-digital converter (ADC). The amplifier is a multicell unit so that up to three electrodes can be monitored simultaneously. It is designed such that the signal range and lower limit can be set to use the full range of the ADC.

For all standard additions, we used a Mettler Instruments Corporation model DV11 digital buret drive with interchangeable 10-mL burets. This setup could deliver titrant volumes as small as 0.001 mL under computer control, or 0.1 mL by manual push button control. A PDP8/I computer using FOCAL computer language (*4*), and a computer system consisting of a GT-44 and PDP11/45 using FORTRAN computer language were used. Both computerized systems used a cathode ray tube to display the potentiometric data as acquired, and Gran and error-function plots when generated. Both were also equipped with a light-sensitive pen and cursors so that positions in the data array could be specified by the operator.

All electrode calibrations and assays were carried out at 25 ± 0.5 °C in 150-mL beakers. A glass stirring paddle and electric motor controlled by a rheostat were used to control the stirring characteristics.

**Reagents.** The Orion Research Inc. iodide reagent (catalogue No. 97-70-10) and acid-buffer reagent (catalogue No. 97-70-09) were used as recommended for some preliminary studies (*3*). For later studies, and all the assays we report here, either reagent-grade KI crystals or a 10% (w/v) solution of KI in 0.025 M NaOH was added directly to the test solution. The pH 4 buffer was prepared by dissolving 243 g of sodium acetate trihydrate and 480 g of glacial acetic acid in enough deionized water to make 1 L, in accordance with the ASTM procedure (*1*, *2*).

**Standards.** Chlorimine-T trihydrate (Aldrich Chem. Co., Inc., catalogue No. 85,731-9) and calcium hypochlorite (Fischer Sci-

[1] Present address, The University of Wales Institute of Science and Technology, King Edward VII Avenue, Cathays Park, Cardiff, CF 1 3 NU, Wales, United Kingdom.

0003-2700/78/0350-0465$01.00/0 © 1978 American Chemical Society

Table I. Residual-Chlorine Assay Using Chloramine-T Standard; 180 Data Points Taken in 180 s[a]

| Chloramine-T taken, ppb | No. of runs | Residual chlorine found, ppb | Rel std dev | Error, ppb |
|---|---|---|---|---|
| Blank[b] | 5 | 0.16 | 0.10 | +0.16 |
| 4 | 5 | 3.44 | 0.25 | −0.56 |
| 10 | 5 | 10.21 | 0.89 | +0.21 |
| 20 | 5 | 20.65 | 1.39 | +0.65 |
| 40 | 5 | 40.03 | 0.41 | +0.03 |
| 80 | 6 | 79.25 | 1.65 | −0.75 |

[a] Standard addition initiated 1 min after iodide reagent was added. [b] No blank corrections applied to chloramine-T samples.

entific Co., catalogue No. C-100) were used to prepare active chlorine standards. All standards and reagents were prepared with water distilled over potassium permanganate or deionized water, each being finally deaerated with highly pure nitrogen. For electrode calibrations, a 0.01 M solution of chloramine-T was prepared and serially diluted when ready for use. Fresh stock standards were prepared daily to contain 2 g of chlorine (15.882 g of chloromine-T per liter), and 1-mL aliquots were diluted to 1 L to give 2 ppm. We assayed stock solutions by titrating with sodium thiosulfate using starch indicator (6). Both chloramine-T and a filtered calcium hypochlorite solution provide a suitable direct source of active chlorine standards, but chloramine-T is considerably more stable, showing less than 2% loss of chlorine after 226 hours storage in glass. Calcium hypochlorite lost 14% and 35% of chlorine when stored for 216 hours in glass and polyethylene bottles, respectively. We prepared iodate standards by dissolving the calculated amount of primary-standard grade $KH(IO_3)_2$ (G. Frederick Smith Co., Inc.) in deionized water. Generally a stock 0.01 N solution was serially diluted as needed for electrode calibrations and standard-addition assays. Alternatively, the Orion iodate reagent (catalogue No. 97-70-07) can be employed (3).

**Procedure.** A 50- or 100-mL aliquot of sample in a 150-mL beaker is mixed with 1 mL of buffer, and the electrode is submerged so that the iodide-sensing element is about 0.5 cm below the liquid surface. The stirring motor is adjusted to give a well-stirred solution with minimum vortex and in which no visible air bubbles are entrained. Either 50 to 100 mg of KI, or 1 mL of 10% KI in basic solution is added, and after 1 min the potential is recorded and the standard addition initiated. Then, a standard containing 2 ppm of active chlorine or its equivalent is added in 180 increments of 0.005 to 0.010 mL each. One increment is added each 0.72 s. The potential is recorded just before each addition. The data are plotted on the cathode ray tube and transformed to a Gran plot, and the error-function minimum is determined. Then the concentration of active chlorine is calculated from the error-function minimum. The electrode is rinsed thoroughly and blotted dry with tissue before the start of each assay.

## RESULTS AND DISCUSSION

**Blank and Interference by Oxygen.** We conducted experiments to determine the level of oxygen interference in aerated water and the effect of stirring rate on possible oxygen absorption during assay. First we aerated deionized water by bubbling air through it for 7 to 10 min and then assayed the water by the above procedure to test for dissolved oxygen. An average of 0.16 ppb with a relative standard deviation of 0.1 ppb was found (Table I).

To study the effect of stirring on oxygen absorption, we deaerated deionized water by bubbling highly pure nitrogen through it for 7 to 10 min. The nitrogen stream was stopped, 1 mL each of buffer solution and 10% KI were added, and the potential was measured at 0.72-s intervals for 6 min. The effect on these measurements of two greatly different stirring rates was determined. The minimum stirring rate generated a small vortex and brought no air bubbles into the bulk of the solution; while at the maximum stirring rate, the vortex

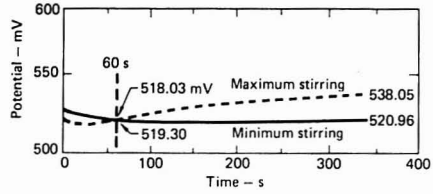


Figure 1. Effect of stirring rates (adsorption of oxygen) on the potential from the Orion 97-70 chlorine electrode

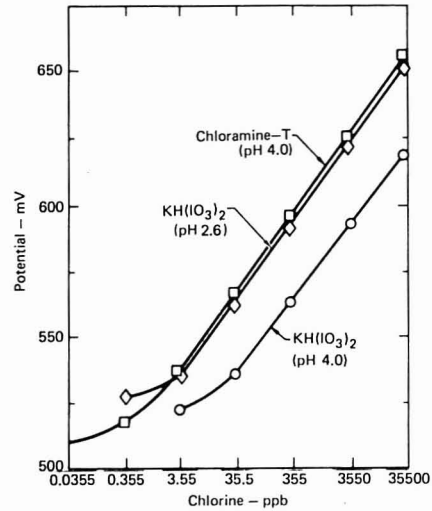


Figure 2. Computer calibration of an Orion 97-70 residual-chlorine electrode under three different conditions

extended nearly to the bottom of the solution and many small air bubbles were continually entrained into the bulk of the solution. The electrode took about 60 s to equilibrate at the start of each run. The total increases in potential after 60 s were 1.66 mV for the minimum rate and 20.02 mV for the maximum. These potentials are equivalent to about 0.6 and 20 ppb of chlorine respectively (Figure 1).

Iodate oxidizes iodide to iodine in acid solution according to:

$$IO_3^- + 5I^- + 6H^+ \rightarrow 3I_2 + 3H_2O \quad (7)$$

Orion Inc. and ASTM recommend $KIO_3$ and $KH(IO_3)_2$, respectively, as a standard instead of a compound yielding active chlorine because primary standard-grade iodate is readily available and iodate solutions are much more stable than active chlorine solutions. Iodate appears to be a satisfactory standard for the manual iodometric ASTM methods for assaying active chlorine, but we have not investigated this point.

However, iodate is unsatisfactory below 35 ppb for the Orion standardization procedure with the 97-70 chlorine electrode (Figure 2). At pH 4 the reaction is too slow, but at pH 2.6 it is fast enough for satisfactory use at chlorine levels of 4 ppb or more. Thus calibrations were investigated with $KH(IO_3)_2$ and chloramine-T using acetic acid sodium acetate buffer at pH 4, and also with iodate solutions adjusted to pH 2.6 with 0.2 M acetic acid. We placed the electrode in the buffered

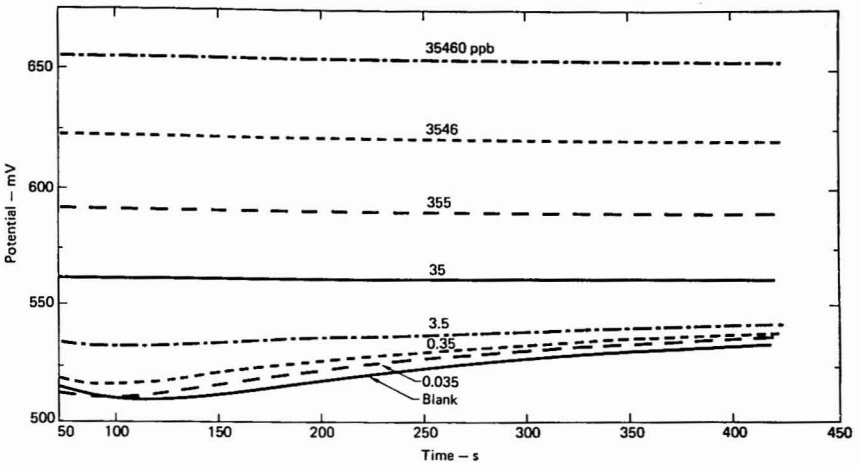


**Figure 3.** Response of the Orion 97-70 chloride electrode to chloramine-T in pH 4 acetate buffer

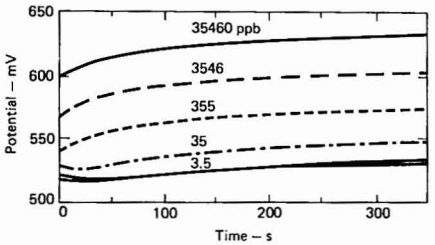


**Figure 4.** Response of the Orion 97-70 chlorine electrode to $KH(IO_3)_2$ in pH 4 acetate buffer

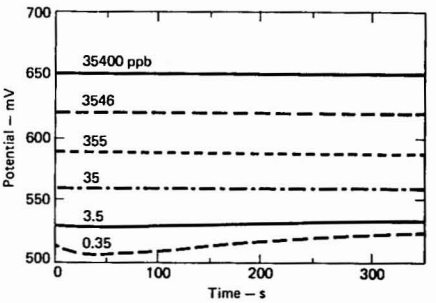


**Figure 5.** Response of the Orion 97-70 chlorine electrode to $KH(IO_3)_2$ in 0.2 M acetic acid at pH 2.6

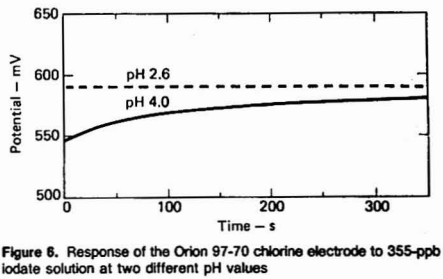


**Figure 6.** Response of the Orion 97-70 chlorine electrode to 355-ppb iodate solution at two different pH values

solutions and initiated Reaction 7, or of course Reaction 4, by injecting 1 mL of KI solution. We then measured the potential at least once per second for 6 min with continuous, minimum stirring. Typical potential vs. time curves are shown in Figures 3 through 6 and typical electrode-calibration curves are shown in Figure 7, where the potential (measured 60 s after addition of KI) is plotted against the equivalent concentration of active chlorine. An example of a typical potentiometric curve, Gran plot, and error function are shown in Figure 8.

**Iodide Reagent.** Some lots of Orion 97-70-10 iodide reagent gave blanks ranging from 5 to 15 ppb of chlorine when 20 drops were added to 50 mL of water. We also found that a 10% aqueous solution of KI slowly turned brown with increased storage time and yielded increasingly high blanks, presumably because of the oxidation of iodide by oxygen in air. Adding KI crystals to the sample is a satisfactory means of correcting the problem of iodide-reagent oxidation. However, the initial potential varies with the amount of iodide (Reactions 1 and 2). Therefore, the iodide concentration must be the same for electrode calibrations. There was no effect on the assay when 50 to 250 mg of KI was added to 50 mL of samples, while a 10% solution of KI in 0.025 M NaOH was stable for at least several weeks. It is recommended that aliquots of such a solution be used even for routine assays.

**Loss of Gaseous Iodine.** To appraise the error that might result from loss of iodine gas, we monitored potential vs. time for 6 min at chlorine concentrations from 10 to 80 ppb and at the minimum stirring rate. Changes in potential observed between 1 and 6 min for the stirred solutions were between 0.2 and 0.3 mV.

**Standard Additions.** To determine the effect of the amount of chlorine added per increment, 500 additions of standard chloramine-T containing 2 ppm of chlorine were added in increments of 0.002 to 0.015 mL to assay solutions containing 10 ppb of chlorine in deaerated water. Over the range tested, there is no significant difference in the results (Table II). The average amount found was 9.59 ppb with a relative standard deviation of 0.23 ppb.

Table II. Effect of the Size of the Incremental Titrant Additions for Known-Addition Assay of 10-ppb Standard Chloramine-T[a]

| Incremental volume of chloramine-T, mL | Amount found, ppb[b] |
|---|---|
| 0.002 | 9.56 |
| 0.005 | 9.98 |
| 0.007 | 9.40 |
| 0.010 | 9.76 |
| 0.015 | 9.26 |

[a] The data show no significant change with increment size. The assay used 1 mL of 10% KI in basic solution and pH 4 acetate buffer. [b] No blank correction applied.

A series of blanks and standard assay solutions were prepared using deaerated water. The average chlorine found for blanks was only 0.16 ppb. The data indicate that the precision of the assay tends to overlap the level of the blank, and careful control of stirring to minimize absorption of oxygen is more crucial than a blank correction. The data for the standard assay solutions are given in Table II.

In addition to using deionized water to prepare assay standards, water from two sources of public water supply and one swimming pool was used to prepare 10-ppb assay standards. We allowed these waters to stand for several days and deaerated them with nitrogen for 7 to 10 min to remove any residual chlorine before adding the standard (*1*, *2*). Recoveries of the 10-ppb additions were 9.59, 9.14, 9.62, and 9.06 ppb.

**Electrode Calibrations, Gran and Error-Function Plots.** We calibrated two different Orion 97-70 electrodes, both manually and using the computer, and found them to be linear from about 3.5 to 35 460 ppb. The mean slope for 30 calibrations was 29.59 mV per decade with a standard deviation of 1.12 mV. Figure 7 shows the calibration of two electrodes determined simultaneously in the same solution, with the computer used to measure the potentials 1 min after iodide reagent was added. There is some difference between the two electrodes, but the linear range extends to about 3.5 ppb. The lower limit of the assay is probably governed more by absorption of oxygen than by the sensitivity of the electrode.

Although the calibration curves shown in Figure 7 appear linear over a five-decade concentration range (3.5 to 35 460 ppb), if one expands the curve around the 3.5-ppb level, some curvature is observed. The error function locates the region where the electrode response is most linear (*4*, *5*), and uses only a small set of standard additions to extrapolate the initial concentration. This, coupled with this method's capacity for very small and precise additions of standard, allows one to obtain reasonably accurate results even when the electrode response is not linear with concentration over the range added. For example, the Gran plot in Figure 8 shows some curvature with increasing concentration of standard. If we extrapolate the initial concentration using the entire data set, the error is greater than when we used a small subset of data near the beginning of the standard addition. In this example, 40 data points were used in successive estimates with a 10-point increment (shown by the error-function plot in Figure 8). The error-function minimum occurs where 51 to 91 additions have been made.

## CONCLUSION

This method of using the 97-70 electrode exhibits no liquid junction problem and gives reproducible slopes. More than 300 assays have been made without any noticeable deterioration of the electrode response. In addition to providing a rapid, simple means for determining low-level active chlorine, this method could be varied for determination of many other species, for example ozone.

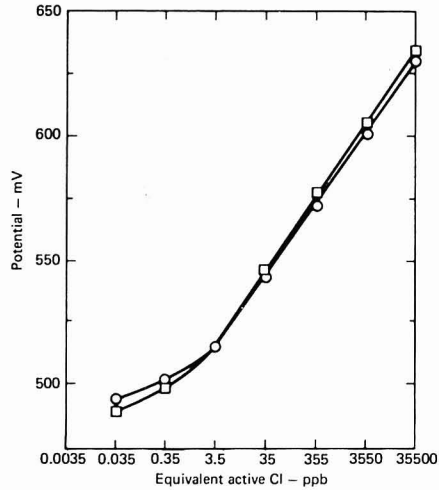


Figure 7. Simultaneous computer-based calibration of two Orion 97-70 residual-chlorine electrodes with chloramine-T in pH 4 buffer. Slopes are 30.0 and 29.55 mV per decade of concentration

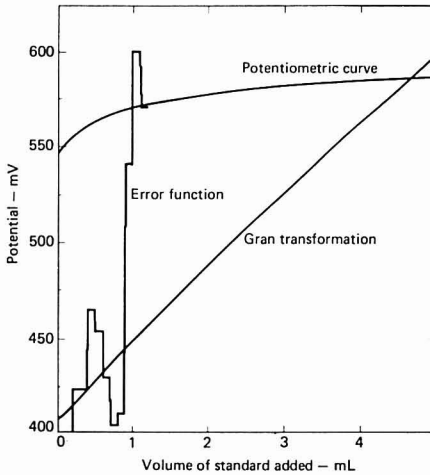


Figure 8. Potentiometric curve, Gran transformation, and error-function plots for the determination of 10 ppb of active chlorine

## LITERATURE CITED

(1) "Annual Book of ASTM Standards", Standard D-1427-68, American Society for Testing and Materials, Philadelphia, Pa., 1976, Vol. 31, p 283.
(2) "Annual Book of ASTM Standards", Standard D-1253-76, American Society for Testing and Materials, Philadelphia, Pa., 1976, Vol. 31, p 276.
(3) Instruction Manual for Model 97-90, Residual Chlorine Electrode, Orion Research, Inc., Cambridge, Mass., 1976.
(4) Jack W. Frazer, A. M. Kray, W. Selig, and R. Lim, *Anal. Chem.*, **47**, 869 (1975).
(5) Jack W. Frazer, Walter Selig, and Lester P. Rigdon, *Anal. Chem.*, **49**, 1250 (1977).

(6) W. C. Pierce and E. L. Haenisch, "Quantitative Analysis", John Wiley and Sons, New York, N.Y., 1948, Chap. 13.

RECEIVED for review September 13, 1977. Accepted November 7, 1977. Work performed under the auspices of the U.S. Energy Research and Development Administration, under contract No. W-7405-Eng-48, and the Environmental Protection Agency, under interagency agreement D7-0321. Mention of a company or product name does not imply approval or recommendation of the product by the University of California or the U.S. Energy Research and Development Administration to the exclusion of others that may be suitable.

# Determination of Sub-Nanogram Amounts of Silver in Rainwater by Stable Isotope Dilution

**M. E. Bickford,* Lyle R. Silka,[1] Robert D. Shuster, Ernest E. Angino, and Charles R. Ragsdale**

*Department of Geology, University of Kansas, Lawrence, Kansas 66045*

**Methods for the collection of rainwater and its analysis for silver were developed in connection with AgI cloud-seeding programs in Kansas. $^{109}Ag$ tracer is added in the field and Ag is removed by electrodeposition without processing or preconcentration for mass spectrometric analysis. Tests indicate that accuracy is about ±6% for concentrations of 0.10 ng/g or greater. Absolute errors averaging ±0.007 ng/g for solutions containing 0.01 ng/g Ag indicate that the method is probably limited by contamination or absorptive effects in the collecting bottles. Data for Ag concentration in Kansas rainwater over a two-year period are given.**

There is currently great interest in weather modification through seeding of cloud systems with AgI in Kansas as well as most of the other plains states. The cloud seeding process is not completely understood with respect to efficiency and down-wind effects. This has suggested monitoring of the Ag concentration in precipitation across the state both before and after cloud seeding experiments. Moreover, although Ag has been introduced into the atmosphere during cloud seeding for at least 25 years, virtually nothing is known about its distribution in rainwater, surface water, or ground water.

With these concerns in mind, we were asked by the Kansas Water Resources Board to design systems for the collection and Ag analysis of rainwater within the state. This paper presents the details of analysis of Ag in concentrations ranging from 0.01 to 10.4 ng/g in Kansas rainwater by stable isotope dilution analysis. We chose isotope dilution as an analytical technique partly because of our experience in the determination of U, Pb, Rb, and Sr by this method in connection with the measurement of isotopic ages of geological samples. However, we have found the technique to be ideally suited to the demands of the present research and we believe that it offers advantages over other analytical methods currently in use.

Others have reported the analysis of Ag in natural water in sub-nanogram quantities by neutron activation (*1*), flame atomic absorption with microsampling boat (*2*, *3*), and flameless atomic absorption (*4*, *5*). Neutron activation analysis is subject to rather large reproducibility errors (on the order of ±25% at nanogram concentrations) and is expensive. Atomic absorption methods are relatively inexpensive but require some preconcentration of water samples, with attendant possibilities for sample contamination, to obtain reasonable precision of measurements. All methods, including isotope dilution, are subject to additional errors which result from adsorption of Ag onto the walls of sample containers (*6*, *7*) unless steps are taken to prevent this.

[1] Present address, U.S. Environmental Protection Agency, 401 M. Street, S.W., Washington, D.C. 20460.

## EXPERIMENTAL

**Collection and Field Procedure.** We collect rainwater in devices such as those illustrated in Figure 1. A box, placed upon a 4-ft wooden tower and sealed around the top with weatherstripping, contains a child's ordinary plastic swimming pool of about 1-m diameter. The swimming pool has a hole in its center to which a funnel is attached with epoxy cement. The funnel leads to a 2-L polyethylene collecting bottle, in a wooden traveling case, through a short length of Tygon tubing to which an inverted funnel is attached to prevent dust contamination of the sample bottle. Sample bottles, filled with dilute (0.10 N) $HNO_3$ solution, are shipped to our collecting sites. When rainfall begins, the top of the collector is opened and the swimming pool is washed with the 2 L of dilute $HNO_3$ from the sample bottle. Then the bottle is placed, still in its traveling case, on a shelf beneath the collector and the Tygon tube is inserted into the mouth of the bottle.

After the rainfall stops, about 4 μg of $^{109}Ag$ spike in 3.5 N $HNO_3$ is added from a 50-mL bottle which has been sent to the site from our laboratory. Immediately, the spike bottle is rinsed with about 30 mL of distilled 3.5 N $HNO_3$ containing about 10 μg of 99.9999% pure Au; this solution is added to the sample bottle to complete the transfer of spike, acidify the solution, and make the resulting spiked rainwater sample about 5 ppb Au. Then the bottle is agitated for 7 min to equilibrate the isotopic tracer with the Ag present in the rainwater. If the rainfall is enough to completely fill the 2-L sample bottle, water is decanted until the volume is about 1.8 L before the spike and acid are added. This procedure minimized problems associated with adsorption of Ag on the walls of the sample bottle, for the Au is evidently preferentially adsorbed and the quantitative information resides only in the $^{107}Ag/^{109}Ag$ ratio after the spike has been equilibrated with the sample. We began adding Au to our samples at the suggestion of I. L. Barnes, National Bureau of Standards, who found that Au stabilized Hg in ng/g concentrations in water solutions, and that the addition of Au to such solutions quantitatively released Hg which had been adsorbed on the container walls. Following the addition of the spike, the sample bottles are returned to our laboratory for mass spectrometric analysis.

**Electroplating and Isotope Dilution Analysis.** In the laboratory, we separate the Ag from the rainwater sample by electroplating it directly onto high purity Pt wire electrodes at a potential of 2 V. We use Pt wires about 12 cm long and place them directly in the sample bottle, thus eliminating losses or contamination through transfer or preconcentration procedures. We electroplate for at least 12 h and have obtained a yield greater than 95% when the solution is about 0.07 N in $HNO_3$. As will be discussed below, we can obtain stable ion beams for mass

0003-2700/78/0350-0469$01.00/0 © 1978 American Chemical Society

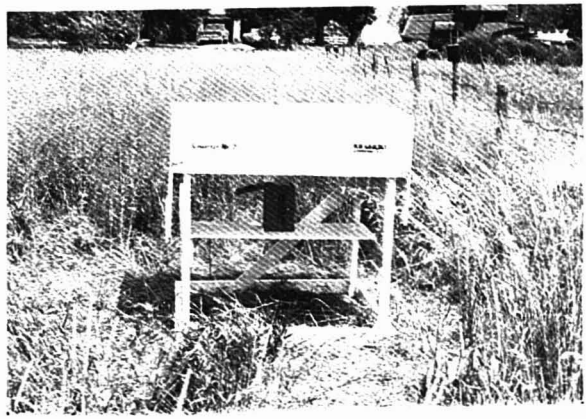

**Figure 1.** Rainwater collector on site near Lawrence, Kansas

**Table I. Isotope Ratio Measurements on $^{109}Ag$ Tracer and Normal Ag Standard**

| Material | $^{107}Ag/^{109}Ag \pm 1\sigma$ | Material | $^{107}Ag/^{109}Ag \pm 1\sigma$ |
|---|---|---|---|
| Tracer | 0.00792 ± 0.00230 | NBS SRM 978 | 1.0727 ± 0.0021 |
| Tracer | 0.00787 ± 0.00220 | | 1.0801 ± 0.0066 |
| Av. | 0.00790 | | 1.0783 ± 0.0064 |
| ORNL value | 0.00746 | | 1.0798 ± 0.0020 |
| | | | 1.0766 ± 0.0182 |
| | | | 1.0789 ± 0.0026 |
| | | Av. | 1.0777 |
| | | NBS value | 1.0760 |

spectrometry with samples of 50 to 100 ng so that yield in the electroplating process is not critical. During electroplating, the rainwater sample is stirred on a magnetic stirplate using a Teflon stir-bar which has been cleaned in distilled $HNO_3$ and distilled and deionized water. After electroplating is complete, the Ag is stripped from the cathode with distilled $HNO_3$, transferred to a 5-mL Pyrex beaker, and evaporated to dryness.

Nitric acid for use in this work is distilled in a Vycor glass sub-boiling still from reagent-grade starting material. We prepare water by distilling it in a Pyrex glass still and then passing it through a mixed-bed deionizing column.

The mass spectrometer used is a 6-inch radius of curvature, single-focusing, 60°-sector instrument with a thermionic emission ion source. The Ag samples are loaded onto a single 20-mil rhenium filament on a bed of silica gel in the presence of 0.28 N $H_2PO_3$ following the technique of Cameron and others (8). This technique is now routinely used for mass spectrometric analysis of Pb and the similarities of Pb and Ag, especially with respect to ionization potential, suggested that it might also be suitable for Ag mass spectrometry. We found, after some experimentation, that we could obtain stable beams of Ag ions producing output signals of 30 to 100 mV with about 50 ng of Ag on a filament. We have obtained beams at lower intensities with total samples of only 0.10 ng, but our results are much more consistent with somewhat larger amounts of sample on the filament. Isotope ratios are recorded on our instrument by an automatic peak-hopping magnet current control circuit and a vibrating-reed electrometer. The output of the electrometer goes to a voltage-to-frequency converter whose output is counted and fed to a printer. Resolution of Ag isotopes by this instrument is excellent (Figure 2) and isotope ratios can be measured routinely with precision better than ±1%. Precision falls to about ±6% for extremely small samples which yield low ion currents.

## RESULTS

**Spike Composition and Accuracy of Isotopic Measurements.** We obtained 50 mg of approximately 99% enriched $^{109}Ag$ from Oak Ridge National Laboratory (ORNL) for use as the spike. After making a solution of this material in distilled $HNO_3$ we measured its isotopic composition on our mass spectrometer (Table I) and found that our results agreed very closely with those given by ORNL. The spike was then calibrated by isotope dilution against an Ag shelf solution carefully prepared from NBS $Ag(NO_3)$ SRM 978. The calibration value agreed with the gravimetric value of concentration of the spike solution within 0.5%. In addition, we have measured the isotopic composition of the shelf solution. These measurements (Table I) agree closely with the composition determined by NBS.

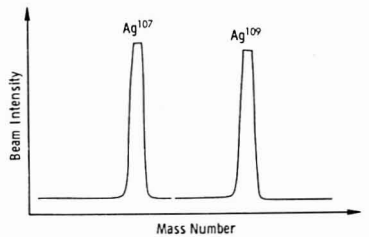


**Figure 2.** Silver mass spectrum

**Analytical Accuracy.** We made several tests to determine the accuracy of our analytical scheme. We obtained ultra pure water and determined that its Ag concentration was 0.0029 ng/g of $H_2O$. Using this water and several of our 2-L rainwater sample bottles, we prepared solutions of varying amounts of normal Ag in about 1.85 L of water, made them about 5 ppb Au, and spiked them with $^{109}Ag$ tracer. Silver was then

Table II. Isotope Dilution Tests

| Ag concn in test solution, ng/g | Ag concn by isotope dilution, ng/g | Difference, ng/g |
|---|---|---|
| 201.6 | 203.2 | +1.6 |
| 22.41 | 22.49 | +0.08 |
| 12.00 | 11.66 | −0.34 |
| 9.62 | 10.34 | +0.72 |
| 8.51 | 7.38 | −1.13 |
| 0.970 | 0.919 | −0.051 |
| 0.024 | 0.050 | +0.026 |
| 0.132 | 0.127 | −0.005 |
| 0.018 | 0.023 | +0.005 |
| 0.014 | 0.024 | +0.010 |
| 0.010 | 0.0045 | −0.0055 |

separated from these by electroplating and the $^{107}Ag/^{109}Ag$ ratio was measured on the mass spectrometer. Ag concentrations were calculated from the isotope ratios and compared with the known Ag concentrations of the test solutions. The results of these tests are given in Table II.

The data in Table II indicate that our absolute errors in analyzing the test solutions are about 6% for concentrations of 0.1 ng/g or greater, although one result (8.51 ng/g test solution) is in error by 13%. The absolute errors for the analyses of test solutions whose concentrations are in the 0.02 to 0.01 ng/g range are small, averaging about 0.007 ng/g, but these errors are a quite large percentage of the Ag concentrations of the test solutions. The results suggest that we are limited in the analysis of these very dilute solutions by contamination, adsorptive effects on the laboratory ware, or both. Our results in the 0.01 to 0.02 ng/g range are accurate only to within plus or minus a factor of two.

In a similar series of tests, done before we began the addition of Au to our solutions, we consistently found that our isotope dilution results were low by 15 to 25% suggesting that Ag was being lost to the walls of the 2-L sample bottles. The present results evidently confirm that the addition of 5 to 10 ppb Au to the solutions inhibits or prevents adsorption of Ag on container walls. As mentioned earlier, we are indebted to I. L. Barnes of the National Bureau of Standards, who suggested the addition of Au as a means of solving the adsorption problem.

The tests are probably a fair measure of the accuracy with which we can measure Ag concentrations in rainwater, for we used the same sample bottles and other apparatus, and followed the same procedures as in our regular analytical method. In the analysis of field samples, additional uncertainties arise from potential contamination of collectors and from the presence of dust or other particulate matter in the atmosphere during rainfall.

**Concentration of Ag in Kansas Rainwater and Snow.** Table III gives the results of analyses of over 100 rainwater samples and of several snow samples that we have collected in Kansas. We began stabilizing samples by the addition of Au in April 1977. We currently have eight collecting stations: two are located at Lawrence, Kansas; the others are on Agricultural Experiment Stations at Colby, Garden City, Scandia, Hays, Tribune, and St. John, Kansas. The data in Table III should be representative of background Ag levels in rainwater in Kansas, and may be compared with values from several sources which are given in Table IV.

## DISCUSSION

The isotope dilution technique described here offers two major advantages for the analysis of nanogram quantities of Ag (or other elements) in natural waters. First, the tracer may be added directly to the sample in the field immediately after collection, thus minimizing errors which arise from adsorption

Table III. Range of Ag Concentrations in Kansas Rainwater Samples

| Location | Collection interval | Ag Concn, g/g |
|---|---|---|
| Lawrence, Kansas | 6/75–4/77 | $0.1–104 \times 10^{-10}$ |
| Lawrence, Kansas (Nelson Tract) | 9/75–4/77 | $0.5–2.9 \times 10^{-10}$ |
| Colby Exp. Field, Colby, Kansas | 6/75–4/77 | $0.15–41.6 \times 10^{-10}$ |
| Garden City, Kansas | 8/75–4/77 | $0.1–31.0 \times 10^{-10}$ |
| Scandia, Kansas | 1/76–4/77 | $0.2–5.4 \times 10^{-10}$ |
| Hays, Kansas | 2/76–1/77 | $0.2–10.0 \times 10^{-10}$ |
| Tribune, Kansas | 4/76–4/77 | $0.7–3.5 \times 10^{-10}$ |
| St. John, Kansas | 1/76–4/77 | $0.1–29.6 \times 10^{-10}$ |

Table IV. Representative Ag Concentrations in Rainwater and Snow

| Location and Reference | Date | Ag Concn, g/g |
|---|---|---|
| Southwest Montana (*4*) | 2/71–7/71 | $0.1–0.9 \times 10^{-10}$ (snow) |
| Eastern Sierra Nevada (*1*) | 1966–1969 | $0.04 \times 10^{-10}$ av. (snow) |
| Lake Erie, New York State (*1*) | 1968–1969 | $0.21 \times 10^{-10}$ av. (snow) |
| Climax, Colorado (*1*) | 1966–1969 | $0.4 \times 10^{-10}$ av. (snow) |
| Quillayute, Washington (*9*) | 12/68 | $0.1–10 \times 10^{-10}$ (rain) |
| Nebraska–South Dakota (*10*) | 4/70 | $0.05–0.5 \times 10^{-10}$ (rain) |
| Coral Gables, Florida (*5*) | 6/73–10/73 | $0.5 \times 10^{-10}$ av. (rain) |
| Seawater (*1*) | | $15.0–29.0 \times 10^{-10}$ |

of the sample onto the walls of the sample container. Second, electroplating of the Ag directly from the sample bottles without preconcentration eliminates errors or contamination from such procedures.

The great sensitivity of the mass spectrometer permits the measurement of isotope ratios from samples of Ag as small as 0.1 ng, and this in turn permits working with relatively small water samples. We currently collect 2-L samples, but we could probably work with 1 L or less. Much of the sensitivity of the techniques we are using results from the remarkable improvement in mass spectrometry of Pb (and by extension Ag) since the development of the silica gel–phosphoric acid method by Cameron and others.

The method described here is quite simple to carry out. It has the disadvantage of requiring a mass spectrometer for measurement of isotope ratios.

## LITERATURE CITED


(1) J. A. Warburton and L. G. Young, *Anal. Chem.*, **44**, 2043 (1972).
(2) Denver, Colorado Meeting, May 18, 1971, on "The determination of silver in terrestrial and aquatic ecosystems" (Details available from M. L. Teller, Colorado State University, Fort Collins, Colo.).
(3) H. L. Kahn, G. E. Peterson, and J. E. Schallis, *At. Absorp. Newsl.*, **7**, 35 (1968).
(4) R. Woodriff, B. R. Culver, D. Shrader, and A. B. Super, *Anal. Chem.*, **45**, 230 (1973).
(5) J. Wisniewski, W. R. Cotton, and R. I. Sax, 4th Conf. on Weather Modification, Fort Lauderdale, Fla., 1974, p 73.
(6) F. K. West, P. W. West, and F. A. Iddings, *Anal. Chem.*, **38**, 1566 (1966).
(7) T. T. Chao, E. A. Jenne, and L. M. Heppting, *U.S. Geol. Surv. Prof. Pap.*, **600-D**, 13 (1968).
(8) A. E. Cameron, D. H. Smith, and R. L. Walker, *Anal. Chem.*, **41**, 525 (1969).
(9) A. K. Chakraburtty, C. M. Stevens, H. C. Rushing, and E. Anders, *J. Geophys. Res.*, **69**, 505 (1964).
(10) L. A. Ranticelli, R. W. Perkins, T. M. Tanner, and C. W. Thomas, *AEC Sym. Ser.*, **22** (CONF – 700601), 99 (1970).


RECEIVED for review April 12, 1976. Resubmitted October 24, 1977. Accepted December 1, 1977. This research was supported by the Kansas Water Resources Board.

# Solubility Products of Bis(*O*,*O*′-diethyldithiophosphato)copper(II) and *O*,*O*′-dimethyldithiophosphatocopper(I)

**Walter Rudzinski and Quintus Fernando***

*Department of Chemistry, University of Arizona, Tucson, Arizona 85721*

**The ammonium salt of *O*,*O*′-diethyldithiophosphonic acid reacts with copper(II) in aqueous solution to give a mixture of the copper(I) and copper(II) complexes of *O*,*O*′-diethyldithiophosphonic acid. The solubility product of the copper(II) complex was found to be $10^{-15.22}$ in a $KNO_3$ medium of ionic strength 0.1. The reaction of copper (II) with the ammonium salt of *O*,*O*′-dimethyldithiophosphonic acid gave a mixture of several complexes. The dimeric copper(I) complex of *O*,*O*′-dimethyldithiophosphonic acid was readily synthesized and an approximate value for its solubility product was obtained.**

A large number of sulfur-containing compounds are employed as flotation agents and among these are the dithiophosphonic acids and their sodium, potassium, or ammonium salts (aerofloats). Unlike most flotation agents, the dithiophosphonic acids are stable in the presence of strong acids and are potentially useful in certain hydrometallurgical processes that make use of strong acids for the partial disruption of an ore matrix. A disadvantage of the dithiophosphonic acids is the relatively high solubility of their transition metal complexes. Of special interest to us are the values of the solubility products of a series of bis(*O*,*O*′-dialkyldithiophosphato)copper(II) compounds that were first reported by Kakovsky (*1*) and subsequently by Tulyupa (*2*). Both sets of solubility products decreased as the number of carbon atoms in the alkoxy substituents on the phosphorus atoms increased. There were considerable discrepancies, however, in the magnitude of the solubility products reported by the two workers. For example, the values reported for the solubility product of bis(*O*,*O*′-diethyldithiophosphato)copper(II), $Cu(dtp)_2$, differed by a factor of $10^4$. This large discrepancy raises a question concerning the identity of the copper complex that was synthesized by the two investigators. Wasson has reported that attempts to prepare (*O*,*O*′-dialkyldithiophosphato)copper(II) complexes as solids were unsuccessful probably because the dithiophosphate ligand acted as a reducing agent to form copper(I) complexes (*3*).

The formation of bis(*O*,*O*′-dimethyldithiophosphato)copper(II), $Cu(dmp)_2$, is of particular importance because it is the basis for a proposed titrimetric method for the determination of malathion by Hill and co-workers (*4*). In a subsequent report, Hill presented evidence which indicated that the copper(II) complex existed in equilibrium with the corresponding copper(I) complex and the disulfide formed by the oxidation of the dithiophosphate ligand (*5*).

The work that is described below was carried out to resolve the widely divergent values of the solubility products that have been reported for $Cu(dtp)_2$ and $Cu(dmp)_2$. In the course of this work, it was essential to determine the oxidation state of the copper in the complexes that were synthesized and to verify that the complexes had the predicted composition.

## EXPERIMENTAL

**Synthesis of $NH_4[(S)SP(OC_2H_5)_2]$, $NH_4$(dtp).** The preparation was adapted from the method of Coldberry, Fernelius, and Shamma (*6*). One hundred mL of ethanol was added slowly over a period of 1.5 h to 110 g of finely powdered $P_2S_5$ (Eastman Chemical Co.). The reaction mixture was heated under reflux for 3 h and the $H_2S$ that was evolved was passed through scrubbers containing $H_2O_2$ and NaOH. The reaction product which consisted of a black oily liquid was filtered without suction and the filtrate was extracted with three 50-mL portions of water. Gaseous ammonia was bubbled through the extract containing the *O*,*O*′-diethyldithiophosphonic acid. Two hundred mL of acetone was added and the mixture was concentrated to one half of its original volume. White crystals of the ammonium salt which formed on standing were filtered, dried, and recrystallized from ethyl acetate. Titration of the ammonium salt, dissolved in 90% ethanol, with NaOH showed that the purity of the salt was 99.3%.

**Synthesis of $Cu[S(S)P(OC_2H_5)_2]_2$, $Cu(dtp)_2$ and $Cu[(S)SP(OCH_3)_2]_2$, $Cu(dmp)_2$.** Attempts were made to prepare $Cu(dtp)_2$ and $Cu(dmp)_2$ by the slow addition of $NH_4$(dtp) or $NH_4$(dmp) (Aldrich Chemical Co.) to an aqueous solution of copper(II) nitrate. In each case, a yellowish brown oil was formed when the reaction was complete. The components of the oily brown liquid that was obtained in the synthesis of $Cu(dtp)_2$ were separated on silica gel plates with a solvent mixture that consisted of 92% v/v toluene and 8% v/v ethyl acetate.

**Synthesis of $Cu[(S)SP(OCH_3)_2]$, Cu(dmp).** An aqueous solution of copper(II) nitrate was added to a solution containing an excess of $NH_4$(dmp). When a pale yellow precipitate was obtained, $SO_2$ was passed through the solution to reduce any $Cu(dmp)_2$ that may have formed. The pale yellow precipitate was washed repeatedly with water and dried in a vacuum desiccator. (Cu: 28.8% calcd, 28.9% found; P: 14.04% calcd, 14.15% found.)

**Infrared Spectra.** A Perkin-Elmer Infracord Spectrophotometer was used to record all infrared spectra in the range 4000–700 $cm^{-1}$. A Beckman IR 12 double beam spectrophotometer was used to record the spectra in the region 700–200 $cm^{-1}$.

The infrared spectra of $Cu(dtp)_2$ and $Cu(dmp)_2$ which were obtained as oily liquids were run as Nujol mulls and as neat oils on AgCl disks. The infrared spectrum of the pale yellow compound, Cu(dmp), was run as a KBr pellet in the region 4000–200 $cm^{-1}$.

**Mass Spectrum of Cu(dmp).** The mass spectrum of Cu(dmp) was obtained with a Hewlett-Packard Model 5930A mass spectrometer with an electron energy of 8 eV. The compound was introduced into the sample chamber which was maintained at 200 °C by the direct insertion method.

**Photoelectron Spectroscopy.** X-ray photoelectron spectra were obtained with a McPherson ESCA 36 Photoelectron spectrometer equipped with a Sargent-Welch turbomolecular pumping system ($10^{-7}$ to $10^{-8}$ Torr). The sample was irradiated with Al K$\alpha$ x-rays (1482.6 eV). A finely powdered sample of the compound was spread on double-stick adhesive tape (3M) which was attached to an aluminum planchet. The sample holder was cooled with liquid nitrogen. The binding energies of the photoelectrons were determined by assuming that the carbon electrons from the adhesive tape had a binding energy of 285.0 ± 0.24 eV.

**Atomic Absorption Spectrophotometry.** The total copper concentrations in solutions that were in equilibrium with solid $Cu(dtp)_2$ were determined with a Varian Model AA-5 atomic absorption spectrophotometer. The copper concentrations of solutions that were in equilibrium with Cu(dmp) were determined with a Heath Model 703 atomic absorption spectrophotometer. Single slot burners designed for use with an air–acetylene flame were employed. A standard copper hollow cathode lamp was used as the source and the copper resonance line at 3248.8 Å was used for all the measurements.

**Fluorescence Measurements.** The concentrations of the ligand, dmp, in solutions that were in equilibrium with the pale

0003-2700/78/0350-0472$01.00/0 © 1978 American Chemical Society

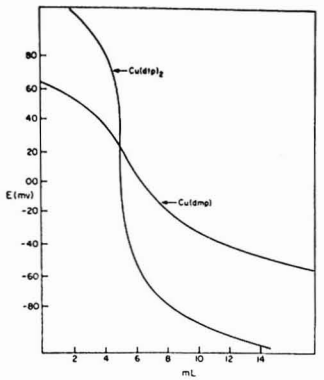


**Figure 1.** Potentiometric titrations of copper(II) nitrate ($2.166 \times 10^{-3}$ M) with $NH_4$dtp ($2.232 \times 10^{-2}$ M) and copper(II) nitrate ($2.211 \times 10^{-3}$ M) with $NH_4$dmp ($2.241 \times 10^{-2}$ M) with a cupric ion selective electrode

yellow solid, Cu(dmp), were determined fluorimetrically. A Perkin-Elmer Model 204A fluorescence spectrophotometer was used for the fluorescence measurements; the excitation wavelength was 384 nm and the fluorescence intensities were measured in a 1-cm quartz cell at 385 nm.

**Potentiometric Measurements.** All potentiometric determinations were carried out in a water-jacketed vessel that was maintained at 25 °C. The potentiometric measurements were made with an Orion Model 701 digital pH/mV meter with a cupric ion selective electrode (Model 94-29) and a double-junction reference electrode (Model 90-02-00). Standard solutions of copper(II) nitrate were made with sufficient $KNO_3$ to maintain a constant ionic strength of 0.1. The calibration and determination of the response of the cupric ion selective electrode have been described before (*7*).

Twenty-five mL of a $2.166 \times 10^{-3}$ M solution of Cu(II) nitrate was titrated with a $2.232 \times 10^{-2}$ M solution of $NH_4$(dtp). The solution was stirred at a constant rate throughout the titration. The concentration of $Cu^{2+}$ was calculated from the measured potential difference between the Orion cupric ion selective electrode and the double-junction reference electrode at each point in the course of the titration. It was found essential to keep the cupric ion electrode surface free of precipitated $Cu(dtp)_2$. This was accomplished by removing the electrode from the titration vessel and wiping the electrode surface to free it from any adhering precipitate. Failure to do this at least three or four times in the course of a titration resulted in nonreproducible potential differences. All titrations were carried out in triplicate to ensure that the potential differences were reproducible.

The above titrimetric procedure was repeated with $NH_4$(dmp) as the titrant. Twenty-five mL of a $2.211 \times 10^{-3}$ M solution of copper(II) nitrate was titrated with a $2.241 \times 10^{-2}$ M solution of $NH_4$(dmp). Examples of the experimental curves are shown in Figure 1.

## RESULTS AND DISCUSSION

Attempts to synthesize $Cu(dtp)_2$ resulted in the formation of a yellowish brown oil which was separated into two components by thin-layer chromatography with a mixture of toluene and ethyl acetate (92:8 v/v) as the developing solvent. The yellowish brown oil separated into two zones, a colorless zone which contained the dimeric copper(I) complex ($R_f = 0$) and a pale yellow zone which contained the $Cu(dtp)_2$ complex ($R_f = 0.55$). The dimeric copper(I) complex was identified as the 1:1 complex of copper(I) and dtp by the characteristic bands in its infrared spectrum (*9*). The pale yellow zone contained $(Cu(dtp)_2$ which has an absorption band in the visible region at 420 nm; neither the disulfide oxidation product nor the 1:1 complex of copper(I) absorbed in this

**Table I. Infrared Absorption Bands of $Ni(dtp)_2$ and Related Compounds ($cm^{-1}$)**

| Yellowish brown oil | $Ni(dtp)_2$[a] | $Cu(dtp)$[b] |
|---|---|---|
| 1302 | ... | ... |
| 1235 | ... | ... |
| 1162 | 1159 | 1150 |
| 1095 | 1103 | 1098 |
| 1040 | 1049 | 1035 |
| 1008 | 1004 | 1015 |
| 964 | 970 | 965 |
| 955 | ... | 955 |
| 822 | 823 | ... |
| 806 | 807 | ... |
| 786 | ... | 785 |
| 774 | ... | 775 |
| 690 | ... | ... |
| 630 | 643 | 640 |
| 518 | 544 | 538 |
| 502 | ... | 524 |
| 482 | ... | ... |
| 401 | 396 | ... |

[a] Ref. (*8*). [b] Ref. (*9*).

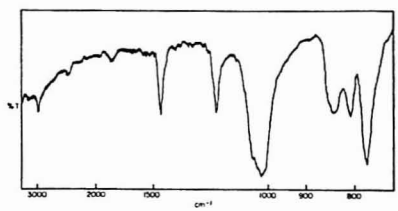


**Figure 2.** Infrared spectrum of the copper(I) complex of dmp in KBr

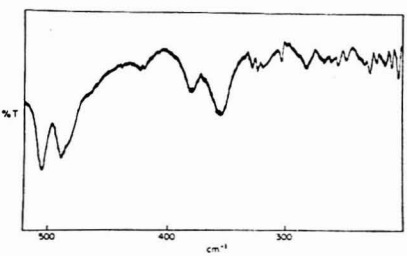


**Figure 3.** Infrared spectrum of the copper(I) complex of dmp in KBr in the low frequency region

region of the spectrum (*5*). The colorless zone at $R_f = 0$ was extracted with chloroform. The solution gradually darkened and after about 2 h it had an absorption band at 420 nm. This indicated that $Cu(dtp)_2$ was formed in the chloroform solution of the copper(I) complex and existed in equilibrium with the copper(I) complex and the disulfide (*5*).

$$R_2P(S)S\text{-}S(S)PR_2 + Cu_2[S(S)PR_2]_2 \rightleftharpoons 2\,Cu[S(S)PR_2]_2 \quad (1)$$

where $R = OC_2H_5$.

A comparison of the infrared frequencies that have been reported for $Ni(dtp)_2$ (*8*) and the copper(I) complex of dtp (*9*), with the frequencies that were observed for the yellowish brown oil (Table I) confirmed the finding that it is a mixture of the copper(I) and copper(II) complexes of dtp.

The infrared spectrum of the copper(I) complex of dmp, which is a pale yellow solid, has two prominent bands at 840 $cm^{-1}$ and 489 $cm^{-1}$ (Figures 2 and 3) which are not found in the infrared spectra of either the copper(I) complex of dtp

Table II. Mass Spectrum of the Copper(I) Complex of dmp

| m/e | Relative intensity | m/e | Relative intensity |
|---|---|---|---|
| 76 | 5.5 | 314 | 39.3 |
| 93 | 100 | 315 | 4.2 |
| 125 | 65.0 | 316 | 7.6 |
| 157 | 10.5 | 370 | 2.5 |
| 158 | 9.1 | 377 | 2.9 |
| 188 | 11.3 | 379 | 1.8 |
| 220 | 6.0 | 440 | 0.3 |
| 222 | 0.9 | 442 | 0.4 |
| 250 | 7.1 | | |

(*9*) or $Ni(dmp)_2$ (*8*). The presence of these two bands may be attributed either to the contamination of the copper(I) complex of dmp with a small amount of $Cu(dmp)_2$ or to the presence of the disulfide oxidation product. The former is unlikely since these two bands are not found in the infrared spectra of either $Ni(dtp)_2$ or $Ni(dmp)_2$. Moreover, the presence of a copper(II) complex could not be detected in the x-ray photoelectron spectrum of the pale yellow copper(I) complex of dmp. The $2p_{1/2}$ peak was found at 953 eV (FWHM = 3 eV) and $2p_{3/2}$ peak at 933 eV (FWHM = 2 eV). The satellite or secondary peaks that are usually associated with the x-ray photoelectron spectra of copper(II) compounds were absent.

It is conceivable that the copper(I) complex of dmp can have additional infrared absorption bands that arise as a consequence of ring puckering and alteration of the symmetry of the molecule. It was decided, therefore, to obtain the mass spectrum of the compound with the expectation that any copper-containing peaks would be readily identifiable since the $^{63}Cu$:$^{65}Cu$ isotope ratio is 7:3. The values of $m/e$ with the corresponding relative intensities for the mass spectrum of the copper(I) complex of dmp are given in Table II. The low molecular weight fragments at $m/e$ values of 93 and 125 are characteristic of all dithiophosphate compounds (*10*) and may be assigned to the fragments $P(OCH_3)_2$ and $P(OCH_3)_2(S)$, respectively. By analogy to the fragmentation patterns that have been observed for $Ni[(S)SP(CH_3)_2]_2$, (*11*, *12*), the fragments observed at $m/e$ values of 314, 250, 157, and 188 may be attributed to the following disulfide fragments: $(CH_3O)_2P(S)$-S-S-(S)$P(OCH_3)_2$; $(CH_3O)_2P$-S-S-$P(OCH_3)_2$; $(CH_3O)_2P$-S-S-$PO_2$; $(CH_3O)_2PS_2$ and $(CH_3O)_2P$-S-S-P.

Unfortunately, no copper containing peaks could be identified. The peaks at $m/e$ values of 377 and 379 may be attributed to $Cu(dmp)_2$ even though the ratio of the peak intensities do not correspond to a value of 7/3. It is possible that $Cu(dmp)_2$ is formed when $Cu_2(dmp)_2$ is subjected to electron impact. The peaks at 440 and 442 may be indicative of the presence of a fragment of the dimer, but the peaks are too weak to be interpretable. The only conclusion that can be drawn is that the 1:1 complex of copper(I) with the ligand, *O,O'*-dimethyldithiophosphate, is nonvolatile and probably dimeric or polymeric.

It has been established from the foregoing experiments that the yellowish brown oil formed by the interaction of copper(II) nitrate with $NH_4(dtp)$ in an aqueous solution is a mixture of the copper(I) and copper(II) complexes of dtp. The reducing action of the ligand, dtp, results in the formation of the copper(I) complex as well as the disulfide, and the following equilibria are established in the aqueous solution.

$$Cu^{2+} + 2[S(S)PR_2]^- \rightleftarrows Cu[S(S)PR_2]_2 \quad (2)$$

i.e., $Cu^{2+} + 2\ dtp^- \rightleftarrows Cu(dtp)_2$, and

$$Cu[S(S)PR_2]_2 \rightleftarrows {}^1/_2Cu_2[S(S)PR_2]_2 + {}^1/_2[R_2P(S)S\text{-}S(S)PR_2] \quad (3)$$

disulfide

where $R = OC_2H_5$.

It can be inferred from Equations 2 and 3 that copper(II) reacts with the ligand, dtp, in the stoichiometric ratio of 1:2 to form not only the copper(II) complex of dtp but also the copper(I) complex of dtp and the disulfide. It should be possible to verify the stoichiometry of the reaction and to follow the course of the titration of a solution of copper(II) nitrate with $NH_4(dtp)$ with a cupric ion selective electrode. If there are no other complexes of importance in solution, it should be possible to calculate the solubility product of $Cu(dtp)_2$ from the titrimetric data in the manner outlined below.

The solubility product of $Cu(dtp)_2$ at a constant ionic strength of 0.1 is defined by:

$$K_{sp} = [Cu^{2+}][dtp^-]^2 \quad (4)$$

where the terms in square brackets are molar concentrations. If the equilibrium concentrations of $Cu^{2+}$ and dtp are determined, $K_{sp}$ can be calculated. This can be accomplished by the addition of an excess of dtp to a solution containing copper(II); the uncomplexed $Cu^{2+}$ can be measured with the cupric ion selective electrode and the unreacted dtp can be calculated from the stoichiometric excess of $NH_4(dtp)$ added, i.e., after the equivalence point in the titration of copper(II) nitrate with $NH_4(dtp)$,

$$[dtp^-] = \frac{C_L V_L - 2C_m V_o}{V_o + V_L} \quad (5)$$

where $C_m$ and $C_L$ are the initial molar concentrations of copper(II) nitrate and $NH_4(dtp)$, respectively; $V_o$ represents the initial volume, in mL, of copper(II) nitrate and $V_L$ the volume of $NH_4(dtp)$ added. At the equivalence point, $V_e$ mL of the titrant has been added and,

$$2C_m V_o = C_L V_e \quad (6)$$

Substitution of Equations 5 and 6 in 4 and rearrangement gives,

$$\frac{(V_o + V_L)}{[Cu^{2+}]^{1/2}} = \frac{C_L}{(K_{sp})^{1/2}} \cdot V_L - \frac{C_L V_e}{(K_{sp})^{1/2}} \quad (7)$$

A plot of values of $(V_o + V_L)/[Cu^{2+}]^{1/2}$ as ordinates and the corresponding values of $V_L$ as abscissa should give a straight line of slope $C_L/(K_{sp})^{1/2}$. Values of $[Cu^{2+}]$ were obtained from the equation

$$[Cu^{2+}] = 10^{(E-E')/29.58}\ (\text{at } 25\ ^\circ C) \quad (8)$$

where $E$ is the potential difference, in millivolts, between the cupric ion selective electrode and the double junction reference electrode and $E'$ is a constant, the value of which depends on the standard electrode potential of the cupric ion selective electrode, the liquid junction potential, the potential of the reference electrode, and the activity coefficient of $Cu^{2+}$ in solution. The constant $E'$ was evaluated by substitution in Equation 8 of the calculated values of $[Cu^{2+}]$ before the equivalence point and the corresponding values of $E$ that were obtained experimentally. Before the equivalence point, the concentration of $Cu^{2+}$ ions can be calculated on the assumption that the only equilibria that govern the free $Cu^{2+}$ concentration are represented by Equations 2 and 3. Hence,

$$[Cu^{2+}] = \frac{C_m V_o - 0.5\, C_L V_L}{V_o + V_L} \quad (9)$$

Measured values of $E$ and the calculated constant $E'$ were employed in obtaining values of $[Cu^{2+}]$ after the equivalence point.

The average value of the slope of the straight line given by Equation 7 was found to be $9.088 \times 10^5$ for three replicate

titrations. The initial concentration of the ligand, $C_L$, was $2.232 \times 10^{-2}$ M and the calculated value of $K_{sp}$, the solubility product of $Cu(dtp)_2$, is $10^{-15.22}$

The basis for the above calculation is, (a) that $Cu^{2+}$ reacts stoichiometrically with the ligand, dtp, in the ratio 1:2 and (b) that in the presence of an excess of the ligand, the only copper-containing species in solution is the uncomplexed $Cu^{2+}$. The stoichiometry of the reaction was verified by determination of the $x$ intercept of the straight line given by Equation 7. The maximum difference between the value of $V_e$ that was determined from the $x$ intercept and the calculated value on the basis of the assumed stoichiometry for the three replicate titrations was 0.08 mL which represented an error of +1.6%.

The total copper concentration in a solution containing an excess of the ligand was determined by atomic absorption spectrophotometry. A 25-mL aliquot of a standard solution of copper(II) nitrate ($\sim 10^{-3}$ M) was titrated with a standard solution of $NH_4(dtp)$ ($\sim 10^{-2}$ M). The titrant was added until the dtp was in slight excess. The yellow-brown oil was removed by filtration, first through a 5-$\mu$m Millipore filter and then through a 0.2-$\mu$m Millipore filter. Three successive filtrations removed the oil as well as any suspended particles that were present in solution. The total concentration of copper in solution was determined by atomic absorption spectrophotometry and the free ligand concentration, $[dtp^-]$, was calculated from Equation 5. In a typical experiment, the total copper concentration determined by atomic absorption spectrophotometry and assumed to be the value of $[Cu^{2+}]$ in solution was $1.42 \times 10^{-6}$ M. The concentration of the free ligand, $[dtp^-]$, that was calculated from Equation 5 was $1.86 \times 10^{-5}$. Hence the calculated solubility product of $Cu(dtp)_2$, from Equation 4 is $10^{-15.3}$. This value is in reasonable agreement with the value of $K_{sp}$ determined potentiometrically with the cupric ion selective electrode, and the assumptions on which the calculation is based are valid.

The thermodynamic solubility product of $Cu(dtp)_2$ reported by Kakovsky (*1*) is $10^{-15.85}$; if an approximate correction is made for ionic strength effects, the solubility product in 0.1 M $KNO_3$ is $10^{-15.13}$ which is in fair agreement with the value of $10^{-15.22}$ that was measured potentiometrically with the cupric ion selective electrode. The solubility product of $10^{-20.3}$ reported by Tulyupa (*2*) is in error.

Replacement of the ethoxy groups on the phosphorus atom in dithiophosphonic acid by methoxy groups results in a marked change in the properties of the ligand. The reaction products of *O,O'*-dimethyldithiophosphonic acid, (dmp), or its ammonium salt, $NH_4(dmp)$, and copper(II) nitrate are quite different from those obtained with *O,O'*-diethyldithiophosphonic acid. The predominant complex is a copper(I) complex of dmp instead of the expected copper(II) complex, $Cu(dmp)_2$. In addition, experimental evidence was obtained for the successive formation of a series of copper-containing complexes. A solution of copper(II) nitrate was titrated with $NH_4(dmp)$ and the concentration of $Cu^{2+}$ was monitored throughout the course of the titration with a cupric ion selective electrode. A plot of the potential differences between the cupric ion selective electrode and the reference electrode as ordinates and the volume of the titrant added as abscissa did not give the expected sigmoid-shaped curve with a well-defined vertical segment at the end point. Instead, a titration curve with a long drawn out end point was obtained (Figure 1) which indicated that the concentration of $Cu^{2+}$ gradually decreased over a wide concentration range of added ligand. It may be deduced from the absence of a sharp drop in $Cu^{2+}$ concentration in solution that the successive formation of several copper-containing complexes contributes to the gradual decrease in the concentration of $Cu^{2+}$ in solution.

Although the copper(II) complex of dmp could not be prepared in aqueous solution as a stable species, the dimeric copper(I) complex of dmp, $Cu_2(dmp)_2$, was readily synthesized as a pale yellow solid. An approximate value for the solubility product of $Cu_2(dmp)_2$ was obtained by two methods: (a) The solid $Cu_2(dmp)_2$ was equilibrated with an aqueous solution containing copper(II) nitrate at an ionic strength of 0.1. The unreacted $Cu_2(dmp)_2$ was separated by filtration and the total copper in solution was measured by atomic absorption spectrophotometry. (b) The solid $Cu_2(dmp)_2$ was equilibrated in an aqueous solution containing $NH_4(dmp)$. The unreacted $Cu_2(dmp)_2$ was separated by filtration and the total dmp in solution was determined fluorimetrically. In this experiment, no inert electrolyte was added to control the ionic strength because of the quenching effect exerted by most common anions.

The solubility product of $Cu_2(dmp)_2$ is given by

$$K_{sp} = [Cu^+][dmp] \qquad (10)$$

When $Cu_2(dmp)_2$ is equilibrated with aqueous solutions of copper(II) nitrate ($1.11 \times 10^{-6}$ M to $5.53 \times 10^{-5}$ M) the total copper in solution varied from $2.21 \times 10^{-5}$ M to $7.42 \times 10^{-5}$ M. The excess copper in solution was produced by the dissociation of $Cu_2(dmp)_2$ and was assumed to be present only as $Cu^+$. On the basis of this assumption, the calculated solubility product of $Cu_2(dmp)_2$ varied between $10^{-9.45}$ and $10^{-9.35}$.

When $Cu_2(dmp)_2$ is equilibrated with a known excess of the ligand, the solubility product of the complex may be calculated from Equation 10 in which $[dmp^-]$ is the sum of the concentrations of added $NH_4(dmp)$ and the dmp produced by the dissociation of $Cu_2(dmp)_2$. The added ligand varied from $1.12 \times 10^{-6}$ M to $5.61 \times 10^{-6}$ M, and the total dmp found in solution by the fluorimetric method varied from $3.60 \times 10^{-5}$ M to $4.09 \times 10^{-5}$ M. Hence, the concentration of dmp introduced into solution by the dissociation of $Cu_2(dmp)_2$ ranged from $3.49 \times 10^{-5}$ M to $3.53 \times 10^{-5}$ M. The solubility product therefore, of $Cu_2(dmp)_2$ calculated from Equation 10 varied between $10^{-8.90}$ and $10^{-8.84}$. In the absence of any added $NH_4(dmp)$, the concentration of dmp in solution measured fluorimetrically in solution was $3.17 \times 10^{-5}$ M and the solubility product of $Cu_2(dmp)_2$ calculated from Equation 10 was $10^{-9.00}$.

There are many uncertainties in the experimental techniques and in the assumptions involving the molecular and ionic species that are present in solution. The above measurements therefore, give only an order of magnitude of the solubility product of $Cu_2(dmp)_2$.

## LITERATURE CITED


(1) I. A. Kakovsky, "Proceedings of the Second International Congress of Surface Activity, London", Vol. IV, Academic Press, New York, N.Y., 1957, p 225–237.
(2) F. M. Tulyupa, *Khim. Tekhnol.*, **15**, 115 (1969); *Chem. Abstr.*, **74**, 68389s (1969).
(3) J. R. Wasson, G. M. Woltermann, and H. J. Stoklosa, *Fortschr. Chem. Forsch.*, **35**, 65 (1973).
(4) A. C. Hill, M. Akhtar, M. Mumtaz, and J. A. Osmani, *Analyst (London)*, **92**, 496 (1967).
(5) A. C. Hill, *J. Sci. Food Agric.*, **20**, 4 (1969).
(6) D. E. Coldberry, W. C. Fernelius, and M. Shamma, *Inorg. Synth.*, **6**, 142 (1960).
(7) H. Wada and Q. Fernando, *Anal. Chem.*, **43**, 751 (1971).
(8) W. Rudzinski, G. T. Behnke, and Q. Fernando, *Inorg. Chem.*, **16**, 1206 (1977).
(9) K. Sakata and M. Nanjo, *Tohoku Daigaku Senko Seiren Kenkyusho Iho*, **26**, (*1*), 1 (1970); *Chem. Abstr.*, **74**, 93038j (1971).
(10) J. N. Damico, *J. Assoc. Offic. Anal. Chem.*, **49**, 1027 (1966).
(11) R. G. Cavell, W. Byers, and E. D. Day, *Inorg. Chem.*, **10**, 2110 (1971).
(12) S. E. Livingstone and A. E. Mihkelson, *Inorg. Chem.*, **9**, 2545 (1970).


RECEIVED for review November 9, 1977. Accepted December 27, 1977.

# Investigations of the Ferricyanide–Ferrocyanide System by Pulsed Rotation Voltammetry

**W. J. Blaedel* and R. C. Engstrom**

*Department of Chemistry, University of Wisconsin, Madison, Wisconsin 53706*

**The technique of pulsed rotation voltammetry (PRV) at a rotated disk electrode involves switching the rotation rate of the electrode between two values, and measuring a difference current while maintaining a constant applied potential. Extremely low background signals are achieved at glassy carbon electrodes, allowing a detection limit of $1 \times 10^{-6}$ M ferricyanide. Well defined current–potential curves are obtained for the ferricyanide–ferrocyanide system, and estimates of the heterogeneous rate constant ($k^0$) and the transfer coefficient ($\alpha$) are reported.**

The attainment of reproducible current–voltage data for low concentrations of electroactive compounds at solid electrodes is difficult using conventional voltage scanning techniques. Several procedures have been devised to improve the quality of the voltammograms, including that of steady-state voltammetry (SSV). As described in the literature (*1*), SSV involves the application of a constant potential to the electrodes, and waiting for the transient current to decay, until a current is reached that is constant with time. The steady-state current is the component that is due to transport of the electroactive material in solution, uncomplicated by the transients that represent charging and electrochemical reactions of the electrode surface. With these transients eliminated, background steady-state currents are very low, permitting discernment of very low concentrations of electroactive materials. The technique has been successfully applied to the electrochemical study of nicotinamide adenine dinucleotide at the micromolar level (*2*). One drawback to SSV is the time required to reach a true steady-state. As long as an hour may be required for the transient currents to decay to nanoampere levels, so that acquisition of data for an entire voltammogram may require many hours. Also, error sources like drifting backgrounds and slow decomposition of the electroactive material may become important over a long experiment that are usually unimportant for short experiments.

Instead of waiting to achieve the true steady-state current, a difference current may be measured between two different rotational speeds of a rotated disk electrode. The difference current is purely convective and is not influenced significantly by transient surface reactions of the electrode. The difference current may be measured before steady-state is reached, and the time of the experiment may be greatly reduced.

The concept of hydrodynamic modulation is not new. It has been used in the determination of rate constants at rotated disk electrodes by measuring current as a function of linearly increasing rotation rate (*3*) and linearly increasing square-root of rotation rate (*4*, *5*). Miller, Bruckenstein, and co-workers have done a great deal of work in developing the theory and practice of hydrodynamic modulation at rotated disk and ring-disk electrodes. In addition to a simple square-root function of rotation rate (*6*), they have designed a system for programming the speed of rotation to give any of a number of modulations that can be superimposed on a constant or monotonically increasing rotation rate (*7*). The analytical usefulness of hydrodynamic modulation has been demonstrated using a sinusoidally modulated rotation rate with phase sensitive detection to obtain scanning voltammograms at the $5 \times 10^{-8}$ M concentration level (*8*). The rate constants for a quasi-reversible electron transfer reaction were obtained, also using a sinusoidal rotation rate (*9*). Pulsed flow work in a laminar flow regime through tubular electrodes has also been reported (*10*).

The purpose of the following work is to demonstrate the technique of pulsed rotation voltammetry (PRV), in which the rotation rate of a rotated disk electrode is switched between a high and low value, while the potential is held constant. By measuring the difference currents at a number of discrete applied potentials, a voltammogram may be developed and plotted pointwise. The advantages and limitations of this experiment are demonstrated using the ferricyanide–ferrocyanide redox system at a glassy carbon rotated disk electrode. The heterogeneous rate constant ($k^0$) and the transfer coefficient ($\alpha$) of the electron transfer reaction of that system are evaluated using equations based on mass transport coefficients such as those presented originally by Jordan (*11*) and later by other workers (*12*, *13*).

## THEORY

For the electron transfer reaction,

$$\mathrm{O} + ne \underset{k_b}{\overset{k_f}{\rightleftharpoons}} \mathrm{R} \tag{1}$$

the faradaic current, in terms of mass transport coefficients, is given by (*11–14*):

$$i = \frac{\dfrac{i_{l,c}}{M_O} + \dfrac{i_{l,a}}{M_R}\theta}{\dfrac{1}{M_O} + \dfrac{\theta}{M_R} + \dfrac{1}{k_f}} \tag{2}$$

In Equation 2,

$$k_f = k^0 \exp\left[\frac{-\alpha nF}{RT}(E - E^\circ)\right] \tag{3}$$

$$k_b = k^0 \exp\left[\frac{(1-\alpha)nF}{RT}(E - E^\circ)\right] \tag{4}$$

$$\theta = \frac{k_b}{k_f} = \exp\left[\frac{nF}{RT}(E - E^\circ)\right] \tag{5}$$

$$i_{l,c} = nFAM_O C_O^* \tag{6}$$

$$i_{l,a} = -nFAM_R C_R^* \tag{7}$$

In Equations 2–7: $C^*$ represents the bulk concentration (mol/cm$^3$) of the species denoted by the subscript; $M$ represents the mass transport coefficient (cm/s) of the species denoted by the subscript; $i_{l,c}$ and $i_{l,a}$ represent the limiting cathodic and anodic currents of the voltammogram of a

0003-2700/78/0350-0476$01.00/0 © 1978 American Chemical Society

mixture of O and R; and the other terms have their usual electrochemical significance. In practice, formal rate constants ($k_f'$, $k_b'$, $k^{0\prime}$ and $\theta'$) and a formal standard potential ($E^{\circ\prime}$) are determined and used at a constant ionic strength, instead of the thermodynamic values designated in Equations 2–7.

For the work in this paper, it will be assumed that transport coefficients of the oxidized and reduced species are equal ($M_O = M_R = M$). This assumption is supported by an estimate of 1.11 for the ratio $M_O/M_R$ for the ferricyanide–ferrocyanide system (*15*). Only when $\theta$ is close to unity will this approximation cause significant error. Such error will be avoided in treating data, and currents at potentials close to $E^{\circ\prime}$ will not be used in the computation of kinetic parameters.

A more rigorous derivation has been worked out for the case where $M_O$ and $M_R$ are not equal (*16*). The equations are quite complicated algebraically, and their use does not seem justified for the treatment of the ferricyanide–ferrocyanide system, whose oxidized and reduced forms are similar in weight and size.

With the approximation that $M_O = M_R$, Equation 2 becomes

$$i = \frac{i_{l,c} + i_{l,a}\theta}{1 + \theta + \frac{M}{k_f}} \tag{8}$$

For purposes of calculating rate constants, it is simpler and more accurate to deal only with solutions of the oxidized form (ferricyanide) alone, or of the reduced form (ferrocyanide) alone, in which cases, Equation 8 becomes

$$i_c = \frac{i_{l,c}}{1 + \theta + \frac{M}{k_f}} \tag{9}$$

$$i_a = \frac{i_{l,a}}{1 + \frac{1}{\theta} + \frac{M}{k_b}} \tag{10}$$

The cathodic difference current ($\Delta i_c$) between a high and a low rotation rate may be expressed as:

$$\Delta i_c = \frac{i_{l,c,2}}{1 + \theta + \frac{M_2}{k_f}} - \frac{i_{l,c,1}}{1 + \theta + \frac{M_1}{k_f}} \tag{11}$$

In Equation 11, the subscripts 1 and 2 designate the values of $M$ and of $i_{l,c}$ at low and high rotational speeds, respectively. Equation 11 may be solved for $k_f$ in terms of the quadratic formula

$$k_f = \frac{-B + \sqrt{B^2 - 4AC}}{2A} \tag{12}$$

where

$$\left.\begin{aligned} A &= (\theta + 1)^2 - \frac{\Delta i_{l,c}}{\Delta i_c}(\theta + 1) \\ B &= (M_1 + M_2)(\theta + 1) \\ C &= M_1 M_2 \end{aligned}\right\} \tag{13}$$

The negative square-root term results in negative rate constants, and is not used.

In practice, $k_f'$ may be calculated using Equations 12 and 13 from a voltammogram of $\Delta i_c$ vs. $E$. For the calculation, $M_1$, $M_2$, and $E^{\circ\prime}$ must be known. $M_1$ and $M_2$ may be calculated from the SSV limiting currents at low and high rotational speeds, using Equation 6. Alternatively, $M_1$ may be calculated from the SSV limiting current, and $M_2$ may be calculated from $M_1$, using the verified square-root dependence of current upon rotation rate.

When the rates of mass transport and electron transfer are similar, that is, for a quasi-reversible system, a simple relationship between $E^\circ$ and $E_{1/2}$ does not exist. A more accurate method of estimating $E^{\circ\prime}$ is to find the potential at which $\Delta i$ becomes zero for a solution containing known concentrations of ferricyanide and ferrocyanide:

$$E_{(\Delta i = 0)} = E^{\circ\prime} + \frac{RT}{nF} \ln \frac{C_O}{C_R} \tag{14}$$

A similar argument for the oxidation of the reduced form results in a quadratic expression for $k_b$, with

$$\left.\begin{aligned} A &= (\theta + 1)^2 - \frac{\Delta i_{l,a}}{\Delta i_a}(\theta + 1)\theta \\ B &= (M_1 + M_2)(\theta + 1)\theta \\ C &= M_1 M_2 \theta^2 \end{aligned}\right\} \tag{15}$$

## EXPERIMENTAL

**Apparatus.** A rotated disk electrode system was constructed similarly to one described previously (*2*), but with several modifications. The motor speed controller (Model S-47, Gerald K. Heller Co., Las Vegas, Nev.) was modified by putting an additional speed control potentiometer into the circuit. A two-position rotary switch was used to select which potentiometer controlled the speed of the rotated disk electrode. Voltages were applied to the two-electrode system with a battery powered potentiometer circuit and monitored with a digital voltmeter (Model 282, B&K Precision, Chicago, Ill.) of sufficiently high input impedance so as not to load the circuit. Currents were measured with a picoammeter equipped with a current suppression option (Model 414S, Keithley Instruments, Inc., Cleveland, Ohio). The output of the picoammeter was monitored on a strip-chart recorder (Model A5113-2I, Houston Instruments, Austin, Texas). The rotation counting system consisted of a combination LED-phototransistor fitted over a twelve-slotted wheel attached to the electrode chuck. Voltage pulses produced by light passing through the slots were counted by an events counter (Model IM-4100, Heath Co., Benton Harbor, Mich.) modified to have a 5-s count time. The display therefore read revolutions per minute directly. The counting-rotation system was found to have a standard deviation of 0.74% (95% confidence limit).

**Electrodes.** A 0.5-cm length of 3-mm glassy carbon rod (Grade 30S, Tokai Mfg. Co., Tokyo, Japan) was epoxied into the end of a 0.5-in. o.d. Lucite rod (Rohm and Haas Co., Philadelphia, Pa.) with Epotek 349 (Epoxy Technology Inc., Watertown, Mass.) and polished with successively finer polishing paper, followed by a 0.1-$\mu$m alumina slurry, until a mirrorlike finish was obtained.

The reference electrode was a chloridized silver wire in 0.0100 M KCl (*2*). A frit permeated with agar gave very low leakage between the reference and sample compartments of the cell.

**Reagents.** Tap distilled water was redistilled from alkaline permanganate and this was used to prepare all solutions. The supporting electrolyte was 0.1 M phosphate buffer (pH 7.50), prepared from reagent grade potassium salts (Fisher Scientific, Fair Lawn, N.J.). $K_3Fe(CN)_6$ and $K_4Fe(CN)_6{\cdot}3H_2O$ (Mallinckrodt Chemical Works, St. Louis, Mo.) were used without further purification for 0.01 M stock solutions of the oxidized and reduced forms. For an electrochemical experiment, aliquots of the stock solutions were injected into the supporting electrolyte to give the desired concentration. Ferrocyanide solutions were prepared with deaerated buffer just before use.

**Procedure.** All work was performed in a thermostated cell at 25.0 ± 0.2 °C. A 100-mL aliquot of buffer was pipetted into the cell and pretreatment of the electrode begun. This consisted of cycling the applied potential between +1.0 V and −1.0 V for two cycles, allowing 10 min at each voltage. The system was deaerated during pretreatment by bubbling water-saturated nitrogen through the solution. At the end of this time, the nitrogen delivery tube was raised just above the surface of the liquid for the remainder of the experiment. A background voltammogram

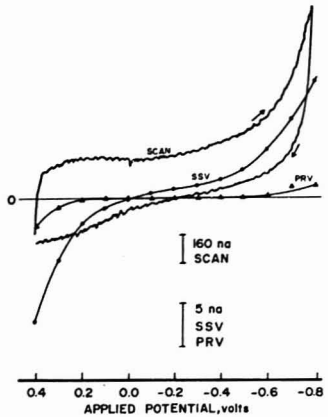


**Figure 1.** Background current–potential curves for 0.1 M phosphate buffer, pH 7.5. Rotation rate, 500 rpm for scan and SSV, 500 and 1500 rpm for PRV. Pulsing frequency, ~15 s

was obtained by setting the applied potential to the initial value. The current was allowed to decay until the baseline no longer changed rapidly (this usually took no more than a minute), then the rotation rate was switched from its lower value (500 rpm) to its higher value (1500 rpm). The switching was done three times at each potential, about 15 s being allowed at each rotation rate. After three pulses, the potential was reset to the next value and the pulsing repeated. For rate constant calculations, the current was allowed to reach a steady-state at the final potential, and its absolute value recorded for the calculation of mass transport coefficients. The potential was then reset to the starting point, and an appropriate amount of the analyte stock solution added with an Oxford Sampler (Oxford Laboratories, Foster City, Calif.). Five minutes of deaeration was performed before beginning the voltammogram of the analyte.

**Data Treatment.** The strip chart recordings of the picoammeter output were read by means of a digitizer (Numonics Corp., North Wales, Pa.) interfaced to a desk-top programmable calculator (TEK 31, Tektronix Inc., Beaverton, Ore.). The calculator was programmed to compute the average difference current for each potential on the voltammogram. It also performed the calculations for the estimation of $k_f$ or $k_b$. Plots were made of ln $k_f$ or ln $k_b$ vs. $E - E^{0\prime}$, and $k^{0\prime}$ and $\alpha$ were determined from the intercept and slope, respectively.

## RESULTS AND DISCUSSION

**Mass Transport.** The dependence of limiting current on rotation rate was evaluated using 10 $\mu$M potassium ferricyanide over the range of 200–2000 rpm. A log–log plot of current against rotation rate was completely linear with a slope of 0.495 ± 0.003 (90% confidence limit) (*17*), indicating nearly ideal behavior for the rotating disk electrode. This relationship was used to calculate $M_2$ from the SSV measurement of $M_1$.

**Background Voltammogram.** Figure 1 shows a comparison of the background current–voltage curves of the phosphate buffer obtained from a conventional scanning mode, a steady-state mode, and a pulsed rotation mode. The scanned background is very large due to the current associated with double layer charging. It is also comparatively noisy, and the magnitude depends on the direction and rate of scan. The steady-state current is much smaller than the scanned current because there are no charging currents. Slow surface reactions at the electrode and electrolyte decomposition are postulated to account for the major portion of the SSV current. The pulsed mode shows an extremely low background, indicating good correction for electrode surface currents and electrolyte

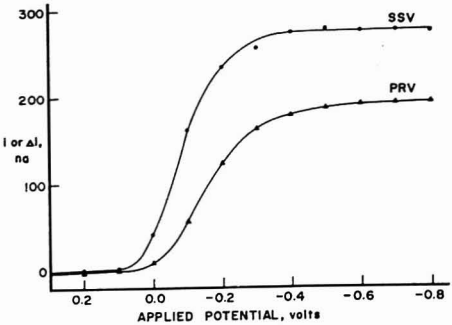


**Figure 2.** Current–potential curves for 10 $\mu$M ferricyanide in 0.1 M phosphate buffer, pH 7.5. Conditions: As in Figure 1

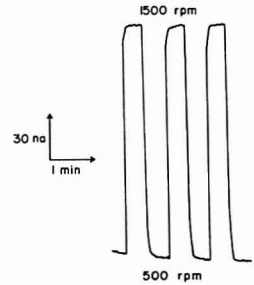


**Figure 3.** PRV current–time record for 10 $\mu$M ferricyanide. Conditions: As in Figure 1, at −0.6 V

decomposition. The PRV curve also indicates the virtual absence of electroactive impurities in the potential range of +0.2 to −0.6 V. The nonconvective nature of solvent decomposition observed in SSV and in PRV should permit measurement to be made over a wider voltage range than for conventional scanning voltammetry. It should be noted that the PRV data was taken in about 20 min, compared to several hours for the SSV curve.

**Calculation of Electron Exchange Rate Constants in the Ferricyanide–Ferrocyanide System.** Reduction of 10 $\mu$M $Fe(CN)_6^{3-}$, corrected for background, by SSV and by PRV is shown in Figure 2. Very well defined waves and plateaus were obtained by both techniques. Figure 3 is the current–time record for a point on the plateau of the PRV curve of Figure 2.

To evaluate the mass transfer coefficients from the limiting current and Equation 6, the electrode area must be known. This was done both electrochemically and optically. The electrochemical determination was done using literature values of the diffusion coefficient of ferricyanide in 0.1 M KCl (*15*), and calculating the area from the limiting current in that medium, based on the Levich equation, and using the experimentally determined exponent of rotation rate. A value of 0.0847 $cm^2$ was found. Microscopic measurement of the electrode diameter using a calibrated micrometer eyepiece yielded an area of 0.0873 ± 0.0018 $cm^2$. A 3.1% difference exists between the two measurements, and the optically determined value was used in further calculations.

The formal standard potential was determined by preparing an equimolar solution of both redox species in phosphate buffer, and by PRV in the region of zero current, observing

Table I. Rate Constants for the Ferricyanide–Ferrocyanide System[a]

| Potential region | $k^{0\prime}$ cm/s × $10^3$ | $\alpha$ |
|---|---|---|
| Cathodic | 4.7 ± 0.7 | 0.23 ± 0.03 |
| Anodic | 5.4 | 0.69 |

[a] Tabled values accompanied by 90% confidence limits.

the potential where the current crosses the voltage axis. Triplicate determinations of $E^{o\prime}$ gave 0.054 ± 0.003 V (90% confidence limit).

Triplicate voltammograms of 10 $\mu$M ferricyanide reduction was obtained, and values of ln $k_f$, calculated from Equation 12, were plotted against the applied potential. The values of $k^{0\prime}$ and $\alpha$ obtained from cathodic reduction data are reported in Table I. Values are also given from the anodic oxidation of ferrocyanide. The values of $k^{0\prime}$ from the oxidation and reduction agree reasonably well with one another. They are similar to determinations (0.0015–0.0071 cm/s) reported under various conditions at carbon paste rotated disk electrodes (*18*), and somewhat larger than values around 0.002 cm/s reported for glassy carbon tubular electrodes (*13*). Discrepancies among literature values of $k^{0\prime}$ for the ferricyanide–ferrocyanide system at solid electrodes are prevalent, and may be ascribed largely to differences in history and pretreatment of the electrodes. A thorough study of modes of preparation and pretreatment of solid electrodes is called for.

The values of the transfer coefficient, $\alpha$, obtained from oxidation and reduction data, are decidedly not in agreement with one another. Associated with this is the observation that all of the plots of ln $k_f$ or ln $k_b$ vs. $E - E^{o\prime}$ show a deviation from linearity at low values of overpotential. The deviation for cathodic data is in a direction that approaches the slope for anodic data, and vice-versa. This phenomenon is not unique to the experimental method presented here, but has been observed in a similar chemical system at glassy carbon turbulent tubular electrodes, where a definite change in slope occurs near zero overpotential for solutions containing both ferricyanide and ferrocyanide (*13*). This indicates that there is a different transfer coefficient for the oxidation than for the reduction, implying that something more than a simple electron transfer between the two species is taking place. Apparently this is not restricted to glassy carbon electrodes. At graphite rotating-disk electrodes, the formation of a dimer consisting of one molecule of ferricyanide and one molecule of ferrocyanide, which reacts more readily than either form alone, has been postulated (*19*). Other possible explanations for nonlinearity in Tafel plots of the ferricyanide–ferrocyanide system have been suggested: they include a potential-dependent transfer coefficient (*20*), and an influence on the electron transfer by ion-pairing (*21*). At micromolar concentrations, this last idea can be ruled out.

**Sensitivity of PRV.** Two separate experiments were performed to determine the linearity between the difference current ($\Delta i$) and the ferricyanide concentration, for an applied potential in the current-limited region of Figure 2. The concentration range 0–10 $\mu$M gave a least squares slope of 19.4 ± 0.2 nA/$\mu$M (90% confidence limits) and the range of 0–100 $\mu$M yielded 19.2 ± 0.2 $\mu$A/$\mu$M.

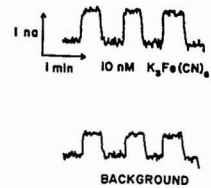


Figure 4. PRV current–time record for 10 nM ferricyanide. Conditions: As in Figure 1, at –0.6 V

Although the blank has a definite $\Delta i$ signal, its noise level in this system is only nA. Based on a signal-to-noise ratio of 1, the limit of detection for ferricyanide should be around 10 nM. Current–time traces are given in Figure 4 for 10 nM potassium ferricyanide and for blank buffer solution, verifying experimentally the detectability of that concentration.

## CONCLUSIONS

The technique of pulsed rotation voltammetry is designed primarily to compensate and correct for nonconvective background currents that trouble conventional voltammetric techniques at solid electrodes. It is a potentiostatic technique that is considerably more rapid than steady-state voltammetry without sacrifice of data quality. It offers both qualitative and quantitative information on the measurement of electroactive material, and on electron transfer kinetics. Instrumentation is relatively simple, and the experiment is easy to perform. PRV has been used to obtain the rate constants for heterogeneous electron transfer in the ferricyanide–ferrocyanide system at a glassy carbon rotated disk electrode. Electrochemical kinetic studies with PRV are in progress on systems involving riboflavin, nicotinamide adenine dinucleotide, and porphyrin compounds.

## LITERATURE CITED

(1) W. J. Blaedel and R. A. Jenkins, *Anal. Chem.*, **46**, 1952 (1974).
(2) W. J. Blaedel and R. A. Jenkins, *Anal. Chem.*, **47**, 1337 (1975).
(3) K. Prater, *J. Electrochem. Soc.*, **115**, 27C (1968).
(4) S. C. Creason and R. F. Nelson, *J. Electroanal. Chem.*, **21**, 548 (1969).
(5) S. C. Creason and R. F. Nelson, *J. Electroanal. Chem.*, **27**, 189 (1970).
(6) B. Miller and S. Bruckenstein, *J. Electrochem. Soc.*, **117**, 1032 (1970).
(7) B. Miller, M. I. Bellavance, and S. Bruckenstein, *Anal. Chem.*, **44**, 1983 (1972).
(8) B. Miller and S. Bruckenstein, *Anal. Chem.*, **46**, 2026 (1974).
(9) B. Miller and S. Bruckenstein, *J. Electrochem. Soc.*, **121**, 1558 (1974).
(10) W. J. Blaedel and D. Iverson, *Anal. Chem.*, **48**, 2027 (1976).
(11) J. Jordan, *Anal. Chem.*, **27**, 1708 (1955).
(12) R. N. Adams, "Electrochemistry at Solid Electrodes", Marcel Dekker, New York, N.Y., 1969.
(13) W. J. Blaedel and G. W. Schieffer, *J. Electroanal. Chem.*, **80**, 259 (1977).
(14) A detailed derivation of Equation 2 is available upon request.
(15) D. Sawyer and J. L. Roberts, Jr., "Experimental Electrochemistry for Chemists", John Wiley and Sons, New York, N.Y., 1974, p 77.
(16) Younghee Hahn, unpublished work, University of Wisconsin–Madison, 1977.
(17) W. J. Blaedel and D. Iverson, *Anal. Chem.*, **48**, 1240 (1976).
(18) Z. Galus and R. N. Adams, *J. Phys. Chem.*, **67**, 866 (1963).
(19) R. Sohr, L. Miller, and R. Landsberg, *J. Electroanal. Chem.*, **50**, 55 (1974).
(20) D. N. Angell and T. Dickenson, *J. Electroanal. Chem.*, **35**, 55 (1972).
(21) D. J. Bieman and W. R. Fawcett, *J. Electroanal. Chem.*, **34**, 27 (1972).

RECEIVED for review September 15, 1977. Accepted December 5, 1977. This work was supported in part by a grant (No. CHE-7615128) from the National Science Foundation.

# Determination of the Electrochemically Effective Electrode Area

**Timothy E. Cummings and Philip J. Elving***

*The University of Michigan, Ann Arbor, Michigan 48109*

**The factors are discussed which affect diffusion controlled behavior in dc polarography at a controlled drop-time dropping mercury electrode (DME) and in cyclic voltammetry at a hanging mercury drop electrode (HMDE) with respect to the evaluation of the electrochemically effective area. The measurement of the latter in terms of capacity, the results obtained, and the difference in the effective area for faradaic and nonfaradaic processes are described. Based on published values of the diffusion coefficient of Cd(II) in 0.1 M KCl, the dc polarographic diffusion current at a controlled drop-time DME is found to obey the theory for diffusion to an expanding sphere; depletion effects are considerably reduced by convection resulting from use of a mechanical drop-knocker, and current–time behavior for single drops is very reproducible, even at times as short as 0.2 s. Contrary to published theory, shielding effects from the glass capillary decrease with time after drop-birth. An experimental technique for calibration of HMDE areas using the trioxalatoiron(III) species is described, which gives a precision of 2 to 4%. Use of Cd(II) for evaluation of HMDE areas is subject to errors due to trace adsorbates. Use of slow scan rates is recommended for precise HMDE area evaluation, and a mathematical procedure is detailed which accounts for the extant sphericity effects.**

**DME.** Mathematical theories for describing the polarographic diffusion current at a dropping mercury electrode (DME) have been reviewed (*1*). Because of both its simplicity and satisfactory description of the physical relations under normal conditions, the original Ilkovic equation (*2*) continues to be used, despite considerable advancement in the mathematical sophistication used to solve the DME boundary value problem. In a study of current–time behavior at a DME (*3*), the experimental data at times shorter than one second showed a marked deviation from published theories.

While it was, at one time, difficult to use a DME having a short drop-time because of the necessarily large mercury flow-rates and the concomitant polarographic maxima induced by the rapid mercury flow, the mechanical drop-knocker has made work at short drop-times feasible. Use of short drop-times has several advantages. A wider drop-time range increases the capability to study chemical kinetics. The current flow at the end of a mechanically controlled drop-life can be made much smaller than for a natural drop-life, which reduces $iR$ losses in solution, a fact of particular importance in ac polarography and cyclic voltammetry at the DME. Furthermore, controlled drop-times are used in analysis to speed determinations and, in general, to avoid dependence of the natural drop-time and, hence, of the drop area on the applied potential.

Until recently, it was generally assumed that the contact area between the mercury drop and the DME was small and that shielding effects from the glass capillary were minor; however, no reliable method was known for experimentally evaluating these effects. Recently, Mohilner et al. (*4*), in connection with differential capacity measurement, reported a useful relationship for evaluation of the effective electrode area that is not available because of shielding and orifice contact (this combined effect will be referred to as the effective contact area). A previously reported method (*5*) for evaluating the effective contact area was more complex in introducing correction for back pressure; the authors underemphasized the importance of the effective contact area correction by stating that it approximately equaled the orifice area and by failing to report the determined values.

Because of the importance of knowing the true area for many purposes, e.g., evaluations of diffusion coefficients and of the relation between polarographic limiting current and mercury column height, the effects of effective contact area and sphericity at the DME on measured parameters were systematically studied with the aim of determining the simplest set of equations which could, within a given tolerance of error, be employed.

**HMDE.** For much work employing the hanging mercury drop electrode (HMDE), the electrochemically effective electrode area must be known. Regardless of which type of HMDE is employed, e.g., platinum contact or syringe, for precise work, the area must be experimentally evaluated.

Determination of the HMDE area from cyclic peak current relations (*6*, *7*) and experimental voltammograms for a reversible compound with a known diffusion coefficient, $D$, suffers from two problems. Since $D$ is a function of temperature, solvent, and ionic strength, only $D$ values determined in a solution of ionic strength sufficient for electrochemical work may be used. Furthermore, the literature is replete with contradictory $D$ values.

One intent of the present study is to present an internally consistent method for HMDE area evaluation using dc polarographic and cyclic voltammetric data obtainable in the same laboratory, thereby avoiding reliance on externally obtained values which may not have been obtained under identical conditions. The method has the advantages of the precision with which the DME effective area can be evaluated and the accuracy obtainable through comparison of measurements on the same solution.

## EXPERIMENTAL

**Chemicals.** Reagent grade $CdCl_2 \cdot 2.5\ H_2O$ (Baker) was dried at 110 °C for several days. Reagent grade $Fe_2(SO_4)_3 \cdot 6H_2O$ (Merck), $K_2C_2O_4 \cdot H_2O$ (Mallinckrodt) and KCl were used without further purification. Mercury for electrodes was chemically purified and distilled. Water was suitably distilled.

**Instrumentation.** All data were obtained using a jacketed, three-compartment cell thermostated at 25 ± 0.1 °C. The DME capillary was a 20.8-cm length of Corning Code No. 215670 marine barometer tubing. The mechanical drop-knocker was a solenoid with a metal pin attached to the solenoid plunger. The pin moved horizontally, striking the DME capillary with a force which was dependent on the electrically regulated solenoid current. The HMDE was a Metrohm E 410 Micro-Feeder. The potentiostat was a standard configuration, similar to one described (*8*). Triangular waveforms were supplied by a Wavetek Model 112 function generator. Potentials were monitored by a Hewlett-Packard Model 3440A digital voltmeter with a Model 3443A high gain/auto range unit. Data were recorded on a Houston Model 2000 x-y recorder.

0003-2700/78/0350-0480$01.00/0 © 1978 American Chemical Society

**Procedures.** Solutions were deaerated with purified nitrogen for 30 min; a nitrogen atmosphere was maintained in the electrochemical cell during experiments. Reported potentials are vs. an aqueous saturated calomel electrode.

*DC Polarography.* For 0.183 mM Cd(II) in 0.3 M KCl solution, the potential was scanned at 4 mV/s, starting at −0.3 V. For all other solutions, the potential was held constant at a value on the diffusion plateau, −0.700 V for Cd(II) and −0.350 V for Fe(III), and the currents for 10 to 20 drops were recorded, using the time-base sweep on the recorder $x$-axis; an identical procedure used for background alone permitted background subtraction.

To minimize long term stirring effects, the mechanical drop-knocker was adjusted to deliver the minimum striking force necessary to dislodge the drop.

*Cyclic Voltammetry.* A drop corresponding to 10% of one rotation (two divisions) of the micro-feeder piston mechanism was used. The precision of thus setting the piston is about 1%. A new drop was used for each cyclic voltammogram.

## THEORY

Because most read-out instruments in current use respond sufficiently rapidly to measure the instantaneous polarographic current, the theory will be considered for such currents. Conversion for mean currents should be readily apparent.

**DC Polarography.** The original Ilkovic equation (2), which does not account for sphericity effects at the DME, is:

$$i_d = 709\, nD^{1/2} Cm^{2/3} t^{1/6} \quad (1)$$

where $i_d$ is the maximum diffusion current in $\mu$A, $n$ is the number of electrochemical equivalents per mole of species electrolyzed, $D$ is its diffusion coefficient in cm$^2$/s, $C$ is its bulk solution concentration in mM, $m$ is the mean mercury flow rate in mg/s, and $t$ is the life-time of the drop in s.

Derivations which accounted for sphericity effects (*9–16*) have produced, after truncating a series expression, equations of the following type, in which only the coefficient $B$ differs:

$$i_d = 709\, nD^{1/2} Cm^{2/3} t^{1/6} (1 + BD^{1/2} t^{1/6}/m^{1/3}) \quad (2)$$

In Matsuda's solution (*15*), which appears to be the most rigorous (*1*), $B$ is 36.3 for a freely hanging sphere and 23.5 when the shielding effect of the glass capillary is considered.

Mohilner et al. (*4*) equated the electrochemically effective electrode area, $A$, to the difference between the area computed from drop volume assuming a spherical shape, $A_s$, and the effective contact area of the drop, $A_0$. The accuracy of the spherical shape assumption has been shown to be sufficient (*17–19*). On substituting for $A_s$, based on the mercury flow rate and drop-time, Mohilner et al. obtained

$$A = (6\, m\pi^{1/2}/d)^{2/3} t^{2/3} - A_0 \quad (3)$$

where $d$ is the density of Hg. A useful (and obvious) relationship is

$$A = A_s(1 - A_0/A_s) \quad (4)$$

Since the Ilkovic equation is linear in $A_s$ (incorporated in terms of $m$ and $t$), one can correct for the effect of $A_0$, i.e., replace $A_s$ by $A$, by substitution of Equation 4 into Equation 1, which, upon further substitution for $A_s$, yields

$$i_d = 709\, nD^{1/2} Cm^{2/3} t^{1/6} (1 - 117.8\, A_0/m^{2/3} t^{2/3}) \quad (5)$$

where $A_0$ is in cm$^2$. Since the effective electrode area does not appear in the derivation of Equation 2 in places leading to the second term in the parentheses (at least not in a manner amenable to correction of $A_s$ for $A_0$), Equation 4 can be introduced into Equation 2 analogously to the substitution into Equation 1, so that

$$i_d = 709\, nD^{1/2} Cm^{2/3} t^{1/6} (1 + BD^{1/2} t^{1/6}/m^{1/3})(1 - 117.8\, A_0/m^{2/3} t^{2/3}) \quad (6)$$

**AC Polarography.** Although Mohilner et al. (*4*) were solving for the differential capacitance, this approach is readily adaptable to ac polarographic current measurements, which can be used to determine the DME drop area in the absence of a faradaic process. Since the measured ac current, $i_{ac}$, equals the product of the ac current density, $j_{ac}$, and the electrode area, substitution of Equation 3 for the electrode area relates $i_{ac}$ and $j_{ac}$:

$$i_{ac} = j_{ac}(6\, m\pi^{1/2}/d)^{2/3} t^{2/3} - j_{ac} A_0 \quad (7)$$

Thus, at constant $E_{dc}$, a plot of $i_{ac}$ vs. $t^{2/3}$ should be linear with a slope, $U$, equal to $j_{ac}(6\, m\pi^{1/2}/d)^{2/3}$ and an intercept, $Z$, equal to $-j_{ac}A_0$. Values of $U$ and $Z$ can be determined by least-squares; if $m$ is known, $A_0$ can then be evaluated from

$$A_0 = -Z(6\, m\pi^{1/2}/d)^{2/3}/U \quad (8)$$

Because of resistance in solution and through the DME, the measured ac currents must be corrected for $iR$ loss (*20*), which also results in a phase shift of the working electrode ac voltage, $\Delta E_w$, relative to the applied ac voltage, $V$. If the in-phase, $i_{0°}$, and quadrature, $i_{90°}$, components of the ac current are measured, the total ac current, $i_t$, is given by

$$i_t = (i_{0°}^2 + i_{90°}^2)^{1/2} \quad (9)$$

Correction for the $iR$ loss is then made using Equation 10.

$$i_{ac} = i_t/\sin[\arctan(i_{90°}/i_{0°})] \quad (10)$$

**Cyclic Voltammetry.** Nicholson and Shain (*7*) have tabulated the current functions, $\pi^{1/2}\chi(at)$ and $\phi(at)$, for a reversible charge-transfer for Equation 11, where $r_0$ is the HMDE radius and $v$ is the scan rate.

$$i = 6.02 \times 10^5 n^{3/2} AD^{1/2} Cv^{1/2} [\pi^{1/2}\chi(at) + 0.16(D^{1/2}/r_0 n^{1/2} v^{1/2})\phi(at)] \quad (11)$$

At fast $v$, the second term in brackets in Equation 11 becomes negligible and Equation 11 can be accurately approximated for the peak current by

$$i_p = 2.687 \times 10^5 n^{3/2} AD^{1/2} Cv^{1/2} \quad (12)$$

At slow $v$, the assumption made in obtaining Equation 12 is not valid. If $D^{1/2}$ is not large and $r_0$ and $v$ are not very small, $i_p$ will still appear 28.5 mV past $E_{1/2}$ and Equation 11 can be written for $i_p$ as

$$i_p = 6.02 \times 10^5 n^{3/2} AD^{1/2} Cv^{1/2} [0.4463 + 0.1203\, D^{1/2}/r_0 n^{1/2} v^{1/2}] \quad (13)$$

For a rapidly diffusing species, a very small $r_0$ or a very slow $v$, the second term in brackets in Equation 11 causes a shift of $E_p$ to slightly more negative values (for a reduction), and different numerical values of $\pi^{1/2}\chi(at)$ and $\phi(at)$ are required (*7*).

**HMDE Area Evaluation.** Several relationships may be used to obtain the HMDE area. If Equation 1 satisfactorily describes the dc polarographic current and Equation 12 accurately describes the cyclic peak current, the area calculation is straightforward. Equation 15 is readily deduced from Equations 1, 12, and 14; the HMDE area is then evaluated using experimental values of $i_p/Cv^{1/2}$ and $I_d$.

$$I_d = i_d/Cm^{2/3} t^{1/6} \quad (14)$$

$$(i_p/Cv^{1/2})/I_d = 3.790 \times 10^2 n^{1/2} A \quad (15)$$

In the event that Equation 5 is assumed to be valid, $I_d'$, defined by Equation 16, replaces $I_d$ in Equation 15.

$$I_d' = i_d/C(m^{2/3} t^{1/6} - 117.8\, A_0/t^{1/2}) \quad (16)$$

If sphericity effects at the DME are important, it is necessary to evaluate $D^{1/2}$. Using Equation 2, $I_d$ is given by

Table I. AC Polarographic Currents and Current Densities[a]

| $t$, s | $i_{ac}$, μA | $A_s$,[b] cm² | $i_{ac}/A_s$, μA/cm² | $i_{ac}/(A_s - A_0)$,[c] μA/cm² | $i_{ac}/(A_s - A_0)$,[d] μA/cm² |
|---|---|---|---|---|---|
| 2.10 | 2.06 | 0.00903 | 228.3 | 258.6 | 251.4 |
| 2.22 | 2.15 | 0.00938 | 229.3 | 258.6 | 251.6 |
| 2.39 | 2.26 | 0.00986 | 229.5 | 257.2 | 250.6 |
| 2.54 | 2.37 | 0.01028 | 230.5 | 257.0 | 250.8 |
| 2.69 | 2.48 | 0.01069 | 231.9 | 257.5 | 251.5 |
| 2.85 | 2.59 | 0.01112 | 232.8 | 257.4 | 251.6 |
| 2.98 | 2.67 | 0.01147 | 232.8 | 256.5 | 251.0 |
| Mean | | | 230.7 | 257.5 | 251.2 |
| Std dev | | | 1.82 | 0.78 | 0.41 |
| Rel std dev, % | | | 0.79 | 0.30 | 0.16 |
| Range | | | 4.58 | 2.09 | 1.01 |
| Rel range, % | | | 1.98 | 0.81 | 0.40 |

[a] 0.4 M $K_2C_2O_4$; $E_{dc} = -0.090$ V; $h = 39.5$ cm. [b] Based on $m$ calculated from Equation 22 with $m/h_c = 0.01429$ mg/cm s. [c] $A_0 = 0.00106$ cm², based on $i_{ac}$ vs. $t^{2/3}$. [d] $A_0 = 0.00083$ cm², based on $i_{ac}$ vs. $(mt)^{2/3}$.

Equation 17, which is a quadratic equation in $D^{1/2}$; hence, $D^{1/2}$ is given by Equation 18.

$$I_d = 709\, nD^{1/2}(1 + BD^{1/2}\, t^{1/6}/m^{1/3}) \quad (17)$$

$$D^{1/2} = [(1 + 4\, Bt^{1/6} I_d/709\, nm^{1/3})^{1/2} - 1]m^{1/3}/2Bt^{1/6} \quad (18)$$

If Equation 6 is employed, $I_d'$ replaces $I_d$ in Equations 17 and 18.

When sphericity effects at the HMDE are negligible, $D^{1/2}$ can be used with cyclic voltammetric results to evaluate $A$ directly from Equation 12. If $v$ is sufficiently slow that sphericity effects are not negligible, Equation 13 must be used. To simplify the calculation, advantage can be taken of the fact that $A$ equals $4\pi r_0^2$; substitution of $A^{1/2}/2\pi^{1/2}$ for $r_0$ in Equation 13 leads to

$$i_p = 6.02 \times 10^5 n^{3/2} AD^{1/2} Cv^{1/2}[0.4463 + 0.4263(D/Anv)^{1/2}] \quad (19)$$

Since Equation 19 is a quadratic equation in $A^{1/2}$,

$$A = \{[(0.1817\, D/nv + 2.965 \times 10^{-6}\, i_p/n^{3/2}D^{1/2}Cv^{1/2})^{1/2} - 0.4263(D/nv)^{1/2}]/0.8926\}^2 \quad (20)$$

## RESULTS AND DISCUSSION: DC POLAROGRAPHY

**Contact Area.** A 0.4 M $K_2C_2O_4$ solution was employed for the contact area evaluation by ac polarography. A plot of $i_{ac}$ vs. $t^{2/3}$ (Table I) yielded a slope of 1.422 μA/s$^{2/3}$ and an intercept of −0.2736 μA, giving an $A_0$ of 0.00106 cm², based on $m = 0.525$ mg/s. An identical $A_0$ was obtained for the same capillary using 0.3 M KCl, suggesting that $A_0$ is independent of the nature and concentration of the supporting electrolyte.

Because of the short drop-times employed, back-pressure effects can be significant; since $A_0$ is evaluated by a long extrapolation, a nonconstant $m$ can result in an erroneous $A_0$. To test the effect of variations in $m$ on $A_0$, the data in Table I were analyzed as follows. Equation 7 indicates that a plot of $i_{ac}$ vs. $(mt)^{2/3}$ should be linear with a slope of $j_{ac}\,(6\pi^{1/2}/d)^{2/3}$ and an intercept of $-j_{ac}A_0$, so that $A_0$ can be evaluated analogously to the method employing Equation 8. The proposed method requires experimental evaluation of either $m$ as a function of $t$ at the column height, $h$, employed or the relation between $m$ and the corrected column height, $h_c$, since $h_c$ is related to $h$ and $t$ through the back-pressure term, $h_b$ [given by $3.1/(mt)^{1/3}$ (21), assuming the surface tension is 400 dyne/cm], i.e.,

$$h_c = h - 3.1/(mt)^{1/3} \quad (21)$$

Since, for a given capillary, $m/h_c$ is a constant, symbolized by $K$, multiplication of Equation 21 by $K$, yields Equation 22, where $Kh_c$ is replaced by $m$, which permits calculation of $m$ for any values of $h$ and $t$, once $K$ is determined.

$$m = Kh + 3.1\, K/(mt)^{1/3} \quad (22)$$

For $h$ of 39.6 and 63.4 cm at 2.10 s and 39.6 cm at 2.85 s, $m$ of 0.5225, 0.8694, and 0.5277 mg/s, respectively, were experimentally determined at open circuit; the corresponding $h_c$, determined from Equation 21, were 36.6, 60.8, and 36.9 cm, respectively. The average $m/h_c$ or $K$, 0.01429 mg/cm s (relative average deviation of 0.06%), was used in Equation 22 to calculate $m$ at the various drop-times employed for the ac data (Table I) obtained at an $h$ of 39.5 cm. A plot of $i_{ac}$ vs. $(mt)^{2/3}$ yielded a slope of 2.132 μA/mg$^{2/3}$ and an intercept of −0.2075 μA; the $A_0$ of $8.3 \pm 0.8 \times 10^{-4}$ cm² is 22% less than that obtained from the $i_{ac}$ vs. $t^{2/3}$ plot.

Since $i_{ac}$ is related to the differential capacity by drop-time independent terms except for the electrode area, the ratio of $i_{ac}$ to the effective electrode area should be drop-time independent. Values of $i_{ac}/A_s$, and $i_{ac}/(A_s - A_0)$ for $A_0$ of 0.00106 and 0.00083 cm² are shown in Table I. The results indicate that $A = A_s - 0.00083$ cm² is the best of the three values. For either value of $A_0$, the precision of the mean $i_{ac}/(A_s - A_0)$ is better than the precision of the data; however, using $A_0 = 0.00083$ cm², no systematic trend is observed between $i_{ac}/(A_s - A_0)$ and $t$ as is the case with the larger $A_0$. The importance of using the correct $A_0$ is evident from the difference between the two mean values of $i_{ac}/(A_s - A_0)$.

The results in Table I indicate that the value of $A_s$, determined from $m$ and $t$, is accurate to better than 0.5% over the time range of 2 to 3 s; for shorter times, the accuracy may be slightly poorer, depending on the validity of Equations 21 and 22.

Several points must be made regarding the results just presented and the work of Mohilner et al. (4). Mohilner's procedure was developed for evaluation of differential capacitance data based on the slope of a plot of $i_{ac}$ vs. $t^{2/3}$; he was not interested in the value of $A_0$ based on the intercept. However, the intercept and slope of a straight line fit to data are not independent, and differential capacitance (or current density) values based on intercept calculated contact area corrections should agree with corresponding values calculated from the slope of the plot. The values of $i_{ac}/(A_s - A_0)$, based on the slopes, were 0.1 μA/cm² lower than the respective mean values in Table I in both cases, so that a plot, which yields an incorrect intercept calculated $A_0$, will also give incorrect values based on slope evaluation. Because evaluation of $m$ at several values of $h$ and/or $t$ is tedious, it is desirable to avoid such a task whenever possible; as use of $m$ values in calculations introduces the errors associated with evaluation of $m$, e.g., precise back-pressure calculation, it is advisable to use Mohilner's approach, i.e., to obtain values of $i_{ac}$ at long drop-times, since $m$ becomes relatively independent of $t$ after a few seconds. Since the linear least-squares method will preferentially fit data at large values of $t$, the data at long drop-times should lead to proper evaluation of $A_0$ from a plot of $i_{ac}$ vs. $t^{2/3}$. However, data at short drop-times, e.g., down to 2 s, should also be used in the fit to prevent the need for a long extrapolation to the intercept. The need to consider back-pressure effects on $m$ at the shorter drop-times confirms the complex evaluation procedure of Nancollas and Vincent (5).

**Cadmium(II).** Using the diaphragm method, Rulfs (22) obtained $7.0 \times 10^{-6}$ cm²/s for the diffusion coefficient of 1 mM Cd(II) in 0.1 M KCl; a later study (23) reported a weighted average of $7.0 \pm 0.13 \times 10^{-6}$ cm²/s based on published results of four independent workers using different techniques. Because $D$ for Cd(II) in 0.1 M KCl has been carefully eval-

**Table II. Diffusion Coefficients for 1.012 mM Cd(II) in 0.1 M KCl[a]**

| $h_c$, cm | $I_d$[b] | $I_d'$[b] | $D_{Cd(II)}^{1/2} \times 10^3$, cm/s$^{1/2}$ | | | | | |
|---|---|---|---|---|---|---|---|---|
| 36.5 | 4.15 | 4.59 | 2.93[c] | 3.23[d] | 2.58[e] | 2.69[f] | 2.82[g] | 2.71[h] |
| 41.1 | 4.15 | 4.57 | 2.93 | 3.23 | 2.59 | 2.69 | 2.82 | 2.71 |
| 46.9 | 4.16 | 4.56 | 2.93 | 3.19 | 2.61 | 2.71 | 2.81 | 2.72 |
| 50.9 | 4.15 | 4.54 | 2.93 | 3.17 | 2.61 | 2.71 | 2.81 | 2.72 |
| 53.8 | 4.16 | 4.54 | 2.93 | 3.16 | 2.62 | 2.72 | 2.81 | 2.72 |
| 55.9 | 4.15 | 4.53 | 2.93 | 3.15 | 2.62 | 2.71 | 2.80 | 2.72 |
| 58.7 | 4.15 | 4.52 | 2.93 | 3.15 | 2.62 | 2.72 | 2.80 | 2.72 |
| 60.8 | 4.14 | 4.51 | 2.92 | 3.13 | 2.62 | 2.72 | 2.79 | 2.72 |
| Mean | 4.15 | 4.55 | 2.93 | 3.18 | 2.61 | 2.71 | 2.81 | 2.72 |
| Std dev | 0.004 | 0.028 | 0.003 | 0.037 | 0.015 | 0.011 | 0.012 | 0.003 |
| Rel std dev, % | 0.10 | 0.61 | 0.10 | 1.16 | 0.57 | 0.41 | 0.42 | 0.11 |
| Range | 0.014 | 0.084 | 0.010 | 0.100 | 0.040 | 0.030 | 0.030 | 0.009 |
| Rel range, % | 0.34 | 1.85 | 0.34 | 3.17 | 1.54 | 1.11 | 1.07 | 0.33 |

[a] $t$ = 2.1 s; $m/h_c$ = 0.01376 mg/cm s; literature value, $D^{1/2}$ = 2.65 ± 0.025 × 10$^{-3}$ cm/s$^{1/2}$ (23). [b] Units are $\mu$A s$^{1/2}$/mM mg$^{2/3}$; $I_d'$ is for $A_0$ = 0.00083 cm$^2$. [c] Expanding plane model, Equation 1 (Ilkovic equation). [d] Expanding plane model, Equation 5, $A_0$ = 0.00083 cm$^2$ (Ilkovic equation with contact area correction). [e] Expanding sphere model, Equation 2, $B$ = 36.3 (Matsuda equation). [f] Expanding sphere model, Equation 2, $B$ = 23.5 (Matsuda equation accounting for shielding effect). [g] Expanding sphere model, Equation 6, $B$ = 36.3, $A_0$ = 0.00083 cm$^2$ (Matsuda equation with contact area correction). [h] Expanding sphere model, Equation 6, $B$ = 36.3, $A_0$ = 0.00047 cm$^2$ (Matsuda equation with contact area correction).

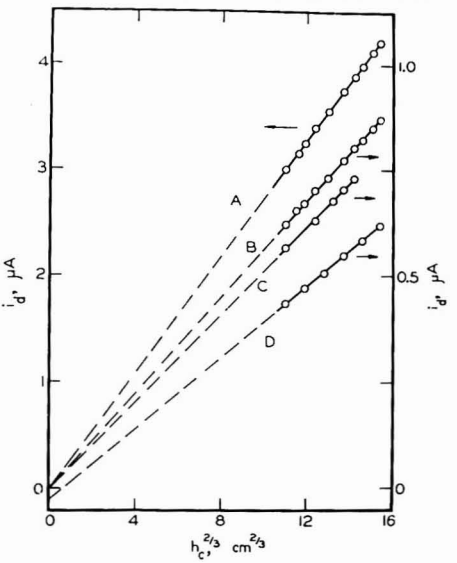


**Figure 1.** Variation of dc polarographic diffusion current with corrected mercury column-height, $h_c$ (calculated from $h$ and $m/h_c$ using Equations 21 and 22; $t$ = 2.10 s). (A) 1.012 mM Cd(II) in 0.1 M KCl; $m/h_c$ = 0.01376 mg/cm s. (B) 0.212 mM Cd(II) in 0.1 M KCl; $m/h_c$ = 0.01376 mg/cm s. (C) 0.183 mM Cd(II) in 0.3 M KCl; $m/h_c$ = 0.01521 mg/cm s and $t$ = 2.07 s. (D) 0.341 mM Fe(III) in 0.4 M $K_2C_2O_4$; $m/h_c$ = 0.01429 mg/cm s

uated, this system should serve as a good check on the contact area correction value for faradaic processes.

The diffusion current for 1.012 mM Cd(II) in 0.1 M KCl was measured at −0.700 V at ten column heights, using a controlled 2.10-s drop-time. Similar measurements were made on 0.212 mM Cd(II) in 0.1 M KCl and 0.183 mM Cd(II) in 0.3 M KCl. Because $t$ was controlled, only $m$ was dependent on $h_c$; the expanding plane model predicts that $i_d$ should be linear with $h_c^{2/3}$ and have a zero intercept. The latter relationships are verified by curves A to C of Figure 1; however, when $i_d$ is corrected for the effect of $A_0$ on the electrode area, a nonzero intercept results (curves A to C of Figure 2). If the polarographic diffusion current is best described by the form of Equation 2 or 6, $i_d$ is not linear with $h_c^{2/3}$ because of the spherical correction term, and a linear extrapolation of $i_d$ vs. $h_c^{2/3}$ should have a nonzero intercept, a fact borne out by theoretically predicted $i_d$–$h_c^{2/3}$ relations (Figure 3). It is also obvious from Figure 3 that a positive value of $A_0$ alters the apparent intercept, which is a function of $A_0$, $m/h_c$, $t$, $D$, and the range of $h_c$ values at which data are fitted (the apparent linearity over the entire range of curve B of Figure 3 is merely a fortuitous consequence of the theoretical parameter values).

**Table III. Diffusion Coefficients for 0.212 mM Cd(II) in 0.1 M KCl[a]**

| $h_c$, cm | $I_d$[b] | $I_d'$[b] | $D_{Cd(II)}^{1/2} \times 10^3$, cm/s$^{1/2}$ | | |
|---|---|---|---|---|---|
| 36.5 | 4.09 | 4.53 | 2.55[c] | 2.65[d] | 2.79[e] |
| 41.1 | 4.08 | 4.50 | 2.55 | 2.65 | 2.79 |
| 46.9 | 4.08 | 4.47 | 2.56 | 2.66 | 2.78 |
| 50.9 | 4.08 | 4.47 | 2.57 | 2.67 | 2.79 |
| 53.6 | 4.09 | 4.47 | 2.58 | 2.67 | 2.80 |
| 55.9 | 4.08 | 4.45 | 2.58 | 2.67 | 2.79 |
| 58.7 | 4.08 | 4.44 | 2.58 | 2.67 | 2.79 |
| 60.8 | 4.08 | 4.44 | 2.59 | 2.68 | 2.79 |
| Mean | 4.08 | 4.47 | 2.57 | 2.67 | 2.79 |
| Std dev | 0.006 | 0.030 | 0.014 | 0.010 | 0.004 |
| Rel std dev, % | 0.15 | 0.67 | 0.54 | 0.39 | 0.14 |
| Range | 0.018 | 0.09 | 0.037 | 0.027 | 0.011 |
| Rel range, % | 0.44 | 2.01 | 1.45 | 1.01 | 0.39 |

[a] $t$ = 2.1 s, $m/h_c$ = 0.01376 mg/cm s; literature value for 1 mM Cd(II), $D^{1/2}$ = 2.65 ± 0.025 × 10$^{-3}$ cm/s$^{1/2}$ (23). [b] Units are $\mu$A s$^{1/2}$/mM mg$^{2/3}$. [c] Expanding sphere model, Equation 2, $B$ = 36.3 (Matsuda equation). [d] Expanding sphere model, Equation 2, $B$ = 23.5 (Matsuda equation accounting for shielding effect). [e] Expanding sphere model, Equation 6, $B$ = 36.3, $A_0$ = 0.00083 cm$^2$ (Matsuda equation with contact area correction).

The diffusion coefficient for Cd(II) in 0.1 M KCl was evaluated from the data in curves A to C of Figure 1, using various theoretical relationships (Tables II to IV); points deviating noticeably from the fitted line were not included.

From the results in Table II, the simple Ilkovic equation gives the best precision for $D^{1/2}$, but the deviation from the reported value (23) is 10%. Equation 6 with $B$ = 36.3 and

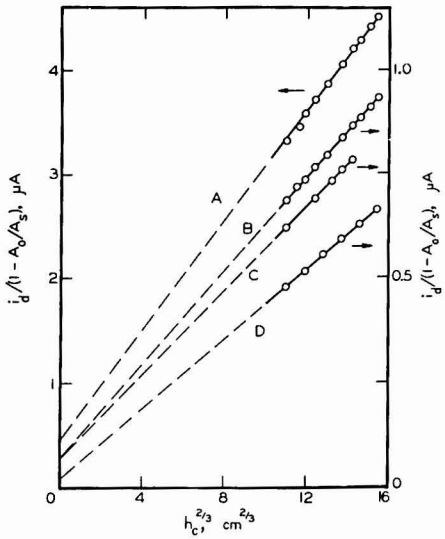


**Figure 2.** Variation of dc polarographic diffusion current (corrected for contact area effect) with corrected mercury column-height. Conditions and curve designations are as in Figure 1; $A_o$ = 0.00083 cm²

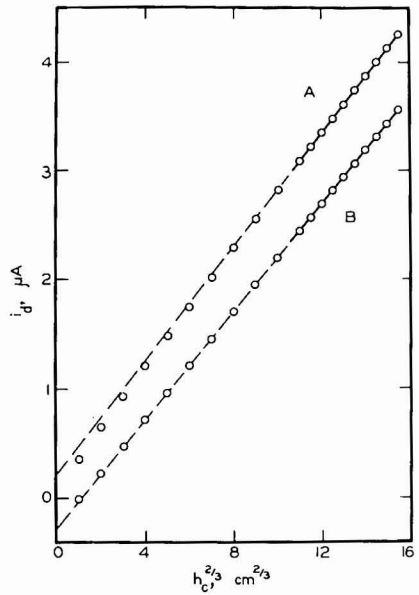


**Figure 3.** Theoretical relation of dc polarographic diffusion current to corrected mercury column height. Parameters: $D = 7 \times 10^{-6}$ cm²/s; $C$ = 1 mM; $n$ = 2; $t$ = 2.10 s; $m/h_c$ = 0.014 mg/cm s. (A) $i_d$ relation defined by Equation 2 with $B$ = 36.3. (B) $i_d$ relation defined by Equation 6 with $B$ = 36.3 and $A_o$ = 0.00083 cm². Lines represent estimated linear relation of $i_d$ to $h_c^{2/3}$ for $h_c^{2/3} \geq 11$ cm$^{2/3}$

**Table IV. Diffusion Coefficients for 0.183 mM Cd(II) in 0.3 M KCl[a]**

| $h_c$, cm | $I_d$[b] | $I_d'$[b] | $D_{Cd(II)} \times 10^3$, cm/s$^{1/2}$ | | |
|---|---|---|---|---|---|
| 36.6 | 4.05 | 4.44 | 2.54[c] | 2.63[d] | 2.76[e] |
| 43.6 | 4.04 | 4.38 | 2.54 | 2.64 | 2.74 |
| 48.3 | 4.02 | 4.34 | 2.54 | 2.63 | 2.72 |
| 50.9 | 4.04 | 4.35 | 2.56 | 2.65 | 2.74 |
| 53.9 | 4.02 | 4.32 | 2.55 | 2.64 | 2.72 |
| Mean | 4.03 | 4.37 | 2.55 | 2.64 | 2.74 |
| Std dev | 0.012 | 0.049 | 0.010 | 0.007 | 0.014 |
| Rel std dev, % | 0.31 | 1.11 | 0.37 | 0.28 | 0.50 |

[a] $t$ = 2.07 s; $m/h_c$ = 0.01521 mg/cm s; literature value for 1 mM Cd(II) in 0.1 M KCl, $D^{1/2} = 2.65 \pm 0.25 \times 10^{-3}$ cm/s$^{1/2}$(23). [b] Units are μA s$^{1/2}$/mM mg$^{2/3}$. [c] Expanding sphere model, Equation 2, $B$ = 36.3 (Matsuda equation). [d] Expanding sphere model, Equation 2, $B$ = 23.5 (Matsuda equation accounting for shielding effects). [e] Expanding sphere model, Equation 6, $B$ = 36.3, $A_o$ = 0.00083 cm² (Matsuda equation with contact area correction).

$A_o$ = 0.00083 cm² gives $D^{1/2}$ values 4 to 6% higher than the published value. Matsuda's relations predict $D^{1/2}$ in close agreement with that reported, being 1.5 to 3.8% low if a freely suspended sphere is assumed, and, in the case of a shielded sphere, within less than 1% for the two lower concentrations.

**Iron(III).** The Fe(III)/Fe(II) couple in high $K_2C_2O_4$ concentration has been reported to be an uncomplicated, rapid electron-transfer couple at mercury (*24–28*). A recent investigation (*8*) of Fe(III) reduction in 1 M $K_2C_2O_4$ showed that the ac polarographic peak current was linear with the square root of frequency up to 15 kHz (upper limit of the study) and that the cyclic voltammetric cathodic–anodic peak potential separation was that expected for a simple reversible electron-transfer at scan rates up to 4000 V/s (fastest scan rate employed). Because of its reversible nature and noninvolvement of amalgam formation, the Fe(III)/Fe(II) couple in $K_2C_2O_4$ should be excellent for evaluation of the effective DME and HMDE areas.

The Fe(III) dc polarographic $i_d$–$h_c$ relation was examined, analogously to the Cd(II) study (curve D in Figures 1 and 2). Trioxalatoiron(III) diffusion current constant and coefficient data are given in Table V.

Lingane (*28*) reported an $I_d$ for Fe(III) in 0.2 M $Na_2C_2O_4$ based on average currents which, when converted to the maximum current value, is 1.75 ± 0.035, in agreement with the mean value of 1.75 ± 0.011 in Table V, but 8% below the mean $I_d'$ of 1.90 ± 0.09. Smith and Reinmuth (*29*) obtained $4.95 \times 10^{-6}$ cm²/s for $D$ of Fe(III) in 0.3 M $K_2C_2O_4$ + 0.1 M $H_2C_2O_4$ + 0.05 M KCl, based on the slope of a plot of ac polarographic peak current vs. frequency; the corresponding value of $D^{1/2}$, $2.22 \times 10^{-3}$ cm/s$^{1/2}$, is in excellent agreement with that of $2.23 \times 10^{-3}$ cm/s$^{1/2}$ in Table V, based on the Matsuda equation for a freely suspended sphere. The latter agreement may reflect apparently identical definition of the electrode area as $A_s$, and Smith and Reinmuth's use (*29*) of Koutecky's theory (*16*) to obtain the value of $D$ by ac polarography. (Koutecky's $B$ of 39.5 is quite close to Matsuda's $B$ of 36.3.)

**The Apparent Area.** It is well established that, at a naturally dropping mercury electrode, the drop fall does not cause sufficient convection to homogenize the solution. Consequently, after the growth of the first drop under conditions of faradaic activity, there is some depletion of electroactive species in the solution region into which new drops grow, and the faradaic current for the first drop may be 10–20% larger than for succeeding drops (*30*). Thus, $i_d$ for 1 mM Cd(II) in 0.1 M KCl would be expected to predict diffusion coefficients lower than those measured by nonpo-

Table V. Diffusion Coefficients for 0.341 mM Fe(III) in 0.4 M $K_2C_2O_4$[a]

| $h_c$, cm | $I_d$[b] | $I_d'$[b] | $D_{Fe(III)}^{1/2} \times 10^3$, cm/s$^{1/2}$ | | | | | |
|---|---|---|---|---|---|---|---|---|
| 36.5 | 1.73 | 1.91 | 2.45[c] | 2.69[d] | 2.20[e] | 2.28[f] | 2.48[g] | 2.31[h] |
| 41.1 | 1.74 | 1.90 | 2.45 | 2.68 | 2.21 | 2.28 | 2.40 | 2.31 |
| 45.8 | 1.74 | 1.89 | 2.46 | 2.67 | 2.22 | 2.30 | 2.40 | 2.32 |
| 50.9 | 1.76 | 1.90 | 2.48 | 2.67 | 2.24 | 2.31 | 2.40 | 2.34 |
| 55.8 | 1.76 | 1.89 | 2.48 | 2.66 | 2.25 | 2.32 | 2.41 | 2.34 |
| 60.8 | 1.76 | 1.89 | 2.48 | 2.66 | 2.26 | 2.33 | 2.41 | 2.34 |
| Mean | 1.75 | 1.90 | 2.47 | 2.67 | 2.23 | 2.30 | 2.40 | 2.33 |
| Std dev | 0.011 | 0.085 | 0.016 | 0.012 | 0.025 | 0.022 | 0.005 | 0.015 |
| Rel std dev, % | 0.65 | 0.45 | 0.65 | 0.45 | 1.11 | 0.97 | 0.20 | 0.64 |
| Range | 0.027 | 0.024 | 0.038 | 0.034 | 0.064 | 0.057 | 0.013 | 0.035 |
| Rel range, % | 1.54 | 1.27 | 1.54 | 1.27 | 2.87 | 2.47 | 0.54 | 1.50 |

[a] $t$ = 2.1 s; $m/h_c$ = 0.01429 mg/cm s; literature value, $D^{1/2}$ = 2.22 × 10$^3$ cm/s$^{1/2}$ (29). [b] Units are $\mu$A s$^{1/2}$/mM mg$^{2/3}$; $I_d'$ is for $A_0$ = 0.00083 cm$^2$. [c] Expanding plane model, Equation 1 (Ilkovic equation). [d] Expanding plane model, Equation 5, $A_0$ = 0.00083 cm$^2$ (Ilkovic equation with contact area correction). [e] Expanding sphere model, Equation 2, $B$ = 36.3 (Matsuda equation). [f] Expanding sphere model, Equation 2, $B$ = 23.5 (Matsuda equation accounting for shielding effect). [g] Expanding sphere model, Equation 6, $B$ = 36.3, $A_0$ = 0.00083 cm$^2$ (Matsuda equation with contact area correction). [h] Expanding sphere model, Equation 6, $B$ = 36.3, $A_0$ = 0.00047 cm$^2$ (Matsuda equation with contact area correction).

larographic techniques; since the results in Table II agree with or, in most cases, exceed the reported value, stirring due to the drop knocker must homogenize the solution and may even slightly enhance $i_d$ because of convective effects extant at the drop fall.

To investigate the possible presence of stirring effects, the following procedure was used to examine the $i$–$t$ profiles for single drops: (a) At $E$ = –0.700 V, several drops were allowed to grow and fall at a controlled 2.10-s drop-time; (b) the drop-knocker was shut off as a drop was dislodged so that the next drop grew and fell with a natural drop-time (this drop will be referred to as the first natural drop) and its $i$–$t$ behavior was recorded; (c) $i$–$t$ profiles of successive drops with natural drop-times were recorded (these will be referred to as the second natural drop, etc.). A similar procedure on the background solution permitted background subtraction. Some qualitative conclusions were immediately obvious. Comparison of $i$–$t$ profiles for several controlled drops indicated very reproducible $i$–$t$ behavior for $t$ > 0.1 s (the recorder response time under the conditions employed). The $i$–$t$ behavior of the first natural drop during its first 2.10 s was the same as that of controlled drops, a rather obvious expectation. The $i$–$t$ behaviors of the second and third natural drops were identical within experimental uncertainty for $t$ < 9 s. At any given instant in the drop-life, the current for the first natural drop was larger than that for succeeding drops.

Curve A of Figure 4 represents the current for the first natural drop to grow into relatively undepleted solution beyond the region traversed by a 2.10-s controlled drop. Although the second drop (curve C) grows into a region depleted by the previous drop, the extent of the depletion decreases with increasing distance from the capillary orifice and, with increasing time into the drop-life, the drop grows into a solution region for which diffusion has had additional time to reduce depletion due to the previous drop; hence, the depletion effect on the current decreases with time after drop-birth.

The profound difference in current at short times between the first and second natural drops indicates that the mechanical drop-knocker introduces stirring effects which reduce or eliminate depletion due to the previous drop; however, the matter of whether such stirring merely homogenizes the solution or enhances the current, even 2.10 s after drop-birth, relative to theoretical prediction is unanswered. Although the behavior of the effective contact area corrected currents for the first natural drop (curve B of Figure 4) indicates that stirring influences the current even 2.5 s after drop-birth, this may be an artifact due to the effective contact area for faradaic processes being smaller than that determined by ac polarographic charging currents and/or a breakdown in the $m/h_c$ relationship at short times. The latter seems unlikely, since the apparent effect is seen for drop areas which are intermediate between those for which the $m/h_c$ ratio was found to be constant.

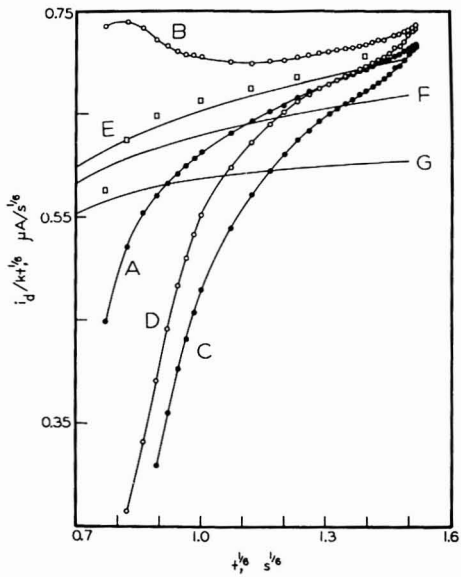


Figure 4. DC polarographic current–time profiles for single drops. (A) First drop after drop-knocker shut-off; $k$ = 1; 0.212 mM Cd(II) in 0.1 M KCl; $h$ = 49.7 cm; $m/h_c$ = 0.01376 mg/cm s. The small rectangles represent the data in curve A for $k$ = 1 – 0.00047/$A_s$. (B) Same as A except $k$ = 1 – 0.00083/$A_s$. (C) Second drop after drop-knocker shut-off; $k$ = 1. (D) Same as C except $k$ = 1 – 0.00083/$A_s$. (E) Behavior predicted by Equation 2 for $n$ = 2, $C$ = 0.212 mM, $D$ = 7 × 10$^{-6}$ cm$^2$/s. $B$ = 36.3, $h$ = 49.7 cm, $m/h_c$ = 0.01376 mg cm/s and $k$ = 1. (F) Same as E except $B$ = 23.5. (G) Behavior predicted by Equation 1; parameters same as for E. The factor $k$ is a means of area correction

An alternative estimate of $A_0$ can be obtained from theoretical relationships between $i_d$, and $m$ and $t$. To a first approximation, the contact area predicted by the Matsuda equation with shielding effects (Equation 2 with $B$ = 23.5)

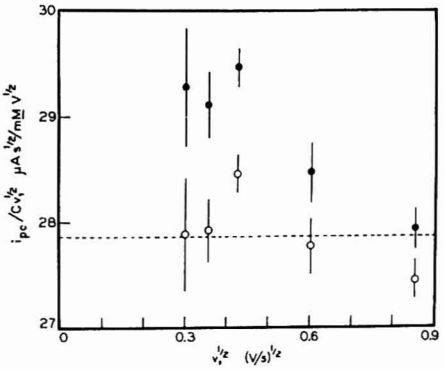


**Figure 5.** Variation with scan rate of the cyclic voltammetric reduction peak current function for 0.183 mM Cd(II) in 0.3 M KCl. (●) experimental values. (O) calculated planar current function values, based on the difference between the observed value and the spherical current function value calculated using $A = 0.0144$ cm$^2$ and $D^{1/2} = 2.55 \times 10^{-3}$ cm/s$^{1/2}$. Dashed line is the predicted planar current function value based on the indicated values of $A$ and $D^{1/2}$. Uncertainties represent the standard deviation of 2 to 3 measurements

can be estimated as the difference between the sphericity terms (in the absence and presence of shielding effect correction) times the spherical electrode area, $(36.3 - 23.5)\ D^{1/2}\ t^{1/6}\ A_s/m^{1/3}$ or $12.8(6\pi^{1/2}/d)^{2/3}\ D^{1/2}\ t^{5/6}\ m^{1/3}$; this approach indicates an average effective electrode area for the data in Tables II and III, which is 0.00047 cm$^2$ smaller than the calculated spherical area (range of 0.00042 to 0.00050 cm$^2$). Correction of points on curve A for a contact area of 0.00047 cm$^2$ yields the results shown in Figure 4. Contact area corrected currents should obey relationships for a freely suspended drop and, indeed, the corrected curve A data do parallel the theoretical predictions (curve E) over the range of 0.5 to ca. 7.5 s; although these corrected $i_d$ values lie above curve E, the deviation is well within the uncertainty of the $D$ value for Cd(II).

The difference in apparent effective contact areas indicated by ac and dc polarography may result from several factors, e.g., an electrode may have different effective areas for faradaic and nonfaradaic processes. It is well established that the faradaically effective area for solid planar electrodes, e.g., Pt and graphite, is the projected area, which more closely approximates the macroscopic rather than the microscopic area (*31*, *32*) because the diffusion layer extends far beyond the surface roughness. This projected area phenomenon is precisely the reason why a spherical Hg electrode supports a larger current than a planar Hg electrode of the same geometric area, since the projected area for a spherical electrode is larger than its geometric area. Although the spherical term of Equation 2 accounts for the projection, the expression for a freely suspended sphere cannot properly account for the projection in the region of the neck or movement of the drop's center of mass; the latter projection may partially compensate for the effective contact area determined by ac polarography. Because the ac polarographic charging current does not involve diffusion and because the double layer is very thin compared to the drop radius, the true, unprojected area is determined by the ac polarographic charging current method.

## RESULTS AND DISCUSSION: CYCLIC VOLTAMMETRY

**Cadmium(II).** To minimize problems associated with *iR* loss, cyclic voltammetric data were acquired on 0.183 mM Cd(II) in 0.3 M KCl. The peak current function at varying scan rate (Figure 5) clearly shows the effects of electrode sphericity, i.e., it decreases with increasing $v$. Using the Table IV data and either Equation 15 or 20, the HMDE area was evaluated (Table VI); the results using Equation 15 show a trend with $v$ due to sphericity. Even at the fastest $v$, where sphericity is relatively negligible (less than a 2% contribution), Equation 15 predicts an area ca. 10% smaller than that obtained from Equation 20 with the best estimate of $D^{1/2}$.

Subtraction of the spherical contribution from the observed current yields the planar current contribution, described by Equation 12 for a reversible system, for which $i_p/cv^{1/2}$ should be scan-rate independent. The results of such a subtraction (Figure 5) show that the calculated planar term is, indeed, essentially constant with no point deviating by more than 2% from the expected value.

**Iron(III).** Cyclic voltammetric peak current function data for 0.341 mM Fe(III) in 0.4 M $K_2C_2O_4$ (Figure 6) were analyzed

**Table VI. Area of the HMDE Based on dc Polarographic and Cyclic Voltammetric Data for 0.183 mM Cd(II) in 0.3 M KCl[a]**

| $v$, V/s | $A$, cm$^2$ | | | | |
|---|---|---|---|---|---|
| 0.091 | 0.0144[b] | 0.0139[c] | 0.0134[d] | 0.0136[e] | 0.0125[f] |
| 0.128 | 0.0145 | 0.0139 | 0.0134 | 0.0135 | 0.0124 |
| 0.182 | 0.0147 | 0.0142 | 0.0137 | 0.0136 | 0.0126 |
| 0.365 | 0.0144 | 0.0138 | 0.0133 | 0.0132 | 0.0122 |
| 0.730 | 0.0142 | 0.0137 | 0.0132 | 0.0129 | 0.0119 |
| Mean | 0.0144 | 0.0139 | 0.0134 | 0.0134 | 0.0123 |
| Std dev | 0.0002 | 0.0002 | 0.0002 | 0.0003 | 0.0003 |
| Rel std dev, % | 1.3 | 1.3 | 1.4 | 2.3 | 2.3 |
| Range | 0.0005 | 0.0005 | 0.0005 | 0.0007 | 0.0007 |
| Rel range, % | 3.5 | 3.6 | 3.7 | 5.2 | 5.7 |

[a] Calculated from data in Figure 5 and Table IV.
[b] From Equation 20; $D^{1/2} = 2.546 \times 10^{-3}$ cm/s$^{1/2}$.
[c] From Equation 20; $D^{1/2} = 2.638 \times 10^{-3}$ cm/s$^{1/2}$.
[d] From Equation 20; $D^{1/2} = 2.735 \times 10^{-3}$ cm/s$^{1/2}$.
[e] From Equation 15; $I_d = 4.035\ \mu$A s$^{1/2}$/mM mg$^{2/3}$.
[f] From Equation 15; $I_d = 4.369\ \mu$A s$^{1/2}$/mM mg$^{2/3}$.

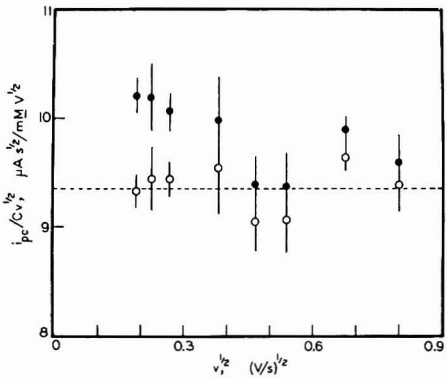


**Figure 6.** Variation with scan rate of the cyclic voltammetric reduction peak current function for 0.341 mM Fe(III) in 0.4 M $K_2C_2O_4$. (●) experimental values. (O) calculated planar current function values, based on the difference between the observed value and the spherical current function value calculated using $A = 0.0151$ cm$^2$ and $D^{1/2} = 2.30 \times 10^{-3}$ cm/s$^{1/2}$. Dashed line is the predicted planar current function value based on the indicated values of $A$ and $D^{1/2}$. Uncertainties represent the standard deviation of 3 to 8 measurements

Table VII. Area of the HMDE Based on dc Polarographic and Cyclic Voltammetric Data for 0.341 mM Fe(III) in 0.4 M $K_2C_2O_4$[a]

| $v$, V/s | $A$, cm² | | | |
|---|---|---|---|---|
| 0.036 | 0.0151[b] | 0.0144[c] | 0.0154[d] | 0.0142[e] |
| 0.051 | 0.0153 | 0.0146 | 0.0154 | 0.0142 |
| 0.073 | 0.0152 | 0.0146 | 0.0152 | 0.0140 |
| 0.146 | 0.0154 | 0.0147 | 0.0151 | 0.0139 |
| 0.218 | 0.0146 | 0.0140 | 0.0142 | 0.0131 |
| 0.291 | 0.0146 | 0.0140 | 0.0140 | 0.0130 |
| 0.457 | 0.0156 | 0.0147 | 0.0149 | 0.0138 |
| 0.641 | 0.0152 | 0.0145 | 0.0145 | 0.0134 |
| Mean | 0.0151 | 0.0144 | 0.0149 | 0.0137 |
| Std dev | 0.0004 | 0.0003 | 0.0005 | 0.0005 |
| Rel std dev, % | 2.4 | 2.0 | 3.5 | 3.5 |
| Mean[f] | 0.0153 | 0.0146 | 0.0151 | 0.0139 |
| Std dev[f] | 0.0002 | 0.0001 | 0.0003 | 0.0003 |
| Rel std dev, %[f] | 1.2 | 0.8 | 2.3 | 2.2 |

[a] Calculated from data in Figure 6 and Table V.
[b] From Equation 20; $D^{1/2} = 2.304 \times 10^{-3}$ cm/s$^{1/2}$.
[c] From Equation 20; $D^{1/2} = 2.402 \times 10^{-3}$ cm/s$^{1/2}$.
[d] From Equation 15; $I_d = 1.748$ μA s$^{1/2}$/mM mg$^{2/3}$.
[e] From Equation 15; $I_d = 1.895$ μA s$^{1/2}$/mM mg$^{2/3}$.
[f] Based on six points not including values at $v = 0.218$ V/s and 0.291 V/s.

analogously to the cadmium data to determine the electrode area (Table VII) and to calculate the planar current function (Figure 6). As with Cd(II), a trend in the calculated area using Equation 15 indicates the effect of sphericity. If the data at scan rates between 0.2 and 0.3 V/s are neglected, the standard deviations of the determined area are about 1%, the same as the Cd(II) data; however, the mean areas determined using the two chemical systems differ by 0.0005 to 0.0015 cm² or 5 to 12% of the area obtained using Fe(III), which always gives larger areas.

**Effect of Chemical System on Determined HMDE Area.** Because the uncertainties in the parameters associated with the calculation of $D^{1/2}$ and $A$ are considerably below the level which could account for the 5 to 12% discrepancy in the areas determined using Cd(II) and Fe(III), the difference is likely to be significant. In fact, although the $F$-test indicates no significant difference between the variances at the 5% uncertainty level, i.e., $S_1^2/S_2^2$ is smaller than the value of $F$ which would be exceeded by chance 5% of the time, there is a significant difference between the mean areas determined by Cd(II) and Fe(III) even at the 99% confidence level.

The probable source of the discrepancy is a difference in behavior of the chemical systems. Some often overlooked reports suggest that Cd(II)/Cd(Hg) is not a satisfactory model system. Delahay and Trachtenberg (*33, 34*) showed that, when "normal care" is taken in chemical purification, small amounts of adsorbable impurities may be present, which can drastically alter the heterogeneous rate constant ($k_{s,h}$) measured at an HMDE but which have little effect on work at a DME. They observed a decrease of more than two orders-of-magnitude in the Cd(II) $k_{s,h}$ when the exposure of the HMDE to the solution before measurement varied from a few minutes to two hours. Randles and Somerton (*35, 36*) noted a change of over three orders-of-magnitude in $k_{s,h}$ upon variation in the concentration of added surfactant. The extreme sensitivity of $k_{s,h}$ to adsorbed impurities is probably due to the close proximity of the Cd(II) reduction potential to the potential-of-zero-charge.

The cyclic voltammograms, from which the data in Figure 5 and Table VI were derived, showed a seemingly peculiar phenomenon. For a two-electron reduction, the difference between cathodic and anodic peak potentials, $E_{pc} - E_{pa}$, should be 0.030 V; the observed values, even at $v = 0.09$ V/s, were 0.02 V. However, the difference between $E_{pc}$ and the potential at half peak height, $E_{pc/2}$, which should be 0.014 V, was 0.03 V, which, because of the observed value of $E_{pc} - E_{pa}$, cannot be due to $iR$ loss in solution. In light of the reported effect of impurities on the cadmium behavior, the drawn-out nature of the cathodic peak is probably the result of a small $k_{s,h}$. However, regardless of the reason for the drawn-out nature of the Cd(II) peaks, their deviation from the theoretically predicted behavior for a reversible system suggests that HMDE areas calculated from Cd(II) data, assuming reversible behavior, will be erroneous and, because of the drawn-out nature of the peaks, will be low.

## EVALUATION OF THEORIES AND PROCEDURES

**DC Polarography.** The results clearly indicate that, for controlled 2-s drop-times, the Ilkovic equation does not accurately describe either the $i_d$–$h_c$ or $i$–$t$ relations for a single drop. Application of Equation 5 and the effective contact area determined by ac polarography results in calculated diffusion coefficients for Cd(II), which are at variance with previously reported results by over 40% (20% for $D^{1/2}$).

The remarkably good agreement between the $D$ values in Table III, calculated using Equation 2 with $B = 23.5$, and the published value is a fortuitous consequence of the drop-time employed for data acquisition, as is obvious from the time (1.87 s) at which experimental curve A of Figure 4 and curve F for the theoretical behavior predicted by Equation 2 with $B = 23.5$, cross, and by the fact that the difference between curves A and F at 2.10 s is only 0.3%. It is evident from Figure 4 that, in the time range from 1 to 4 s, the experimental data (curve A) are within 3% of the theoretical prediction based on Equation 2 with $B = 23.5$ (curve F); the same accuracy is obtained for $B = 36.3$ (curve E) in the range of 2.3 to greater than 12 s on the first drop with natural drop-time; however, use of long controlled drop-times may result in eventual development of depletion in the solution region encountered by the electrode surface near the end of its drop-life, since the stirring effects accompanying mechanical dislodgment may not completely homogenize the solution far from the capillary orifice. Within the range of 2 to 4 s, either form of the Matsuda equation will apparently give comparable accuracy.

The change at about 3.4 s in the value of $B$ for Equation 2, which better describes the $i$–$t$ relation, probably reflects the assumption used in Matsuda's derivation (*15*), that the drop is spherical throughout its life. The assumed spherical shape defines a certain fraction of the drop for which (a) the drop is nearly contacting the glass capillary or (b) the distance between drop and capillary is less than the expected diffusion layer thickness, so that supply of electroactive species to that region of the electrode is greatly reduced; based on Matsuda's theory, the fraction of the drop area suffering from one of these two phenomena increases during drop-life. Early in the drop-life, the shape probably is relatively spherical; however, the drop is actually pendant-shaped, particularly later in its life when the weight is relatively large. The pendant shape results in the major portion of the drop's mass—and, hence, area—being below the neck and, consequently, farther removed from the capillary than would be the case for a spherical shape, with concomitantly reduced shielding by the capillary. Thus, early in the drop-life, when the shape approaches spherical, the equation accounting for shielding more accurately describes the $i$–$t$ behavior; later, as the mass increases and the drop neck stretches, the shielding effect diminishes and the $i$–$t$ behavior is more nearly approximated by the equation for a freely suspended drop.

For very accurate measurement of $D$, i.e., 1 to 2% accuracy, it is evident from the factors discussed in the previous paragraph and the fact that the Hg flow-rate influences the

time at which the $i$–$t$ behavior is more accurately described as that of a freely suspended drop, that calibration data should be obtained under the drop-time and Hg flow-rate conditions to be employed. For the purpose of calibration, the system of 1 mM Cd(II) in 0.1 M KCl appears to be excellent, since $D$ for Cd(II) under these conditions is accurately known.

Considerable debate has recently centered on the questions of whether polarographic behavior at controlled drop-times of less than 1 s is accurately described by the Ilkovic equation and whether the back-pressure term in the calculation of $h_c$—and, hence, $m$—is properly described by $3.1/(mt)^{1/3}$. Canterford (*37*) has reviewed the various reports and has presented evidence which indicates that the Ilkovic equation does not properly describe the currents at short drop-times. The results of the present study also clearly indicate that use of a mechanical drop-knocker tends to diminish or eliminate the depletion effects, which, under conditions of natural drop-fall, counterbalance sphericity effects and permit the Ilkovic equation to describe accurately the $i$–$h_c$ relation.

**Cyclic Voltammetry.** For accurate determination of the HMDE area using cyclic voltammetry or linear potential scan amperometry, a chart recorder is preferable to an oscilloscope as a read-out device because of the inherently greater accuracy of the former; however, because of the relatively slow response time of a recorder, it is generally not possible to employ scan rates exceeding 0.5 to 1 V/s; even with scan rates of ca. 0.5 V/s, low current axis sensitivities must be employed to prevent recorder response degradation, thus reducing the precision with which peak currents can be measured. (The danger associated with using too high a current axis sensitivity is exemplified by the points in Figure 6 for $v^{1/2}$ of 0.47 and 0.54 $V^{1/2}/s^{1/2}$.) Thus, one must evaluate the electrode area under conditions of slow scan rate, for which it is necessary to use the cyclic voltammetric peak current equation which accounts for sphericity.

The variability of the HMDE area, as indicated by the standard deviations for the peak current functions (Figures 5 and 6) is less than 3%.

Because of the previously mentioned problems associated with the Cd(II)/Cd(Hg) system, this system should not be employed for HMDE area evaluation. The Fe(III)/Fe(II) couple seems to be an excellent choice for such area evaluation.

## LITERATURE CITED


(1) J. M. Markowitz and P. J. Elving, *Chem. Rev.*, **58**, 1047 (1958).
(2) D. Ilkovic, *Collect. Czech. Chem. Commun.*, **6**, 498 (1934).
(3) J. M. Markowitz and P. J. Elving, *J. Am. Chem. Soc.*, **81**, 3518 (1959).
(4) D. M. Mohilner, J. C. Kreuser, H. Nakadomari, and P. O. Mohilner, *J. Electrochem. Soc.*, **123**, 359 (1976).
(5) G. H. Nancollas and C. A. Vincent, *Electrochim. Acta*, **10**, 97 (1965).
(6) W. H. Reinmuth, *J. Am. Chem. Soc.*, **79**, 6358 (1957).
(7) R. S. Nicholson and I. Shain, *Anal. Chem.*, **36**, 706 (1964).
(8) T. E. Cummings, M. A. Jensen, and P. J. Elving, to be submitted for publication.
(9) H. Strehlow and M. von Stackelberg, *Z. Elektrochem.*, **54**, 51 (1950).
(10) M. von Stackelberg, *Z. Elektrochem.*, **57**, 338 (1953).
(11) M. von Stackelberg and V. Toome, *Z. Elektrochem.*, **58**, 226 (1954).
(12) T. Kambara and I. Tachi, "Proc. I. Internat. Polarograph. Congress", Vol. 1, Prirodovedeche Vydavatelstvi, Prague, 1951, p 126.
(13) T. Kambara and I. Tachi, *Bull. Chem. Soc. Jpn.*, **23**, 226 (1950).
(14) R. S. Sabrahmanya, *Can. J. Chem.*, **40**, 289 (1962).
(15) H. Matsuda, *Bull. Chem. Soc. Jpn.*, **36**, 342 (1953).
(16) J. Koutecky, *Czech. J. Phys.*, **2**, 50 (1953).
(17) W. M. MacNevin and E. W. Balis, *J. Am. Chem. Soc.*, **65**, 660 (1943).
(18) G. S. Smith, *Trans. Faraday Soc.*, **47**, 63 (1952).
(19) J. W. Perram, J. B. Hayter, and R. J. Hunter, *J. Electroanal. Chem.*, **42**, 291 (1973).
(20) D. E. Smith, in "Electroanalytical Chemistry", Vol. 1, A. J. Bard, Ed., Dekker, New York, N.Y., 1966.
(21) J. Heyrovsky and J. Kuta, "Principles of Polarography", Academic Press, London, 1966, p 37.
(22) C. L. Rulfs, *J. Am. Chem. Soc.*, **76**, 2071 (1954).
(23) D. J. Macero and C. L. Rulfs, *J. Electroanal. Chem.*, **7**, 328 (1964).
(24) M. von Stackelberg and H. Freyhold, *Z. Elektrochem.*, **46**, 120 (1940).
(25) J. J. Lingane, *Chem. Rev.*, **29**, 1 (1941).
(26) J. E. B. Randles and D. W. Somerton, *Trans. Faraday Soc.*, **48**, 937 (1952).
(27) R. deLeeuwe, M. Sluyters-Rehbach, and J. H. Sluyters, *Electrochim. Acta*, **14**, 1183 (1969).
(28) J. J. Lingane, *J. Am. Chem. Soc.*, **68**, 2448 (1946).
(29) D. E. Smith and W. H. Reinmuth, *Anal. Chem.*, **33**, 482 (1961).
(30) J. Kuta and I. Smoler, in "Progress in Polarography", Vol. 1, P. Zuman and I. M. Kolthoff, Ed., Interscience, New York, N.Y., 1962, p 43.
(31) P. J. Elving and D. L. Smith, "Analytical Chemistry 1962", Elsevier, Amsterdam, 1963, pp 204-213.
(32) C. N. Reilley, G. W. Everett, and R. H. Johns, *Anal. Chem.*, **27**, 483 (1955).
(33) P. Delahay and I. Trachtenberg, *J. Am. Chem. Soc.*, **80**, 2094 (1958).
(34) P. Delahay, *J. Chim. Phys.*, **54**, 369 (1957).
(35) J. E. B. Randles and K. W. Somerton, *Trans. Faraday Soc.*, **48**, 951 (1952).
(36) J. E. B. Randles, *Faraday Soc. Discuss.*, **1**, 11 (1947).
(37) D. R. Canterford, *J. Electroanal. Chem.*, **77**, 113 (1977).


RECEIVED for review October 21, 1977. Accepted December 7, 1977. The authors thank the National Science Foundation, which helped support the work described.

# Solvent Extraction of Chromium(III) by Salicylic, Thiosalicylic, and Phthalic acids

**Dennis G. Sebastian[1] and David C. Hilderbrand***

*Department of Chemistry, South Dakota State University, Brookings, South Dakota 57007*

**The use of salicylic, thiosalicylic, and phthalic acid complexing agents for the solvent extraction of Cr(III) from aqueous solution was investigated. *N*-Butanol was used as the organic solvent. The extraction efficiency was optimized with respect to pH, heating period, choice of buffer, and concentration of a salting-out agent. An extraction efficiency of greater than 97% was obtained using a mixed phthalic–thiosalicylic complexing system.**

Quantitative solvent extraction of many first row transition metal elements can be readily achieved at room temperature using a variety of complexing agents. The solvent extraction of chromium is much more difficult with quantitative extraction occurring only after extraction at elevated temperature for a prolonged period of time. One cause of chromium's poor extractability is the lability of the hexaquochromium ion. The half-life of the exchange of water molecules has been reported as 40 h (*1*) and corresponding rate constants for the exchange reaction of $2 \times 10^{-5}$ (*2*) to $4.8 \times 10^{-6}$ $s^{-1}$ (*1*) have been reported. By comparison the rate constants for exchange of hydrated copper(II) and iron(III) ions are $2 \times 10^{8}$ $s^{-1}$ and $2.5 \times 10^{2}$ $s^{-1}$ (*2*). Chromium(III) was chosen as the oxidation state for extraction because of its stability compared to chromium(II). Acetylacetone, thenoyltrifluoroacetone, hydroxyquinoline, diethyldithiocarbamate, and 1-phenyl-3-methyl-4-benzoylpyrazolone have previously been used to extract

[1] Present address, Agrico Chemical Co., South Pierce Chemical Works, Bartow, Fla. 33830.

0003-2700/78/0350-0488$01.00/0 © 1978 American Chemical Society

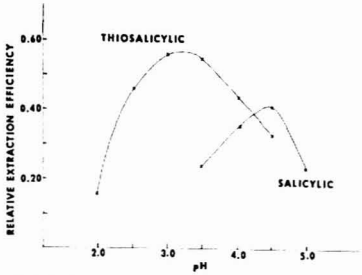


**Figure 1.** Relative extraction efficiency of chromium(III) by salicylic and thiosalicylic acids in the presence of an acetate buffer

chromium at elevated temperatures (3-6). Extraction of chromium with neither salicylic, thiosalicylic, nor phthalic acids has been thoroughly studied. Salicylic acid has, however, been used in the extraction of trivalent ions such as aluminum(III) and iron(III) (7).

## EXPERIMENTAL

The solvent extraction studies were performed using equal volumes of aqueous and organic solvents. The organic solvent selected was 1-butanol. Complexing agents were dissolved in the 1-butanol to provide concentrations of 0.15 M for salicylic and thiosalicylic acids and 0.10 M for phthalic acid. A mixed complexing agent solution that was 0.15 M in thiosalicylic acid and 0.10 M in phthalic acid was also used.

The pH's of the extraction solutions were controlled by use of acetate or phthalate buffer systems. The pH of buffer-free systems was adjusted using dilute HCl or NaOH as appropriate. The pH range investigated was from 2.0 to 5.0.

The organic solvent and aqueous sample were refluxed for 20–60 min prior to separation. Sodium chloride was added to the extraction system to determine the effect of salting-out agents on the efficiency of extraction processes.

After separation, the organic layer was analyzed to determine the percent extraction of chromium from the aqueous layer. For selected extractions, aliquots of both the organic and aqueous layer were analyzed for chromium to permit calculation of the distribution ratios. Solutions to be analyzed for chromium were prepared by a wet digestion procedure. Samples were initially digested with dilute nitric acid until all readily oxidizable material had been destroyed. Sample digestion was completed using a mixture of nitric, perchloric, and sulfuric acids.

Chromium was determined using a Perkin-Elmer model 303 atomic absorption spectrophotometer. The spectrophotometer was equipped with a premix burner chamber and digital signal averaging unit. A fuel rich air–acetylene flame was used to inhibit the formation of refractory oxides of chromium. From these data, percent extractions and distribution ratios were determined.

## RESULTS AND DISCUSSION

The relative extraction efficiencies of salicylic, thiosalicylic, and phthalic acids in the presence of different pH values and buffer systems are discussed below.

Figure 1 presents the relative extraction efficiencies of salicylic and thiosalicylic acid in the presence of a sodium acetate–acetic acid buffer system. The optimum pH for the extraction of chromium(III) with salicylic acid is 4.5 and for thiosalicylic acid is between 3.0 and 3.5. The efficiency of the extraction initially increases with increasing pH. This change is due to the higher degree of ionization of the complexing acid. After passing through a maximum, the efficiency beings to decrease. This results from the formation of nonextractable complexes that compete effectively with the complexing agent for the chromium. The pH at which the maximum occurs is dependent on the dissociation constants of the complexing acid and the formation constants of all of the complexes. The competing complex could be either a hydroxide complex or an acetate complex. The optimum extraction efficiency achieved using thiosalicylic acid in the presence of acetate buffer was 40% greater than for salicylic acid.

**Table I. Effect of Heating Time on Extraction Efficiency[a] (mixed phthalic acid-thiosalicylic acid extraction)**

| Duration of heating, min | Extraction, % |
|---|---|
| 20 | 90.4 |
| 25 | 93.8 |
| 30 | 96.5 |
| 35 | 97.6 |
| 60 | 97.4 |

[a] Extraction conditions where pH = 3.0 and 7.6 g NaCl/25 mL of aqueous solution.

**Table II. Distribution Ratios and % Extraction (mixed phthalic acid-thiosalicylic acid extraction)**

| Extraction condition[a] | $D$ | % $E$ from $D$ | % $E$ from recovery |
|---|---|---|---|
| 20-min heating, pH 3.5 | 8.12 | 88.9 | 86.3 |
| 20-min heating, pH 3.0 | 13.8 | 93.1 | 90.5 |
| 60-min heating, pH 3.0 | 19.1 | 95.1 | 97.4 |

[a] 6.5 g NaCl/25 mL aqueous solution.

Since acetate is known to form a competitive nonextractable complex with chromium(III) (8), the extraction efficiency of chromium by thiosalicylic acid in the absence of buffer was determined. The pH of the solution to be extracted was adjusted to the desired value prior to introduction of the organic solvent-complexing agent solution. The extraction efficiency vs. pH is shown in Figure 2. The pH of the solution decreases after introduction of the complexing agent because of dissociation of the agent. The extraction efficiency achieved was greater at high pH values than was achieved in the presence of acetate. This indicates that the acetate competes effectively with the thiosalicylic acid for the chromium at pH values where a large fraction of the acetate is in the ionized form. The extraction efficiency at higher pH values is ultimately limited by the formation of hydroxide complexes.

The effect of adding sodium chloride as a salting-out agent in combination with thiosalicylic acid as a complexing agent is also presented in Figure 2. The maximum extraction efficiency was increased by 20% and occurred at a lower pH where the formation of insoluble hydroxides is less troublesome. The salt concentration was 0.2 g/mL aqueous solution.

Control of pH by use of a potassium hydrogen phthalate–phthalic acid buffer system was studied as an alternative to the acetate buffer system. Phthalic acid itself is a complexing agent and was found to give extraction efficiencies in the presence of a salting-out agent similar to those obtained by use of thiosalicylic acid. When phthalic acid and thiosalicylic acid were used as the complexing agents in combination with a potassium hydrogen phthalate buffer, the highest extraction efficiencies for chromium were obtained. Addition of NaCl further increased the extraction efficiency as shown in Figure 3. The pH range of optimum extraction efficiency was 3.0–4.0.

The effect of heating time for the refluxing process on the extraction efficiency was determined. Table I indicates that the extraction efficiency was not increased by heating times exceeding 35 min. Distribution ratios and percent extractions for selected extraction conditions are presented in Table II.

Mole ratio plots for thiosalicylic and phthalic acid indicates that two moles of ligand combine with one mole of chromium.

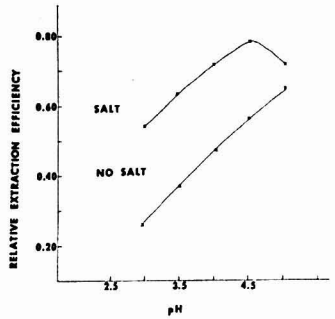


**Figure 2.** Relative extraction efficiency of chromium(III) by thiosalicylic acid from an unbuffered solution in the presence and absence of a salting-out agent

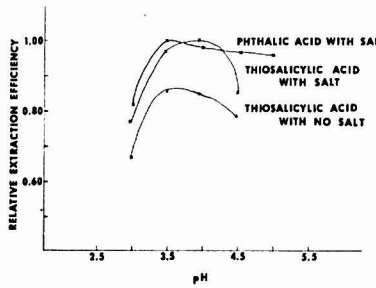


**Figure 3.** Relative extraction efficiency of chromium(III) by thiosalicylic and phthalic acids from a phthalate buffered solution

This agrees with the finding of Aggett for salicylic acid as the complexing agent (7).

A plot of the absorbance of a series of solutions of constant concentration of chromium and phthalic acid and variable concentrations of thiosalicylic acid is shown in Figure 4. The absorbance increased linearly with increasing concentration of the thiosalicylic acid. This indicates that a mixture of complexes is present in the system. If phthalic acid was not being replaced by thiosalicylic acid, the absorbance would remain constant at concentrations of thiosalicylic acid greater than 1:1 mole ratio which corresponds to complexation of all chromium. If phthalic acid was quantitatively replaced by thiosalicylic acid at the stoichiometric concentration of thiosalicylic acid, the absorbance would be constant at

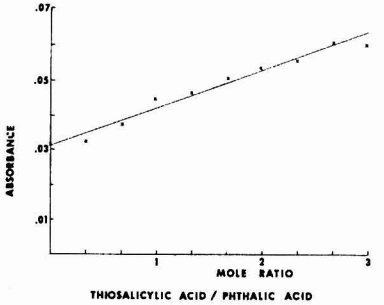


**Figure 4.** Mole ratio plot for a constant concentration of phthalic acid and chromium (1:1 mole ratio) and a variable concentration of thiosalicylic acid

concentrations of thiosalicylic acid greater than a 2:1 mole ratio of thiosalicylic acid to chromium. Since the absorbance continues to increase at mole ratios of thiosalicylic acid to chromium of up to at least 3:1, a gradual replacement of phthalic acid by thiosalicylic acid is indicated. Thus it appears that the formation constants for the two complexes are of the same order of magnitude and the one which predominates is primarily dependent on the relative concentrations of the two ligands. The line through the data points is a least squares fit with the equation $y = 0.00344/x + 0.0316$.

An efficient new method of chromium extraction has been demonstrated. The extraction efficiency of a combination of phthalic and thiosalicylic acid yields extraction efficiencies in excess of 95% in conjunction with a potassium hydrogen phthalate buffer system and a salting-out agent. The optimum pH for extraction is 3.0. No further increase in extraction efficiency was seen with heating periods exceeding 35 min. Use of sodium chloride as a salting-out agent increased the extraction efficiency of all systems studied.

## LITERATURE CITED

(1) I. P. Hunt and H. Taube, *J. Chem. Phys.*, **19**, 602 (1951).
(2) R. E. Dickerson, H. B. Gray, and G. P. Haight, Jr., "Chemical Principles", 2nd ed., W. A. Benjamin, Melo Park, Calif. 1974, p 796.
(3) S. V. Froeger, A. S. Lozovik, and M. I. Ovrutskii, *J. Anal. Chem. U.S.S.R.*, **26**, 2133 (1971).
(4) E. E. Cary and O. E. Olson, *J. Assoc. Off. Anal. Chem.*, **58**, 433 (1975).
(5) S. S. Leitner and J. Savoy, *Anal. Chim. Acta*, **74**, 133 (1975).
(6) D. C. Hilderbrand and E. E. Pickett, *Anal. Chem.*, **47**, 424 (1975).
(7) J. Aggett, P. Crossley, and R. Haneork, *J. Inorg. Nucl. Chem.*, **31**, 3241 (1969).
(8) E. W. Berg, "Physical and Chemical Methods of Separation", McGraw-Hill, New York, N.Y., 1963, p 349.

RECEIVED for review August 8, 1977. Accepted December 19, 1977.

# Liquid Chromatographic Analysis of Pharmaceutical Syrups Using Pre-Columns and Salt-Adsorption on Amberlite XAD-2

**Hussain Y. Mohammed and Frederick F. Cantwell***

*Department of Chemistry, University of Alberta, Edmonton, Alberta, Canada T6G 2G2*

**Twenty-nine drug compounds are chromatographed in acidic, neutral, and alkaline solutions containing varying amounts of water and methanol on a column of Amberlite XAD-2 nonionic resin. Cationic conjugate acids of amine drugs are adsorbed via "salt-adsorption". Their retention volumes depend on concentration and type of anion (e.g. $Cl^-$, $ClO_4^-$) added to the mobile phase as well as on its pH and solvent composition. Pharmaceutical syrups can be analyzed without prior treatment when short pre-columns containing anion-exchange resin and XAD-2 are added. As examples, synthetic and commercial syrups are analyzed for phenylephrine hydrochloride, acetaminophen, glyceryl guaiacolate, and dextromethorphan hydrobromide.**

Pharmaceutical syrups are complex mixtures containing one to ten "active" drug ingredients along with up to several dozen "inert" components such as dyes, flavoring agents, sweeteners, preservatives, and buffers. For this reason, gas chromatography and high efficiency liquid chromatography have been popular for their analysis. Gas chromatographic assay methods require an initial liquid–liquid extraction of the drugs from the aqueous syrup to eliminate water (*1*) and sometimes to eliminate interfering inert ingredients (*2*). Furthermore, some polar amines like phenylephrine must be converted to less polar derivatives before gas chromatography (*3*). Using liquid chromatography, Sprieck (*4*) analyzed phenylpropanolamine, chlorpheniramine, pseudoephedrine, and pheniramine in syrups on a pellicular cation-exchange column by direct injection. The liquid chromatographic behavior of a number of drugs on nonpolar bonded phases has also been reported (*5, 6*) but syrup samples with their multitude of potentially interfering "inert" ingredients were not analyzed and amine drugs showed considerable tailing (*5*). Chromatography of syrup samples on a nonpolar bonded phase (octadecylsilyl) required preliminary liquid–liquid extraction (*7*) to eliminate interferents. When chromatographing amines on nonpolar bonded phases, the pH was adjusted to a value at which the nonionized free-base was the adsorbed species (*5–8*).

In another approach to syrup analysis, Doyle and Levine (*9, 10*) have popularized gravity-flow liquid–liquid partition chromatography employing ion-pair distribution of the salts of amine drugs with simple anions such as $Cl^-$, $Br^-$, and $NO_3^-$. Although the chromatographic column must be prepared fresh before each analysis, and it has a very low column efficiency, the approach of Doyle and Levine has remained popular.

High efficiency ion-pair partition chromatography of amines has been demonstrated using aqueous (*11–13*) and nonaqueous (*11*) stationary liquid phases supported on silica gel. Recently, octadecylsilyl bonded packings have been used as stationary phases for reverse-phase "ion pair" chromatography of cationic sample components using a large organic anion as the counterion (*14, 15*), and for anionic sample components using quaternary ammonium counterions (*15–18*). Horvath et al. (*19, 20*) have investigated the retention of charged species from aqueous solutions on octadecylsilyl phases and interpreted the results in terms of "solvophobic theory". None of these high efficiency techniques has been applied to the assay of syrups.

Amberlite XAD-2 is a rigid, nonionic, macroreticular copolymer of styrene and divinylbenzene which is stable at all pH in aqueous solution (*21*). It is capable of adsorbing both neutral and ionic chemical species from solution (*22, 23*) and has been shown to be suitable as a stationary phase for liquid chromatography of a variety of chemical classes (*24–27*). A previous study (*28*) has demonstrated the utility of this stationary phase in the chromatographic analysis of preservatives in pharmaceutical syrups. In that study a short pre-column was used to facilitate on-column clean-up, allowing direct injection of the syrup.

In the present study the chromatographic retention, on XAD-2, of 29 drugs which are common components of cough–cold preparations, has been investigated as a function of mobile phase composition. Both neutral and ionic conjugate species are retained, and retention volumes depend on percent methanol, pH, and nature and concentration of anion. The observed retention diagrams are used to predict appropriate mobile phase composition for a given analysis. When combined with short pre-columns of XAD-2 and anion-exchange resin, the resulting chromatographic system is used for the analysis of phenylephrine hydrochloride, acetaminophen, glyceryl guaiacolate, and dextromethorphan hydrobromide in commercial syrups.

## EXPERIMENTAL

**Apparatus.** Pump $P_1$, all valves, chromatographic columns, injectors, fittings, and Teflon tubing were of the "Cheminert" variety, obtained from Laboratory Data Control, Riviera Beach, Fla. The chromatograph used for the analysis of syrups is pictured in Figure 1. With valve $V_3$ (Model R6031 SVP) in the position shown, pump $P_1$ (Model CMP-2VK) pumped Solvent 1 through the sample injection valve, $V_1$ (Model CSV), the pre-column, $C_1$, and the analytical column, $C_3$. Simultaneously, pump $P_2$, which was based on the design of Fritz (*29*), pumped Solvent 2 to waste. When valve $V_3$ was switched (dashed lines) it allowed Solvent 1 to flow directly into the analytical column and diverted Solvent 2 through $C_1$. In the analysis of dextromethorphan hydrobromide, the injection valve was moved to $V_2$ instead of $V_1$ and an additional pre-column was added at $C_2$. The use of the chromatograph is described below. The UV detector was a Model 770 Spectroflow Monitor (Schoeffel Instrument Corp., Westwood, N.J.); the recorder, a Model SR (Sargent-Welch Co., Skokie, Ill.); and the electronic integrator, a Model CSI-38 (Columbia Scientific Industries, Austin, Texas). The glass analytical column $C_3$ was either 30 cm × 0.20 cm or 15 cm × 0.28 cm (Type MB) packed with 0.25 g of <325 mesh Amberlite XAD-2. Pre-column $C_1$ was 3 cm × 0.28 cm and $C_2$ was 2 cm × 0.28 cm. All columns were dry packed. Pre-column packings are described below. Experiments were performed at ambient temperature.

When measuring adjusted retention volumes, pump $P_2$ was connected directly to the 30 cm × 0.20 cm analytical column via a septum injector (Model 183A8), and 5 μL of sample solution containing 2.5–5.0 μg of a soluble drug salt was injected with a Pressure-Lok microsyringe (Precision Sampling, Baton Rouge, La.). Adjusted (Net) retention volumes were calculated as $V_N = V_R - V_M$. Here $V_R$ is the sample retention volume and $V_M$ is

0003-2700/78/0350-0491$01.00/0 © 1978 American Chemical Society

**Table I. Drug Composition of Blank Syrups[a]**

| Drug | mg/mL | Blank for phenylephrine·HCl and acetaminophen | Blank for glyceryl guaiacolate | Blank for dextromethorphan·HBr |
|---|---|---|---|---|
| Acetaminophen | 20.0 | A | + | + |
| Phenylephrine·HCl | 2.0 | A | + | + |
| Glyceryl guaiacolate | 20.0 | + | A | + |
| Dextromethorphan·HBr | 3.0 | + | + | A |
| Codeine phosphate | 2.4 | − | + | + |
| Methoxyphenamine maleate | 3.4 | − | + | + |
| Diphenhydramine·HCl | 2.0 | − | + | + |
| Diphenylpyraline·HCl | 0.4 | + | + | + |
| Ephedrine·HCl | 6.0 | + | + | + |
| Brompheniramine maleate | 0.8 | + | + | + |
| Chlorpheniramine maleate | 0.4 | + | + | + |
| Phenylpropanolamine·HCl | 4.0 | + | + | + |
| Pheniramine maleate | 1.5 | + | + | + |
| Pyrilamine maleate | 2.5 | + | + | + |
| Promathazine·HCl | 1.0 | + | + | + |
| Phenyltoloxamine citrate | 2.0 | + | + | −[b] |
| Methdilazine·HCl | 0.4 | + | + | + |

[a] A (+) indicates presence in blank syrup. An (A) indicates the analyte component, which is absent from the blank. A (−) indicates drugs omitted from blank. [b] Not found in combination with dextromethorphan·HBr in commercial syrups.

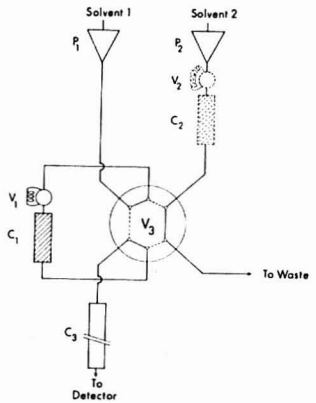


**Figure 1.** Diagram of the liquid chromatograph (description in text)

the retention volume of an unretained component (0.70 mL in this case). $V_N$ is readily found by injecting a small amount of water into a mobile phase containing a high percent methanol. Water is unretained and produces a peak as it elutes, due to a large change in refractive index.

**Resins, Chemicals, Solvents, and Syrups.** The preparation of <325 mesh Amberlite XAD-2 resin and 120–325 mesh Amberlyst A-26 strong base anion-exchange resin (Rohm and Haas Co., Philadelphia, Pa.) has been described (*28*). Water, methanol, dyes, flavors, and caramel coloring were as previously reported (*28*), and all drug substances were USP or equivalent grades. All the chemicals were reagent grade. Dextromethorphan hydrobromide was analyzed by Fajan's titration and by nonaqueous titration as 95.4%. Phenylephrine hydrochloride was analyzed by Fajan's titration as 100.0%. Glyceryl guaiacolate and acetaminophen were analyzed spectrophotometrically using USP and NF Reference Standards as 99.6% and 99.4%, respectively.

All methanol–water mobile phase solvents were prepared volumetrically by transferring measured volumes of water and aqueous reagent solutions into a volumetric flask and diluting to volume with methanol. Solvent composition is therefore reported as v/v percent water.

Mobile phases used to measure the dependence of $V_N$ on chloride and perchlorate concentration shown in Figure 4 were prepared to contain $1.0 \times 10^{-3}$ M HCl or $HClO_4$ plus a sufficient amount of added NaCl or $NaClO_4$ to yield the desired anion concentration, in 100% water (i.e., no methanol).

Commercial cough–cold syrups were purchased at a local pharmacy. The undiluted syrup was drawn into the sample injection valve and injected directly onto the pre-column.

**Blank and Spiked Blank Syrups.** In order to demonstrate the lack of interference by other likely active and inert syrup components, blank syrups were prepared to contain the drugs shown in Table I. Blank syrups also contained the dyes, excipients, flavors, and other ingredients listed in Table I of reference (*28*) along with 1 mg/mL of cinnemaldehyde. Quantitative recovery of the analyte component was demonstrated with a spiked blank syrup prepared by adding a known concentration of analyte compound to a portion of the appropriate blank syrup before injecting it.

## RESULTS AND DISCUSSION

**Retention of Drugs.** Twenty-nine different drugs were chromatographed on a 30 cm × 0.20 cm column of XAD-2 using acidic, neutral, and alkaline mobile phases, each containing various ratios of water and methanol. The chromatographic behavior is presented in Figure 2 as plots of log $V_N$ vs. percent water. (Tables of all of the data in Figure 2 are available directly from the authors upon request.) Adjusted retention volumes above about 17 mL are too long and those below about 0.1 mL are too short to measure accurately. In the 0.010 M ammonia mobile phases (Figure 2, A and B) compounds 1–24 are present as neutral species and are adsorbed on the resin as such. (See Table II for compound names and identifying numbers.) Many of the compounds exhibit a linear relationship, as has been observed before (*28*, *30*).

Compounds 25–29 possess a phenolic or carboxyl proton. They are ionized in ammonia solution and show greatly reduced retention volumes. Their retention behavior was studied in water–methanol mobile phase without added base (Figure 2E) as well as in 0.10 M HCl (Figure 2, compounds 25–27). Of this group of compounds, only phenylephrine (No. 27) possesses a basic functional group. Consequently, the neutral conjugate species for all but phenylephrine is the predominent species in both water and 0.10 M HCl and the plots of net retention volumes vs. percent water are similar

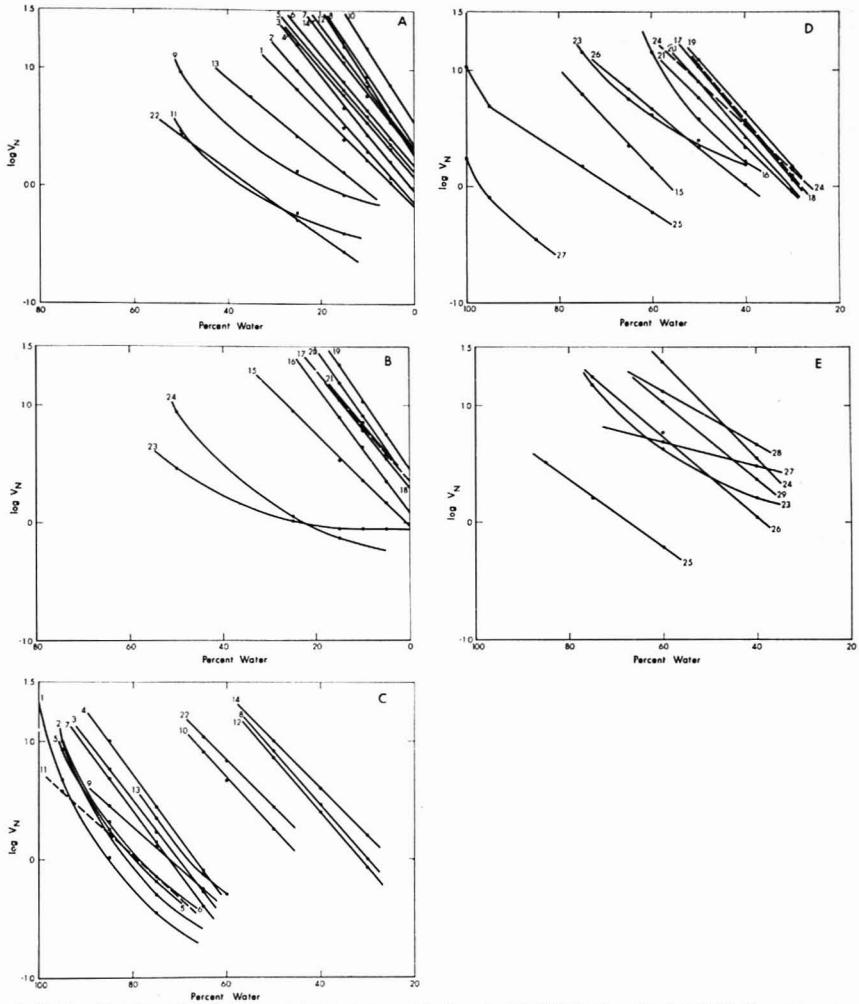


**Figure 2.** Relationship between log $V_N$ and percent water in the mobile phase for 0.010 M $NH_3$ (A and B), 0.10 M HCl (C and D), and with no added acid or base (E), on a 30 cm × 0.20 cm column of Amberlite XAD-2. Compounds identified in Table II

for these compounds in both acidic and neutral solvents.

Compounds 22–24 are not significantly ionized in 0.10 M HCl, water, or 0.01 M $NH_3$ and their retention behavior is similar in all three.

In 0.10 M HCl mobile phases (Figure 2, C and D) compounds 1–21 (except 14) and phenylephrine are cations. Of this group, compounds 1–8 are divalent cations and the remainder are univalent. These cationic species are adsorbed by Amberlite XAD-2. It is recognized that the adsorption of ionic species at the interface between a hydrophobic resin and a solution will likely differ mechanistically from their partitioning between two bulk liquid phases. For this reason the term "salt-adsorption" (*26*) will be used for the former. It is shown below, however, that there are similarities between the retention behavior of ions in both the adsorption and liquid–liquid ion-pair partition systems.

Compound 14, phenothiazine, is actually too weak a base to be protonated in 0.10 M HCl and its retention volume is the same in acidic mobile phases as in those containing 0.01 M $NH_3$. However, the compound is rapidly decomposed in an acidic solvent and the decomposition product elutes with a much shorter retention volume then phenothiazine. The curve for compound 14 in Figure 2C is that of its decomposition product.

For a given methanol–water composition, the retention volume of a monofunctional acid or base can be predicted as a function of pH from a knowledge of its ionization constant and the net retention volumes of its two conjugate species (*19*,

Table II. Names and Identifying Numbers of Drugs Studied

| | |
|---|---|
| 1. Pheniramine·(maleate) | 16. Diphenhydramine·(HCl) |
| 2. Doxylamine·(succinate) | 17. Diphenylpyraline·(HCl) |
| 3. Chlorpheniramine·(maleate) | 18. Dimethoxanate·(HCl) |
| 4. Brompheniramine·(maleate) | 19. Promethazine·(HCl) |
| 5. Methapyriline·(maleate) | 20. Phenyltoloxamine·(citrate) |
| 6. Tripelennamine·$(HCl)_2$ | 21. Dextromethorphan·(HBr) |
| 7. Pyrilamine·(maleate) | 22. Glyceryl guaiacolate |
| 8. Chlorcyclazine·$(HCl)_2$ | 23. Caffeine |
| 9. Ephedrine·(HCl) | 24. Phenacetin |
| 10. Methdilazine·(HCl) | 25. Acetaminophen |
| 11. Phenylpropanolamine·(HCl) | 26. Salicylamide |
| 12. Caramiphen·(ethanesulfonate) | 27. Phenylephrine·(HCl) |
| 13. Codeine·(phosphate) | 28. Salicylic acid |
| 14. Phenothiazine[a] | 29. Acetylsalicylic acid |
| 15. Methoxyphenamine·(HCl) | |

[a] See text for anomalous behavior of this compound.

*26, 31*). Likewise for difunctional bases (e.g., No. 1–8), retention volumes intermediate between those for the divalent cation and free-base are obtained with mobile phase pH's between those of 0.10 M HCl and 0.010 M $NH_3$.

**Predicting Separation Conditions.** The plots in Figure 2 may be used to select the column length and mobile phase composition required to separate any two syrup components $i$ and $j$, where $j$ has a larger retention volume than $i$. The following symbols are defined:

$V_{N,i}$, $V_{N,j}$ = adjusted retention volumes in mL for $i$ and $j = V_{R,i} - V_M$, $V_{R,j} - V_M$

$k_i'$, $k_j'$ = capacity factors for $i$ and $j = \frac{V_{N,i}}{V_M}, \frac{V_{N,j}}{V_M}$ (1)

$W_i$, $W_j$ = band width of eluted peaks $i$ and $j$ in mL

$H$ = height equivalent to a theoretical plate in cm

$L$ = column length in cm

$N$ = number of theoretical plates in the column = $\frac{L}{H} = 16\left(\frac{V_{R,j}}{W_j}\right)^2$ (2)

$\alpha_{j/i}$ = separation factor for $j$ and $i = \frac{V_{N,j}}{V_{N,i}}$ (3)

$R_S$ = resolution between $i$ and $j \equiv \frac{2(V_{N,j} - V_{N,i})}{W_j + W_i} \approx \frac{\sqrt{N}}{4}\left(\frac{\alpha_{j/i} - 1}{\alpha_{j/i}}\right)\left(\frac{k_j'}{1 + k_j'}\right)$ (4)

Equation 2 implies that the plate height, $H$, is independent of the sample component whose peak is used to calculate $N$, which is only approximately true. Also the right hand form of Equation 4 assumes that the retention volumes for peaks $i$ and $j$ are not too different, so that their widths may be considered approximately equal (*32*).

Figure 2 and Equations 1–4 are used as follows. If columns are packed with resin in a reproducible manner, then the column void volume, $V_M$, and the retention volume, $V_R$, are both directly proportional to the amount of packing in the column, and the values in Figure 2 can be adjusted to apply to any column size. Thus, for a given column, one first selects a mobile phase composition from Figure 2 to give the desired $k_j'$ Since $N$ is known for the column then Equation 4 can be used to predict the minimum $\alpha_{j/i}$ required to achieve the desired resolution. An example will illustrate the approach: The 15 cm × 0.28 cm column used for syrup analyses exhibited plate heights ($H$) between 0.1 and 0.2 cm for a variety of methanol–water compositions, at linear velocities between 0.14 and 0.4 cm/s (0.5 and 1.0 mL/min). Thus $N \approx 100$ plates for this column. In order to separate dextromethorphan (No. 21) from promethazine (No. 19) with a resolution $R_S = 1.0$ (i.e., about 2% mutual overlap of similar size peaks), one would proceed by first selecting a mobile phase that will elute the more strongly retained promethazine with $k_j'$ between 2 and 10. Using Equation 1 and the measured value of $V_M = 0.70$ mL, it is evident that $V_{N,j}$ should be about 3.5 mL ($\log V_{N,j} = 0.54$) in order to have $k_j' = 5$. Either 0.010 M $NH_3$ in 2% water or 0.10 M HCl in 38% water would be satisfactory. (At intermediate mobile phase pH's, intermediate methanol–water compositions are appropriate.) From Equation 4 the value of $\alpha_{j/i}$ necessary to produce $R_S = 1.0$ is 1.9 ($\log \alpha_{j/i} = 0.28$). This corresponds in Figure 2 to a vertical distance between the lines for compounds 19 and 21 of 0.28. The observed distance in the ammoniacal solvent is 0.12 and in the acidic solvent it is 0.28. Hence $R_S = 1$ separation can be achieved in this case by salt-adsorption chromatography but not by chromatography of the free bases. Since $R_S$ is proportional to $\sqrt{N}$ it would require a 34-cm column to achieve $R_S = 1.0$ with the ammoniacal mobile phase.

**Chromatography of Inert Ingredients.** The azosulfonate dyes used to color syrups are adsorbed on XAD-2 and alter the retention volumes of amine drugs (*28*). They are readily removed from the injected syrup and prevented from reaching the XAD-2 adsorbent by placing a short pre-column of Amberlyst A-26 macroreticular anion-exchange resin immediately downstream from the sample injection valve. After 30 syrup injections, a 1-cm length of the ion exchanger showed no sign of dye breakthrough. Any UV absorbing components in the common syrup ingredients sucrose, sorbitol, and caramel coloring elute nearly unretained from the XAD-2 column and present no interference in the analyses. Adjusted retention volumes of the preservatives methyl and propyl *p*-hydroxybenzoate, of the flavor components vanillin, benzaldehyde and cinnemaldehyde, and of their decomposition products benzoic acid, vanillic acid, *p*-hydroxybenzoic acid, and cinnamic acid can be estimated for any XAD-2 column with an acidic mobile phase from Figure 2 in Ref. 28 by multiplying the net retention volume from that figure by the ratio of the weight of resin in the two columns. Maleic acid, from maleate salts of the drugs, has $k' \approx 1$ in a 100% water acidic mobile phase and is nearly unretained when the methanol content is increased. In an alkaline mobile phase, all of these compounds except benzaldehyde and cinnemaldehyde exist as anions and are trapped on the anion-exchange resin along with the azosulfonate dyes.

**Analysis of Syrups.** Application of the data in Figure 2 to the analysis of real syrups will be illustrated by three examples: determination of phenylephrine hydrochloride and acetaminophen; determination of glyceryl guaiacolate; and determination of dextromethorphan hydrobromide. In these analyses, the analytical column, $C_3$, was 15 cm × 0.28 cm. In each case blank syrup chromatograms showed straight baselines in the region of interest. Quantitation was based on comparison with standard curves obtained by injecting aqueous solutions of the analyte drug. Both peak height and peak area measurements yielded linear calibration curves and similar syrup assay values. Relative standard deviations for replicate injections were about 1.4% for area measurements and 1.6% for height measurements. Assay values reported in Table III are the average of both height and area values. The three spiked blank syrups and eight commercial syrups,

**Table III. Results of Syrup Analyses**

| Product | Found mg/mL (Label claim mg/mL) Phenylephrine·HCl | Acetaminophen | Glyceryl guaiacolate | Dextromethorphan·HBr | Other drugs present |
|---|---|---|---|---|---|
| Spiked blank[a] | 1.10 (1.10) | 20.4 (20.3) | 10.6 (10.6) | 2.49 (2.50) | Table I |
| A | ... | ... | 10.1 (10.0) | 1.91 (2.00) | Phenylpropanolamine·HCl |
| B | 0.46 (0.50) | 21.7 (21.6) | 10.1 (10.0) | 1.48 (1.50) | ... |
| C | 2.04 (2.00) | ... | ... | ... | Diphenylpyraline·HCl |
| D | 0.92 (1.00) | ... | 19.8 (20.0) | ... | Phenylpropanolamine·HCl<br>Brompheniramine maleate |
| E | ... | 16.4 (16.0) | ... | ... | Triprolidine·HCl<br>Pseudoephedrine·HCl |
| F | ... | ... | 20.1 (20.0) | 2.89 (3.00) | Phenylpropanolamine·HCl<br>Pheniramine maleate<br>Pyrilamine maleate |
| G | ... | ... | ... | 2.80 (3.00) | Diphenhydramine·HCl |
| H | 0.4, (1.00)[b] | ... | ... | 0.94 (1.00) | Carbinoxamine maleate |

[a] Amount in parentheses in this row is amount added to spiked blank. [b] Peak height data only.

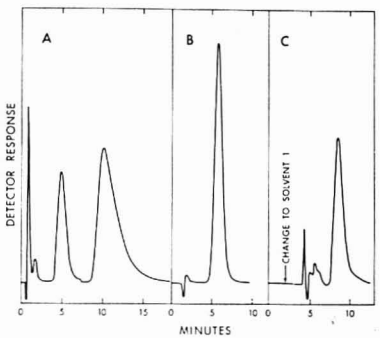


**Figure 3.** Typical syrup chromatograms of phenylephrine·HCl (AUFS = 0.1, λ = 275 nm) and acetaminophen (AUFS = 1.0, λ = 275 nm) (A); glyceryl guaiacolate (AUFS = 1.0, λ = 275 nm) (B); and dextromethorphan·HBr (AUFS = 0.4, λ = 280 nm) (C), on a 15-cm column

each containing two or more of the four drug compounds of interest, were analyzed. Assay values are compared with the known amounts added to spiked blanks and with label claims of commercial syrups, in Table III. Typical chromatograms of syrups are shown in Figure 3.

**Phenylephrine and Acetaminophen.** Using 0.10 M HCl in 100% water these two compounds are well resolved from one another ($\Delta \log V_N = 0.8$). Of the 27 other drugs investigated, all are well resolved from phenylephrine and only ephedrine and phenylpropanolamine might interfere with acetaminophen. At 275 nm, however, both of these potential interferents have sufficiently low molar absorptivities that they do not interfere with the acetaminophen peak. In 0.10 M HCl, the resolution between phenylephrine and acetaminophen is actually too large so that when acetaminophen elutes with $k' \approx 12$ phenylephrine has $k' \approx 2$ and overlaps components such as maleic acid which are nearly unretained. Since phenylephrine is retained via "salt-adsorption", while acetaminophen is adsorbed as a neutral species, it is possible to selectively increase the retention volume of the former by an increase in anion concentration (*31*). Figure 4 shows the effect of chloride concentration on $V_N$ of both compounds. The relatively small increase in $V_N$ for acetaminophen above 0.1 M $Cl^-$ is a "salting-out" effect (*33, 34*). An increase in chloride concentration evidently does not sufficiently reduce $\alpha_{j/i}$ for acetaminophen and phenylephrine. Changing to a perchlorate-containing mobile phase, however, results in a much

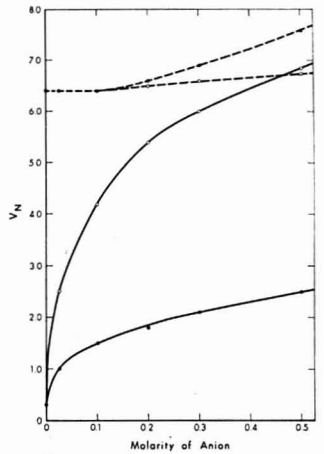


**Figure 4.** Dependence of $V_N$ for acetaminophen (---) and phenylephrine (—) on concentration of chloride (●) and perchlorate (○) on a 15 cm × 0.28 cm column of Amberlite XAD-2

larger $V_N$ for phenylephrine and a nearly unchanged $V_N$ for acetaminophen.

There are similarities between the retention behavior of cations (exemplified by phenylephrine) in this system and in a liquid–liquid ion-pair partition system (*11*). First, the marked increase in $V_N$ with anion concentration, though nonlinear in the former system, is common to both. Second, the effectiveness of the anion in promoting adsorption of the organic cation improves in the order $Cl^- < ClO_4^-$. (Experiments with other organic cations and a wider range of anions show the order $Cl^- < Br^- < ClO_4^- <$ *d*-camphorsulfonate). However, since the adsorption of ion-pairs has not yet been proved as a major retention mechanism on XAD-2, we employ the less specific term "salt-adsorption".

For this determination the liquid chromatograph shown in Figure 1 had no valve $V_2$ or column $C_2$ and employed 0.030 M $HClO_4$ in 100% water as Solvent 1 and 0.030 M $HClO_4$ in 5% water as Solvent 2. The upper one-third of pre-column $C_1$ contained anion-exchange resin and the lower two-thirds contained XAD-2. With Solvent 1 pumping through $P_1$, $C_1$, and $C_3$, a 10-μL sample was injected. After 6.0 min, when phenylephrine and acetaminophen had quantitatively eluted

from $C_1$ onto $C_3$, but before the other drugs, preservatives or flavor ingredients had eluted from $C_1$, valve $V_3$ was switched, and Solvent 2 washed all of these components from $C_1$ to waste, while Solvent 1 continued to pass through the analytical column. After the elution of acetaminophen, $V_3$, was switched back and another injection made after a 3-min equilibration period. If the syrup contains drugs which elute right after acetaminophen (e.g., No 1) then some fraction of them may be transferred onto column $C_3$ along with acetaminophen. These are washed off by the "slug" of Solvent 2 from $C_1$ which passes through $C_3$ when valve $V_3$ is switched back.

The phenylephrine-HCl content of Syrup "H" is well below label claim and the phenylephrine chromatographic peak for this sample is overlapped by another peak with a longer retention time. A similar peak appears in chromatograms of aerated alkaline solutions of phenylephrine-HCl that have been stored at elevated temperature and is accompanied by a decrease in the phenylephrine peak. This presumed decomposition product can be resolved from phenylephrine on a 30-cm column of XAD-2 using a mobile phase 0.010 M $HClO_4$ plus 0.10 M $NaClO_4$.

**Glyceryl Guaiacolate.** In an alkaline mobile phase, glyceryl guaiacolate is well resolved from all 28 other drugs studied except caffeine and phenylpropanolamine (Figure 2, A and B). The former is not present in commercial syrups along with glyceryl guaiacolate and the latter has such a low molar absorptivity at 275 nm that it shows negligible absorbance at the detector sensitivity employed. The chromatograph for this determination was identical to that used for phenylephrine and acetaminophen except that Solvent 1 was 0.010 M NaOH in 50% water, Solvent 2 was 0.010 M NaOH in 5% water, and column $C_1$ contained 2.0 cm of anion-exchange resin followed by 1.0 cm of XAD-2.

With Solvent 1 flowing through $P_1$, $C_1$ and $C_3$, a 2-$\mu$L syrup sample was injected. After 2.5 min, the glyceryl guaiacolate had all been eluted from column $C_1$ onto $C_3$ and valve $V_3$ was then switched to allow Solvent 2 to wash off the syrup components that were retained on $C_1$. With Solvent 1 as mobile phase, all of the preservatives, flavor ingredients, and their decomposition products except benzaldehyde and cinnemaldehyde were trapped on the anion-exchange resin, while the latter two compounds were retained on the XAD-2 resin in Column $C_1$, along with the other drug components, and subsequently washed off to waste by Solvent 2.

**Dextromethorphan Hydrobromide.** This compound is the major nonnarcotic cough suppressant used in syrups. With 0.10 M HCl in 35% water as mobile phase, the only unresolved drugs, of those which are found in combination with dextromethorphan, are diphenhydramine hydrochloride and diphenylpyraline hydrochloride. At 280 nm both of these compounds are too weak absorbers to interfere with dextromethorphan. The chromatograph for this determination had no $V_1$. Pre-column $C_1$ contained 3 cm of XAD-2 while pre-column $C_2$ contained 2 cm of anion-exchange resin. Solvent 1 was 0.10 M HCl in 35% water and Solvent 2 was 0.010 M NaOH in 35% water. Before injecting the sample, valve $V_3$ was set to allow Solvent 2 to pump through $V_2$, $C_2$, and $C_1$ to waste, while Solvent 1 passed through the analytical column only. When a 10-$\mu$L sample was injected, the components which are anions in an alkaline solution were trapped on the anion-exchange resin, while dextromethorphan was adsorbed on pre-column $C_1$. Weakly retained compounds, like the drugs glyceryl guaiacolate and codeine and the flavor components benzaldehyde and cinnemaldehyde, elute from $C_1$ to waste during this time. After 2.5 min, $V_3$ was switched to allow Solvent 1 to pass through pre-column $C_1$ eluting dextromethorphan through both $C_1$ and $C_3$. Compounds such as methdilazine and promethazine, which are adsorbed onto $C_1$ from an alkaline solvent, elute from $C_3$ either before or after dextromethorphan. After a total of 12 min, valve $V_3$ is switched back to its original position and the next injection is made after a short equilibration period.

## CONCLUSIONS

Retention volumes of drugs on columns of Amberlite XAD-2 can be controlled by variation of mobile phase pH, solvent composition, counterion type, and counterion concentration. The moderate efficiency ($H \approx 1$–$2$ mm), compatability with solvents of all pH, long column life, and low cost of such columns make them an attractive alternative to low efficiency liquid–liquid partition systems (*9*, *10*) for many applications. When combined with suitable pre-columns, the use of this resin eliminates the need for syrup clean-up prior to injection. Finally, it is obvious from the principles outlined in the Discussion and from the data in Figure 2 that separation factors for many drug pairs are large enough that quantitative separation can be achieved on very short columns with low pressures or gravity flow (*28*).

## ACKNOWLEDGMENT

Samples of drugs, dyes, and flavors were kindly provided by Lester Chatten of the College of Pharmacy, University of Alberta, and by C. F. Hiskey of Endo Laboratories, Inc.

## LITERATURE CITED

(1) F. L. Fricke, *J. Assoc. Off. Anal. Chem.*, **55**, 1162 (1972).
(2) E. Mario and L. G. Meehen, *J. Pharm. Sci.*, **59**, 539 (1970).
(3) J. R. Watson and R. C. Lawrence, *J. Pharm. Sci.*, **66**, 560 (1977).
(4) T. Sprieck, *J. Pharm. Sci.*, **63**, 591 (1974).
(5) I. L. Honigberg, J. T. Stewart, and A. P. Smith, *J. Pharm. Sci.*, **63**, 767 (1974).
(6) P. J. Twitchett and A. C. Moffat, *J. Chromatogr.*, **111**, 149 (1975).
(7) A. Menyharth, F. P. Mahn, and J. E. Heveran, *J. Pharm. Sci.*, **63**, 430 (1974).
(8) "Analysis of Pharmaceutical Products", Technical Bulletin, Waters Associates, Inc., Milford, Mass., 1976.
(9) T. D. Doyle and J. Levine, *Anal. Chem.*, **39**, 1282 (1967).
(10) T. D. Doyle and J. Levine, *J. Assoc. Off. Anal. Chem.*, **51**, 191 (1968).
(11) S. Eksborg, P.-O. Lagerström, R. Modin, and G. Schill, *J. Chromatogr.*, **83**, 99 (1973).
(12) S. Eksborg and G. Schill, *Anal. Chem.*, **45**, 2092 (1973).
(13) B.-A. Persson and B. L. Karger, *J. Chromatogr. Sci.*, **12**, 521 (1974).
(14) E. Fitzgerald, *Anal. Chem.*, **48**, 1734 (1976).
(15) "Paired-Ion Chromatography", Technical Bulletin, Waters Associates, Inc., Milford, Mass., 1976.
(16) D. P. Wittmer, N. O. Nuessle, and W. G. Haney, Jr., *Anal. Chem.*, **47**, 1422 (1975).
(17) S. P. Sood, L. E. Sartori, D. P. Wittmer, and W. G. Haney, *Anal. Chem.*, **48**, 796 (1976).
(18) J. Korpi, D. P. Wittmer, B. J. Sandmann, and W. G. Haney, Jr., *J. Pharm. Sci.*, **65**, 1087 (1976).
(19) C. Horvath, W. Melander, and I. Molnár, *Anal. Chem.*, **49**, 142 (1977).
(20) I. Molnár and C. Horvath, *Clin. Chem. (Winston-Salem, N.C.)*, **22**, 1497 (1976).
(21) "Amberlite XAD-2", Technical Bulletin, Rohm and Haas Co., Philadephia, Pa., 1972.
(22) R. L. Gustafson, R. L. Albright, J. Heisler, J. A. Lirio, and O. T. Reid, Jr., *Ind. Eng. Chem., Prod. Res. Dev.*, **7**, 107 (1968).
(23) J. Paleos, *J. Colloid Interface Sci.*, **31**, 7 (1969).
(24) M. W. Scoggins and J. W. Miller, *Anal. Chem.*, **40**, 1155 (1968).
(25) L. L. Zaika, *J. Chromatogr.*, **49**, 222 (1970).
(26) D. J. Pietrzyk and C.-H. Chu, *Anal. Chem.*, **49**, 757 (1977).
(27) D. J. Pietrzyk and C.-H. Chu, *Anal. Chem.*, **49**, 860 (1977).
(28) F. F. Cantwell, *Anal. Chem.*, **48**, 1854 (1976).
(29) J. S. Fritz and R. B. Willis, *J. Chromatogr.*, **79**, 107 (1973).
(30) K. Fuzita, *Nippon Kagaku Kaishi*, **1975** (5), 846.
(31) S. Puon and F. F. Cantwell, *Anal. Chem.*, **49**, 1256 (1977).
(32) B. L. Karger, L. R. Snyder, and C. Horvath, "An Introduction to Separation Science", Wiley-Interscience, Toronto, 1973.
(33) M. D. Grieser and D. J. Pietrzyk, *Anal. Chem.*, **45**, 1348 (1973).
(34) F. A. Long and W. F. McDevitt, *Chem. Rev.*, **51**, 119 (1952).
(35) R. G. Baum and F. F. Cantwell, *Anal. Chem.*, **50**, 280 (1978).

RECEIVED for review August 23, 1977. Accepted November 21, 1977. This work was supported by the National Research Council of Canada and the University of Alberta.

# Effect of Solute Ionization on Chromatographic Retention on Porous Polystyrene Copolymers

**Donald J. Pietrzyk,* Eugene P. Kroeff, and Terry D. Rotsch**

*Chemistry Department, The University of Iowa, Iowa City, Iowa 52242*

**The effect of solute ionization on the chromatographic retention of weak monoprotic and diprotic acids and bases and ampholytes on Amberlite XAD-2 was investigated. This stationary phase, which is a polystyrene–divinylbenzene copolymer, is particularly suited to these kinds of studies because of its stability throughout the entire pH range. Equations relating the capacity factor to pH, in which all equilibria are accounted for, were described for each type of ionogenic substance. Each equation was experimentally verified. For monoprotic and diprotic acids and bases, retention is high as the neutral form and low as the dissociated form. The greatest change in retention for the diprotic acids and bases occurs during the formation of the singly charged species. For ampholytes, the retention as a function of pH passes through either a minimum or a maximum.**

Several years ago we had shown that the retention of weak monoprotic acids (*1*) and bases (2) on the nonpolar adsorbent Amberlite XAD-2 (a polystyrene–divinylbenzene copolymer) could be quantitatively described by considering the effects of solute ionization. These equations were also shown to hold for XAD-4 (a polystyrene–divinylbenzene copolymer with a larger surface area and smaller pore size than XAD-2) and for XAD-7 (a cross-linked acrylic ester copolymer). Although the initial equations were expressed in terms of batch distribution coefficients as a function of hydrogen ion concentration, these same equations are readily expressed in capacity factors or retention times or volumes (*3–5*) since these parameters are directly related to the batch distribution coefficient. Recently, the effect of solute ionization on the retention of the solute on the nonpolar bonded phase, octadecylsilica (ODS), was considered (*6*). Equations describing retention of monoprotic acids and bases, diprotic acids, and diprotic ampholytes were considered.

This paper emphasizes two main points. First, it is shown that the XAD copolymers are useful stationary phase models for studying the effect of solute ionization on chromatographic retention. The XAD copolymers are stable throughout the entire pH range, unlike ODS which is stable only in the pH range of 2–8, and thus, retention of monoprotic and polyprotic acids and bases and ampholytes can be studied. Second, the equations describing retention of the acids, bases, and ampholytes are shown experimentally to be valid. Because of the pH limitation of ODS, experimental verification is limited to acids, bases, and ampholytes having ionization constants within certain limits.

## EXPERIMENTAL

The chromatographic equipment used and procedures for cleaning and sizing of XAD copolymers and conditioning of columns have been described previously (*2–5*). The column used to collect the data reported here was 25.0 cm × 0.236 cm and contained 0.310 g of 45 to 65 μm XAD-2 except for valine which was studied on a XAD-4 column. Experiments were repeated with new solutions and samples using a second column of similar dimensions and also with a longer column. Buffers were 0.01 M and were prepared with analytical grade phosphate salts, NaOH, and HCl. Ionic strength was maintained at 0.1 M by adding appropriate amounts of KCl to the buffer solution. All mixed solvents were prepared as percent by volume.

## RESULTS AND DISCUSSION

Retention of a weak monoprotic organic acid on XAD-2 (*1–5*) and on ODS (*6*) will be large in acid solution where the weak acid is undissociated and low in basic solution where the weak acid is dissociated. The equation relating capacity factor to pH is given by

$$k' = \frac{k_0}{1 + \frac{K_a}{[H^+]}} + \frac{k_{-1}}{1 + \frac{[H^+]}{K_a}} \quad (1)$$

where $k_0$ and $k_{-1}$ are the capacity factors for the undissociated and dissociated form of the weak acid and $K_a$ is its ionization constant. The reverse, or high retention in basic solution and low retention in acidic solution, is found for weak organic monoprotic bases (*2–4, 6*) where retention is given by

$$k' = \frac{k_1}{1 + \frac{[OH^-]}{K_b}} + \frac{k_0}{\frac{K_b}{[OH^-]} + 1} \quad (2)$$

and $k_1$ and $k_0$ are the capacity factors for the dissociated and undissociated form of the weak base and $K_b$ is its ionization constant. Equation 2 can also be derived in terms of the conjugate acid $HB^+$, $K_a$, and $H^+$ (*2–6*).

**Weak Acids.** Verifying Equation 1 with the ODS support is limited since this support will decompose in strongly acidic and basic solutions. In many cases, more acidic and more basic conditions than provided by this pH range are required to experimentally determine $k_0$ and $k_{-1}$ values. Consequently, only organic acids in the $pK_a$ range of 2.8 to 4.4 were studied on ODS and shown to follow Equation 1 (*6*). Alternatively, the $K_a$ values can be calculated from Equation 1 by experimentally determining the capacity factors as a function of pH (*1, 2, 6*).

The XAD copolymer does not suffer from the pH limitation and can be used over the entire pH range. Thus, Equation 1 can be tested with several different weak acids. For example, Equation 1 was shown to describe the retention of chlorinated and nitrated phenols ($pK_a$ 0.71 to 9.98) (*1*), phenoxyacetic acid derivatives ($pK_a \simeq 2.8$) (*3, 4*), and benzoic acid derivatives ($pK_a$ = 2.1 to 4.6) (*1, 3, 4*) as a function of pH by experimentally determining $k_0$ and $k_{-1}$, generating a plot of $k'$ vs. pH with Equation 1, and then experimentally determining $k$ values at intermediate pH values for comparison (*1, 3, 4*).

**Weak Bases.** Equation 2 which describes the effect of ionization of weak organic bases on their retention was not tested with the ODS column (*6*). However, there is no reason to expect that it would not predict the chromatographic retention of weak organic bases on this column. As with the weak acids, the pH limitation of ODS permits its use only in examining organic bases that are in the $pK_b$ range of ap-

0003-2700/78/0350-0497$01.00/0 © 1978 American Chemical Society

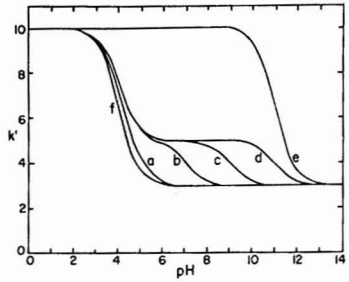


**Figure 1.** Plots of the capacity factors for diprotic acids vs pH calculated by Equation 3 using the variables

| Curve | $k_0$ | $k_{-1}$ | $k_{-2}$ | $pK_{a_1}$ | $pK_{a_2}$ |
|---|---|---|---|---|---|
| a | 10 | 5 | 3 | 4 | 5 |
| b | 10 | 5 | 3 | 4 | 7 |
| c | 10 | 5 | 3 | 4 | 9 |
| d | 10 | 5 | 3 | 4 | 11 |
| e | 10 | 10 | 3 | 4 | 11 |
| f | 10 | 3 | 3 | 4 | 11 |

proximately 6 to 10. For stronger or weaker bases, the determination of $k_0$ and $k_1$ requires a stronger basic and acidic condition then can be tolerated by ODS.

The XAD-2 copolymer with its pH stability was shown to follow Equation 2 by comparing experimental $k'$ data to calculated $k'$ data (*3*). Aniline and pyridine derivatives covering a $pK_b$ range of 4 to 11 were studied.

In general, the buffered solutions used to evaluate Equations 1 and 2 with XAD-2 contained 10% alcohol (*1–4*). Reasonable agreement was obtained at higher alcohol concentrations even though aqueous $K_a$ and $K_b$ values were used. Good agreement was also obtained for XAD-4 and XAD-7; however, the latter copolymer was not studied as extensively as the XAD-2 and -4.

**Diprotic Acids.** A second ionization step, such as provided by a diprotic acid can be accounted for (*6*). Thus, it can be shown that

$$k' = \frac{k_{-1} + k_0\frac{[H^+]}{K_{a_1}} + k_{-2}\frac{K_{a_2}}{[H^+]}}{1 + \frac{[H^+]}{K_{a_1}} + \frac{K_{a_2}}{[H^+]}} \qquad (3)$$

where $k_0$, $k_{-1}$, and $k_{-2}$ are the capacity factors for the undissociated, half-dissociated, and fully dissociated diprotic acid, respectively, and $K_{a_1}$ and $K_{a_2}$ are the two ionization constants. (Equation 3 has been arranged into a different algebraic form than that provided elsewhere (*6*).)

Since ODS is limited in its useful pH range, testing Equation 3 is limited to acids within a specific $K_a$ range. Good agreement between Equation 3 and $k'$ data was found for *o*-phthalic acid ($pK_{a_1}$ = 2.95 and $pK_{a_2}$ = 5.41) (*6*). For weaker acids, the base conditions required to convert the acid into the dissociated form would decompose the ODS column.

Figure 1 illustrates how $k'$ for a diprotic acid changes with pH according to Equation 3. The parameters are arbitrarily chosen to illustrate the factors which determine the shape of the $k'$–pH curve.

As $K_{a_2}$ approaches $K_{a_1}$ for a diprotic acid, the $k'$–pH curve tends to fuse into a single break with its $^1/_2$-break position approaching a pH equal to $^1/_2(pK_{a_1} + pK_{a_2})$. This is illustrated in curves a to d in Figure 1, where it is assumed that the capacity factor for the intermediate species, $k_{-1}$ in Equation 3, is significantly different than $k_0$ and $k_{-2}$.

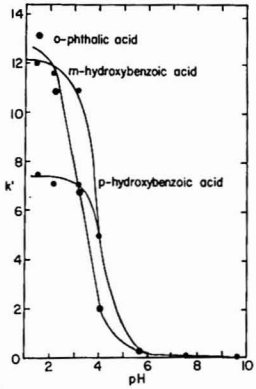


**Figure 2.** Capacity factors for several diprotic acids as a function of pH with $k_0$, $k_{-1}$, and $k_{-2}$ calculated by Equation 3 using a nonlinear least squares fit. $K_{a_1}$, $K_{a_2}$, $k_0$, $k_{-1}$, and $k_{-2}$ are given, respectively, for *o*-phthalic acid: $1.29 \times 10^{-3}$, $3.09 \times 10^{-6}$, 13.3, 1.9, 0; for *m*-hydroxybenzoic acid: $8.70 \times 10^{-5}$, $1.20 \times 10^{-10}$, 11.8, 0, 0; and for *p*-hydroxybenzoic acid: $3.31 \times 10^{-5}$, $4.78 \times 10^{-10}$, 7.3, 0, 0. A 45 to 65 μm, 0.31 g, 25 × 0.236 cm XAD-2 column at a flow rate of 0.94 mL/min, $V_0$ = 0.89 mL was used with phosphate buffers at 0.01 M concentration made to ionic strength 0.1 M with NaCl in 4% $CH_3CN$–96% water

If the retention is largely affected by the concentration of the singly charged species formed in the first ionization step; that is $k_{-1} \rightarrow k_{-2}$, then a single break in the $k'$–pH curve is approached. This is shown in Figure 1 as curve f for the extreme case where $k_{-1} = k_{-2}$. In contrast, if the retention is affected only by the doubly charged species that is formed in the second ionization step, the single break in the $k'$–pH curve that is approached is shown as curve e in Figure 1 for the extreme case where $k_0 = k_{-1}$. In the first case the $^1/_2$-break corresponds to the pH where $pk_{a_1}$ = pH and in the second where $pk_{a_2}$ = pH.

Figure 2 illustrates experimental data for several diprotic acids on XAD-2. Small amounts of $CH_3CN$ were used to reduce the $k'$ values since in aqueous acidic solutions retention times are very large. Although the ionization constants for the hydroxybenzoic acids are sufficiently different, a stepwise $k'$–pH curve is not obtained. The $k'$–pH curve indicates that the capacity factor, $k_{-1}$, for the intermediate singly charged species approaches the $k_{-2}$ value and that the $^1/_2$-break pH value corresponds closely to the $pK_{a_1}$. Hence, the major change in retention is the result of conversion of the undissociated acid to the singly charged species and further dissociation has little effect on the retention.

*o*-Phthalic acid, which is a stronger diprotic acid that has closely related dissociation constants, undergoes a major change in retention during the first ionization step. However, the data in Figure 2 also indicate that retention of the singly charged species occurs. Similar results were reported for the retention of *o*-phthalic acid on ODS (*6*). Although not reported here, $k'$ data for 3-nitro- and 4-nitro-*o*-phthalic acid were collected as a function of pH and were found to follow Equation 3. In strong acid solution, where retention of the neutral form occurs, the order of retention is *o*-phthalic > 4-nitro- > 3-nitro-.

The $k'$ values for *o*-phthalic acid are larger on XAD-2 (Figure 2) in comparison to ODS (*6*). For example, in aqueous solutions, $k'$ values greater than 30 were observed on XAD-2 while the maximum $k'$ on ODS was reported to be 6 (*6*).

The values for $k_0$, $k_{-1}$, and $k_{-2}$ cited in Figure 2 were calculated from the experimental data from Equation 3 using a nonlinear least squares fit of the data and were used to calculate the solid line. Alternatively, the limits of the experimental $k'$ data can be used as values for $k_0$ (strong acid) and $k_{-2}$ (strong base). These values and a $k'$ at an intermediate pH are used to calculate $k_{-1}$. From these data and the $K_a$ values, the entire $k'$–pH curve can be calculated by Equation 3 and compared to other experimentral $k'$ data.

**Diprotic Bases.** For a diprotic base, B, the ionization steps are

$$B + H_2O \rightleftharpoons HB^+ + OH^-$$

$$HB^+ + H_2O \rightleftharpoons H_2B^{+2} + OH^-$$

and are described by the equilibrium constants

$$K_{b_1} = \frac{[HB^+][OH^-]}{[B]}$$

$$K_{b_2} = \frac{[H_2B^{2+}][OH^-]}{[HB^+]}$$

If $k_0$, $k_1$, and $k_2$ are the capacity factors for the retention of the neutral, half-dissociated, and fully dissociated species, respectively, it can be shown using procedures outlined elsewhere (*1–6*) that

$$k' = \frac{k_1 + k_0\frac{[OH^-]}{K_{b_1}} + k_2\frac{K_{b_2}}{[OH^-]}}{1 + \frac{[OH^-]}{K_{b_1}} + \frac{K_{b_2}}{[OH^-]}} \quad (4)$$

Equation 4 can be rewritten in $H^+$ concentration and $K_a$ values for the conjugate acid form of the base, B, by appropriate substitution or derived directly by considering ionization of the conjugate acid $H_2B^{2+}$. It should be noted that Equation 4 in terms of $H^+$ and $K_{a_1}$ and $K_{a_2}$ for the base, B, is not the same as Equation 3.

A discussion of the retention of diprotic bases on ODS and the XAD copolymers would follow that for diprotic acids, with the exception that a large $k'$ would be obtained in basic solution (conditions for sorption of the undissociated form) and a small one in acidic solution (conditions for sorption of the dissociated form). As with diprotic acids, the pH limitations of ODS prevent its use in evaluating Equation 4 except over a narrow $pK_{b_1}$ and $pK_{b_2}$ range. XAD-2, in contrast, can be used to test the validity of Equation 4 throughout the entire pH region.

The effect of pH and $K_b$ values on the chromatographic retention of diprotic bases according to Equation 4 is illustrated in Figure 3. As $K_{b_2}$ approaches $K_{b_1}$, assuming an intermediate value for $k_1$, a single break in the $k'$–pH curve is approached and is located at a $^1/_2$-break position where the pH = $pK_w - {}^1/_2(pK_{b_1} + pK_{b_2})$. This is shown in curves a to d in Figure 3. As $k_1 \rightarrow k_2$ or the case where the retention is determined by the formation of the singly charged species in the first ionization step, curve e in Figure 2 (the extreme case where $k_1 = k_2$) is approached. Its $^1/_2$-break position corresponds to a pH where pH = $pK_w - pK_{b_1}$. For the case of $k_1 \rightarrow k_0$, or where retention is determined by the doubly charged species formed in the second ionizatin step, curve f in Figure 2 (the extreme case where $k_0 = k_1$) is approached. Its $^1/_2$-break position corresponds to a pH where pH = $pK_w - pK_{b_2}$.

Previously, it was shown that formation of the singly charged species in the first ionization step provided the most significant influence on reducing the retention of the diprotic bases 2-aminopyridine and 2-amino-4-methylpyridine on XAD-2 (*2*). Increasing the acidity in order to convert the base to the doubly charged species appeared to have little effect on its retention. However, the $K_{b_2}$ values for these two bases are very small and these diprotic bases are not ideal compounds to test Equation 4.

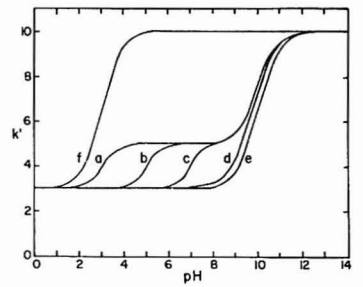


**Figure 3.** Plots of the capacity factors for diprotic bases vs. pH calculated by Equation 4 using the variables

| Curve | $k_0$ | $k_1$ | $k_2$ | $pK_{b_1}$ | $pK_{b_2}$ |
|---|---|---|---|---|---|
| a | 10 | 5 | 3 | 4 | 11 |
| b | 10 | 5 | 3 | 4 | 9 |
| c | 10 | 5 | 3 | 4 | 7 |
| d | 10 | 5 | 3 | 4 | 5 |
| e | 10 | 3 | 3 | 4 | 11 |
| f | 10 | 10 | 3 | 4 | 11 |

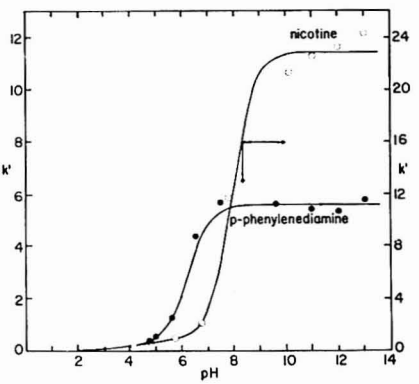


**Figure 4.** Capacity factors for several diprotic bases as a function of pH with $k_0$, $k_1$, and $k_2$ calculated by Equation 4 using a nonlinear least-squares fit. $K_{b_1}$, $K_{b_2}$, $k_0$, $k_1$, and $k_2$ are given, respectively, for *p*-phenylenediamine: $1.45 \times 10^{-8}$, $6.31 \times 10^{-12}$, 5.6, 0.12, 0; and for nicotine: $1.05 \times 10^{-6}$, $1.32 \times 10^{-11}$, 23.0, 1.05, 0. A 45 to 65 μm, 0.31 g, 25 × 0.236 cm XAD-2 column at a flow rate of 0.97 mL/min, $V_0$ = 0.83 mL was used with phosphate buffers at 0.01 M concentration made to ionic strength 0.1 M with NaCl in 4% $CH_3CN$–96% water (10% $CH_3CN$ for nicotine)

Figure 4 shows the experimentally determined $k'$ data for two different diprotic bases on XAD-2. Similar results were found for *m*-phenylenediamine. Acetonitrile was used in the eluting mixture for nicotine to avoid the large $k'$ value that would be found in basic solution if aqueous solutions were used.

A stepwise change in the $k'$–pH graph was not obtained indicating that the formation of the singly charged species in the first ionization step has the greatest effect on reducing the retention of the base. That is, $k_1 \rightarrow k_2$ in value. Also, the

$^1/_2$-break positions in the curves in Figure 4 are predictable as outlined previously.

The potential locations of charge differ for the bases studied in Figure 4. Nicotine contains a tertiary amine side group ($pK_{b_2}$) which is not in conjugation with the pyridine-N ($pK_{b_1}$) in the molecule. In contrast, both amine groups ($pK_{b_1}$ and $pK_{b_2}$) are directly joined to a benzene ring in the phenylenediamines. This difference in types of charge sites does not cause a deviation from Equation 4.

The values for $k_0$, $k_1$, and $k_2$ cited in Figure 4 were calculated by a nonlinear least squares fit of the data using Equation 4. Alternatively, the limits of the experimental data can be used as values for $k_2$ (strong acid) and $k_0$ (strong base). With an experimentally determined $k'$ at an intermediate pH, $k_1$ can be calculated. These data and the $K_b$ values are then used to calculate the entire curve which can be compared to all the experimental data. No attempts were made to test ODS because of its pH limitations.

**Polyprotic Acids and Bases.** Equations can be derived to describe retention of any polyprotic acid and base. Each ionization step must be considered and the resultant equation will be in terms of the capacity factor for the retention of each of the dissociated and undissociated forms, the $K_a$ values, and $H^+$ concentration. Experimental verification of these equations becomes more difficult as the number of ionization steps increases since a capacity factor must be determined not only for the undissociated form but also for each of the dissociated forms. Since it appears that the initial ionization step with the formation of the singly charged species has the greatest effect on reducing the retention of the neutral species, an independent measurement of capacity factors for additional charged species is not always possible.

The differences in the $K_a$ (or $K_b$) values for polyprotic systems are also significant factors. The closer they are numerically, the more difficult it is to achieve an experimental condition which ensures that the intermediate dissociated species are at a high concentration relative to the other species. Also, depending on the magnitude of the $K_a$ (or $K_b$) values, it may even be difficult to achieve an acidic and basic condition that ensures a complete conversion to the undissociated and dissociated forms of the weak acid (or base).

Based on present and past observations (*1–5*), it appears in general, that the chromatographic behavior of polyprotic acids and bases on nonpolar stationary phases can be predicted by considering only the first ionization step. For more fundamental studies, an exact expression accounting for all the equilibria can be derived.

**Ampholytes.** The chromatographic behavior of an ampholyte on a nonpolar stationary phase should not be the same as a typical diprotic system since the intermediate species will be electrostatically neutral. Two possibilities for the effect of pH on $k'$ can be predicted. Consider glycine as a typical ampholyte where the ionization steps are

$$\underset{H_2Gly^+}{H_3{}^+NCH_2CO_2H} + H_2O \overset{K_{a_1}}{\rightleftharpoons} \underset{HGly}{H_2NCH_2CO_2H} + \underset{H_3O^+}{} \quad (5)$$

$$\underset{HGly}{H_2NCH_2CO_2H} + H_2O \overset{K_{a_2}}{\rightleftharpoons} \underset{Gly^-}{H_2NCH_2CO_2^-} + \underset{H_3O^+}{} \quad (6)$$

In strong acid solution, glycine is present as $H_2Gly^+$ and its capacity factor on a nonpolar type phase should be small. Increasing the pH converts glycine into the form HGly which will exist in the zwitterion form, $H_3{}^+NCH_2CO_2^-$. Thus, the capacity factor should be even smaller since the solute species is now highly charged even though it is electrostatically neutral. If the HGly form were not to exist in a zwitterion form, the solute species would have no charge and the capacity factor should increase as the concentration of this neutral species increases. As the pH is made basic the anion form Gly is formed and the capacity factor should increase relative to the capacity factor for HGly if it exists as a zwitterion or decrease if it is not a zwitterion.

The ionization expressions for Equation 5 and 6 are given by

$$K_{a_1} = \frac{[H^+][HGly]}{[H_2Gly^+]} \quad (7)$$

$$K_{a_2} = \frac{[H^+][Gly^-]}{[HGly]} \quad (8)$$

Since the overall capacity factor is

$$k' = \theta \frac{[H_2Gly^+]_R + [HGly]_R + [Gly^-]_R}{[H_2Gly^+]_S + [HGly]_S + [Gly^-]_S} \quad (9)$$

where R and S are the resin and solution state, respectively, it can be shown (*1–6*) that chromatographic retention as a function of pH is given by

$$k' = \frac{k_0 + k_1\frac{[H^+]}{K_{a_1}} + k_{-1}\frac{K_{a_2}}{[H^+]}}{1 + \frac{[H^+]}{K_{a_1}} + \frac{K_{a_2}}{[H^+]}} \quad (10)$$

In this equation, which can be represented in several algebraic forms, $k_0$ is the capacity factor for the retention of the neutral form (HGly), $k_1$ for retention of the cationic form ($H_2Gly^+$), $k_{-1}$ for retention of the anionic form ($Gly^-$), and $K_{a_1}$ and $K_{a_2}$ are the ionization constants for the diprotic ampholyte.

An expression describing the retention of ampholytes on ODS as a function of pH was recently described (*6*) and differs from Equation 10, in that $K_{a_1}$ and $K_{a_2}$ values were apparently defined as hydrogen ion loss from the zwitterion state and as a hydrogen loss from the cationic form of the ampholyte, respectively. Substitution of literature $K_{a_1}$ and $K_{a_2}$ values as customarily defined (see Equations 5 to 8) into the equation derived in reference 6 will lead to incorrect results.

Figure 5 illustrates how the different capacity factors ($k_0$, $k_1$, $k_{-1}$) and ionization constants ($K_{a_1}$, $K_{a_2}$) will affect retention according to Equation 10. The ionization constants selected in Figure 5a are typical of the amino acids while the rest (curves b to d) were chosen to illustrate the effect of the $K_a$'s on the $k'$–pH graph, assuming that the intermediate species is a zwitterion and that its retention is low; that is, $k_0 < k_1$ and $k_{-1}$. According to Equation 10, a broad minimum in the vicinity of the isoelectric pH value is predicted assuming a small $k_0$ value. The range of this minimum can be correlated to a fraction plot whereby the fraction of the ampholyte in solution as the neutral form is plotted as a function of pH. Where the fraction of the neutral form is large in concentration (the isoelectric pH), the retention is at a minimum. As the difference in $K_{a_1}$ and $K_{a_2}$ decreases, assuming zwitterion formation, the broadness of the minimum decreases. This is shown in Figure 5b to 5d.

If zwitterion formation for the intermediate species does not occur, then a maximum in $k'$ would be expected and Equation 10 would still apply. This is shown as Figure 5e. Although not shown, it is readily concluded that decreasing the difference in $K_{a_1}$ and $K_{a_2}$ will reduce the broadness of the maximum. This also correlates to the fraction plot but, in this case, the maximum in the $k'$–pH plot is at some pH range at which the fraction plot is at a maximum. It should be noted

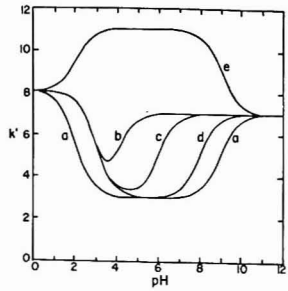


**Figure 5.** Plots of the capacity factors for ampholytes vs. pH calculated by Equation 10 using the variables

| Curve | $k_0$ | $k_1$ | $k_{-1}$ | $pK_{a_1}$ | $pK_{a_2}$ |
|---|---|---|---|---|---|
| a | 3 | 8 | 7 | 2 | 9 |
| b | 3 | 8 | 7 | 3 | 4 |
| c | 3 | 8 | 7 | 3 | 6 |
| d | 3 | 8 | 7 | 3 | 8 |
| e | 11 | 8 | 7 | 2 | 9 |

that the theoretical curves shown in Figure 5 do not agree with those previously shown (*6*) because of the differences in selecting the parameters.

The pH limitations of ODS prevent its being used to test Equation 10 with ampholytes, such as amino acids, because of their widely different $K_{a_1}$ and $K_{a_2}$ values. The XAD polymers, not having this limitation, can be used to test Equation 10. Figure 6 contains a plot of experimentally determined $k'$ data for valine (Val) as a function of pH using a XAD-4 column. The values for $k_1$, $k_0$, and $k_{-1}$ were calculated by a nonlinear least squares fit of the data using Equation 14 and were used to calculate the solid line. Alternatively, the $k'$ values at the isoelectric pH ($k_0$), in strong acid solution ($k_1$), and in strong base solution ($k_{-1}$) can be used to verify Equation 10 by calculating the $k'$–pH curve and comparing it to the remaining experimentally determined $k'$ data.

A minimum corresponding to the isoelectric pH is observed. Thus, retention for valine is high in acidic solutions (pH $\lesssim$ 3) where $H_2Val^+$ is present, low at intermediate pH values (pH $\lesssim$ 3 to 8) where the zwitterion $^+HVal^-$ is present, and then high again (pH > 9) where Val is the principal species. Details of additional examples and a discussion of other factors, such as an additional ionization step, on the retention of amino acids and peptides on the XAD copolymers will be described elsewhere (*7*).

It was possible to study the retention of anthranilic acid as a typical ampholyte on ODS because its $K_{a_1}$ and $K_{a_2}$ are within the stable pH region of an ODS column (*6*). A maximum was found suggesting that the intermediate form does not exist appreciably in the zwitterion form. Thus, retention is low in acid solution where the $H_2A^+$ species is present (pH $\lesssim$ 2.2), high at intermediate pH's (pH $\simeq$ 2.2 to 5.3) where the HA species is present, and low (pH $\gtrsim$ 5.3) where the $A^-$ species is present.

This same result was found on XAD-2 and these data are shown in Figure 6. A small amount of $CH_3CN$ was used in the eluting mixture in order to reduce the magnitude of the $k'$ values which are much larger than that found on ODS.

**Limitations.** In calculating the capacity factor values from the experimental $k'$–pH data by a nonlinear squares fit, it was assumed that the ionization constants were precisely known for the ionic strength conditions used in the chromatographic experiment. This is not always the case and the error in the $K_a$ or $K_b$ values can be significant. For example, the literature

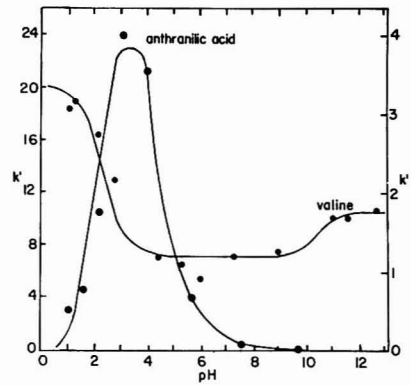


**Figure 6.** Capacity factors for two ampholytes as a function of pH with $k_1$, $k_0$, and $k_{-1}$ calculated by Equation 10 using a nonlinear squares fit. $K_{a_1}$, $K_{a_2}$, $k_1$, $k_0$, and $k_{-1}$ are given, respectively, for anthranilic acid: $8.13 \times 10^{-3}$, $1.62 \times 10^{-5}$, 0, 25.3, 0.49; and for valine: $4.47 \times 10^{-3}$, $1.35 \times 10^{-10}$, 3.38, 1.20, 1.75. Column conditions for anthranilic acid are listed in Figure 2. For valine, a 45 to 65 μm, 0.46 g, 30 × 0.236 cm XAD-4 column at flow rate of 0.50 mL/min, with detection at 208 nm, $V_0$ = 0.83 mL was used with phosphate buffers at 0.02 M concentration made to ionic strength 0.2 M with NaCl in 100% water

values reported for the $pK_{b_1}$ and $pK_{b_2}$ for *p*-phenylenediamine range from 7.66 to 7.92 and 10.89 to 11.33, respectively (*8*).

The errors introduced by the uncertainty in the $K_a$ or $K_b$ values have their greatest effect in the calculation of the capacity factor for retention of the intermediate species for the diprotic acids and bases and for the neutral form of the ampholytes. Although these errors are present, the examples studied here clearly demonstrate that Equations 3, 4, and 10 accurately describe how solute ionization affects chromatographic retention. Furthermore, they demonstrate that a significant change in the retention of polyprotic acids and bases, at least for the XAD copolymers, occurs during the formation of the singly charged species during the first ionization step. For the ampholytes the major effect is more complex because of the retention of the intermediate form.

## CONCLUSION

The effect of solute ionization on chromatographic retention of these solutes as discussed here and elsewhere (*1–6*) is not limited to the bonded phase ODS and the nonpolar adsorbent XAD copolymer but, in fact, should apply to many other types of stationary phases providing the stationary phase does not itself participate in an acid–base interaction with the solute. If the latter does occur, as for example with ion exchangers, formulism describing the retention can still be derived. These equations must include consideration of the effect of the exchange site on the reaction (*9, 10*).

From a theoretical standpoint, the XAD copolymers appear to be more suitable for evaluating the effects of pH on retention of widely different organic acids and bases since these copolymers do not decompose in strong acid or base as does the ODS stationary phase. Although the XAD copolymers can be used for analytical separations, their chromatographic efficiencies are much less than that provided by the microparticulate ODS stationary phase, and the latter stationary phase would be preferred in many applications. However, where strong acidic (pH < 2) or basic (pH > 8) solutions are required for optimum elution, the XAD copolymers would have the advantage. What remains to be quantitatively established is whether the data obtained over wide pH

conditions on the XAD copolymers, can be used to predict retention behavior in the limited useful pH range of the ODS or other similar bonded phases.


## ACKNOWLEDGMENT

We thank Kenneth Sando for advice and help in developing and carrying out the computer operations.


## LITERATURE CITED


(1) M. D. Grieser and D. J. Pietrzyk, *Anal. Chem.*, **45**, 1348 (1973).
(2) C. H. Chu and D. J. Pietrzyk, *Anal. Chem.*, **46**, 330 (1974).
(3) D. J. Pietrzyk and C. H. Chu, *Anal. Chem.*, **49**, 757 (1977).
(4) D. J. Pietrzyk and C. H. Chu, *Anal. Chem.*, **49**, 860 (1977).
(5) H. Takahagi and S. Seno, *J. Chromatogr.*, **108**, 354 (1975).
(6) C. Horvath, W. Melandar, and I. Molnar, *Anal. Chem.*, **49**, 142 (1977).
(7) E. P. Kroeff and D. J. Pietrzyk, *Anal. Chem.*, following paper in this issue.
(8) D. D. Perrin, "Dissociation Constants of Organic Bases in Aqueous Solutions", Butterworth and Co., London, England, 1965; A. Albert and E. P. Serjeant, "Ionization Constants of Acids and Bases", Methuen and Co., London, England, 1962.
(9) F. E. Cantwell and D. J. Pietrzyk, *Anal. Chem.*, **46**, 344 (1974).
(10) F. E. Cantwell and D. J. Pietrzyk, *Anal. Chem.*, **46**, 1450 (1974).



RECEIVED for review August 31, 1977. Accepted December 22, 1977. Part of this work was presented at the 12th Midwest Regional ACS Meeting, Kansas City, Mo., 1976, and part at the Pittsburgh Conference of Analytical Chemistry and Applied Spectroscopy, Cleveland, Ohio, 1977. This investigation was supported by Grant Number CA 18555, awarded by the National Cancer Institute, DHEW.


# Investigation of the Retention and Separation of Amino Acids, Peptides, and Derivatives on Porous Copolymers by High Performance Liquid Chromatography


**Eugene P. Kroeff and Donald J. Pietrzyk***

*Chemistry Department, The University of Iowa, Iowa City, Iowa 52242*



**Conditions are described for the separation of amino acids, derivatives, and peptides by high performance liquid chromatography on Amberlite XAD-2, -4, and -7 copolymers which act as reversed stationary phases. Retention changes in the order XAD-7 ≥ XAD-4 > XAD-2 while resolution changes in the order XAD-4 > XAD-7 ≥ XAD-2. Water, water–ethanol, or water–acetonitrile mixtures with or without pH control are potential eluting conditions. As the organic solvent concentration increases, retention decreases. In acid and base solution, retention is high while at the isoelectric pH, retention is low. The effect of amino acid and peptide structure and of peptide chain length on chromatographic retention is evaluated. DNP, dansyl, and PTH amino acid derivatives were studied. An equation which describes capacity factor as a function of pH and accounts for all the equilibria that influence the retention was verified for amino acids and peptides. Several separations which are predicted from these data are listed.**


Reversed phase liquid chromatography employing a bonded phase is perhaps one of the most used and versatile techniques in high performance liquid chromatography (HPLC). Bonded phases have the advantage of good reproducibility, high efficiency, and often require only aqueous-alcohol or -acetonitrile eluting mixtures. Their main disadvantage is that they can be used only over a narrow pH range of about 2 to 8.

The separation and subsequent determination or purification of amino acids, small and large molecular weight peptides, and other biologically significant compounds are important analytical procedures. Usually, thin-layer and ion-exchange chromatographic techniques have been used (*1*).

Recently, reversed phase packings have been used for these separations. For example, several aromatic amino acids were separated on an ODS column (*2–5*) and on a bonded optically active tripeptide stationary phase (*6*). The effects of pH, salt, and solvent on the retention of five nonapeptides on several reversed bonded phases were studied (*7*). The optimum conditions for their HPLC determination in pharmaceutical dosage forms were developed and these results were compared to those obtained by bioassay (*8*). Phenyl-corasil, Poragel PN, and Poragel PS were used to investigate di- to decapeptide retention (*9*). Several amino acid and peptide derivatives were studied on bonded phases (*1, 5, 9*) and related adsorbents (*10*).

In our laboratory, studies were initiated several years ago to investigate the chromatographic properties of the nonpolar, porous Amberlite XAD-2 (a polystyrene–divinylbenzene copolymer) and related adsorbents which function as reversed phase adsorbents. Organic acids (*11–13*), bases (*14*), and nonionic compounds, such as steroids and hydrocarbons (*12*), were separated by HPLC on these stationary phases using aqueous-alcohol and acetonitrile solutions. Although the bonded phases are more efficient than the XAD copolymers, these latter supports have the advantage of being stable throughout the entire pH range and have larger loading capacities (*14, 15*).

A detailed study of the ionization equilibria, which influence the chromatographic retention of organic acids (*11–13*) and bases (*11*) on the XAD copolymers, was reported. Recently, this was extended to diprotic acids (*15, 16*) and bases (*13, 15*) and to amphoteric compounds (*15, 16*).

The chromatographic retention of amino acids, small chain peptides, and amino acid derivatives on XAD-2 and related adsorbents is described in this report. With these data, it is possible to predict separations, to discuss the influence of amino acid structure and elution conditions on the retention of the amino acids, and to establish quantitatively the equilibria that influence the retention.

## EXPERIMENTAL

**Reagents.** Amino acids, amino acid derivatives, and peptides were obtained from Aldrich Chemical Company, Eastman Kodak Chemical, Fischer Scientific, Matheson Coleman and Bell, and Sigma Chemical Company, and were used as obtained. Absolute ethanol and pesticide quality acetonitrile was used in the preparation of mixed solvents. Inorganic salts, acids, and bases were of analytical reagent grade.

Amberlite XAD-2, -4, and -7 were purchased from Rohm and Haas or Mallinckrodt Chemical Works. The preparation of these

0003-2700/78/0350-0502$01.00/0 © 1978 American Chemical Society

Table I. Capacity Factors for Nonpolar and Aromatic Type Amino Acids on XAD-2, -4, and -7 as a Function of Ethanol–Water Composition

| | Capacity factor, $k'$ | | | | | | | | | |
|---|---|---|---|---|---|---|---|---|---|---|
| | XAD-2[a] % Ethanol | | | XAD-4[b] % Ethanol | | | XAD-7[c] % Ethanol | | | |
| Amino acid | 0 | 5 | 10 | 0 | 5 | 10 | 0 | 5 | 10 | 15 |
| Glycine, Gly | 0.30 | 0.29 | 0.30 | 0.75 | 0.72 | 0.69 | 1.29 | 1.15 | 1.09 | 1.04 |
| DL-Alanine, Ala | 0.31 | 0.29 | 0.30 | 0.79 | 0.72 | 0.67 | 1.13 | 1.12 | 1.08 | 1.01 |
| DL-Valine, Val | 0.47 | 0.39 | 0.40 | 1.42 | 0.94 | 0.91 | 1.38 | 1.31 | 1.15 | 1.10 |
| DL-Isoleucine, Ile | 0.96 | 0.65 | 0.58 | 3.11 | 1.61 | 1.43 | | | | |
| DL-Leucine, Leu | 1.08 | 0.71 | 0.63 | 3.79 | 1.82 | 1.55 | 1.73 | 1.67 | 1.43 | 1.24 |
| DL-Tyrosine, Tyr[d] | 1.38 | 0.89 | 0.76 | | | 2.00 | 4.07 | 3.23 | 2.48 | 1.81 |

[a] 45 to 54 μm, 0.72 g, 45 × 0.236 cm XAD-2 column at a flow rate of 0.50 mL/min, $V_0$ = 1.30 mL. [b] 45 to 65 μm, 0.46 g, 30 × 0.236 cm XAD-4 column at a flow rate of 0.50 mL/min, $V_0$ = 0.83 mL. [c] 45 to 65 μm, 0.39 g, 45 × 0.236 cm XAD-7 column at a flow rate of 0.50 mL/min, $V_0$ = 1.10 mL. [d] Data for other aromatic amino acids are provided in ref 13.

copolymers for column experiments has been previously described (*11–15*).

**Procedures.** Stainless steel tubing (0.236 cm i.d.) and fritted end fittings were purchased from Waters Associates. Columns were 30 and 45 cm and were dry packed with 45 to 65 μm (250 to 325 mesh) particles of the desired copolymer. Column preparation and conditioning procedures have been discussed earlier (*11–15*).

A Waters Liquid Chromatograph, Model-202 equipped with an M-6000 pump, 254-nm UV detector with 8-μL flow cell, and a U6K sample injector fitted with a 2-mL sample loop, was used. A modular system, comprised of an Altex M-100 pump, Rheodyne 905-19 injector system (with 175-μL sample loop), and a Tracor 970 variable wavelength detector fitted with an 8-μL Teflon flow cell was also employed. Gradients were generated with a Tracor Model 920 solvent programmer.

Sample solutions were prepared by dissolving 0.5 to 7.0 mg of the desired compound per 1 mL of water or water–ethanol mixture. Samples were stored in 6-mL Hypovials fitted with Hycar Septa and sealed with aluminum caps (Pierce Chemical). Pressure Lok Series B-110 10-μL or 25-μL syringes (Precision Sampling Corporation) were used to inject 3 to 10 μL of a sample into the chromatographic system.

Flow rates were 0.4 to 2.0 mL/min for the various experiments and inlet pressures were 250 to 1500 psig, depending upon the flow rate and the composition of the eluting solvent. Aromatic amino acids were detected at 254 nm, while nonaromatic amino acids were monitored at 208 nm.

Water–organic solvent mixtures are expressed as percent by volume. Phosphate salt buffer systems, and dilute solutions of HCl and NaOH were used to control the pH of the eluting agent. A constant ionic strength was maintained by adding NaCl to the buffer solutions. All pH values were determined with a pH meter. Capacity factors were calculated by

$$k' = \frac{V_R - V_0}{V_0}$$

where $V_R$ is the elution volume for the chromatographic peak and $V_0$ is the column void volume.

## RESULTS AND DISCUSSION

Amino acids (AA) will ionize according to

$$\underset{\text{H}_2\text{AA}^+}{\overset{\text{R}}{\overset{|}{\text{H}_3^+\text{NCHCO}_2\text{H}}}} + \text{H}_2\text{O} \overset{K_{a_1}}{\rightleftharpoons} \text{H}_3\overset{+}{\text{O}} + \underset{\text{HAA}}{\overset{\text{R}}{\overset{|}{\text{H}_2\text{NCHCO}_2\text{H}}}} \quad (1)$$

$$\underset{\text{HAA}}{\overset{\text{R}}{\overset{|}{\text{H}_2\text{NCHCO}_2\text{H}}}} + \text{H}_2\text{O} \overset{K_{a_2}}{\rightleftharpoons} \text{H}_3\overset{+}{\text{O}} + \underset{\text{AA}^-}{\overset{\text{R}}{\overset{|}{\text{H}_2\text{NCHCO}_2^-}}} \quad (2)$$

and these ionization steps have a strong influence on their chromatographic behavior. The structure of the R group will also influence the chromatographic behavior by providing a hydrophobic center rather than having a strong influence on the $K_{a_1}$ and $K_{a_2}$ values (these values are similar for the different amino acids). In reversed phase chromatography, both factors will influence the interaction between the AA and the solid nonpolar stationary phase since pH changes will alter the charge sites while a change in R will affect the hydrophobic sites.

**Effect of Support.** Table I lists capacity factor data for several amino acids on three different Amberlite supports. XAD-2 and XAD-4 are polystyrene–divinylbenzene copolymers and differ in that the surface area is larger and the pore size smaller for the XAD-4 (*11–15*). Both act as nonpolar stationary phases (*11–15*). The fact that retention (see Table I) is larger on XAD-4 is consistent with these properties.

XAD-7, which is also porous, is a cross-linked acrylic ester type copolymer which exhibits characteristics of an intermediate polar stationary phase. The tendency for larger $k'$ values on the XAD-7 is consistent with the more polar character of this support (see Table I).

In comparing the three XAD supports in Table I, the order of retention of the AA on the supports is XAD-7 ≥ XAD-4 > XAD-2. However, the capacity factors for the different AA cover a larger range on XAD-4. Thus, the order of resolution would be XAD-4 > XAD-7 ≥ XAD-2.

Although Table I considers only a few AA using water and water–alcohol eluting mixtures, these same conclusions would be drawn when considering other AA and derivatives (see Table II) and the effect of pH in the eluting mixture (see Table III).

**Amino Acid Structural Effects.** The AA in Table I can be divided into two groups according to the magnitude of the $k'$ values. The lower values were found for those AA that do not contain aromatic or conjugated groups in the R portion of the AA molecule; while those that do, have the higher $k'$ values. Within each group, the order of selectivity is consistent with what might be predicted based on the influence of the R group on the interaction. For example, the $k'$ decreases in the order Leu > Ile > Val > Ala > Gly which is also the order of a decrease in the hydrophobic nature of R, that is, $(CH_3)_2CHCH_2- > CH_3CH_2CH(CH_3) > (CH_3)_3CH- > CH_3- > H$. The polar –OH group in Tyr causes its $k'$ to be smaller than that for Phe while the double ring system of Trp causes its $k'$ to be larger than Phe.

Polar changes in the R group will affect the chromatographic behavior of the AA. This is illustrated in the data in Table II where $k'$ data for other naturally occurring AA are listed as a function of EtOH–water concentration. These AA were investigated only on XAD-4 and XAD-7 since the re-

Table II. Capacity Factors for Polar Amino Acids on XAD-2, -4, and -7 as a Function of Ethanol–Water Composition

| | Capacity factor, $k'$ | | | | | | |
|---|---|---|---|---|---|---|---|
| | XAD-4[a] % Ethanol | | | XAD-7[b] % Ethanol | | | |
| Amino acid | 0 | 5 | 10 | 0 | 5 | 10 | 15 |
| DL-Aspartic acid, Asp | 0.51 | 0.48 | 0.36 | 0.54 | 0.55 | 0.53 | 0.51 |
| DL-Serine, Ser | 0.76 | 0.69 | 0.70 | 1.40 | 1.21 | 1.17 | 1.04 |
| DL-Threonine, Thr | 0.87 | 0.80 | 0.76 | 1.49 | 1.32 | 1.22 | 1.04 |
| DL-Cysteine, Cys | 1.00 | 0.97 | 0.88 | 1.57 | 1.54 | 1.24 | 1.09 |
| DL-Glutamic acid, Glu | 0.58 | 0.57 | 0.53 | 0.76 | 0.54 | 0.58 | 0.59 |
| DL-Glutamine, Gln | 0.87 | 0.80 | 0.67 | 1.21 | 1.12 | 1.10 | 1.01 |

[a] Same column as in Table I, footnote *b*. [b] Same column as in Table I, footnote *c*.

Table III. Effect of pH on the Capacity Factors for Amino Acids on XAD-2, -4, and -7

| | Capacity factor, $k'$, on XAD-2[a] | | | | | | |
|---|---|---|---|---|---|---|---|
| | pH | | | | | | |
| Amino acid | 2.2 | 4.7 | 5.9 | 6.5 | 8.1 | 8.9 | 11.5 |
| DL-Tyrosine | 0.35 | 0.25 | 0.22 | 0.22 | 0.29 | 0.22 | |
| DL-Phenylalanine, Phe | 0.83 | 0.69 | 0.66 | 0.68 | 0.78 | 0.79 | 0.91 |
| DL-Tryptophan, Trp | 2.44 | 1.64 | 1.60 | 1.68 | 2.65 | 1.73 | 1.58 |

| | Capacity factor, $k'$, on XAD-4[b] | | | | |
|---|---|---|---|---|---|
| | pH | | | | |
| | 2.3 | 4.8 | 6.5 | 8.9 | 11.4 |
| Glycine | 0.46 | 0.34 | 0.30 | 0.35 | 0.22 |
| DL-Alanine | 0.45 | 0.36 | 0.35 | 0.45 | 0.30 |
| DL-Valine | 0.97 | 0.56 | 0.57 | 0.64 | 0.68 |
| DL-Isoleucine | 2.08 | 1.10 | 1.02 | 1.20 | 1.53 |
| DL-Leucine | 2.27 | 1.30 | 1.25 | 1.45 | 1.71 |
| DL-Tyrosine | 3.33 | 1.75 | 1.56 | 1.94 | 0.25 |
| DL-Phenylalanine | 8.18 | 5.13 | 4.54 | 6.75 | 7.28 |

| | Capacity factor, $k'$, on XAD-7[c] | | | | | | |
|---|---|---|---|---|---|---|---|
| | pH | | | | | | |
| | 1.15 | 2.70 | 4.40 | 5.80 | 7.22 | 8.83 | 11.38 |
| DL-Valine | 1.41 | 1.20 | 1.13 | 1.14 | 1.10 | 1.08 | 1.22 |
| DL-Leucine | 2.39 | 1.77 | 1.32 | 1.26 | 1.26 | 1.29 | 1.29 |
| DL-Threonine | 1.09 | 1.04 | 1.02 | 1.00 | 0.99 | 1.01 | |
| DL-Tyrosine | 4.59 | 2.88 | 1.90 | 1.86 | 1.80 | 1.65 | 0.88 |
| DL-Phenylalanine | 5.77 | 3.59 | 2.34 | 2.28 | 2.29 | 2.33 | 2.31 |

[a] 45 to 65 μm, 0.72 g, 45 × 0.236 cm XAD-2 column at a flow rate of 0.50 mL/min, $V_o$ = 1.30 mL. Phosphate buffers were 0.02 M and the solvent was 10% ethanol–90% water by volume. [b] 45 to 65 μm, 0.46 g, 30 × 0.236 cm XAD-4 column at a flow rate of 0.50 mL/min, $V_o$ = 0.76 mL. Phosphate buffers were 0.02 M and the solvent was 5% ethanol–95% water by volume. [c] 45 to 65 μm, 0.39 g, 45 × 0.236 cm XAD-7 column at a flow rate of 0.50 mL/min, $V_o$ = 1.10 mL. Phosphate buffers were 0.04 M with the ionic strength maintained at 0.2 M by adding NaCl and the solvent was 100% water.

tention is greater on these copolymers in comparison to XAD-2 (see Table I). It was expected that the modifications in the AA would lead to lower $k'$ values.

A change in the polar nature of the R group and its effect on $k'$ values can be seen by comparing the data in Table I and Table II. For example, $k'$ decreases in the order Cys > Ala > Ser > Asp where the respective change in carbon 3 is –SH, –H, –OH, $-CO_2H$. Introducing another $-CH_3$ onto carbon-3 as in Thr increases the $k'$ value (compare $k'$ for Thr to Ser in Table II).

The large influence of the $-CO_2H$ group on the R chain, which is readily dissociated, is evident by comparing the data for Glu to Gln in Table II. The $k'$ value for the latter AA, where the R contains a terminal amide group, is almost twice that of Glu, where the R contains a terminal carboxyl group.

**Effect of Organic Solvent.** The data in Table I and II demonstrate that the capacity factors for the AA on XAD-2, -4, and -7 decrease sharply as the ethanol concentration increases. This is consistent with previous observations of the eluting power of ethanol–water mixtures (*11–15*). Using other organic solvents will also alter the eluting power. In general, the order reported previously (*11–15*) is observed for the amino acids, that is, the eluting power decreases in the order $CH_3CN$ > EtOH > MeOH.

**Effect of pH.** Large capacity factors for organic acids on the XAD copolymers are favored by acidic conditions where the acids exist as the undissociated form. In basic solution, where the dissociated form is present, $k'$ values are much lower (*11–13*). The reverse is found for organic bases (*14*). Since AA have both an acidic and basic site, the influence of solute ionization should be expected to be more complex.

Table III lists the $k'$ data for several AA on XAD-2, -4, and -7 as a function of pH. If these data are graphed, a minimum is found at the isoelectric point pH except for XAD-7 where the $k'$ tends to level off in basic solution. Tyr, unlike the other AA, is triprotic and the $k'$ decreases at higher pH values since a doubly charged species forms because of dissociation of the phenolic group ($pK_{a_3}$ = 10.13).

The AA–XAD copolymer interaction at the two pH extremes and at the isoelectric pH can be viewed as

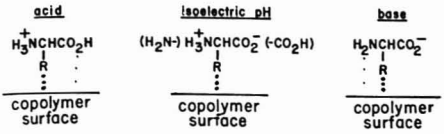


The interaction between the (nonionizable) R group and the copolymer surface will be constant throughout the entire pH range. Thus, any variations in the $k'$ value will be the result of a change in the ionization of the $-CO_2H$ and/or $-NH_2$ groups. In the region of the isoelectric pH both groups are fully ionized (zwitterion form) and will be directed away from the nonpolar copolymer surface. For an acidic solution, the $-CO_2H$ group is unionized, while, in basic solution, the $-NH_2$ group is unionized. Under these conditions, they will participate in the adsorption process, thereby increasing the $k'$ value.

Alternatively, the XAD copolymer, being aromatic, can be viewed as having good electron donor properties. Thus, its interactions with the different groups (-R, $-NH_2$, and $-CO_2H$) could be described by a donor–acceptor type interaction. Evidence of a broad nature which supports this type of interaction includes (1) observation of the order in which substituents influence the chromatographic retention of organic acids and bases (*12, 13*), (2) the elution order observed for different solvents (*11–14*), (3) the solvent uptake order observed for the XAD copolymes (*12, 17*), (4) the fact that retention on the XAD copolymers is much larger than on the ODS stationary phase (*15, 16*), and (5) the observed retention order of the AA. Additional experiments, which should more clearly define this interaction, particularly in the case of the AA, are currently underway and will be described later.

In all the $k'$-pH studies of AA (see Table III and Figure 1), the $k'$ values in acidic solution were always found to be larger than those observed in basic solution. This is attributed to the greater interaction of the $-CO_2H$ group over the $-NH_2$ group.

A comparison of the three XAD copolymers in Table III at a given pH condition leads to conclusions outlined previously about the chromatographic performance of each support. That is, XAD-4 appears to be the most versatile with respect to resolving mixtures. Furthermore, structural changes within the amino acids as discussed previously, have the same chromatographic effect at the different pH conditions. Also, the $k'$ values will decrease at a given pH if the alcohol concentration is increased or if the organic solvent used is one of higher eluting power than ethanol (*11–15*).

**Calculation of Adsorption Data.** It was previously shown that the adsorption of weak monoprotic organic acids and bases on the XAD copolymers is influenced by ionization equilibria (*11–15*). Thus, the change in capacity factor, $k'$, for the retention of a weak organic acid as a function of pH is given by

$$k' = k_0\left(\frac{1}{1 + K_a/[H^+]}\right) + k_{-1}\left(\frac{1}{1 + [H^+]/K_a}\right) \qquad (3)$$

where $k_0$ and $k_{-1}$ are the capacity factors for the undissociated and dissociated form of the weak acid, respectively, and $K_a$ is its ionization constant. A similar equation can be derived for the retention of weak organic bases. These equations have been shown to hold for the adsorption of monoprotic phenol, carboxylic acid, phenoxyacetic acid, amine, and pyridine derivatives (*11–15*).

The usefulness of such equations is twofold. (1) They define the equilibria that influence the sorption of organic acids and bases in reversed phase chromatography, and (2) they permit the prediction of elution behavior as a function of a minimum number of measurements. That is, the $K_D$, $k'$, or retention time or volume can be calculated as a function of pH providing the $K_a$ (or $K_b$) and the $K_D$, $k$, or retention time or volume for the neutral form and the dissociated forms are known.

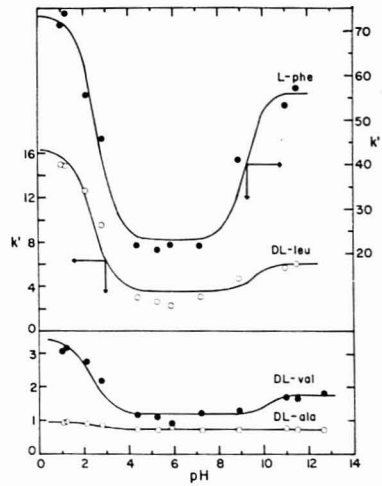


**Figure 1.** Capacity factors for several amino acids on XAD-4 as a function of pH with $k_1$, $k_0$, and $k_{-1}$ calculated by Equation 4 using a nonlinear squares fit. For the following amino acids, $K_{a_1}$, $K_{a_2}$, $k_1$, $k_0$, and $k_{-1}$ are respectively: DL-alanine, $4.47 \times 10^{-3}$, $1.35 \times 10^{-10}$, 0.94 ± 0.02, 0.74 ± 0.01, 0.73 ± 0.02; DL-valine, $5.13 \times 10^{-3}$, $1.91 \times 10^{-10}$, 3.38 ± 0.15, 1.19 ± 0.09, 1.75 ± 0.12; DL-leucine, $4.68 \times 10^{-3}$, $1.82 \times 10^{-10}$, 16.35 ± 0.89, 3.56 ± 0.57, 6.07 ± 0.96; L-phenylalanine, $2.63 \times 10^{-3}$, $5.75 \times 10^{-10}$, 73.2 ± 2.6, 23.0 ± 1.9, 56.8 ± 2.9. 45 to 65 μm, 0.46 g, 30 × 0.236 cm XAD-4 column at a flow rate of 0.50 mL/min (L-Phe 2.0 mL/min), $V_0$ = 0.83 mL. Phosphate buffers in water at 0.04 M and ionic strength made to 0.2 M with NaCl

Recently, an equation was derived which relates the capacity factor of a weak diprotic acid to the pH of the eluting solution. The equation, which is in terms of the ionization constants of the diprotic acid and of the capacity factors for the retention of the undissociated, half-dissociated, and fully dissociated forms of the diprotic acid, was shown to hold for the nonpolar octadecylsilica stationary phase (*16*) and for the XAD supports (*15*). Similarly, an equation for weak diprotic bases was derived and shown to hold for the XAD supports (*15*).

For substances that have the potential to exist as zwitterions, such as amino acids, the equation describing its sorption is

$$k' = \frac{k_0 + k_1\left(\frac{[H^+]}{K_{a_1}}\right) + k_{-1}\left(\frac{K_{a_2}}{[H^+]}\right)}{1 + \frac{[H^+]}{K_{a_1}} + \frac{K_{a_2}}{[H^+]}} \qquad (4)$$

where $k_0$, $k_1$, and $k_{-1}$ are the capacity factors for the zwitterion ion form, cationic form, and anionic form, respectively, and $K_{a_1}$ and $K_{a_2}$ are ionization constants for the two-step ionization, respectively (*15, 16*).

Verification of Equation 4 was accomplished in two ways. Figure 1 shows plots of experimentally determined $k'$ values on XAD-4 for several AA as a function of pH at controlled ionic strength. The $k_0$, $k_1$ and $k_{-1}$ values listed in Figure 1 were calculated by Equation 4 using a nonlinear least-squares fit of the data. Semiquantitatively, the solid line in Figure 1 can

Table IV. Effect of Salt Concentration on the Capacity Factor for Amino Acids on XAD-2

| | Capacity factor, $k'$[a] | | | | | | |
|---|---|---|---|---|---|---|---|
| | Concentration of NaCl, M | | | | | | |
| Amino acid | 0 | 0.001 | 0.005 | 0.010 | 0.050 | 0.100 | 0.500 |
| DL-Tyrosine | 0.34 | 0.23 | 0.27 | 0.29 | 0.29 | 0.32 | 0.25 |
| DL-Phenylalanine | 0.83 | 0.67 | 0.68 | 0.74 | 0.74 | 0.79 | 0.77 |
| DL-Tryptophan | 2.06 | 1.74 | 1.73 | 1.71 | 1.76 | 1.95 | 2.04 |

[a] 45 to 65 μm, 0.72 g, 45 × 0.236 cm XAD-2 column at a flow rate of 0.5 mL/min, and a solvent mixture of 10% ethanol–90% water, $V_0$ = 1.30 mL.

be calculated with Equation 4 using the three experimental points, $k_1$ at pH 1.00, $k_0$ at the isoelectric pH, and $k_{-1}$ at pH 12.65. Excellent agreement demonstrates that Equation 4 accurately describes the equilibria that influence the chromatographic retention of AA. Secondly, it confirms that potential eluting conditions based on pH can be predicted from a minimum set of column $k'$–pH measurements.

Equation 4 also describes the chromatographic retention of AA on XAD-7. This was demonstrated by carrying out these same kinds of calculations using the $k'$–pH data for XAD-7 listed in Table III, where $k_1$, $k_0$, and $k_{-1}$ are the capacity factors at pH 1.15, 5.80, and 11.38, respectively.

If the AA has a third ionization constant, an equation which accounts for the third ionization step can be derived. An AA of this type is Tyr which contains a phenolic group in addition to the $-CO_2H$ and $-NH_2$ group. Thus, the three ionization steps are given by Equations 1 and 2 where

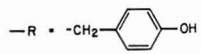


and Equation 5.

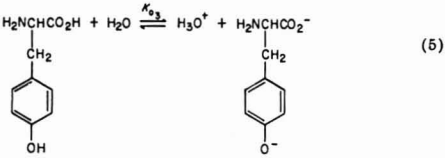


(5)

Using the approach outlined elsewhere (*15*), an equation which describes the influence of the three ionization steps on the relationship of $k'$ to $H^+$ can be derived as

$$k' = \frac{k_0 + k_1\left(\frac{[H^+]}{K_{a_1}}\right) + k_{-1}\left(\frac{K_{a_2}}{[H^+]}\right) + k_{-2}\left(\frac{K_{a_2}K_{a_3}}{[H^+]^2}\right)}{1 + \frac{[H^+]}{K_{a_1}} + \frac{K_{a_2}}{[H^+]} + \frac{K_{a_2}K_{a_3}}{[H^+]^2}} \quad (6)$$

where $k_0$, $k_1$, $k_{-1}$, $k_{-2}$ are the capacity factors for the zwitterion, protonated species, anionic species, and doubly charged anionic species, respectively, and $K_{a_1}$, $K_{a_2}$, and $K_{a_3}$ are the three ionization constants.

Experimentally determined $k'$ values for tyrosine as a function of pH are shown in Figure 2. Like the other AA, the retention of Tyr is high at low pH values, where it exists as a singly charged cation. The $k'$ value then decreases and levels off at the isoelectric point pH and stays constant. As the pH is increased to pH values where the doubly negative charged species is formed, the $k'$ value decreases again. The values of $k_1$, $k_0$, $k_{-1}$, and $k_{-2}$ were calculated from the experimental data by a nonlinear least-squares fit of the data to Equation 6. The $K_a$ values are taken from the literature (*18*, *19*). Limitations in these calculations are discussed elsewhere (*15*).

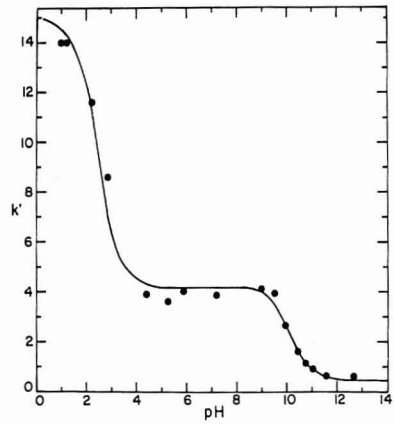


Figure 2. Capacity factors for tyrosine on XAD-4 as a function of pH. For tyrosine, $K_{a_1}$ = 4.57 × $10^{-3}$, $K_{a_2}$ = 7.73 × $10^{-10}$, $K_{a_3}$ = 7.38 × $10^{-11}$, $k_1$ = 15.1 ± 0.4, $k_0$ = 4.20 ± 0.28, $k_{-1}$ = 4.04 ± 0.66, and $k_{-2}$ = 0.48 ± 0.33. Column conditions are given in Figure 1

Several other AA and related derivatives have three ionization steps and their retention should follow Equation 6. However, the calculation of $k'$–pH data with Equation 6 and a minimum set of $k'$ data is more difficult since as the number of ionization steps increases in the molecule or the more closely related they are, the more difficult it becomes to experimentally determine the capacity factor for the retention of the undissociated form and for each of the dissociated forms of the molecule.

**Effect of Salt.** Addition of salt to the eluting mixture will affect the sorption of organic acids or bases on the XAD copolymers when the experimental condition ensures that the acid or base is in the dissociated form, particularly, for strong acids like sulfonic acids (*12*, *13*). Two major effects were observed in these studies as salt concentration was increased: (1) the retention volumes and capacity factors increased, and (2) the peaks tended to be sharper.

Since the AA are in a charged form at different pH conditions, the effect of added salt was evaluated. Table IV lists the $k'$ data for three aromatic AA as a function of NaCl concentration in the absence of pH control. Under these conditions, the AA should be in its zwitterion form. Although the changes are small, they are consistent in that the $k'$ values for the three AA decrease initially and then slowly increase as salt concentration is increased.

In buffered solution near the isoelectric pH (studied in the pH range of 5.88 to 7.20 at a buffer concentration of 0.02 M) little salt effect was noted upon the addition of NaCl (0.05 to 0.25 M). Apparently, the salt components of the buffer itself were sufficient to influence the $k'$ value and for this

Table V. Capacity Factors for Small Chain Peptides on XAD-2 as a Function of Ethanol-Water Concentration

| | Capacity factor, $k'$[a] | | | |
|---|---|---|---|---|
| | % Ethanol | | | |
| Peptide | 10 | 15 | 20 | 30 |
| Gly-DL-Phe | 0.5 | 0.3 | 0.1 | 0.1 |
| DL-Ala-DL-Phe | 1.0 | 0.6 | | |
| L-Val-L-Phe | 1.7 | 1.0 | | |
| DL-Leu-DL-Phe | 7.3 | 5.1 | | |
| L-Ser-L-Phe | 0.5 | 0.3 | | |
| L-Pro-L-Phe | 2.2 | 1.4 | | |
| L-Met-L-Phe | 4.6 | 3.1 | | |
| L-Phe-Gly | 0.6 | 0.4 | 0.3 | 0.3 |
| L-Phe-L-Ala | 0.6 | 0.4 | 0.3 | 0.3 |
| L-Phe-L-Val | 1.4 | 0.8 | | |
| L-Phe-L-Leu | 6.9 | 4.7 | 3.2 | 1.6 |
| Gly-L-Tyr | 0.1 | 0.1 | 0.1 | 0.1 |
| Gly-DL-Phe | 0.5 | 0.3 | 0.1 | 0.1 |
| Gly-L-Trp | 1.1 | 0.6 | 0.4 | 0.3 |
| L-Phe-Gly-Gly | 0.4 | 0.2 | 0.1 | 0 |
| Gly-Gly-L-Phe | 0.5 | 0.3 | 0.2 | 0.2 |
| DL-Tyr | 0.2 | 0.2 | 0.3 | 0.2 |
| DL-Phe | 0.6 | 0.6 | 0.5 | 0.3 |

[a] 45 to 65 μm, 0.32 g, 30 × 0.19 cm XAD-2 column at a flow rate of 0.5 mL/min, $V_o$ = 0.7 mL.

Table VI. Capacity Factors for Small Chain Peptides on XAD-2 as a Function of pH

| | Capacity factor, $k'$[a] | | | |
|---|---|---|---|---|
| | pH | | | |
| Peptide | 3.68 | 5.70 | 7.40 | 10.35 |
| Gly-DL-Phe | 2.44 | 1.44 | 1.56 | 2.66 |
| DL-Ala-DL-Phe | 4.33 | 2.56 | 2.67 | 4.56 |
| L-Val-L-Phe | 5.89 | 3.11 | 7.78 | 21.2 |
| DL-Leu-DL-Phe | | 10.67 | | |
| L-Ser-L-Phe | 2.22 | 1.33 | 1.44 | 2.11 |
| L-Pro-L-Phe | 3.56 | 1.89 | 3.00 | |
| L-Met-L-Phe | 13.4 | 6.89 | 16.2 | |
| L-Phe-Gly | 1.89 | 1.56 | 2.67 | 4.11 |
| L-Phe-L-Ala | 1.78 | 1.22 | 3.22 | 5.89 |
| L-Phe-L-Val | 4.11 | 2.33 | 14.6 | |
| L-Phe-Gly-Gly | 1.56 | 1.33 | 2.56 | 3.78 |
| Gly-Gly-L-Phe | 3.00 | 1.44 | 1.56 | 2.00 |

[a] 45 to 65 μm, 0.71 g, 45 × 0.236 cm XAD-2 column at a flow rate of 0.50 mL/min, $V_o$ = 0.90 mL. Phosphate buffers were at 0.1 M concentration in a solvent of 10% ethanol–90% water.

reason salt effects in strong acid or base solution were not examined.

The major salt effect is noted when comparing data determined in alcohol–water mixtures to that in buffered alcohol–water mixtures. This is illustrated by comparing the data in Table I to the data at the isoelectric pH in Table III for the same ethanol concentration. In all cases, the $k'$ data are lower in the presence of the buffer. Although there is a salt effect it is less significant than observed with other organic acids and bases at least for the conditions examined.

**Peptides and Amino Acid Derivatives.** Since R groups in the AA were shown to have a significant influence on the chromatographic retention of the AA, it was of interest to establish R group effects in peptide systems. Several potential factors were considered. These included the effects of structure of each AA unit in the peptide, the position of each AA unit in the peptide, and the length of the peptide.

Capacity factor data on XAD-2 were determined for several dipeptides and a few tripeptides, as a function of ethanol concentration and pH. As shown in Table V, an increase in the ethanol concentration decreases the $k'$ value while a minimum in $k'$, as shown in Table VI, was found near the isoelectric point pH when the pH of the eluting mixture was varied. These general trends are the same as found for the simple AA.

Examination of the $k'$ data in Tables V and VI reveals several trends in the effect of structure on chromatographic retention. Since one AA unit of the dipeptide is held constant, the effect of the other unit on retention can be ascertained. (Although examined in less detail, similar results were found for Tyr- and Trp-containing dipeptides.)

As observed with the individual nonpolar AA, increasing the hydrophobic character of the R group in the varying AA subunit of the Phe-derived peptide (see Table V and VI) results in an increase in retention. That is, $k'$ for the peptides changes in the order Leu > Val > Ala > Gly. This trend is observed regardless of whether these AA units provide the free $-NH_2$ group or the free $-CO_2H$ group in the dipeptide.

In the absence of salt or buffer (see Table V) and at the isoelectric point pH (see Table VI), retention is the largest when the Phe unit provides the free–$CO_2H$ group in the dipeptide. In acid and base solution, this trend is not observed suggesting that the terminal $-NH_2$ and $-CO_2H$ groups in the dipeptide are influencing its retention.

The dipeptide-XAD copolymer interaction can be viewed as

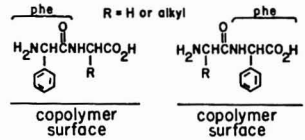


In acid solution, the larger $k'$ is favored by the dipeptide in which the Phe provides the $-CO_2H$ group. Under these conditions this group, which is closest to the phenyl ring, is undissociated. In base solution, the reverse is found, that is, a smaller $k'$ is favored by the dipeptide where the Phe provides the $-CO_2H$ group. Under these conditions the $-CO_2H$ is dissociated and the phenyl ring is close to the charged site.

This trend is consistent with the observation that the aromatic AA are much more highly retained than the nonpolar AA (see Tables I to III). Thus, any large change in polarity in the vicinity of the phenyl ring should have a significant influence on the retention. A change in polarity close to the R group in the dipeptide will also influence its interaction with the XAD copolymer; however, the dominating factor in the case of this series of dipeptides is the phenyl group.

This is further illustrated by comparing the tripeptides Gly-Gly-Phe to Phe-Gly-Gly. In base solution, high retention is favored by the Phe group providing the free $-NH_2$ group or at position 1 in the tripeptide while, in acid solution, high retention is favored by the Phe being at position 3. In both cases, the highest retention occurs when the aromatic ring of Phe is the furthest from the charge site.

If a polar group is introduced into one of the AA units, retention is decreased. This is illustrated by comparing Ser-Phe (where a –OH group is introduced in Ser) to Ala-Phe. In Met-Phe a S heteroatom is introduced in the Met AA unit but it is introduced as a methyl–thio ether. This group is less polar than the –OH group and the corresponding –SH group. Thus, the retention of Met-Phe is intermediate between Val-Phe and Leu-Phe suggesting that it is acting similar to a 4 C-unit R chain. Based on these results the dipeptide Cys-Phe would be predicted to have a larger $k'$ than that for Ser-Phe but less than that for Leu-Phe, and probably similar to Val-Phe (see Table V). Since Pro is also a 4 C-unit R chain, it is not surprising to find that retention of Pro-Phe is similar to that for Val-Phe even though the C-unit R chain is bound

Table VII. Capacity Factors on XAD-4 for a Series of Alanine Peptides

| Peptide | Mol. wt | $k'^a$ |
|---|---|---|
| DL-Alanine | 89.10 | 0.46 |
| L-Alanyl-L-alanine | 160.2 | 1.28 |
| Tri-L-alanine | 231.2 | 1.77 |
| Tetra-L-alanine | 302.3 | 1.99 |
| Penta-L-alanine | 373.4 | 2.47 |
| Hexa-L-alanine | 444.5 | 6.69 |
| Poly-DL-alanine | 1800 (Avg.) | |

[a] 45 to 65 μm, 0.46 g, 30 × 0.236 cm XAD-4 column at a flow rate of 0.50 mL/min, $V_e$ = 0.83 mL. Eluting mixture was 10% ethanol-90% water.

to the nitrogen within the Pro molecule.

For mixtures of dipeptides and perhaps tripeptides, it should be possible to qualitatively predict elution order by considering the structure of the R groups in the AA units and their positions relative to the charge sites if pH is to be used as an eluting variable. The data for simple AA in Tables I to III would serve as the guidelines. Using these, the trends observed in Tables IV and V are consistent with the predictions.

AA are frequently converted into derivatives in order to facilitate chromatographic separation and detection. Two such classes of derivatives are the DNP-AA, formed by the reaction of an AA with 2,4-dinitrofluorobenzene, and the dansyl-AA, formed by the reaction of an AA with *N,N*-dimethyl-1-naphthylamine-5-sulfonic acid chloride (dansyl chloride). In both cases the reaction site is at the amine group. For glycine the derivatives are

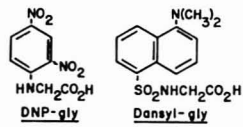


Because of the structural changes in the derivatives (increased number of functional groups and reduction of zwitterion ion formation), the chromatography of the derivatives on the XAD copolymers should be different than for the simple AA. Although detailed studies were not carried out it was readily shown that: (1) the derivatives acted as weak acids in response to a pH change in the eluting mixture, (2) the derivatives were more retained than the corresponding simple AA and stronger eluting conditions were required for their removal off the column, and (3) the order of elution of the derivatives was the same as for the simple AA, that is retention changes in the order Phe > Leu > Val > Ala > Gly.

Preliminary experiments were also carried out with the PTH-AA derivatives which are formed by the reaction of an amino acid with phenylisothiocyanate. In these derivatives both the amine and carboxyl group are involved in the reaction. Retention was greater in comparison to the simple AA (examined on XAD-7) and strong eluting conditions were required (30 to 50% $CH_3CN$–$H_2O$ was studied). The elution order for the PTH derivatives was found to be similar to the simple AA.

**Peptide Chain Length.** Since the XAD resins have large porosities, experiments were conducted to evaluate whether peptide size had a significant effect on its retention. XAD-4 was chosen as the stationary phase since it provides high retention and has the smallest average pore size of the three XAD copolymers (*11, 12, 14*). Thus, if peptide molecular size is significant, it should be more readily observed with this stationary phase.

Table VII lists the capacity factor data for a series of alanine peptides. As the molecular weight increases, the retention

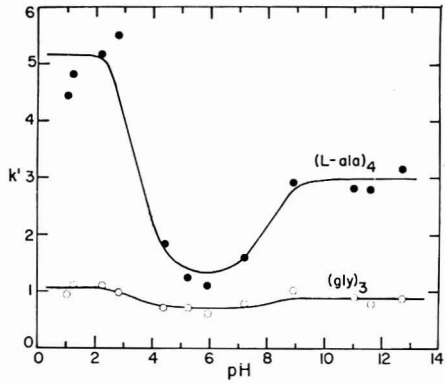


Figure 3. Capacity factors for two peptides on XAD-4 as a function of pH with $k_1$, $k_0$, and $k_{-1}$ calculated by Equation 4 using a nonlinear squares fit. For tri-glycine: $K_{a_1} = 5.89 \times 10^{-4}$, $K_{a_2} = 8.13 \times 10^{-9}$, $k_1 = 1.07 \pm 0.05$, $k_0 = 0.71 \pm 0.04$, $k_{-1} = 0.89 \pm 0.04$. For tetra-L-alanine, $K_{a_1} = 3.80 \times 10^{-4}$, $K_{a_2} = 1.15 \times 10^{-8}$, $k_1 = 5.18 \pm 0.25$, $k_0 = 1.33 \pm 0.25$, $k_1 = 2.98 \pm 0.24$. Column conditions are given in Figure 1

increases. Intermediate peptides between hexa-L-alanine and poly-DL-alanine, which would more clearly define the change in retention, were not available. However, the data still clearly indicate that as molecular weight increases the retention increases and thus, XAD-4 is not acting as a size or exclusion type stationary phase but rather as a typical adsorbent.

The effect of pH and organic solvent on retention followed the trends observed for simple AA and dipeptides. Elution of the poly-DL-alanine was not observed even with changes in the eluting mixtures up to 80% acetonitrile which represents a sharp increase in eluting power. A more detailed study of eluting conditions for large molecular weight peptides is currently underway.

A glycine peptide series analogous to the alanine peptide series listed in Table VII was also examined. Although some difficulty was encountered due to the limited solubilities of the glycine series, the trend of an increase in capacity factor with increase in molecular weight was observed. Also, as anticipated from comparison of retention of alanine to glycine, the $k'$ values for the alanine peptides were larger than for the corresponding glycine peptides.

**Calculation of Peptide Adsorption Data.** Di-, tri-, etc. peptides will still contain the acidic $-CO_2H$ site at one end of the molecule and the basic $-NH_2$ site at the other end of the molecule. If the peptide does not contain any AA units with additional acidic or basic sites, such as Tyr, the equilibria influencing the retention of the peptide should still be ionization of the acidic and basic site. Thus, Equation 4 should describe the change in $k'$ as a function of pH.

Figure 3 shows plots of experimentally determined $k'$ values on XAD-4 as a function of pH at a constant ionic strength for two peptides. Peptide $k'$ data on XAD-7 are shown in Figure 4. These results are similar to those found for the AA. In acid and base solution, retention occurs as the cation and anion, respectively, while in the intermediate pH region, zwitterion formation, which leads to a highly charged species, reduces the extent of the retention.

The $k_1$, $k_0$, and $k_{-1}$ values listed in Figure 3 and 4 were calculated by a nonlinear least-squares fit of the experimental data to Equation 5. It should be noted that a minimum set of data was used in the fitting of data in Figures 3 and 4. The $K_a$ values are taken from the literature (*18*). Limitations in

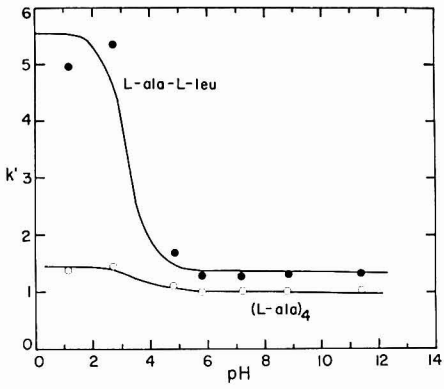


**Figure 4.** Capacity factors for two peptides on XAD-7 as a function of pH with $k_1$, $k_0$, and $k_{-1}$ calculated by Equation 4 using a nonlinear squares fit. For tetra-L-alanine, $K_{a_1} = 3.80 \times 10^{-4}$, $K_{a_2} = 1.15 \times 10^{-8}$, $k_1 = 1.43 \pm 0.04$, $k_0 = 1.03 \pm 0.03$, $k_{-1} = 1.00 \pm 0.04$. For L-alanyl-L-leucine, $K_{a_1} = 5.01 \times 10^{-4}$, $K_{a_2} = 7.24 \times 10^{-9}$, $k_1 = 5.53 \pm 0.35$, $k_0 = 1.35 \pm 0.27$, $k_{-1} = 1.30 \pm 0.34$. 45 to 65 μm, 0.39 g, 45 × 0.236 cm XAD-7 column at a flow rate of 0.50 mL/min, $V_0$ = 1.09 mL. Phosphate buffers in water at 0.04 M and ionic strength made to 0.2 M with NaCl

these calculations are discussed elsewhere (*15*). Alternatively, the $k'$–pH relationship can be calculated by using Equation 4 and the capacity factors determined at three pH conditions as previously described for the amino acids.

Thus, it can be concluded that Equation 4 provides a quantitative description of the equilibria that influence the retention of diprotic peptides on the XAD copolymers. If the peptide has additional ionization sites, these can be accounted for by modification of Equation 4 (see Equation 6). Since the $k'$ data are readily determined as a function of pH, Equation 4 can also be used to determine the $K_a$ values for the peptide. Finally, eluting conditions based on pH are readily predicted from a $k'$–pH plot which can be calculated from a minimum number of experimentally determined $k'$ data.

**Separations.** Changes in capacity factors for the AA and derivatives can be achieved by controlling variables in the eluting mixture, such as pH, organic solvent–water ratio, the type of organic solvent used, or the addition of salt and by choice of the XAD copolymer as the stationary phase. The separations cited here were designed to illustrate the scope of the XAD copolymers in separating AA and derivatives through the control of these variables.

Initial experiments showed that plate heights (2 to 5 mm) were similar to those found for retention of organic acids and bases (*11–14*) and that sample loading could be done up to 1 to 2 mg/g of support without sacrificing plate height. All separations reported here were done at loading capacities well below this level.

Figure 5 illustrates a separation of nonpolar and aromatic amino acids on XAD-4 using 1% $CH_3CN$–99% water as the eluting mixture. The XAD-4 support is preferred over the XAD-2 because retention of the nonpolar AA is much higher on the XAD-4. If only aromatic amino acids, which have large $k'$ values, were being separated, XAD-2 would be a suitable support. The conditions for the separation of a DL-Tyr, DL-Phe, DL-Trp mixture on XAD-2 has been reported previously (*13*).

If Trp were included in the mixture in Figure 5, its peak would appear at a much higher $R_v$ relative to DL-Phe. For convenience, a larger flow rate was used to elute the DL-Phe.

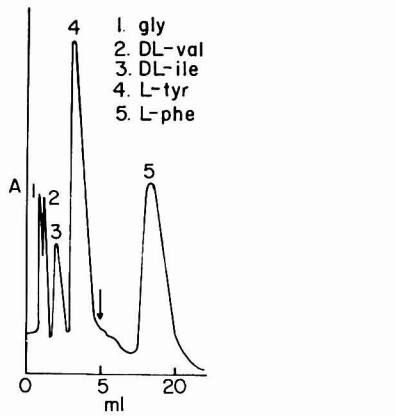


**Figure 5.** Separation of amino acids on XAD-4. 45 to 65 μm, 0.46 g, 30 × 0.236 cm XAD-4 column at a flow rate of 0.5 mL/min (increased to 1.0 mL/min at ↓) and using 1% $CH_3CN$–99% $H_2O$. Sample: (1) 27 μg, (2) 29 μg, (3) 35 μg, (4) 3.3 μg, and (5) 3.3 μg, and detection at 208 nm

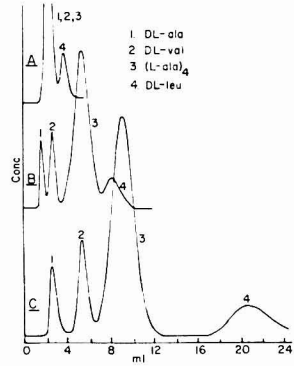


**Figure 6.** Increasing resolution through pH control in the separation of amino acids on XAD-4. 45 to 65 μm, 0.46 g, 30 × 0.236 cm XAD-4 column at a flow rate of 0.8 mL/min using detection at 208 nm where (A) pH 5.89, phosphate buffer, ionic strength 0.2 M, (B) pH 2.53, HCl solution, ionic strength 0.2 M, and (C) pH 1.99, HCl solution, ionic strength 0.2 M, all 100% $H_2O$

The separation of compounds 1 to 4 can be improved by utilizing a gradient in which $CH_3CN$ is introduced slowly into water up to the 1% level and then increased more rapidly to reduce the $R_v$ for DL-Phe and DL-Trp (if in the sample).

Figure 6 illustrates both the utilization of pH to bring about a separation and the use of Equation 4 to predict the separation. If faced with having to separate a mixture of DL-Ala, DL-Val, tetra-L-Ala, and DL-Leu the $k'$ value for each would be measured in strong acid solution ($k_1$), at the isoelectric pH ($k_0$), and in strong base solution ($k_{-1}$). With these data and the ionization constants, graphs of $k'$ vs. pH can be calculated by Equation 4 (see Figures 1 and 3). Comparison of these graphs allows the prediction of the optimum pH condition for the separation.

In Figure 6A, the isoelectric point pH is used for the separation. As predicted from Figures 1 and 3, $k'$ values at this pH are not significantly different for the three AA and

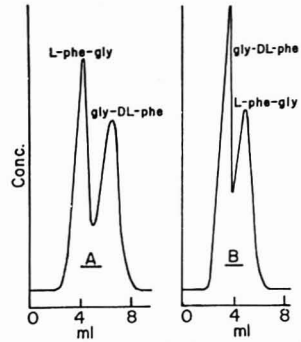


**Figure 7.** Reversal in elution order for the separation of a dipeptide mixture on XAD-2 by a change in the pH of the eluting agent. 45 to 65 μm, 0.31 g, 21 × 0.236 cm XAD-2 column at a flow rate of 0.5 mL/min using detection at 208 nm, a sample of 2.7 μg of each dipeptide, and (A) pH 2.73, phosphate buffer at ionic strength 0.2 M in 2% EtOH–98% water, and (B) pH 11.03 phosphate buffer at ionic strength 0.2 M in 2% EtOH–98% water

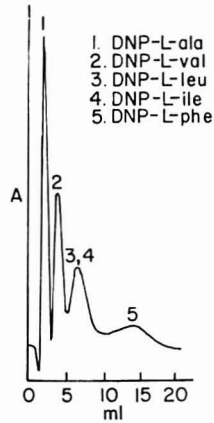


**Figure 8.** Separation of DNP derivatives of amino acids on XAD-2. 45 to 65 μm, 0.71 g, 45 × 0.236 cm XAD-2 column at a flow rate of 1.0 mL/min and using 15% $CH_3CN$–85% $H_2O$. Sample: (1) 3.6 μg, (2) 3.9 μg, (3) 2.3 μg, (4) 2.3 μg, and (5) 8.3 μg, and detection at 254 nm

the peptide, and only two peaks are obtained, the first containing two AA and the peptide and the second containing Leu. Although increasing the pH in the eluting mixture to pH 12 would increase the difference in $k'$ values, the difference would not be as large as that possible in acid solution. Figure 6B illustrates the complete separation at pH 2.53. Increasing the acidity, as shown in Figure 6C, increases the resolution; however, the time for the complete separation is also increased. Considering both the time and resolution factor, the optimum pH for the separation is in the range of pH 2 to 3.

As noted previously, the type and position of the R group in the AA subunits in the peptide have an effect on the chromatographic retention at different pH conditions. This effect can be large enough to cause a reversal in the elution order and can be used advantageously in many practical applications. An example of this is shown in Figure 7 where L-Phe-Gly and Gly-L-Phe are separated under acidic (Figure

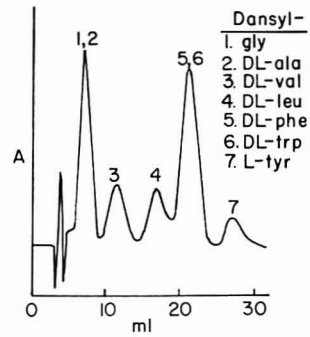


**Figure 9.** Separation of dansyl derivatives of amino acids on XAD-2. Same column as in Figure 8 using gradient described in the text. Sample: (1) 6 μg, (2) 5 μg, (3) 5 μg, (4) 6 μg, (5) 8 μg, (6) 9 μg, and (7) 8 μg, and detection at 254 nm

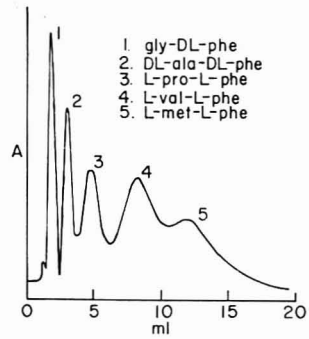


**Figure 10.** Separation of a dipeptide mixture on XAD-2. 45 to 65 μm, 0.71 g, 45 × 0.236 cm column at a flow rate of 0.5 mL/min and using 0.1 M $NaHCO_3$ in 10% EtOH–90% $H_2O$. Sample: (1) 5 μg, (2) 10 μg, (3) 15 μg, (4) 23 μg, and (5) 20 μg, and detection at 254 nm

7A) and basic (Figure 7B) eluting conditions. As predicted from Table VI, in acid L-Phe-Gly appears first, while in base it appears second.

Figures 8 and 9 illustrate separations of AA as the DNP and dansyl derivatives, respectively. XAD-2 was used over XAD-4 because the derivatives already have large $k'$ values and the stronger adsorption power of XAD-4 is not necessary. Since both AA derivatives contain free carboxyl groups, pH, which was not explored in detail, is also a variable that can be used to effect the separation.

The initial mixture for the gradient used in Figure 9 was 23% $CH_3CN$–77% water containing 0.11 M NaCl. The mixture was changed by adding 1.25 mL $CH_3CN$/min until 35% $CH_3CN$ was reached; the eluting mixture was then maintained at this level. In the absence of the salt, the peaks in Figure 9 were broader and the resolution was reduced. This type of salt effect was previously found when separating other organic acids (*12, 13*).

Examination of the $k'$ values in Table V and VI suggest that a wide variety of dipeptide combinations are readily separated. Figure 10 illustrates the separation of a mixture of 5 dipepties on XAD-2. If the $k'$–pH graphs for each dipeptide were determined, as outlined for Figure 6, the optimum pH condition for the separation is readily predicted. Several other dipeptide mixtures such as Gly-L-Tyr, Gly-DL-Phe, Gly-L-Trp were also separated.

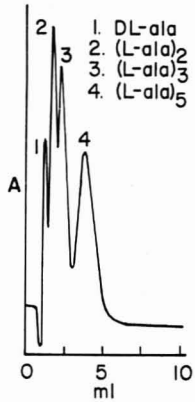


**Figure 11.** Separation of a peptide mixture on XAD-4. 45 to 65 μm, 0.46 g, 30 × 0.236 cm XAD-4 column at a flow rate of 0.4 mL/min and using 5% EtOH–95% $H_2O$. Sample: (1) 11 μg, (2) 2.7 μg, (3) 3.7 μg, and (4) 4.7 μg, and detection at 208 nm

Figure 11 illustrates the separation of a mixture of alanine peptides on XAD-4. The tetra-L-Ala was not included in the mixture because, under these eluting conditions, its peak would not be resolved from the tri-L-Ala peak.

Several attempts were made to separate small chain peptides that differed only in optical activity. Enough success was experienced to warrant further examination since it presently appears that resolution is going to be achieved for certain structural arrangements.


## ACKNOWLEDGMENT

We thank Kenneth Sando for advice and help in developing and carrying out the computer operations.


## LITERATURE CITED


(1) H. F. Walton, *Anal. Chem.*, **48**, 52R (1976).
(2) K. Tsuzi and J. H. Robertson, *J. Chromatogr.*, **112**, 663 (1975).
(3) C. Horvath, W. Melandar, and I. Molnar, *J. Chromatogr.*, **125**, 129 (1976).
(4) R. W. Frei, L. Michel, and W. Santl, *J. Chromatogr.*, **126**, 665 (1976).
(5) R. Burgus and J. Rivier, 14th European Peptide Symposium, April 1976.
(6) E. J. Kikta, Jr., and E. Grushka, *J. Chromatogr.*, **135**, 367 (1977).
(7) K. Krummen and R. W. Frei, *J. Chromatogr.*, **132**, 27 (1977).
(8) K. Krummen and R. W. Frei, *J. Chromatogr.*, **132**, 429 (1977).
(9) J. J. Hansen, T. Greibrokk, B. L. Currie, K. Nils-Gunnar Johansson, and K. Folkers, *J. Chromatogr.*, **135**, 155 (1977).
(10) A. Niederwieser, *J. Chromatogr.*, **61**, 81 (1971).
(11) M. D. Grieser and D. J. Pietrzyk, *Anal. Chem.*, **46**, 330 (1974).
(12) D. J. Pietrzyk and C. H. Chu, *Anal. Chem.*, **49**, 757 (1977).
(13) D. J. Pietrzyk and C. H. Chu, *Anal. Chem.*, **49**, 860 (1977).
(14) C. H. Chu and D. J. Pietrzyk, *Anal. Chem.*, **46**, 330 (1974).
(15) D. J. Pietrzyk, E. D. Kroeff, and T. D. Rotsch, *Anal. Chem.*, preceding paper in this issue.
(16) C. Horvath, W. Melander, and I. Molnar, *Anal. Chem.*, **49**, 142 (1977).
(17) D. J. Pietrzyk, *Talanta*, **16**, 169 (1969).
(18) D. D. Perrin, "Dissociation Constants of Organic Bases in Aqueous Solutions", Butterworth and Co., London, England, 1965.
(19) R. B. Martin, J. T. Edsall, D. B. Wetlaufer, and B. R. Hollingworth, *J. Biol. Chem.*, **233**, 1429 (1958).



RECEIVED for review September 30, 1977. Accepted December 16, 1977. This investigation was supported by Grant Number CA 18555, awarded by the National Cancer Institute, DHEW. Part of this work was presented at the Federation of Analytical Chemistry and Spectroscopy Societies, Paper No 135, Detroit, Mich., 1977, at the Pittsburgh Conference on Analytical Chemistry and Applied Spectroscopy, Paper No 448, Cleveland, Ohio, 1977, and at the 12th Midwest ACS Regional Meeting, Paper No 113, Kansas City, Mo., 1976.


# Evaluation of Benzene as a Charge Exchange Reagent


**S. C. Subba Rao[1] and Catherine Fenselau***

*Department of Pharmacology and Experimental Therapeutics, Johns Hopkins University School of Medicine, Baltimore, Maryland 21205*



**The feasibility of utilizing benzene as a reagent gas is explored. Under chemical ionization conditions $C_6H_6^{+\cdot}$ is the reactant ion in benzene. $C_6H_6^{+\cdot}$ ions ionize compounds with ionization potentials below 9.2 eV by charge exchange. These spectra contain prominent molecular ion peaks with evidence of very little fragmentation and no peaks beyond the $M^+$ group. The $C_6H_6^{+\cdot}$ species has been found to ionize only the unsaturated fatty acids in a mixture of saturated and unsaturated fatty acids.**


Charge exchange reagents offer the potential of selectively ionizing only those components of a mixture which have lower ionization potentials (*1*). Thus a charge exchange reagent with recombination energy in the middle of the range of ionization potentials of most organic compounds, 7–11 eV, should be a useful reagent gas for chemical ionization mass spectrometry. Einolf and Munson have evaluated a number of small gaseous molecules with ionization potentials in this range (*1*), and subsequent work with nitric oxide has been reported from a number of laboratories (*2–4*). However, the selectivity of nitric oxide as a charge exchange reagent (see reaction 1), was found to be compromised by other ion molecule reactions, including electrophilic addition (reaction 2), and hydride abstraction (reaction 3) which also lead to ionization of the sample. Thus nitric oxide at pressures used in chemical ionization sources will ionize most compounds, regardless of their ionization potentials.

$$NO^+ + R \rightarrow NO + R^{+\cdot} \quad (1)$$

$$NO^+ + R \rightarrow R{\cdot}NO^+ \quad (2)$$

$$NO^+ + R \rightarrow HNO + (R\text{-}H)^+ \quad (3)$$

Charge exchange ionization has also been reported by methane at chemical ionization pressures (*5*). However, the charge exchange reactions of alkanes are usually superseded by ion molecule reactions involving proton transfer.

[1] On Sabbatical leave from Lincoln University, Lincoln University, Pa.

0003-2700/78/0350-0511$01.00/0 © 1978 American Chemical Society

Table I. Mass Spectra of $C_6H_6$ at Various Source Temperatures and 0.4 Torr[a]

| | Relative intensity | | | | | |
|---|---|---|---|---|---|---|
| m/e | 100 °C | 140 °C | 170 °C | 185 °C | 200 °C | 230 °C |
| 63 | 2 | 1.7 | 1.9 | 1.9 | 2.2 | 2.2 |
| 77 | 1.7 | 2.2 | 4.0 | 4.3 | 5.0 | 6.0 |
| 78 | 100 | 100 | 100 | 100 | 100 | 100 |
| 79 | 12 | 10.0 | 10.0 | 10.0 | 10.0 | 10.0 |
| 115 | 2.5 | 2.2 | 2.2 | 2.0 | 2.0 | 2.0 |
| 128 | 3.2 | 1.7 | 1.6 | 1.6 | 1.6 | 1.6 |
| 154 | 7.0 | 1.7 | 1.7 | 1.7 | 1.7 | 1.7 |
| 155 | 25.0 | 9.0 | 7.0 | 7.0 | 7.0 | 7.0 |
| 156 | 2.7 | 1.2 | 1.2 | 1.2 | 1.2 | 1.2 |

[a] Not corrected for isotope peaks.

Thus the ideal reagent for selective ionization by charge exchange alone would appear to be a molecule which undergoes neither electrophilic addition nor proton transfer readily. Additional considerations require that the substance have a high enough vapor pressure for use in the CI source and that its recombination energy fall within the range of ionization potentials of most organic compounds.

Previous studies (*6–8*) of the ion-molecule reactions occurring in gaseous benzene suggest that it is a candidate for the kind of selective charge exchange reagent being sought. At a pressure of 0.5 Torr and temperature of 200 °C, benzene produces predominantly $C_6H_6^{+\cdot}$ ions. The recombination energy of $C_6H_6^{+\cdot}$ is approximately 9.3 eV (*9*) mid-range in the ionization potentials of most organic compounds. The proton affinities of most organic molecules are generally lower than that of the phenyl radical and thus most samples are not expected to be ionized through proton transfer. The $C_6H_6^{+\cdot}$ ion is not a good electrophile and does not generally attach itself to organic molecules; therefore charge exchange should be the only ionizing event to result from most $C_6H_6^{+\cdot}$ ion–molecule collisions.

The objectives of this study are (1) to investigate the competitive occurrence of charge exchange, proton transfer, and ion attachment in ion–molecule reactions of $C_6H_6^{+\cdot}$ at approximately 0.4 Torr; (2) to examine the specificity of $C_6H_6^{+\cdot}$ as a charge exchange reagent; and (3) to apply $C_6H_6^{+\cdot}$ charge exchange ionization to the analysis of mixtures.

## EXPERIMENTAL

All mass spectra were recorded on a DuPont 21-491 double focusing mass spectrometer equipped with a dual EI/CI source and interfaced to a Varian 2700 gas chromatograph through a glass jet separator. The source has a separate introduction port for reagent gas. The source temperature was maintained at 185 °C (unless otherwise specified) and the reagent gas pressure in the source at 0.4 Torr.

All the CI mass spectra were recorded with a sample concentration of ≤0.5% of the reagent gas. For reactant ion monitoring, the sample concentration was maintained at 1–2% of the reagent gas.

Samples were introduced from the batch inlet system at 150 °C. Samples were introduced from the gas chromatograph using a 6-ft glass column packed with 3% OV-101. Column temperatures are reported with each chromatogram. The GC-MS interface line was maintained at 300°.

An Incos data system was used for the acquisition and processing of data. Gas chromatograms were reconstructed by computer from electron impact scans made under computer control throughout the time of the chromatographic elution. Reagent ion records (*m/e* 78) were reconstructed by computer from repetitive scans made under CI conditions. For ion intensity studies, a spectrum averaged from 50 scans of the benzene reagent gas was subtracted from a spectrum obtained as the average of 50 scans of reagent gas and sample additive.

Benzene was Photorex Reagent grade from J. T. Baker Chemical Company. Benzene-$d_6$ was obtained from Merck Sharp and Dohme, Canada, Ltd., labeled minimum isotopic purity 99.96 atom % D.

Table II. Mass Spectrum of $C_6D_6$ at 185 °C and 0.4 Torr[a]

| m/e | Relative intensity |
|---|---|
| 66 | 1.04 |
| 82 | 3.96 |
| 84 | 100 |
| 85 | 6.5 |
| 86 | 2.6 |
| 122 | 1.0 |
| 136 | 1.2 |
| 166 | 5.0 |

[a] Not corrected for isotope peaks.

Table III. Ionization Potential of Some Substituted Benzenes (*12*) and $\Delta H$ for the Reaction $C_6H_6^{+\cdot} + XC_6H_5 \rightarrow C_6H_5\cdot + (XC_6H_5H)^+$

| Compound | Ionization potential, eV | $\Delta H$, kcal/mol |
|---|---|---|
| 1. Aniline | 7.7 | −10 |
| 2. Anisole | 8.2 | −0.1 |
| 3. Iodobenzene | 8.7 | |
| 4. Toluene | 8.8 | 9.3 |
| 5. Chlorobenzene | 9.1 | 16.6 |
| 6. Fluorobenzene | 9.2 | 16.4 |
| 7. Benzaldehyde | 9.5 | 0.2 |
| 8. Benzonitrile | 9.7 | 4.2 |
| 9. Nitrobenzene | 9.9 | 6.7 |

## RESULTS AND DISCUSSION

The mass spectra of $C_6H_6$ at a pressure of 0.4 Torr and over a source temperature range from 110 to 230 °C are presented in Table I. The $C_6H_6^{+\cdot}$ ions contribute the base peak at all temperatures. The next most intense peak, at *m/e* 155, corresponds to $C_6H_6{\cdot}C_6H_5^+$ ions. The intensity of the $C_6H_6{\cdot}C_6H_5^+$ peak decreases with increasing temperature. The dimer $[C_6H_6]_2^{+\cdot}$ is not significant at any temperature. Both the intensities of $C_6H_6{\cdot}C_6H_5^+$ and $[C_6H_6]_2^{+\cdot}$ and the effect of temperature were more pronounced in an earlier study (*8*), and the differences probably reflect primarily the shorter residence time of ions in the source used in the present work. The mass spectrum of $C_6D_6$ at 0.4 Torr and 185 °C is presented in Table II. The base peak corresponds to $C_6D_6^{+\cdot}$ and $C_6D_6{\cdot}C_6D_5^+$ ions contribute the second most intense peak. The correspondence between the spectra of $C_6H_6$ and $C_6D_6$ is straightforward.

**Charge Exchange Mass Spectra of Monosubstituted Benzenes.** Several monosubstituted benzenes (Table III) with ionization potentials in the range of 7 to 10 eV were used as model compounds to study charge exchange ionization by $C_6H_6^{+\cdot}$ ions. The $C_6H_6^{+\cdot}$ ions would be expected to undergo reaction 4 if the ionization potential of compound A is lower than that of benzene or reaction 5 if the proton affinity of compound B is greater than that of the phenyl radical (*10*).

$$C_6H_6^{+\cdot} + A \rightarrow A^{+\cdot} + C_6H_6 \quad (4)$$

$$C_6H_6^{+\cdot} + B \rightarrow BH^+ + C_6H_5\cdot \quad (5)$$

For aniline the calculated value of $\Delta H$ for reaction 5 is −10 Kcal/mol (*10*). $\Delta H$ values for reaction 5 with other monosubstituted benzenes are estimated using the $\Delta H$ value for aniline and proton affinities of monosubstituted benzenes (*11*). These are presented in Table III.

Compounds with ionization potentials lower than that of benzene (9.2 eV) were found to be ionized by $C_6H_6^{+\cdot}$ and the spectra produced are reported in Table IV. The spectra exhibit the following features: (1) $M^{+\cdot}$ is the base peak; (2)

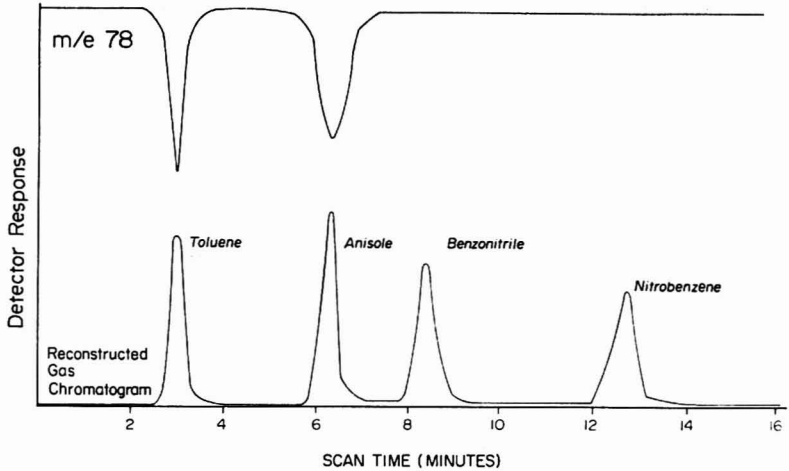


**Figure 1.** Reconstructed gas chromatogram (RGC) (electron impact) and reactant ion trace (RIM) ($C_6H_6^{+\cdot}$ ions) for a mixture of monosubstituted benzene compounds. The gas chromatogram was programmed from 70 °C at 10°/min

very little fragmentation occurs; (3) no peaks are present beyond the molecular ion peak group.

Compounds with ionization potentials greater than 9.2 eV were found to produce very weak spectra. The $(M + H)^+$ ions contribute the base peaks in these spectra, and $M^{+\cdot}$ ions have little or no abundance. Thus ionization is not occurring by charge exchange. The $(M + H)^+$ ions could be formed from a reaction of a molecular ion of the sample with a molecule of the sample

$$M^{+\cdot} + M \rightarrow (M + H)^+ + (M - H)\cdot \quad (6)$$

or proton transfer from any hydrogen-containing reactant ion in the reagent gas to a molecule of the sample (*13*).

$$XH^+ + M \rightarrow MH^+ + X \quad (7)$$

Reactions between molecules of sample were deemed unlikely to occur under the present experimental conditions because the partial pressures of the samples were kept at a low value and the proton affinities of the compounds used are low. Benzene-$d_6$ was used as the reagent gas to determine whether or not proton transfers occur between $C_6H_6^{+\cdot}$ ions and the compounds with ionization potentials greater than 9.2 eV. If protons are transferred from $C_6H_6^{+\cdot}$ ions, then deuteron transfer would be expected to occur from $C_6D_6^{+\cdot}$ ions yielding $(M + D)^+$ peaks. However, no ionization at all took place with $C_6D_6$ as the reagent gas, indicating that the $(M + H)^+$ peaks observed previously were caused by either a contaminant in benzene or in the mass spectrometer.

Benzene-$d_6$ was also used as a reagent gas for compounds with ionization potentials lower than 9.2 eV. The spectra produced are presented in Table IV, and are almost identical with those obtained with $C_6H_6$ as a reagent gas except in the case of aniline. The $C_6D_6$ charge exchange spectrum of aniline contains $M^{+\cdot}$ as the base peak and a small $(M + D)^+$ peak. This is the only compound studied for which $\Delta H$ in reaction 5 is significantly negative; thus proton transfer competes, though weakly, with charge exchange from $C_6H_6^{+\cdot}$ to aniline.

Further evidence that ion–molecule reactions do indeed occur between $C_6H_6^{+\cdot}$ and only those compounds with ionization potentials below 9.2 eV is obtained by monitoring the reactant ion current. In the reactant ion monitoring technique (*14*), the intensity of the reactant ion is monitored as a function

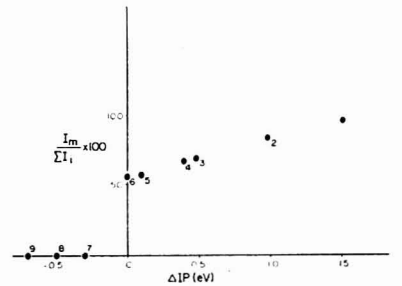


**Figure 2.** Molecular ion current/Total ion current × 100 as a function of the difference between the ionization potential of benzene and that of the sample. Samples are (1) Aniline, (2) Anisole, (3) Iodobenzene, (4) Toluene, (5) Chlorobenzene, (6) Fluorobenzene, (7) Benzaldehyde, (8) Benzonitrile, (9) Nitrobenzene

of time. The intensity of reactant ions decreases when these ions react with a sample, e.g., a sample eluted into the source of the mass spectrometer from the GC. A trace of reactant ion current vs. time resembles a gas chromatogram. The area of a peak depends on the amount of substance passing into the mass spectrometer and it has been proposed (*14*) that the area depends on the rate constant for the ion–molecule reaction.

A mixture of toluene, anisole, benzonitrile, and nitrobenzene was injected through the GC (total ion current, Figure 1). As toluene and anisole were eluted into the source of the mass spectrometer, there was a momentary decrease in the reactant ion current. As benzonitrile and nitrobenzene were eluted into the source, there was no detectable decrease in the reactant ion current. The trace of reactant ion current vs. time is shown in Figure 1. Ionization potentials of benzonitrile and nitrobenzene are higher than that of benzene and no reaction takes place with $C_6H_6^{+\cdot}$ ions.

A graph of the ratios of molecular ion current to total ion current as a function of the difference between the ionization potential of benzene and the ionization potentials of com-

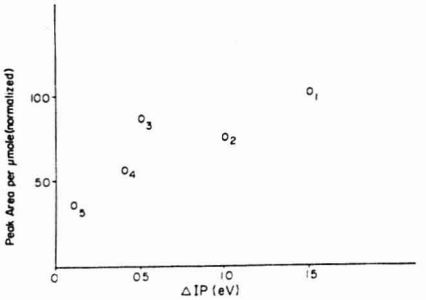


**Figure 3.** Normalized area per μmole of the reactant ion peak as a function of the difference between the ionization potential of benzene and that of the sample. Samples are the same as in Figure 2

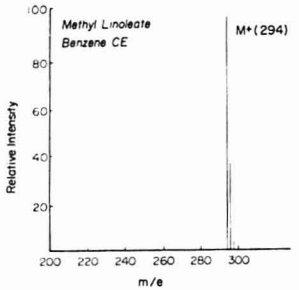


**Figure 4.** Benzene charge exchange mass spectrum of methyl linoleate

pounds 1–9 is shown in Figure 2. It is interesting to note that as $\Delta IP$ increases, the value of $I_m/\Sigma I_i$ also increases. It is likely that the efficiency of charge exchange ionization increases as the difference in the ionization potential of the reagent gas and the additive increases, at least in the close interval examined here. In order to test this, known amounts of compounds with ionization potentials below 9.2 eV were injected through the GC. The area per μmole of the sample as a function of $\Delta IP$ is shown in Figure 3. It is observed that the area/μmole increases as the $\Delta IP$ increases. This indicates that the relative rate constants for the ion–molecule reaction between $C_6H_6^{+\cdot}$ and these compounds increase with increasing $\Delta IP$.

**Charge Exchange between $C_6H_6^{+\cdot}$ and Fatty Acid.** In order to demonstrate the utility of $C_6H_6^{+\cdot}$ as a reagent ion for charge exchange reactions with mixtures encountered in bio-organic problems, seven esters of saturated and unsaturated fatty acids were examined (Table V). Only the esters of unsaturated fatty acids were found to be ionized by $C_6H_6^{+\cdot}$. All the spectra contain intense molecular ion peaks, small M + 1 peaks and few fragment peaks. The molecular ion is the base peak in all the spectra except in the case of methyl oleate. In this spectrum $[M - 32]^{+\cdot}$ ions contribute the base peak and the relative intensity of the $M^+$ peak is about 40%. The spectrum of methyl linoleate is shown in Figure 4. Although ionization potentials of fatty acids do not appear to have been measured, it is apparent from the present findings that the ionization potentials of unsaturated fatty acids lie below 9.2 eV. The ionization potentials of some model compounds are given in Table V, in which unsaturated hydrocarbons are seen to have ionization potentials below that of benzene.

The esters of saturated fatty acids were ionized much less efficiently, and then apparently by proton transfer, since the spectra contained $(M + H)^+$ peaks as the base peaks in addition to other fragments. Evidence that this was not caused by proton transfer from $C_6H_6^{+\cdot}$ was obtained by reactant ion monitoring. A mixture of five esters was prepared and injected through the GC. As the ester of each unsaturated fatty acid was eluted into the source, a decrease in the reactant ion current was observed. As the esters of the saturated fatty acids were eluted, no change in the reactant ion current was recorded. The trace of the reactant ion current vs. time is shown in Figure 5, along with the gas chromatogram reconstructed by the computer from electron impact spectra of the same mixture.

**$C_6H_6^{+\cdot}$ Charge Exchange Spectra of Miscellaneous Compounds.** In order to demonstrate the versatility of this reagent, the benzene charge exchange spectra of nalorphine, cholesterol, and the methyl ester of tryptophan (introduced by direct probe) are shown in Figures 6 to 8. Each of the

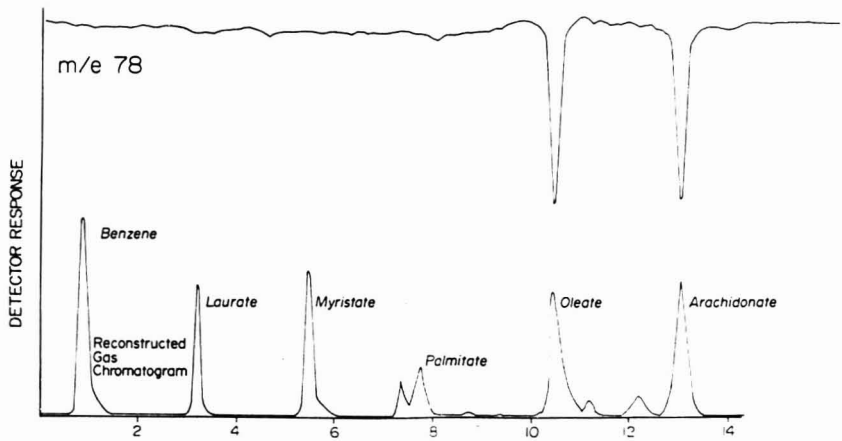


**Figure 5.** Reconstructed gas chromatogram (RGC) (electron impact) and reactant ion trace (RIM) ($C_6H_6^{+\cdot}$ ions) for a mixture of fatty acid esters. The gas chromatograph was programmed from 175 °C at 6°/min

Table IV. $C_6H_6^{+\cdot}$ and $C_6D_6^{+\cdot}$ Charge Exchange Mass Spectra of Monosubstituted Benzenes[a]

| | $C_6H_6^{+\cdot}$ | | | $C_6D_6^{+\cdot}$ | | | |
|---|---|---|---|---|---|---|---|
| Substituent | $(M-1)^+$ | $M^{+\cdot}$ | $(M+1)^+$ | $(M-1)^+$ | $M^{+\cdot}$ | $(M+1)^+$ | $(M+2)^+$ |
| $NH_2$ | 2 | 100 | 11 | 1.5 | 100 | 8 | 4 |
| $OCH_3$ | - | 100 | 9 | - | 100 | 8 | - |
| I | - | 100 | 7 | - | 100 | 7 | - |
| $CH_3$ | 35 | 100 | 8 | 25 | 100 | 8 | - |
| Cl | | 100 | 7 | | | | |
| F | | 100 | 7 | | | | |

[a] Not corrected for isotope peaks.

Table V. Fatty Acid Esters and Related Compounds

| Compound | Number of double bonds | *IP* (*12*) |
|---|---|---|
| Methyl laurate | 0 | - |
| Methyl myristate | 0 | - |
| Methyl palmitate | 0 | - |
| Methyl oleate | 1 | - |
| Methyl linoleate | 2 | - |
| Methyl linolinate | 3 | - |
| Ethyl arachidonate | 4 | - |
| Methyl pentanoate | 0 | 10.40 |
| *N*-hexane | 0 | 10.18 |
| 1-Hexene | 1 | 9.46 |
| *trans*-3-Hexene | 1 | 8.95 |
| 2,4-Hexadiene | 2 | 8.48 |

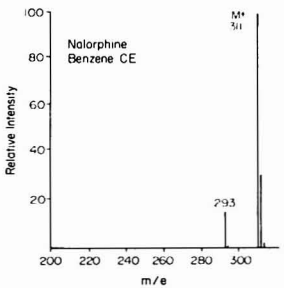


Figure 6. Benzene charge exchange mass spectrum of nalorphine

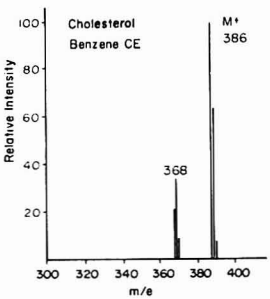


Figure 7. Benzene charge exchange mass spectrum of cholesterol

spectra contains a molecular ion peak as the base peak, accompanied by little fragmentation. The intensity of $(M+1)$ ions is somewhat larger than the expected isotopic value, presumably reflecting proton transfer from species other than $C_6H_6^{+\cdot}$. No attachment ions are detected. The intense molecular ions and the fragmentation greatly reduced relative to electron impact or proton transfer chemical ionization

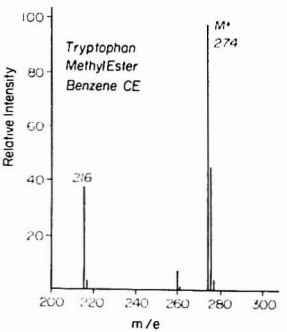


Figure 8. Benzene charge exchange mass spectrum of tryptophan methyl ester

recommend this charge transfer technique for certain analytical problems.

## CONCLUSION

Benzene ions can be used quite satisfactorily for charge exchange of samples with ionization potentials below 9.2 eV. Benzene ions have the advantage over many other reagent ions in that proton transfer, hydride abstraction, and ion attachment do not occur significantly in competition with charge exchange. Benzene ions will ionize unsaturated fatty acids by charge exchange in the presence of saturated fatty acids.

## ACKNOWLEDGMENT

We thank L. D. Smucker and Y. Kishimoto for gifts of fatty acid esters.

## LITERATURE CITED

(1) N. Einolf and B. Munson, *Int. J. Mass Spectrom. Ion Phys.*, **9**, 145 (1972).
(2) D. F. Hunt and J. F. Ryan, *J. Chem. Soc., Chem. Commun.*, 620 (1972).
(3) B. Jelus, B. Munson, and C. Fenselau, *Anal. Chem.*, **46**, 729 (1974).
(4) I. Jardine and C. Fenselau, *Anal. Chem.*, **47**, 730 (1975).
(5) R. L. Foltz, D. A. Knowlton, D. K. Lin, and A. F. Fentiman, Jr., "Proceedings of the Second International Conference on Stable Isotopes, Oakbrook, Ill., October 1975", National Technical Information Service, U.S. Department of Commerce, Springfield, Va.
(6) F. H. Field, P. Hamlet, and W. F. Libby, *J. Am. Chem. Soc.*, **89**, 6035 (1967).
(7) S. Wexler and R. P. Clow, *J. Am. Chem. Soc.*, **90**, 3940 (1968).
(8) F. H. Field, P. Hamlet, and W. F. Libby, *J. Am. Chem. Soc.*, **91**, 2839 (1969).
(9) E. Lindholm, in "Ion-Molecular Reactions", J. L. Franklin, Ed., Plenum Press, New York, N.Y., 1972, Vol. 2, p 466.
(10) E. C. Horning, M. G. Horning, D. I. Carrol, I. Dzidic, and R. N. Stillwell, *Anal. Chem.*, **45**, 938 (1973).
(11) Y. K. Lau and P. Kebarle, *J. Am. Chem. Soc.*, **98**, 7452 (1976).
(12) H. M. Rosenstock, K. Draxl, B. W. Steiner, and T. J. Herron, *J. Phys. Chem. Ref. Data*, Vol. 6, Supplement 1 (1977).
(13) R. L. Foltz, paper presented at the 19th Annual Conference on Mass Spectrometry of the American Society for Mass Spectrometry, Atlanta, Ga., May 1971.
(14) F. Hatch and B. Munson, *Anal. Chem.*, **49**, 731 (1977).

RECEIVED for review September 6, 1977. Accepted December 22, 1977. This work was supported by U.S.P.H.S. grants GM-21248, GM-70417, and MARC Fellowship GM-05709.

# Determination of Dissolved Iron in Seawater by Radioisotope Dilution and the Chelating Agent Bathophenanthroline

**G. M. Sharma* and Henry R. DuBois**

*Department of Chemical Oceanography, New York Ocean Science Laboratory, Montauk, New York 11954*

**A new radioisotope dilution method for the direct determination of ionic iron in a small volume of ocean water is described. Known amounts of unlabeled ferrous ions are added to the aliquots of the radioactive ferrous ions ($^{59}Fe^{2+}$) and the mixtures are reacted with bathophenanthroline to yield [iron-(batho)$_3$]$^{2+}$ complex. A standard curve is constructed by plotting % batho-bound radioactivities against the amounts of unlabeled ferrous ions on logit-log paper. The concentration of iron in an unknown sample is obtained by observing the % radioactivity of the labeled iron bound by bathophenanthroline after radiodilution by the unlabeled iron present in a known volume of the sample; the concentration is read from the standard curve. The interference due to cuprous ions is eliminated by complexing them with neocuproine. The method is simple and suitable for routine determination of soluble iron on shipboard.**

Although biologically essential trace elements (Fe, Cu, Co, Mn, Zn, Mo, V, etc.) occur at low concentrations in ocean waters, marine organisms are able to absorb them in quantities far in excess of their biological needs (*1*). This is well demonstrated by autotrophic algae which contain trace elements at concentrations as high as $10^6$ times of their seawater concentrations (2). Biological uptake processes of this magnitude should produce seasonal variations in the distribution of elements being consumed. Experimental verification of this phenomenon would require analysis of a large number of samples per season. Projects of this type would be speeded up considerably if the analysis could be carried out on shipboard. For this, simple methods for the direct determination of trace elements in a small volume of seawater (1 mL or less) are needed. In this paper we describe a radioisotope dilution method for the determination of ionic iron which enjoys these features. The method is based on the observation that after reduction to the ferrous state, the ionic iron in seawater samples or in standard solutions competes with the added radioactive ferrous ions ($^{59}Fe^{2+}$) for complexing with the iron specific binder, 4,7-diphenyl-1,10-phenanthroline (bathophenanthroline or simply batho) on an equal basis. In competitive binding experiments, the radioactivity bound usually represents the degree of isotope dilution (3, 4). In view of this we can write Equations 1-3.

$$\frac{B}{B_0} = \frac{m}{m+x} \tag{1}$$

Let $B/B_0 = P$, then

$$\frac{P}{1-P} = \frac{m}{x} \tag{2}$$

$$\ln \frac{P}{1-P} \equiv \text{logit } P = \ln (m) - \ln (x) = \ln (m) - 2.303 \log_{10} (x) \tag{3}$$

In these equations, $B_0$ is the radioactivity bound when $a$ units (substoichiometric amount) of bathophenanthroline is reacted with $m$ units of the labeled ferrous ions and $B$ is the radioactivity bound by $a$ units of bathophenanthroline when reacted with a mixture of $m$ units of the labeled and $x$ units of the unlabeled ferrous ions. The expressions $B/B_0 = P$ and $m/(m + x)$ represent the % batho-bound radioactivity and degree of isotope dilution respectively. When $x$ is known and $P$ is plotted vs. $x$ on a logit-log paper, a linear standard curve is obtained. The slope of the line will be $-1$ when $\log_e x$ is used or the slope will be $-2.303$ when $\log_{10} x$ is used. Any large deviation of the slope of the experimental line from the constant value should indicate interference from some other element or elements to the binding of ferrous ions with bathophenanthroline. Using this criterion it was discovered that, except for ionic copper, no other ions present at their normal concentration in seawater compete with ferrous ions for binding to bathophenanthroline. The interference due to copper ions was eliminated by complexing them with the copper specific binder 2,9-dimethyl-1,10-phenanthroline (neocuproine). The concentration of iron in an unknown sample is obtained by adding a known volume of the sample to the aliquot of the radioactive iron and observing the percent radioactivity bound by bathophenanthroline from this mixture. The concentration is read from the standard curve. The sensitivity range of the method appears to extend from the lowest to the highest values of iron encountered in ocean waters. For other applications of this technique, Ref. 5 may be consulted.

## EXPERIMENTAL

**Apparatus.** Radioactivity was measured with a Baird Atomic Gamma Counter (Baird-Atomic, Inc., Cambridge, Mass.) equipped with a well type scintillation detector (Model 810), a general purpose scaler (Model 132), and a timer (Model 960A). Reagents used in the assay were pipetted with a Schwarz/Mann "biopipet" or a "dialamatic microdispenser" (calibration 0–100 $\mu$L) made by Drummond Scientific Company, Broomall, Pa., (distributor, Fisher Scientific Co.). Logit-log graph papers were purchased from Schwarz/Mann, Mountain View Ave., Orangeburg, N.Y. 10962. Whatman GF/C filter pads for filtering seawater were obtained from VWR Scientific Company. All reactions were carried out in polypropylene tubes. Polypropylene tubes and other plastic apparatus used in assays were cleaned thoroughly by immersing in 50% v/v hydrochloride acid for 2 h and then washing liberally with double-distilled water.

**Chemicals.** Iron-59 solutions containing on the day of calibration ~100 $\mu$Ci of $^{59}$Fe as ferric chloride in 1.0 mL of 0.1 N HCl were purchased from Amersham/Searle Corporation. Total iron in each vial was ~13 $\mu$g. Bathophenanthroline and neocuproine were purchased from G. Frederick Smith Chemical Company, Columbus, Ohio. Analytical grade sodium acetate, hydroxylamine hydrochloride, and hydrochloric acid were obtained from J. T. Baker Chemical Company. Isoamyl alcohol was purchased from Fisher Scientific Company. Redistilled ethanol was used to prepare bathophenanthroline and neocuproine solutions.

**Preparation of Reagents.** *Bathophenanthroline Solution (Batho-solution).* A stock batho-solution was prepared by dissolving 0.0700 g of 4,7-diphenyl-1,10-phenanthroline in 100 mL of ethyl alcohol and then adding 100 mL of distilled water. The stock solution was kept in a well stoppered polyethylene bottle. Working solutions containing 350, 700, and 1230 ng batho-

0003-2700/78/0350-0516$01.00/0 © 1978 American Chemical Society

phenanthroline in 100 μL of the solvent were prepared by diluting 0.1, 0.2, and 0.35-mL aliquots of the stock solution to 10 mL with 50% v/v ethanol–water mixture. These solutions are respectively $1.05 \times 10^{-6}$, $2.11 \times 10^{-6}$, and $3.68 \times 10^{-5}$ M bathophenanthroline.

*Neocuproine Solution.* A stock solution of neocuproine was prepared by dissolving 100 mg of 2,9-dimethyl-1,10-phenanthroline in 100 mL of ethanol. The working solution was prepared by diluting 1 mL of the stock solution to 10 mL with 50% v/v ethanol–water mixture.

*Iron-Free Hydroxylamine Hydrochloride.* The reagent grade hydroxylamine hydrochloride was crystallized twice from 10% v/v hydrochloric acid and then from double distilled water. The crystallized material was dried. The dried salt, 10.0 g, was dissolved in 100 mL of distilled water. The solution was made iron-free by reacting with bathophenanthroline and extracting the red iron-batho complex with isoamyl alcohol as described by Strickland and Parsons (6). The iron-free hydroxylamine solution was stored in a well-stoppered polyethylene bottle.

*Iron-Free Sodium Acetate Buffer.* Reagent grade sodium acetate trihydrate, 75 g, was dissolved in 100 mL of distilled water and the solution was made iron-free according to the procedure described by Strickland and Parsons (6).

*Iron and Copper-Free Seawater.* Seawater was filtered through a GF/C filter pad. A 100-mL aliquot of the filtrate was mixed with 10 mL of 0.48 N HCl and 2.0 mL of hydroxylamine hydrochloride solution in a clean Nalgene separatory funnel and the mixture was allowed to stand for 5 min to complete the reduction of ferric to ferrous and cupric to cuprous ions. Then 2.0 mL of acetate buffer and 5 mL of batho-solution were added and, after mixing, the mixture was let stand for 10 min. The complexes of ferrous and cuprous ions with bathophenanthroline were extracted with 30 mL of isoamyl alcohol. The aqueous layer was separated and boiled in a flask for 10 min to expel most of the isoamyl alcohol. This iron and copper-free seawater was stored in a well-stoppered polyethylene bottle.

*Iron-59 Solutions.* Solutions containing ~15 ng, 50 ng, and 100 ng of $Fe^{2+}$/100 μL and having 5000–17 000 cpm/100 μL were prepared by mixing appropriate volumes of 10 ppm ferric chloride solution and radioiron solution in 10-mL volumetric flasks. After the addition of 2.0 mL of hydroxylamine hydrochloride solution and 0.4 mL of concentrated HCl, the volumes were brought to 10 mL by adding double-distilled water. The solutions were stored at 4 °C in well-stoppered plastic tubes. The quantity of hydroxylamine present in these solutions is sufficient to reduce the progressively increasing amounts of ferric ions used in the competitive binding experiments.

*Cold Iron Solutions.* The solutions containing 10, 1, and 0.1 μg ferric ions in 1.0 mL of distilled water were prepared daily from 1000 ppm $Fe^{3+}$ stock solution. The 1000 ppm $Fe^{3+}$ stock solution was prepared by dissolving 0.5000 g of analytical grade iron wire in 20 mL of 6 N HCl and making the volume to 500 mL with distilled water.

*Copper Solutions.* Working solutions containing 10, 1.0, and 0.1 μg of $Cu^{2+}$ in 1.0 mL of distilled water were prepared by serial dilutions of 1000 ppm copper solution purchased from Fisher Scientific Company.

**Saturation Curve.** One milliliter of distilled water was placed in each of the 18 sequentially numbered polypropylene tubes. For duplicate runs, the tubes were arranged in pairs and progressively increasing amounts of radioactive ferrous ions were added to them. After counting the radioactivity in each tube, the pH of the solutions was brought within the range 4–4.5 by adding 50 μL of acetate buffer and mixing. To each tube, 100 μL of $3.68 \times 10^{-5}$ M batho-solution was added and, after mixing, the tubes were allowed to stand at ambient temperature for 20 min. During this period the tubes were vortexed three times (after 5, 10, and 20 min) so that the iron–batho complex produced during the reaction could coat the sides of the tubes. The aqueous solutions were poured into another set of similarly numbered tubes. By measuring the radioactivity in these tubes, the counts due to uncomplexed iron were obtained. Rinsing the assay tubes with water did not improve the precision on counting the uncomplexed iron. The radioactivities bound to bathophenanthroline were calculated by subtracting the counts due to uncomplexed iron from the total counts. The calculated batho-bound radioactivities were almost identical with the ones obtained by counting iron–batho complex directly. The iron–batho complex coated to the sides of the assay tubes was dissolved in 2 mL of isoamyl alcohol prior to counting. The saturation curve shown in Figure 1 was obtained by plotting total counts vs. the bound counts.

**Table I. Counting Data of a Typical Competitive Binding Experiment: Iron$^{59}$ = 100 ng; total cpm, 16 712**

| Tube No. | Cold Fe, ng | Free cpm | Bound cpm | $B/B_0 \times 100$ |
|---|---|---|---|---|
| 1 | 0 | 5 100 | 11 612 | $B_0$ = 11835 |
| 2 | 0 | 4 948 | 11 764 | |
| 3 | 0 | 4 584 | 12 128 | |
| 4 | 10 | 6 366 | 10 346 | 87.4 |
| 5 | 10 | 5 906 | 10 806 | 91.3 |
| 6 | 10 | 5 620 | 11 092 | 93.7 |
| 7 | 20 | 6 782 | 9 930 | 83.9 |
| 8 | 20 | 6 392 | 10 320 | 87.2 |
| 9 | 20 | 7 016 | 9 696 | 81.9 |
| 10 | 50 | 8 392 | 8 320 | 70.3 |
| 11 | 50 | 8 242 | 8 470 | 71.6 |
| 12 | 50 | 8 264 | 8 448 | 71.4 |
| 13 | 100 | 10 102 | 6 610 | 55.9 |
| 14 | 100 | 10 080 | 6 632 | 56.0 |
| 15 | 100 | 10 130 | 6 582 | 55.6 |
| 16 | 200 | 12 406 | 4 306 | 36.4 |
| 17 | 200 | 12 352 | 4 360 | 36.8 |
| 18 | 200 | 12 028 | 4 684 | 39.6 |
| 19 | 500 | 14 728 | 1 984 | 16.8 |
| 20 | 500 | 14 748 | 1 964 | 16.6 |
| 21 | 500 | 14 728 | 1 984 | 16.8 |
| 22 | 1 000 | 16 018 | 694 | 5.9 |
| 23 | 1 000 | 15 890 | 822 | 6.9 |

**Competitive Binding Studies.** The experiments were done either in duplicate or in triplicate in well-cleaned polypropylene tubes using distilled water, filtered seawater, and seawater made free of iron and copper ions. The amounts of labeled iron used in these experiments are not to be taken too exactly, rather they are intended to indicate a concentration that is orders of magnitude higher than the $1/K$ value of bathophenanthroline. The concentration of batho-solutions were such that 100-μL aliquot would bind 40–70% of the labeled iron when the dose of the unlabeled iron was zero. Actual amounts of radioactive ferrous ions and bathophenanthroline used in the experiments are listed in the legend of the curves of the experimental data (see Figures 2 and 3). Progressively increasing amounts of the unlabeled iron added to the labeled iron may be read from the abscissa of the graphs. The procedure for obtaining data in triplicate is described below.

Water, 1.0 mL, was added to 24 sequentially numbered polypropylene tubes. The tubes were arranged in sets of three, and to sets 2–8 progressively increasing amounts of unlabeled ferric ions were added. Then, 100 μL of iron-59 solution was added to each tube. After mixing, the tubes were allowed to stand at room temperature for 5 min to complete the reduction of the unlabeled ferric ions to the ferrous state by the hydroxylamine present in the iron-59 solution. During this period, the radioactivities in tubes 1–3 were counted and averaged to give total counts for the experiment. Finally, 50 μL of acetate buffer and 100 μL of batho-solution of appropriate molarity were added to each tube and the contents of the tubes were mixed thoroughly using a vortex mixer. The procedure for separating the iron–batho complex from the uncomplexed iron was the same as described under "Preparation of the Saturation Curve". The counts due to uncomplexed iron were determined and subtracted from the total counts to give counts bound by bathophenanthroline. The bound counts in tubes 1, 2, and 3 were averaged and the averaged counts were represented by the symbol $B_0$. The counts bound by bathophenanthroline in all other tubes were represented by the symbol $B$. Percent radioactivities bound by bathophenanthroline were calculated using the expression $P = B/B_0 \times 100$. By plotting $P$ against the amounts of cold iron on logit-log papers, the curves shown in Figures 2 and 3 were obtained. Counting data of a typical experiment and calculation of $P$ from it is shown in Table I.

Table II. Inhibition of the Binding of Iron to Bathophenanthroline by Copper. $Iron^{59}$ = 100 ng; total cpm = 7751; batho = 100 μL $3.68 \times 10^{-5}$ M Solution

| Tube | Cu, ng | Neocuproine, μL | Free cpm | Bound cpm | $B/B_0 \times 100$ |
|---|---|---|---|---|---|
| 1 | 0 | 0 | 3253 | 4498 | $B_0$ = 4522 |
| 2 | 0 | 0 | 3195 | 4556 | |
| 3 | 0 | 100 | 3295 | 4456 | |
| 4 | 10 | 0 | 3471 | 4280 | 94.6 |
| 5 | 10 | 0 | 3521 | 4230 | 93.5 |
| 6 | 10 | 100 | 3207 | 4544 | 100.5 |
| 7 | 20 | 0 | 4157 | 3594 | 79.5 |
| 8 | 20 | 0 | 3859 | 3890 | 86.1 |
| 9 | 20 | 100 | 3167 | 4584 | 101.4 |
| 10 | 50 | 0 | 4885 | 2866 | 63.4 |
| 11 | 50 | 0 | 4883 | 2868 | 63.4 |
| 12 | 50 | 100 | 3399 | 4352 | 96.2 |
| 13 | 100 | 0 | 6107 | 1644 | 36.4 |
| 14 | 100 | 0 | 5835 | 1916 | 42.4 |
| 15 | 100 | 100 | 3169 | 4582 | 101.3 |
| 16 | 200 | 0 | 7457 | 294 | 6.5 |
| 17 | 200 | 0 | 7275 | 476 | 10.5 |
| 18 | 200 | 100 | 3425 | 4326 | 95.7 |

Curve B of Figure 3 is the graphical representation of these data.

**Interference due to Copper.** Distilled water, 1.00 mL, and radioiron, 100 ng, were added to each of the 18 sequentially numbered polypropylene tubes. The tubes were arranged in sets of three, and to sets 2–6 known amounts of cupric ions were added (see Table II). After mixing, the contents of the tubes were allowed to stand at room temperature for 5 min to complete the reduction of cupric to cuprous ions. During this period the radioactivities in tubes 1–3 were counted and averaged to give total counts used in the experiment. After adding 50 μL of acetate buffer to all tubes, 100 μL of neocuproine solution was pipetted to one tube of each set (i.e., tubes 3, 6, 9, 12, 15, and 18). This was followed by the addition of 100 μL of $3.68 \times 10^{-5}$ M batho-solution to each tube. The experimental procedure for determining the radioactivities bound to bathophenanthroline was the same as described in the preceding experiments. The counting data of this experiment are given in Table II. The line shown in Figure 4 was obtained by plotting % batho-bound radioactivities vs. the amounts of copper added on a logit-log paper.

**Preparation of the Standard Curve.** The data for the construction of the standard curve was gathered in iron and copper-free seawater. Except for the addition of 100 μL of neocuproine solution prior to the reaction with bathophenanthroline the procedure for obtaining the data was the same as described under the "Competitive Binding Studies". The standard curve constructed from the data obtained by reacting 100-μL aliquots of $2.11 \times 10^{-5}$ M batho-solution with mixtures of 50 ng of radioactive iron and progressively increasing amounts of the unlabeled iron had a slope of −2.20.

**Assay Procedure.** The seawater samples were filtered through GF/C filter pads to remove particulate iron. One-milliliter aliquots of the filtrates were placed in polypropylene tubes and the same amounts of radioactive iron, acetate buffer, neocuproine and batho-solutions as used in the preparations of the standard curve were added to each tube. The % radioactivities bound to bathophenanthroline were determined and the concentrations were read from the standard curve. These samples were also analyzed by the colorimetric method described in Ref. 6. The results are compared in Table III.

Table III. Comparison of the Results of Iron Determination of Seawater by the Radioisotope Dilution Method and by the Colorimetric Method Described by Strickland and Parsons (6)

| Isotopic method (duplicate analysis),[a] μg/L | Strickland and Parsons method (single determination),[b] μg/L |
|---|---|
| 6.0, 4.2 | 4.9 |
| 5.0, 4.8 | 4.3 |
| 4.1, 4.5 | 5.0 |
| 7.0, 7.5 | 6.0 |
| 5.2, 5.8 | 5.8 |

[a] 1.0 mL of seawater was used for each determination. [b] 100 mL of seawater was used for each determination by colorimetric method.

## RESULTS AND DISCUSSION

The determination of iron by competitive binding techniques would require three components: (1) A radioisotope of iron having high specific activity, (2) a substance that binds specifically and avidly to ionic iron, and (3) some technique for separating the iron-binder complex from the uncomplexed iron. Preparation of ferric chloride labeled with iron-59, a strong γ emitter, are commercially available. The bidentate heterocyclic amine, bathophenanthroline, is known to react with ferrous ions almost specifically to give $[Fe(batho)_3]^{2+}$ complex (7). The formation constant (8), $K$, of the complex is $10^{10}$ which suggests that even at parts per billion level the ferrous ions will react with substoichiometric amounts of bathophenanthroline to give theoretical yield of $[Fe(batho)_3]^{2+}$ complex. Thus two of the three components needed for the radiochemical determination of iron are readily available.

In order to develop a technique for separating the iron–batho complex from the uncomplexed iron, known amounts (20–100 ng) of radioactive ferrous ions were reacted with 100-μL aliquots of $3.68 \times 10^{-5}$ M batho-solution in polypropylene tubes. Interestingly, the iron–batho complex produced during the reaction was found to coat the sides of the tubes very tenaciously when the contents of the tubes were swirled using a vortex mixer. The aqueous solutions containing the uncomplexed iron were poured into another set of tubes. The counts in these tubes were determined and subtracted from the total counts to give counts due to iron–batho complex coated to the sides of the first set of tubes. When batho-bound radioactivities were plotted vs. the total counts, the saturation curve shown in Figure 1 was obtained. This curve clearly demonstrates that even at low concentrations the reaction between ferrous ions and stoichiometric amount of bathophenanthroline practically goes to completion. The coating of the iron-batho complex to the sides of the assay tubes makes the quantitative separation of the uncomplexed iron from the bound iron an easy process.

Competitions between known amounts of labeled and unlabeled ferrous ions for binding with bathophenanthroline were studied in three separate media: viz, distilled water, seawater, and seawater made free of iron and copper ions. The curves A, B, and C of Figure 2 represent data obtained in distilled water using, respectively, 15, 50, and 100 ng of hot iron. The amounts of cold iron added to the aliquots of hot iron may be read from the abscissa of the graphs. The slopes of these curves lie in the range −2.20 to −2.30, which is in close agreement with the slope of −2.303 expected for a theoretical curve. In sharp contrast to this the data obtained in filtered seawater gave a curve (Figure 3, curve A) which had a slope of −2.80. The increase in the slope of the curve upon going from distilled water to seawater was attributed to the competition of cuprous ions, present in the later medium, with ferrous ions for binding to bathophenanthroline. This view was substantiated when the curve (curve B; Figure 3) constructed from the data obtained in copper-free seawater exhibited a slope of −2.30.

It is well known that neocuproine binds specifically with cuprous ions (7). When the competitive binding experiments were repeated by including this reagent in the protocol, the interference due to copper was found to have been eliminated. The data gave curves which had slopes close to the expected value of −2.303.

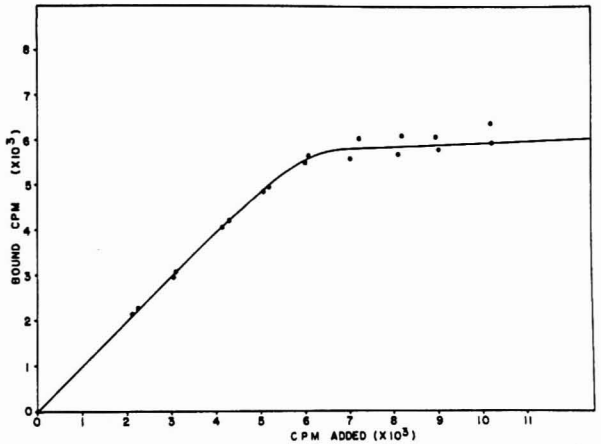


**Figure 1.** Saturation of bathophenanthroline with iron in distilled water. Reactants: batho, 100 μL of 3.68 × $10^{-5}$ M solution; $iron^{59}$ = 20–100 ng (1000 cpm ~10 ng)

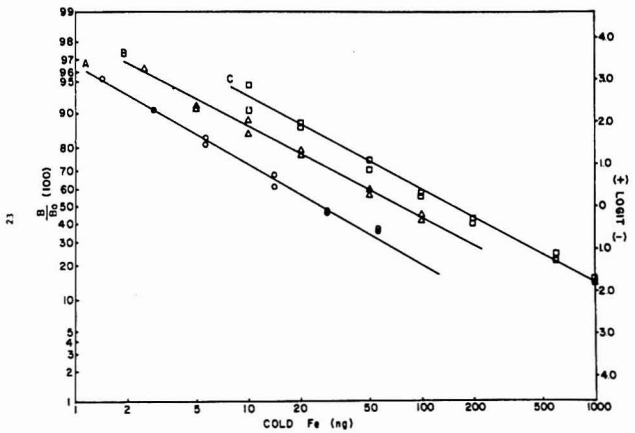


**Figure 2.** Competitive binding curves in distilled water. Curve A: $iron^{59}$ ~15 ng, cpm = 6462; batho, 100 μL of 1.05 × $10^{-5}$ M solution; $B_0$ = 66.5%; slope = −2.30. Curve B: $iron^{59}$ ~50 ng, cpm = 11095; batho, 100 μL of 2.11 × $10^{-5}$ M solution; $B_0$ = 61.8%; slope = −2.20. Curve C: $iron^{59}$ ~100 ng, cpm = 17524; batho, 100 μL of 3.68 × $10^{-5}$ M solution; $B_0$ = 59.4%; slope = −2.20

Unequivocal proof for the interference of copper in the binding of iron to bathophenanthroline and for the ability of neocuproine to eliminate this interference was provided by the results of the following experiment. Progressively increasing amounts of cupric ions were added to the aliquots of radioiron solution and the mixtures were reacted with bathophenanthroline both in the presence and in the absence of neocuproine. The counting data of this experiment are collated in Table III. It may be noticed that less and less radioactivity binds to bathophenanthroline as the dose of copper added to the radioiron is increased from 0–200 ng. In the presence of neocuproine, bathophenanthroline binds the expected amount of radioactivity irrespective of the quantity of copper added to the radioiron. When percent batho-bound radioactivity is plotted vs. added copper on a logit-log paper, the curve shown in Figure 4 is obtained. The linearity of this curve (slope −3.20) suggests that it should be possible to determine the concentrations of copper in seawater by exploiting the ability of cuprous ions to stoichiometrically reduce the binding of iron to bathophenanthroline. The only requirement is that a technique for eliminating the interference due to iron present in seawater should be developed. Work on this problem is being actively pursued.

In Figures 2 and 3, 50% dilution of the radioactivity should correspond to a point where the dose of cold iron added is equal to the amount of labeled iron used. It may be pointed out that in nearly every competitive binding experiment, the quantity of hot iron read from the logit-log plots was ~10–25 ng greater than the actual amount of iron-59 used in the experiments. This discrepancy was attributed to the contamination of polypropylene tubes by iron although precautions were taken to clean them thoroughly. Nevertheless, this contamination does not affect the reproducibility of the assay when all the tubes are cleaned in exactly the same way.

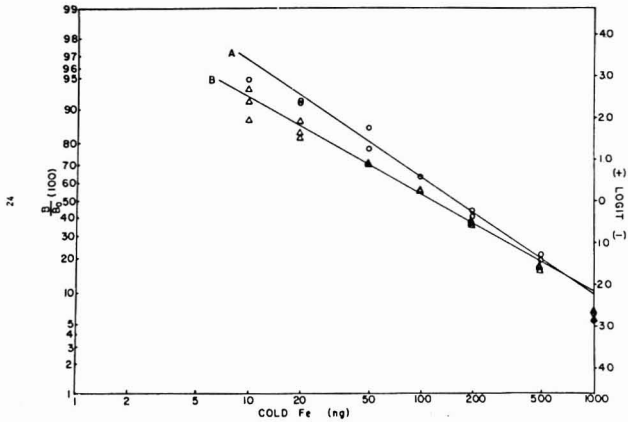


**Figure 3.** Competitive binding curves in filtered seawater and iron and copper-free seawater. Curve A: filtered seawater; iron$^{59}$ ~100 ng, cpm = 16540; batho, 100 μL 3.68 × $10^{-5}$ M solution; $B_0$ = 52.5%; slope = −2.80. Curve B: iron and copper-free seawater: iron$^{59}$ ~100 ng, cpm = 16457; batho, 150 μL of 3.68 × $10^{-5}$ M solution; $B_0$ = 71.8%; slope = −2.30

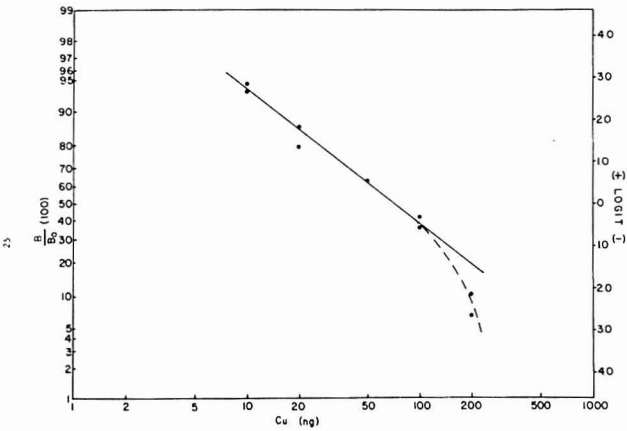


**Figure 4.** Inhibition of iron–batho complex formation due to copper. Reactants: iron$^{59}$ ~100 ng, cpm = 7751; copper = 0–200 ng; batho, 100 μL of 3.68 × $10^{-5}$ M solution; $B_0$ = 58.3%; slope = −3.20

The tubes cleaned in identical fashion are expected to contain the same quantity of residual iron.

In the procedure for the preparation of the standard curve and determination of iron in unknown samples, neocuproine was used to complex copper ions which otherwise interfere with the binding of iron to bathophenanthroline. Several seawater samples were analyzed for the concentration of the dissolved iron by the isotopic method and by the colorimetric method described in the literature (*6*). The results (Table III) indicated a fair agreement between the two methods.

It may be pointed out that, to approximate shipboard conditions, we carried out all experiments in a laboratory which was neither air conditioned nor kept solely for trace element work. The major source of contamination, under these conditions, was the air-borne dust which completely voids the assay if the tubes are not kept capped at all times except for the addition of reagents. With this precaution, the values obtained in replicate determinations agreed well among themselves in the range 10–100 ng Fe/mL. The relative standard deviation at 10 and 20 ng Fe/mL was 13.6 and 12.4%, respectively. In the range around 1–5 ng Fe/mL level, the scatter of individual determinations around the mean was found to be much larger if all sources of contamination were not scrupulously eliminated. This point is well demonstrated by the data reported in Table III.

## LITERATURE CITED

(1) H. J. M. Bowen, "Trace Elements in Biochemistry", Academic Press, London and New York, 1966, pp 68–69.
(2) J. P. Riley and R. Chester, "Introduction to Marine Chemistry", Academic Press, London and New York, 1971, p 92.
(3) A. Zettner, *Clin. Chem.* (*Winston-Salem, N.C.*), **19**, 699–705 (1973).
(4) A. Zettner and P. E. Duly, *Clin. Chem.* (*Winston-Salem, N.C.*), **20**, 5–14 (1974).
(5) J. Ruzicka and J. Stary, "Substiochiometry in Radiochemical Analysis", Pergamon Press, Oxford, 1968.
(6) J. D. H. Strickland and T. R. Parsons, "A Practical Handbook of Seawater Analysis", J. C. Stevenson, Ed., Fisheries Research Board of Canada, Ottawa, 1968, pp 99–107.

(7) J. P. Riley "Chemical Oceanography," Vol. 2, J. P. Riley and G. Skirrow. Ed., Academic Press, London and New York, 1965, pp 378–381, 384.
(8) E. König, *Coord. Chem. Rev.*, 3, 471–495 (1968).

RECEIVED for review September 6, 1977. Accepted January 3, 1978. This work was supported by New York State Contract No. C108738 and by grants from Nassau and Suffolk Counties in New York State. New York Ocean Science Laboratory Contribution No. 83.

# Determination of Phentolamine in Blood and Urine by High Performance Liquid Chromatography

**Frederic de Bros***

*Anesthesia Laboratory of Harvard Medical School, Massachusetts General Hospital, Boston, Massachusetts 02114*

**Ernest M. Wolshin**[1]

*Astra Pharmaceutical Laboratory of Clinical Pharmacology, St. Vincent Hospital, Worcester, Massachusetts*

**A high performance liquid chromatographic method for the analysis of phentolamine in blood and urine is described. The procedure requires 1 mL of biological fluids and involves the addition of a double internal standard, alkalinization, extraction into ether, followed by back extraction into sulfuric acid. Separation of drug and internal standards is accomplished by HPLC on a reverse phase column with octane sulfonic acid in the mobile phase as an ion pairing reagent. Chromatographic separation is complete in less than 12 minutes. The assay is linear for concentrations from 15 to 5000 ng/mL. The limit of detection is 15 ng/mL for a 1-mL sample. Relative standard deviations for replicate samples average 4.57%. The assay is specific for phentolamine. There is no interference from commonly coadministered drugs.**

Phentolamine or 2-(*N'-p*-tolyl-*N'-m*-hydroxyphenylaminomethyl)imidazoline (Figure 1) is an $\alpha$ adrenergic blocking agent (*1–5*) with a slight $\beta$ stimulating effect (*6*). It was introduced in 1950 (*7*) as a vasodilating drug for intravenous and oral administration (*8*). It has been reported as a useful agent for therapy in congestive heart failure, myocardial infarction, arrhythmia, angina pectoris, shock, and bronchial asthma (*9*). Current pharmacologic investigations of phentolamine have been summarized in the proceedings of a symposium (*10*). Because of the recent interest for use of this drug as a continuous infusion or for long-term therapy, a simple, specific, quantitative assay in biological media is desirable.

Techniques applied to the analysis of pharmaceutical preparations include titrimetry (*2*), gravimetry (*1*), UV spectrophotometry (*11*), colorimetry (*12–14*), gas chromatography (*15*), and high pressure liquid chromatography (*16*). The colorimetric reaction (*17*) has been adapted for use in biological samples (*18*), but was not found to be specific for phentolamine. The HPLC analysis of phentolamine utilizes an ion-exchange column (*16*); however, the method is characterized by asymmetric peaks and poor resolution ($R < 1.0$). Analysis of imidazoline compounds in biological samples with TLC (*19*) is specific for phentolamine, but is limited to quantities greater than 1 $\mu$g. In addition, the TLC technique is time consuming but may be of value for monitoring of drug concentrations in urine. Although gas–liquid chromatography is employed to assess the purity of pharmaceutical preparations and possibly may be adaptable to clinical determinations, the technique for derivatization of phentolamine and its measurement in nanogram quantities has not been reported.

A rapid and specific, clinically applicable assay with nanogram sensitivity for phentolamine has not previously been published. This paper presents an analytic method which meets the above criteria for phentolamine in biological fluids. It can measure the drug in a broad concentration range and is suitable for pharmaceutical development purposes as well as drug monitoring in a clinical laboratory.

## EXPERIMENTAL

**Reagents and Solvents.** Phentolamine mesylate was provided by Ciba-Geigy, Summit, N.J. Antazoline base and naphazoline hydrochloride were obtained from Pfaltz and Bauer, Stanford, Conn. Sodium octane sulfonic acid was purchased from Eastman Chemicals, Rochester, N.Y. Triple distilled methanol, diethyl ether, and cyclohexane were obtained from Burdick and Jackson Laboratories, Muskegon, Mich. Distilled, deionized, neutral, charcoal filtered, and bacteria free water was used for all solutions. All other reagents were analytical grade or better.

**Apparatus.** A liquid chromatograph with a Milton Roy Minipump (Milton Roy Company, Riviera Beach, Fla.) was used. A pulseless solvent flow was obtained with a $\pi$ configuration of dampers and restrictors (Waters Associates, Milford, Mass.). Pressure was monitored continuously with a glycerine filled, 5000 psig Lenz gauge through a high pressure manifold connected to a 10000 psig Circle Seal adjustable relief valve, set for a 5000-psig cracking pressure. The mobile phase was continuously filtered through the solvent inlet line by a 30-$\mu$m filter (No. 25531, Waters Associates). Further particulate matter was removed from the solvent by a 2- and 0.5-$\mu$m filter (Swagelok SS2F-2 and SS-2000-SR12, respectively) placed in series after the pulse damping network. Samples were injected through a 7000-psig, six-port Valco valve, with a 50-$\mu$L loop. A Glenco sample injection syringe (Model VIS 50-700) and filling port (VISF-1) were used. Separations were accomplished on a Microbondapak/$C_{18}$ column (Waters Associates) maintained at constant temperature in a 20-L water bath. The drug concentration in the column effluent was monitored by a variable wavelength detector (model SF770, Schoeffel Instruments, Westwood, N.J.). Chromatograms were recorded with a model 252A Linear Instruments strip chart recorder.

**Chromatographic Conditions.** Separations were performed at 2.4 mL/min and at a back pressure of 4000 psig. The column

[1]Present address, Astra Pharmaceutical Products, Inc., Framingham, Mass. 01701.

0003-2700/78/0350-0521$01.00/0 © 1978 American Chemical Society

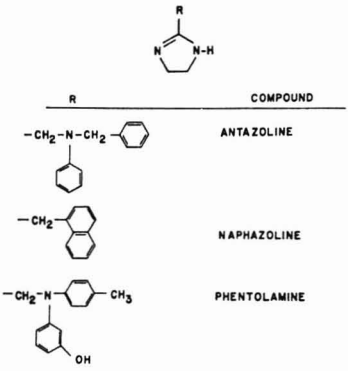


**Figure 1.** Imidazolines and their generic names

was maintained at 25 ± 0.05 °C and the effluent was monitored at 280 nm.

**Stock Solutions.** Phentolamine stock solution was prepared by dissolving 5 mg of the mesylate salt in 100 mL of distilled deionized water. The solution was used for preparation of standard curves and absolute recovery studies.

The internal standard solution contained 50 μg/mL antazoline base and 1 μg/mL naphazoline HCl in water. All stock solutions were stored at 4 °C in the dark.

**Mobile Phase.** The mobile phase was prepared from a methanol and an aqueous component. Each component contained 6.16 mM 1-octane sulfonic acid and 1% v/v glacial acetic acid. The methanol solution was adjusted to pH 4.0 with 1.0 N potassium hydroxide in methanol and the aqueous solution was adjusted to the same pH with 5.0 N sodium hydroxide in water. One percent acetonitrile was added to the aqueous component as a preservative. The mobile phase solution was made by adding 52 parts of the methanolic component to 48 parts of the aqueous component.

**Extraction Procedure.** The extraction was performed by pipetting 1.0 mL of blood or urine, 100 μL of internal standard solution, 500 μL of 1.0 M ammonium hydroxide, and 6.0 mL of water-saturated ether into a 15-mL, conical bottom, centrifuge tube. After capping the tube with a polyethylene stopper, it was mixed for 20 min at 18 rpm on a Drummond Scientific Rotary Mixer. The organic and aqueous phases were separated by centrifugation of 20 min at 1500 rpm (400 × *g*). Five milliliters of the water-saturated ether were transferred to a clean 15-mL centrifuge tube and mixed with 25 μL of 0.2 M sulfuric acid, by vortexing for 1 min. The ether and sulfuric acid were separated by the addition and mixing of 6 mL of cyclohexane, followed by centrifugation for 20 min at 1500 rpm (400 × *g*). As much as possible of the cyclohexane–ether layer was aspirated off and the sample was warmed for 5 min at 70 °C in a water bath to eliminate residual organic solvent. The recovered aqueous volume (45–50 μL) was deposited in the sample loop for injection.

**Standard Curves.** Samples for the standard curves in the 250 to 5000 ng/mL range were prepared from drug-free blood, or urine, by the addition of microliter volumes of the phentolamine mesylate stock solution (50 μg/mL). For samples in the 15 to 250 ng/mL range, the stock solution was diluted to 5 μg/mL.

**Study of Blood Concentrations.** A 60-kg patient undergoing surgery for a pheochromocytoma received a 30-mg intravenous "bolus" injection of phentolamine mesylate (Regitine, Ciba-Geigy). Samples of arterial blood were drawn at the appropriate times and stored at 4 °C in heparinized vacutainers for 18 h prior to analysis.

## RESULTS AND DISCUSSION

When blood and urine samples were alkalinized with ammonia hydroxide, phentolamine could be extracted by using water saturated ether. The average pH of extraction was 10.3.

**Table I. Recoveries of Naphazoline (N), Phentolamine (P), and Antazoline (A) from Blood and Urine**

| | N | P | P | P | A |
|---|---|---|---|---|---|
| medium | blood | blood | blood | urine | blood |
| μg added | 0.1 | 0.05 | 0.5 | 5 | 5 |
| μg recovered, $\bar{m}$ | 0.081 | 0.041 | 0.389 | 4.23 | 3.2 |
| SD, $n = 4$ | 0.0092 | 0.0065 | 0.0833 | 0.645 | 0.452 |
| RDS, % | 11 | 16 | 21 | 15 | 14 |
| Mean recovery, % | 81 | 82 | 78 | 85 | 64 |

Ether yielded a macroscopically clean phase after extraction and had a reasonably equal affinity for the drugs of interest. Direct evaporation of the ether extract gave residues which were insoluble in small volumes (<100 μL) of mobile phase. The precipitates did not form when the drug was back-extracted into 0.2 M sulfuric acid. The back-extraction was further enhanced by the addition of cyclohexane. This procedure concentrates the drug in the relatively small, particulate free volume by reducing its solubility in the organic phase.

Recoveries were determined by comparing the peak heights of extracts with those of stock solutions. Phentolamine yielded an average recovery of 83% over the range 15–5000 ng/mL. Naphazoline and antazoline had recoveries of 81 and 64%, respectively (Table I).

A second extraction was performed to ascertain the amount of drug and internal standard remaining in the alkaline aqueous phase; 4% of the naphazoline and 8% of the phentolamine and antazoline were found. The effectiveness of back-extraction was determined by evaporation of the ether–cyclohexane mixture. The residue was chromatographed and traces (<1%) of antazoline were found. Phentolamine or naphazoline were absent. The back-extraction recovered all of the drugs of interest.

Ion-pair chromatography is an application of the ion-pair extraction of amine drugs which has been extensively studied (*20*). In an ion-pair extraction, an anionic reagent such as bromthymol blue pairs by mutual charge attraction with a cation such as protonated amine. The ion pair exhibits a lipophilic solubility not shown by the individual components and may be extracted into an organic phase from an aqueous phase. Likewise a cation can be used to extract a desired anion.

Recently it was reported that the addition of various alkyl quaternary ammonium salts to a methanol, water, formic acid mobile phase could be used to increase the retention and resolution of a UV absorbing sulfonic acid dye on a lipophilic column such as Bondapak/$C_{18}$ (*21*). The lipophilic column is analogous to the organic phase of extraction. From this it was postulated that various UV-absorbing amines could be chromatographed by the addition of an appropriate non-UV-absorbing lipophilic sulfonic acid. Octane sulfonic acid was chosen for experimentation and found to have useful properties. A pH was selected such that both compounds would be ionized. Use of an ion-pair reagent in the mobile phase produces high resolution between homologous compounds as well as symmetrical peaks which are characteristics not normally associated with the chromatography of ionized substances.

An alternate way to render an amine lipophilic and hence retained, is to suppress its ionization by the selection of a mobile phase pH above its p$K_a$. These values, usually above pH 7.0 cause dissolution of the column silica. Ion-pair chromatography lengthens column life by employing a mobile phase pH where the silica is more stable, such as pH 4.0.

Phentolamine, naphazoline, and antazoline were chromatographed by reverse phase, ion-pair chromatography as symmetrical peaks with excellent resolution (Table II). A

Table II. Chromatographic Parameters of Phentolamine (P), Naphazoline (N), and Antazoline (A)[a]

| Compound | N | P | A |
|---|---|---|---|
| Capacity factor $K'$ | 2.70 | 4.4 | 6.6 |
| Theoretical plates $N$ | 860 | 1218 | 1156 |
| Retention time, min | 5.5 | 7.5 | 11.0 |

[a] Flow rate 2.4 mL/min.

Table III. Effect of the Ion Pairing Reagent Octane Sulfonic Acid (OSA) on Retention Times and Theoretical Plate Counts of Naphazoline (N), Phentolamine (P), and Antazoline (A)

| | Retention volume, mL | | | Theoretical plate count | | |
|---|---|---|---|---|---|---|
| OSA, mM | N | P | A | N | P | A |
| 0 | 7.09 | 9.27 | 12.0 | 676 | 740 | 860 |
| 1.50 | 9.27 | 12.0 | 16.4 | 1056 | 1239 | 961 |
| 3.08 | 10.9 | 14.7 | 20.2 | 1124 | 1797 | 1081 |
| 4.50 | 12.0 | 16.2 | 22.3 | 1354 | 1827 | 1183 |
| 6.16 | 12.4 | 17.5 | 25.5 | 1504 | 1936 | 1296 |

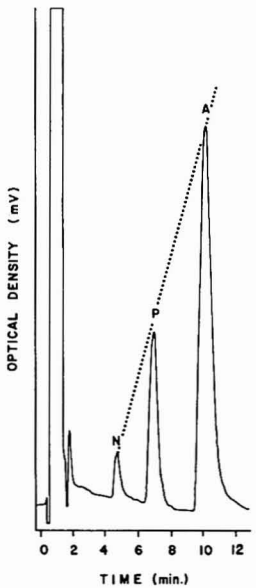


Figure 2. Chromatogram of a patient's urine sample containing 500 ng/mL of phentolamine (P). Internal standards: N = naphazoline, A = antazoline. Graphical quantitation: The dotted line connecting the tops of the antazoline and naphazoline peaks nearly intercepts the top of a 500-ng phentolamine peak. Chromatographic parameters: Column: μBondapak/$C_{18}$, Mobile phase 48% $H_2O$, 52% methanol, 6.16 mM octane sulfonic acid, 1% acetic acid, pH 4. Flow rate: 2.4 mL/min. Temperature 25 °C, UV scale 0.01 aufs at 280 nm

decrease in the concentration of octane sulfonic acid caused a decrease in both retention volume and theoretical plate count (Table III). Conversely, a decrease in the concentration of methanol increased the value of these parameters (Table IV).

It is possible that, as the concentration of the octane sulfonic acid is reduced, the acetate ion also present in the mobile phase may associate more with the chromatographed compounds and become the dominant ion-pair adduct. In our present system, the only function ascribed to the acetic acid is control of pH. Future research should elucidate this point.

Table IV. Effect of the Water/Methanol Ratio in the Mobile Phase on Retention Volumes and Theoretical Plate Counts of Naphazoline (N), Phentolamine (P), and Antazoline (A)

| Volume ratio of water to methanol | Retention volume, mL | | | Theoretical plate count | | |
|---|---|---|---|---|---|---|
| | N | P | A | N | P | A |
| 44/56 | 6.48 | 8.64 | 11.9 | 829 | 1024 | 1102 |
| 50/50 | 10.1 | 15.1 | 21.6 | 1394 | 1760 | 1600 |
| 56/44 | 23.4 | 40.3 | 58.0 | 1878 | 2478 | 2454 |

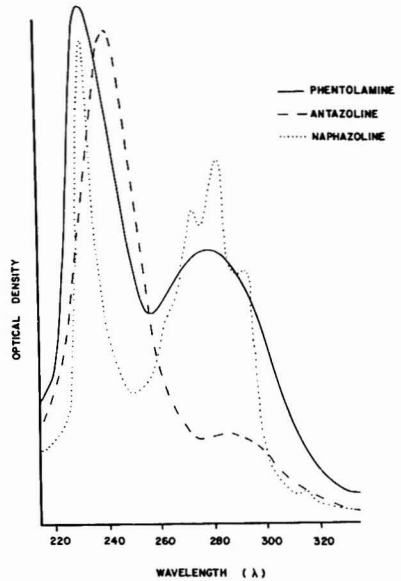


Figure 3. Superimposed UV spectra of the drug and the two internal standards in mobile phase. 0.202 mM naphazoline HCl, 0.132 mM phentolamine mesylate, and 0.180 mM antazoline base. Spectra obtained with a model 25 Beckman spectrophotometer and recorder

Antazoline and naphazoline were chosen as internal standards because they are readily available and have structural as well as chromatographic properties similar to phentolamine. Both are agents for topical use and are never coadministered with phentolamine because of antagonistic physiological properties. Thus, blood levels related to their use are unlikely to occur. A dual internal standard was chosen for several reasons. First, one may quantify accurately both low and high levels of phentolamine with minimal attenuation changes. Second, if an interfering substance coincides with one of the internal standards, quantitation is still feasible with the other. Third, one may rapidly approximate the concentration of phentolamine as being more than or less than 500 ng/mL by drawing a line from the top of the antazoline peak to the top of the naphazoline peak (Figure 2). The peak height ratios using either internal standard were linear over a three-decade concentration range for both blood and urine (Tables V and VI ) with a minimum correlation coefficient of 0.997.

The UV spectra of phentolamine, naphazoline, and antazoline are shown in Figure 3. Although sensitivity is higher

Table V. Standard Curves for Phentolamine in Whole Blood

| μg phentolamine/mL of blood | Naphazoline as internal standard | | | | Antazoline as internal standard | | | |
|---|---|---|---|---|---|---|---|---|
| | PHR[a] ($\bar{m}$) | SD | RSD, % | $n$ | PHR ($\bar{m}$) | SD | RSD, % | $n$ |
| 0.015 | 0.0978 | 0.0061 | 6.2 | 4 | 0.0125 | 0.0004 | 3.2 | 4 |
| 0.050 | 0.327 | 0.0218 | 6.7 | 4 | 0.0350 | 0.0028 | 8.0 | 4 |
| 0.1 | 0.664 | 0.0356 | 5.4 | 4 | 0.0651 | 0.0029 | 4.5 | 4 |
| 0.2 | 1.12 | 0.0440 | 3.6 | 4 | 0.143 | 0.0047 | 3.3 | 4 |
| 0.5 | 3.06 | 0.103 | 3.4 | 4 | 0.349 | 0.0215 | 6.2 | 4 |
| 1 | 6.56 | 0.125 | 1.9 | 4 | 0.652 | 0.031 | 4.8 | 4 |
| 2 | 13.78 | 0.372 | 2.7 | 4 | 1.375 | 0.065 | 4.7 | 4 |
| $r^2$ | 0.998 | | | | 0.997 | | | |
| Intercept | 0.0245 | | | | 0.0023 | | | |
| Slope | 0.1426 | | | | 1.461 | | | |

[a] PHR = peak height ratio of drug to internal standard.

Table VI. Standard Curves for Phentolamine in Urine

| Phentolamine μg added to 1 mL urine | Naphazoline as internal standard | | | | Antazoline as internal standard | | | |
|---|---|---|---|---|---|---|---|---|
| | mean PHR[a] | SD | RSD, % | $n$ | mean PHR[a] | SD | RSD, % | $n$ |
| 0.038 | 0.238 | 0.023 | 9.7 | 5 | 0.0381 | 0.0033 | 8.6 | 5 |
| 0.05 | 0.433 | 0.0207 | 5.0 | 5 | 0.0551 | 0.0032 | 5.8 | 5 |
| 0.45 | 3.51 | 0.1747 | 4.9 | 5 | 0.507 | 0.0114 | 2.2 | 5 |
| 5 | 43.0 | 2.2623 | 5.3 | 5 | 5.66 | 0.0215 | 3.8 | 5 |
| $r^2$ | 0.997 | | | | 0.998 | | | |
| Intercept | 0.0214 | | | | 0.0064 | | | |
| Slope | 0.1157 | | | | 0.8809 | | | |

[a] PHR = peak height ratio of drug to internal standard.

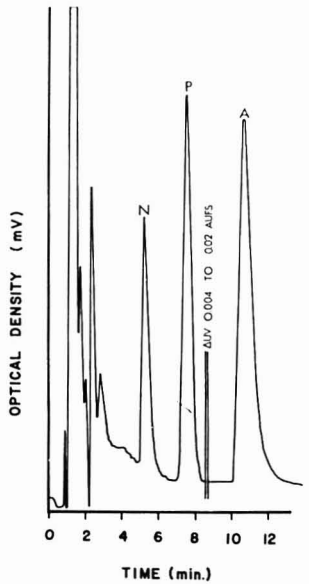


Figure 4. Chromatogram of a patient's blood sample containing 244 ng/mL of phentolamine. N = naphazoline, P = phentolamine, A = antazoline. Chromatographic parameters: Column: μBondapak/$C_{18}$. Mobile phase 48% $H_2O$, 52% methanol, 6.16 mM octane sulfonic acid, 1% acetic acid, pH 4. Flow rate: 2.4 mL/min. Temperature: 25 °C. Wavelength: 280 mn

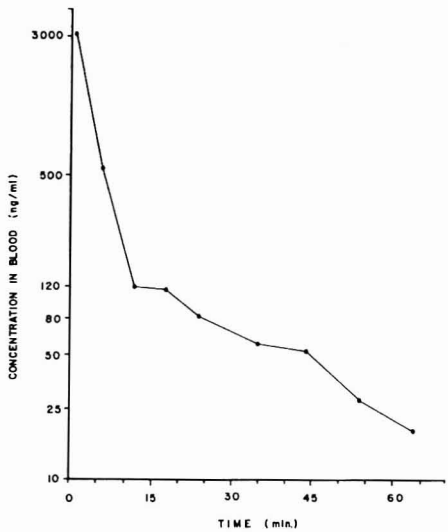


Figure 5. Blood levels of phentolamine measured after a "bolus" injection of 30 mg of phentolamine mesylate (Regitine) to a 60-kg patient. The measureable terminal half-life is 19 min

at 240 nm, the assay was developed for 280 nm to allow the use of a low cost fixed wavelength detector. The minimum detectable quantity was 15 ng for a 1.0-mL sample. This is based on a peak height of twice baseline noise.

With this assay, the pharmacokinetic properties of phentolamine are now under investigation. A chromatogram of a patients's blood sample containing 240 ng/mL is shown in Figure 4. Figure 5 shows a typical example of phentolamine blood concentrations measured after an intravenous injection

of 30 mg of phentolamine to a 60-kg patient. The curve observed during this experiment reflects the phases of distribution and elimination. The measurable terminal half-life of 19 minutes suggests a high degree of drug metabolization.

## ACKNOWLEDGMENT

The authors are indebted to B. Covino, Vice President, Astra Pharmaceutical Products, for generously allowing free use of the laboratory facilities at St. Vincent Hospital, Worcester, Mass. We thank Melvin B. Meyer and David Watkins for encouragements and Carl V. Manion for helpful suggestions on the manuscript; L. Franconi, Waters Associates, for providing us with a new column; and A. Fain and Charles A. Browley, Research Department, Pharmaceutical Division, Ciba-Geigy, Summit, N.J., for the donation of phentolamine. The technical assistance of Carol Reardon, Susan Wolshin, Mary Cavanaugh, Sandi Thibodeau, and Trudy DiBello is gratefully acknowledged.

## LITERATURE CITED

(1) "National Formulary", XIV Edition, Mack Publishing, Co., Easton, Pa., 1973, p 572.
(2) "The United States Pharmacopeia", XIX Revision, Mack Publishing Co., Easton, Pa., 1973, p 375.
(3) E. A. Herroid, A. Cameron, A. Earl, F. Roth, N. Smith, E. Sorenson, and B. N. Craver, *Fed. Proc.*, **8**, 302 (1949).
(4) M. R. Warren, R. A. Woodbury, and J. H. Trapold, *Fed. Proc.*, **8**, 343 (1949).
(5) R. Meier, F. F. Yonkmann, B. N. Craver, and F. Gross, *Proc. Soc. Exp. Biol. Med.*, **71**, 70 (1949).
(6) J. B. Singh, W. B. Hood, and W. H. Abelmann, *Am. J. Cardiol.*, **26**, 660 (1970).
(7) K. Miescher, A. Marxer, and E. Urech, U.S. Patent, No. 2503059 (1950).
(8) E. D. Freis, J. G. MacKay, and W. F. Oliver, *Circulation*, **3**, 254 (1951).
(9) L. Gould and C. V. Ramana Reddy, *Am. Heart J.*, **92** (3), 397 (1976).
(10) Phentolamine Workshop, The CIBA Foundation, London, Nov. 25, 1975.
(11) H. Abdine, A. M. Wahbi, and M. A. Korany, *J. Pharm. Pharmacol.*, **23**, 552 (1972).
(12) S. C. Slack and W. J. Mader, *J. Am. Pharm. Assoc., Sci. Ed.*, **46**, 742 (1957).
(13) S. A. Ismaiel and A. D. Yassa, *Pharmazie*, **28**, 407 (1973).
(14) S. A. Ismaiel, *Pharmazie*, **29**, 210 (1974).
(15) P. F. G. Boon and W. Sudds, *J. Pharm. Pharmacol. Suppl.*, **19**, 885 (1967).
(16) J. A. Mollica, G. R. Padmanabhan, and R. Strusz, *Anal. Chem.*, **45**, 1859 (1973).
(17) E. Edgar, *J. Org. Chem.*, **8**, 417 (1943).
(18) P. A. Jones, H. A. Walker, and A. P. Richardson, *Proc. Soc. Exp. Biol. Med.*, **73**, 366 (1950).
(19) S. Goenecha, *J. Chromatogr.*, **36**, 375 (1968).
(20) "Ion Exchange and Solvent Extraction", Vol. 6, J. A. Marinsky, and Y. Marcus, Ed., Marcel Dekker, New York, N.Y., 1974, pp 1–57.
(21) D. P. Wittmer, N. O. Nuessle, and W. G. Haney, Jr., *Anal. Chem.*, **47**, 1422 (1975).

RECEIVED for review August 29, 1977. Accepted January 3, 1978. Frederic de Bros was supported by Grant NIH GTO1GMO1273.

# Evaluation of a Self-Scanned Photodiode Array Spectrometer for Flame Atomic Absorption Measurements

**F. S. Chuang, D. F. S. Natusch, and K. R. O'Keefe***

*Department of Chemistry, Colorado State University, Fort Collins, Colorado 80523*

**A self-scanned photodiode array is evaluated in terms of its utility as a detector for flame atomic absorption measurements. The relative quantum efficiency of the device is presented and is shown to offer an advantage over conventional detectors for multiwavelength atomic absorption measurements. Sensitivity and detection limits of the atomic absorption spectrometer are established for eight elements over the wavelength range 213.8 to 589.0 nm in a single element mode and are shown to be generally comparable to conventional systems. The use of two or more absorption lines for a single element is shown to extend the range of concentrations that can be measured without additional solution manipulations or instrumental changes. Applications of the spectrometer to multielement determination for two or three elements are presented and the major limitations in this technique are seen to be multiplexing several light sources, optimizing flame conditions for several elements simultaneously, and a limited wavelength coverage with high resolution.**

The utilization of multidetector arrays in spectrometry has increased dramatically recently largely because of the introduction of vidicon tube and silicon photodiode array devices with adequate wavelength coverage and sensitivity for many spectrochemical applications and because of the widespread availability of laboratory scale computers with adequate computing capability to process the data output from these devices. The major limitations of these devices are recognized as low sensitivity as compared to a photomultiplier tube and limited spectral range with high resolution (*1–4*). Although the sensitivity limitation may be severe when application to atomic or molecular emission measurements is considered, absorption measurements are feasible as long as intense sources are available for the spectral region in which measurements are to be made. Resolution limitations are generally not a problem in molecular spectrometric measurements where the resolution of the photodiode array is adequate ($\Delta\lambda/\lambda = 10^{-3}$). In atomic spectrometry, however, spectral coverage generally has to be limited to ensure adequate resolution. Atomic absorption measurements using these array detectors are thus practical since limited spectral resolution usually yields satisfactory results when using hollow cathode lamp sources and since the hollow cathode lamps are sources of intense radiation at appropriate wavelengths.

In the past few years several reports have described the use of silicon vidicons (*1, 2*) and photodiode arrays (*3*) as detectors for flame atomic absorption measurements. Although the significant advantages of these detectors, including multielement analysis, extension of the linear concentration region by use of atomic lines of different sensitivities, background correction by use of nonspecifically absorbed atomic lines, and relative simplicity and stability of instrumentation are widely recognized, evaluations of the photodiode array have thus far been largely qualitative. Horlick (*5*) has discussed in detail the characteristics of this device as a transducer for spectrochemical measurements; however, the evaluation of his

0003-2700/78/0350-0525$01.00/0 © 1978 American Chemical Society

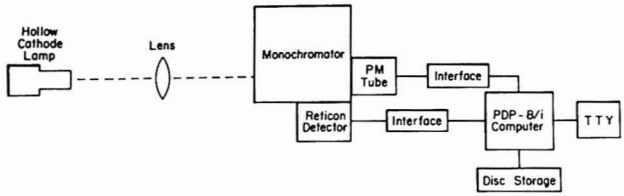


**Figure 1.** Block diagram of optical configuration used for quantum efficiency measurements

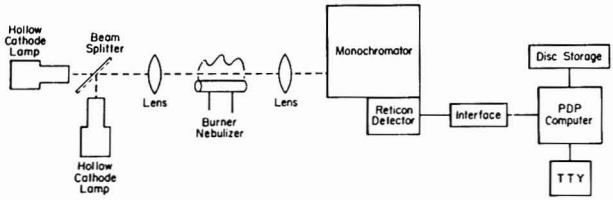


**Figure 2.** Block diagram of optical configuration used for flame atomic absorption measurements

results with respect to application in a specific case, e.g., flame atomic absorption measurements, is difficult.

Characteristics of the source, detector, and data processing algorithms each contribute to atomic absorption measurements in ways that must be determined before the ultimate utility of the system can be established. Source characteristics of interest include how to multiplex atomic lines of all desired elements along the same optical path without reducing intensity to unacceptable levels or introducing spectral interferences. These characteristics are in addition to conventional criteria of stability, source life, cost, etc. Criteria for the sample presentation system, e.g., a nebulizer/burner in flame atomic absorption measurements, are basically the same as those of importance in conventional measurements, although optimization of flame conditions for multielement analysis may represent a fundamental limitation for such techniques. Factors such as sensitivity over the wavelength range of interest, noise, stability, and resolution are critical with respect to the suitability of a proposed detector. In addition, the data processing algorithms may be evaluated in terms of their stability to accurately extract as much chemical information as possible from the spectral data obtained. Finally, the application of an analytical technique in several typical situations may provide a great deal of information about its utility for practical analysis.

The purpose of this report is to evaluate a self-scanned photodiode array spectrometer for flame atomic absorption measurements. Toward this goal, the system components are individually characterized and the system as a whole is evaluated for single and multielement analysis.

## EXPERIMENTAL

The polychromator/photodiode array and associated pseudo-random access electronics and computer control system used in this work are described elsewhere (6). Both 512 and 1024 element photodiode arrays (Models 1024C/17 and 512C, Reticon Corp., Sunnyvale, Calif.) were used in this work. The 512-element array was used without a window for quantum efficiency measurements; the 1024-element array with the standard quartz window for atomic absorption measurements. Both devices were operated at about −10 °C to reduce dark current. The polychromator used in this work provided wavelength coverages of about 26 and 52 nm with the two arrays since the former covered only half the portion of the focal plane covered by the latter.

A block diagram of the optical configuration used for the measurement of the relative quantum efficiency of the photodiode array is shown in Figure 1. The photomultiplier tube module used in this work is the model EU 701-30 (GCA-McPherson, Acton, Mass.) with data acquisition as described elsewhere (7). The monochromator's exit folding mirror is removed when measurements are made with the photodiode array. The radiation from the hollow cathode lamp is focused on the entrance slit of the monochromator by the quartz lens and is masked at the slit

Table I. Experimental Conditions for the Measurement of the Relative Quantum Efficiency of the Photodiode Array Detector[a]

| Element | Wavelength, nm | Integration time, s | Hollow cathode lamp current, mA |
|---|---|---|---|
| Zn | 213.8 | 1.0 | 12 |
| Fe | 248.3 | 2.0 | 20 |
| Mg | 285.2 | 0.2 | 20 |
| Ag | 328.1 | 0.5 | 15 |
| Cr | 357.9 | 0.1 | 20 |
| Ca | 422.7 | 2.0 | 25 |
| Sr | 460.7 | 2.0 | 25 |
| Ba | 553.6 | 2.0 | 25 |
| Ne[b] | 585.2 | variable | variable |
| Ne | 633.6 | 0.1 | 20 |

[a] Monochromator slit width = 100 μm. [b] Ne line emitted from each hollow cathode lamp.

Table II. Experimental Conditions for Flame Atomic Absorption Measurements with the Photodiode Array Detector[a]

| Element | Wavelength, nm | Integration time, s | Hollow cathode lamp current, mA |
|---|---|---|---|
| Zn | 213.8 | 2.0 | 12 |
| Fe | 248.3 | 1.5 | 20 |
| Mn | 279.5 | 1.0 | 25 |
| Mg | 285.2 | 0.8 | 20 |
| Cu | 324.7 | 1.3 | 20 |
| Cr | 357.9 | 0.6 | 20 |
| Ca | 422.7 | 1.0 | 20 |
| Na | 589.0 | 2.5 | 25 |

[a] Slit width of monochromator was set at 100 μm.

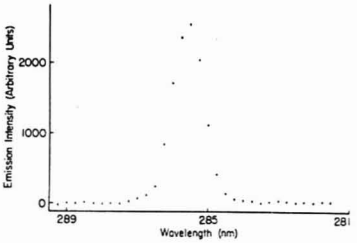


Figure 3. Mg hollow cathode emission spectrum near 285.2 nm atomic line

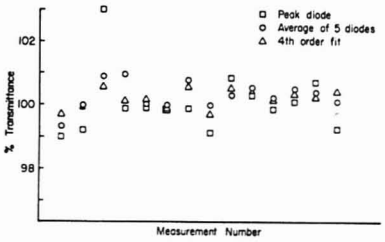


Figure 4. Results for three different methods of measuring atomic line intensity

by a mask 400 μm high. The experimental conditions used for the quantum efficiency measurements are shown in Table I.

The optical configuration used for flame atomic absorption measurements is shown in Figure 2. One of the hollow cathode lamps and the beam splitter is removed during single element measurements. The experimental conditions for flame atomic absorption measurements are shown in Table II.

The burner/nebulizer used in this work was that provided with the Model 303 atomic absorption spectrometer (Perkin-Elmer Corp., Norwalk, Conn.). Gas regulators and flowmeters were from the same model instrument manifold (Perkin-Elmer Corp.). Gas flow rates and burner height were optimized for each set of experimental data reported, except as noted.

## RESULTS AND DISCUSSION

An emission spectrum of a Mg hollow cathode lamp near the 285.2 nm atomic line is shown in Figure 3 as acquired using the photodiode array spectrometer and displayed using a point plotting output option. From this figure, it is clear that determining the atomic line intensity and, hence, subsequently atomic absorption, is not necessarily straightforward. Although one can use the intensity value of the peak diode, it is not always possible to ensure that the peak diode is on the peak of the atomic line, especially in multielement measurements. In addition, using only the peak diode as a measure of atomic line intensity disregards information that is contained in adjacent diodes and that may improve the precision of atomic line intensity measurements. Methods that take advantage of this information include averaging or summing several diodes on the atomic line or fitting an equation to several diodes across the peak and calculating the maximum value of the fitted curve. The results of using the different methods to measure the peak intensity of the magnesium 285.2 nm atomic line emitted from a hollow cathode lamp using an 0.8-s integration time are shown in Figure 4. Three methods were applied to data collected at 1-s intervals after the lamp had warmed up for about an hour. The three methods included taking the intensity of the peak diode, taking the average of the five diodes exposed to the most intense irradiation, and determining the maximum of a fourth-order curve fit to the seven most intense diodes. In the latter two cases, the same diodes were always used, and in all cases correction for background (dark current, detector and electronic offset, etc.) was made by applying the same method to the signal obtained with emission from the hollow cathode lamp blocked. With the first measurement in each case arbitrarily set to 100% $T$ the results show a standard deviation for the peak diode measurement of 1.3% $T$, of 0.48% $T$ for the average, and 0.37% $T$ for the quartic fit. The stability of the lamp over the measurement interval is expected to be better than 0.1% (8).

The use of either the quartic fit or the average is indicated by the good measurement precisions of these algorithms; however, measurement bias is difficult to evaluate for the quartic fit. Because the measured intensity distribution may change with increasing absorbance because of the presence of nonabsorbed lines in the monochromator bandpass or variations in the absorption geometry in the flame, the calculated maximum intensity as well as the apparent position of the maximum intensity may change when the quartic fit is utilized. Work is continuing in our laboratory to characterize this behavior; however, because of the uncertain bias of the technique, it was not adopted for the remainder of the work reported. Rather, the average of the five diodes experiencing the most intense irradiation by the atomic line during the 100% transmittance measurement was used for subsequent atomic line intensity measurements.

A major factor in determining the utility of a spectral detector for high precision atomic absorption spectrometry is the quantum efficiency of the device over the spectral range of interest, e.g., 200–600 nm. The relative quantum efficiency of the photodiode array was determined by comparing its response to a reference photomultiplier tube detector whose quantum efficiency as a function of wavelength was known.

The signal obtained when observing an emission line from the hollow cathode lamp can be expressed as

$$S_D = N_\lambda \cdot f_m \cdot f_c \cdot f_D \cdot \phi_D \cdot k_D \quad (1)$$

or as

$$S_{PM} = N_\lambda \cdot f_m \cdot f_{mi} \cdot f_c \cdot f_{PM} \cdot \phi_{PM} \cdot k_{PM} \quad (2)$$

for the diode array or the photomultiplier tube detector, respectively. In these expressions, $S_D$ and $S_{PM}$ are the signals obtained for a given measurement time (units are "number"); $N_\lambda$ is the number of photons with wavelengths in the bandpass of the monochromator emitted by the source during the measurement interval (photons), $f_c$ and $f_m$ are the fractions of emitted light, $N_\lambda$, collected by and transmitted through the monochromator (unitless); $f_D$ or $f_{PM}$ is the fraction of light that exits the monochromator that illuminates the detector, subscripted to indicate which detector is illuminated (unitless); $\phi$ is the quantum efficiency of the detector indicated by the subscript (photoelectrons/photon); and $k$ is the transfer function corresponding to the conversion of photoelectrons during the measurement interval to a number by the associated electronics and interface (number/photoelectron). The $f_{mi}$ term is included in Equation 2 because an exit folding mirror is in the monochromator in this case. Note that $f_{mi}$, $f_m$, and $\phi$ are wavelength dependent to a considerable extent and may be tagged to indicate the wavelength at which a measurement is made. The two remaining optical efficiency terms, $f_c$ and $f_{PM}$ or $f_D$ may be slightly wavelength dependent because of changes in optical characteristics of the system with wavelength, but they can generally be considered constant.

If measurements are made on a reference and a sample atomic line, λr and λs, respectively, four equations can be written corresponding to Equations 1 and 2 above for each

Table III. Comparison of Analytical Figures of Merit for Single Element Atomic Absorption

| Element | Wavelength, nm | Sensitivity, ppm[a] | | Detection limit, ppm[b] | | Linear range[c] | Relative[d] std dev, % |
|---|---|---|---|---|---|---|---|
| | | This work | Literature[e] | This work | Literature[e] | | |
| Zn | 213.7 | 0.03 | 0.04 | 0.006 | 0.005 | 1200 | 2.0 (1) |
| Mn | 279.5 | 0.05 | 0.08 | 0.01 | 0.005 | 1700 | 2.0 (1) |
| Mg | 285.2 | 0.02 | 0.02 | 0.006 | 0.003 | 1900 | 1.5 (1) |
| Cu | 324.7 | 0.14 | 0.10 | 0.02 | 0.005 | 2000 | 1.5 (1) |
| Cr | 357.8 | 0.15 | 0.15 | 0.03 | 0.01 | 2500 | 2.0 (3) |
| Ca | 422.7 | 0.08 | 0.10 | 0.01 | 0.01 | 2000 | 1.1 (1) |
| Na | 589.0 | 0.04 | 0.05 | 0.06 | 0.005 | 500 | 1.0 (1) |

[a] Sensitivity = the concentration of analyte which absorbed 1% of the hollow cathode lamp intensity. [b] Detection limit = the concentration which gave an absorbance signal of 2 × rms noise level. [c] Linear range = the range over which a linear log-log plot resulted within ±5%. [d] Rel std dev = $S_c/C \times 100\%$, where $S_c$ was the standard deviation of four measurements of concentration $C$. [e] See Reference 12.

wavelength. Ratioing the sample signal to the reference signal for the photodiode array measurement gives

$$\frac{S_D(\lambda s)}{S_D(\lambda r)} = \frac{N_{\lambda s} \cdot f_m(\lambda s) \cdot f_c \cdot f_D \cdot \phi_D(\lambda s) \cdot k_D}{N_{\lambda r} \cdot f_m(\lambda r) \cdot f_c \cdot f_D \cdot \phi_D(\lambda r) \cdot k_D} \quad (3)$$

Eliminating constant terms,

$$\frac{S_D(\lambda s)}{S_D(\lambda r)} = \frac{N_{\lambda s} \cdot f_m(\lambda s) \cdot \phi_D(\lambda s)}{N_{\lambda r} \cdot f_m(\lambda r) \cdot \phi_D(\lambda r)} \quad (4)$$

Similarly, for measurements made with the photomultiplier tube detector,

$$\frac{S_{PM}(\lambda s)}{S_{PM}(\lambda r)} = \frac{N_{\lambda s} \cdot f_m(\lambda s) \cdot f_{mi}(\lambda s) \cdot \phi_{PM}(\lambda s)}{N_{\lambda r} \cdot f_m(\lambda r) \cdot f_{mi}(\lambda r) \cdot \phi_{PM}(\lambda r)} \quad (5)$$

Dividing Equation 4 by Equation 5 and rearranging gives for the relative quantum efficiency of the photodiode array

$$\frac{\phi_D(\lambda s)}{\phi_D(\lambda r)} = \frac{S_D(\lambda s)}{S_D(\lambda r)} \cdot \frac{S_{PM}(\lambda r)}{S_{PM}(\lambda s)} \cdot \frac{f_{mi}(\lambda s)}{f_{mi}(\lambda r)} \cdot \frac{\phi_{PM}(\lambda s)}{\phi_{PM}(\lambda r)} \quad (6)$$

In Equation 6, the $S$ values are measurable quantities; the efficiency of the front surface aluminized mirror is available in the literature (*9*), as is the relative quantum efficiency of the photomultiplier tube detector as a function of wavelength (*10*); hence, the relative quantum efficiency of the photodiode array detector can be calculated. Using the experimental conditions outlined in Table I with the Ne 585.2 nm emission line taken as the reference line in all cases gave the results shown in Figure 5. These data were all obtained using the same region of the photodiode array, e.g., diodes 290–310, for sample and reference wavelength measurement, although a cursory examination of several different regions of the device showed no significant difference in relative quantum efficiency. Replicate measurements of the data in Figure 5 gave results that generally agreed to within ±5%.

Actual values ranged from a relative quantum efficiency of 0.5 at 328 nm to (by definition) 1.0 at 585.2 nm. This behavior is quite different from that of most photomultiplier tubes, which generally show dramatic decreases in quantum efficiency near the extremes of their wavelength range, at least one of which usually occurs in the 200–600 nm region. For example, the 1P28A photomultiplier tube that was used as a reference in this work shows a maximum quantum efficiency at 340 nm, dropping to 15% relative quantum efficiency at 200 nm and to 19% at 600 nm, a variation of more than a factor of five.

The relatively constant quantum efficiency of the diode array is a distinct advantage in spectrochemical measurements. A fundamental limitation on the precision of photometric measurements is the statistical nature of photon and photoelectron emission (*11*); hence, the ultimate precision of an intensity measurement is directly related to the photon arrival rate at the detector. Because the photodiode array has a constant "gain" for each diode and since, in addition, each diode has a relatively constant quantum efficiency, illumination of the detector at any wavelength allows constant precision measurements insofar as the photon arrival rates are constant. This condition can often be met in the multielement atomic absorption case by controlling lamp current and selectively filtering the output of multielement lamps so the incident intensities of all the atomic lines of interest are approximately equal.

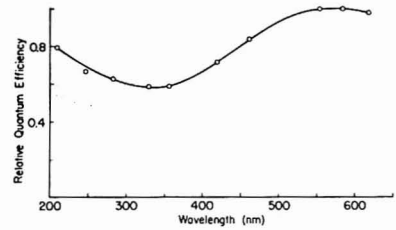


Figure 5. Relative quantum efficiency of photodiode array spectrometer

Single element flame atomic absorption measurements were made on several elements over the wavelength range 200–600 nm in order to evaluate the overall spectrometer performance. The flame conditions and the region viewed by the spectrometer were optimized individually for each element studied and the absorption signal recorded was the result of a single integration of the length specified in Table II. Analytical figures of merit for these studies are shown in Table III. The literature figures of merit, which are included for comparison, are reported for a conventional atomic absorption spectrometer using a burner/nebulizer identical to that used in this work (*12*). The similar sensitivities (analyte concentration required to produce 1% absorption) for all the elements except copper using either type of instrumentation indicates that the photodiode array detection system is equivalent to more conventional detection systems with respect to those factors that influence sensitivity, e.g., resolution, and that the main factors determining the instrumental sensitivity are similar for both spectrometers. It is expected that burner/nebulizer characteristics are the primary factors determining sensitivity in these instruments, which is the reason that the results reported for this work are compared to results obtained on conventional instrumentation equipped with a similar burner/nebulizer. The 30% poorer sensitivity for copper reported in this work is due to the relatively high lamp current used for these studies. This type of behavior is well documented (*13*). The lowered sensitivity was judged to be acceptable for these studies because later multielement work required similar

integration times for all the elements to be determined simultaneously, and the relatively high copper lamp current provided the atomic line intensity that was required to meet this criterion.

The detection limits reported in this work are the analyte concentrations that produce a signal equal to twice the root-mean-square signal obtained during at least ten measurements while water was aspirated into the flame. The detection limits reported in this work are generally about a factor of three poorer than those reported in the literature (*12*). This may be due to any of several factors, although the exact cause is difficult to evaluate because the experimental conditions used to obtain the literature results are not well defined. One of the contributing factors that could be considerably different in this work as compared to the literature is the instrumental time constant or measurement time. Since the sensitivities are about the same in both cases, the detection limit is expected to be inversely proportional to the measurement noise, which in turn is proportional to the square root of the measurement time (*14*). As seen in Table II, measurement times of about 1 s were used in this work; hence, the factor of three difference in detection limits reported in this work and the report cited could be due to a 9-s measurement time having been used in that study. When ten measurements were averaged using the spectrometer described herein, improvements in measurement precision of a factor of about three were generally obtained. The ultimate detection limits, based upon the limit in variance of the 0 absorbance signal at very long measurement times varied from 0.002 ppm for Mg to 0.008 ppm for Cr. This fundamental limit is due both to flame and source flicker noise and long-term lamp drift since a single beam optical arrangement is used in this work. The exact values for these "ultimate" detection limits vary by a factor of 10 or more for the same element if different lamps are used, especially for multielement or very old lamps, and can be treated only as very approximate values.

A second factor that could be important in contributing to poorer detection limits is the presence of a major noise source. This could include a noisy lamp power supply, burner/nebulizer assembly, impure combustion gases, irreproducible gas delivery, or a host of other sources. Although it is impossible to definitely rule out these noise sources, the good "ultimate" detection limit cited for the elements studied and the uniformity of the effect over all the elements studied and over the several months that measurements were made, make these sources unlikely. In addition, several lamps and lamp power supplies were used for various elements, two different burner/nebulizer assemblies were used at various times, and several sources of gas were utilized, all without seeming to affect the results reported.

A third factor that could have contributed to the poorer detection limits reported herein is the use of an inherently poor signal-to-noise ratio detector. As noted earlier, however, the signal-to-noise behavior of the photodiode array detector and measurement system employed closely parallels that of a conventional photomultiplier tube with output current measured using a dc amplifier technique and measurement precision seems to be nebulizer/burner limited. These characteristics rule out this effect as a predominant noise source.

One important potential application of the photodiode array detector in atomic absorption spectrometry is its use for multiline measurements of a single element. Horlick has examined this application with respect to improving the efficiency of utilization of information contained in an atomic absorption spectrum (*3*). Another use of this approach is the measurement of several atomic lines of different sensitivities so that a wider range of analyte concentrations can be directly measured than is possible with conventional single line atomic absorption measurements.

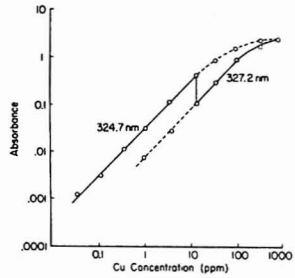


**Figure 6.** Analytical curves obtained using two copper lines of different sensitivities

**Table IV. Some Atomic Lines of Different Sensitivities for Several Elements and Accessible Concentrations**

| Element | Analytical wavelength, nm | Sensitivity, concn (ppm) required for 1% absorption[a] | Concn accessible, ppm[b] |
|---|---|---|---|
| Chromium | 425.4 | 0.26 | 0.1–125 |
| | 427.5 | 0.65 | |
| Copper | 324.7 | 0.04 | 0.02–150 |
| | 327.4 | 0.14 | |
| Iron | 372.0 | 0.38 | |
| | 386.0 | 0.6 | 0.2–1100 |
| | 392.0 | 11 | |
| Lead | 217.0 | 0.16 | 0.05–580 |
| | 261.4 | 5.8 | |
| Nickel | 341.5 | 0.46 | |
| | 352.5 | 1.0 | 0.2–5000 |
| | 362.5 | 49 | |
| Selenium | 196.0 | 0.8 | 0.5–1000 |
| | 204.0 | 11.2 | |
| Tin | 224.6 | 0.4 | 0.2–2000 |
| | 266.1 | 18.7 | |

[a] Sensitivity data: Varian Techtron Hollow Cathode Lamp Data, March 1970. [b] Linear analytical curves ±5% using all the lines listed.

Extension of the analyte concentration range was explored in this work using two copper lines of different sensitivities. The copper lines used were the 324.7 nm line with a sensitivity of 0.029 A/ppm and the 327.4 nm atomic line with a sensitivity of 0.0072 A/ppm. The results of these measurements are shown in Figure 6. The more sensitive 324.7 nm line is linear within 5% on the log–log plot over concentration range 0.02 to 40 ppm while the less sensitive 327.4 nm line is linear over the concentration range 0.1 to 150 ppm copper. Since both atomic lines can be measured simultaneously using the photodiode array spectrometer, concentrations from 0.02 to 150 ppm copper can be measured without dilution by utilizing the appropriate line. The solid line in Figure 6 shows the resulting analytical curve with a transition from using the 324.7 nm to the 327.4 nm atomic line at an analyte concentration of 20 ppm. This measurement concept can be extended to most elements determined by atomic absorption spectrometry since most metals show atomic absorption with different sensitivities at several wavelengths (*15*). Some appropriate multiplets within the 52-nm window of the detector along with atomic absorption sensitivities and analyte concentrations accessible are shown in Table IV.

Perhaps the major utility of the photodiode array detector in atomic absorption spectrometry will be for simultaneous

Table V. Figures of Merit for Simultaneous Multielement Determination of Mn and Mg and Cu, Cr, and Fe

| Element | Wavelength, nm | Sensitivity, ppm[a] | Detection limit, ppm[b] | Linear range[c] | Rel std dev, % (ppm)[d] |
|---|---|---|---|---|---|
| | | Two-element analysis | | | |
| Mn | 279.5 | 0.07 | 0.014 | 1400 | 2.0 (1) |
| Mg | 285.2 | 0.13 | 0.03 | 1300 | 1.7 (1) |
| | | Three-element analysis | | | |
| Cu | 324.7 | 0.29 | 0.07 | 1600 | 2.2 (3) |
| Cr | 357.8 | 0.34 | 0.09 | 1900 | 2.5 (3) |
| Fe | 372.0 | 0.96 | 0.26 | 1100 | 3.7 (5) |

*a*, *b*, *c*, and *d* are defined in Table III.

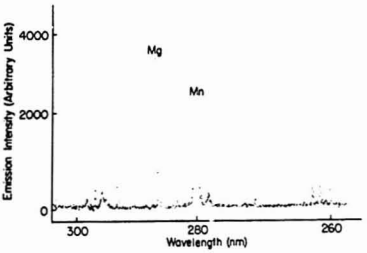


**Figure 7.** Emission spectrum of multiplexed Mn and Mg hollow cathode lamps

multielement analysis. The evaluation of the photodiode array spectrometer with respect to multielement analysis was carried out by performing both two- and three-element analyses. The major limitations as to the number of elements that can be determined simultaneously in this work were the method of multiplexing the hollow cathode lamp outputs and the limited wavelength coverage. Two lamps were the maximum number that could be multiplexed using the beam splitter approach while maintaining an adequate intensity; therefore the number of elements that could be determined simultaneously was limited by both the 52-nm window of the detector and the availability of intense multielement lamps. Efforts are currently underway in our laboratory to devise more suitable multiplexing methods to extend the number of elements that can be determined simultaneously to between six and ten.

The wavelength coverage limitation of the spectrometer is a direct result of the geometric constraints of the detector as well as the optical configuration of the polychromator. With a given detector wavelength, coverage can be increased by reducing the linear dispersion of the polychromator with a concomitant reduction in resolution. In many atomic absorption measurements, a resolution of 0.1 nm is adequate (*15*, *16*), which allows for a wavelength coverage of 102 nm with the present 1024-element device. A 1800-element device is available at the present time which would allow a 180-nm coverage with 0.1-nm resolution.

Multielement determinations were performed with magnesium and manganese as the analytes and also with copper, chromium, and iron as analytes. In the first case, magnesium and manganese single element hollow cathode lamps were used as the sources of atomic radiation. The emission spectrum of the multiplexed lamps is shown in Figure 7 with the entire 52-nm region viewed by the detector displayed. The magnesium singlet at 285.2 nm and the manganese triplet at 279 nm are well resolved in this spectrum. The flame conditions and region viewed by the polychromator were optimized for the determination of manganese in this case. The figures of merit for the measurements are shown in Table V. From this table it is clear that the analytical figures of merit for a given element depend strongly upon experimental conditions. The results for manganese are virtually the same for single element and multielement measurements while the results for magnesium are much poorer in the multielement case, reflecting the fact that the experimental variables were optimized for the determination of the former. Nevertheless, the measurement of magnesium and manganese simultaneously using these conditions is practical.

Copper, chromium, and iron were determined simultaneously using a Zn–Cu–Fe–Mg multielement hollow cathode lamp and a Cr single element lamp. The optimum flame conditions and burner height are considerably different for these three elements (*16*); hence, compromise conditions were chosen so that about equal absorbances were obtained for each element when a solution that was 1 ppm in each element was aspirated into the flame. The figures of merit for this multielement configuration are shown in Table V. In this case the figures of merit for both copper and chromium are considerably worse than in the single element measurements, reflecting the compromise conditions selected.

## ACKNOWLEDGMENT

The authors are grateful for the loan of some of the equipment used in this work from Reticon Corporation, Sunnyvale, Calif.

## LITERATURE CITED

(1) K. W. Jackson, K. M. Aldous, and D. G. Mitchell, *Spectrosc. Lett.*, **6**, 315 (1973).
(2) D. G. Mitchell, K. W. Jackson, and K. M. Aldous, *Anal. Chem.*, **45**, 1215A (1973).
(3) G. Horlick and E. G. Codding, *Appl. Spectrosc.*, **29**, 167 (1975).
(4) K. W. Busch, N. G. Howell, and G. H. Morrison, *Anal. Chem.*, **48**, 575 (1974).
(5) G. Horlick, *Appl. Spectrosc.*, **30** (2), 113 (1976).
(6) K. R. O'Keefe, T. A. Loeske, and P. R. Beaulieu, manuscript in preparation.
(7) K. Ratzlaff, K. R. O'Keefe, D. F. S. Natusch, and F. S. Chuang, manuscript submitted to *Rev. Sci. Instrum.*
(8) P. K. Kuo, Ph.D. Thesis, University of Illinois, Urbana, Ill., 1974.
(9) G. A. Ash, *Opt. Spectra*, **9**, (February) (1975).
(10) Hammatsu TV Co., Ltd., Bulletin C75-2-60, 1975.
(11) M. L. Franklin, G. Horlick, and H. V. Malmstadt, *Anal. Chem.*, **41**, 2 (1969).
(12) Walter Slavin, "Atomic Absorption Instrumentation and Technique: A Review", Perkin-Elmer Corp., Norwalk, Conn.
(13) J. C. Burger, Release ETD–6603, Westinghouse Electric Corp., Elmira, N.Y., 1966.
(14) H. V. Malmstadt, G. G. Enke, S. R. Crouch, and G. Horlick, "Optimization of Electronic Measurements", Benjamin, Menlo Park, Calif., 1974.
(15) K. Fuwa, in "Spectrochemical Methods of Analysis", J. D. Winefordner, Ed., Wiley-Interscience, New York, N.Y., 1971.
(16) C. Veillon in "Flame Emission and Atomic Absorption Spectrometry", J. A. Dean and T. C. Rains, Ed., Vol. III, Marcel Dekker, New York, N.Y., 1971.

RECEIVED for review October 27, 1977. Accepted December 15, 1977. The authors are grateful for partial support of this research by the donors of the Petroleum Research Fund administered by the American Chemical Society. This work was supported in part by grant ERT-74-24276 from the United States National Science Foundation, by grant R-803950 from the United States Environmental Protection Agency, Water Quality Laboratory–Duluth, Minn., and by grant 7-R01-ES 01472 from the National Institute of Environmental Health Sciences, NIH.

# CORRESPONDENCE

## Limitations on the Spectrophotometric Determination of Copper(I) with Ferrozine

*Sir:* The use of Ferrozine (Hach Chemical Co.), the disodium salt of 3(2-pyridyl)-5,6-bis(4-phenylsulfonic acid)-1,2,4-triazine, for the determination of several metallic ions such as iron, cobalt, copper, osmium, etc. has been reported by several workers (*1*–*3*). It has also been used for the indirect determination of species which reduce ferric iron such as ascorbic acid (*4*) and also for determining sulfur dioxide in liquid samples (*5*). In 1974, Kundra et al. (2) showed that copper(I) and iron(II) can be determined simultaneously in samples containing the two ions. They showed that this method yielded quantitative data and that it was free from interference by other ions. Our attention was drawn to this method because of our interest in hemoglobin and other proteins. This seemed to be an attractive method for the determination of copper which is known to be present in several biological macromolecules (*6*). Nagel et al. (*7*) have reported the binding of copper to hemoglobin and showed that this could be a good model for the study of protein metal interaction.

If the precision claimed by Kundra et al. (2) is correct, then it will be possible to determine the equilibrium constant for the binding of copper ions to hemoglobin spectrophotometrically.

We have repeated the work of Kundra et al. after taking cognizance of the modifications suggested by Gibbs (*3*). As a note of caution to other workers, we report the results of our findings. The results show that copper cannot be determined quantitatively and that the precision becomes worse in the presence of iron. Addition of sodium sulfite, however, improves the precision for the determination of copper. The possible reasons why this method fails are discussed in terms of the instability of copper(I) complexes.

### EXPERIMENTAL

**Apparatus.** A Unicam SP 6-200 spectrophotometer and Radiometer 4 pH meter were used.

**Reagents.** Ferrozine purchased from Hach Chemical Co. was recrystallized as suggested by Kundra et al. (2). Ferrozine solution was made according to the method of Gibbs (*3*) since precipitates formed under the high acid conditions suggested by Stookey (*1*); the solution was then made up with doubly (glass) distilled water. All glassware used in this work was soaked in concentrated hydrochloric acid for several hours and later rinsed copiously with doubly distilled water.

All other solutions used were prepared as described by Kundra et al. (2).

**Digestion of Hemoglobin Samples.** Digestion of the protein molecule was carried out by the method of Cameron (*8*). The hemoglobin sample, 0.1 mL, was measured with an Agla microsyringe (Wellcome Ltd) into a 20-mL standard flask, 0.1 mL of perchloric acid and 0.1 mL of hydrogen peroxide were added, and the mixture was digested at 100 °C in a water bath for 30 min. Then 1 mL of 1% hydroxylamine hydrochloride was added to the mixture and heated further for about 7 min. Determination of copper and iron was carried out as suggested by Kundra et al.

### RESULTS AND DISCUSSION

The copper(I)-Ferrozine complex and iron(II)-Ferrozine complex have been shown to have absorption maxima at 470 nm and 562 nm, respectively (2). We find that the absorption of copper(I)–Ferrozine complex is weak at 470 nm. This is not surprising in view of the $d^{10}$ electronic structure of Cu(I). In the presence of iron, this absorption peak is completely masked and is not observed as shown in Figure 1. Besides, the molar extinction coefficient of the Fe(II) complex is much higher than that of the Cu(I) complex at this wavelength. Our experimental results show that at 470 nm, the molar extinction coefficients for Cu(I) and Fe(II) complexes are 4332 and 9802, respectively.

Table I. Determination of Copper in a Solution Containing Copper Alone

| Copper taken, mg/mL | Copper found, mg/mL[a] |
|---|---|
| 1.23 | 1.09 |
| 1.62 | 1.36 |
| 2.02 | 1.67 |
| 2.46 | 2.03 |
| 2.87 | 2.32 |

[a] Each of the data represents the average of at least 5 samples.

Table II. Determination of Iron in a Solution Containing Iron Alone

| Iron taken, mg/mL | Iron found, mg/mL[a] |
|---|---|
| 1.22 | 1.20 |
| 2.44 | 2.42 |
| 3.65 | 3.66 |
| 4.87 | 4.90 |
| 7.37 | 7.31 |

[a] Each of the data represents the average of at least 5 samples.

Table III. Simultaneous Determination of Iron and Copper in a Mixture[a]

| Copper taken, mg/mL | Copper found, mg/mL | Iron taken, mg/mL | Iron found, mg/mL |
|---|---|---|---|
| 1.69 | 1.27 | 1.63 | 1.59 |
| 3.39 | 1.71 | 2.76 | 2.77 |
| 5.08 | 2.66 | 4.12 | 3.92 |
| 7.42 | 3.30 | 6.59 | 6.63 |

[a] Each of the data represents the average of at least 5 samples.

Table I shows the results for copper determined in a solution in which copper was present alone and Table II is that for iron. Comparison of Tables I and II shows that iron is more precisely determined than copper by the Ferrozine method. Table III shows typical data obtained in the simultaneous determination of iron and copper from synthetic mixtures. To verify that results obtained from the digestion of hemoglobin were not affected by the digestion procedure or any biological material present, we determined iron alone by this procedure and the results of such determinations show that iron in the protein samples is determined as precisely

0003-2700/78/0350-0531$01.00/0 © 1978 American Chemical Society

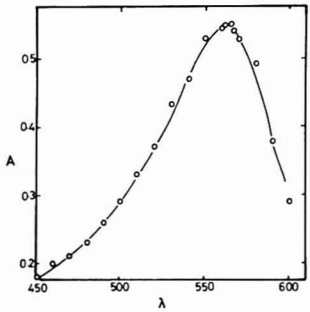


**Figure 1.** Absorbance of a solution containing copper(I) and iron(II) salts after treatment with Ferrozine

**Table IV. Determination of Copper in the Presence of Sodium Sulfite**

| Copper taken, mg/mL | Copper found, mg/mL[a] |
|---|---|
| 1.39 | 1.28 |
| 1.72 | 1.61 |
| 2.77 | 2.58 |
| 3.12 | 3.00 |
| 4.16 | 3.91 |

[a] Each of the data represents the average of at least 5 samples.

as iron in inorganic Fe(II) solutions by this method.

All the results show that the amount of copper found is consistently lower than the expected value. The deviations observed show that the results cannot be attributed to random experimental errors, but rather that copper is underdetermined in all cases. We noticed that the color of the Cu(I)–Ferrozine complex fades on long exposure. This suggests that the complex is unstable. It is known that in aqueous solutions of many low molecular weight copper(I) compounds, univalent copper is almost instantaneously oxidized into copper(II) by molecular oxygen (*9*). This means that many copper(I) complexes will have a limited stability in the presence of oxygen. This can explain our observation that the color of the Cu(I)-Ferrozine complex fades on long exposure and the fact that copper cannot be determined quantitatively by the use of ferrozine. The precision of such determinations for Cu(I) is improved by the addition of sodium sulfite as shown by the results in Table IV.

There is, however, a possibility that this method may be used to determine copper quantitatively if oxygen is completely excluded.

## LITERATURE CITED

(1) L. L. Stookey, *Anal. Chem.*, **42**, 779 (1970).
(2) S. K. Kundra, M. Katyal, and R. P. Singh, *Anal. Chem.*, **46**, 1605 (1974).
(3) C. R. Gibbs, *Anal. Chem.*, **48**, 1197 (1976).
(4) B. Jaselskis and S. J. Nelepathy, *Anal. Chem.*, **44**, 379 (1972).
(5) A. Atari and B. Jaselskis, *Anal. Chem.*, **44**, 1515 (1972).
(6) R. Osterberg, *Coord. Chem. Rev.*, **12**, 309 (1974).
(7) R. L. Nagel, G. Bemski, and P. Pincus, *Arch. Biochem. Biophys.*, **137**, 428 (1970).
(8) B. F. Cameron, *Anal. Biochem.*, **11**, 164 (1965).
(9) A. Zuberbühler, *Helv. Chim. Acta*, **50**, 466 (1967).

**Alphonso C. I. Anusiem***
**Gbeminiyi B. Ojo**

Department of Chemistry
University of Ibadan
Ibadan, Nigeria

RECEIVED for review July 27, 1977. Accepted November 17, 1977.

# AIDS FOR ANALYTICAL CHEMISTS

## Positive Pressure Columns for Solvent Cleanup or Chromatography

**B. P. Semonian, J. A. Lubkowitz,[1] and L. B. Rogers***

*Department of Chemistry, University of Georgia, Athens, Georgia 30602*

There are many applications, such as solvent and sample purifications, which still utilize the classical gravity-feed columns. However, the use of volatile solvents often generates problems in those (gravity-feed) systems. The most common inconveniences are, first, the formation of gas bubbles in the column bed, which renders the column useless and, second, the loss of mobile phase by evaporation from the solvent reservoir. In addition, the dissolution of water vapor (from the air) at the column outlet, can contaminate the sample or solvent. To minimize those problems, a closed system was devised in which the high partial pressure of the solvent provided a protective gas blanket.

The columns were based on the principle of an addition funnel (*1*), and with the aid of a simple mercury pressure valve, the problem of gas bubble formation was eliminated when purifying *n*-pentane over silica gel. The loss of *n*-pentane through evaporation was substantially reduced and water contamination was essentially eliminated. The pseudo-sealed system utilized the partial pressure of the *n*-pentane to generate a pressure of approximately 50 Torr greater than the ambient pressure.

The pressure served several functions. It served to collapse any bubbles already present in the column. At the same time, the positive pressure also kept air from leaking around the sides of the stopcock which often generates additional bubbles in the column packing through evaporation. Since the system was a pseudo-closed one, the liquid vaporized to the point of establishing its characteristic partial pressure. After this pressure had been achieved, further losses due to evaporation were eliminated. This system could also be used to exclude atmospheric gases by employing a purge gas.

### EXPERIMENTAL

**Apparatus.** A diagram of the system is shown in Figure 1. All unions used were 24/40 ground glass unions. The column was

[1] Present address, Apartado 1747, Caracas 101, Venezuela.

0003-2700/78/0350-0532$01.00/0 © 1978 American Chemical Society

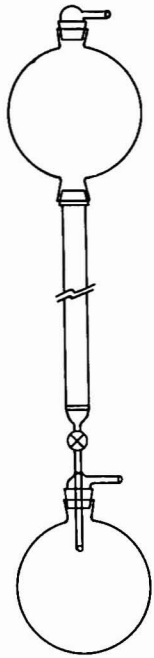

Figure 1. Column with upper and lower (2-L) reservoirs

60 cm × 2.54 cm (o.d.) and 2.24 cm (i.d.). The sintered-glass frit was of medium porosity. The top joint of the reservoir was fitted with a tubing-adapter. A latex rubber tube was used to connect the reservoir tubing adapter, through a glass "T", to the venting arm that followed the column. The third port of the "T" was connected by latex tubing to a 4-mm o.d. glass tube which had been inserted through a two-hole rubber stopper and into the mercury reservoir. (An optional ballast tank could be placed as a branch at any convenient location along the latex tubing.) The pressure was regulated by the mercury reservoir, and it was adjusted by raising or lowering the height of the glass tube in the mercury pool. Once the pressure had been set to a desired value, no other adjustments were necessary.

**Procedure.** The silica gel was first dried overnight at 170 °C. It was then slowly poured into the column which had previously been filled with *n*-pentane. The top reservoir was then attached and also filled with *n*-pentane.

The routine operation of the column consisted of four steps: (a) Filling the reservoir, (b) cleaning the receiver of vapor by blowing filtered house air into it, (c) clamping the receiver to the bottom of the column, and (d) adjusting the flow rate of liquid to a desired level. Once those steps had been taken, the column required no further maintenance.

## RESULTS AND DISCUSSION

We have repeatedly used this technique for cleaning up technical grade *n*-pentane. The advantages of this system are, first, that slow flow rates can be used without vaporization losses of the *n*-pentane becoming a problem. We have used up to 12 h to pass 2 L of *n*-pentane without appreciable loss. Second, more efficient columns were maintained since bed-disrupting bubbles were prevented from forming. Third, safety was increased because an increase in ambient temperature could not generate either higher column pressures or noticeable amounts of gaseous *n*-pentane. (Nevertheless, this system was operated in a good fume hood!) Fourth, the pseudo-closed system eliminated the access of water vapor to the outlet of the column. Finally, accidental degradation of the column material by water adsorption was reduced. Even in cases where the column was accidently allowed to run dry and to remain in that condition for several hours, there was no evidence that atmospheric water had penetrated the system to an extent that deactivated or seriously impaired the operation of the column. Obviously, this type of technique could also be used to exclude atmospheric gases if an appropriate purge gas were employed.

The system was ideal for solvent cleanup, and it can be readily adapted to fraction collection by incorporating several containers inside the receiver flask. In this mode of operation, one would (most probably) use the optional ballast tank.

## LITERATURE CITED

(1) "Separatory funnels, addition, pressure equalizing," Item No. 5237-H10, Arthur H. Thomas Co. Catalog, 1976.

RECEIVED for review August 5, 1977. Accepted November 14, 1977. This work was supported by the U.S. Energy Research and Development Administration through Contract No. E(38-1)-854.

# Preparation of Wet Fish Reference Material from Shark Meat

**Yukiko Dokiya, Masashi Taguchi,[1] Shozo Toda,* and Keiichiro Fuwa[2]**

*Department of Agricultural Chemistry, Faculty of Agriculture, The University of Tokyo, Bunkyoku, Tokyo, Japan, 113*

Standard reference materials or certified reference materials for metal analysis of biological or environmental samples have recently attracted the attention of analytical chemists who deal with those "soft" materials. Since H. J. M. Bowen (*1*) prepared his Kale Powder in the early 1960's, several trials for preparing such materials have been performed, including grass samples by J. B. Jones (*2*), Orchard Leaves and Bovine Liver by NBS research groups (*3, 4*), Cd-rice by N. Yamagata (*5*) and Oyster Powder by R. Fukai (*6*). Among these works, those of NBS research groups are considered to be the most systematic and comprehensive. An unprecedented demand for Orchard Leaves and Bovine Liver is currently reported by J. P. Cali (*7*).

The authors, in a cooperative study with NBS research groups, have performed some researches for new biological reference materials, and the work includes the preparation of Tea Leaves and Pepper Bush samples (*8*). No standard reference materials of fish meat have been successfully

[1] Present address, Department of Fisheries, Faculty of Agriculture, The University of Tokyo, Bunkyoku, Tokyo, Japan, 113.
[2] Present address, Department of Chemistry, Faculty of Science, The University of Tokyo, Bunkyoku, Tokyo, Japan, 113.

0003-2700/78/0350-0533$01.00/0 © 1978 American Chemical Society

Table I. Experimental Conditions for Atomic Absorption and Flame Emission Spectrometry

| Element | K | Na | Ca | Mg | Zn | Fe |
|---|---|---|---|---|---|---|
| Analytical line, nm | 766.5 | 589.0 | 422.7 | 285.2 | 213.9 | 248.3 |
| Mode | FE | FE | FE | AAS | AAS | AAS |
| S.B.W., nm | 0.4 | 0.4 | 0.4 | 1.0 | 1.0 | 0.4 |
| Flame | | | | | | |
| Air flow rate | 15 L/min | | | | | |
| $C_2H_2$ flow rate | 2.4 L/min | | | | | |
| Position | 1.5–1.8 cm above the burner | | | | | |

Table II. Water and Elementary Content of the Raw Material (*Squalus mitsukurii*)

| Shark | T.L., mm[a] | B.W., kg[b] | $H_2O$, % | Na[c] | K | Ca | Mg | Zn | Fe | Hg |
|---|---|---|---|---|---|---|---|---|---|---|
| 1 | 1131 | 8.45 | 73.9 | 795 | 3590 | 43 | 235 | 4.1 | 6 | 1.75 |
| 2 | 1010 | 6.15 | 79.4 | 740 | 3000 | 50 | 210 | 2.9 | 7 | 1.74 |
| 3 | 1055 | 8.48 | 74.4 | 930 | 3670 | 57 | 240 | 2.9 | 7 | 1.83 |
| 4 | 968 | 5.24 | 76.3 | 700 | 4050 | 45 | 250 | 2.8 | 7 | 1.54 |
| 5 | 1045 | 6.85 | 75.2 | 770 | 3320 | 82 | 215 | 3.6 | 6 | 1.40 |
| 6 | 1087 | 6.63 | 75.3 | 975 | 3700 | 43 | 225 | 3.8 | 10 | 2.13 |
| 7 | 1193 | 10.37 | 75.3 | 725 | 3600 | 43 | 225 | 3.6 | 12 | 2.11 |
| 8 | 1080 | 7.80 | 76.5 | 725 | 3050 | 38 | 230 | 3.0 | 5 | 1.83 |
| Av | 1070 | 7.50 | 75.8 | 759 | 3500 | 50 | 229 | 3.3 | 8 | 1.79 |
| Rel std dev, % | 6.5 | 21.6 | 2.2 | 12.9 | 10.1 | 28.1 | 5.7 | 14.8 | 30.7 | 14.0 |

[a] Total length. [b] Body weight. [c] Elements given in μg/g wet.

Table III. Variation of Water and Elementary Composition during the Preparation of "Wet" Shark Reference Material

| Steps of Production | $H_2O$, % | Na, μg/g wet |
|---|---|---|
| 1. Raw material | 78.5 ± 1.7[a] | 759 ± 98 |
| 2. Mixture in silent cutter | 68.1 ± 0.4 | 13800 ± 200 |
| 3. "Wet" shark reference material | 68.5 ± 0.2 | 13700 ± 450 |

| Steps | K[b] | Mg | Ca | Zn | Fe | Hg |
|---|---|---|---|---|---|---|
| 1. | 3500 ± 350 | 229 ± 13 | 50 ± 14 | 3.3 ± 0.5 | 8 ± 2 | 1.79 ± 0.25 |
| 2. | 3560 ± 110 | 221 ± 4 | 68 ± 7 | 3.5 ± 0.8 | 30 ± 7 | 1.94 ± 0.03 |
| 3. | 3650 ± 100 | 220 ± 6 | 59 ± 3 | 3.1 ± 0.6 | 26 ± 5 | 1.96 ± 0.05 |

[a] $(\bar{x} \pm \sigma_{n-1})$. [b] Elements given in μg/g wet.

prepared up to the present, because of the difficulty in realizing homogeneous concentrations of elements, especially that of calcium (*9*). In this study, the white muscle of shark (*Squalus mitsukurii*) was adopted as the raw material, since the distribution of metals in the muscle is known to be comparatively homogeneous owing to the fact that this fish has less bones in the muscle parts (*10, 14*).

In the fields of food science, oceanography, environmental science, etc., where fish meat reference materials are required, metals are often determined in "wet" or "fresh" samples. Although the wet weight is rather hard to define as a scientific unit, it can be practically useful to prepare a reference material of a wet weight basis under given conditions. The procedure of producing Japanese fish paste was adopted for this purpose and a strong preservative, AF-2, which is now forbidden for use in food, was utilized to preserve it for a long period.

## EXPERIMENTAL

**Preparation of "Wet" Shark Reference Material.** Eight fresh sharks of similar size (Table I) were obtained from the fish market of Choshi and the muscle parts of them were dissected and frozen and processed as follows. NaCl and starch were of analytical grade. AF-2(2-furyl)-3-(5-nitro-2-furyl)acrylamide) was obtained from Ueno Pharmaceutical Co.

The white muscle of each fish (ca. 500 g wet) was dissected and cut into small pieces by a stainless steel knife and homogenized by a mixer. The fine bones and the red muscle were discarded.

The meat (2.5 kg) was further homogenized in an ordinary silent cutter for 40 min, and NaCl (75 g) and starch (25 g) were then added to enable the paste to clot after steaming. AF-2 (0.1 g) which was also added caused the paste to become yellow in color.

The resulting paste was steamed in a wooden frame for 15 min. Then the clotted paste was cut into pillars of 2–3 g and put into Pyrex glass bottles with caps and Teflon-coated packings, and sterilized at 120 °C and 1.2 atm for 30 min by a high-pressure sterilizer.

**Determination of Metals.** A random selection of 10 bottles was taken from the products, and the contents were transfered to flasks (300 mL) containing $HNO_3$ (5 mL) and $H_2O_2$ (5 mL) for digestion. The flasks were heated gently with coolers whose tops were connected to traps of acid (*11*). After 10 h, the digested solution volume was adjusted to 50 mL and used for the metal determinations. Wet samples (2 g) of the raw material and the mixture in the silent cutter were digested in the same manner as above.

Na, K, Ca, Mg, Fe, and Zn were determined by flame emission and atomic absorption spectrometry under the conditions specified in Table I, using a Seiko SAS 721 atomic absorption spectrophotometer.

Hg was determined by the reduction-cold vapor atomic absorption method using a 100-cm quartz absorption cell attached to a Hitachi 207 atomic absorption spectrophotometer (*12*).

**Determination of Water Content.** The weight change by drying at 90 °C in an electric oven was used for determining the water content of the raw material, the mixture in the silent cutter, and the products.

**Determination of Microbial Activities.** Fungal activity was determined by counting the colonies. The testing paper

Table IV. Elementary Composition of "Wet" Shark Reference Material (μg/g wet)

| Bottles | Na | K | Ca | Mg | Zn | Fe | Hg |
|---|---|---|---|---|---|---|---|
| a | 13200 | 3720 | 60 | 215 | 3.0 | 25 | 1.92 |
| b | 13600 | 3690 | 66 | 225 | 2.2 | 21 | 1.99 |
| c | 13000 | 3700 | 57 | 210 | 3.0 | 24 | 2.05 |
| d | 13900 | 3710 | 59 | 215 | 3.1 | 21 | 1.92 |
| e | 13900 | 3630 | 60 | 225 | 4.6 | 25 | 2.00 |
| f | 14200 | 3590 | 55 | 220 | 3.4 | 25 | 1.99 |
| g | 14000 | 3650 | 64 | 215 | 2.5 | 35 | 1.92 |
| h | 13300 | 3630 | 57 | 215 | 2.8 | 32 | 1.89 |
| i | 13400 | 3400 | 57 | 230 | 2.8 | 22 | 1.99 |
| j | 13700 | 3750 | 57 | 215 | 3.2 | 28 | 1.92 |
| Av | 13700 | 3650 | 59 | 220 | 3.1 | 26 | 1.96 |
| Rel std dev, % | 3.3 | 2.6 | 5.9 | 2.8 | 20.6 | 17.8 | 2.6 |

Table V. Change of Weight and Microbial Activities in Three Months (from Feb. 1977 to May 1977)

| | Weight change, g[a] | Microbial activity | |
|---|---|---|---|
| | | Fungi | Bacteria |
| Room temperature (Dark) | | | |
| Sterilized[b] | 0, 0, −0.1, 0, 0 | ----- | − |
| Not sterilized | −0.3, −0.2, 0, | −+−+− | ± |
| Cold room (ca. 4 °C) | | | |
| Sterilized[b] | 0, 0, 0, 0, 0 | ----- | − |
| Not sterilized | 0, 0, 0, 0, 0 | ----- | − |
| Freezer (−20 °C) | | | |
| Sterilized[b] | 0, 0, 0, 0, 0 | ----- | − |
| Not sterilized | 0, 0, 0, 0, −0.05 | ----- | − |

[a] Starting sample weight: 1.7-3.0 g. [b] Sterilization: 120 °C, 1.2 atm, 30 min.

Table VI. Metal Concentration of Some Animal Reference Materials

| | Bovine Liver NBS-SRM 1577 (4) | Oyster Powder IAEA-Monaco MA-M-1 (6) | "Wet" Shark Reference Material (Shark Paste) | |
|---|---|---|---|---|
| | μg/g dry | μg/g dry | μg/g dry[a] | μg/g wet[b] |
| K | 9700 ± 600 | | 11600 ± 300 | 3650 ± 100 |
| Na | 2430 ± 130 | | 43400 ± 3000 | 13700 ± 450 |
| Mg | (605) | | 890 ± 13 | 220 ± 6 |
| Ca | (123) | | 187 ± 13 | 59 ± 4 |
| Fe | 270 ± 20 | 300 ± 20 | 83 ± 15 | 26 ± 5 |
| Cu | 193 ± 10 | 310 ± 10 | (3)[c] | (1)[c] |
| Zn | 130 ± 10 | 2630 ± 120 | 10 ± 2 | 3.1 ± 0.6 |
| Mn | 10.3 ± 1.0 | 66 ± 4 | (3)[c] | (1)[c] |
| Hg | 0.016 ± 0.002 | 0.20 ± 0.02 | 6.22 ± 0.16 | 1.96 ± 0.05 |

[a] Calculated values from μg/g wet. [b] Average ± $\sigma_{n-1}$. [c] Approximate value.

"Bactester", purchased from Kanto-Kagaku Co. Ltd., was utilized for the determination of bacterial activities.

## RESULTS AND DISCUSSION

**Characteristics of the Raw Material.** The total length, the body weight of the eight sharks obtained, their water content, and the K, Na, Ca, Mg, Fe, Zn, and Hg contents of the white muscle are summarized in Table II.

The most typical characteristic of this fish is the high concentration of Hg in the muscle, presumably owing to their eating habits. A correlation between the total length and the Hg content in the muscle is also known (*13*). Thus, considering the field of utilization and according to the user's requirements, shark muscle of Hg content ranging from 0.2 to 2.0 μg/g (wet weight basis) can be obtained as the raw material for the reference by chosing the appropriate variety and the total length of the shark.

The K, Na, Ca, Mg, Fe, and Zn contents are similar to those of other fish meat. The variation of Ca content (Rel std dev, 28.1%) between the individual sharks was the greatest among those of the elements examined.

**Changes during Preparation.** The changes of water content and mineral concentrations during the preparation are summarized in Table III, As NaCl was added in the process, the concentration of Na was increased more than ten times that of the raw material. The slight decrease of the water content of the mixture in the silent cutter may be attributed to the addition of starch (1%) and to evaporation. The increase of Fe concentration observed with the mixture in the silent cutter and with the product was considered to be due to contamination from the material of the silent cutter. This contamination should be eliminated by chosing a more suitable cutter material or by changing this process to a less contaminating one.

The variation of metal concentrations was shown to be reduced after the preparation, except in the case of Zn. The situation was best for Ca where the rel std dev value after preparation was 5.9% relative to 28.1% for the raw material. No significant loss of Hg was observed during the preparation.

**Water and Metal Contents of "Wet" Shark Reference Material.** The water and metal contents of samples contained in 10 bottles selected at random are shown in Table IV. The homogeniety with respect to Na, K, Ca, Mg, and Hg was shown to be within 6% (rel std dev value), while that of Zn and Fe

were as much as 20%.

**Preservation of the Sample.** As the samples are wet, long-term preservation should be one of the most difficult factors to realize. Thus, the preservation test was performed periodically after the completion of the preparation. Fifteen bottles were sterilized by a high-pressure sterilizer and sets of 5 bottles were then kept at (1) room temperature, (2) 4 °C, and (3) −20 °C. The weight and microbial activity of each sample was determined. This procedure was repeated for a further 15 sample bottles but omitting sterilization. A summary of the results of these tests after 3-month storage are given in Table V.

Except for the bottles not sterilized and kept at room temperature, microbial activity was not observed, neither fungal nor bacterial, and the change of weight during preservation was shown to be negligible. These tests are being continued for a few years.

**Comparison with Other Animal Reference Material.** The elementary composition of this wet shark reference material was compared with NBS-SRM 1571, Bovine Liver, and with the Oyster Powder produced by R. Fukai (6) of the Marine Research Laboratory (Monaco) of IAEA for the purpose of intercalibration (Table VI).

The most typical characteristics of this shark reference material are the high concentration of Hg and the low concentration of other heavy metals such as Fe, Zn, Cu, and Mn compared with other materials.

## CONCLUSION

As the first trial to make a fish reference material of wet basis, a Japanese-style steamed fish paste reference material was prepared from shark meat. Provided the prerequisites for reference materials are as follows: (1) Availability in large amount, (2) availability at low cost, (3) homogeniety of samples, (4) preservation, (5) safety in transportation, (6) appropriate concentration of elements, this material can be concluded to be a good candidate. For the first two items, the price of shark fish is comparatively low and the fish can be obtained in sufficient numbers at certain markets (about $2 for a fish).

The homogeniety with respect to Hg, K, Na, Ca, and Mg was shown to be within 6% of rel std dev value, using about 2 g of wet sample (ca. 0.6 g dry matter). This material can be preserved for at least 3 months even at room temperature and may be preserved for longer periods in a cold room or in a refrigerator.

Safety in transportation can be readily achieved with careful packing. For the last item, this material can serve as a very good reference material in those fields concerned with the analysis of Hg in fish meat, where Bovine Liver, because it contains too low a concentration of Hg, is difficult to utilize.

## ACKNOWLEDGMENT

The authors express their hearty thanks to T. Taniuchi of the Department of Fisheries, the University of Tokyo, for his help in getting the raw materials and to M. Nose of Tachikawa College of Tokyo for her cooperation in the preparation of this reference material.

## LITERATURE CITED

(1) H. J. M. Bowen, *Analyst (London)*, **92**, 124 (1967).
(2) J. B. Jones, Proceedings of the Pittsburg Conference on Analytical Chemistry and Applied Spectroscopy, Pittsburg, Pa., 1967.
(3) Certificate for Orchard Leaves, U.S. Department of Commerce, National Bureau of Standards, Washington, D.C., 1970.
(4) Certificate for Bovine Liver, U.S. Department of Commerce, National Bureau of Standards, Washington, D.C., 1971.
(5) N. Yamagata, *Bunseki Kagaku*, **20**, 515 (1971).
(6) R. Fukai, Progress Report No. 13, Intercalibration of Analytical Methods on Marine Environmental Samples, International Laboratory of Marine Radioactivity, Principality of Monaco, 1976.
(7) J. P. Cali, *Anal. Chem.*, **48**, 802A (1976).
(8) K. Fuwa et al, *Bull. Chem. Soc., Jpn.*, submitted.
(9) H. L. Rook, Anal. Div., NBS–USA, personal communication, 1976.
(10) T. Taniuchi, "The Sharks", Diving World Pub., Japan, 1976.
(11) S. Hanamura et al., *Proc. Forum Jpn. Soc. Anal. Chem.*, **34**, (1973).
(12) S. Yamazaki et al., *Nihon Kagaku Kaishi*, **1977**, 1148.
(13) C. R. Forester, K. S. Ketchen, and C. C. Wong, *J. Fish. Res. Board Can.*, **29**, 1487 (1972).
(14) M. Taguchi et al., *Bunseki Kagaku*, **26**, 438 (1977).

RECEIVED for review August 18, 1977. Accepted November 2, 1977.

# Use of Electron Capture-Induced Products for Confirmation of Identity in Pesticide Residue Analysis

**Walter A. Aue* and Shubhender Kapila**

*5637 Life Sciences, Dalhousie University, Halifax, N.S., Canada*

The products of reactions taking place in the electron capture detector (ECD) are sometimes capable of reacting with electrons themselves; in fact, this secondary reaction has so far been the only means of detecting their presence (*1-3*). Some of these EC-induced products have been tentatively identified by retention data (*3*).

Some pesticides yield distinct product patterns (e.g., pentachloronitrobenzene yields pentachlorobenzene and the possible tetrachlorobenzenes) and these could conceivably be used to confirm the presence of the pesticide in an analytical sample. The need for confirmation of GC peak identity needs no belaboring; the publications on this subject are far too numerous to cite. They include GC-MS, UV photolysis, use of multiple selective detectors, and, most prevalent, a wide variety of derivatization reactions.

Derivatization usually involves reaction of the total sample, rather than reaction of a single GC peak. While the latter would be preferable on theoretical grounds—i.e. the probability of mistaking another compound for the expected de-

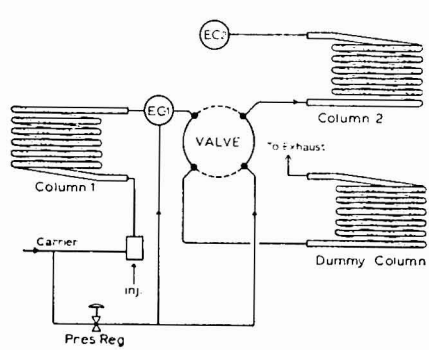


**Figure 1.** Flow schematic

0003-2700/78/0350-0536$01.00/0 © 1978 American Chemical Society

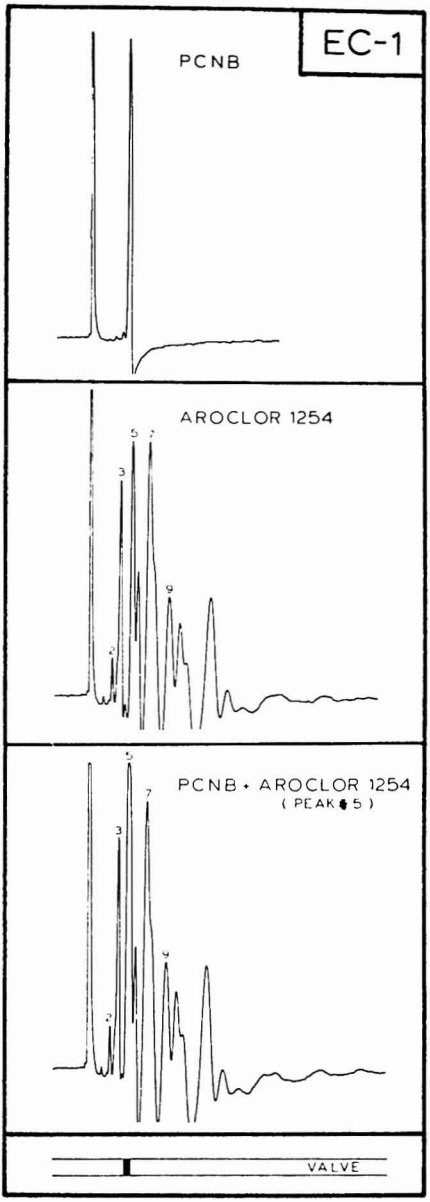


**Figure 2.** Chromatograms obtained from EC-1 for 100-pg injections of pentachloronitrobenzene and 1.5 ng of Aroclor 1254; alone and in mixture. Temperatures: Column 1, 145 °C; column 2, 105 °C; EC-1, 250 °C. Carrier: Argon/isooctane, 30 mL/min through column 1. Same attenuation throughout

rivative is reduced—the technical difficulties in such an approach are formidable and, in most cases, forbidding.

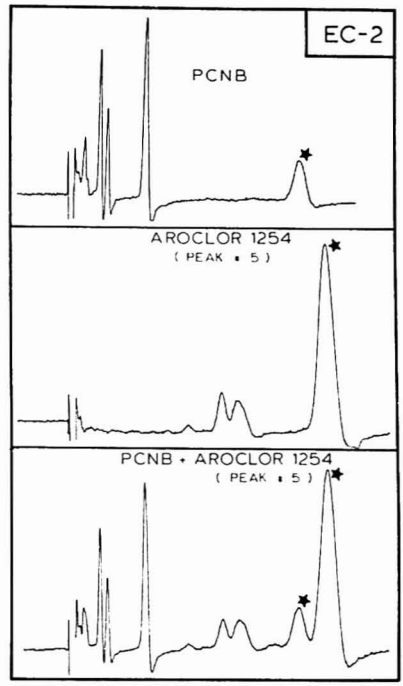


**Figure 3.** Chromatograms of products and residual analyte as seen by EC-2 for cuts taken as indicated in Figure 2. Residual analyte peaks are starred. Same attenuation throughout

Electron capture as a derivatization reaction appears much more restricted in its application than the other methods, but it is one approach which could be used on a single peak right in the chromatograph itself. Analysis would thus be combined with confirmation (similar to GC-MS) and the amount of injected analyte could be in the picogram range.

The present study attempts to demonstrate the feasibility of this approach; a demonstration called for by the hazards of prediction when the temperamental EC detector and thermolabile compounds in very low concentration ranges are involved.

## EXPERIMENTAL

Figure 1 provides a self-explanatory flow chart of the apparatus. The two detectors were regular Mikrotek (Tracor) Ni-63 models. The carrier gas, prepurified argon, was saturated with the vapor of purified isooctane to favor product formation (*3*). The high-temperature 4-port valve was a Valco product, and the steel diaphragm pressure regulator served to keep both inputs to the valve at the same pressure. This setting was chosen such that a significant flow of carrier entered EC-1, adding to the effluent from column 1.

Column 1, and column 2 plus the dummy column, were independently thermostated, the former at higher temperature than the latter two. Columns 1 and 2 were packed with 3% OV-101 on Carbowax 20M-modified (*4*) Chromosorb W, 45/60 mesh. The dummy column (a column of similar resistance as column 2, used to avoid pressure and flow fluctuations) was packed with bare Chromosorb of the same mesh.

Figure 1 shows the usual flowpath, i.e., pure carrier sweeps column 2 and EC-2, while the effluents from column 1 are shunted

to an exhaust duct via the dummy column. The valve is turned only to let the peak of interest pass on to column 2; an operation noted by the dark rectangle on the time axis of Figure 2.

## RESULTS AND DISCUSSION

Figure 2 shows regular chromatograms obtained from EC-1 for PCNB (pentachloronitrobenzene, a much-used fungicide) and Aroclor 1254 (a typical polychlorinated biphenyl product), followed by a mixture of the two, in which PCNB overlaps with peak 5 of the Aroclor.

In each case, the valve was turned at the same time, allowing PCNB, Aroclor peak 5, and their EC-induced products to enter column 2. Residual analyte (starred) and products were monitored by EC-2 as shown in Figure 3. As expected, the product patterns of pentachloronitrobenzene and the polychlorinated biphenyl(s) are drastically different and allow unequivocal distinction, even in mixture.

It should be noted that, even though columns 1 and 2 are packed with the same stationary phase, the analyte peaks overlap severely in Figure 2 but are almost resolved in Figure 3. This is caused by the temperature difference between the two columns and the superior chromatographic conditions for resolution on the second one. The effect could have been easily enhanced by using a different column packing in column 2; and, mutatis mutandis, there are obvious analytical advantageous to such an approach.

While the method appears to work well, an obvious limitation and caveat should be kept in mind. First, not all compounds which respond well in the EC detector give rise to useable product patterns. Second, the requirement for a "clean" system, so typical of EC-GC, is even more stringent in this case, where peaks in the picogram range are being manipulated. This taken into account, the described approach should prove valuable for the detection and confirmation of pesticide residues.

## LITERATURE CITED

(1) C. R. Hastings, T. R. Ryan, and W. A. Aue, *Anal. Chem.*, **47**, 1169 (1975).
(2) S. Kapila and W. A. Aue, *J. Chromatogr.*, **108**, 13 (1975).
(3) S. Kapila, Ph.D. thesis, Dalhousie University, 1976.
(4) C. R. Hastings and W. A. Aue, *J. Chromatogr.*, **89**, 369 (1974).

RECEIVED for review August 19, 1977. Accepted October 10, 1977. This study was supported by AC grant 6099 and NRC grant 9604.

# Tantalum Treated Graphite Atomizer Tubes for Atomic Absorption Spectrometry

**Vladimir J. Zatka**

*J. Roy Gordon Research Laboratory, INCO Metals Company, Sheridan Park, Mississauga, Ontario, Canada, L5K 1Z9*

Atomic absorption analysis in electrically heated graphite atomizers has found widespread acceptance as a routine method in many research and application laboratories. Atomization of the sample in graphite tubes heated up to 3000 °C makes the method exceptionally sensitive and capable of determining a large number of trace elements directly in diverse sample matrices.

Unfortunately, practicing analysts have not always been able to take full advantage of the high temperatures. The tubes rapidly deteriorate and a frequent use of standards is then required due to a steadily changing response. At 2700 °C a useful lifetime of 30 to 50 firings is not unusual. By lowering the atomization temperature, the lifetime of a tube can be increased but sensitivity for many elements is thus sacrificed and potential problems from an incompletely volatilized sample matrix may be generated.

To alleviate the sensitivity problems, matrix modification (*1*, *2*) or various pre-treatments of the graphite tube, sometimes of questionable value, have been tried (*3–5*) including the in situ coating with pyrolytic graphite (*6–9*). In all these approaches, only the interior of the tube is affected and the exterior surface is left unprotected towards oxidation. No substantial improvement in the lifetime of the tube is so achieved.

Obviously, a much more useful approach is one where the whole graphite tube surface, both interior and exterior, is involved in the protective treatment. Tubes with a complete pyrolytic coating are available from Varian-Techtron. It is the purpose of the present paper to document the outstanding properties of tantalum carbidized graphite tubes. Developed originally for handling lanthanum matrices, the treated tubes showed such a steady response and long lifetime at 2700–2800 °C that they are now being used for over two years for general electrothermal atomic absorption practice. In the meantime, two papers were published dealing with specific determinations of silicon in tungsten (*10*) and beryllium in biological material (*11*) for which tubes impregnated with tungsten, tantalum, or zirconium salts were used. In the present paper, a rapid soaking method is described. The procedure is simple enough to be carried out in any laboratory and is easily amenable to commercial mass production of carbidized tubes. The general performance of the tantalum carbidized tubes is distinctly superior to that of tubes with internal pyrolytic coating (*9*).

## EXPERIMENTAL

**Apparatus.** The work was done on a Perkin-Elmer Model HGA 74 graphite furnace atomizer mounted in a Model 306 AA spectrophotometer with a Model 165 recorder. Also used were a Leeds and Northrup disappearing-filament optical pyrometer, a Cameca Model MS 64 electron microprobe, and a Siemens x-ray diffraction unit.

Regular graphite tubes were utilized for the treatment by tantalum. Sample solutions were injected by Eppendorf microliter pipets. The atomizer system was operated in the gas-stop mode with argon as the purge gas.

**Tantalum Soaking Solution (6% Ta).** Weigh 3 g of tantalum metal into a 100-mL PTFE beaker, add 10 mL of dilute hydrofluoric acid (1 + 1), 3 g of oxalic acid dihydrate, and 0.5 mL of 30% hydrogen peroxide. Heat carefully to dissolve the metal. Add more peroxide when the reaction becomes too slow. When dissolution is complete, add 4 g of oxalic acid and approximately 30 mL of water. Dissolve the acid and dilute to 50 mL. Store in a plastic bottle.

**Tube Treatment.** Vertically immerse the graphite atomizer tubes in the 6% tantalum soaking solution contained in a plastic vial. Transfer the vial into a desiccator, evacuate (water pump), and maintain under reduced pressure for 20–30 s. Release the air bubbles formed on the tube walls by tapping the exterior of the desiccator. Restore the atmospheric pressure in the desiccator, remove the tubes from the bath and dry them first in the air (30 min) and then at 105 °C (1 h). Mount each tube in the atomizer unit fitted with new unused graphite rings and, while the argon purge gas flow and the water cooling are on, raise the temperature gradually (30 s) to 1000 °C and then for a few seconds to 2500 °C.

Repeat the treatment once again but soak the tubes for only

0003-2700/78/0350-0538$01.00/0 © 1978 American Chemical Society

**Table I. Precision and Accuracy with Tantalum Carbidized Tubes[a]**

| Material | Sample | Parts per million | | | | | | | |
|---|---|---|---|---|---|---|---|---|---|
| | | As (RSD[b]) | Bi (RSD[b]) | Co (RSD[b]) | Mn (RSD[b]) | Pb (RSD[b]) | Sb (RSD[b]) | Sn (RSD[b]) | Te (RSD[b]) |
| Nickel Metal (ASTM 871) | 1 | - | 1.39 (5%) | 22.7 (1%) | 2.28 (3%) | 2.40 (2%) | 0.92 (17%) | 2.18 (16%) | 1.18 (2%) |
| | 2 | - | 1.41 (1%) | 22.5 (2%) | 2.13 (3%) | 1.77 (1%) | 1.04 (30%) | 1.76 (9%) | 1.35 (4%) |
| | 3 | - | 1.47 (1%) | 22.9 (2%) | 2.42 (3%) | 2.12 (2%) | 0.86 (16%) | 1.84 (10%) | 1.38 (4%) |
| | 4 | - | 1.44 (2%) | 23.5 (5%) | 2.10 (2%) | 1.94 (3%) | 1.15 (18%) | 1.84 (5%) | 1.28 (9%) |
| | 5 | - | 1.46 (3%) | 22.5 (2%) | 2.06 (1%) | 2.09 (1%) | 1.02 (22%) | 1.91 (3%) | 1.37 (4%) |
| | 6 | - | 1.40 (4%) | 22.4 (2%) | 2.17 (2%) | 1.78 (2%) | - | 1.96 (9%) | 1.34 (11%) |
| Mean, $\bar{x}$ | | - | 1.43 | 22.8 | 2.19 | 2.00 | 1.00 | 1.92 | 1.32 |
| RSD[c] ($n = 6$) | | - | 2.3% | 1.8% | 6.1% | 11.9% | 11.3% | 7.7% | 5.7% |
| Tube history (No. of firings) | | - | 100 | 30 | 140 | 140 | 40 | 180 | new |
| Found by other method, ppm | | - | 1.3[d] | 23[e] | 1.9[f] | 1.5[d] | 1.4[f] | 3[f] | 2.2[f] |
| Nickel Metal (ASTM 872) | 1 | 9.56 (1%) | 9.79 (1%) | 12.8 (2%) | - | 7.86 (2%) | 9.80 (3%) | 9.98 (4%) | 10.81 (2%) |
| | 2 | 9.62 (2%) | 9.97 (1%) | 12.5 (1%) | - | 7.62 (1%) | 9.99 (4%) | 9.83 (1%) | 10.86 (1%) |
| | 3 | 9.44 (2%) | 10.04 (1%) | 12.6 (1%) | - | 7.82 (1%) | 9.83 (3%) | 10.07 (2%) | 11.05 (1%) |
| | 4 | 9.68 (1%) | 9.78 (1%) | 12.4 (4%) | - | 7.81 (2%) | 10.04 (2%) | 9.86 (4%) | 11.34 (3%) |
| | 5 | 9.78 (2%) | 9.87 (2%) | 12.4 (2%) | - | 7.81 (1%) | 9.95 (3%) | 9.78 (4%) | 10.95 (3%) |
| | 6 | 9.37 (2%) | 9.81 (2%) | 12.4 (1%) | - | 7.71 (1%) | - | 9.68 (3%) | 11.44 (1%) |
| Mean $\bar{x}$ | | 9.58 | 9.88 | 12.5 | - | 7.77 | 9.92 | 9.87 | 11.08 |
| RSD[c] ($n = 6$) | | 1.6% | 1.1% | 1.3% | | 1.1% | 1.0% | 1.4% | 2.3% |
| Tube history (No. of firings) | | 100 | 140 | 60 | | 180 | 30 | 240 | 50 |
| Found by other method, ppm | | 8[g] | 10.0[d] | 13[e] | - | 7.8[d] | 10[f] | 10[f] | 12[f] |
| Instrument parameters | | | | | | | | | |
| Wavelength, nm | | 193.7 | 223.1 | 252.1 | 279.5 | 283.3 | 217.6 | 286.3 | 214.3 |
| Slit setting | | 4 | 3 | 3 | 3 | 4 | 3 | 3 | 3 |
| Char, °C | | 800 | 600 | 800 | 800 | 400 | 400 | 500 | 600 |
| Atomize, °C | | 2600 | 2500 | 2700 | 2600 | 2500 | 2600 | 2600 | 2500 |

[a] 2% nickel nitrate solution in 5% v/v nitric acid; aliquot analyzed 10 μL. [b] Repeatability of replicate analyses ($n = 4$; for Co, $n = 3$). [c] Reproducibility of 6 independent sample means; for Sb, $n = 5$. [d] TOPO extraction, AA (ASTM method). [e] Direct conventional AA with matched matrix. [f] Lanthanum hydroxide collection, conventional AA. [g] Iodide extraction, molybdenum blue.

Table II. Accuracy in Copper Metal Analysis[a]

| | Parts per million | | | | | | | |
|---|---|---|---|---|---|---|---|---|
| | Bi | | Pb | | Sb | | Sn | |
| NBS Designation | Found | NBS | Found | NBS | Found | NBS | Found | NBS |
| SRM 394 (Cu I) | 0.3 | 0.35 | 28. | 26.5 | 3.7 | 4.8 | – | 65 |
| SRM 395 (Cu II) | 0.4 | 0.50 | 3.4 | 3.25 | 7.8 | 7.5 | 1.7 | 1.5 |
| SRM 396 (Cu III) | 0.1 | 0.07 | 0.44 | 0.41 | <.2 | (.2) | 0.9 | 0.8 |

[a] 2% copper nitrate solution in 5% v/v nitric acid; aliquot analyzed, 10 μL; instrument parameters as in Table I; all data are single analysis results.

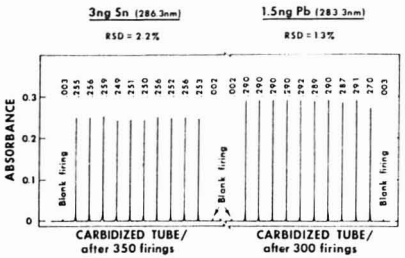


**Figure 1.** Repeatability of signals in old tantalum carbidized tube (solution matrix 5 mg $mL^{-1}$ La and 2 mg $mL^{-1}$ Fe in 5% $HNO_3$). Temperature program: Sn, 120°/20 s, 500°/20 s, 2700°/6 s. Pb, 120°/20 s, 400°/20 s, 2700°/6 s

10 s under the reduced pressure.

## RESULTS AND DISCUSSION

To form a thermally protective layer of refractory metal carbide over the entire graphite tube surface, tantalum is the obvious first choice. It forms a thermodynamically stable interstitial carbide, TaC, with very high melting point of 4270 K (*12*) and a very low vapor tension. It is electroconductive, is not decomposed by water, and is chemically inert. This ensures the longevity of the treatment without altering the physical properties of the parent graphite tube.

**Composition of Soaking Solution.** It is essential that the solution be free of strong mineral acids, such as sulfuric or nitric, as they destroy the graphite surface on evaporation and contribute to both a reduced tube lifetime and poor repeatability of atomization signals. The hydrofluoric–oxalic acid medium is suitable for holding a sufficiently high tantalum concentration (6%) required for the graphite treatment. The solution is stable and keeps indefinitely even when only a small excess of free hydrofluoric acid is present.

**Treatment of Graphite Atomizer Tubes.** By using reduced pressure, the penetration of the soaking solution inside the graphite tube is fast and the whole operation takes only a few minutes or so as compared to 24 h at atmospheric pressure (*10*) or 6 h at 175 °C in an autoclave (*11*). After one treatment, electron microprobe analysis of the cross section of the tube showed a uniform tantalum penetration through the whole wall thickness. In the second treatment, tantalum was deposited at the tube surface only, approximately 0.1 mm deep. X-ray diffraction examination showed tantalum carbide, TaC, and carbon as the only major phases. The carbidizing reduces the porosity of the graphite tubes but does not seal the surface completely.

**Temperature Calibration.** The temperature meter on the HGA power supply unit was calibrated in the range of 1500–2700 °C by measuring the actual temperature inside the heated tube. The radiation from the inner wall of the tube was focused through the sample introduction port at the viewing lens of the optical pyrometer. The estimated accuracy of the measurement was ±50 °C. Temperatures achieved in the double tantalum carbidized tubes did not differ from those in the regular tubes and a re-calibration of the meter is therefore not necessary.

**Response and Lifetime of Treated Tubes.** The carbidizing of the graphite atomizer tubes greatly improves the repeatability of replicate atomization signals even after extended use of the tube at temperatures of 2700 °C. The refractory coating of the entire tube surface assists in maintaining the tube in uniformly good condition and effectively retards the aging effect caused by high temperatures.

For example, trace elements are routinely determined in this laboratory by electrothermal atomic absorption after collection on mixed lanthanum–ferric hydroxides. Problems were encountered in the past when the regular untreated graphite tubes were used. Some of the lanthanum always remained in the tube as carbide. As an ionic type, the lanthanum carbide was hydrolyzed by the next sample aliquot or, simply, by humidity in the air and this led to rapid destruction of the tube surface and deterioration of tube performance. For this reason, the recommended lanthanum treatment of the tube interior (*3, 4*) does not appear advantageous. In the tantalum carbidized tubes, it is possible to ensure a complete matrix removal at an atomization temperature of 2700 °C without sacrificing the useful lifetime and a steady response of the tube. Figure 1 shows the chart recorder tracings and peak height readings on 10 replicate analyses of 1.5 ng of Pb and 3 ng of Sn in a La-Fe matrix as they were obtained in a tantalum carbidized tube with a history of 300 and 350 firings at 2700 °C, respectively. Aliquots of 5 and 10 μL, respectively, were added manually. The excellent precision of 1.3% and 2.2% (RSD) for such an old tube is remarkable. The useful lifetime of this particular tube was over 400 firings, which is not unusual for the tantalum treated tubes operated at 2700 °C.

No difficulties have been encountered at the trace level determinations of Ag, Al, As, Bi, Cd, Co, Mn, Pb, Sb, Se, Sn, Te, and Zn in a variety of inorganic matrices using the tantalum carbidized atomizer tubes. Examples of achieved precision, i.e., the repeatability of replicate analyses of identical aliquots and the reproducibility of results from independent samples, and of accuracy in the analysis of ASTM nickel test samples and of NBS copper SRM's are given in Tables I and II. Potential interferences remain the same as are those observed in the regular untreated graphite tubes.

## CONCLUSIONS

The lifetime and the long-term response stability of the graphite atomizer tubes is substantially improved by tantalum carbidization of their entire surface. Even at high atomization temperatures of 2700 °C, the carbidized tubes survive 350–400 firings with continued high precision on replicate analyses. The useful lifetime of a regular tube is thus extended by a factor of 8 or better. The decrease in sensitivity due to aging is minimal; for instance, a loss of only 25% was recorded for selenium during the course of 350 firings at 2700 °C.

The tantalum treatment does not alter the temperature calibration of the furnace by more than 50 °C. The carbidized

tubes are suitable for general electrothermal atomic absorption analysis of trace elements in various matrices. They failed, however, in the determination of platinum group metals by effectively suppressing their atomization. While the tubes may not be suitable for a tantalum determination, a similar treatment with the second highest boiling niobium carbide, NbC, may make it possible.

The developed procedure is simple and inexpensive. It uniformly affects the whole surface of the graphite tube. The extent of the carbide formation can be easily controlled by the number of sequential treatments and by the concentration of the tantalum solution.

## LITERATURE CITED

(1) E. L. Henn, *Anal. Chem.*, **47**, 428 (1975).
(2) E. L. Henn, ASTM STP 618, 1977, p 54.
(3) J. H. Runnels, R. Merryfield, and H. B. Fisher, *Anal. Chem.*, **47**, 1258 (1975).
(4) K. C. Thompson, K. Wagstaff, and K. C. Wheatstone, *Analyst (London)*, **102**, 310 (1977).
(5) R. Cioni, G. Ottonello, and A. Mazzucotelli, *Anal. Chim. Acta*, **82**, 415 (1976).
(6) D. D. Siemer, R. Woodriff, and B. Watne, *Appl. Spectrosc.*, **28**, 582 (1974).
(7) S. A. Clyburn, T. Kantor, and C. Veillon, *Anal. Chem.*, **46**, 2213 (1974).
(8) K. C. Thompson, R. G. Godden, and D. R. Thomerson, *Anal. Chim. Acta*, **74**, 289 (1975).
(9) D. C. Manning and R. D. Ediger, *At. Absorpt. Newsl.*, **15**, 42 (1976).
(10) H. M. Ortner and E. Kantuscher, *Talanta*, **22**, 581 (1975).
(11) T. Stiefel, K. Schulze, G. Tölg, and H. Zorn, *Anal. Chim. Acta*, **87**, 67 (1976).
(12) A. K. Holliday, G. Hughes, and S. M. Walker "Carbon" in "Comprehensive Inorganic Chemistry", Vol. 1, J. C. Bailar, Jr., H. J. Emeléus, R. Nyholm, and A. F. Trotman-Dickenson, Ed., Pergamon Press, Oxford, 1973, p 1211.

RECEIVED for review October 3, 1977. Accepted November 23, 1977.

# Contamination-Free Adjustment of pH during Trace Analysis

**J. E. Riley, Jr.**

*Bell Laboratories, Murray Hill, New Jersey 07974*

Determinations of trace elements in high purity materials often require dissolution of the sample followed by adjustment of the pH prior to chemical separations or preconcentration. These adjustment steps are sources of contamination even when efforts are made to use high-purity reagents (*1–3*). Very high purity reagents are produced by a number of excellent nonboiling distillation procedures (*1–6*). However, assuming reagents of acceptable quality are produced, storage for periods of time can result in contamination of the reagent by even extensively precleaned storage vessels (*2*).

Circumventing the problem of reagent contamination during storage can be accomplished by using gaseous reagents generated when needed for trace analyses. Gaseous acids and bases have been used occasionally in industrial applications (*7, 8*). Use of such reagents in the trace analysis laboratory could be more extensive (*9*). This paper reports a study of the application of gaseous reagents to trace analysis with data to exhibit the utility and advantages.

## EXPERIMENTAL

**Equipment.** Important considerations in the design of the apparatus are: (1) total amount of reagent to be transferred, (2) accuracy and precision of transfer, (3) speed of reagent transfer, and (4) number of samples to be treated. In the majority of trace analytical work in our laboratory, a relatively small number of valuable samples are processed. Precise control of pH in small volumes of solution (2–5 mL) is essential for quantitative recovery of trace elements during chemical separations.

The apparatus in Figure 1 is basically an isopiestic distillation system. The container was a cut-off 2000-mL beaker placed on a glass plate with multiple samples accommodated around a single reservoir. Isopiestic distillation will proceed until stopped or until the volatile reagent has attained an equilibrium distribution in all solutions. Initially, for control, an extra sample solution with indicator was used in one of the beakers; but after several runs the transfer rate was characterized for the particular experimental arrangement and the indicator was omitted. To increase the speed of distillation, a small disk of aluminum with a radially bored hole for a small cartridge heater was placed under the reservoir. To minimize leaching by the sample solutions, only the reservoir and not the entire apparatus was heated. When used, this heater did little more than supply the heat of vaporization to the reagent reservoir. The reagent in the reservoir was not boiled since violent bubbling would transfer droplets to the open sample beakers.

The gas stream apparatus (Figure 2) processed single samples quickly with exact control of pH. The rate of reagent generation was controlled by the temperature of the reservoir. There were two reagent delivery modes in this system, one for rapid transfer with coarse control (left side) and one "diluting" system for exact control of the final pH adjustments (right side). For the higher rate of transfer, the "wand" portion of the generator directed the output to the surface of the sample solution. Although transfer of reagent is more efficient and the sample is stirred by bubbling from the submerged tip of the capillary, this contact should be avoided unless great care is taken in choosing and cleaning the capillary in order to minimize leaching impurities into the sample.

Exact control of the pH was achieved by metering into the sample small amounts of the reagent or reagent and pure carrier gas mixtures with a syringe. To avoid drawing sample solution into the capillary due to a low flow of highly soluble gaseous reagent, a constant stream of pure, filtered carrier gas ($N_2$ or He at <100 mL/min) was bubbled through the solution. Careful selection of capillary bore and gas flow rate was essential to avoid excessive bubbling, which leads to contamination or loss of sample. The positive, inert atmosphere over the sample surface also aided in the exclusion of airborne contamination. Gaseous reagent, a mixture of reagent and carrier gas, or pure carrier gas was drawn into the syringe through a mixing valve consisting of two Teflon stopcocks with staggered opening angles. A syringe valve allowed filling from the mixing valve and discharge through a fine Teflon needle into the carrier gas stream at the top of the capillary. Construction of the apparatus with all-plastic or Teflon-coated stainless steel minimized opportunities for inorganic contamination. For the ultimate in pH control, the gaseous reagent in the syringe was diluted with carrier after each small injection, thus successively decreasing the amount of reagent added per unit volume of the syringe. For the final additions, the syringe was disconnected and all but a small fraction of its contents ejected before further dilution.

Because of the evolution of toxic gases and the need to minimize chances for sample contamination, both apparatus and samples were housed in a laminar-flow clean hood with exhaust.

**Contamination Measurements.** *Radiotracer Studies.* One hundred milliliters of reagent grade HCl and $NH_4OH$ were added to their respective reservoirs for experiments with the gas stream system. Both reagents were then spiked with 1–4 μg per mL with each of the following cations: Na, Cr, Mn, Fe, Co, and Zn. The spiking solutions had been tagged with sufficient $^{22}Na$, $^{51}Cr$, $^{54}Mn$, $^{59}Fe$, $^{60}Co$, and $^{65}Zn$ so that there would be on the order of 50 cpm/ng of each element. A 0.1-mL aliquot of the HCl solution was counted on a lithium-drifted germanium detector to acquire the spectrum shown in Figure 3.

Multiple samples of $HNO_3$ (8 M) and NaOH (10 M) were neutralized with gaseous reagents from the radioactive reservoirs.

0003-2700/78/0350-0541$01.00/0 © 1978 American Chemical Society

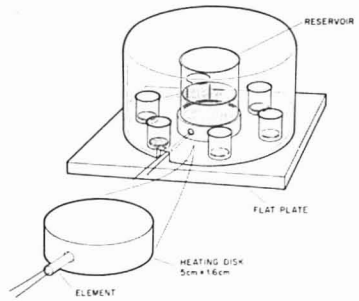


**Figure 1.** Reagent chamber transfer apparatus

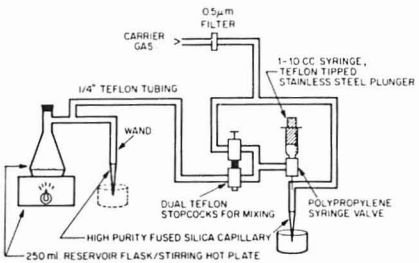


**Figure 2.** Gas stream transfer apparatus

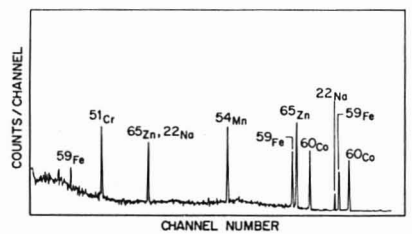


**Figure 3.** γ-ray spectrum of spiked HCl reservoir

The reservoirs were stirred and heated gently to the point where gas bubbles were formed. At the phenyl red end point, the samples were counted in a 7.62-cm (3-inch) well-type NaI detector wired to an amplifier and timer/scaler. Also counted were 2-μL aliquots of each radioactive reagent. This volume contained 4.0, 5.6, 4.2, 4.0, 8.0, and 3.6 ng of Na, Cr, Mn, Fe, Co, and Zn, respectively, on the basis of the added dopants. All γ-ray activity from 0.3 to 1.4 MeV was integrated for a period of 2000 s for samples, reservoir aliquots, and backgrounds.

*X-ray Fluorescence Measurements.* Blank samples were prepared containing 0.1 mL of 44% perchloric acid (high purity), 2 μg of Ti coprecipitant, and 2.5 mL of high purity water. After adjusting the pH with gaseous or high purity aqueous ammonia to 4.0 ± 0.1, 2 drops of 2% aqueous solution of diethyldithiocarbamate were added (*10, 11*). The subsequent Microdot samples were examined with a nondispersive x-ray fluorescence (XRF) instrument incorporating: (1) a Ag target x-ray tube operating at 50 kV and 10 mA with a 0.050-inch aperture, (2) a lithium-drifted silicon detector, (3) a Princeton Gamma Tech PGT-1000 Analyzer system.

*Reagent Chamber Transfer Rates.* Solutions of HCl and KOH were neutralized to the phenyl red end point with $NH_3$ and HCl, respectively, in the reagent chamber apparatus. The initial concentrations of the 10-mL sample solutions of HCl and KOH extended through the 0.1 to 1.0 M range with duplicates run at each point. The reagent reservoir, a 250-mL beaker containing 100 mL of concentrated $NH_4OH$ or HCl, was warmed by a small heater to prevent self-chilling of the reagent to below room temperature. The reservoir was filled with fresh reagent prior to each neutralization, and the cover was put into place immediately. The entire assembly was agitated slightly on a regular basis during the course of the neutralization in order to mix the sample solutions and to facilitate end-point detection.

Table I. Total γ-ray Activities of Neutralized $HNO_3$ Solutions

| Sample[a] | Activity, cpm |
|---|---|
| 1 | 219 |
| 2 | 217 |
| 3 | 213 |
| 4 | 217 |
| 5 | 218 |
| Mean | 217 ± 2 |
| Background | 215 |
| A[b] | 1881 |
| B[b] | 1846 |

[a] 4 mL, 8 M $HNO_3$. [b] 2 μL $NH_4OH$ from reservoir, diluted to 4 mL.

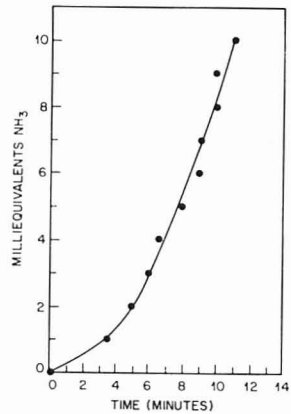


**Figure 4.** $NH_3$ transfer with reagent chamber

## RESULTS AND DISCUSSION

Tables I and II show the results of the contamination studies. As can be seen, there is no detectable transfer of the doped elements into the nonactive samples from the reservoirs of reagent containing contaminants at a level one hundred times normal. The spectrum acquired with the Ge(Li) detector showed that the γ-ray activity levels measured approximately the same for the six tracers. Dividing the average measured reservoir activity equally among the elements (total: 29.4 ng) yields roughly 60 cpm for 1 ng of all elements combined. From this and the measured background, a minimum detectable level (*12*) can be set at 0.3 ng of total impurities in the 4-mL sample (0.08 ppb). Therefore, it can be estimated that the largest total weight of the six elements that could have been transferred without being detected in the tracer studies was less than 0.3 ng during the transfer of 32 mequiv of $NH_4OH$ and 40 mequiv of HCl.

While the tracer work indicated that no detectable contamination was transferred to samples from the reservoir, information was also necessary concerning the introduction of contaminants by other parts of the apparatus. XRF data taken on blanks prepared with pH adjustment by either gaseous or high purity aqueous $NH_3$ showed no measurable

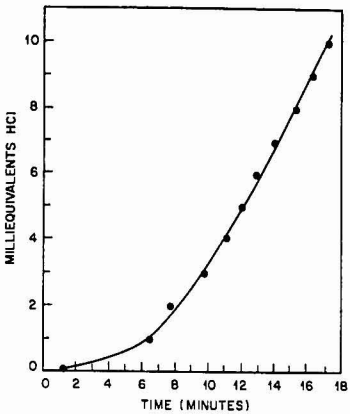


Figure 5. HCl transfer with reagent chamber

difference between the two methods for Cu, Ni, Co, Fe, Mn, Cr, and Zn. This information complemented that from the radiotracer studies by indicating that the contamination introduced between the reservoir and the sample was also negligible. The contribution of this gaseous technique for pH adjustment is further enhanced by the facts that during the preparation of the XRF blanks (1) there was a negligible increase in sample solution volume, (2) precise control of the pH adjustment of small, unbuffered solutions was maintained easily to better than ± 0.1 pH unit, (3) with a high degree of control the adjustments were performed more quickly than with aqueous reagents, and (4) reagent grade $NH_4OH$ was used as the source for the high purity gas.

In Figure 4 are plotted data from neutralizations of 10-mL HCl solutions in 50-mL beakers with $NH_3$ using the reagent chamber. On the average, the rate of $NH_3$ uptake from the 250-mL reservoir is 0.7 mequiv/min. Figure 5 shows a similar plot of the reverse situation where basic solutions (KOH) were neutralized from HCl (12 M) reservoirs. The average rate of HCl transfer was 0.4 mequiv/min. When 30-mL sample beakers were used, the transfer rate decreased by 30%.

Table II. Total γ-ray Activities of Neutralized NaOH Solutions

| Sample[a] | Activity, cpm |
|---|---|
| 1 | 255 |
| 2 | 250 |
| 3 | 248 |
| 4 | 249 |
| 5 | 248 |
| Mean | 250 ± 3 |
| Background | 249 |
| A[b] | 1946 |
| B[b] | 1950 |

[a] 4 mL 10 M NaOH. [b] 2 μL HCl from reservoir, diluted to 4 mL.

## ACKNOWLEDGMENT

The author thanks J. E. Kessler for his able assistance with the Microdot analyses and for his many helpful discussions.

## LITERATURE CITED

(1) E. C. Kuehner, R. Alvarez, P. J. Paulsen, and T. J. Murphy, *Anal. Chem.*, 44, 2050 (1972).
(2) R. W. Dabeka, A. Mykytiuk, S. S. Berman, and D. S. Russell, *Anal. Chem.*, 48, 1203 (1976).
(3) M. Zief and J. W. Mitchell, "Contamination Control in Trace Analysis", John Wiley and Sons, New York, N.Y., 1976, Chapter 6.
(4) H. Irving and J. J. Cox, *Analyst (London)*, 83, 526 (1958).
(5) J. M. Mattinson, *Anal. Chem.*, 44, 1715 (1972).
(6) K. Little and J. D. Brooks, *Anal. Chem.*, 46, 1343 (1974).
(7) O. Wein, K. Wichterle, P. Mitschka, J. Sulc, and M. Patek, *Chem. Prum.*, 24 (12), 604 (1974).
(8) Mississippi Chemical Corp., French Patent 2187692, February 1974.
(9) J. W. Mitchell and D. L. Nash, *Anal. Chem.*, 46, 326 (1974).
(10) C. L. Luke, *Anal. Chim. Acta*, 41, 237 (1968).
(11) J. E. Kessler and S. M. Vincent, unpublished work.
(12) L. A. Currie, *Anal. Chem.*, 40, 586 (1968).

RECEIVED for review October 6, 1977. Accepted November 1, 1977.

# Rapid Packing of Coiled Glass Gas Chromatography Columns

**Geraldine Olerich**

*Analytical Chemistry Division, Oak Ridge National Laboratory, Oak Ridge, Tennessee 37830*

Many methods have been tried in our laboratory to pack gas chromatographic columns of high efficiency and reproducibility. Because of the fragile nature of the majority of our columns, 20 ft × $^1/_8$ in. o.d. glass, delicate handling is necessary. Until now, the most efficient method we have found was to place a small plug of glass wool in one end of the column and attach the column to a vacuum line. A 3 ft × $^1/_4$ in. o.d. Teflon tube was filled with the packing material and, using Swagelok fittings, one end of the tube was attached to the column and the other end to a dry nitrogen source. The packing was forced into the column with a nitrogen head pressure of 50 psig and vibration. Several hours were required to pack the columns, apparently because of static electricity generated by the friction of the packing against the glass. The static charge caused the packing to coat the inside of the column and prevented it from moving freely to give a high density packed column. The problem can be alleviated somewhat by packing the column following heat treatment in the gas chromatographic oven. The front of the column is connected to the inlet of the chromatograph and the empty column is heated to ~200 °C for 5 min. After cooling, the column is removed from the oven and again attached to the vacuum and nitrogen lines.

We realized then that most of our problems could be solved if the columns could be packed directly in the GC oven. The column packer described in this paper is a simple, inexpensive device which allows this to be done. This device (Figure 1) was constructed to fit a Perkin-Elmer Model 3920 but could be adapted to any gas chromatograph.

A small glass wool plug is placed in the back end of the glass column. Two or three inches of packing is pulled into the column with vacuum to allow compacting of the glass wool plug. The column is then placed in the GC oven and the front end attached to the inlet as usual. The system retainer nut and the metal and glass liner are removed from the inlet and the $^1/_4$-in. o.d. copper tube of the column packer is inserted as far as it will go into the inlet. The Swagelok is tightened to hold the packer in place. Using a small funnel, the reservoir

0003-2700/78/0350-0543$01.00/0 © 1978 American Chemical Society

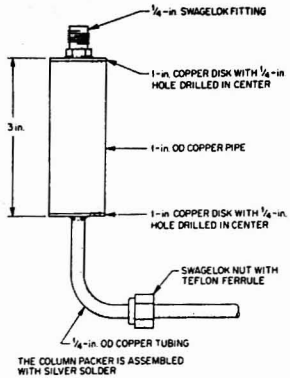


**Figure 1.** Column packing reservoir

is filled with packing material. A $^1/_4$-in. o.d. copper tube is attached to the top Swagelok fitting and the other end is connected to a nitrogen or helium tank. By applying a pressure of 60 psig and vibrating the copper tube just under the reservoir, the packing will flow into the column. When the column appears to be full, each coil is lightly vibrated with the vibro-tool and the copper tube is again vibrated until no more packing will flow into the column. If static electricity slows the movement of the packing, close the oven and heat to ~200 °C. Immediately cool the oven and the packing will continue to flow. After gradually reducing the pressure to atmospheric, the column is removed from the oven and a glass wool plug is inserted in the front of the column.

By this method, we have been able to reproducibly pack 20 ft × $^1/_8$ in. o.d. coiled glass columns of high density in 5 to 10 min.

RECEIVED for review September 12, 1977. Accepted October 17, 1977. Research sponsored by the U.S. Energy Research and Development Administration under contract with Union Carbide Corporation.

## CORRECTION

### Precision of Flame Atomic Absorption Measurements of Copper

In this article by N. W. Bower and J. D. Ingle, Jr., *Anal. Chem.*, 48, 686 (1976), Equation 15 should read:

$$\xi_3 = [E_s\ 2.303\ A]^{-1}[\sigma_{st}^2 - (\xi_1^2 + \xi_2^2)(E_r T)^2 - mGKE_r T - \sigma_{ot}^2 - \sigma_e^2]^{1/2}$$

The correct form of the equation shown here was used for all calculations presented as well as in a more recent paper (N. W. Bower and J. D. Ingle, Jr., *Anal. Chem.*, 49, 574 (1977)).

0003-2700/78/0350-0544$01.00/0 © 1978 American Chemical Society

# Author Index



---

# Future Articles

**Practical Solutions to Matrix Effects in X-ray Fluorescence Analysis by Mathematical Methods**
M. T. Haukka and I. L. Thomas

**Microdetermination of Molecular Species of Oligo- and Polyunsaturated Diacylglycerols by Gas Chromatography–Mass Spectrometry of Their *tert*-Butyldimethylsilyl Ethers**
J. J. Myher, A. Kuksis, L. Marai, and S. K. F. Yeung

**Band-Broadening Phenomena in Microcapillary Tubes under the Conditions of Liquid Chromatography**
T. Tsuda and M. Novotny

**Solvent Enhancement Effects in Thin-Layer Phosphorimetry**
J. N. Miller, D. L. Phillipps, D. T. Burns, and J. W. Bridges

**Analysis of Commercial Sodium Tripolyphosphates by Phosphorus-31 Fourier Transform Nuclear Magnetic Resonance Spectrometry**
S. A. Sojka and R. A. Wolfe

**Quantitative Determination of D- and L-Amino Acids: Reaction with *tert*-Butyloxycarbonyl-L-leucine *N*-Hydroxysuccinimide Ester and Chromatographic Separation as L,D and L,L Dipeptides**
A. R. Mitchell, S. B. H. Kent, I. C. Chu, and R. B. Merrifield

**Determination of the Leachability of Solids**
O. U. Anders and J. F. Bartel

**Automated Three-Dimensional Plotter for Fluorescence Measurements**
J. H. Rho and J. L. Stuart

**Simultaneous Multielement Determination by Atomic Emission with an Echelle Spectrometer Interfaced to Image Dissector and Silicon Vidicon Tubes**
H. L. Felkel and H. L. Pardue

**Optimization of Reverse-Phase Liquid Chromatographic Separation of Weak Organic Acids**
S. N. Deming and M. L. H. Turoff

**Determination of Ruthenium in Automobile Exhaust Emissions by Negative Ion Chemical Ionization Mass Spectrometry**
S. R. Prescott and T. H. Risby

**Microcomputer Assisted, Single Beam, Photoacoustic Spectrometer System for Solids**
E. H. Eaton and J. D. Stuart

**Determination of the Benzodiazepine Anticonvulsants in Plasma by High Pressure Liquid Chromatography**
R. J. Perchalski and B. J. Wilder

**Determination of Main Components and Impurities in Lithium–Boron Alloys**
L. E. DeVries and E. Gubner


# Want the only dispenser with a Teflon®-coated plunger?

# Ask for the 'Teflon Dispenser.'

Why does a Brinkmann Dispensette seem to work more smoothly than other bottle-top dispensers?

The secret is its Teflon-coated plunger.

Dispensers with glass or polypropylene plastic plungers often 'freeze' or 'stick' when used with alkaline reagents. On a Dispensette, the Teflon coating on the plunger insures smooth operation with any reactive chemical (except HF), even with concentrated acids and bases.

Of course, it takes more than a smoothly-working plunger to make a dependable dispenser. Instead of external glass tubing that could break or chip, Dispensettes are equipped with flexible Teflon filling and discharge tubes that can easily be cut to any desired length. Simply pull them off and a Dispensette is ready for autoclaving at 120°C without further disassembly.

Dispensette offers a wide selection of models for fast, accurate dispensing of volumes from 0.1 to 50ml, with better than ±1.0% accuracy and ±0.1% reproducibility. There is hardly a standard size screw-neck reagent bottle, can or container (even STJ 24/40 and 29/42 glassware) which a Dispensette will not fit, either directly or with optional screw-in adapters.

Some Dispensette design features have been copied by other dispensers, but none has its smooth, foolproof operation. That's because only Dispensette has a Teflon-coated plunger. Write for literature: Brinkmann Instruments, Inc., Cantiague Rd., Westbury, N.Y. 11590. In Canada: Brinkmann Instruments (Canada), Ltd.

**Brinkmann Dispensette®**

*Available from:* Ace Scientific
Beckman Instruments, Science Essentials Operations
Bio-Rad Laboratories/Cole-Parmer Instrument Co.
Curtin Matheson Scientific/Fisher Scientific
General Scientific/Markson Scientific/Preiser Scientific
Sargent Welch/Scientific Products/SGA Scientific
Arthur H. Thomas/VWR Scientific/Wilkens-Anderson Co.

Dispensette® is a registered trademark of R. Brand Co.
Teflon® is a Du Pont trademark.

CIRCLE 21 ON READER SERVICE CARD

23 AA 2521